

Contract No. N00014-95-1-0013 and N00014-97-1-0409

Program Officer: R. Miller/J. Goldwasser

Title: Experimental Charge Densities and Electrostatic Potentials in Energetic
Materials and Infrastructure Upgrade for an X-ray Crystallography
Laboratory

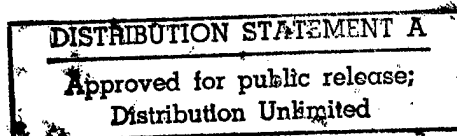
PI: A. Alan Pinkerton

Department of Chemistry, University of Toledo, Toledo, OH 43606

tel. (419) 530-4580, FAX (419) 530-4033, email apinker@uoft02.utoledo.edu

FINAL TECHNICAL REPORT

Submitted by A. Alan Pinkerton 2.11.99



DTIC QUALITY INSPECTED 4

1 999 0222 041

A Description of the scientific research goals

1. To install a state-of-the-art X-ray crystallography laboratory with a new diffractometer using CCD area detector technology and develop data collection and data reduction protocols for charge density studies. To compare charge density results from a CCD detector to those obtained by conventional diffractometers. To fully evaluate the suitability of CCD detectors for the experimental study of electron density distributions and the derived electrostatic potentials. To develop, optimize and calibrate a new helium cooling system for X-ray diffraction for ultra low temperature measurements.
2. To experimentally map the electron density distribution and derived electrostatic potentials in series of related solid energetic materials of differing shock sensitivities from high angle, low temperature X-ray diffraction data. To develop methods of graphical representation of charge densities and electrostatic potentials.
3. To measure the anisotropy of thermal expansion parameters for energetic materials. To relate the thermal expansion to molecular thermal motion.
4. To develop the necessary protocols for compressibility studies on a CCD diffractometer. To measure the compressibilities of energetic materials.
5. To investigate possible cations compatible with the dinitramide anion to form high density salts.
6. To provide crystal structures of energetic materials to others in the field.

B Significant results

The results obtained for the six goals are summarized below. Full details have been collected in appendices as listed in the text. Results that have been published, are in press or submitted for publication are provided as reprints or preprints; others are attached as unpublished technical reports.

1. A Siemens X-ray diffractometer with a CCD detector was installed with additional funding from ONR (N00014-95-1-1252). It allows much more efficient data collection, especially for charge density studies.

The investment of ONR into X-ray diffraction at the University of Toledo has been used to leverage additional state funding (Ohio Board of Regents) of \$815,000 to create a center for state-wide cooperation in the discipline of X-ray crystallography (the Ohio Crystallography Consortium). Relevant to the current contract, a second diffractometer with a CCD detector was installed thus doubling the measuring capacity of the X-ray laboratory. In addition to the hardware obtained from this funding, a short-term commitment of technical manpower support was also made (\$150,000 over two years).

With additional funding from ONR (N00014-97-1-0409) one of our two CCD diffractometers has now been upgraded by the addition of a 2K CCD detector, thus increasing the measuring area by a factor of four with a concomitant increase in measuring speed. This is currently the only small molecule laboratory in the country thus equipped.

The importance of the presence of harmonics of the primary radiation as a source of systematic errors when using CCD detectors has been evaluated. It is primarily a function of the tube voltage with a minor modification due to absorption by the tube window. A method to measure the amount of $\lambda/2$ contamination in the primary beam using Mo-K α radiation has been developed and it is now possible to correct the data observed under normal operating conditions. It was shown that for routine structural measurements, the effect on the final refinement was negligible. However, without correction, incorrect unit cells are easily obtained for strongly diffracting samples. In addition, incorrect space group assignments may easily be made. The influence on charge density determinations is not yet clear due to the small number of studies carried out. The software to determine and correct for the effect has been written. **Appendix 1a.**

The ability to obtain data of the required quality for charge density studies has been demonstrated using a crystal of oxalic acid cooled to 100 K. The first experiment demonstrated two drawbacks to the

method and the data collection protocol used; i) using the same frame time for high and low angle data is not appropriate, ii) the data was contaminated with $\lambda/2$ reflections. Another data set has now been collected with modified frame times to take care of i) while using an accelerating voltage that eliminates contributions from ii). These results compare well with those obtained by a commission of the International Union of Crystallography using conventional serial diffractometers. This data has been analyzed both statistically and by carrying out parallel refinements of the charge density with an existing high quality data set using a point detector. The results are very encouraging, in particular, some charge redistribution effects appear more clearly using the CCD data. A possible explanation for this is the observation that weak data is measured systematically higher with a CCD detector than with a point detector, whereas the agreement with stronger data is very good. Thus the suitability of CCD data for charge density studies has been established. **Appendix 1b.**

In order to obtain even better data for charge density studies, a prototype helium-cooling device has been fabricated. The cooling system has been tested and cools to below 30 K. The temperature calibration is based on unit cell and refined thermal parameters obtained with data on oxalic acid at various temperatures, as well as the observation of a known phase change observed for TbVO_4 (32 K). Currently, the rate of helium consumption is ca. 4 L per hr. With higher flow rates, temperatures < 14 K have been obtained (calibrated with the known phase transition of DyVO_4). Although developed for the 1 k CCD detector, the liquid helium cooling system has been adapted for use with the 2k detector with only minor modifications. Applications of this system in the field of protein crystallography have been established by demonstrating the feasibility of using this system to flash cool protein crystals to liquid helium temperatures (in collaboration with Dr. G. Bunick at ORNL). **Appendix 1c and 1d.**

The change in structure of the magnetic material TbVO_4 associated with the phase change at 32 K has been established by analysis of diffraction data on the twinned low temperature phase at 20 K. **Appendix 1e.**

The ability of a CCD machine to handle very small crystals was demonstrated by the determination of the structure of HFNX from a crystal which had approximate dimensions $30 \times 20 \times 20 \mu$. The experiment was a success in that this size of sample was shown to be tractable, however, it was a failure in that the material was not a new polymorph.

The quality of the data from the new 2k detector has been evaluated with respect to charge density measurements using Mo- $K\alpha$ radiation and found to be at least as good as the 1 k system with a reduction of one third in measuring time. The possibility of increasing efficiency by the use of shorter wavelengths (Ag- $K\alpha$) is currently in progress.

The increased size of the 2 k detector makes the use of longer wavelength radiation viable. The possibility of exploiting the λ^3 dependence of the scattered intensity to measure crystals smaller than 20μ by using longer wavelength radiation (Cu- $K\alpha$) has been established. In addition, the ability to obtain absolute configurations from "routine" measurements of all light atom structures using Cu- $K\alpha$ radiation has also been demonstrated. **Appendix 1f.**

2. The electron density distribution for three compounds (ADN , BIGH.DN and $\text{BIGH}_2\text{.(DN)}_2$) has been determined from 85 K X-ray diffraction data measured to $\sin(\theta)/\lambda = 1.35 \text{ \AA}^{-1}$. The electron density has been refined using an atom centered multipole model with terms up to octupoles for C, N and O, and a monopole and atom directed dipole for H. Mapped as the deformation density, features due to chemical bonding in the cations and in the anions are clearly seen, as well as clearly resolved lone pair regions (two per O atom). Calculations of the corresponding electrostatic potentials have been carried out and, for the dinitramide anion, the most electronegative regions are on either end of the molecule and out of the plane of the terminal nitrogens. Comparison of the experimental and theoretical (A.B. Kunz) charge density distribution for $\text{BIGH}_2\text{.(DN)}_2$ has been carried out at several levels of sophistication. Using simple spherical atom models with expansion and contraction of the valence shell with a variable population, the experimental atomic point charges are close to those obtained from theory. However, agreement of the theoretical crystallographic structure factors with either the experimental values or those calculated from a complete multipole refinement is not as good. This is believed to be due to truncation of the lattice sums

used in the theoretical calculations of the structure factors. Diffraction data to determine the charge density distribution and electrostatic potential for TNAZ has been collected as well as for a new trinitrodiazapentalene (TDAP). At present, data analysis for these last two studies is incomplete. **Appendix 2a - e.**

Additionally, the deformation density and electrostatic potential for the three experiments described above have been mapped using 3D computer graphics. Computer programs have been written to interface the crystallographic software to that of the graphics modules. A number of static 3D images have been produced, as well short movies. New visualization schemes have been devised to allow the use of virtual reality and ray tracing techniques to show electron density or electrostatic potential isosurfaces at the same time as ball and stick models of the molecules. Computer programs have been modified or new interfaces written to allow integration across a wider platform of machines due to the introduction of new computer hardware (SGI and PowerPC) associated with the new diffractometer. Examples of these representations may be viewed on our web site:

<http://www.icenter.utoledo.edu/icenter/projects.htmlx#apinkerton1>

3. Variable temperature X-ray diffraction experiments have been carried out over a 200 degree range for the following compounds: ADN, KDN, BIGH.DN, BIGH₂.DN₂, ε-CL20, γ-CL20, AP, RDX, TNAZ, TDAP. In all cases the anisotropy in the thermal expansion parameters have been determined as well as the temperature dependence of the volume (and hence the density). The complete thermal expansion tensors have also been determined for most of these compounds. Complete structure refinements have been carried out at all temperatures (except for AP and ADN) and, where appropriate, libration and translation tensors for rigid molecules have been derived. The anisotropy in the thermal expansion may be interpreted in terms of changing intermolecular contacts as well as individual atomic thermal motion, however, the only study completed to this level of interpretation is for KDN. **Appendix 3a - j.**

4. In collaboration with Dr. Tom Russell at NRL and Dr. G.J. Piermarini at NIST, a new design of diamond anvil cell for high pressure crystallography has been tested on the CCD diffractometers. A protocol for the determination of unit cell parameters has been developed and the variation of the unit cell parameters with hydrostatic pressure up to 25 kbar for ε-CL20 has been determined. Some progress towards a protocol for obtaining Bragg intensity data from the same experiment has been made, however, the structural refinement from such data is still unsatisfactory. However, a number of problems associated with the above cell have been established, thus, a new cell has been designed and fabricated and performance evaluation is currently in progress. **Appendix 4a.**

5. A number of salts of melamine (MEL) and biguanide (BIG) have been prepared and structurally characterized - MELH₂.(ClO₄)₂, MELH.NO₃, MELH.DN, BIGH.ClO₄, BIGH₂.(ClO₄)₂, BIGH.NO₃, BIGH₂.(NO₃)₂, BIGH.DN, BIGH₂.(DN)₂. All are characterized by strong hydrogen bonded networks. The variability and asymmetry in the geometry of the dinitramide anion has been noted. In addition a TGA/MS analysis of the thermal decomposition of BIGH₂.(ClO₄)₂ has been carried out. **Appendix 5a - f.**

6. Four structures of molecules from the research program of Dr. Alan Marchand have been determined. These were of crystals that had proven to be intractable with the resources available to him at the University of North Texas. **Appendix 6a - d.**

Papers published in refereed journals:

121. Melaminium Diperchlorate Hydrate.
Martin, A.; and Pinkerton, A.A., *Acta Crystallogr.*, **1995**, C51, 2174-2177.
 122. Charge Densities and Electrostatic Potentials for Energetic Materials.
Pinkerton, A.A.; and Martin, A., *Mat. Res. Soc. Symp. Proc.*, **1996**, 418, 49-53.
 123. Energetic Materials. The Biguanidinium Nitrates.
Martin, A.; Pinkerton, A.A.; and Schiemann, A.; *Acta Crystallogr.*, **1996**, C52, 966-970.
 124. Two Energetic Ionic Materials: the Biguanidinium Perchlorates.
Martin, A.; and Pinkerton, A.A., *Acta Crystallogr.*, **1996**, C52, 1048-1052.
 126. A Study of the Thermal Decomposition of Biguanidinium Diperchlorate using Thermogravimetry and Mass Spectroscopy.
Dollimore, D.; Martin, A.; and Pinkerton, A.A., *Thermochim. Acta*, **1996**, 285, 109-117.
 130. Energetic Materials - The Preparation and Structural Characterization of Three Biguanidinium Dinitramides.
Martin, A.; Pinkerton, A.A.; Gilardi, R.D.; and Bottaro, J.C., *Acta Crystallogr.*, **1997**, B53, 504-512.
 133. $\lambda/2$ Contamination in CCD Area Detector Data.
Kirschbaum, K.; Martin, A.; and Pinkerton, A.A.; *J. Appl. Cryst.*, **1997**, 30, 514-516.
 137. Intermolecular [2 + 2] Photocyclization of Ethyl 5-oxo-1a,2,5,5a,6,6a-hexahydro-2,6-methano-2aH-indeno-[5,6-b]oxirene-2a-carboxylate.
Pinkerton, A.A.; Martin, A.; Marchand, A.P.; and Devasagayaraj, A.; *J. Chem. Crystallogr.*, **1997**, 27, 701-705.
 139. Charge Density Studies Using CCD Detectors - Oxalic Acid at 100 K Revisited.
Martin, A.; and Pinkerton, A.A.; *Acta Crystallogr.*, **1998**, B54, 471-478.
 142. An Open Flow Helium Cryostat for X-ray Diffraction.
Hardie, M.J., Kirschbaum, K., Martin, A.; and Pinkerton, A.A., *J. Appl. Cryst.*, **1998**, 31, 815-817.
- Charge Density Data from CCD Detectors.
Pinkerton, A.A. in "Electron, Spin and Momentum Densities and Chemical Reactivity," P.G. Mezey and B. Robertson, eds., Kluwer, 1998, in press.
- Structure of 1,2,3,4,9,9-Hexachloro-6,7-tetrahydro-1,4-methanonaphthalene: A Facially Differentiated, Annulated 1,3-Cyclohexadiene.
Pinkerton, A.A.; Burckel, P.M.; Marchand, A.P.; and Dong, E.Z.; *J. Chem. Crystallogr.*, in press.
- Energetic Materials: The Preparation and Structural Characterization of Melaminium Dinitramide and Melaminium Nitrate.
Tanbug, R.; Kirschbaum, K.; and Pinkerton, A.A.; *J. Chem. Crystallogr.*, in press.
- Use of an Open Flow Helium Cryostat for Macromolecular Cryocrystallography.
Hanson, B.L.; Martin, A.; Harp, J.M.; Bunick, C.G.; Parrish, D.A.; Kirschbaum, K.; Bunick, G.J.; and Pinkerton, A.A.; *J. Appl. Cryst.*, submitted for publication.

Cooperative Jahn-Teller Induced Phase Transition of TbVO_4 : Single Crystal Structure Analyses of the Tetragonal High Temperature Phase and the Twinned Orthorhombic Phase Below 33 K.
Kirschbaum, K.; Martin, A.; Parrish, D.A.; and Pinkerton, A.A.; *J. Phys. Condens. Matt.*, submitted for publication.

Meeting papers and abstracts

American Crystallographic Association Meeting, Atlanta, June 25 - 28, 1994.
"Experimental Electron Density Distribution of Biguanidinium Bis(dinitramide)." A. Martin, and A.A. Pinkerton.

The 52nd Annual Pittsburgh Diffraction Conference, Pittsburgh, November 3-5, 1994.
"Hydrogen Bonding in Three High Density Perchlorate Salts." A. Martin and A.A. Pinkerton.

Contemporary Inorganic Chemistry: A Symposium in Honor of F.A. Cotton, College Station, Texas, March 12-15, 1995.
"Energetic Nitrogen Compounds - a Charge Density Study." A.A. Pinkerton and A. Martin.

DEA 5660 Group 4 Workshop, Paris, France, June 19-21, 1995.
"An Experimental Electron Density and Electrostatic Potential Study for Biguanidinium Dinitramide." A.A. Pinkerton and A. Martin.

Gordon Conference on "Electron Distribution and Chemical Bonding", Plymouth, NH, July 2-7, 1995.
"The Use of 3D Computer Graphics to Display Deformation Densities and Electrostatic Potentials - an Example." A. Martin and A.A. Pinkerton.

American Crystallographic Association Meeting, Montreal, July 23 - 28, 1995.
"The Use of 3D Computer Graphics to Display Deformation Densities and Electrostatic Potentials - an Example." A. Martin and A.A. Pinkerton.

ONR Energetic Materials Workshop, Houghton, Michigan, October 3 - 4, 1995.
"Charge Densities and Electrostatic Potentials from X-ray Diffraction Data," A.A. Pinkerton.

Materials Research Society Meeting, Boston, November 27 - December 1, 1995.
"Charge Densities and Electrostatic Potentials for Energetic Materials." A. Martin and A.A. Pinkerton.

Gordon Conference on Energetic Materials, New Hampton, NH, June 16 - 21, 1996.
"Experimental and Theoretical Studies of the Charge Density Distribution of ADN." A.A. Pinkerton, K. Kirschbaum, A. Martin and A.B. Kunz.

International Union of Crystallography XVII Congress, Seattle, WA, August 8 - 18, 1996.
"Preliminary Analysis of CCD Data for Oxalic Acid Dihydrate at 100 K," A.A. Pinkerton, A. Martin, C.F. Campana and M.R. Pressprich.
"Comparing 90 K Data to Solid State Ab Initio Calculations from Crystal92," A. Martin, A.A. Pinkerton and A.B. Kunz.
"Beyond Routine Structure Determination - The Renaissance of Small Molecule Crystallography," A.A. Pinkerton.

ONR Energetic Materials Workshop, Annapolis, MD, December 3-6, 1996.
"New Technology for X-ray Diffractometry and Associated New Experimental Capabilities," A.A. Pinkerton.

Siemens' Area Detector Users Group Meeting, Athens, GA, April 17 - 19, 1997.

"Chemical Crystallography, Past, Present and (Mainly)Future," A.A. Pinkerton.

" $\lambda/2$ Contamination in Area Detector Data," K. Kirschbaum, A. Martin and A.A. Pinkerton.

"Charge Density Data from CCD Diffractometers - Oxalic Acid at 100 K Revisited," A. Martin and A.A. Pinkerton.

"A Helium Cooling Device for a SMART CCD Diffractometer," K. Kirschbaum, A. Martin and A.A. Pinkerton.

American Crystallographic Association Meeting, St. Louis, MO, July 19 - 27, 1997.

"Significance of Harmonics of λ in CCD Data Sets," A.A. Pinkerton, K. Kirschbaum and A. Martin.

"A Simple Affordable Open Flow Helium Cryostat for Area Detector Diffractometers," A. Martin, A.A. Pinkerton, K. Kirschbaum and M.J. Hardie.

"High Pressure Crystallography of Hexanitrohexaazaisowurtzite on a SMART CCD Diffractometer," M.J. Hardie, K. Kirschbaum, A. Martin, R. Tanbug, T.P. Russell and G.J. Piermarini.

American Physical Society, Shock and Compression Conference, Amherst, MA, July 27 - Aug 1, 1997.

"Determination of Unit Cell Parameters of Molecular Organic Crystals Under Hydrostatic Compression at Pressures up to 5.0 GPa," T.P. Russell, M.J. Hardie, K. Kirschbaum, A. Martin, A.A. Pinkerton, R. Tanbug and G.J. Piermarini.

Sagamore XII, IUCr Commission on Charge, Spin and Momentum Densities, Waskesiu, Saskatchewan, Canada, July 27 - August 1, 1997.

"Charge Density Data from a CCD Detector," A.A. Pinkerton.

ONR Energetic Materials Workshop, Annapolis, MD, January 27-29, 1998.

"Thermal Expansion and Compressibility Studies of Energetic Crystals," A.A. Pinkerton.

American Crystallographic Association Meeting, Arlington, VA, July 18 - 23, 1998.

"Phase Transition of TbVO_4 : Non-merohedral Twinning at He-Temperature," A.A. Pinkerton, K.Kirschbaum, A. Martin and D.A. Parrish.

"Energetic Materials: The Preparation and Structural Characterization of Two Melaminium Salts," R. Tanbug and A.A. Pinkerton.

"Variable Temperature Measurements and Thermal Expansion Tensors of Five Energetic Materials," A. Martin, A.A. Pinkerton, R. Tanbug and M.J. Hardie.

"Use of an Open Flow Helium Cryostat in Macromolecular Crystallography," B.L. Hanson, A. Martin, J. M. Harp, D.A. Parrish, K. Kirschbaum, G.J. Bunick and A. A. Pinkerton.

Gordon Conference on "Electron Distribution and Chemical Bonding", Oxford, UK, August 30 - September 4, 1998.

"Experiences with Charge Density Data Collected with a 2k CCD Detector." A.A. Pinkerton.

European SMART User's Meeting, Bergen, Norway, September 11 - 13, 1998.

"New Experiences with New Technology - the Impact of the 2K CCD Detector," A.A. Pinkerton.

Contract No. N00014-95-1-0013 and N00014-97-1-0409

Program Officer: R. Miller/J. Goldwasser

**Title: Experimental Charge Densities and Electrostatic Potentials in Energetic
Materials and Infrastructure Upgrade for an X-ray Crystallography
Laboratory**

PI: A. Alan Pinkerton

Department of Chemistry, University of Toledo, Toledo, OH 43606

tel. (419) 530-4580, FAX (419) 530-4033, email apinker@uoft02.utoledo.edu

APPENDIX 1a

$\lambda/2$ Contamination in CCD Area Detector Data.

**Kirschbaum, K.; Martin, A.; and Pinkerton, A.A.; *J. Appl. Cryst.*, 1997, 30,
514-516.**

FAST COMMUNICATIONS

Contributions intended for this section should be submitted to any of the Co-editors of the *Journal of Applied Crystallography*. In the letter accompanying the submission, authors should state why rapid publication is essential. The paper should not exceed two printed pages (about 2000 words or eight pages of double-spaced typescript including tables and figures) and figures should be clearly lettered. If the paper is available on a 3.5 or 5.25 in IBM PC compatible or 3.5 in Apple Macintosh diskette, this should be sent with the manuscript together with details of the word-processing package used. Papers not judged suitable for this section will be considered for publication in the appropriate section of the *Journal of Applied Crystallography*.

J. Appl. Cryst. (1997), **30**, 514–516

$\lambda/2$ Contamination in charge-coupled-device area-detector data

KRISTIN KIRSCHBAUM, ANTHONY MARTIN AND A. ALAN PINKERTON at *Department of Chemistry, University of Toledo, Toledo, OH 43606, USA. E-mail: apinker@uoft02.utoledo.edu*

(Received 9 January 1997; accepted 14 March 1997)

Abstract

A method is proposed to estimate the amount of $\lambda/2$ contamination inherent in area-detector [charge-coupled device (CCD) or image plate] data using Mo radiation. The intensity increase due to the Mo $\lambda/2$ contribution to I_{hkl} has been determined by measurement of the intensity for reflections where h , k or l is half-integral, i.e. reflections where there is no contribution from λ , for three crystals using two different CCD diffractometers. This information is present in all data sets obtained with area detectors but is usually ignored. The correction thus determined has been applied to nine data sets. The improvement to the data, as measured from the least-squares refinement, is shown to be insignificant for routine data sets, even for the weak low-angle reflections. Some reduction in the number of 'observed' systematic absences is noted, thus improving space-group assignments. In addition, for strongly diffracting crystals, incorrect unit cells may be obtained owing to the presence of strong $\lambda/2$ reflections at the reciprocal-lattice nodes.

1. Introduction

When a sealed-tube X-ray source or a rotating-anode generator is used, the characteristic radiation (usually $K\alpha$) employed for a typical diffraction experiment is commonly obtained using a crystal monochromator. It is well known that harmonics of λ contributing to the primary beam leaving the X-ray source also contribute to the primary 'monochromatic' beam arriving at the sample. For Mo radiation, only $\lambda/2$ is important under normal operating conditions (50 kV); however, for Cu radiation, harmonics through $\lambda/6$ are present. In the present paper, we limit ourselves to the Mo case. Following Bragg's Law, for any reflection $2h2k2l$ due to λ , there will be a contribution to the intensity of the reflection hkl due to $\lambda/2$ if this harmonic is present in the primary beam. When a scintillation counter is used to detect the scattered radiation, this unwanted effect can be removed by energy discrimination. With the advent of area detectors, both charged-coupled devices (CCDs) and image plates (but not multiwire detectors), this contamination has become a potential source of systematic errors because these devices cannot discriminate with respect to energy. In particular, weak low-angle reflections are observed with higher intensities than required by the structure. This also leads to incorrect

space-group assignment as some space-group extinctions may actually be 'observed', or, for strongly diffracting crystals, $\lambda/2$ reflections for odd indices may be observed at lattice nodes (half-integral hkl values) leading to incorrect unit cells.

There are four approaches to remove or account for this effect: (i) primary radiation that is free of the $\lambda/2$ radiation can be produced; (ii) an Si or Ge monochromator may be used; (iii) the $\lambda/2$ component of the scattered radiation in the experiment can be determined; (iv) an independent determination of the amount of $\lambda/2$ scattering may be carried out. In the following, we examine these approaches, estimate the contribution of the $\lambda/2$ scattering to the observed intensities and evaluate its effect on structure refinement.

2. $\lambda/2$ -free radiation

The only way to produce a primary beam that is free of $\lambda/2$ radiation is to reduce the accelerating voltage below that required for $\lambda/2$ generation. The lower limit of the wavelength corresponds to the transformation of the kinetic energy of an electron into a single photon (*International Tables for X-ray Crystallography*, 1995):

$$\lambda_{\min} = hc/eV = 12398(1/V),$$

where e is the charge on the electron, h is Planck's constant, c is the speed of light, V is the accelerating potential in volts and λ is in Å. For Mo $K\alpha$ radiation, $\lambda/2 = 0.3554$ Å and the corresponding accelerating voltage is 34.9 kV. Although operating an X-ray source at this potential will indeed remove all $\lambda/2$ contamination, it will also result in a drastic reduction in the intensity of the desired characteristic radiation (*International Tables for X-ray Crystallography*, 1995):

$$I(K\alpha) = k(V - V_0)^{1.63},$$

where V is the accelerating voltage, V_0 is the minimum voltage necessary to excite $K\alpha$ (20.0 kV for Mo $K\alpha$) and k is a constant. Thus, reducing the potential from a typical value of 50.0 kV to 34.9 kV for Mo $K\alpha$ radiation will reduce the intensity of the desired radiation by 68%. Although some of this loss in intensity may be recovered by an increase of the filament current, this is not a convenient solution for most crystallographic experiments. However, for samples that are strongly diffracting, e.g. minerals, this is a reasonable approach. Indeed,

we have found that for such samples, e.g. ruby, the intensity of the $\lambda/2$ components at reciprocal-lattice nodes is so intense at 50 kV that some (or all) cell axes appear doubled using autoindexing routines.

3. Use of Si or Ge monochromators

The structure amplitude of F_{222} for Si or Ge is close to zero; therefore, the contribution of $\lambda/2$ to the 111 reflection is zero. We may therefore use the 111 reflection from an Si or Ge monochromator to obtain $\lambda/2$ -free radiation. The most common choice for a monochromator crystal for commercial diffractometers is graphite. Changing to Si would reduce the intensity of the primary beam by almost 50% owing to the difference in scattering power between Si and graphite. This is less of a problem for Ge; however, the absorption coefficient for Ge is more than two orders of magnitude higher than that for carbon, which makes this also a poor solution.

4. Experimental determination

For any structure factor obtained from an experiment where there is $\lambda/2$ contamination, we may write it as the sum of two components:

$$F'_{hkl} = F_{hkl} + kF_{2h2k2l}$$

Thus, we may, in principle, obtain a best value for k from a modification of the normal least-squares procedure. As we expect k to be $\ll 1$, F'_{hkl} will only significantly differ from F_{hkl} when the amplitude of F_{hkl} is small and that of F_{2h2k2l} is large, i.e. the reflections carrying the most information about k are those very reflections that are poorly observed and that will have small weights in the least-squares procedure. Thus, this is not a reliable method for most experiments.

5. Independent determination of the $\lambda/2$ contribution to the scattering

A method for correcting observed intensities for film data was proposed by Guinier (1963). In this method, two films were used, separated by a metal filter that was designed to absorb λ radiation and let the more penetrating $\lambda/2$ radiation pass through. Thus, subtraction of the intensities on the second film from those on the first gave intensities free from $\lambda/2$ contamination.

A better way to measure the contribution of the $\lambda/2$ contribution to the observed intensity* at any reciprocal-lattice point was proposed by Rees (1977) for neutron data and is equally applicable to X-ray data. By comparing the observed intensity of strong reflections with at least one index odd with that of the $\lambda/2$ reflections (which now have corresponding half-integral indices and no λ component), we obtain a direct measure of the two components. With a serial diffractometer, this information was usually unavailable (and happily unnecessary). With an area detector, this information is contained in the measured diffraction pattern but is normally ignored if the reflections have been correctly indexed. The easiest way to extract this information using existing software is to define a new unit cell in which all the axes have been doubled and hence all of the indices likewise. Now all of the original reflections in

the data set have even indices; all of those with an odd index are pure $\lambda/2$ reflections. The only odd reflections that are observable will be those where the corresponding even reflection is strong and hence has a negligible $\lambda/2$ component. From the comparison of pairs of reflections of this type, we can determine the ratio of the intensities due to the λ and $\lambda/2$ components of the primary beam. This information may then be used to correct the intensities of the affected reflections in the original data set, primarily weak reflections at low angles. As this is a property of the primary beam, it is best performed as a separate experiment designed to optimize the integration of the half-integral reflections under standard (or several standard) operating conditions. It is, of course, a function of the accelerating voltage but not of the filament current. The value should be stable with time except for effects due to changes in the absorption of the window of the X-ray source. The difference between diffractometers is small but not negligible (see below).

We also note that, for a strong absorber, the $\lambda/2$ corrections should be determined from absorption-corrected data and then applied to the raw data before the absorption correction is repeated. This follows from the fact that the $\lambda/2$ component is more penetrating and less affected by absorption.

6. Experiment

We have chosen three spherical crystals, the standard ylid crystal provided by Siemens Analytical Instrumentation, ruby and ammonium hydrogen tartrate (Enraf-Nonius standard crystal), and carried out an experiment such as that described above using two SMART CCD diffractometers. In a typical experiment, we collected approximately a hemisphere of data using 0.3° (ω) frames. A number of different frame times were used in order to maximize the number of useful intensity ratios, the stronger reflections being measured with short frames and less intense reflections measured at longer frame times where the strong reflections overflowed the detector.† Before integration (SAINT, Siemens Analytical Instrumentation, 1996), all of the cell axes were multiplied by 2. Duplicate measurements were then averaged, and all odd reflections with values of $F^2 > 15$ estimated standard deviations (e.s.d.'s) as normalized in XPREP (Sheldrick, 1986) were compared with the reflection with double the indices to obtain the best value of k for the expression $F'_{hkl} = kF_{2h2k2l}$, where at least one value of h , k or l is odd.‡ The average values of k obtained for the two diffractometers were 0.0014 (2) and 0.00106 (5).

These values were used to correct the intensities for nine representative data sets, organic crystals, organometallics and minerals.§ only the reflections hkl for which the corresponding reflection $2h2k2l$ exists in the same data set being corrected. The structures are either known or will be published elsewhere. The data were compared with respect to systematic absences and space-group assignment (i) with no corrections to the data,

† In the current version of the SMART software, a detector overflow results in the frame being remeasured at $8\times$ the scan speed. Any reflection still overflowing is discarded.

‡ The value of 15 was chosen because the use of weaker data rapidly increased the variance of k .

§ 1, 2: $C_{11}H_{10}SO_2$ ($P2_12_12_1$, 10 and 20 s frames); 3: $C_{34}H_{38}N_4O_6$ ($P2_1/c$); 4: $C_{17}H_{10}N_4O_3ClRe$ ($P2_1$); 5, 6: ruby ($R\bar{3}c$, 10 and 20 s frames); 7: $C_{42}H_{35}Te_3As$ ($P2_1/n$); 8: $C_4H_9NO_6$ ($P2_12_12_1$); 9: $C_{36}H_{37}N_3O_3S$ ($P2_1$).

* Although we speak of intensities, these must be L_p corrected, so the real values are F_o^2 .

(ii) with an absorption correction (*SADABS*; Sheldrick, 1996),[¶] (iii) with only $\lambda/2$ correction and (iv) with both absorption and $\lambda/2$ correction. Analogously four different refinements per sample were carried out based on F^2 .

The magnitudes of the corrections varied quite widely over the nine data sets; however, the average correction was typically less than one e.s.d. The maximum correction also varied quite widely. The smallest maximum correction was for structure 9, 1.7σ for the raw data and 1.2σ for the absorption-corrected data. The largest maximum correction on the raw data was for structure 6, 47.4σ , and for structure 3 on the absorption-corrected data 26.9σ . The average maximum correction over the nine data sets was 26.9σ for the raw data and 5.8σ for the absorption-corrected data. The reduction in the apparent correction after absorption correction is mainly due to the modified e.s.d.'s generated by the program *SADABS*.

In all cases, there was an improvement in the number of 'observed' systematic absences, although not one as dramatic as that produced by the modification in the e.s.d.'s produced by *SADABS*. Using the criteria in *XPREP* (Sheldrick, 1986) to suggest the space group, using raw data, only structures 4 and 9 were correct. After correction for $\lambda/2$, structures 1, 3, 4, 5, 8 and 9 were now correctly determined. Correction with *SADABS* alone produced the correct space group for all but data sets 3 and 7. Subsequent $\lambda/2$ correction obtained the correct space group for all data sets.

The effects of the $\lambda/2$ correction on the final refinements was negligible. There was no significant change in the final agreement factors and the changes in the geometrical parameters were all smaller than 1 e.s.d.

[¶] *SADABS* also performs interframe scaling and modifies (inflates) $\sigma(F^2)$ based on the observed variance in the intensities of equivalent reflections.

7. Conclusions

It is clear that, although the $\lambda/2$ contribution to the scattering can be observed and corrected for, the correction has minimal influence on the final refined structure. However, for extremely accurate work, e.g. in charge-density studies, the correction is probably worthwhile. Perhaps the most important observation in this work is that it is quite easy to obtain the wrong unit cell for strongly scattering samples when pure $\lambda/2$ reflections are included in the array used for cell determination. Some care must also be taken in identifying the space group from the systematic absences as they may also be 'observed' owing to a pure $\lambda/2$ component. It is also abundantly clear that the current integration algorithms seriously underestimate the e.s.d.'s of the intensities.

We thank the College of Arts and Sciences of the University of Toledo and the Ohio Board of Regents for generous financial support of the X-ray diffraction facility and thank the Office of Naval Research for funding this work (Contracts Nos. N00014-95-1-0013 and N00014-95-1-1252).

References

- Guinier, A. (1963). *X-ray Diffraction in Crystals, Imperfect Crystals, and Amorphous Bodies*, p. 175. London: W. H. Freeman.
- International Tables for X-ray Crystallography* (1995). Vol. C. Dordrecht: Kluwer Academic Publishers.
- Rees, B. (1977). *Israel J. Chem.* **16**, 154–158.
- Sheldrick, G. M. (1986). *SHELXTL86. An Integrated System for Solving, Refining and Displaying Crystal Structures from Diffraction Data*, University of Göttingen, Germany.
- Sheldrick, G. M. (1996). *SADABS*. University of Göttingen, Germany, to be published.
- Siemens Analytical Instrumentation (1996). *SAINT. A Program to Integrate and Reduce Raw Crystallographic Area-Detector Data*.

Contract No. N00014-95-1-0013 and N00014-97-1-0409

Program Officer: R. Miller/J. Goldwasser

**Title: Experimental Charge Densities and Electrostatic Potentials in Energetic
Materials and Infrastructure Upgrade for an X-ray Crystallography
Laboratory**

PI: A. Alan Pinkerton

Department of Chemistry, University of Toledo, Toledo, OH 43606

tel. (419) 530-4580, FAX (419) 530-4033, email apinker@uoft02.utoledo.edu

APPENDIX 1b

**Charge Density Studies Using CCD Detectors - Oxalic Acid at 100 K
Revisited.**

Martin, A.; and Pinkerton, A.A.; *Acta Crystallogr.*, 1998, *B54*, 471-478.

Charge Density Data from CCD Detectors.

**Pinkerton, A.A. in "Electron, Spin and Momentum Densities and Chemical
Reactivity," P.G. Mezey and B. Robertson, eds., Kluwer, 1998, in press.**

Charge Density Studies Using CCD Detectors: Oxalic Acid at 100 K Revisited

ANTHONY MARTIN AND A. ALAN PINKERTON*

Department of Chemistry, University of Toledo, Toledo, OH 43606, USA. E-mail: apinker@uoft02.utoledo.edu

(Received 25 August 1997; accepted 27 October 1997)

Abstract

The charge density of oxalic acid dihydrate has been redetermined from 100 K X-ray diffraction data using a SMART CCD diffractometer. The quality of the data has been carefully analyzed and shown to be at least as good as that obtained using a point detector. The positional and thermal parameters obtained from least-squares refinement and the main features of difference density maps are comparable with those obtained by a number of laboratories as part of the IUCr electron density project. In particular, the comparison study has been completed by two multipole refinements carried out in parallel using both the current data set and that of a previous study [Stevens & Coppens (1980). *Acta Cryst. B*36, 1864–1876].

1. Introduction

The advent of CCD detectors for X-ray diffraction experiments has produced a remarkable increase in the speed with which routine structures may be determined. Although the data are perfectly adequate for routine structure determination, it has not been demonstrated that the data quality is sufficient for charge density studies. In an attempt to answer this question, it was decided to remeasure oxalic acid dihydrate and compare the results with those obtained in the 'Project on Comparison of Structural Parameters and Electron Density Maps of Oxalic Acid Dihydrate' commissioned by the IUCr (Coppens, 1984), as well as with later studies on the same structure.

2. Experimental

A well faceted crystal of oxalic acid dihydrate of the dimensions $0.25 \times 0.23 \times 0.18$ mm was glued to the tip of a diamond-cleaved 0.1 mm thin-walled capillary and mounted on a Siemens SMART Platform diffractometer. The sample was cooled to 100.0 (1) K with an Oxford Cryosystems Cryostream cooling device. Preliminary examination and final data collection were carried out with graphite-monochromated Mo $K\alpha$ radiation. In order to avoid any contamination of the data with the $\lambda/2$ harmonic (Kirschbaum *et al.*, 1997), the generator was run at 35 kV and 50 mA. Intensity data were collected using 0.3° ω scans with a detector

distance of 3 cm. The maximum redundancy in the data was obtained using four φ settings $-0, 90, 180, 270^\circ$ – for each detector position. Five detector positions were used, ensuring overlap of the data: $-35, -65, -95, -109$ and -50° in 2θ . 60 s frames were measured for the three lowest-resolution detector positions and 120 s frames for the two high-resolution positions. For the first four detector positions, 600 frames were measured for each φ setting. For the final detector setting only 500 frames were measured.†

3. Data reduction

The unit cell [$a = 6.1024$ (1), $b = 3.4973$ (1), $c = 11.9586$ (2) Å, $\beta = 105.771$ (1)°] and orientation matrix were determined from the XYZ centroids of 8192 reflections with $I > 20\sigma(I)$ obtained from the frames of the first two detector positions (-35 and -65°). These two runs were integrated together (SAINT; Siemens, 1996). Subsequent runs were integrated separately, but with no further refinement of the orientation matrix. The intensities were first corrected for beam inhomogeneity and decay, and the e.s.d.'s adjusted using the program SADABS (Sheldrick, 1998). An absorption correction was then applied ($T_{\min} = 0.949$, $T_{\max} = 0.983$) and symmetry and multiply measured reflections averaged with the program SORTAV (Blessing, 1987). The absorption correction was applied with SORTAV (Blessing, 1987) rather than SADABS (Sheldrick, 1998) in order to obtain reasonable values for T_{bar} in the absence of known face indices and corresponding dimensions. A further revision of the e.s.d.'s was carried out via a bivariate analysis of the data with respect to $\sin \theta/\lambda$ and intensity.

A total of 46 067 reflections was measured [of which 29 753 had $I > 2\sigma(I)$] with only 154 reflections missing to $\sin \theta/\lambda = 1.34$ Å $^{-1}$ ($-16 < h < 16$, $-8 < k < 8$, $-31 < l < 31$). 5166 reflections were unique, of which 2589 had been measured more than nine times (symmetry equivalents plus multiple measurements) and only 650 had been measured less than three times. After rejection

† Lists of atomic coordinates, anisotropic displacement parameters and structure factors have been deposited with the IUCr (Reference: FR0004). Copies may be obtained through The Managing Editor, International Union of Crystallography, 5 Abbey Square, Chester CH1 2HU, England.

Table 1. Summary of least-squares refinements

Hydrogen coordinates for (II), (III) and (IV) fixed at neutron positions with isotropic thermal parameters from (I).

Refinement	(I)	(II)	(III)	(IV)
Sin θ/λ range (\AA^{-1})	0.00–1.20	1.00–1.34	0.00–1.34	0.00–1.20
N_{obs}	3860	2895	5166	3860
N_v	50	37	50	108
Scale factor	1.812 (2)	1.87 (2)	1.813 (4)	1.812 (4)
$R(F^2)^\dagger$	0.0540	0.1170	0.0457	0.0532
$wR(F^2)^\dagger$	0.0769	0.1630	0.0777	0.0299
$R(F)$ [$I > 2\sigma(I)$]	0.0281	0.0423	0.0282	0.0190
S	1.01	0.84	0.86	0.73

† All reflections.

of 2294 abnormal outliers (e.g. clipped reflections from the frame edges) and 5 statistical outliers, the merging R values were $R_1 = 0.032$ and $R_2 = 0.024$ for 4878 means.

4. Refinements

Starting coordinates were taken from Stevens & Coppens (1980), hereafter SC, and all refinements were carried out on F^2 using the *XD* (Koritsanszky *et al.*, 1995) suite of programs. Four different refinements were carried out using statistical weights throughout and the results are summarized in Table 1. Refinement (I) is a traditional independent atom refinement. Refinement (II) is a high-angle refinement ($1.00 < \sin \theta/\lambda < 1.34 \text{ \AA}^{-1}$) with the H atoms fixed at the neutron positions (values from Feld *et al.*, 1978) and isotropic thermal parameters fixed at the values obtained from refinement (I). Refinement (III) is a kappa refinement to assign atomic charges (Coppens *et al.*, 1979). The hydrogen positional and thermal parameters were fixed as in refinement (II). A complete atom-centered multipole refinement was carried out in (IV), where the nonspherical atomic electron density (Coppens, 1997) is given by

$$\rho_{\text{at}}(\mathbf{r}) = P_c \rho_{\text{core}}(r) + P_v \kappa^3 \rho_{\text{valence}}(\kappa r) + \sum_{l=1}^{l_{\text{max}}} \kappa^3 R_l(\kappa' r) \sum_{m=0}^l P_{lm\pm} d_{lm\pm}(\theta, \varphi).$$

The H atoms were treated as in (II) with one atom-directed dipole and quadrupole population varied. All other atoms were refined as previously described (Stevens & Coppens, 1980) up to the hexadecapole level

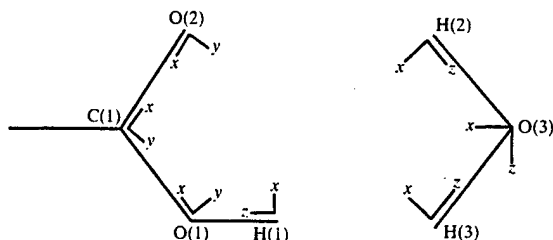


Fig. 1. Local coordinate system used to define multipoles.

with mirror symmetry imposed in the plane of the oxalic acid molecule and in the bisecting plane perpendicular to the plane of the water molecule. The local coordinate systems used to define the multipoles is shown in Fig. 1. Isotropic extinction was included in all four refinements, however, the value obtained from refinement (I) was held constant for the high-angle refinement. For purposes of comparison, particularly of the multipole refinements, an identical set of refinements was carried out using the SC data and the results compared. As the SC data only extend to $\sin \theta/\lambda = 1.2 \text{ \AA}^{-1}$, the current data were also limited to this resolution for refinement (IV).

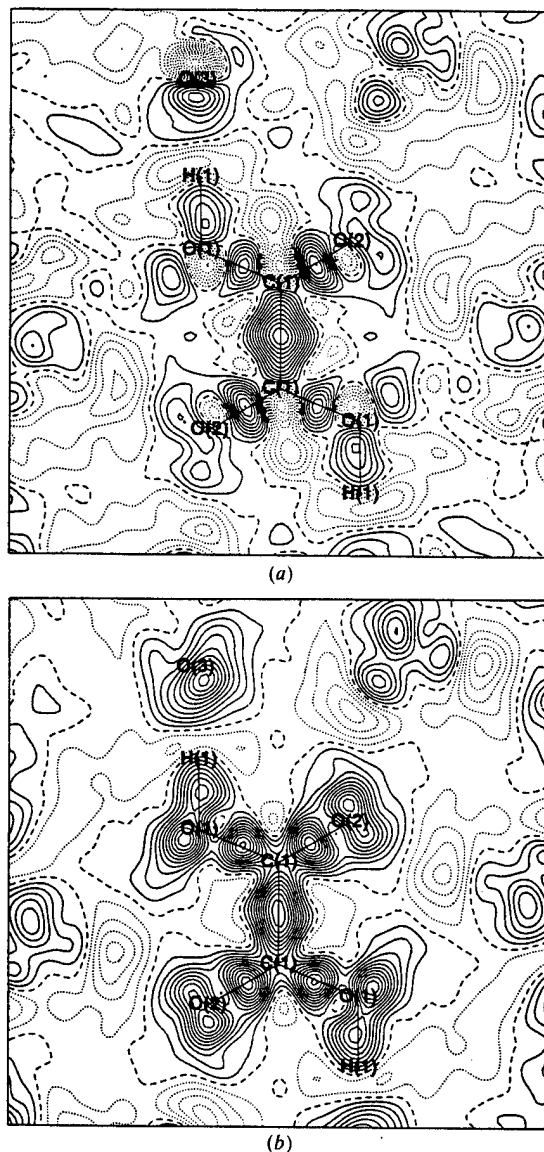


Fig. 2. Difference map after high-order refinement – data cut-off at $\sin \theta/\lambda = 0.9 \text{ \AA}^{-1}$ for reflections with $F^2 > 2\sigma(F^2)$; (a) this work; (b) SC. Contour level: 0.05 e \AA^{-3} .

Table 2. Comparison of unit-cell parameters

This work	IUCr study
$a = 6.1024 (1) \text{ \AA}$	$\bar{a} = 6.102 (6) \text{ \AA}$
$b = 3.4973 (1) \text{ \AA}$	$\bar{b} = 3.501 (7) \text{ \AA}$
$c = 11.9586 (2) \text{ \AA}$	$\bar{c} = 11.964 (17) \text{ \AA}$
$\beta = 105.771 (1)^\circ$	$\bar{\beta} = 105.80 (5)^\circ$

5. Charge density maps

Difference density maps in the molecular plane were computed (*XD*; Koritsanzky *et al.*, 1995) after the high-angle refinements. To make the comparison as meaningful as possible, a cut-off of $\sin \theta/\lambda = 1.2 \text{ \AA}^{-1}$ was also imposed for the present data during this refinement. For the case of the SC data the scale factor was refined on all the data after the high-order refinement owing to the incompleteness of the high-order data, as previously discussed (Stevens & Coppens, 1980). Comparison maps with a $\sin \theta/\lambda$ cut-off of 0.9 \AA^{-1} are presented in Fig. 2. In both cases only reflections with $F_o^2 > 2\sigma(F_o^2)$ were included in the summations.

Model deformation density maps after the multipole refinement were also computed for the same plane with the same cut-offs and are compared in Fig. 3. The coefficients for the summations are $(F_{\text{mul}} - F_{\text{iam}})$. In addition, in order to judge the completeness of the refinement and the quality of the data, the corresponding residual maps were computed after the multipole refinement (Fig. 4).

6. Discussion

Why choose to collect data at 100 K? In order to compare point-detector data with those obtained with a CCD it was important to choose a temperature for which there was already extensive data available. The most common temperature of the IUCr study (Coppens, 1984) was 100 K and this was also the temperature of the SC data which we have chosen for the most detailed comparison.

A comparison of unit-cell parameters is given in Table 2. All metric parameters fall well within the range previously quoted (Coppens, 1984).

Examination of the reflection statistics (Table 3) with respect to $F_o^2/\sigma(F_o^2)$ (Q) and $\sin \theta/\lambda$ (S), as obtained from *SORTAV* (Blessing, 1987), indicates the expected trends with respect to the merging R values *versus* Q or S , and suggests that the data should be adequate for a charge density study.

Positional parameters of the non-H atoms obtained from refinements (I) and (II) have been compared with those obtained from similar refinements by SC or Dam *et al.* (1984), hereafter DHF, from X-ray data as well as those obtained from neutron data (Koetzle & McMullan, unpublished). Refinement (I) agrees well with SC [average positional discrepancy $0.0010 (5) \text{ \AA}$], less well with DHF [average positional discrepancy

$0.0017 (3) \text{ \AA}$] and, not surprisingly, poorly with the neutron data [average positional discrepancy $0.0018 (8) \text{ \AA}$]. Better agreement was obtained from the high-order refinement (II), the corresponding average discrepancies being $0.0012 (9)$, $0.0012 (3)$ and $0.0007 (6) \text{ \AA}$. The largest discrepancy in all cases is for O(3), which, in the worst case, is close to 0.002 \AA .

Although the Hirschfeld (1976) rigid-bond test is obeyed in the current study (differences of mean-square displacement amplitudes along the bonds being $\leq 0.001 \text{ \AA}^2$), there are some striking differences in the thermal displacement parameters compared with other

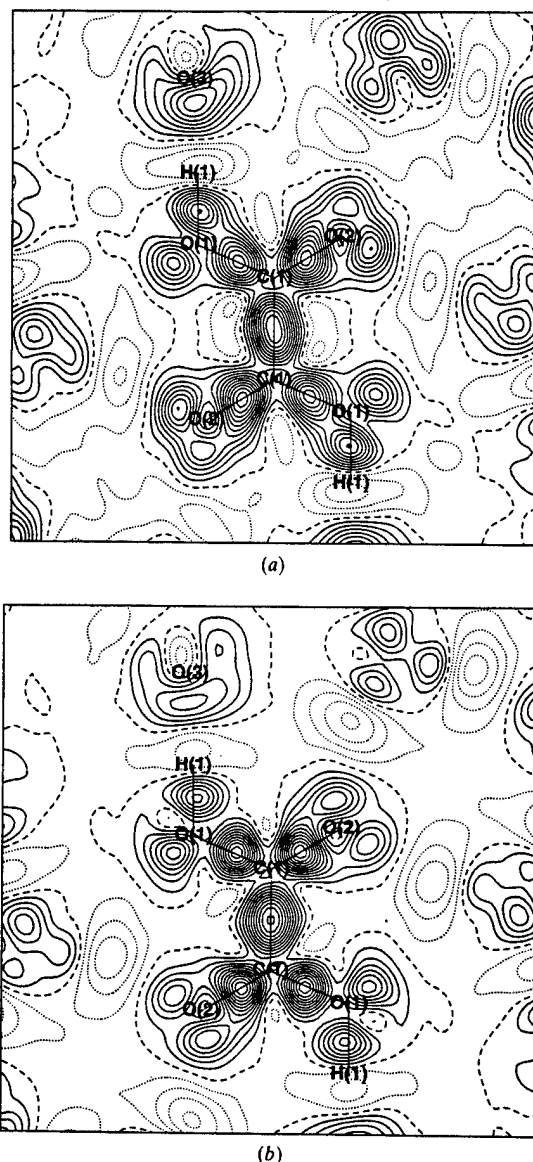


Fig. 3. Model map after multipole refinement: data cut-off at $\sin \theta/\lambda = 0.9 \text{ \AA}^{-1}$ for reflections with $F^2 > 2\sigma(F^2)$; (a) this work; (b) SC. Contour level: 0.05 e \AA^{-3} .

Table 3. Reflection statistics with respect to (a) intensity and (b) resolution

	R_1	R_2	wR	N_{terms}	N_{means}
(a)					
$Q < -2.0$	0.0527	0.0610	0.0758	8	4
$-2.0 < Q < -1.0$	0.4186	0.4591	0.4343	156	41
$-1.0 < Q < 0.0$	0.9073	0.9195	0.8695	3157	443
$0.0 < Q < 1.0$	0.8215	0.8215	0.8745	8342	1033
$1.0 < Q < 2.0$	0.3585	0.3668	0.4385	4621	566
$2.0 < Q < 3.0$	0.2105	0.2358	0.2622	3449	404
$3.0 < Q < 4.0$	0.1380	0.1622	0.1732	2522	292
$4.0 < Q < 6.0$	0.0963	0.1137	0.1194	4499	468
$6.0 < Q < 8.0$	0.0710	0.0856	0.0866	3551	333
$8.0 < Q < 10.0$	0.0543	0.0666	0.0656	2553	230
$10.0 < Q < 20.0$	0.0346	0.0417	0.0418	7804	634
$20.0 < Q < 50.0$	0.0219	0.0288	0.0252	5232	382
$50.0 < Q$	0.0144	0.0173	0.0161	547	48
(b)					
$S < 0.500$	0.0192	0.0235	0.0227	3891	313
$0.500 < S < 0.600$	0.0241	0.0245	0.0304	3262	214
$0.600 < S < 0.650$	0.0286	0.0265	0.0370	1900	129
$0.650 < S < 0.700$	0.0327	0.0295	0.0431	2126	155
$0.700 < S < 0.750$	0.0385	0.0345	0.0483	2790	181
$0.750 < S < 0.800$	0.0467	0.0391	0.0571	3343	207
$0.800 < S < 0.850$	0.0479	0.0378	0.0575	2998	213
$0.850 < S < 0.900$	0.0533	0.0423	0.0608	3682	270
$0.900 < S < 0.950$	0.0657	0.0502	0.0730	3872	289
$0.950 < S < 1.000$	0.0772	0.0577	0.0854	3343	298
$1.000 < S < 1.050$	0.1026	0.0750	0.1140	3418	352
$1.050 < S < 1.100$	0.1119	0.0778	0.1197	3169	386
$1.100 < S < 1.150$	0.1081	0.0823	0.1253	2296	388
$1.150 < S < 1.200$	0.1449	0.1041	0.1642	2393	451
$1.200 < S < 1.250$	0.1334	0.1054	0.1520	2347	480
$1.250 < S < 1.300$	0.1525	0.1165	0.1821	1253	396
$1.300 < S < 1.350$	0.1433	0.1139	0.1776	358	156

$Q = F_o^2/\sigma(F_o^2)$, $S = \sin \theta/\lambda$, $R_1 = \Sigma|Y - \bar{Y}|/\Sigma|Y|$, $R_2 = [\Sigma(Y - \bar{Y})^2/\Sigma Y^2]^{1/2}$, $wR = \{\Sigma w[(Y - \bar{Y})/\sigma(Y)]^2/\Sigma w[Y/\sigma(Y)]^2\}^{1/2}$, where $Y = F_o^2$.

studies. The values fall in the same range as reported in the IUCr study (Coppens, 1984), however, all three refinements gave values that were systematically smaller than those obtained by SC. The mean of the ratios of the U^{ii} parameters for the two studies is 0.95 (3). In contrast, the values are quite similar to the values reported by DHF, the average ratio for the two comparable refinements (I) and (II) being 1.02 (2). It is tempting to suggest that the thermal parameters are too small owing to the presence of TDS contamination in the intensity data, as argued by DHF. However, no TDS correction was applied to the data in the SC study either. It is, of course, possible that the experimental temperatures were not identical, although all three experiments were calibrated in the same way (potassium dihydrogen phosphate, KDP, 122 K), or that there was a difference in crystal quality. At first sight, the agreement of thermal parameters from refinement (II) with those obtained from neutron data (Koetzle & McMullan, unpublished results) appears more satisfying, the average ratio being 1.01 (4). However, the ratio for U^{11} [0.965 (6)] is systematically smaller than for the two other principal

components [1.037 (12)]. The values obtained from a second neutron study (Feld, 1980) reported for the same temperature differed by 15%, again suggesting a problem with temperature calibration across these experiments.

If, as has been suggested, the integrated intensities of the weak reflections are overestimated by the current integration algorithm (SAINT; Siemens, 1996) the displacement parameters would indeed be reduced. To examine this possibility, the ratio between F_o^2 for the current data and that of SC, appropriately scaled using

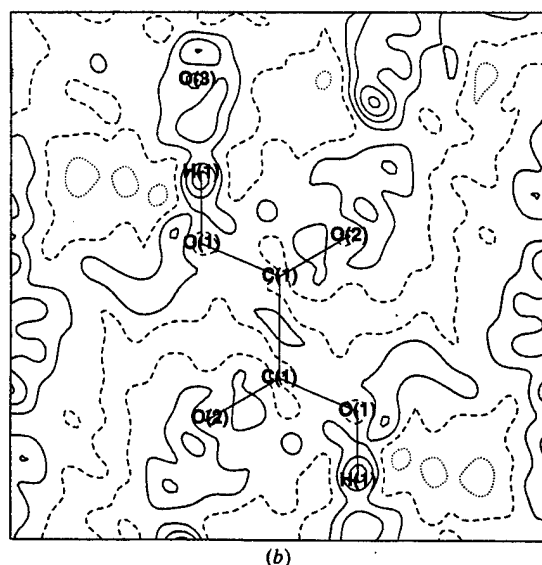
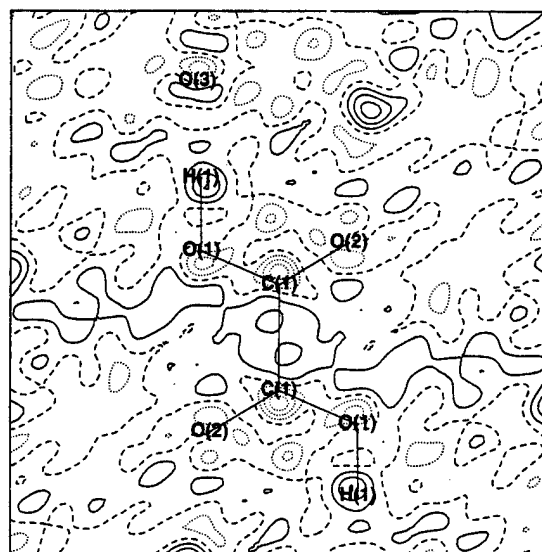


Fig. 4. Residual map after multipole refinement; data cut-off at $\sin \theta/\lambda = 0.9 \text{ \AA}^{-1}$ for reflections with $F^2 > 2\sigma(F^2)$; (a) this work; (b) SC. Contour level: 0.05 e \AA^{-3} .

Table 4. Comparison of the results of the kappa refinements

	This work		SC	
	q	κ	q	κ
O(1)	-0.42 (3)	0.976 (3)	-0.18 (3)	0.986 (3)
O(2)	-0.51 (2)	0.972 (3)	-0.32 (3)	0.973 (3)
O(3)	-0.63 (3)	0.960 (3)	-0.44 (4)	0.968 (4)
C(1)	0.27 (3)	1.032 (5)	-0.06 (5)	0.990 (7)
H(1)	0.49 (2)	1.49 (6)	0.29 (3)	1.20 (3)
H(2)	0.41 (2)	1.34 (3)	0.35 (2)	1.22 (3)
H(3)	0.41 (2)	1.34 (3)	0.35 (2)	1.22 (3)

the scale factors from the final multipole refinements, has been calculated for all reflections common to the two data sets and the results are reported in Fig. 5. It can be seen that the agreement for the strong reflections is good, however, either the CCD detector has indeed overestimated the weak intensities or else they are underestimated by the scintillation counter.

The main purpose of this study was to examine the charge density and compare with previous studies. First the atomic charges were estimated from a kappa refinement. The results are given in Table 4 and compared with those obtained from the SC data. The most striking difference is the positive charge obtained for the C atom from the CCD data compared with a small negative charge obtained using the point-detector data. Indeed, in agreement with chemical intuition, a charge of +0.69 on C is predicted by *ab initio* calculations for the gas phase oxalic acid molecule (6-31G* basis set, SPARTAN; Wavefunction, Inc., 1995), hence, this observed difference is satisfying.

Difference density maps from the current data and the SC data are presented in Fig. 2. The maps were prepared after high-order refinements, as described above. It is clear that the main features of the maps are the same with respect to the bonding and lone-pair regions, however, there are much deeper negative regions close to the nuclear positions for the current data, particularly for the C atom. In contrast, a similar map reported by DHF also has negative regions of similar magnitude.

Comparison of the model maps (Fig. 3) again shows qualitative agreement. All regions agree to within one contour level ($0.05 \text{ e } \text{\AA}^{-3}$), except for the lone-pair regions for O(2) and O(3), which are significantly sharpened in the current study compared with those obtained with the SC data. We note that the differences in the data are real as parallel refinements were carried out using the original SC data and the current data, and identical maps prepared. Indeed, although the current data set extends to $\sin \theta/\lambda = 1.34 \text{ \AA}^{-1}$, it was truncated at 1.20 \AA^{-1} in the refinement to make the comparison as meaningful as possible. However, in the present study all the data were available, whereas in the previous study, only data calculated to be observable was measured for $\sin \theta/\lambda > 0.90 \text{ \AA}^{-1}$.

Examination of the multipole populations gives no indication of this discrepancy observed in the model maps, most populations from the parallel refinements agreeing to within 2 e.s.d.'s (Table 5). The striking exception is the difference in the monopole populations (P_v). This must be a simple difference in the partitioning of the charge density between atom centers in the model as there is no discernible difference in the model maps

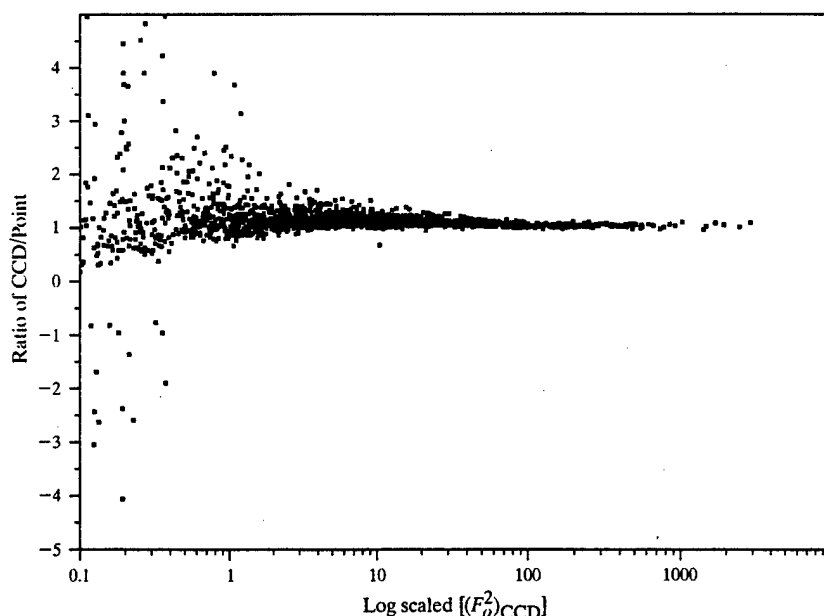


Fig. 5. Ratio between scaled F^2 for CCD and point-detector data with respect to $\log F^2$.

Table 5. Comparison of refined multipole parameters

	C(1)		O(1)		O(2)		O(3)	
	This work	SC	This work	SC	This work	SC	This work	SC
κ'	0.981 (3)	0.974 (4)	0.974 (3)	0.987 (2)	1.000 (5)	0.978 (2)	1.014 (6)	0.999 (3)
P_v	3.87 (4)	4.31 (3)	6.22 (3)	6.06 (2)	6.47 (3)	6.27 (2)	5.83 (5)	5.77 (3)
P_{+11}	0.026 (14)	0.063 (8)	-0.015 (9)	-0.028 (4)	-0.051 (10)	-0.045 (6)	-0.100 (9)	-0.082 (5)
P_{-11}	-0.015 (11)	0.018 (6)	0.001 (7)	-0.055 (5)	0.010 (8)	0.010 (4)	-0.021 (8)	0.011 (5)
P_{20}	-0.264 (12)	-0.255 (7)	-0.032 (10)	-0.008 (6)	-0.078 (10)	-0.062 (7)	-0.015 (8)	-0.037 (5)
P_{+22}	0.072 (12)	0.069 (7)	-0.045 (9)	-0.040 (4)	-0.003 (9)	-0.039 (6)	-0.022 (8)	-0.016 (5)
P_{-22}	-0.044 (11)	-0.031 (6)	0.027 (9)	0.022 (5)	0.040 (8)	0.003 (5)	-0.013 (8)	-0.006 (5)
P_{+31}	0.031 (13)	0.017 (7)	0.012 (10)	0.019 (4)	-0.014 (10)	0.005 (5)	0.124 (8)	0.090 (4)
P_{-31}	0.009 (11)	-0.013 (6)	-0.028 (9)	-0.039 (4)	-0.015 (9)	-0.012 (4)	0.020 (8)	0.024 (4)
P_{+33}	0.287 (14)	0.301 (7)	0.079 (9)	0.076 (4)	0.057 (9)	0.034 (4)	0.013 (8)	-0.001 (4)
P_{-33}	0.030 (16)	0.067 (7)	0.012 (10)	-0.011 (4)	0.016 (8)	-0.007 (4)	0.006 (8)	-0.006 (4)
P_{40}	0.038 (16)	0.026 (8)	0.010 (13)	0.017 (6)	-0.001 (13)	0.006 (6)	-0.019 (11)	-0.002 (5)
P_{+42}	0.009 (17)	0.016 (8)	0.021 (12)	0.014 (5)	-0.003 (11)	-0.013 (5)	0.062 (10)	0.071 (5)
P_{-42}	-0.018 (17)	-0.010 (8)	0.007 (11)	-0.005 (6)	-0.010 (11)	-0.000 (5)	-0.001 (10)	0.018 (5)
P_{+44}	-0.061 (20)	-0.031 (9)	-0.001 (10)	0.028 (5)	-0.008 (10)	-0.007 (5)	-0.010 (10)	0.012 (5)
P_{-44}	-0.051 (15)	-0.007 (8)	0.032 (10)	0.029 (4)	0.010 (10)	-0.002 (4)	-0.003 (10)	-0.009 (5)

	H(1)		H(2)		H(3)	
	This work	SC	This work	SC	This work	SC
κ	1.00	1.00	1.00	1.00	1.00	1.00
P_v	0.75 (2)	0.87 (1)	0.93 (2)	0.86 (1)	0.93 (2)	0.86 (1)
P_{10}	0.197 (21)	0.253 (12)	0.392 (20)	0.384 (11)	0.392 (20)	0.384 (11)
P_{20}	0.330 (31)	0.330 (20)	0.275 (22)	0.243 (13)	0.275 (22)	0.243 (13)

H(3) populations are constrained equal to H(2).

around the carbon position, however, it is also in accordance with the result obtained from the kappa refinement. We note that the e.s.d.'s of the multipole parameters (Table 5) for the CCD study are approximately twice those from the SC data. This implies that the SC data are of superior quality, however, the e.s.d.'s from the CCD data are still as good as those typically reported for similar studies.

The residual maps (Fig. 4) both show similar inadequacies in the model for the H atoms. The most striking difference between the CCD and SC data is the deeper negative regions close to the nuclear positions obtained with the CCD data. Elsewhere, the noise levels are of similar magnitude, but more randomly distributed from the CCD study.

7. Conclusions

Clearly the data obtained are adequate for a charge density analysis. It is also possible that the weak data, contrary to popular wisdom, are actually better than those from point detectors (Fig. 5). Following informal discussions at the 1997 ACA meeting† it seems possible that even better data will be obtained using narrower frames (e.g. 0.1°). From our own observations (Kirschbaum *et al.*, 1997) it is not necessary to eliminate the $\lambda/2$

contamination by reducing the generator voltage as was performed in the present study. However, although the effect on routine structure refinement has been shown to be negligible, the effect of applying the small correction to the intensity data has yet to be determined for charge density studies.

We thank Professor E. D. Stevens for providing the data for the 1980 study, the College of Arts and Sciences of the University of Toledo and the Ohio Board of Regents for generous financial support of the X-ray diffraction facility and thank the Office of Naval Research for funding this work (contract numbers N00014-95-1-0013 and N00014-95-1-1252).

References

- Blessing, R. H. (1987). *Cryst. Rev.* **1**, 3–57.
- Coppens, P. (1984). *Acta Cryst.* **A40**, 184–195.
- Coppens, P. (1997). *X-ray Charge Densities and Chemical Bonding*. Oxford University Press.
- Coppens, P., Guru Row, T. N., Leung, P., Stevens, E. D., Becker, P. J. & Yang, Y. W. (1979). *Acta Cryst.* **A35**, 63–72.
- Dam, J., Harkema, S. & Feil, D. (1984). *Acta Cryst.* **B39**, 760–768.
- Feld, R. H. (1980). Ph.D. thesis. Philipps Universität Marburg/Lahn.
- Feld, R. H., Brown, P. J. & Lehmann, M. S. (1978). *Acta Cryst.* **A34**, S28.

† Contributors to the discussion were the authors, Drs W. Clegg, P. Coppens, C. S. Frampton, T. Koritsanszky, F. K. Larsen, P. M. Mallinson, M. R. Pressprich and E. D. Stevens.

- Hirschfeld, F. L. (1976). *Acta Cryst.* A32, 239–244.
- Kirschbaum, K., Martin, A. & Pinkerton, A. A. (1997). *J. Appl. Cryst.* 30, 514–516.
- Koetzle, T. F. & McMullan, R. Unpublished results.
- Koritsanzky, T., Howard, S., Mallison, P. R., Su, Z., Richter, T. & Hansen, N. K. (1995). *XD. A Computer Program Package for Multipole Refinement and Analysis of Electron Densities from Diffraction Data. User's Manual.* University of Berlin, Germany
- Sheldrick, G. M. (1998). *SADABS.* University of Göttingen, Germany. To be published.
- Siemens (1996). *SAINT. Program to Integrate and Reduce Raw Crystallographic Area Detector Data.* Siemens Analytical X-ray Instruments Inc., Madison, Wisconsin, USA.
- Stevens, E. D. & Coppens, P. (1980). *Acta Cryst.* B36, 1864–1876.
- Wavefunction, Inc. (1995). *SPARTAN4.0.* Wavefunction, Inc., Irvine, California, USA.

CHARGE DENSITY DATA FROM CCD DETECTORS

A. ALAN PINKERTON
Department of Chemistry
University of Toledo
Toledo
OH 43606
USA.

Introduction

The advent of CCD detectors for X-ray diffraction experiments has raised the possibility of obtaining charge density data sets in a much reduced time compared to that required with traditional point detectors. This opens the door to many more studies and, in particular, comparative studies. In addition, the length of data collection no longer scales with the size of the problem, thus the size of tractable studies has certainly increased but the limit remains unknown. Before embracing this new technology, it is necessary to evaluate the quality of the data obtained and the possible new sources of error. The details of the work summarized below has either been published or submitted for publication elsewhere [1-3].

As area detectors (other than multiwire systems) are not energy discriminating devices, a potential source of error lies in the contamination of the data with harmonics of the assumed wavelength of the primary beam. The importance of this effect has been estimated for molybdenum $K\alpha$ radiation using a graphite monochromator [1].

The quality of the intensity data obtainable has been assessed from an experiment on oxalic acid obtained at 100 K with a CCD detector. In this experiment the contamination of $\lambda/2$ to the measured intensities was eliminated by appropriate choice of the generator voltage. Various criteria for judging the quality of the data are discussed below [2].

The advantages of measuring at very low temperatures are well established [4]. Because of the increased speed of data collection, it now becomes feasible to consider the use of liquid helium as a cryogen. A prototype open-flow helium cooling device using mainly off-the-shelf components has been developed [3].

$\lambda/2$ contamination

The characteristic radiation employed for a typical diffraction experiment is commonly obtained by using a crystal monochromator. Harmonics of λ contributing to the primary beam leaving the X-ray source also contribute to the "monochromatic" beam arriving at the sample. Limiting ourselves to Mo- $K\alpha$ radiation, only $\lambda/2$ is important under normal operating conditions (50kV). For any reflection $2h2k2l$ due to λ , there will be a contribution due to $\lambda/2$ to the intensity of the reflection hkl if this harmonic is present in the primary beam. When using a scintillation counter to detect the scattered radiation, this can be removed by energy discrimination. With CCD detectors (and also

image plates), this contamination is a potential source of systematic errors because these devices cannot discriminate with respect to energy.

There are four approaches to remove or account for this effect: i) primary radiation free of any $\lambda/2$ component can be produced; ii) a Si or Ge monochromator may be used; iii) the $\lambda/2$ component of the scattered radiation can be determined; iv) an independent determination of the amount of $\lambda/2$ scattering may be carried out.

$\lambda/2$ free radiation - A primary beam that is free of $\lambda/2$ radiation is produced when the accelerating voltage is reduced below the threshold required for $\lambda/2$ generation. This is given by [5]

$$\lambda_{\min} = \frac{hc}{eV} = 12398 \frac{1}{V}$$

For Mo-K α radiation, $\lambda/2 = 0.3554 \text{ \AA}$ which is produced at a threshold voltage of 34.9 kV. Operating an X-ray source at this potential also results in a drastic reduction in intensity of the desired characteristic radiation [5].

$$I(K\alpha) = k(V - V_0)^{1.63}$$

Thus, reducing the potential from 50.0 kV to 34.9 kV will reduce the intensity of the desired radiation (Mo-K α) by 68 %. Although some of this loss in intensity may be recovered by increasing the filament current, this is not a convenient solution for most experiments. For samples which are strongly diffracting, e.g. minerals, this is a reasonable approach.

Use of Si or Ge monochromators - The amplitude of F_{222} for Si or Ge is close to zero, therefore the contribution of $\lambda/2$ to the 111 reflection is zero. Hence, the 111 reflection from a Si or Ge monochromator is used to obtain $\lambda/2$ free radiation. However, these monochromators also drastically reduce the intensity of the primary beam compared to the graphite monochromators found in most commercial diffractometers.

Experimental determination - A structure factor obtained from an experiment where there is $\lambda/2$ contamination may be written as

$$F'_{hkl} = F_{hkl} + kF_{2h2k2l}$$

Thus, we may obtain a best value for k from a modification of the normal least squares procedure. As $k \ll 1$, F'_{hkl} will only significantly differ from F_{hkl} when F_{hkl} is small and F_{2h2k2l} is large. i.e. the reflections carrying the most information about k are those very reflections which are poorly observed. Hence, this is not a reliable method.

Independent determination of the $\lambda/2$ contribution to the scattering - A method for correcting intensities from film data was proposed by Guinier [6] where two films were used. These were separated by a metal filter designed to absorb radiation λ and let the more penetrating $\lambda/2$ radiation through. Subtraction of the intensities on the second film from those on the first gave intensities free from $\lambda/2$ contamination.

A method to measure the $\lambda/2$ contribution to the observed intensity at any reciprocal lattice point was proposed by Rees [7] for neutron data and is equally applicable to X-rays. By comparing the intensity of strong reflections with at least one index odd with that of pure $\lambda/2$ reflections (which appear at reciprocal lattice nodes) we obtain a direct measure of the two components. With an area detector, this information is always contained in the measurement but is normally ignored if the

reflections have been correctly indexed. This information may be extracted using existing software by defining a new unit cell in which all the axes have been doubled. Now all of the original reflections in the data set have even indices; all of those with any odd index are pure $\lambda/2$ reflections. From the comparison of appropriate pairs of reflections, the ratio of the intensities of the two components of the primary beam may be estimated. As this is a property of the primary beam, it is best performed as a separate experiment designed to optimize the integration of the half integral reflections under standard operating conditions. It is, of course, a function of the accelerating voltage but not of the filament current. The value should be stable with time except for effects due to changes in the absorption of the window of the X-ray source. The difference between diffractometers is small but not negligible (see below).

Using three spherical crystals - the standard ylid crystal provided by Siemens Analytical Instrumentation, ruby and ammonium hydrogen tartrate (Enraf-Nonius standard crystal) - such an experiment has been carried out using two SMART CCD diffractometers. Before integration [8], all of the cell axes were multiplied by 2. Duplicate measurements were then averaged, and all odd reflections with values of $F^2 > 15$ esd's were compared with the reflection with double the indices to obtain the best value of k for the expression $F_{hkl}^2 = kF_{2h2k2l}^2$. The average values of k obtained for the two diffractometers were 0.0014(2) and 0.00106(5).

These values were used to correct the intensities for nine representative data sets, organic crystals, organometallics and minerals and the data compared with respect to systematic absences and space group assignment i) with no corrections to the data, ii) with an absorption correction (SADABS [9]), iii) with only $\lambda/2$ correction, and iv) with both absorption and $\lambda/2$ correction. Analogously four different refinements per sample were carried out based on F^2 .

The magnitudes of the corrections varied quite widely over the nine data sets, the average correction being less than one esd, however the maximum correction was 47.4σ . In all cases there was an improvement in the number of "observed" systematic absences and, hence, space group assignment.

The effects of the $\lambda/2$ correction on the final refinements of these routine data sets was negligible. There was no significant change in the final agreement factors and the changes in the geometrical parameters were all smaller than 1 esd. However, although it has been suggested that this is also the case for charge density data sets, it has yet to be rigorously demonstrated.

Oxalic acid

Experiment - An extensive data set on oxalic acid dihydrate was obtained at 100.0(1) K using a Siemens SMART Platform diffractometer and graphite monochromated Mo- $K\alpha$ radiation. $\lambda/2$ contamination was eliminated by running the generator at 35 kV and 50 mA. Intensity data was collected using 0.3° omega scans with a detector distance of 3 cm. Maximum redundancy in the data was obtained by using four phi settings - 0, 90, 180, 270° - for each of five detector positions - -35° , -65° , -95° , -109° and -50° in 2θ . 60 sec frames were measured for the three lowest resolution detector positions, and 120 sec frames for the two others. For the first four detector positions, 600 frames were measured for each phi setting and 500 for the final detector position.

Data Reduction - The unit cell (Table 1) and orientation matrix were determined from the XYZ centroids of 8,192 reflections with $I > 20\sigma(I)$. The intensities (SAINT [8]) were corrected for beam inhomogeneity and decay, and the esd's adjusted using SADABS [9]. An absorption correction was

applied (T_{\min} 0.949, T_{\max} 0.983) and symmetry and multiply measured reflections averaged with SORTAV [10].

Of 46,135 reflections measured (29,973 with $I > 2\sigma(I)$), only 156 reflections were missing to $\sin\theta/\lambda = 1.34 \text{ \AA}^{-1}$. 5,102 reflections were unique of which 2,681 had been measured more than nine times (symmetry equivalents plus multiple measurements). The merging R values were $R1 = 0.037$ and $R2 = 0.024$ for 4,809 accepted means. Examination of the reflection statistics (Table 2) with respect to $F_o^2/\sigma(F_o^2)$ (Q) and $\sin\theta/\lambda$ (S) indicate the usual trends and suggest that the data should be adequate for a charge density study.

Refinements - Starting coordinates were taken from Stevens and Coppens (hereafter SC) [11] and all refinements were carried out on F^2 using the XD suite of programs [12]. Four different refinements were carried out using statistical weights throughout and the results are summarized in Table 3. Refinement I is an independent atom refinement; II is a high angle refinement ($1.00 < \sin\theta/\lambda < 1.34 \text{ \AA}^{-1}$) with the hydrogen atoms fixed at the neutron positions [13] with isotropic thermal parameters fixed at the values obtained from I; III is a kappa refinement to assign atomic charges [14] with hydrogen parameters fixed as in II; a complete atom centered multipole refinement [15] was carried out in IV with hydrogen atoms treated as in II with one atom directed dipole and quadrupole population varied. All other atoms were refined as previously [11] up to the hexadecapole level with mirror symmetry imposed in the plane of the oxalic acid molecule and in the bisecting plane perpendicular to the plane of the water molecule. Isotropic extinction was included in all four refinements, however, the value obtained from refinement I was held constant for the high angle refinement. For purposes of comparison, particularly of the multipole refinements, an identical set of refinements was carried out using the SC data [11] and the results compared. As the SC data only extend to $\sin\theta/\lambda = 1.2 \text{ \AA}^{-1}$, the current data was also limited to this resolution for refinement IV.

Positional parameters of the non-hydrogen atoms obtained from refinements I and II are in good agreement with those of SC (1980) or Dam, Harkema and Feil (hereafter DHF) [16] from X-ray data as well as those from neutron data [13,17].

The values for the thermal displacement parameters fall in the same range as reported in the IUCr study [18], however, all refinements gave values that were systematically smaller than those obtained by SC [11]. In contrast, the values are quite similar to the values reported by DHF [16]. It is tempting to suggest that the thermal parameters are too small due to the presence of TDS contamination in the intensity data, however, it is more likely that the experimental temperatures were not identical. The agreement of thermal parameters from refinement II with those obtained from one neutron data set [17] is quite satisfying, however, agreement with a second neutron study [13] reported for the same temperature differed by 15%, again suggesting a problem with temperature calibration across these experiments.

Charge densities - The atomic charges estimated from a kappa refinement are given in Table 4 as well as those obtained from the SC data [11]. The main difference is the positive charge obtained for the C atom from the CCD data (in agreement with chemical intuition) compared to a small negative one obtained using the point detector data.

Difference density maps from the current data and the SC [11] data after high order refinements are shown in Fig. 1a,b. The main features of the maps agree with respect to the bonding and lone pair

regions, however, there are much deeper negative regions close to the nuclear positions for the current data. In contrast, a similar map reported by DHF [16] also has similar negative regions.

Comparison of the model maps (Fig. 1c,d) again show qualitative agreement. All regions agree to within one contour level ($0.05 \text{ e } \text{\AA}^{-3}$) except for the lone pair regions for O(2) and O(3) which are significantly sharpened compared to those obtained with the SC data.

Examination of the multipole populations gives no indication of the discrepancy observed in the model maps, all populations from parallel refinements agreeing to within 2 esd's (Table 5). The one striking exception is the monopole population (P_v) for carbon. This must be a simple difference in the partitioning of the charge density between atom centers in the model as there is no discernable difference in the model maps around the carbon position.

It has been suggested that the integrated intensities of weak reflections are overestimated by the current integration algorithm (SAINT, [8]). The ratio between F_o^2 for the current data and that of SC [11], scaled from the multipole refinements, has been calculated for all common reflections (Fig. 2). The agreement for the strong reflections is good, however, either the CCD detector has indeed overestimated the weak intensities or else they are underestimated by the scintillation counter.

Helium cooling

Most previous attempts to obtain X-ray diffraction data at very low temperatures ($< 80 \text{ K}$) have used custom built systems with closed cycle helium refrigerators mounted on large, robust four circle diffractometers. In order to remove the inherent disadvantages of these systems - cost, single application, absorption and scattering of the windows - we have built an open flow system from mainly off the shelf components which uses liquid helium as the cryogen. This is not the first open flow helium system [19,20] but is the first that is mainly off the shelf and is mountable on any diffractometer. It is based on an ADP Helitran ESR cryostat with modifications to the nozzle assembly and to the direction of the gas flow. The lowest temperature is estimated to be $< 30 \text{ K}$. At the current price for liquid helium in the US, with the increase in measuring speed available with a CCD detector, the economics per data set are comparable with those using liquid nitrogen on a conventional diffractometer.

Concluding remarks

Clearly the CCD data is adequate for a charge density analysis. It is also possible that the weak data, contrary to popular wisdom, is actually better than that from point detectors. Following informal discussions at the 1997 ACA meeting¹ it seems possible that even better data will be obtained by using narrower frames (e.g. 0.1°).

Acknowledgments

We thank Professor E.D. Stevens for providing the data for the 1980 study, the College of Arts and Sciences of the University of Toledo and the Ohio Board of Regents for generous financial support of the X-ray diffraction facility and thank the Office of Naval Research for funding this work. (Contract Nos. N00014-95-1-0013 and N00014-95-1-1252).

¹Contributors to the discussion were the author, Drs. W. Clegg, P. Coppens, C.S. Frampton, T. Koritsanszky, F.K. Larsen, P.M. Mallinson, A. Martin, M.R. Pressprich, E.D. Stevens.

References

1. Kirschbaum, K., Martin, A. and Pinkerton, A.A. (1997). *J. Appl. Cryst.*, **30**, 514-516.
2. Martin, A. and Pinkerton, A.A. (1998) *Acta Cryst.*, **B**, in press.
3. Kirschbaum, K., Martin, A. and Pinkerton, A.A. *J. Appl. Cryst.*, in press.
4. F.K. Larsen, *Acta Cryst.*, **B51**, 468 (1995).
5. International Tables for X-Ray Crystallography, Vol. C, Kluwer Academic Publishers, Dordrecht, 1995.
6. Guinier, A. (1963) X-Ray Diffraction in Crystals, Imperfect Crystals, and Amorphous Bodies, W.H. Freeman and Co., pp. 175.
7. Rees, B. (1977). *Israel J. Chem.*, **16**, 154-158.
8. Siemens Analytical Instrumentation (1996). SAINT, a program to integrate and reduce raw crystallographic area detector data.
9. Sheldrick, G.M. (1996). SADABS, University of Göttingen, Germany, to be published.
10. Blessing, R.H. (1987). *Cryst. Rev.*, **1**, 3-57.
11. Stevens, E.D. and Coppens, P. (1980). *Acta Cryst.*, **B36**, 1864-1876.
12. Koritsanszky, T., Howard, S., Mallison, P.R., Su, Z., Richter, T. and Hansen, N.K. (1995). XD, a program for refinement and display of charge densities.
13. Feld, R.H., Brown, P.J. and Lehmann, M.S. (1978). *Acta Cryst.*, **A34**, S28; Feld, R.H. (1980) Ph.D. thesis, Philipps-Universität Marburg/Lahn.
14. Coppens, P., Guru Row, T.N., Leung, P., Stevens, E.D., Becker, P.J. and Yang, Y.W. (1979). *Acta Cryst.*, **A35**, 63-72.
15. Hansen, N.K. and Coppens, P. (1978), *Acta Cryst.*, **A34**, 909-921.
16. Dam, J., Harkema, S. and Feil, D. (1984). *Acta Cryst.*, **B39**, 760-768.
17. Koetzle, T.F and McMullan, R., unpublished results.
18. Coppens, P. (1984). *Acta Cryst.*, **A40**, 184-195.
19. Greubel, K.H., Gmelin, E., Moser, H., Mensing, C. and Walz, L. (1990) *Cryogenics*, **30** (suppl.), 457-462.
20. Teng, T., Schildkamp, W., Dolmer, P. and Moffat, K. (1994) *J. Appl. Cryst.*, **27**, 133-139.

Figure captions

1. Difference map after high order refinement - data cutoff at $\sin\theta/\lambda = 0.9 \text{ \AA}^{-1}$ for reflections with $F^2 > 2\sigma(F^2)$; a) this work, b) SC. Model map after multipole refinement - data cutoff at $\sin\theta/\lambda = 0.9 \text{ \AA}^{-1}$ for reflections with $F^2 > 2\sigma(F^2)$; c) this work, d) SC.
2. Ratio between scaled F^2 for CCD and point detector data with respect to $\log F^2$.

Table 1. Comparison of unit cell parameters

This work	IUCr study
$a = 6.1024(1) \text{ (\AA)}$	$\bar{a} = 6.102(6)$
$b = 3.4973(1) \text{ (\AA)}$	$\bar{b} = 3.501(7)$
$c = 11.9586(2) \text{ (\AA)}$	$\bar{c} = 11.964(17)$
$\beta = 105.771(1) \text{ (}^\circ\text{)}$	$\bar{\beta} = 105.80(5)$

Table 2a. Reflection statistics with respect to intensity.^a

				R1	R2	Rw	Nterms	Nmeans	
	Q	<	-2.0	0.0527	0.0610	0.0758	8	4	
-2.0	<	Q	<	-1.0	0.4186	0.4591	0.4343	156	41
-1.0	<	Q	<	0.0	0.9073	0.9195	0.8695	3157	443
0.0	<	Q	<	1.0	0.8215	0.8215	0.8745	8342	1033
1.0	<	Q	<	2.0	0.3585	0.3668	0.4385	4621	566
2.0	<	Q	<	3.0	0.2105	0.2358	0.2622	3449	404
3.0	<	Q	<	4.0	0.1380	0.1622	0.1732	2522	292
4.0	<	Q	<	6.0	0.0963	0.1137	0.1194	4499	468
6.0	<	Q	<	8.0	0.0710	0.0856	0.0866	3551	333
8.0	<	Q	<	10.0	0.0543	0.0666	0.0656	2553	230
10.0	<	Q	<	20.0	0.0346	0.0417	0.0418	7804	634
20.0	<	Q	<	50.0	0.0219	0.0288	0.0252	5232	382
50.0	<	Q			0.0144	0.0173	0.0161	547	48

Table 2b. Reflection statistics with respect to resolution.^a

				R1	R2	Rw	Nterms	Nmeans	
	S	<	0.500	0.0192	0.0235	0.0227	3891	313	
0.500	<	S	<	0.600	0.0241	0.0245	0.0304	3262	214
0.600	<	S	<	0.650	0.0286	0.0265	0.0370	1900	129
0.650	<	S	<	0.700	0.0327	0.0295	0.0431	2126	155
0.700	<	S	<	0.750	0.0385	0.0345	0.0483	2790	181
0.750	<	S	<	0.800	0.0467	0.0391	0.0571	3343	207
0.800	<	S	<	0.850	0.0479	0.0378	0.0575	2998	213
0.850	<	S	<	0.900	0.0533	0.0423	0.0608	3682	270
0.900	<	S	<	0.950	0.0657	0.0502	0.0730	3872	289
0.950	<	S	<	1.000	0.0772	0.0577	0.0854	3343	298
1.000	<	S	<	1.050	0.1026	0.0750	0.1140	3418	352
1.050	<	S	<	1.100	0.1119	0.0778	0.1197	3169	386
1.100	<	S	<	1.150	0.1081	0.0823	0.1253	2296	388
1.150	<	S	<	1.200	0.1449	0.1041	0.1642	2393	451
1.200	<	S	<	1.250	0.1334	0.1054	0.1520	2347	480
1.250	<	S	<	1.300	0.1525	0.1165	0.1821	1253	396
1.300	<	S	<	1.350	0.1433	0.1139	0.1776	358	156

^a $Q = F_o^2/\sigma(F_o^2)$, $S = \sin\theta/\lambda$, $R1 = \Sigma |Y - \bar{Y}| / \Sigma |Y|$, $R2 = \sqrt{(\Sigma(Y - \bar{Y})^2 / \Sigma Y^2)}$, $RW = \sqrt{(\Sigma w((Y - \bar{Y}) / \sigma(Y))^2 / \Sigma w(Y / \sigma(Y))^2)}$ where $Y = F_o^2$

Table 3. Summary of Least-squares refinements

Refinement	I	II ^a	III ^a	IV ^a
$\sin\theta/\lambda$ range (\AA^{-1})	0.00-1.20	1.00-1.33	0.00-1.33	0.00-1.20
N_{obs}	3860	2895	5166	3860
N_{v}	50	37	50	108
Scale Factor	1.812(2)	1.87(2)	1.813(4)	1.812(4)
$R(F^2)^b$	0.0540	0.1170	0.0457	0.0532
$R_w(F^2)^b$	0.0769	0.1630	0.0777	0.0299
$R(F)$ ($I > 2\sigma(I)$)	0.0281	0.0423	0.0282	0.0190
GOF	1.01	0.84	0.86	0.73

^a Hydrogen coordinates fixed at neutron positions with isotropic thermal parameters from I.

^b All reflections.

Table 4. Comparison of the results of the kappa refinements.

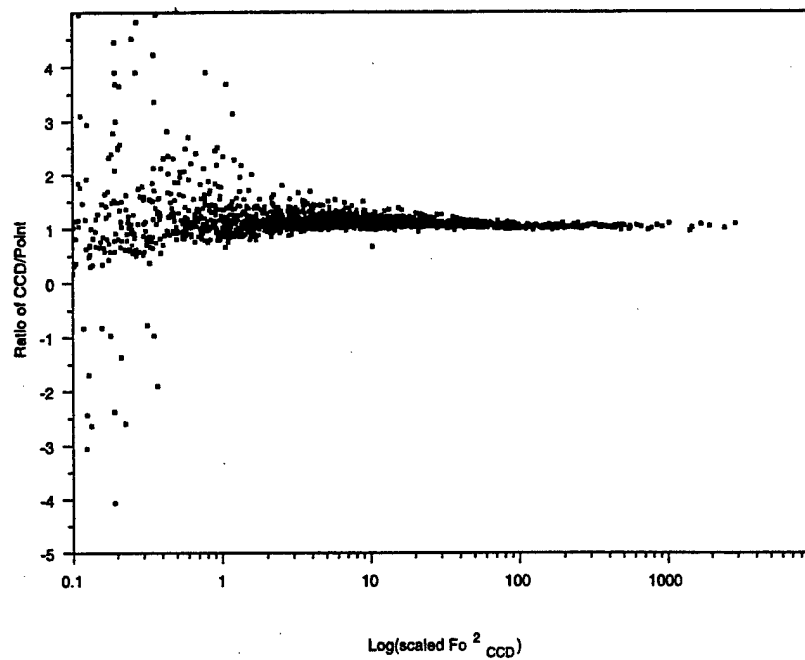
	This work		SC	
	q	κ	q	κ
O(1)	-0.42(3)	0.976(3)	-0.18(3)	0.986(3)
O(2)	-0.51(2)	0.972(3)	-0.32(3)	0.973(3)
O(3)	-0.63(3)	0.960(3)	-0.44(4)	0.968(4)
C(1)	0.27(3)	1.032(5)	-0.06(5)	0.990(7)
H(1)	0.49(2)	1.49(6)	0.29(3)	1.20(3)
H(2)	0.41(2)	1.34(3)	0.35(2)	1.22(3)
H(3)	0.41(2)	1.34(3)	0.35(2)	1.22(3)

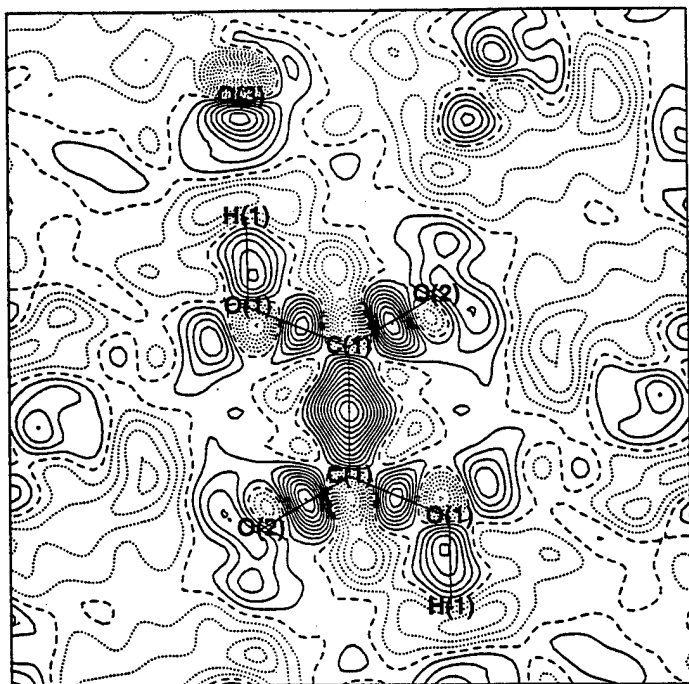
Table 5. Comparison of refined Multipole Parameters

	C(1)		O(1)		O(2)		O(3)	
	This work	SC	This work	SC	This work	SC	This work	SC
κ'	0.981(3)	0.974(4)	0.974(3)	0.987(2)	1.000(5)	0.978(2)	1.014(6)	0.999(3)
P_v	3.87(4)	4.31(3)	6.22(3)	6.06(2)	6.47(3)	6.27(2)	5.83(5)	5.77(3)
P_{+11}	0.026(14)	0.063(8)	-0.015(9)	-0.028(4)	-0.051(10)	-0.045(6)	-0.100(9)	-0.082(5)
P_{-11}	-0.015(11)	0.018(6)	0.001(7)	-0.055(5)	0.010(8)	0.010(4)	-0.021(8)	0.011(5)
P_{20}	-0.264(12)	-0.255(7)	-0.032(10)	-0.008(6)	-0.078(10)	-0.062(7)	-0.015(8)	-0.037(5)
P_{+22}	0.072(12)	0.069(7)	-0.045(9)	-0.040(4)	-0.003(9)	-0.039(6)	-0.022(8)	-0.016(5)
P_{-22}	-0.044(11)	-0.031(6)	0.027(9)	0.022(5)	0.040(8)	0.003(5)	-0.013(8)	-0.006(5)
P_{+31}	0.031(13)	0.017(7)	0.012(10)	0.019(4)	-0.014(10)	0.005(5)	0.124(8)	0.090(4)
P_{-31}	0.009(11)	-0.013(6)	-0.028(9)	-0.039(4)	-0.015(9)	-0.012(4)	0.020(8)	0.024(4)
P_{+33}	0.287(14)	0.301(7)	0.079(9)	0.076(4)	0.057(9)	0.034(4)	0.013(8)	-0.001(4)
P_{-33}	0.030(16)	0.067(7)	0.012(10)	-0.011(4)	0.016(8)	-0.007(4)	0.006(8)	-0.006(4)
P_{40}	0.038(16)	0.026(8)	0.010(13)	0.017(6)	-0.001(13)	0.006(6)	-0.019(11)	-0.002(5)
P_{+42}	0.009(17)	0.016(8)	0.021(12)	0.014(5)	-0.003(11)	-0.013(5)	0.062(10)	0.071(5)
P_{-42}	-0.018(17)	-0.010(8)	0.007(11)	-0.005(6)	-0.010(11)	-0.000(5)	-0.001(10)	0.018(5)
P_{+44}	-0.061(20)	-0.031(9)	-0.001(10)	0.028(5)	-0.008(10)	-0.007(5)	-0.010(10)	0.012(5)
P_{-44}	-0.051(15)	-0.007(8)	0.032(10)	0.029(4)	0.010(10)	-0.002(4)	-0.003(10)	-0.009(5)

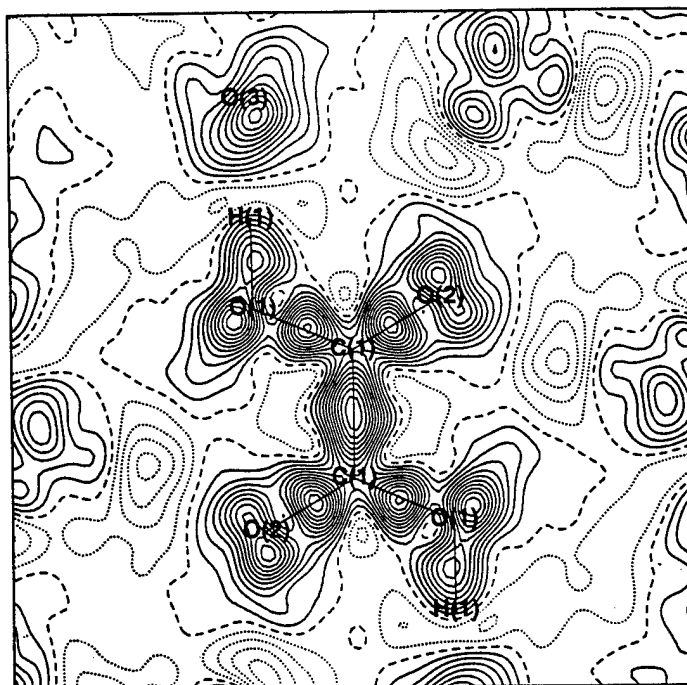
	H(1)		H(2)		H(3)*	
	This work	SC	This work	SC	This work	SC
κ	1.00	1.00	1.00	1.00	1.00	1.00
P_v	0.75(2)	0.87(1)	0.93(2)	0.86(1)	0.93(2)	0.86(1)
P_{10}	0.197(21)	0.253(12)	0.392(20)	0.384(11)	0.392(20)	0.384(11)
P_{20}	0.330(31)	0.330(20)	0.275(22)	0.243(13)	0.275(22)	0.243(13)

*H(3) populations are constrained equal to H(2).

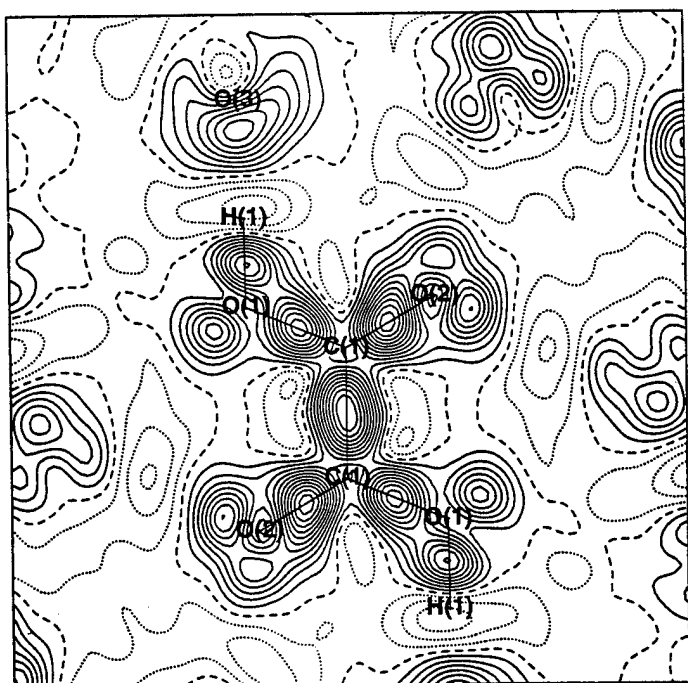




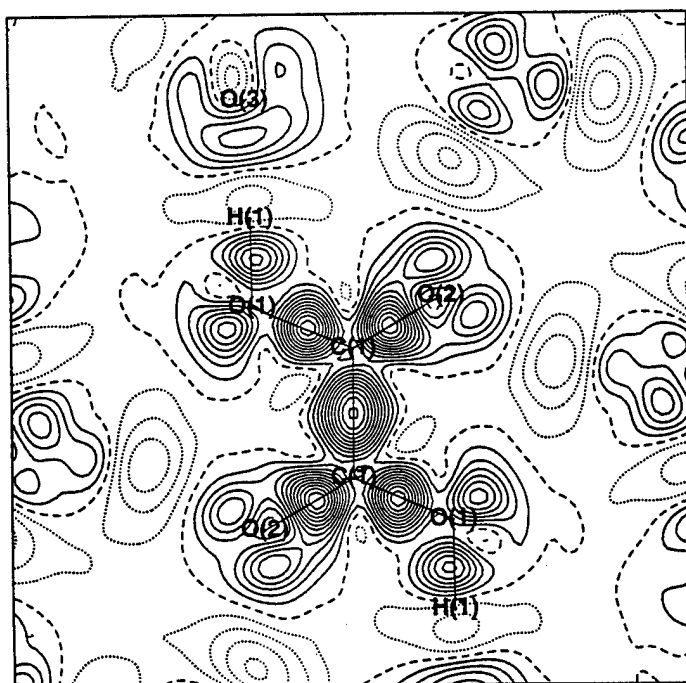
a



b



c



d

Contract No. N00014-95-1-0013 and N00014-97-1-0409

Program Officer: R. Miller/J. Goldwasser

**Title: Experimental Charge Densities and Electrostatic Potentials in Energetic
Materials and Infrastructure Upgrade for an X-ray Crystallography
Laboratory**

PI: A. Alan Pinkerton

Department of Chemistry, University of Toledo, Toledo, OH 43606

tel. (419) 530-4580, FAX (419) 530-4033, email apinker@uoft02.utoledo.edu

APPENDIX 1c

An Open Flow Helium Cryostat for X-ray Diffraction.

Hardie, M.J., Kirschbaum, K., Martin, A; and Pinkerton, A.A., *J. Appl. Cryst.*, 1998, *31*, 815-817.

J. Appl. Cryst. (1998). **31**, 815–817

An open-flow helium cryostat for single-crystal X-ray diffraction experiments

M. J. HARDIE, K. KIRSCHBAUM, A. MARTIN AND A. A. PINKERTON* at *Department of Chemistry, University of Toledo, Toledo, OH 43606, USA. E-mail: apinker@uoft02.utoledo.edu*

(Received 12 November 1997; accepted 26 February 1998)

Abstract

An open-flow helium cryostat for single-crystal X-ray diffraction experiments capable of reaching 14 K has been developed using off-the-shelf components. Solid/liquid air build-up is prevented using the transfer-line helium back-flow and a heated nozzle. The system has run for over 30 h with no frost build-up.† The effectiveness of the system has been demonstrated using test data for oxalic acid, terbium vanadate and dysprosium vanadate.

1. Introduction

The advantages of low temperatures for crystallography are well understood (Larsen, 1995). Several commercial systems that use liquid nitrogen, such as the Oxford Cryosystems Cryostream, are available and easily attain cooling to 100 K. However, crystal cooling systems that can provide much lower temperatures are less common and less straightforward to build and operate. The 'traditional method' uses a closed-cycle helium refrigerator mounted onto a large four-circle diffractometer (Copley *et al.*, 1997). This allows very low temperatures (10 K) to be held for long periods. Neutron diffraction experiments using such systems are much more common than similar experiments using X-rays. One of the major drawbacks of such systems for X-ray diffraction is the need for Be windows, which obscure the view of the crystal, produce significant background scatter and absorb X-rays. Another disadvantage is the relatively high level of technical expertise and expense needed to create such a system, making it prohibitive for everyday use.

An alternative methodology is to use liquid helium in a manner similar to that employed for nitrogen systems. The biggest barrier to developing such open-flow helium cryostats has always been the price of the cryogen. However, with the advent of area detectors, the time required for data collection has been drastically reduced and is essentially independent of the number of atoms in a structure. Thus, with measurement of a normal 'small molecule' data-set taking as little as 6 h on a CCD (charge-coupled device) diffractometer, the economic barrier has been largely removed.

We describe below an open-flow helium cryostat built from essentially off-the-shelf components. This is not the first open-flow cryostat to use liquid helium as the cryogen, at least two others have been documented (Greubel *et al.*, 1990; Teng *et al.*, 1994). However, both of these custom-built systems require a high level of expertise to assemble and, while showing the basic idea is sound, are unlikely to become common. It is the authors' belief that the system described here is both simple enough and economical enough to make helium-temperature data collection far more common than it is currently.

† In a recent experiment the system has run for over 60 h with no frost build-up.

2. Description of the helium cryostat

An APD Heli-tran ESR cryostat (APD Cryogenics Inc., Allentown, PA, USA; Fig. 1) was modified for use with a SMART CCD platform diffractometer. However, the arrangement would work as well on any other type of diffractometer where space is available to mount a stationary low-temperature device.

As with other open-flow systems, a warm gas flow is used to shield the cold gas. In this case, the warm stream is obtained from the helium transfer-line back-flow and fed into the cryostat via the normal (ESR) exhaust port [Fig. 1, B].

The following modifications to a commercially available Heli-tran are necessary for successful operation. The quartz Dewar with an aluminium sleeve (Fig. 2) supplied with the Heli-tran must be shortened such that the end of the dewar is level with the end of the helium nozzle. Alternatively, the quartz/aluminium assembly may be replaced with a single piece constructed entirely of aluminium.

The second modification is the removal of the sample thermocouple, situated at the bottom of the cold-helium nozzle in the commercial product. This is necessary to ensure a smooth flow of both helium streams.

The third modification is the addition of a heater affixed to the portion of the quartz dewar which extends from the bottom

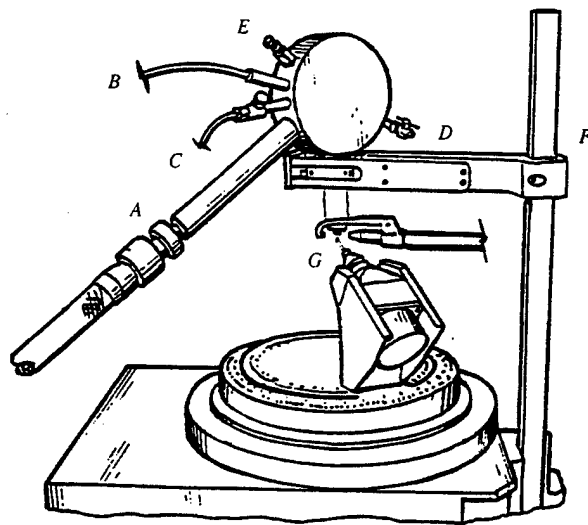


Fig. 1. A schematic of the cryostat mounted on a platform diffractometer. A Helium transfer-line insert, controlled by a screw thread and a needle valve; B transfer-line back-flow gas feed into the cryostat (provides warm stream); C instrumentation/control port for thermocouple(s) and electric heater; D vacuum port; E safety valve; F locally manufactured clamp; G output nozzle.

of the nozzle assembly (Fig. 2). This heater is formed by wrapping a small piece of lead foil round the 11 mm quartz dewar and adding a coil of insulated Nichrome resistance heating wire. The whole assembly is kept in place with an *O* ring at the top. The lead foil is an integral part of the heater, for, without the foil, the heat transfer to the dewar walls is insufficient and frost builds on the tip of the dewar. The bottom of the lead foil is turned up into a rim, in which the coil sits. The coil is connected to a Variac to control the electric heating. The heating is adjusted such that no frost builds up on the outside of the nozzle. A similar heater is required for the all-aluminium nozzle assembly; however, less heating is necessary because of the natural heat leak due to the higher thermal conductivity of the metal compared to quartz.

The Heli-tran is coupled to the storage dewar with an 8 ft (2.44 m) flexible transfer line with a right-angle exit from the helium dewar. The transfer line has a needle valve in the end which controls the flow of the liquid helium and also allows the cryostat to be turned off.

The supply dewar is pressurized from helium gas cylinders connected such that the cylinders can be changed with no loss of pressure. This arrangement is preferable to pressurizing the dewar internally, both in order to conserve liquid helium and to allow finer pressure control.

Finally a clamp is needed to hold the Heli-tran in position. As the nozzle is only 2 mm in diameter, accurate alignment is critical to keep the sample in the center of the cold stream; hence it is vital that the clamp be both stable and rigid with precise translational adjustments.

The cryostat temperature controller is only used to monitor the temperature of the cryogen in the cryostat; the current design does not measure the temperature at the sample.

3. Operation

Operation is straightforward. The crystal should be mounted on a short (2.0 mm) diamond-cleaved 0.1 mm glass capillary. The length of the capillary is critical in order to prevent sample vibration and condensation of air or moisture (capillary too long) or condensation on the metal pin (capillary too short). The cryostat is mounted on the diffractometer and the nozzle aligned using a metal pin to reference the crystal position. The nozzle should be 2–3 mm above the crystal. At this point the

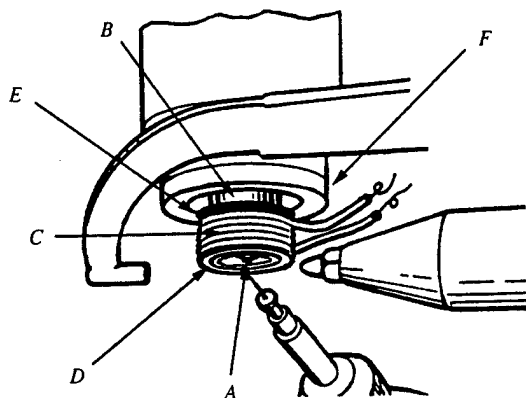


Fig. 2. Detail of the nozzle assembly. A Output nozzle (inner cold stream, outer warm stream); B evacuable dewar assembly; C heat coil; D lead foil; E coil *O* ring; F aluminium sleeve.

cryostat should be evacuated. One end of the transfer line is then placed in the dewar (cathedral ceilings are helpful) and the line connected to the cryostat [Fig. 1. A]. The dewar is attached to the helium gas cylinders, pressurized to 5–8 psi (35–55 kPa) and the transfer-line back-flow connected *via* a flow gauge to the cryostat. Once the dewar is pressurized, the system takes 10–15 min to cool down which provides time to make any necessary fine adjustments to the nozzle position. Below about 150 K ice builds up rapidly if the warm stream heater is not activated. The heater voltage is adjusted to prevent any build-up of frost on the nozzle. The cryostat is ready to use when the internal temperature has stabilized and the system cryopumps. The cold helium flow may be stopped by closing the transfer-line needle valve before mounting or changing samples (note that the heater must also be stopped to prevent overheating). Finally the needle valve is reopened, the heater reactivated and data collection can begin within a few minutes. In our experience, condensation has not been a problem; however, rotating the crystal regularly may be advisable.

4. Test results

Feasibility was established and temperature calibration was obtained from three experiments. Using the quartz nozzle in a first experiment, a data-set was collected for oxalic acid dihydrate on a Siemens SMART CCD platform diffractometer with Mo $K\alpha$ radiation. The system ran continuously for over 30 h using 250 l of liquid helium. During data collection, there was no frost build-up on the nozzle and only a small amount of solid air on the fiber. In this first experiment, the nozzle was 6 mm above the crystal, which necessitated a higher pressure [10 psi (70 kPa)] on the dewar and, hence, more rapid consumption of helium than under the conditions described above. During this test we discovered a small vacuum leak (due to a pinhole in the evacuable quartz dewar assembly) which prevented the system from cryopumping and also increased the consumption of liquid helium.

There are no special requirements for data collection; however, because of the proximity of the nozzle to the crystal, part of the detector is masked by the dewar and heater assembly. A frame of data collected with a glass rod in place of the crystal shows the shadow of the nozzle on the detector which may be used as an active pixel mask during data integration.

The exact temperature at the crystal during the experiment was unknown; however, after normal data reduction and refinement of the structure, the temperature was estimated as follows. By using the literature values of oxalic acid at various temperatures (Stevens & Coppens, 1980; Dam *et al.*, 1983; Coppens *et al.*, 1984; Wang *et al.*, 1985; Zobel *et al.*, 1992) and performing a linear regression analysis on the U_{ii} values of the non-H atoms, a temperature of 34 (3) K was obtained for this experiment. The validity of this method was tested by using a similar data-set collected at 100 (1) K using an Oxford Cryosystems Cryostream. The estimated temperature in that case was 99 (5) K.

The second experiment was a study of terbium vanadate (crystals were kindly provided by Dr L. Boatner of Oak Ridge National Laboratory). In this experiment the quartz nozzle assembly was replaced by the all-aluminium piece which eradicated the vacuum leak and the system cryopumped. Terbium vanadate is known to undergo a second-order phase

transition from tetragonal to orthorhombic at 33 K (Will *et al.*, 1972). A crystal was mounted on a capillary 2.0 mm in length and a quadrant of data collected with the cryostat in operation. The expected twinned orthorhombic phase was observed and by comparison of the unit-cell parameters with those reported in the literature, the temperature at the crystal was estimated to be <20 K. Details of the indexing, integration and structure refinement of the twin will be published elsewhere; however, the successful refinement of the structure from the twinned data ($R = 0.06$) and the small e.s.d.'s of the unit-cell parameters refined from the complete data-set indicate reasonable temperature stability.

In a final third experiment to estimate the temperature at the sample, terbium vanadate was replaced with a crystal of the dysprosium analog (crystals were kindly provided by Dr. L. Boatner of Oak Ridge National Laboratory) which undergoes a similar phase transition at 14 K (Taylor *et al.*, 1985). Again, splitting of the tetragonal reflections was observed indicating formation of the twinned orthorhombic phase and, thus, a temperature below 14 K.

5. Concluding remarks

The use of a modified ESR helium cryostat is a novel, economical and straightforward way of reaching temperatures below 77 K for single-crystal X-ray crystallography. It also offers some significant advantages over other systems: (i) economical construction; (ii) ease of use – the system is essentially 'off-the-shelf' technology, which only requires small (but crucial) modifications; (iii) the crystal can be aligned optically; (iv) there is no increase in background or absorption due to beryllium windows; (v) use of the transfer-line back-flow ensures a dry warm stream and improves the economics of operation. However, there are some disadvantages to the

system: (i) helium is consumed at a rapid rate (*circa* 4 l h^{-1} in the 20 K experiment, more for the 14 K experiment); (ii) there is no provision at the present time for measuring or controlling the temperature at the crystal.

We thank Dr L. Boatner for providing the terbium and dysprosium vanadate crystals, Dr D. White and Mr. L. Gu for assistance with the regression analysis, Mr W. Burger for help in the design and machining of the all-aluminium nozzle and clamp, and OBOR and ONR (contract N00014-95-1-0013) for financial support.

References

- Copley, R. C. B., Goeta, A. E., Lehmann, C. W., Cole, J. C., Yufit, D. S., Howard, J. A. K. & Archer, J. M. (1997). *J. Appl. Cryst.* **30**, 413–417 (and references therein).
- Coppens, P., Dam, J., Harkema, S., Feil, D., Feld, R., Lehmann, M. S., Goddard, R., Krüger, C., Hellner, E., Johansen, H., Larsen, F. K., Koetzle, T. F., McMullan, R. K., Maslen, E. N., Stevens, E. D. & Coppens, P. (1984). *Acta Cryst.* **A40**, 184–195.
- Dam, J., Harkema, S. & Feil, D. (1983). *Acta Cryst.* **B39**, 760–768.
- Gruebel, K. H., Gmelin, E., Moser, N., Mensing, Ch. & Walz, L. (1990). *Cryogenics*, **30**(Suppl.), 457–462.
- Larsen, F. K. (1995). *Acta Cryst.* **B51**, 468–482.
- Stevens, E. D. & Coppens, P. (1980). *Acta Cryst.* **B36**, 1864–1876.
- Taylor, D. R., Smith, S. R. P. & Page, J. H. (1985). *J. Phys. C*, **18**, 3285–3296.
- Teng, T., Schildkamp, W., Dolmer, P. & Moffat, K. (1994). *J. Appl. Cryst.* **27**, 133–139.
- Wang, Y., Tsai, C. J., Liu, W. L. & Calvert, L. D. (1985). *Acta Cryst.* **B41**, 131–135.
- Will, G., Göbel, H., Sampson, C. F. & Forsyth, J. B. (1972). *Phys. Lett.* **38A**, 207–208.
- Zobel, D., Luger, P., Dreissig, W. & Koritsanszky, T. (1992). *Acta Cryst.* **B48**, 837–848.

Contract No. N00014-95-1-0013 and N00014-97-1-0409

Program Officer: R. Miller/J. Goldwasser

**Title: Experimental Charge Densities and Electrostatic Potentials in Energetic
Materials and Infrastructure Upgrade for an X-ray Crystallography
Laboratory**

PI: A. Alan Pinkerton

Department of Chemistry, University of Toledo, Toledo, OH 43606

tel. (419) 530-4580, FAX (419) 530-4033, email apinker@uoft02.utoledo.edu

APPENDIX 1d

**Use of an Open Flow Helium Cryostat for Macromolecular
Cryocrystallography.**

**Hanson, B.L; Martin, A.; Harp, J.M.; Bunick, C.G.; Parrish, D.A.;
Kirschbaum, K.; Bunick, G.J.; and Pinkerton, A.A.; *J. Appl. Cryst.*,
submitted for publication.**

Use of an Open Helium Cryostat in Macromolecular Cryocrystallography

B. Leif Hanson*, Anthony Martin[#], Joel M. Harp*, Chris G. Bunick*, Damon A. Parrish[#], Kristin Kirschbaum[#], Gerard J. Bunick* and A. Alan Pinkerton[#]

* Life Sciences Division, Oak Ridge National Laboratory, Oak Ridge, TN 37831

[#] Department of Chemistry, University of Toledo, Toledo, OH 43606

ABSTRACT

A helium cryostat developed at the University of Toledo was recently described in the Journal of Applied Crystallography. We have tested this helium cooling system on macromolecules, using crystals of chicken egg lysozyme and sperm whale myoglobin. Phase changes in terbium vanadate crystals indicate that temperatures delivered by the cryostat were less than 33 K. This value is supported by the observed unit cell contraction in the protein crystals. Large crystals approaching suitability for neutron diffraction studies were successfully flash cooled and a large crystal of lysozyme was rescued for data collection after undergoing a cycle of macromolecular crystal annealing (MCA) following poor flash-cooling. The results of these studies show that this device could be an especially useful adjunct to neutron diffraction studies and at high intensity synchrotron X-ray sources, and could find uses in the standard macromolecular crystallography laboratory.

INTRODUCTION

Liquid N₂ has provided an acceptable standard for X-ray data collection at cryogenic temperatures for a variety of reasons including cost, ease of use, safety and availability. Most macromolecular crystals capable of being flash-cooled are stable for data collection at a temperature of 90-100 K with conventional X-ray devices as well as with first and second generation synchrotron sources. However, the questions asked of structural biologists have become more complex than can be answered by the shape of the molecule. To answer some of these questions, devices that provide lower temperatures than liquid N₂ are needed. Although these instruments will not supplant N₂ cryostats, their presence in the armamentarium of the crystallographer will increase the scientific questions answerable by crystallography.

The crystal cooling process frequently increases the mosaic spread with a concomitant deleterious effect on the resulting diffraction data. It is thought that the faster the solvent within a crystal reaches a vitrified state the lower the mosaic distortion (Teng and Moffat, 1998). Therefore, the cooling medium which most rapidly lowers the temperature of a crystal should minimize the mosaic spread and provide superior diffraction data. The best material for crystal

cooling purposes is helium. At room temperature, helium gas has 6 fold greater thermal conductivity than N₂ gas, and 10 fold greater than water (Weast, 1983). As it is inert, it has none of the ancillary problems associated with liquid propane use, and is adaptable to the paraphernalia (holders, tongs, etc.) used with N₂ cold streams. The most serious impediment to its use is cost, especially outside of North America. Therefore a helium cryostat capable of delivering reliable low temperatures with a parsimonious expenditure of material is the necessary first step to broadened use of decakelvin delivery devices.

Our interest in helium cooling of macromolecular crystals began with the development at Toledo of an open flow helium cryostat for low temperature studies on inorganic and organic crystals. Details of this cryostat and small molecule experimental studies are found in Hardie *et al.* (1998). The open flow helium cryostat detailed in this paper has several advantages over current commercial He cryostats that make it more adaptable for macromolecular studies. Crystals can be flash-cooled in the He stream of this device. The open flow allows crystals to be optically aligned, and there are no beryllium windows to increase background or absorption. The design of the cryostat also prevents significant icing problems. When used in concert with a CCD diffractometer the consumption rate is low enough to permit collection of a complete dataset of a macromolecular crystal using one 250 L tank. Although other reports exist of macromolecule X-ray diffraction data collected at decakelvin temperatures (Shlichting *et al.*, 1994; Teng *et al.* 1994), to our knowledge no previous helium cold stream experiments have been reported using a sealed tube X-ray source. The use of this cryostat provided us an opportunity to show that a series of experiments could be completed quickly even with a low intensity, local X-ray source, without travel to a synchrotron source.

Four different circumstances suggest a rationale for the use of liquid helium cooling in macromolecular crystallography. Anecdotal reports suggest that the increased flux at third generation synchrotron sources is proving too damaging for crystals cooled by N₂ cryostats. Along with pulsed-beam data collection techniques and the use of small crystals, a helium cryostat should provide heat transfer rates rapid enough to diffuse the heat generated by third generation synchrotron X-ray beams, thus lengthening the lifetime of crystals used in diffraction experiments.

Liquid helium temperature X-ray data collection has already been used to capture photo activated kinetic processes (Shlichting *et al.*, 1994; Teng *et al.* 1994). The photolyzed myoglobin-carbon monoxide structure represents the initial successful efforts in a field that could eventually include elucidation of enzyme and photosynthetic mechanisms, and receptor-ligand interactions. Liquid helium temperatures or lower will be necessary to capture photo activated processes in mid-stride.

In principle, one of the most significant helium temperature applications could occur in macromolecular neutron diffraction studies. These would include experiments using polarized neutrons which would need to be at millikelvin temperatures to facilitate the elimination of incoherent scattering from hydrogen. Because of the lower flux of available neutron beams compared with X-rays, even larger crystals than those used in conventional X-ray experiments will be needed for neutron crystallographic studies. In addition to larger size, diffraction is enhanced from these crystals at liquid He temperatures because of the decreased thermal motion. The practice of bringing such large crystals to such low temperatures will need to be well established to facilitate the routine use of a neutron beam for macromolecular data collection. Helium cryostats may be the only means of successfully cooling the millimeter plus sized crystals needed for neutron diffraction studies.

Finally, NASA has proposed that crystals grown at the space station be harvested on orbit and flash cooled at peak condition prior to return to earth. The experience of our group has demonstrated that larger crystals are more readily produced in space, and we consider this one of the best methods of growing neutron sized crystals in a reasonable time frame (i.e., within the normal 2 -3 year funding cycles of most granting agencies). An effective means of flash-cooling these crystals is needed to preserve the merits of space grown crystals. High thermal transfer rates will be necessary to preserve the integrity of large flash cooled crystals. In addition to high thermal transfer rates, its low weight and inertness make helium the safest mechanism for flash-cooling on manned spaceflight missions.

We approached this study with two immediate objectives. First we wanted to show that macromolecule crystals approaching the size needed for neutron diffraction studies could be successfully flash cooled in the helium stream. Secondly, we wished to establish that the cryostat produced temperatures as low as those seen in the inorganic crystal experiments done previously. In addition to these initial objectives we wished to develop the techniques that would become part of the protocols for helium cryostat work. Finally we wanted to determine the helium consumption and demonstrate the durability of the cryostat by collecting an extended dataset from a representative crystal.

DATA COLLECTION

Crystal growth and flash-cooling

Chicken egg lysozyme (USB Biochemicals) was purified by gel filtration over a 50 cm (150 ml) column of S-100HR resin (Pharmacia). Pooled aliquots corresponding to the monomeric peak were concentrated and prepared for crystallization using 0.9 M NaCl as precipitant, following the protocol for production of P4₃2₁2 crystals at the Biological Macromolecular Crystallization Database (BMCD) website for vapor diffusion experiments

(Gilliland *et al.*, 1994). One plate of lysozyme hanging drop crystallization experiments 3 years old provided the largest crystals, cubes with dimensions ranging from 0.75 to 1.8 mm. Lysozyme crystals were prepared for flash-cooling by dragging through a 30% glycerol solution of the well buffer (50 mM NaOAc, pH 4.5, 0.9M NaCl). After successful flash-cooling was demonstrated under these cryoprotectant conditions, viscous perfluoroether (magic oil) was used as a cryoprotectant for experiments lacking sufficient well material for making a protectant solution. This also proved acceptable.

Sperm whale myoglobin (kindly provided by Allen Edmundson, Oklahoma Medical Research Foundation) was crystallized following the protocols for P2₁ crystal production at the BMCD website. Myoglobin crystals were cryoprotected by dragging through a 30% glycerol solution of 0.1 M Phosphate (pH 6.9), 2.8 M Ammonium Sulfate.

Crystals were harvested from the droplets using the rayon cryoloops of the CrystalCap system (Hampton Research). The most perilous aspect of data collection was the flash-cooling process. Because of the need to maintain low temperature and reduce He consumption, the nozzle of the cryostat was within 5 mm of the crystal, and the width of the He stream was 2 mm. To assure proper placement of the crystal, the empty loop was precentered on the goniometer head. This was a reasonably successful methodology, as only 3 out of 22 different flash-cooling attempts were outside the He stream, becoming so iced as to be unusable. However, we were able to rescue one of the crystals using the MCA techniques described by Harp *et al.* (1998). More traumatic for us was the occasional loss of crystals from the cryoloop because the velocity of the He stream was great enough to dislodge them. We resolved the crystal loss problem by making the loop smaller than the cross section of the crystal with the loop supporting the crystal against the force of the stream. Alternative strategies will be pursued in future experiments.

X-ray data collection and processing

The X-ray system used with the helium cryostat consisted of a sealed copper tube run at 50kV, 40mA, and a SMART 2K CCD from Siemens. All measurements were made with the detector distance at 10 cm. For unit cell determinations (lysozyme and myoglobin), a minimum of 10 frames at 2 or 3 phi settings were collected with a width of 0.3°/frame. These data, collected in Toledo, were processed using the SAINT software package. The temperature within the stream was verified as >33K by observation of the known phase changes in a terbium vanadate crystal diffraction pattern (crystal graciously provided by Lynn Boatner ORNL). This providing an upper limit on the temperature at the crystal position in the He stream.

We noted that the flash cooled myoglobin crystals appeared to diffract to high resolution. A dataset was collected overnight from one crystal, omega scans of 4 different phi orientations

with 2 theta set at 30 and 45 . A total of 700 frames were collected; 100 for 3 minutes, 600 for 60 seconds.

A comparative dataset was collected at Oak Ridge on a myoglobin crystal from the same lot as those used in the He experiments, in a N₂ cryostream using a Rigaku RU200 rotating anode X-ray generator with copper target, double focusing mirrors and an 18 cm Mar image plate area detector. The generator ran at 50 kV, 100 mA. These data are more complete but extend only to 2.02 Å, the limit determined by the detector configuration. Distance to the 18 cm Mar image plate was 9 cm, and the duration was 90 sec/image. Data collected at Oak Ridge were processed using the HKL suite (Otwinowski and Minor, 1995). Tables of the data collection parameters are seen in Table 1. The apparent differences in the quality of data from the two crystals should be considered in light of the higher powered, mirrored rotating anode X-ray source at Oak Ridge which provides a much more intense beam than the sealed tube X-ray generator in Toledo.

For both datasets, after the data were reduced the F² reflection values were converted to F using TRUNCATE of the CCP4 software package (CCP4, 1994). Coordinates from the PDB file 1VXA, collected at 4 °C, (Yang and Philips, 1996) were used as the molecular replacement model (including ordered solvent molecules) using the AMoRe program (Navaza, 1994) to provide an initial fit. Each dataset went through one round (400 cycles) of positional refinement followed by simulated annealing, B-factor refinement and a final round (250 cycles) of positional refinement using XPLOR 3.851 (Brunger, 1992). Maps and molecular models were imaged with O version 5.9 software (Jones *et al.*, 1991).

DISCUSSION

Low temperature determination

Although the low temperature in the helium stream was verified first by low temperature induced twinning in terbium vanadate crystals, subsequently we looked at the unit cell contraction of crystals of sperm whale myoglobin and chicken egg lysozyme. Temperature induced contraction in the unit cell parameters are shown in Table 2. N₂ stream data for myoglobin were derived from data collected at Oak Ridge. Other unit cell parameters were taken from the literature (Yang and Philips, 1996; Young *et al.*, 1994). Teng and Moffat (1998) suggest that a unit cell contraction of 5-7% is to be expected when a crystal cools from ambient to liquid N₂ temperatures, although Frauenfelder *et al.* (1987) noted a 3% decrease in their studies with myoglobin crystals. Our values show a unit cell volume decrease from the ambient value of 4% for myoglobin in the N₂ cryostream, and 5% and 8% in the He coldstream for myoglobin and lysozyme, respectively.

We felt it important to describe the environment within the coldstream accurately. Because of the variation in experimental configurations, descriptions of low temperature

macromolecular data have tended to rely on the measured temperature of the coldstream and not the actual temperature of the crystal. A thermocouple in the head of our open flow system consistently registered 4 to 6 K while in operation. However despite staying in the He stream, moving the nozzle of the cryostat 4 to 8 mm away from crystal can raise the temperature by > 10 K. Hence, we feel the more realistic measure of the crystal temperature is shown by the temperature induced twinning in the terbium vanadate.

Our data for the compaction of the unit cell at low temperature do not suggest that the contraction is linear function of temperature. These results differ from those of Tilton *et al.* (1992) who noted linear expansion in ribonuclease crystals with a greater number of data points. Frauenfelder *et al.* (1987) suggest that differences in the unit cell parameters associated with thermal expansion are the result of relaxation within secondary structural elements of the protein. If so, the variation between the lysozyme and the myoglobin contraction rates is surprising since both proteins are close to the same size and have α -helical secondary structural elements, and have similar crystal solvent contents. The anisotropy of the contraction of lysozyme compared with that of myoglobin suggests thermal contraction of the unit cell is more complex than previously thought the macromolecular community. One complicating factor relates to data processing itself: our general experience has been that the same full dataset from the same crystal will result in differing unit cell parameters when reprocessed with the same or different data analysis and reduction programs. Further, studies with crystals of varying solvent contents may demonstrate whether the secondary protein structure or the solvent environment contributes more to the unit cell contraction.

Flash cooled large crystal

Tetragonal lysozyme crystals with their cubic shape provide a good test of the cooling efficiency of a He stream. These crystals have a lowest surface to volume ratio of any regular crystalline form, approaching 3 for a perfect cube. The efficient dissipation of heat is a necessity for the solvent in the crystal to reach an amorphous state without crystallizing. To show that neutron diffraction sized crystals can be flash cooled in a He stream, a lysozyme crystal measuring 1.8 mm X 1.6 mm X 1.6 mm (surface to volume ratio equal to 3.61) was placed in the helium stream after dragging the crystal through magic oil for cryoprotection. The crystal diffracted to 2.3 Å, the limit of resolution for the detector orientation. Data from this crystal contributed the unit cell parameters seen in Table 2.

Large macromolecular crystals represent a sizable investment in specialized knowledge of growth conditions and in the time required to reach a large size. It would be useful to know that data collection from such a crystal has a reasonable chance of success if the crystal is flash cooled. Intuitively there exists a limit on the maximum size of crystal that can be successfully

flash frozen. How much this limit will fluctuate from macromolecule to macromolecule and whether this variation is primarily the result of the precipitant and solvent content needs to be determined. If cryogenic storage and low temperature data collection of neutron sized crystals are to become a reality, further experimentation with large crystals are necessary. As with the thermal contraction data, these crystals should represent a variety of solvent contents and cryoprotectants.

Macromolecular crystal annealing (MCA)

The rescue of crystals in limited supply that have been improperly flash-cooled is one of the primary benefits of MCA. During these experiments, a large crystal (0.8 mm x 0.6 mm x 0.6 mm) of lysozyme was placed in the helium path for flash-cooling. The crystal was run through a cryoprotectant solution of 30% glycerol in the original precipitant buffer (50 mM NaOAc, pH 4.5, 0.9M NaCl). When the crystal was initially mounted it accidentally contacted the cold stream diverter, resulting in the formation of ice rings seen in figure 1a. After this frame was taken, the crystal was subjected to a cycle of annealing, with the crystal placed in 300 μ l of cryoprotectant solution for \sim 3 minutes, then re-flash cooled, as per Harp *et al.* (1998). Figure 1b shows the resulting X-ray diffraction frame.

Rescue of large crystals is also a matter for concern. The annealed crystal of lysozyme represents to our knowledge the largest crystal successfully annealed. Is the flash-cooling size limit equivalent to the size limit for MCA, or can this process successfully occur only in smaller crystals? This experiment does show that the lower temperature of the He stream does not inhibit annealing and that despite moving from a lower temperature, any transitory ice formation during the reheating of the crystal did not catastrophically disrupt the crystallinity.

Myoglobin data

Our results show that, with a sensitive detector, a dataset on a small unit cell protein can be collected to high resolution in a reasonable time frame. Data were collected for 15 hours, 1/4 of the 60 hour lifetime of a commercially supplied single He dewar. These data are > 50% complete to 1.7 Å for a monoclinic crystal. Utilizing optimized data collection strategies would have appreciably increased our data completeness. Extrapolating from our experience, it appears likely that a complete dataset for nearly any protein could be collected within the lifetime of a 250 L liquid He tank.

Previously flash-cooled crystals can be stored in liquid N₂ prior to use in the He stream. A crystal of myoglobin stored in liquid N₂ was mounted in the He stream and showed reasonable diffraction (i.e. diffracted to the limits of the detector range in 2 phi orientations). If this crystal became permeated with liquid N₂, the solvent did not manifestly solidify within the crystal at He

coldstream temperatures, nor did it disrupt the protein crystal matrix when the temperature dropped. Therefore, as might happen during crystal transport to a data collection facility, storage of crystals initially flash-cooled in He in liquid N₂ for later use in a helium stream appears possible. This would allow transport when storage in liquid helium is either too expensive or infeasible.

The broad based use of He cryostreams, beyond the special circumstances outlined in the introduction, will be dependent on whether He data are of higher quality than standard cryogenic data. The datasets collected from myoglobin crystals differ greatly from one another in the machine parameters (CCD vs image plate). With that potential limitation in mind, the myoglobin data from both the He and the N₂ coldstream have undergone molecular refinement. Since the N₂ data extended only to 2.0 Å, this was chosen as the cutoff point in refinement. After refinement, both datasets had similar R-factors (23.4 for the He, 22.9 for the N₂). No manual fitting was performed. Although better electron density maps were not ubiquitous from the He data, an example of map improvement over the N₂ data is shown in figure 2. Comparisons were made of the 2Fo-Fc electron density maps with a 1.75 σ (F) cutoff. The helium dataset manifested some truncation errors due to incompleteness of the data; however the current experiments appear to justify the expectation that helium cryostream temperatures will improve electron density maps.

ACKNOWLEDGEMENTS

We thank the College of Arts and Sciences of the University of Toledo and the Ohio Board of Regents for generous support of the X-ray diffraction facility and the Office of Naval Research for funding this work (Contract No. N00014-95-1-0013).

REFERENCES

- Brunger, A. T. 1992. *X-PLOR 3.1 Manual*. Yale University Press New Haven and London.
- Collaborative Computational Project, Number 4. 1994. *Acta Cryst.* **D50**: 760-763.
- Frauenfelder, H., H. Hartmann, M. Karplus, I. D. Kuntz Jr., J. Kuriyan, F. Parak, G. A. Petsko, D. Ringe, R. F. Tilton Jr., M. L. Connolly, and N. Max. 1987. *Biochemistry* 26(1): 254-261.
- Gilliland, G. L., M. Tung, D. M. Blakeslee and J. Ladner. 1994. *Acta Cryst.* **D50**:408-413.
- Hardie, M. J., K. Kirschbaum, A. Martin and A. A. Pinkerton. 1998 *J. Appl. Cryst.* 31: 815-817.
- Harp, J. M., D. E. Timm and G. J. Bunick. 1998. *Acta Cryst.* **D54**: 622-628
- Jones, T. A., J-Y. Zou, S. W. Cowan and M. Kjeldgaard. (1991) *Acta Cryst.* **A47**: 110-119.
- Navaza, J. 1994. *Acta Cryst.* **D50**: 157-163.
- Otwinowski, Z. and V. Minor. 1997. *Meth. Enzymol.* 276: 307-326.
- Shlichting, I., Berendzen, J., Phillips, G. N. Jr. and R. M. Sweet. (1994) *Nature* 371: 808-812.
- Teng, T.-Y. and K. Moffat. (1998). *J. Appl. Cryst.* 31:252-257.
- Teng, T.-Y. V. Srajer and K. Moffat. (1994) *Nature struct. Biol.* 1:701-705.
- Weast, R. C., ed. (1983). *CRC Handbook of Chemistry and Physics, 64th edition*. CRC Press, Inc. Boca Raton, Florida
- Tilton, R. F. Jr., J. C. Dewan and G. A. Petsko. (1992). *Biochemistry* 31(9): 2469-2481.
- Yang, F. and G. N. Phillips, Jr. (1996). *J. Mol. Biol.* 256: 762-774.
- Young, A. C. M., R. F. Tilton and J. C. Dewan. 1994. *J. Mol. Biol.* 235:302-317.

PROTEIN	Unit Cell Parameters			β	Unit cell volume (\AA^3)
	a	b	c		
Myoglobin					
< 33 K	63.60	30.60	34.26	105.55	64250
~100 K	63.72	30.68	34.32	106.62	64297
277 K	64.65	30.92	35.53	106.80	67992
Lysozyme					
< 33 K	77.10	77.10	36.95		219646
~100 K	78.42	78.42	36.98		227416
298 K	79.19	79.19	38.02		238426

Table 2. Values of unit cell parameters showing contraction associated with lower temperature. Values of N_2 stream temperatures are based on extrapolated temperature increase from thermocouple at the nozzle of cryostat.

Shell Resolution		% Completeness	R_{shell}	Mean I/σ
Upper Limit	Lower Limit			
10.02 [30.00]	3.00	80.8 [99.1]	0.040 [0.036]	19.3
3.00	2.30	75.7 [97.8]	0.051 [0.063]	8.2
2.30	2.10	68.2 [96.7]	0.080 [0.086]	4.2
2.10	1.90 [2.02]	62.6 [90.5]	0.135 [0.091]	2.9
1.90	1.70	51.6	0.191	1.7
1.70	1.50	7.7	0.246	1.4
1.50	1.394	5.8	0.332	0.9
Total Reflections		38.4 [97.5]	0.056 [0.053]	7.43 [28.9]

Table 1. Data collection statistics for sperm whale myoglobin with He cryostat (sealed tube X-ray source) and [N₂ cryostat] (rotating anode X-ray source). Shells pooled in N₂ to match He data. Bold values indicate highest resolution reflections for individual dataset. Mean I/σ for the data collected in the N₂ coldstream exceeded 20 to the limits of diffraction.

Figure 1. Images of diffraction for a lysozyme crystal. (A) Ice rings in diffraction pattern after contacting the cold stream diverter prior to flash-cooling. (B) Same crystal after macromolecular crystal annealing.

Figure 2. Electron density maps around the side chain of Phe 110 of sperm whale myoglobin. Both maps are 2F₇₀₀-Fc and are scale at 1.75 σ (F). (A) Map based on He cryostream data. (B) Map based on N₂ cryostream data.

Figure 1: Large Lysozyme crystal cooled to 20K

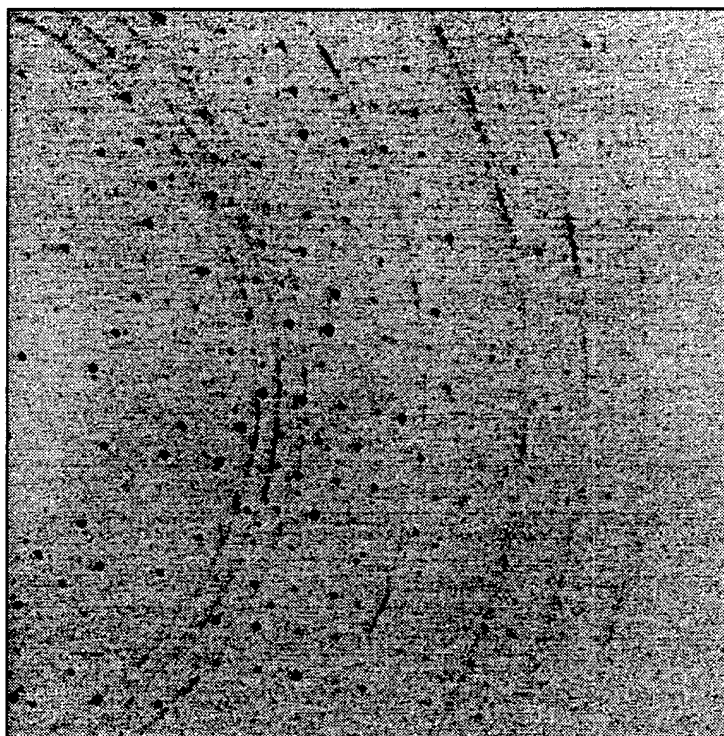


Figure 2a: Lysozyme crystal before annealing

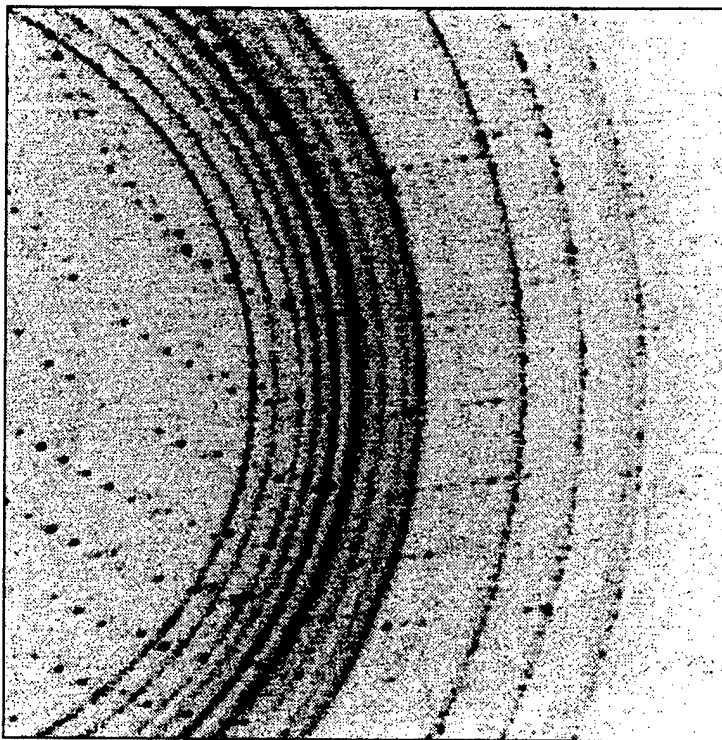
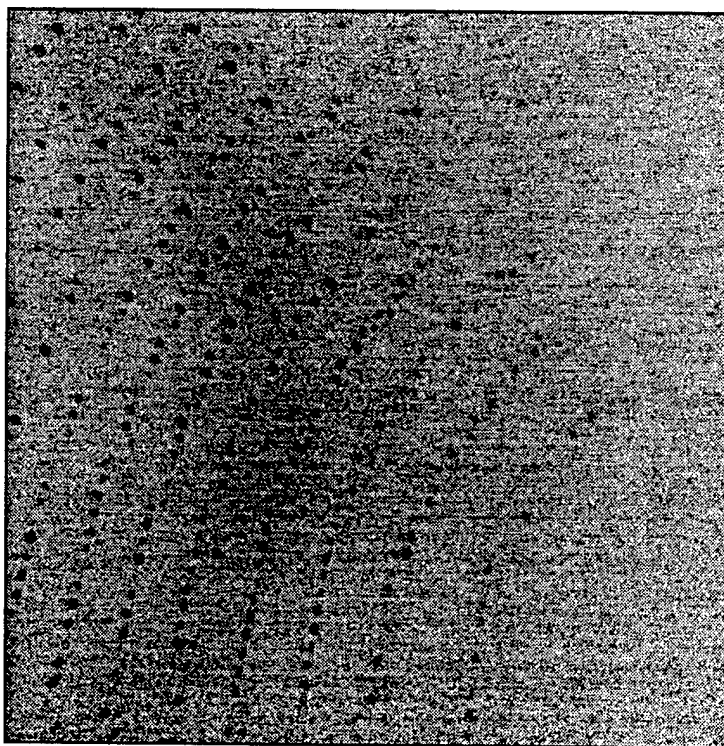


Figure 2b: Lysozyme crystal after annealing



Contract No. N00014-95-1-0013 and N00014-97-1-0409

Program Officer: R. Miller/J. Goldwasser

**Title: Experimental Charge Densities and Electrostatic Potentials in Energetic
Materials and Infrastructure Upgrade for an X-ray Crystallography
Laboratory**

PI: A. Alan Pinkerton

Department of Chemistry, University of Toledo, Toledo, OH 43606

tel. (419) 530-4580, FAX (419) 530-4033, email apinker@uoft02.utoledo.edu

APPENDIX 1e

**Cooperative Jahn-Teller Induced Phase Transition of TbVO_4 : Single Crystal
Structure Analyses of the Tetragonal High Temperature Phase and the Twinned
Orthorhombic Phase Below 33 K.**

**Kirschbaum, K.; Martin, A.; Parrish, D.A.; and Pinkerton, A.A.; *J. Phys. Condens.
Matter*, submitted for publication.**

Cooperative Jahn-Teller induced phase transition of TbVO₄: single crystal structure analyses of the tetragonal high temperature phase and the twinned orthorhombic phase below 33 K

Kristin Kirschbaum, Anthony Martin, Damon A. Parrish, A. Alan Pinkerton

Dedicated to Prof. Dr. Bernt Krebs on the occasion of his 60th birthday

2801 W. Bancroft St.
Department of Chemistry
University of Toledo
Toledo, OH 43606

Single crystal structure analyses of TbVO₄

kkirsch@uoft02.utoledo.edu
amartin@uoft02.utoledo.edu
dparris2@uoft02.utoledo.edu
apinker@uoft02.utoledo.edu

Abstract

The rare earth vanadate, TbVO_4 , undergoes a crystallographic phase transition below 33 K induced by a cooperative Jahn-Teller effect. Twinning of the crystal occurs upon this transition from the tetragonal high temperature phase to the orthorhombic low temperature phase resulting in a domain structure. Single crystal X-ray analyses of the tetragonal and the twinned orthorhombic phase verify a reduction in the site symmetry of the Tb-ion from D_{2d} ($\bar{4}m2$) for the high temperature phase to D_2 (222) for the low temperature phase. Concomitantly, the space group symmetry is lowered from D_{4h}^{19} ($I4_1/amd$) to D_{2h}^{24} (Fddd). The twinned orthorhombic phase is described as domains related to each other by a 180° rotation about the orthorhombic [110] axis.

1. Introduction

The unexpected discovery of a cooperative Jahn-Teller distortion in a series of rare-earth salts has led to extensive investigations of their structural phase transitions at low temperatures (Bleaney 1988). Further interest in this class of compounds lies in their magnetic properties (Bowden 1998).

Lanthanide zircons with the general formula LaXO_4 ($X = \text{V, As, P}$) crystallize at room temperature in the tetragonal space group D_{4h}^{19} ($I4_1/amd$) with two metal ions on D_{2d} sites related by an inversion center. The tetragonal crystal field creates low lying degenerate or almost degenerate electronic states that split or increase their separation upon lowering the symmetry. The phase transition is initiated by coupling of the degenerate or almost degenerate levels of these electronic states with a singly degenerate lattice mode, resulting in lowering of the symmetry at the metal site (Gehring and Gehring 1975).

Jahn-Teller induced phase transitions were observed for TbPO_4 and LaXO_4 ($\text{La} = \text{Tb, Dy, Tm}$; $\text{X} = \text{V, As}$) (DyVO_4 : Cooke et al. 1970; TbAsO_4 : Klein et al. 1971; TmVO_4 : Cooke et al. 1972; TmAsO_4 : Mangum 1971; TbPO_4 : Nägele et al. 1980; DyAsO_4 : Kahle et al. 1971) and initiated a series of extensive investigations on this phenomenon beginning in the early 1970s (e.g. DyVO_4 : Cooke et al. 1971, Sayetat et al. 1971, Elliott et al. 1971, Gehring et al. 1972, Becker and Laugsch 1971; TbAsO_4 : Wüchner and Laugsch 1973, Wüchner et al. 1972, Berkahn et al. 1973; TbVO_4 : Ergun et al. 1976, Harley et al. 1980, Gehring et al. 1976; TmAsO_4 : Becker et al. 1972, Colwell and Mangum 1972; TbPO_4 : Mensinger et al. 1993, Müller et al. 1993, Anderer et al. 1993).

Optical absorption measurements of Gehring et al. (1971) and Raman studies of Elliott et al. (1972) and Harley et al. (1971) determined the phase change for TbVO_4 to be of second order. A domain structure in the low temperature phase was described and the crystal symmetry for the low temperature phase was concluded to be D_{2h}^{24} (Fddd) with a point symmetry for the metal ion of D_2 (Fddd). These results were in contradiction to powder X-ray diffraction measurement on TbVO_4 , which suggested the space group to be D_2^7 (F222) (Sayetat 1972). Extensive research of Sandercock et al. (1972) on Brillouin scattering, ultrasonic and theoretical studies of acoustic anomalies of TbVO_4 later confirmed the original choice of D_{2h}^{24} (Fddd). Specific heat measurements (Wells and Worswick 1972) confirmed the phase transition temperature to be 33.0(1) K, and X-ray studies on single crystals and powder (Will et al. 1972) showed the temperature dependence of the unit cell parameters at low temperatures; however the crystal symmetry could not be unambiguously determined. Recent efforts on the properties of TbVO_4 were directed towards thermal expansion anomalies (Kazei et al. 1998) and compressibility (Chen et al. 1992) along with thermodynamic (Sirota et al. 1990) and magnetic properties (Bleaney et al. 1997).

Despite these efforts, the complete crystal structure of a low temperature phase of these compounds has not been determined until now. However, short reports on X-ray diffraction experiments on single crystals of DyVO_4 by Forsyth and Sampson (1971) and TbVO_4 (Will et al. 1972) provide unit cell information of the low temperature phases.

The present paper describes the solution of the crystal structure of the low temperature phase of TbVO_4 based on X-ray diffraction study on a twinned crystal below 33 K and compares it to the room temperature phase.

2. Experiment

X-ray diffraction measurement of high temperature phase

A clear brownish crystal of approximate dimensions 0.28 x 0.21 x 0.19 mm was glued to the tip of a diamond cleaved 0.1 mm diameter thin wall glass capillary of approximately 4 mm in length using epoxy resin. Preliminary examination and data collection were performed at room temperature on a Siemens SMART Platform diffractometer. The diffractometer was equipped with a 1k CCD detector located 4.96 cm from the crystal and a graphite monochromated Mo – $K\alpha$ radiation source. 0.3° ω -scans were carried out at three different ϕ settings and a detector position of -30° in 2θ , corresponding to a nominal hemisphere of data, with the frame time set at 20 seconds. Coverage of unique data was 96% complete to a resolution of at least 0.75 Å. The final unit cell was obtained from the xyz centroids of 1108 reflections after integration using the SAINT software package (1996). The intensity data were corrected for decay and absorption using SADABS (Sheldrick 1996). The structure was refined using SHELXL-97 (Sheldrick 1997). The final full matrix least squares refinement with anisotropic displacement parameters converged to $R_1 = 2.37\%$ (F , 114 observed unique data) and $wR_2 = 5.64\%$ (F^2 , all data).

X-ray diffraction measurement of low temperature phase

A transparent brownish TbVO_4 crystal of dimensions $0.08 \times 0.10 \times 0.18$ mm was epoxied to a thin wall glass capillary of 2 mm length. The crystal was mounted on the same Siemens SMART Platform diffractometer. In this data collection, the diffractometer was equipped with the *APD Open Flow Helium Cryostat* (Hardie et al. 1998). The crystal temperature was estimated to be 22 K based on the determined unit cell of the low temperature phase.

The CCD detector was set 5.55 cm from the crystal. The data collection nominally covered over a hemisphere of reciprocal space by a combination of 3 runs of exposures, each set having a different ϕ setting for the crystal. Each 10 seconds exposure covered 0.3° in ω . Coverage of the unique data set is over 97 % complete to a resolution of 0.77 \AA .

Out of this data set, a subset of ca. 200 reflections was selected in order to determine the orientation matrices of the two twin components and the lattice parameters. Using the beta-test twin software from R. A. Sparks (TWINDX 1997), two out of several orientation matrices were identified as the reduced settings of the two twin components and transformed into the orthorhombic unit cells. Based on these matrices, integer numbers (hkl) could be assigned to all but 5 reflections. Further improvement of the orientation matrices was achieved by identifying and removing the reflections that originated from both twin components simultaneously (TWUTIL, TWINDX; Sparks 1997). The resulting unit cell dimensions for the two components are in agreement within 0.02 \AA .

Reflection intensities were obtained by integrating the 1371 frames twice (SAINT 1996), once with each of the orthorhombic orientation matrices describing the two orientations of the twin domains. The program TWHKL (Sparks 1997) identified 2683 single, 1720 fully and 928 partially overlapped reflections in the

resulting two files and prepared a twin-resolved intensity data file containing only the fully separated and the fully overlapped reflections. This file was used in the further calculations with SHELXTL (Sheldrick 1990, 1997) together with lattice parameters which were averaged over the two twin components.

The space group - based on systematic absences - was determined to be $Fddd (D_{2h}^{24})$. Placing Tb and V on the appropriate positions as derived from the known tetragonal high temperature phase solved the structure and least-squares refinements followed by difference Fourier syntheses revealed the O-position. All atoms were refined with isotropic atomic displacement factors. In addition, a scale parameter was included in the refinement describing the ratio of the two twin components. Attempts to refine the structure with anisotropic atomic displacement factors were unsuccessful. This is most likely caused by the high absorption of the crystal ($\mu = 24.34 \text{ mm}^{-1}$), which was not corrected for. The structure is refined to $R_1 = 7.82 \%$ (F, 798 observed unmerged data) and $wR_2 = 20.31 \%$ (F^2 , all data) with a 0.54:0.46 ratio of the twin components.

Further details of the crystal structure refinements for both measurements are reported in table 1.

3. Results and Discussion

The single crystal X-ray diffraction study of the tetragonal crystal structure of the high temperature phase of TbVO_4 ($I4_1/amd$, zircon structure) as derived from the room temperature X-ray diffraction measurement shows alternating VO_4 tetrahedra and TbO_8 triangulated dodecahedra connected over common edges and extending along the c-axis. These results are of no surprise and agree with the Rietveld analysis from powder neutron diffraction data (Chakoumakos et al. 1994) and the single crystal X-ray analysis on the isotypes SmVO_4 , EuVO_4 , GdVO_4 , DyVO_4 (Mullica et al. 1996), CeVO_4 (Range et al. 1990) and NdVO_4 (Baglio and

Sovers 1971). Final refined fractional coordinates are given in table 2. Table 3 shows a comparison of selected geometric parameters of the high and the low temperature phases.

The phase transition below 33 K results from coupling of the low-lying electronic states of the Tb-ions with a B_{2g} phonon causing a distortion of the tetragonal ab-plane along the [110] and [1-10] axes. Concomitantly, the I centered tetragonal crystal lattice is converted into an orthorhombic F-centered lattice where the orthorhombic a- and b-axes are the [110] and [1-1 0] diagonals of the tetragonal unit cell, and the tetragonal and orthorhombic c-axes coincide. During this displacive transformation from higher to lower symmetry, two alternative orientations of the orthorhombic setting are produced resulting in a domain structure (Fig. 1a). Concomitant reduction of the angle between two neighboring domains brings the lattice points at the twin interface into register (Fig. 1b). This mechanism is in agreement with the observed smooth change in lattice parameters over the temperature range of 20 – 33 K (Will and Gobel 1972). The relationship between the two twin components may then be described by a 180° rotation about the orthorhombic [110] axis in direct space. The X-ray diffraction pattern of this twinned orthorhombic phase shows imperfect overlap of some reflections, typical for a 'non-merohedral' twin of type TLQS, $n=1$ (Donnay and Donnay 1974).

Assignment of the collected intensities to two independent orientations - as described in the experimental part - and comparison of the two resulting orientation matrices (TWROT, Sparks 1997) indicate that the two twin components are indeed related by a 180° rotation about the orthorhombic [1 1 0] axis in direct space. Thus Fig. 1b shows two domains of the twinned structure with the orthorhombic crystal face (110) as the coherent twin boundary. It should be mentioned here that the domain structure of $TbVO_4$ and other rare earth vanadates/arsenates is often described as a lattice consisting of domains rotated by 90° to each other (e.g. Becker et al. 1972; Harley et al. 1971; Bleaney et al. 1997). In the present case, a 90° rotation about the crystallographic c-axis [001] results in a similar lattice (see Fig. 1a), however, the unit cell faces at the twin

interface would not exactly match. In addition, the rotation required to transform one set of reciprocal lattice points into the other calculates here as 88.8° ($2 \arctan b_o/a_o$) and is only 90.0° for $b = a$.

An interesting experiment using Bragg-regime diffraction of light originated by the twin interface (Reza and Taylor 1991) not only showed the periodic reoccurrence of this interface,* it also determined the size of the domains to be of the order of $4.1 \mu\text{m}$.

In both phases the Tb atom is coordinated by eight O-atoms to form a triangular dodecahedron (Fig. 2). Spectroscopic data have shown that the point symmetry of the Tb site is reduced during the phase transition from $D_{2d} (\bar{4}m2)$ to $D_2 (222)$. This is confirmed by the crystallographic results. Using the nomenclature of Hoard and Silverton (1963) and Drew (1977) the dodecahedron may be described as two intersecting tetrahedra (one flattened, the other one elongated) corresponding to the A and B sites in fig. 2, respectively. Alternatively, the polyhedron may be described as two trapezoids lying in mutual perpendicular mirror planes (sites 7128 and 5346, respectively). The lower symmetry of the orthorhombic phase is characterized by loss of mirror symmetry, which is manifested by a twist, τ , of the trapezoids by 1.6° about the a edge. As seen from table 3, this twist splits both the b and g polyhedral edges into two sets, the b edges differing by 0.100 \AA and the g edges by 0.032 \AA . The larger of these differences (b edge) is reflected in a 3.5° differentiation in the angle subtended at the metal with a concomitant differentiation of 2.4° in the angle (δ) between the faces forming the b edge of the polyhedron. The vanadate group has $\bar{4}m2$ (D_{2d}) symmetry in the high temperature phase and 222 (D_2) symmetry in the low temperature phase. The coordination polyhedron is an elongated tetrahedron with identical metrical parameters in both phases. Hence, the relative decrease in volume on transforming to the low temperature phase is entirely due to shrinking of the terbium coordination polyhedron.

Acknowledgement

We thank Dr Robert A. Sparks for helpful advice on the twinning law and Dr Lynn A. Boatner for donating TbVO₄ crystals. We thank the College of Arts and Sciences of the University of Toledo and the Ohio Board of Regents for generous financial support of the X-ray diffraction facility and thank the Office of Naval Research for funding this work (Contract Nos. N00014-95-1-0013 and N00014-95-1-1252).

* Reza and Taylor refer to the tetragonal {100} domain walls, which coincide with the orthorhombic {110} faces.

Table 1: Summary of Crystallographic Data for TbVO₄

	293 K	22 K
Lattice Type	Tetragonal	Orthorhombic
Space Group	I4 ₁ /amd	Fddd
Radiation	Mo K α	Mo K α
Wavelength (Å)	0.71073	0.71073
a-axis (Å)	7.1841(3)	10.239(2)
b-axis (Å)	7.1841(3)	10.029(2)
c-axis (Å)	6.3310(4)	6.3154(13)
V (Å ³)	326.75(3)	648.6(2)
Z	4	8
D _x	5.567	5.609
μ (mm ⁻¹)	24.15	24.34
F(000)	480	960
θ (range)	4.29-28.06	4.30-28.49
Extinction	0.023(2)	0.0011(4)
R _{int}	0.0467	N/A
R ₁ (F, >2 σ (I))	0.0237	0.0782
R _w (F ² , all)	0.0564	0.2031
Reflections measured	2232	5331 total 928 rejected, overlapped 2683 singles 1720 mults.
Unique Reflections	117	836, sym. equiv. not merged
Reflections > 2 σ (I)	114	798
Parameters	12	9

Table 2: Fractional coordinates of high^a and low^b temperature phase of TbVO₄

T[K]	293				22			
	x	y	z	U _{eq} (Å ²)	x	y	z	U _{iso} (Å ²)
Tb	0.0	0.75	0.125	0.0036(4)	0.125	0.125	-0.375	0.0014(4)
V	0.0	0.25	0.375	0.0039(7)	0.125	0.125	0.125	0.0028(9)
O	0.0	0.4333(5)	0.2016(7)	0.0070(8)	0.2162(5)	0.0319(5)	-0.0494(9)	0.0045(10)

a) Origin at 2/m

b) Origin at $\bar{1}$

Table 3: Selected distances (Å) and angles (°) of high and low temperature phase of TbVO₄

Temp	293 K	22 K
<u>Terbium coordination^a</u>		
Tb-A	2.452(4) (4x)	2.444(6) (4x)
Tb-B	2.326(4) (4x)	2.312(5) (4x)
M _A /M _B	1.054	1.057
a	2.634(7)	2.642(9)
b	3.360(5)	3.289(10)
		3.389(10)
m	2.727(8)	2.703(12)
g	3.068(1)	3.075(2)
		3.043(2)
θ _A	32.50(9)	32.7(1)
θ _B	77.95(11)	78.1(2)
δ	33.5(1) x 4	34.3(2) x 2
		31.9(2) x 2
τ	0	1.6(6)
O-Tb-O		
12,34	64.99(18) (2x)	65.4(2) (2x)
17,28,35,46	69.54(17) (4x)	69.2(2) (4x)
15,16,25,26,37,38,47,48	79.87(9) (8x)	79.49(14) (4x)
		80.50(14) (4x)
57,58,67,68	92.49(4) (4x)	94.2(3) (2x)
		90.7(3) (2x)
18,27,36,45	134.53(11) (4x)	134.62(13) (4x)
13,14,23,24	135.35(11) (4x)	135.1(2) (4x)
56,78	155.9(2) (2x)	156.2(3) (2x)

Vanadium coordination

V-O	1.714(4) (4x)	1.720(5) (4x)
O-V-O	100.4(3) (2x)	100.4(4) (2x)
O-V-O	114.20(15) (4x)	114.2(4) (4x)

a) Nomenclature for edges and angles for a dodecahedron (fig. 2) is taken from Hoard and Silverton (1963) and Drew (1977).

References

- Anderer C, Hess G and Kahle H G 1993 *J Phys.: Condens. Matter* **5** 945
- Baglio J A and Sovers O J 1971 *J. Solid State Chem.* **3** 458
- Becker P-J and Laugsch J 1971 *Phys. State Sol. (b)* **44** K109
- Becker P J, Leask M J M and Tyte R N 1972 *J. Phys. C: Solid State Phys.* **5** 2027
- Berkhahn W, Kahle H G and Schopper H C 1973 *Phys. Stat. Sol. (b)* **55** 265
- Bleaney B 1988 in: Handbook on the Physics and Chemistry of Rare Earths Vol. 11 Gschneidner K A Jr. and Eyring L (Eds.) 322
- Bleaney B, Pfeffer J Z and Wells M R 1997 *J. Phys.: Condens. Matter* **9** 7469
- Bowden G J 1998 *Aust. J. Phys.* **51** 201
- Chakoumakos B C, Abraham M M and Boatner L A 1994 *J. Solid State Chem.* **109** 197
- Chen G, Haire R G and Peterson J R 1992 *Appl. Spectrosc.* **46** 1495
- Colwell J.H. and Mangum B W 1972 *Solid State Commun.* **11** 83
- Cooke A H, Ellis, C J, Gehring K A, Leask M J M, Martin D M, Wanklyn B M, Wells M R and White R L 1970 *Solid State Commun.* **8** 689
- Cooke A H, Martin D M and Wells M R 1971 *Solid State Commun.* **9** 519
- Cooke A H, Swithenby S J and Wells M R 1972 *Solid State Commun.* **10** 265
- Drew M G B 1977 *Coord. Chem. Rev.* **24** 49
- Donnay G and Donnay J D H 1974 *Canadian Mineralogist* **12** 422
- Elliott R J, Harley R T, Hayes W and Smith S R P 1972 *Proc. R. Soc. Lond A.* **328** 217
- Elliott R J, Gehring G A, Malozemoff A P, Smith S R P, Staude W S and Tyte R N 1971 *J. Phys.C: Solid State Physics* **4** L179
- Ergun H B, Gehring K A and Gehring G A 1976 *J. Phys. C: Solid State Phys.* **9** 1101
- Forsyth J B and Sampson C F 1971 *Phys. Let.* **36A** 223
- Gehring K A, Malozemoff A P, Staude W and Tyte R N 1971 *Solid State Commun.* **9** 511

- Gehring G A, Malozemoff A P, Staude W and Tyte R N 1972 *J. Phys. Chem. Solids* **33** 1499
- Ghering G A and Ghering K A 1975 *Rep. Prog. Phys.* **38** 1
- Gehring G A, Kahle H G, Nägele W, Simon A and Wüchner W 1976 *Phys. Stat. Sol.(b)* **74**, 297
- Hardie M J, Kirschbaum K, Martin A and Pinkerton A A 1998 *J. Appl. Cryst.* **31** 815
- Harley R T, Hayes W and Smith S R P 1971 *Solid State Commun.* **9** 515
- Harley R T Lyons K B and Fleury P A 1980 *J. Phys. C: Solid State Phys.* **13** L447
- Hoard J L and Silverton J V 1963 *Inorg. Chem.* **2** 235
- Kazei Z A, Kolmakova N P, Sidorenko A A and Takunov L V 1998 *Physics of the Solid State* **40** 1513
- Kahle H G, Klein L, Müller-Vogt G and Schopper H C 1971 *Phys. Stat. Sol. (b)* **44** 619
- Klein L, Wüchner W, Kahle H G and Schopper H C 1971 *Phys. Stat. Sol. (b)* **48** K139
- Mangum B W, Lee J N and Moos H W 1971 *Phys. Rev. Lett.* **27** 1517
- Mensinger H, Jakelski J, Kahle H G, Kasten A and Paul W 1993 *J Phys: Condens. Matter* **5** 935
- Müller A U, Jakelski J and Kahle H G 1993 *J Phys.: Condens. Matter* **5** 955
- Mullica D F, Sappenfield E L, Abraham M M, Chakoumakos B C and Boatner L A 1996 *Inorg. Chim. Acta* **248** 85
- Nägele W, Hohlwein D and Domann G 1980 *Z. Phys. B* **39** 305
- Range K-J, Meister H and Klement U 1990 *Z. Naturforsch.* **45b** 598
- Reza K A and Taylor D R 1991 *J. Phys: Cond. Matter* **3** 7533
- SAINT 1996 Siemens Analytical Instrumentation
- Sandercock J R, Palmer S B, Elliott R J, Hayes W, Smith S R P and Young A P 1972 *J. Phys. C: Solid State Phys.* **5** 3126
- Sayetat F, Boucherle J X, Belakhovsky M, Kallel A, Tcheou F, Fuess H 1971 *Phys. Lett.* **34A** 361
- Sayetat F 1972 *Solid State Commun.* **10** 879

Sheldrick G M 1996 *SADABS* University of Göttingen

Sheldrick G M 1997 *SHELXL-97* University of Göttingen

Sirota N N, Novikov A V, Novikova V V and Novikov V V 1990 *Zhurnal Fizicheskoi Khimii* **64** 1750

Sparks R A 1997 *TWIN* Programs, TWINDX, TWUTIL, TWHKL, TWROT

Wells M R and Worswick R D 1972 *Phys. Lett.* **42A** 269

Will G, Goebel H, Sampson C F and Forsyth J B 1972 *Phys. Lett.* **38A** 207

Wüchner W, Böhm W, Kahle H G, Kasten A and Laugsch J 1972 *Phys. Stat. Sol. (b)* **54** 273

Wüchner W and Laugsch J 1973 *Int. J. Magnetism* **5** 181

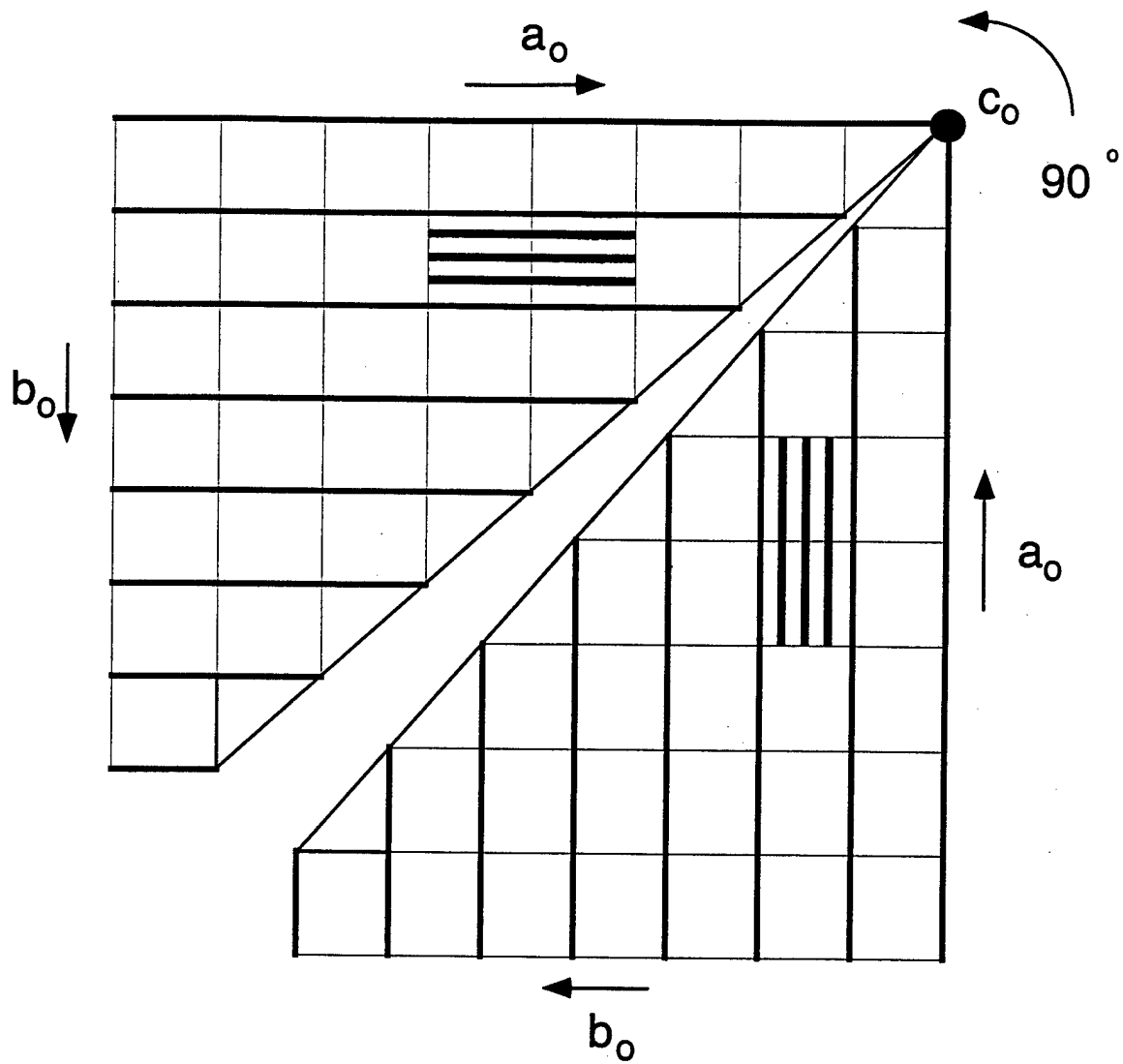
Figure Captions

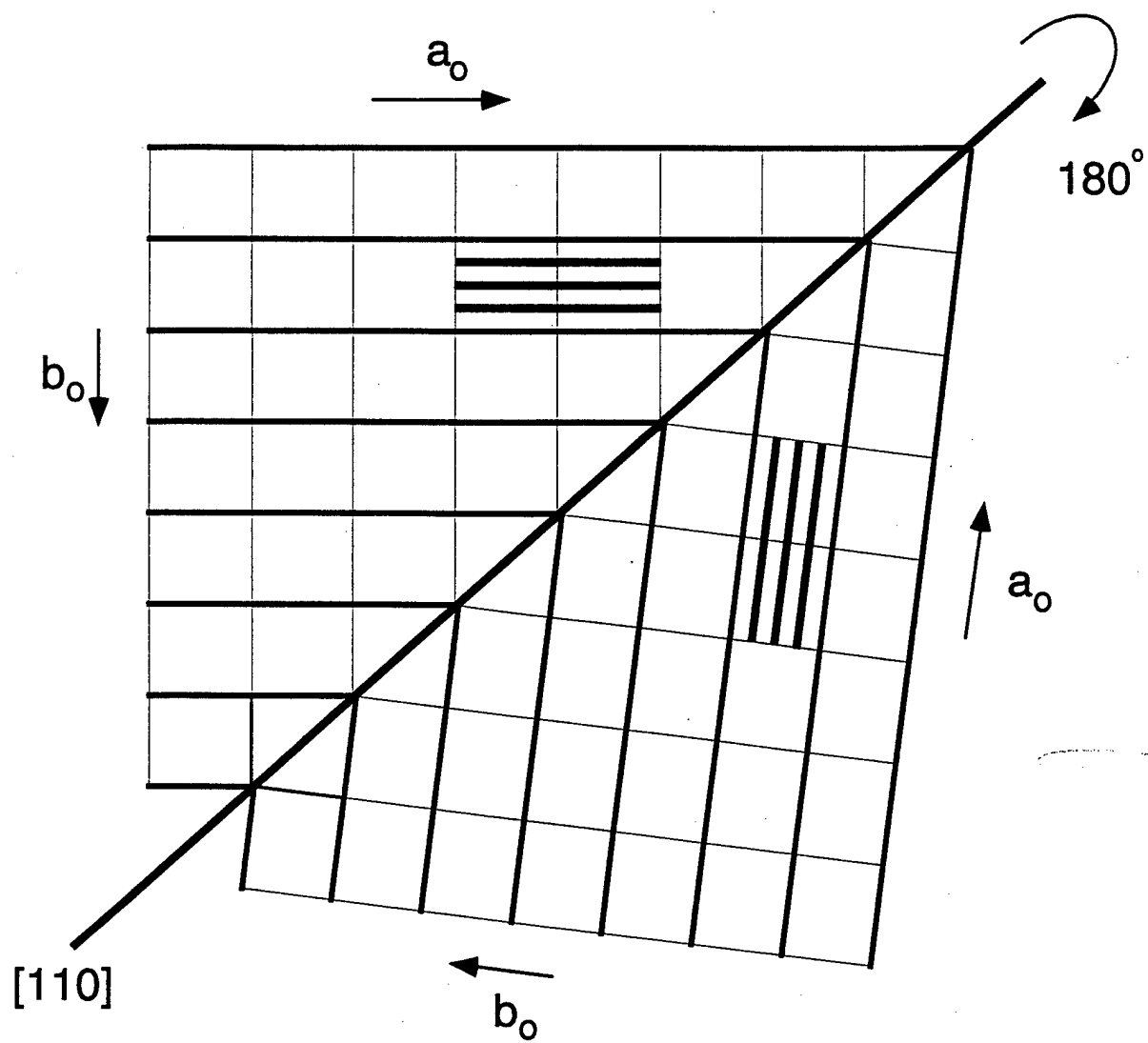
Figure 1

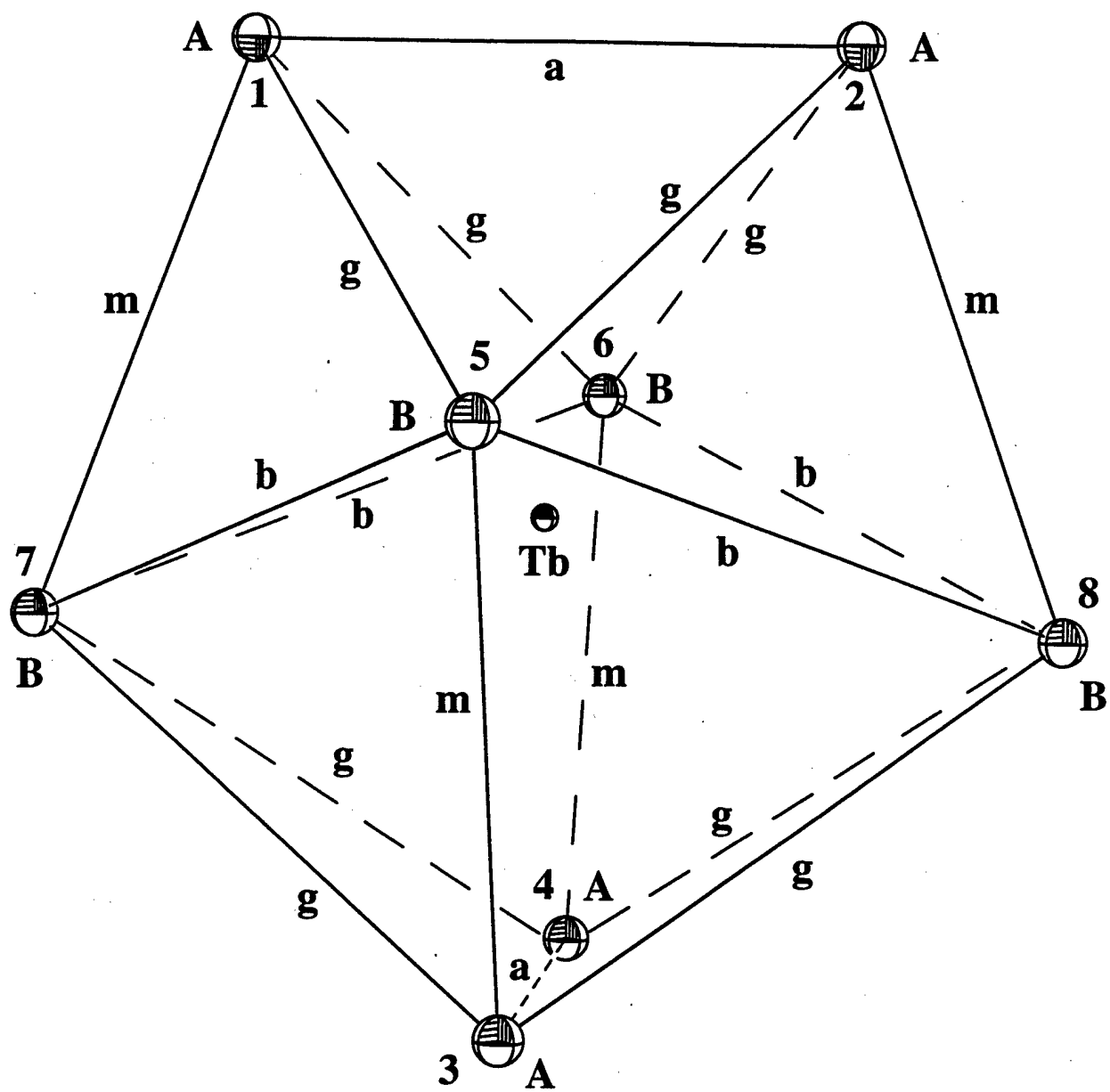
- (a) Schematic of alternative orientations of the orthorhombic unit cells and the result of a twin law of a 90° rotation about $[001]$.
- (b) Schematic of a coherent twin showing the alternative orientations of the orthorhombic unit cells described by a twin law of a 180° rotation about $[110]$.

Figure 2

The dodecahedral coordination of terbium showing the nomenclature due to Hoard, Silverton (1963) and Drew (1977).







Contract No. N00014-95-1-0013 and N00014-97-1-0409

Program Officer: R. Miller/J. Goldwasser

**Title: Experimental Charge Densities and Electrostatic Potentials in Energetic
Materials and Infrastructure Upgrade for an X-ray Crystallography
Laboratory**

PI: A. Alan Pinkerton

Department of Chemistry, University of Toledo, Toledo, OH 43606

tel. (419) 530-4580, FAX (419) 530-4033, email apinker@uoft02.utoledo.edu

APPENDIX 1f

Absolute configuration of all light atom structures from a 2 k CCD detector

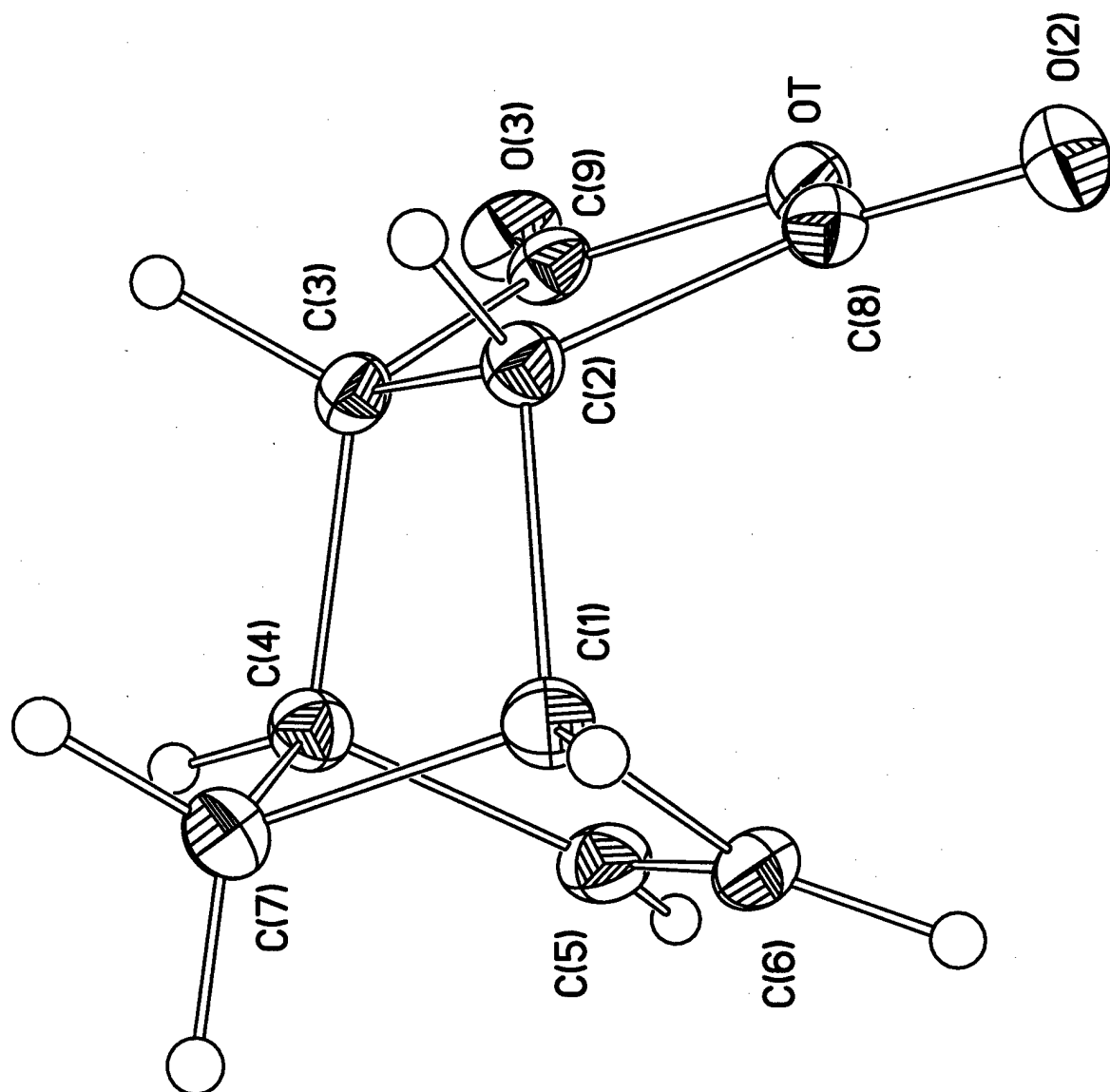


Table 1. Crystal data and structure refinement for Endo(cis-5-norbornene-endo-2,3-dicarboxylic anhydride)

Identification code	endo
Empirical formula	C ₉ H ₈ O ₃
Formula weight	164.15
Temperature	120(1) K
Wavelength	1.54178 Å
Crystal system, space group	Orthorhombic, P2(1)2(1)2(1)
Unit cell dimensions	a = 5.89950(10) Å alpha = 90 deg b = 9.444 Å beta = 90 deg. c = 13.39890(10) Å gamma = 90 deg.
Volume	746.534(14) Å ³
Z, Calculated density	4, 1.461 Mg/m ³
Absorption coefficient	0.925 mm ⁻¹
F(000)	344
Crystal size	0.2 x 0.2 x 0.4 mm
Theta range for data collection	5.73 to 67.07 deg.
Limiting indices	-6<=h<=6, -11<=k<=9, -12<=l<=14
Reflections collected / unique	2609 / 1144 [R(int) = 0.0293]
Completeness to theta = 67.07	89.5 %
Absorption correction Empirical :	Multipole Expansion (Blessing, 1995)
Max. and min. transmission	0.981741 and 0.709383
Refinement method	Full-matrix least-squares on F ²
Data / restraints / parameters	1144 / 0 / 142
Goodness-of-fit on F ²	1.055
Final R indices [I>2sigma(I)]	R1 = 0.0333, wR2 = 0.0892
R indices (all data)	R1 = 0.0341, wR2 = 0.0898
Absolute structure parameter	0.06(24)
Extinction coefficient	0.0112(19)
Largest diff. peak and hole	0.176 and -0.172 e.Å ⁻³

Table 2. Atomic coordinates and equivalent isotropic displacement parameters for Endo(cis-5-norbornene-endo-2,3-dicarboxylic anhydride).

	x	y	z	U(eq)
O1	-0.2299(2)	-0.94597(13)	-0.47512(9)	0.0236(4)
O2	-0.0694(2)	-0.79578(13)	-0.58294(11)	0.0292(4)
O3	-0.4684(3)	-1.08735(13)	-0.39072(10)	0.0289(4)
C1	-0.4321(3)	-0.97606(18)	-0.71491(14)	0.0229(4)
C2	-0.4504(3)	-0.88600(16)	-0.61605(13)	0.0192(4)
C3	-0.5930(3)	-0.98036(17)	-0.54765(13)	0.0198(4)
C4	-0.6496(4)	-1.11216(17)	-0.61503(14)	0.0227(4)
C5	-0.4274(4)	-1.18946(18)	-0.63232(15)	0.0254(5)
C6	-0.2993(4)	-1.10895(18)	-0.69044(15)	0.0258(4)
C7	-0.6753(3)	-1.03513(18)	-0.71624(14)	0.0238(4)
C8	-0.2315(3)	-0.86627(17)	-0.56210(14)	0.0213(4)
C9	-0.4387(3)	-1.01388(17)	-0.46187(13)	0.0212(4)
H1	-0.375(4)	-0.924(2)	-0.7714(16)	0.021(5)
H2	-0.509(4)	-0.794(2)	-0.6267(16)	0.024(5)
H3	-0.734(5)	-0.936(2)	-0.5214(16)	0.029(6)
H4	-0.777(5)	-1.170(2)	-0.5932(16)	0.027(6)
H5	-0.396(4)	-1.274(2)	-0.6021(17)	0.030(6)
H6	-0.140(5)	-1.127(2)	-0.7116(19)	0.040(7)
H7A	-0.704(4)	-1.0987(19)	-0.7728(15)	0.019(5)
H7B	-0.792(4)	-0.960(2)	-0.7168(15)	0.023(5)

Table 3. Bond lengths [Å] and angles [deg] for Endo(cis-5-norbornene-endo-2,3-dicarboxylic anhydride).

O(1)-C(8)	1.387(2)	C(2)-C(3)	1.530(2)
O(1)-C(9)	1.400(2)	C(2)-C(8)	1.491(3)
O(2)-C(8)	1.199(2)	C(3)-C(4)	1.574(2)
O(3)-C(9)	1.192(2)	C(3)-C(9)	1.500(3)
C(1)-C(2)	1.578(2)	C(4)-C(5)	1.518(3)
C(1)-C(6)	1.515(3)	C(4)-C(7)	1.546(3)
C(1)-C(7)	1.539(3)	C(5)-C(6)	1.325(3)
C(8)-O(1)-C(9)	110.42(14)	C(3)-C(4)-C(7)	98.73(13)
C(2)-C(1)-C(6)	107.46(15)	C(5)-C(4)-C(7)	100.19(17)
C(2)-C(1)-C(7)	98.14(15)	C(4)-C(5)-C(6)	107.83(15)
C(6)-C(1)-C(7)	100.62(15)	C(1)-C(6)-C(5)	107.92(18)
C(1)-C(2)-C(3)	103.08(13)	C(1)-C(7)-C(4)	93.96(15)
C(1)-C(2)-C(8)	114.54(16)	O(1)-C(8)-O(2)	119.44(17)
C(3)-C(2)-C(8)	104.98(15)	O(1)-C(8)-C(2)	110.21(15)
C(2)-C(3)-C(4)	103.52(14)	O(2)-C(8)-C(2)	130.35(18)
C(2)-C(3)-C(9)	104.37(15)	O(1)-C(9)-O(3)	119.82(16)
C(4)-C(3)-C(9)	113.68(14)	O(1)-C(9)-C(3)	109.87(14)
C(3)-C(4)-C(5)	106.52(15)	O(3)-C(9)-C(3)	130.29(18)

Table 4. Anisotropic displacement parameters (\AA^2) for Endo(cis-5-norbornene-endo-2,3-dicarboxylic anhydride).

	U11	U22	U33	U23	U13	U12
O1	0.0192(8)	0.0218(6)	0.0299(7)	-0.0031(5)	-0.0056(5)	0.0029(6)
O2	0.0203(8)	0.0248(6)	0.0426(9)	-0.0046(5)	0.0022(6)	-0.0038(6)
O3	0.0345(9)	0.0278(7)	0.0245(7)	0.0027(5)	-0.0025(5)	0.0014(6)
C1	0.0239(12)	0.0238(8)	0.0264(10)	-0.0004(6)	0.0003(7)	-0.0005(7)
C2	0.0173(10)	0.0140(8)	0.0264(10)	-0.0004(6)	0.0002(7)	0.0007(7)
C3	0.0165(11)	0.0189(8)	0.0240(11)	-0.0004(6)	0.0002(7)	0.0007(7)
C4	0.0201(11)	0.0217(9)	0.0262(10)	-0.0004(7)	-0.0028(6)	-0.0063(7)
C5	0.0294(13)	0.0183(8)	0.0286(10)	-0.0050(6)	-0.0085(8)	0.0044(8)
C6	0.0213(12)	0.0273(9)	0.0288(11)	-0.0092(7)	-0.0034(8)	0.0035(8)
C7	0.0225(12)	0.0237(9)	0.0252(10)	-0.0013(7)	-0.0068(7)	0.0023(8)
C8	0.0204(11)	0.0152(7)	0.0283(10)	-0.0047(6)	0.0017(7)	0.0013(8)
C9	0.0200(11)	0.0175(8)	0.0262(11)	-0.0051(6)	-0.0008(7)	0.0013(8)

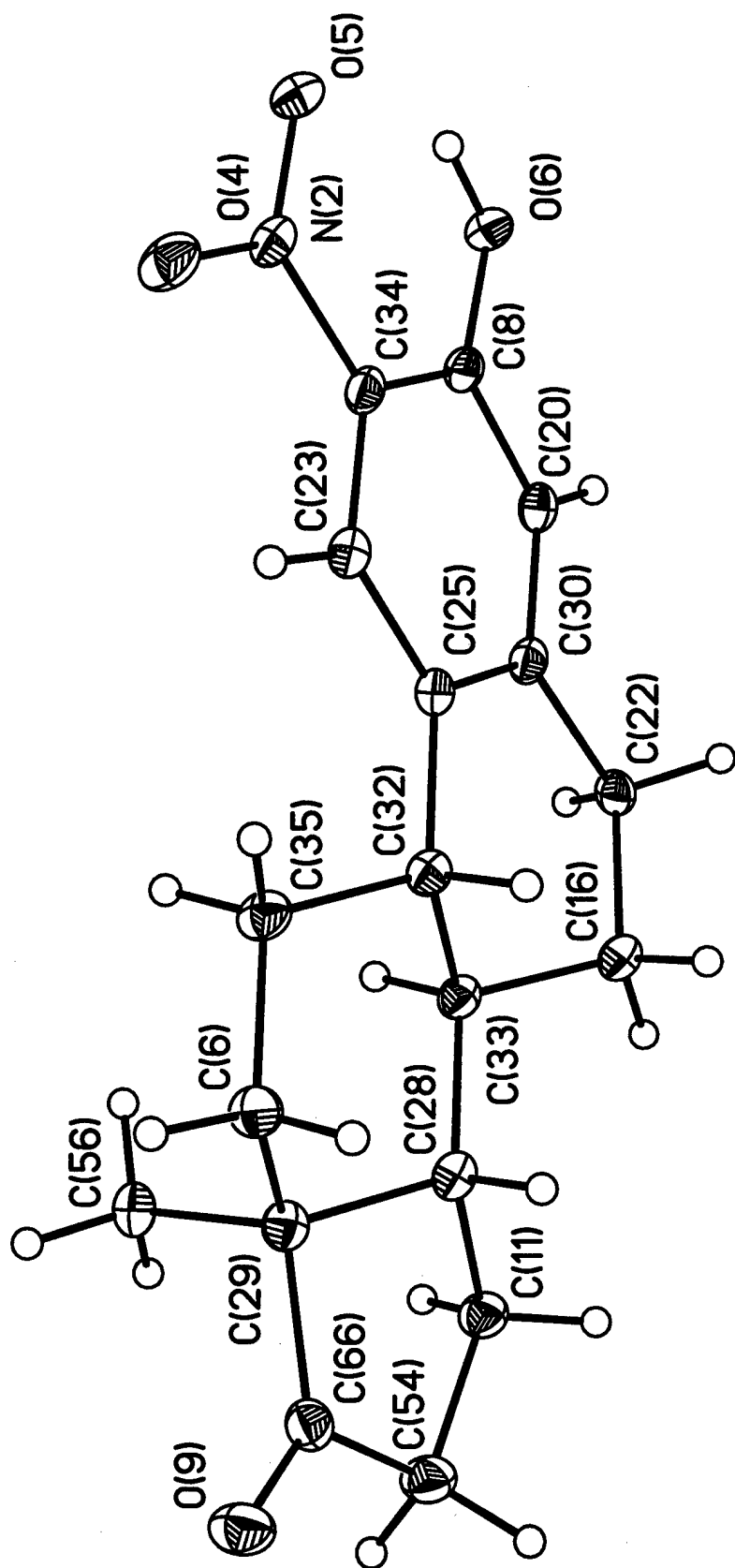


Table 1. Crystal data and structure refinement for nitroestrol

Identification code	nitroestrol
Empirical formula	$C_{18}H_{21}NO_4$
Formula weight	315.36
Temperature	100(1) K
Wavelength	1.54180 Å
Crystal system, space group	Orthorhombic, $P2(1)2(1)2(1)$
Unit cell dimensions	$a = 10.4315(3)$ Å $\alpha = 90$ deg. $b = 11.8495(4)$ Å $\beta = 90$ deg. $c = 25.1265(8)$ Å $\gamma = 90$ deg.
Volume	$3105.84(17)$ Å ³
Z, Calculated density	8, 1.349 Mg/m ³
Absorption coefficient	0.778 mm ⁻¹
F(000)	1344
Crystal size	$0.35 \times 0.25 \times 0.20$ mm
Theta range for data collection	3.52 to 70.11 deg.
Limiting indices	$-11 \leq h \leq 12$, $-14 \leq k \leq 13$, $-25 \leq l \leq 30$
Reflections collected / unique	14604 / 5318 [$R(\text{int}) = 0.0426$]
Completeness to $\theta = 70.11$	94.8 %
Absorption correction	SADABS
Refinement method	Full-matrix least-squares on F^2
Data / restraints / parameters	5318 / 0 / 542
Goodness-of-fit on F^2	0.985
Final R indices [$I > 2\sigma(I)$]	$R1 = 0.0415$, $wR2 = 0.1061$
R indices (all data)	$R1 = 0.0451$, $wR2 = 0.1080$
Absolute structure parameter	$0.07(17)$
Extinction coefficient	$0.00007(9)$
Largest diff. peak and hole	0.248 and -0.241 e.Å ⁻³

Table 2. Atomic coordinates and equivalent isotropic displacement parameters for nitroestrol. U(eq) is defined as one third of the trace of the orthogonalized Uij tensor.

	x	y	z	U(eq)
O(5)	-0.0174(2)	-0.7604(1)	-0.0062(1)	0.028(1)
C(35)	0.4600(2)	-0.4912(2)	-0.1026(1)	0.027(1)
C(34)	0.0891(2)	-0.6177(2)	-0.0515(1)	0.022(1)
C(33)	0.3349(2)	-0.3374(2)	-0.1531(1)	0.022(1)
C(32)	0.3439(2)	-0.4112(2)	-0.1024(1)	0.022(1)
O(6)	-0.1448(2)	-0.6040(1)	-0.0565(1)	0.025(1)
C(30)	0.0995(2)	-0.4188(2)	-0.1093(1)	0.022(1)
C(29)	0.5750(2)	-0.3646(2)	-0.1671(1)	0.024(1)
C(28)	0.4632(2)	-0.2811(2)	-0.1622(1)	0.023(1)
N(2)	0.0880(2)	-0.7210(1)	-0.0206(1)	0.024(1)
C(26)	0.5278(2)	0.0806(2)	-0.0968(1)	0.022(1)
C(25)	0.2159(2)	-0.4688(2)	-0.0919(1)	0.021(1)
C(24)	0.6643(2)	0.2354(2)	-0.1377(1)	0.023(1)
C(23)	0.2077(2)	-0.5694(2)	-0.0637(1)	0.022(1)
C(22)	0.0970(2)	-0.3095(2)	-0.1409(1)	0.023(1)
O(4)	0.1895(2)	-0.7661(1)	-0.0094(1)	0.034(1)
C(20)	-0.0167(2)	-0.4683(2)	-0.0975(1)	0.022(1)
C(19)	0.8981(2)	0.1914(2)	-0.1562(1)	0.022(1)
C(18)	0.6414(2)	0.227(2)	-0.0814(1)	0.022(1)
O(3)	0.2733(2)	-0.0751(1)	-0.0324(1)	0.027(1)
C(16)	0.2273(2)	-0.2518(2)	-0.1461(1)	0.023(1)
C(15)	1.0110(2)	0.273(2)	-0.1147(1)	0.024(1)
C(13)	0.3940(2)	-0.0496(2)	-0.0472(1)	0.022(1)
C(12)	0.4089(3)	0.0449(2)	-0.0795(1)	0.024(1)
C(11)	0.4802(2)	-0.2001(2)	-0.2095(1)	0.027(1)
C(10)	0.6268(2)	-0.0735(2)	-0.0503(1)	0.020(1)
C(9)	0.7730(2)	0.0679(2)	-0.0961(1)	0.022(1)
C(8)	-0.0265(2)	-0.5669(2)	-0.0677(1)	0.021(1)
C(7)	0.7652(2)	0.1441(2)	-0.1462(1)	0.023(1)
C(6)	0.5872(2)	-0.4313(2)	-0.1152(1)	0.026(1)
C(2)	0.8786(2)	-0.219(2)	-0.1002(1)	0.026(1)
C(1)	0.5318(2)	0.1839(2)	-0.1323(1)	0.025(1)
N(1)	0.4977(2)	-0.2081(1)	0.0000(1)	0.024(1)
O(2)	0.5945(2)	-0.2602(1)	0.0109(1)	0.032(1)
O(1)	0.3899(2)	-0.2378(1)	0.0170(1)	0.029(1)
C(52)	1.0003(2)	0.0998(2)	-0.1651(1)	0.025(1)
C(51)	0.5053(2)	-0.1084(2)	-0.0332(1)	0.022(1)
C(58)	0.9750(3)	0.0249(2)	-0.2145(1)	0.031(1)
C(57)	0.9210(2)	0.2769(2)	-0.2014(1)	0.026(1)
C(56)	0.5646(3)	-0.4456(2)	-0.2153(1)	0.030(1)
C(55)	1.0677(3)	0.2812(2)	-0.2052(1)	0.031(1)
C(54)	0.6270(3)	-0.1849(2)	-0.2116(1)	0.032(1)
O(9)	0.7968(2)	-0.2982(1)	-0.1719(1)	0.034(1)
O(10)	1.2277(2)	0.1468(2)	-0.1748(1)	0.038(1)
C(66)	0.6842(2)	-0.2855(2)	-0.1818(1)	0.026(1)
C(63)	1.1151(3)	0.1711(2)	-0.1803(1)	0.028(1)

Table 3. Bond lengths [Å] and angles [deg] for nitroestrol.

O(5)-N(2)	1.248(3)	C(22)-C(16)	1.527(3)
C(35)-C(6)	1.537(3)	C(20)-C(8)	1.392(3)
C(35)-C(32)	1.538(3)	C(19)-C(7)	1.516(3)
C(34)-C(23)	1.397(3)	C(19)-C(52)	1.538(3)
C(34)-C(8)	1.408(3)	C(19)-C(57)	1.540(3)
C(34)-N(2)	1.449(2)	C(18)-C(10)	1.391(3)
C(33)-C(28)	1.512(3)	C(18)-C(9)	1.519(3)
C(33)-C(16)	1.523(3)	O(3)-C(13)	1.346(3)
C(33)-C(32)	1.549(3)	C(15)-C(52)	1.534(3)
C(32)-C(25)	1.523(3)	C(15)-C(2)	1.543(3)
O(6)-C(8)	1.341(3)	C(13)-C(12)	1.392(3)
C(30)-C(20)	1.379(3)	C(13)-C(51)	1.399(3)
C(30)-C(25)	1.420(3)	C(11)-C(54)	1.543(4)
C(30)-C(22)	1.518(3)	C(10)-C(51)	1.401(3)
C(29)-C(66)	1.520(3)	C(9)-C(2)	1.535(3)
C(29)-C(6)	1.532(3)	C(9)-C(7)	1.552(3)
C(29)-C(28)	1.535(3)	N(1)-O(2)	1.214(2)
C(29)-C(56)	1.548(3)	N(1)-O(1)	1.254(2)
C(28)-C(11)	1.537(3)	N(1)-C(51)	1.448(3)
N(2)-O(4)	1.219(3)	C(52)-C(63)	1.514(3)
C(26)-C(12)	1.380(3)	C(52)-C(58)	1.548(3)
C(26)-C(18)	1.422(3)	C(57)-C(55)	1.535(4)
C(26)-C(1)	1.517(3)	C(55)-C(63)	1.529(3)
C(25)-C(23)	1.389(3)	C(54)-C(66)	1.529(3)
C(24)-C(1)	1.516(3)	O(9)-C(66)	1.210(3)
C(24)-C(7)	1.525(3)	O(10)-C(63)	1.218(3)

C(6)-C(35)-C(32)	113.36(17)	C(33)-C(16)-C(22)	111.61(17)
C(23)-C(34)-C(8)	121.30(18)	C(52)-C(15)-C(2)	109.97(19)
C(23)-C(34)-N(2)	118.1(2)	O(3)-C(13)-C(12)	116.4(2)
C(8)-C(34)-N(2)	120.6(2)	O(3)-C(13)-C(51)	126.50(18)
C(28)-C(33)-C(16)	112.11(16)	C(12)-C(13)-C(51)	117.1(2)
C(28)-C(33)-C(32)	108.65(18)	C(26)-C(12)-C(13)	122.0(2)
C(16)-C(33)-C(32)	108.99(18)	C(28)-C(11)-C(54)	102.35(19)
C(25)-C(32)-C(35)	114.54(17)	C(18)-C(10)-C(51)	120.8(2)
C(25)-C(32)-C(33)	110.05(18)	C(18)-C(9)-C(2)	114.88(17)
C(35)-C(32)-C(33)	113.15(18)	C(18)-C(9)-C(7)	110.78(19)
C(20)-C(30)-C(25)	120.50(18)	C(2)-C(9)-C(7)	112.69(18)
C(20)-C(30)-C(22)	117.4(2)	O(6)-C(8)-C(20)	117.1(2)
C(25)-C(30)-C(22)	122.1(2)	O(6)-C(8)-C(34)	126.01(18)
C(66)-C(29)-C(6)	117.5(2)	C(20)-C(8)-C(34)	116.9(2)
C(66)-C(29)-C(28)	101.02(16)	C(19)-C(7)-C(24)	113.10(16)
C(6)-C(29)-C(28)	109.09(18)	C(19)-C(7)-C(9)	107.62(18)
C(66)-C(29)-C(56)	104.25(18)	C(24)-C(7)-C(9)	109.55(18)
C(6)-C(29)-C(56)	110.61(18)	C(29)-C(6)-C(35)	110.0(2)
C(28)-C(29)-C(56)	114.15(19)	C(9)-C(2)-C(15)	113.36(17)
C(33)-C(28)-C(29)	113.60(16)	C(24)-C(1)-C(26)	113.71(19)
C(33)-C(28)-C(11)	119.62(19)	O(2)-N(1)-O(1)	121.77(16)
C(29)-C(28)-C(11)	104.64(18)	O(2)-N(1)-C(51)	119.99(19)
O(4)-N(2)-O(5)	122.27(17)	O(1)-N(1)-C(51)	118.24(18)
O(4)-N(2)-C(34)	119.13(19)	C(63)-C(52)-C(15)	117.5(2)
O(5)-N(2)-C(34)	118.60(19)	C(63)-C(52)-C(19)	101.01(17)
C(12)-C(26)-C(18)	121.06(18)	C(15)-C(52)-C(19)	109.02(18)
C(12)-C(26)-C(1)	117.2(2)	C(63)-C(52)-C(58)	104.62(19)
C(18)-C(26)-C(1)	121.7(2)	C(15)-C(52)-C(58)	110.69(17)
C(23)-C(25)-C(30)	117.5(2)	C(19)-C(52)-C(58)	113.8(2)
C(23)-C(25)-C(32)	121.8(2)	C(13)-C(51)-C(10)	121.82(18)
C(30)-C(25)-C(32)	120.60(18)	C(13)-C(51)-N(1)	120.4(2)
C(1)-C(24)-C(7)	110.90(17)	C(10)-C(51)-N(1)	117.8(2)
C(25)-C(23)-C(34)	121.2(2)	C(55)-C(57)-C(19)	102.87(19)
C(30)-C(22)-C(16)	114.28(18)	C(63)-C(55)-C(57)	105.57(19)
C(30)-C(20)-C(8)	122.5(2)	C(66)-C(54)-C(11)	106.26(19)
C(7)-C(19)-C(52)	113.38(17)	O(9)-C(66)-C(29)	126.9(2)
C(7)-C(19)-C(57)	120.52(19)	O(9)-C(66)-C(54)	125.2(2)
C(52)-C(19)-C(57)	104.45(18)	C(29)-C(66)-C(54)	107.9(2)
C(10)-C(18)-C(26)	117.2(2)	O(10)-C(63)-C(52)	127.1(2)
C(10)-C(18)-C(9)	121.6(2)	O(10)-C(63)-C(55)	124.0(2)
C(26)-C(18)-C(9)	121.15(18)	C(52)-C(63)-C(55)	108.9(2)

Table 4. Anisotropic displacement parameters ($\text{\AA}^2 \times 10^3$) for nitroestrol. The anisotropic displacement factor exponent takes the form: $-2\pi^2 [h^2 a^{*2} U_{11} + \dots + 2hka^*b^*U_{12}]$

	U11	U22	U33	U23	U13	U12
O(5)	0.030(1)	0.021(1)	0.032(1)	0.003(1)	0.001(1)	-0.006(1)
C(35)	0.025(1)	0.023(1)	0.032(1)	0.008(1)	-0.003(1)	0.001(1)
C(34)	0.029(1)	0.016(1)	0.021(1)	-0.002(1)	0.000(1)	0.000(1)
C(33)	0.026(1)	0.018(1)	0.022(1)	0.001(1)	-0.001(1)	0.000(1)
C(32)	0.024(1)	0.020(1)	0.022(1)	0.000(1)	-0.001(1)	-0.001(1)
O(6)	0.026(1)	0.021(1)	0.029(1)	0.002(1)	0.000(1)	-0.004(1)
C(30)	0.028(1)	0.017(1)	0.021(1)	-0.002(1)	0.000(1)	0.001(1)
C(29)	0.025(1)	0.022(1)	0.025(1)	0.000(1)	0.000(1)	0.001(1)
C(28)	0.026(1)	0.020(1)	0.023(1)	0.000(1)	-0.003(1)	0.000(1)
N(2)	0.030(1)	0.017(1)	0.024(1)	-0.001(1)	-0.004(1)	-0.002(1)
C(26)	0.027(1)	0.017(1)	0.023(1)	0.000(1)	-0.004(1)	-0.001(1)
C(25)	0.022(1)	0.018(1)	0.021(1)	-0.003(1)	0.001(1)	0.002(1)
C(24)	0.026(1)	0.018(1)	0.024(1)	0.004(1)	-0.001(1)	-0.001(1)
C(23)	0.025(1)	0.019(1)	0.022(1)	-0.001(1)	-0.001(1)	0.002(1)
C(22)	0.021(1)	0.022(1)	0.026(1)	0.002(1)	0.001(1)	0.006(1)
O(4)	0.032(1)	0.026(1)	0.044(1)	0.012(1)	-0.006(1)	0.002(1)
C(20)	0.022(1)	0.020(1)	0.023(1)	-0.002(1)	-0.004(1)	0.004(1)
C(19)	0.028(1)	0.018(1)	0.021(1)	0.000(1)	-0.002(1)	0.001(1)
C(18)	0.027(1)	0.019(1)	0.020(1)	-0.002(1)	0.001(1)	-0.003(1)
O(3)	0.025(1)	0.024(1)	0.033(1)	0.004(1)	0.000(1)	-0.004(1)
C(16)	0.027(1)	0.019(1)	0.024(1)	0.001(1)	-0.003(1)	0.000(1)
C(15)	0.024(1)	0.020(1)	0.029(1)	0.003(1)	0.000(1)	0.003(1)
C(13)	0.027(1)	0.019(1)	0.022(1)	-0.002(1)	-0.001(1)	-0.004(1)
C(12)	0.025(1)	0.020(1)	0.028(1)	0.000(1)	-0.007(1)	0.003(1)
C(11)	0.027(1)	0.023(1)	0.031(1)	0.006(1)	0.001(1)	0.000(1)
C(10)	0.023(1)	0.017(1)	0.021(1)	-0.002(1)	-0.004(1)	0.001(1)
C(9)	0.025(1)	0.019(1)	0.022(1)	0.000(1)	-0.001(1)	-0.001(1)
C(8)	0.024(1)	0.017(1)	0.022(1)	-0.004(1)	-0.001(1)	-0.003(1)
C(7)	0.029(1)	0.017(1)	0.022(1)	0.001(1)	-0.001(1)	-0.002(1)
C(6)	0.021(1)	0.025(1)	0.032(1)	0.006(1)	-0.002(1)	0.003(1)
C(2)	0.026(1)	0.020(1)	0.031(1)	0.005(1)	0.001(1)	-0.001(1)
C(1)	0.024(1)	0.021(1)	0.030(1)	0.006(1)	-0.002(1)	0.004(1)
N(1)	0.030(1)	0.015(1)	0.025(1)	-0.001(1)	0.000(1)	-0.003(1)
O(2)	0.033(1)	0.022(1)	0.040(1)	0.001(1)	0.005(1)	0.008(1)
O(1)	0.029(1)	0.024(1)	0.034(1)	0.006(1)	0.002(1)	-0.006(1)
C(52)	0.030(1)	0.021(1)	0.023(1)	0.000(1)	-0.001(1)	0.002(1)
C(51)	0.032(1)	0.015(1)	0.021(1)	-0.001(1)	-0.001(1)	-0.001(1)
C(58)	0.037(1)	0.027(1)	0.028(1)	-0.005(1)	0.004(1)	0.009(1)
C(57)	0.030(1)	0.021(1)	0.028(1)	0.005(1)	0.001(1)	0.001(1)
C(56)	0.033(1)	0.024(1)	0.033(1)	-0.006(1)	0.004(1)	0.002(1)
C(55)	0.034(1)	0.027(1)	0.034(1)	0.004(1)	0.006(1)	0.000(1)
C(54)	0.029(1)	0.027(1)	0.039(1)	0.008(1)	0.004(1)	-0.001(1)
O(9)	0.023(1)	0.036(1)	0.045(1)	0.011(1)	0.000(1)	-0.002(1)
O(10)	0.026(1)	0.045(1)	0.043(1)	0.017(1)	0.003(1)	0.002(1)
C(66)	0.029(1)	0.025(1)	0.025(1)	0.000(1)	0.004(1)	0.002(1)
C(63)	0.033(1)	0.029(1)	0.024(1)	0.001(1)	0.004(1)	0.003(1)

Table 5. Hydrogen coordinates and isotropic displacement parameters for nitroestrol.

	x	y	z	U(eq)
H(35A)	0.470(3)	-0.527(2)	-0.0675(11)	0.032
H(35B)	0.445(3)	-0.551(2)	-0.1281(10)	0.032
H(33A)	0.309(3)	-0.387(2)	-0.1840(10)	0.026
H(32A)	0.359(2)	-0.360(2)	-0.0733(10)	0.026
H(6A)	-0.143(3)	-0.660(2)	-0.0361(11)	0.030
H(28A)	0.482(3)	-0.238(2)	-0.1305(10)	0.027
H(24A)	0.688(3)	0.278(2)	-0.1059(10)	0.027
H(24B)	0.662(3)	0.288(2)	-0.1680(10)	0.027
H(23A)	0.279(3)	-0.610(2)	-0.0537(10)	0.026
H(22A)	0.038(3)	-0.259(2)	-0.1244(10)	0.027
H(22B)	0.064(3)	-0.326(2)	-0.1755(11)	0.027
H(20A)	-0.091(3)	-0.438(2)	-0.1078(10)	0.026
H(19A)	0.930(2)	0.231(2)	-0.1232(10)	0.027
H(3A)	0.270(3)	-0.132(3)	-0.0178(12)	0.041
H(16A)	0.223(2)	-0.198(2)	-0.1762(10)	0.028
H(16B)	0.240(2)	-0.209(2)	-0.1158(11)	0.028
H(15A)	1.044(3)	0.074(2)	-0.0861(11)	0.029
H(15B)	1.069(3)	-0.034(2)	-0.1194(10)	0.029
H(12A)	0.335(3)	0.082(2)	-0.0887(10)	0.029
H(11A)	0.449(3)	-0.229(2)	-0.2425(11)	0.032
H(11B)	0.438(3)	-0.129(2)	-0.2033(10)	0.032
H(10A)	0.693(3)	-0.118(2)	-0.0410(10)	0.024
H(9A)	0.803(2)	0.121(2)	-0.0684(10)	0.026
H(7A)	0.739(2)	0.097(2)	-0.1768(10)	0.027
H(6B)	0.608(3)	-0.379(2)	-0.0857(10)	0.031
H(6C)	0.652(3)	-0.482(2)	-0.1140(11)	0.031
H(2A)	0.846(3)	-0.081(2)	-0.1253(10)	0.031
H(2B)	0.889(3)	-0.063(2)	-0.0665(11)	0.031
H(1A)	0.501(3)	0.156(2)	-0.1671(11)	0.030
H(1B)	0.474(3)	0.236(2)	-0.1203(10)	0.030
H(58A)	0.962(3)	0.071(3)	-0.2464(13)	0.046
H(58B)	0.900(3)	-0.019(3)	-0.2091(12)	0.046
H(58C)	1.037(3)	-0.024(3)	-0.2175(12)	0.046
H(57A)	0.885(3)	0.249(2)	-0.2346(10)	0.032
H(57B)	0.885(3)	0.349(2)	-0.1928(10)	0.032
H(56A)	0.637(3)	-0.496(3)	-0.2170(12)	0.045
H(56B)	0.558(3)	-0.408(3)	-0.2485(13)	0.045
H(56C)	0.494(3)	-0.489(3)	-0.2128(12)	0.045
H(55A)	1.101(3)	0.290(2)	-0.2416(11)	0.038
H(55B)	1.105(3)	0.342(2)	-0.1835(11)	0.038
H(54A)	0.659(3)	-0.182(2)	-0.2474(12)	0.038
H(54B)	0.648(3)	-0.114(2)	-0.1938(11)	0.038

Contract No. N00014-95-1-0013 and N00014-97-1-0409

Program Officer: R. Miller/J. Goldwasser

**Title: Experimental Charge Densities and Electrostatic Potentials in Energetic
Materials and Infrastructure Upgrade for an X-ray Crystallography
Laboratory**

PI: A. Alan Pinkerton

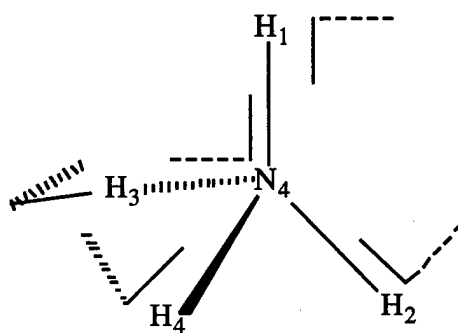
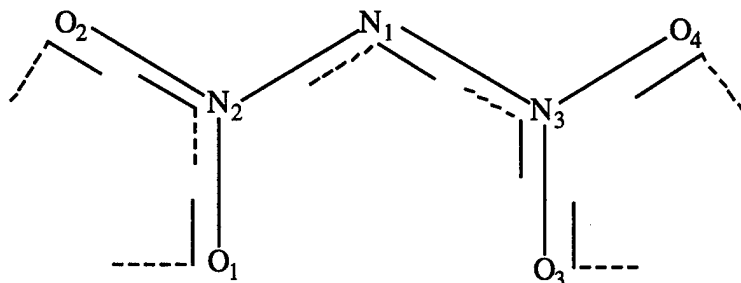
Department of Chemistry, University of Toledo, Toledo, OH 43606

tel. (419) 530-4580, FAX (419) 530-4033, email apinker@uoft02.utoledo.edu

APPENDIX 2a

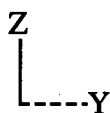
Electron density and electrostatic potential for ADN

Local coordinate system for ADN



The hydrogen coordinates are centered on the nuclei, but they are displaced in the diagram for clarity.

The coordinate scheme for H₃ and H₄ would look identical, if they were in the plane of the paper.



The lines indicate the positive direction of the axis vectors.

The X axis is perpendicular to the Z and Y axis in the usual way

Summary of crystallographic details of ADN from multipole refinement

Empirical formula	N ₄ O ₄ H ₄	Density (calc) (Mg/m ³)	1.81 (293K)
Formula weight	124.06	Absorption coeff. (mm ⁻¹)	0.1798
Wavelength (Å)	0.71073	θ max (°)	73
Crystal system	Monoclinic	Reflections collected	21641
Space group	P2 ₁ /c (# 14)	Independent reflections	5547
Crystal size	0.27 x 0.21 x 0.09 mm	R _{int}	0.0224
Z	4	Data/parameters	5547/231
F(000)	384	Goodness-of-fit on F ²	0.84
Temperature (K)	90±1K	R(F)	0.0297
a (Å)	6.933(1)	Rw(F)	0.0244
b (Å)	11.603(1)	R(F ²)	0.0269
c (Å)	5.567(1)	Rw(F ²)	0.0446
β (°)	100.58(1)		
Volume (Å ³)	440.2		

Fractional coordinates of ADN based on $|F_o^2|$ refinement

ATOM	X	Y	Z
O1	1.29802(5)	0.12783(4)	0.23326(6)
O2	1.56748(4)	0.14295(3)	0.49978(6)
O3	1.01789(5)	0.19366(3)	0.45098(6)
O4	1.01978(5)	0.07174(3)	0.74660(6)
N1	1.30196(4)	0.10834(3)	0.64328(5)
N2	1.38480(4)	0.12980(2)	0.44510(5)
N3	1.10279(4)	0.12527(2)	0.60257(5)
N4	1.27264(4)	-0.11786(3)	0.96677(5)
H1	1.19162	-0.04299	0.93325
H2	1.16100	-0.17706	0.95715
H3	1.35424	-0.13196	0.83301
H4	1.35558	-0.12062	1.14058

Numbers in parentheses are estimated standard deviations in the least significant digits.

Anisotropic means-square atomic displacement parameters ($\times 1.0\text{e}+05$) for ADN based on $|F_o^2|$ refinement

ATOM	U(1,1)	U(2,2)	U(3,3)	U(1,2)	U(1,3)	U(2,3)
O1	1416(10)	1705(12)	751(8)	-17(5)	100(4)	3(4)
O2	903(8)	1795(12)	1366(10)	-44(4)	174(4)	-41(4)
O3	1034(8)	1231(10)	1118(9)	112(4)	19(4)	70(4)
O4	1153(9)	1283(10)	1309(9)	-32(4)	280(4)	64(4)
N1	845(7)	1308(10)	777(8)	73(4)	82(3)	76(4)
N2	880(7)	975(8)	818(7)	3(3)	104(3)	-8(3)
N3	810(6)	896(7)	824(7)	6(3)	82(3)	-3(3)
N4	1198(9)	1226(9)	1044(8)	29(4)	124(3)	21(4)

Numbers in parentheses are estimated standard deviations in the least significant digits.

Bond Distances (\AA) of ADN based on $|F_o^2|$ refinement

Atom 1	Atom 2	Distance
O1	N2	1.2224(3)
O2	N2	1.2555(4)
O3	N3	1.2276(3)
O4	N3	1.2363(5)
N1	N2	1.3570(4)
N1	N3	1.3710(4)

Numbers in parentheses are estimated standard deviations in the least significant digits.

Table 5.7: Bond Angles (°) of ADN based on $|F_o^2|$ refinement

Atom 1	Atom 2	Atom 3	Angle
N2	N1	N3	113.69(2)
O1	N2	O2	122.15(3)
O1	N2	N1	125.12(3)
O2	N2	N1	112.48(3)
O3	N3	O4	123.35(3)
O3	N3	N1	123.21(3)
O4	N3	N1	113.21(3)

Numbers in parentheses are estimated standard deviations in the least significant digits.

Torsion Angles (°) of ADN based on $|F_o^2|$ refinement

Atom 1	Atom 2	Atom 3	Atom 4	Angle
N3	N1	N2	O1	-22.84(0.05)
N3	N1	N2	O2	162.81(0.03)
N2	N1	N3	O3	-27.88(0.04)
N2	N1	N3	O4	157.52(0.03)
O1	N2	N3	O3	-41.62(0.03)

Numbers in parentheses are estimated standard deviations in the least significant digits.

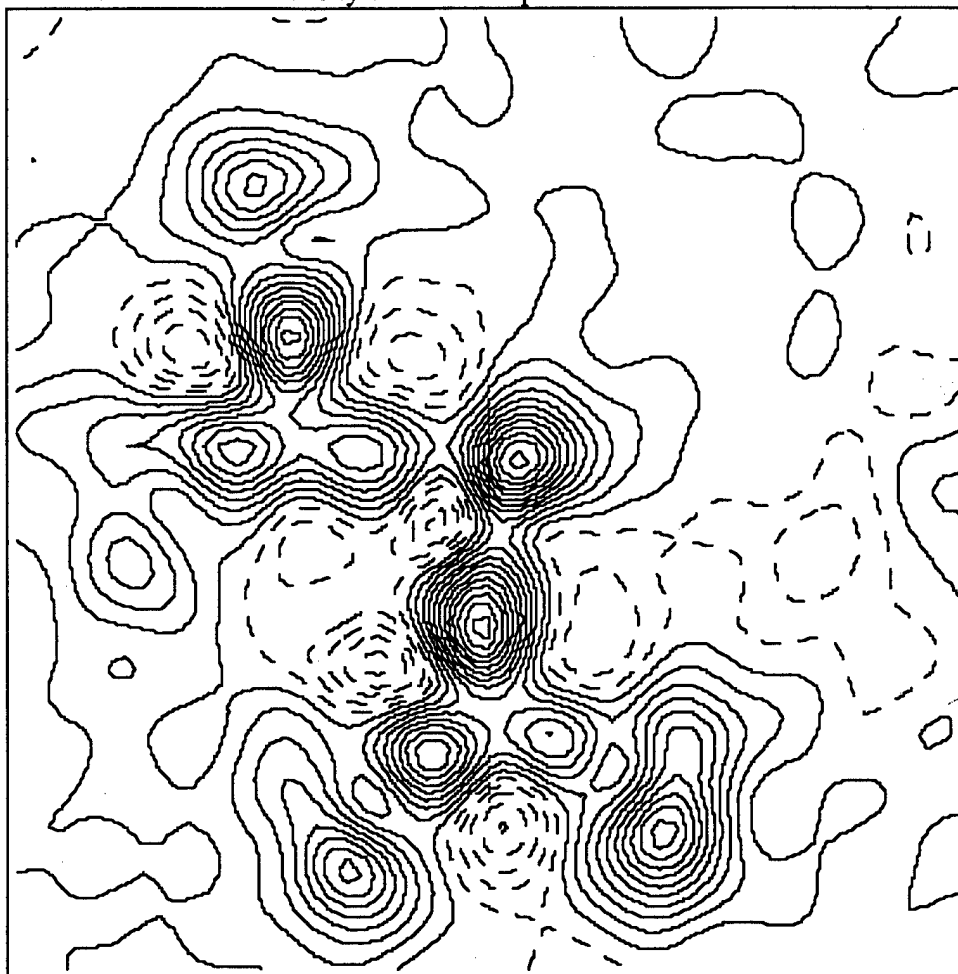
Partial charges for the dinitramide anion from the Kappa refinement

Atom	$P_v (l=0)$ (on F_o^2)	$P_v (l=0)$ (on F_o)	N	$-(P_v-N)$ (on F_o^2)	$-(P_v-N)$ (on F_o)	Theoretical [74]
O1	6.26(4)	6.28(4)	6	-0.26(4)	-0.28	-0.386
O2	6.39(4)	6.45(4)	6	-0.39(4)	-0.45	-0.424
O3	6.45(4)	6.44(4)	6	-0.45(4)	-0.44	-0.411
O4	6.27(4)	6.31(4)	6	-0.27(4)	-0.31	-0.403
N1	5.47(5)	5.45(5)	5	-0.47(5)	-0.45	-0.133
N2	4.55(5)	4.48(5)	5	+0.45(5)	+0.52	+0.506
N3	4.54(5)	4.54(5)	5	+0.46(5)	+0.46	+0.544
TOTAL				-0.93	-0.95	-0.707

Partial charges for the ammonium cation from the Kappa refinement

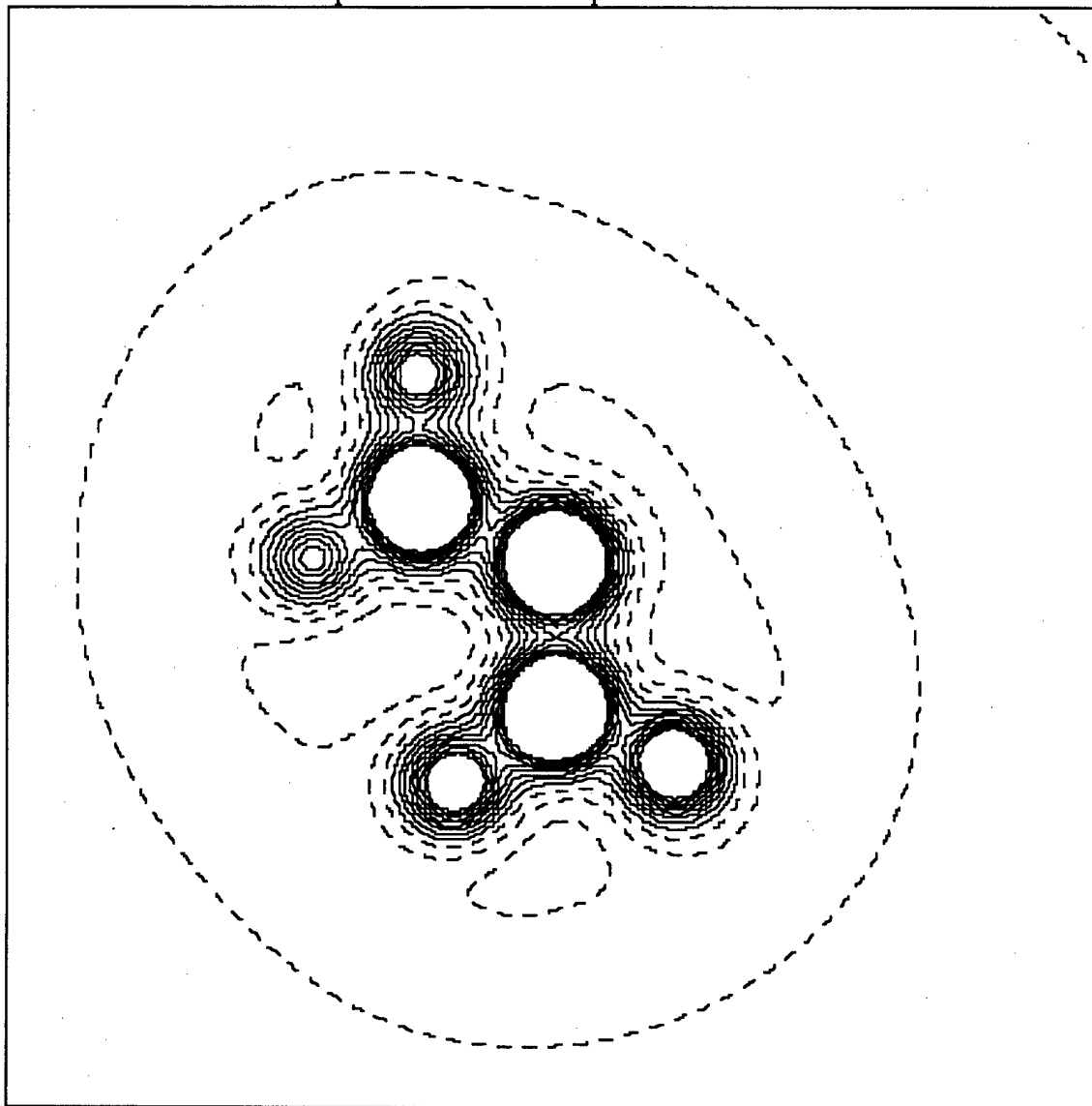
Atom	$P_v (l=0)$ (on F_o^2)	$P_v (l=0)$ (on F_o)	N	$-(P_v-N)$ (on F_o^2)	$-(P_v-N)$ (on F_o)	Theoretical [74]
N4	6.21(7)	6.30(7)	5	-1.21(7)	-1.30	-0.862
H1	0.45(3)	0.43(3)	1	+0.55(3)	+0.57	+0.403
H2	0.46(3)	0.46(3)	1	+0.54(3)	+0.54	+0.396
H3	0.50(3)	0.45(3)	1	+0.50(3)	+0.55	+0.373
H4	0.45(3)	0.42(3)	1	+0.55(3)	+0.58	+0.396
TOTAL				+0.93	+0.95	+0.707

Deformation Density in the NNN plane of dinitramide in ADN



0.05e/Å³ Contour levels. Negative contours dashed

Electrostatic potential in the NNN plane of dinitramide in ADN



0.25 e/Å Contour levels. Negative contours dashed

Value of multipole and associated error for each atom in ADN

	ATOM O1	
MONOPOLE	6.203002	0.017504
DIPOL-X	-0.008000	0.009407
DIPOL-Y	0.026000	0.008952
DIPOL-Z	-0.112000	0.009049
4-POL-ZZ	-0.123000	0.009317
4-POL-ZX	0.009000	0.008936
4-POL-ZY	-0.051000	0.008387
4-PXX-YY	-0.090000	0.008949
4-POL-XY	-0.018000	0.008578
8-POLZZZ	0.028000	0.008552
8-POLXZZ	0.003000	0.007786

8-POLYZZ	0.014000	0.007611
8-PXX-YY	0.024000	0.007831
8-POLXYZ	-0.012000	0.007679
8-POLXXX	0.002000	0.007648
8-POLYYY	-0.004000	0.008021

ATOM O2

MONOPOLE	6.339002	0.017147
DIPOL-X	0.028000	0.009988
DIPOL-Y	0.007000	0.009565
DIPOL-Z	-0.093000	0.010036
4-POL-ZZ	-0.238000	0.010075
4-POL-ZX	-0.018000	0.009453
4-POL-ZY	-0.029000	0.009181
4-PXX-YY	-0.081000	0.009675
4-POL-XY	-0.010000	0.009321
8-POLZZZ	0.015000	0.009427
8-POLXZZ	-0.025000	0.009124
8-POLYZZ	0.012000	0.009187
8-PXX-YY	0.010000	0.009194
8-POLXYZ	0.007000	0.008890
8-POLXXX	-0.002000	0.008466
8-POLYYY	0.003000	0.008456

ATOM O3

MONOPOLE	6.248001	0.016610
DIPOL-X	-0.002000	0.009187
DIPOL-Y	0.004000	0.008957
DIPOL-Z	-0.126000	0.009738
4-POL-ZZ	-0.110000	0.009664
4-POL-ZX	-0.018000	0.008982
4-POL-ZY	0.087000	0.008631
4-PXX-YY	-0.080000	0.008621
4-POL-XY	0.041000	0.008533
8-POLZZZ	0.032000	0.008806
8-POLXZZ	0.009000	0.008141
8-POLYZZ	0.007000	0.008297
8-PXX-YY	-0.015000	0.007929
8-POLXYZ	-0.005000	0.008205
8-POLXXX	0.018000	0.007666
8-POLYYY	0.014000	0.007679

ATOM O4

MONOPOLE	6.182000	0.016647
DIPOL-X	0.010000	0.009708
DIPOL-Y	-0.013000	0.009276
DIPOL-Z	-0.124000	0.010238
4-POL-ZZ	-0.081000	0.009822
4-POL-ZX	0.018000	0.009026
4-POL-ZY	-0.001000	0.008761
4-PXX-YY	-0.061000	0.009074
4-POL-XY	-0.067000	0.008890
8-POLZZZ	0.047000	0.009563
8-POLXZZ	0.016000	0.008849
8-POLYZZ	-0.007000	0.008775
8-PXX-YY	0.006000	0.008441
8-POLXYZ	0.022000	0.008575
8-POLXXX	0.001000	0.008031

8-POLYYY	0.016000	0.008111
----------	----------	----------

ATOM N1

MONOPOLE	5.153001	0.021911
DIPOL-X	-0.018000	0.009039
DIPOL-Y	-0.168000	0.009140
DIPOL-Z	-0.099000	0.009333
4-POL-ZZ	-0.095000	0.008872
4-POL-ZX	0.021000	0.008375
4-POL-ZY	0.028000	0.008407
4-PXX-YY	0.047000	0.008837
4-POL-XY	-0.008000	0.008258
8-POLZZZ	0.079000	0.009718
8-POLXZZ	0.005000	0.008924
8-POLYZZ	0.007000	0.008853
8-PXX-YY	0.041000	0.008925
8-POLXYZ	0.001000	0.008683
8-POLXXX	0.023000	0.008546
8-POLYYY	0.029000	0.008402

ATOM N2

MONOPOLE	5.224001	0.021577
DIPOL-X	0.013000	0.010690
DIPOL-Y	-0.017000	0.013525
DIPOL-Z	-0.004000	0.012658
4-POL-ZZ	0.129000	0.011746
4-POL-ZX	-0.011000	0.010447
4-POL-ZY	0.035000	0.011301
4-PXX-YY	-0.142000	0.011113
4-POL-XY	0.009000	0.009885
8-POLZZZ	0.405000	0.014834
8-POLXZZ	0.030000	0.011871
8-POLYZZ	-0.002000	0.014223
8-PXX-YY	0.290000	0.013111
8-POLXYZ	0.009000	0.012085
8-POLXXX	-0.003000	0.012020
8-POLYYY	0.007000	0.012316

ATOM N3

MONOPOLE	5.305003	0.022468
DIPOL-X	0.024000	0.011218
DIPOL-Y	-0.053000	0.012688
DIPOL-Z	0.029000	0.013641
4-POL-ZZ	0.191000	0.012259
4-POL-ZX	-0.034000	0.010753
4-POL-ZY	0.079000	0.011396
4-PXX-YY	-0.112000	0.010927
4-POL-XY	0.079000	0.010325
8-POLZZZ	0.388000	0.014866
8-POLXZZ	-0.007000	0.012874
8-POLYZZ	-0.061000	0.014375
8-PXX-YY	0.281000	0.013443
8-POLXYZ	-0.046000	0.012694
8-POLXXX	0.004000	0.012035
8-POLYYY	0.024000	0.011869

ATOM N4

MONOPOLE	4.905996	0.043722
----------	----------	----------

DIPOL-X	-0.023001	0.016129
DIPOL-Y	-0.008001	0.016633
DIPOL-Z	-0.023000	0.015445
4-POL-ZZ	-0.033000	0.012847
4-POL-ZX	-0.064000	0.010308
4-POL-ZY	0.051000	0.012619
4-PXX-YY	-0.024000	0.011079
4-POL-XY	0.027000	0.012934
8-POLZZZ	0.084000	0.012585
8-POLXZZ	-0.075000	0.012568
8-POLYZZ	0.255001	0.013858
8-PXX-YY	-0.046000	0.012627
8-POLXYZ	0.017000	0.011398
8-POLXXX	0.114000	0.012292
8-POLYYY	0.159000	0.012180

ATOM H1		
MONOPOLE	0.581999	0.020480
DIPOL-Z	0.284001	0.023210
4-POL-ZZ	0.255001	0.029638

ATOM H2		
MONOPOLE	0.615999	0.021525
DIPOL-Z	0.290002	0.023667
4-POL-ZZ	0.180002	0.032147

ATOM H3		
MONOPOLE	0.634998	0.024102
DIPOL-Z	0.268000	0.026946
4-POL-ZZ	0.215001	0.033081

ATOM H4		
MONOPOLE	0.605999	0.022127
DIPOL-Z	0.315001	0.022847
4-POL-ZZ	0.155002	0.030957

Contract No. N00014-95-1-0013 and N00014-97-1-0409

Program Officer: R. Miller/J. Goldwasser

**Title: Experimental Charge Densities and Electrostatic Potentials in Energetic
Materials and Infrastructure Upgrade for an X-ray Crystallography
Laboratory**

PI: A. Alan Pinkerton

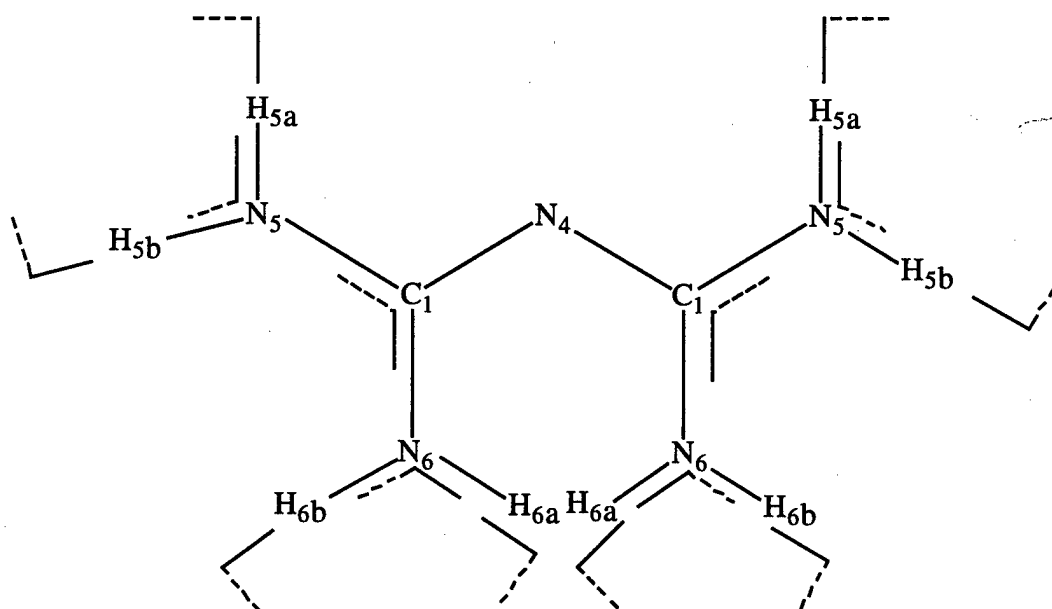
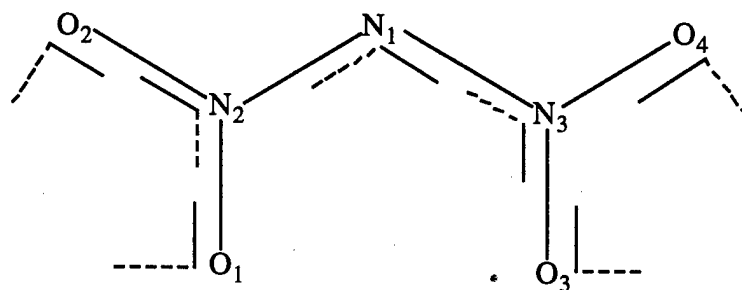
Department of Chemistry, University of Toledo, Toledo, OH 43606

tel. (419) 530-4580, FAX (419) 530-4033, email apinker@uoft02.utoledo.edu

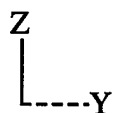
APPENDIX 2b

Electron density and electrostatic potential for BIGH.DN

Coordinate System for biguanidinium dinitramide



The hydrogen coordinates are centered on the nuclei, but they are displaced in the diagram for clarity.



The lines indicate the positive direction of the axis vectors.

The X axis is perpendicular to the Z and Y axis in the usual way

Summary of crystallographic details of BIGHDN from multipole refinement

Empirical formula	$\text{C}_2\text{H}_8\text{N}_8\text{O}_4$	Density (calc) (Mg/m^3)	1.616 (293K)
Formula weight	208.16	Absorption coeff. (mm^{-1})	0.1443
Wavelength (\AA)	0.71073	θ max ($^\circ$)	73
Crystal system	Triclinic	Reflections collected	16752
Space group	$P\bar{1}$ (#2)	Independent reflections	8275
Crystal size	0.21 x 0.15 x 0.13 mm	R_{int}	0.0173
Z	2	Data/parameters	8275/404
F(000)	216	Goodness-of-fit on F^2	1.28
Temperature (K)	90 \pm 1	$R(F)$	0.0445
a (\AA)	4.280(1)	$R_w(F)$	0.0359
b (\AA)	9.288(1)	$R(F^2)$	0.0462
c (\AA)	10.530(4)	$R_w(F^2)$	0.0773
α ($^\circ$)	85.34(2)		
β ($^\circ$)	82.13(2)		
γ ($^\circ$)	81.32(1) $^\circ$,		
Volume (\AA^3)	409.1		

Fractional Coordinates for (BIGH)(DN) based on $|F_o^2|$

ATOM	X	Y	Z
O1	0.56439(13)	-0.27944(5)	0.25571(6)
O2	0.54624(10)	-0.07510(5)	0.14031(4)
O3	-0.23448(13)	-0.09368(6)	0.44486(6)
O4	0.12854(26)	-0.28221(10)	0.44448(11)
N1	0.15705(10)	-0.08738(4)	0.29226(4)
N2	0.43261(9)	-0.15520(4)	0.23070(4)
N3	0.01960(9)	-0.16277(4)	0.39858(4)
N4	1.02455(10)	0.18679(5)	0.08877(4)
N5	0.84960(10)	0.36177(5)	-0.06104(4)
N6	0.61236(10)	0.38332(4)	0.14483(4)
N7	0.37392(12)	0.42323(5)	0.34838(5)
N8	0.52558(12)	0.18608(5)	0.29783(5)
C1	0.82686(9)	0.30799(4)	0.06055(4)
C2	0.51162(10)	0.32785(4)	0.26195(4)
H1	1.02829	0.14012	0.18074
H2	1.18662	0.13738	0.01851
H3	1.04154	0.32996	-0.12768
H4	0.69961	0.45336	-0.08794
H5	0.37604	0.53376	0.33046
H6	0.25269	0.38555	0.43288
H7	0.57391	0.10486	0.23399
H8	0.44160	0.15394	0.39054

Numbers in parentheses are estimated standard deviations in the least significant digits.

Anisotropic means-square atomic displacement parameters (1.0e+05) for (BIGH)(DN)

based on $|F_o^2|$

ATOM	U(1,1)	U(2,2)	U(3,3)	U(1,2)	U(1,3)	U(2,3)
O1	1377(15)	917(13)	1787(18)	77(5)	156(6)	18(6)
O2	1600(14)	1216(12)	1334(14)	-43(5)	229(5)	54(5)
O3	1328(16)	1383(16)	1443(17)	119(6)	199(6)	98(7)
O4	2133(29)	1393(22)	1879(28)	288(9)	356(10)	355(10)
N1	1134(12)	965(11)	1167(13)	49(4)	73(5)	86(5)
N2	1089(11)	900(10)	999(11)	-10(4)	53(4)	-35(4)
N3	1146(11)	932(10)	1000(11)	24(4)	52(4)	47(4)
N4	1408(13)	1340(13)	1273(13)	224(5)	10(5)	72(5)
N5	1519(14)	1205(12)	1038(13)	83(5)	83(5)	72(5)
N6	1495(13)	830(11)	890(12)	58(4)	139(5)	64(4)
N7	2537(19)	983(12)	1188(14)	39(5)	295(6)	-24(5)
N8	2108(17)	793(11)	1218(14)	-49(5)	92(6)	97(5)
C1	1099(12)	906(11)	900(12)	18(4)	33(4)	10(5)
C2	1376(13)	774(11)	982(13)	7(4)	74(5)	59(5)

Numbers in parentheses are estimated standard deviations in the least significant digits.

Bond Distances in Angstroms (Å) for (BIGH)(DN) based on $|F_o^2|$

Atom 1	Atom 2	Distance
O1	N2	1.2304(6)
O2	N2	1.2503(6)
O3	N3	1.2357(7)
O4	N3	1.225(1)
N1	N2	1.3568(5)
N1	N3	1.3807(6)
N4	C1	1.3411(6)
N5	C1	1.3322(6)
N6	C1	1.3431(5)
N6	C2	1.3381(6)
N7	C2	1.3368(6)
N8	C2	1.3348(6)

Numbers in parentheses are estimated standard deviations in the least significant digits.

Bond Angles in Degrees (°) for (BIGH)(DN) based on $|F_o^2|$

Atom 1	Atom 2	Atom 3	Angle
N2	N1	N3	116.46(3)
O1	N2	O2	121.64(4)
O1	N2	N1	126.89(4)
O2	N2	N1	111.47(4)
O3	N3	O4	122.62(7)
O3	N3	N1	111.26(5)
O4	N3	N1	126.12(6)
C1	N6	C2	123.09(4)
N4	C1	N5	117.62(4)
N4	C1	N6	125.83(4)
N5	C1	N6	116.52(4)
N6	C2	N7	116.77(4)
N6	C2	N8	125.59(4)
N7	C2	N8	117.58(4)

Numbers in parentheses are estimated standard deviations in the least significant digits.

Torsion Angles in Degrees (°) for (BIGH)(DN) based on $|F_o^2|$

Atom 1	Atom 2	Atom 3	Atom 4	Angle
N3	N1	N2	O1	3.90(0.07)
N3	N1	N2	O2	-176.45(0.04)
N2	N1	N3	O3	-177.83(0.05)
N2	N1	N3	O4	2.60(0.09)
O1	N2	N3	O3	-173.53(0.07)

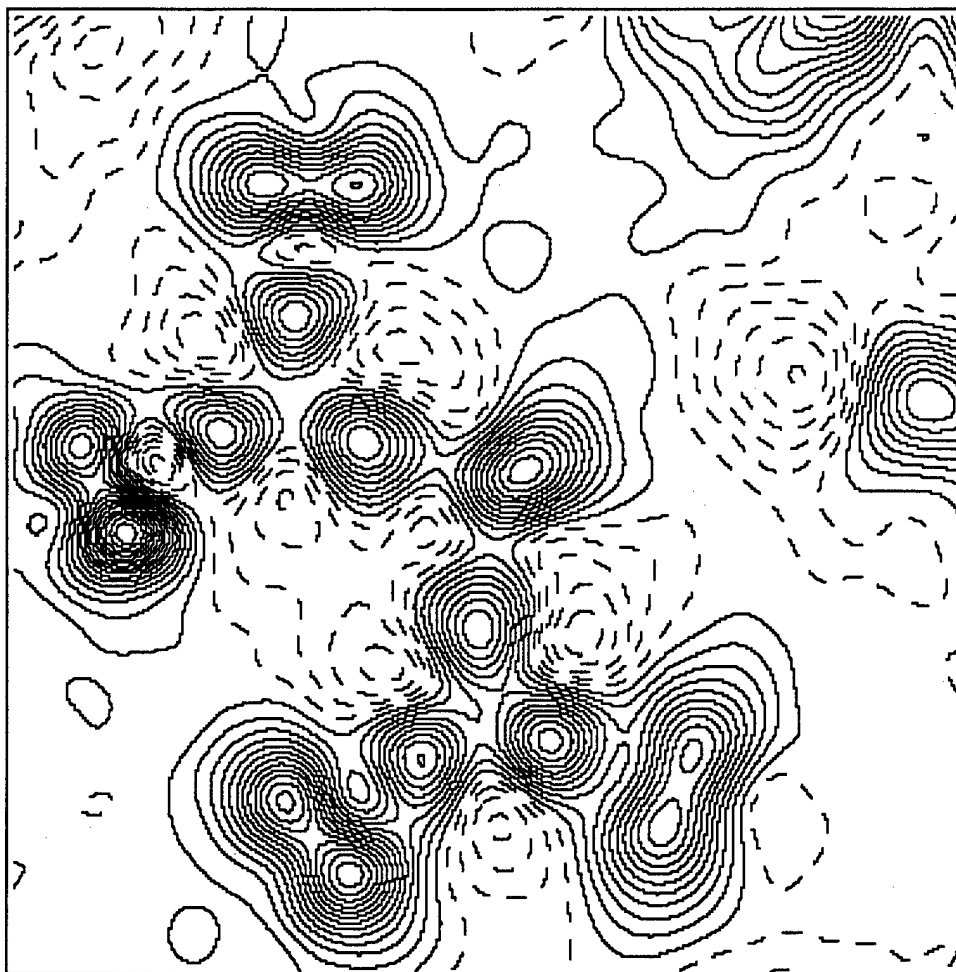
Partial charges for the dinitramide anion from the kappa refinement

Atom	$P_V(l=0)$ (on F_o^2)	$P_V(l=0)$ (on F_o)	N	$-(P_V-N)$ (on F_o^2)	$-(P_V-N)$ (on F_o)	Theoretical [74]
O1	6.32(5)	6.32(5)	6	-0.32(5)	-0.32	-0.169
O2	6.36(5)	6.39(5)	6	-0.36(5)	-0.39	-0.186
O3	6.28(5)	6.34(5)	6	-0.28(5)	-0.34	-0.197
O4	6.27(6)	6.26(5)	6	-0.27(6)	-0.26	-0.205
N1	5.62(6)	5.61(6)	5	-0.62(6)	-0.61	-0.198
N2	4.34(6)	4.37(6)	5	+0.66(6)	+0.63	+0.303
N3	4.19(6)	4.21(5)	5	+0.81(6)	+0.79	+0.302
TOTAL				-0.38	-0.50	-0.350

Partial charges for the monoprotonated biguanidinium cation from the kappa refinement

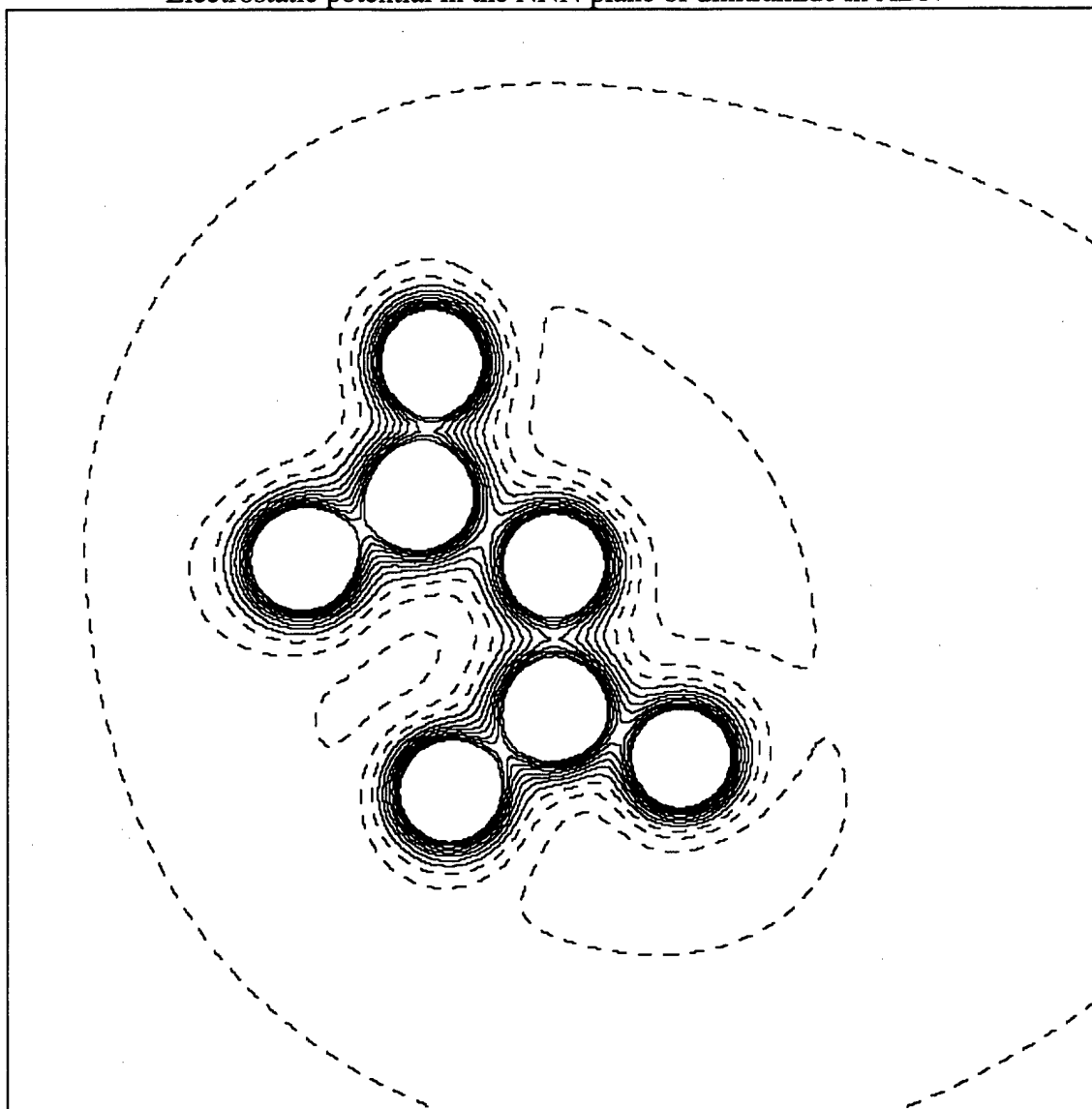
Atom	$P_V(l=0)$ (on F_o^2)	$P_V(l=0)$ (on F_o)	N	$-(P_V-N)$ (on F_o^2)	$-(P_V-N)$ (on F_o)	Theoretical [74]
N4	6.00(7)	5.92(7)	5	-1.00	-0.92	-0.245
N5	6.04(7)	6.08(7)	5	-1.04	-1.08	-0.273
N6	6.01(7)	5.93(6)	5	-1.01	-0.93	-0.225
N7	6.13(7)	6.12(7)	5	-1.13	-1.12	-0.235
N8	5.62(7)	5.55(7)	5	-0.62	-0.55	-0.232
C1	3.37(8)	3.30(7)	4	+0.63	+0.7	+0.332
C2	3.52(9)	3.51(8)	4	+0.48	+0.49	+0.327
H1	0.47(2)	0.50(2)	1	+0.53	+0.5	+0.095
H2	0.52(3)	0.50(2)	1	+0.48	+0.5	+0.134
H3	0.48(2)	0.51(3)	1	+0.52	+0.49	+0.098
H4	0.44(2)	0.46(2)	1	+0.56	+0.54	+0.127
H5	0.54(3)	0.51(2)	1	+0.46	+0.49	+0.121
H6	0.45(2)	0.54(2)	1	+0.55	+0.46	+0.116
H7	0.50(2)	0.57(2)	1	+0.50	+0.43	+0.131
H8	0.53(2)	0.50(2)	1	+0.47	+0.50	+0.081
TOTAL				+0.38	+0.50	+0.352

Deformation Density in the NNN plane of dinitramide in (BIGH)(DN)



0.05e/Å³ Contour levels. Negative contours dashed

Electrostatic potential in the NNN plane of dinitramide in ADN



0.25 e/Å Contour levels. Negative contours dashed

Value of multipole and associated error for each atom in (BIGH)(DN)

	ATOM O1	
MONOPOLE	6.253001	0.024080
DIPOL-X	0.009000	0.013655
DIPOL-Y	-0.001000	0.011115
DIPOL-Z	-0.108001	0.011934
4-POL-ZZ	-0.091000	0.012812
4-POL-ZX	0.021000	0.012727
4-POL-ZY	0.014000	0.011296
4-PXX-YY	-0.088000	0.012421

4-POL-XY	0.075000	0.012660
8-POLZZZ	0.053000	0.011057
8-POLXZZ	0.016000	0.011289
8-POLYZZ	0.008000	0.010304
8-PXX-YY	0.019000	0.010327
8-POLXYZ	-0.001000	0.010731
8-POLXXX	-0.023000	0.010559
8-POLYYY	0.012000	0.010639

ATOM O2

MONOPOLE	6.268002	0.023099
DIPOL-X	-0.007000	0.016548
DIPOL-Y	-0.003000	0.014323
DIPOL-Z	-0.155000	0.016339
4-POL-ZZ	-0.182000	0.015534
4-POL-ZX	0.049000	0.015442
4-POL-ZY	-0.009000	0.014025
4-PXX-YY	-0.044001	0.013726
4-POL-XY	0.025000	0.013987
8-POLZZZ	0.055000	0.015423
8-POLXZZ	-0.049000	0.015695
8-POLYZZ	0.003000	0.014510
8-PXX-YY	-0.003000	0.013712
8-POLXYZ	-0.021000	0.014329
8-POLXXX	0.027000	0.013454
8-POLYYY	0.014000	0.013764

ATOM O3

MONOPOLE	6.190008	0.024788
DIPOL-X	0.016000	0.013428
DIPOL-Y	0.008000	0.010771
DIPOL-Z	-0.094999	0.010781
4-POL-ZZ	-0.098999	0.012148
4-POL-ZX	0.036000	0.013167
4-POL-ZY	0.014000	0.011003
4-PXX-YY	-0.044001	0.012874
4-POL-XY	-0.054000	0.012949
8-POLZZZ	0.033000	0.010569
8-POLXZZ	-0.022000	0.010619
8-POLYZZ	-0.014000	0.009701
8-PXX-YY	0.029000	0.010293
8-POLXYZ	-0.010000	0.010437
8-POLXXX	0.030000	0.010338
8-POLYYY	-0.008000	0.010197

ATOM O4

MONOPOLE	6.142006	0.025617
DIPOL-X	0.084999	0.020101
DIPOL-Y	-0.040000	0.011735
DIPOL-Z	-0.082000	0.011716
4-POL-ZZ	-0.101000	0.014833
4-POL-ZX	-0.019000	0.017853
4-POL-ZY	0.022000	0.012382
4-PXX-YY	-0.090001	0.016207
4-POL-XY	0.028000	0.018899
8-POLZZZ	-0.008000	0.011485

8-POLXZZ	-0.030000	0.012354
8-POLYZZ	0.011000	0.009368
8-PXX-YY	0.080000	0.011145
8-POLXYZ	-0.019000	0.011127
8-POLXXX	0.063000	0.012049
8-POLYYY	0.032000	0.012143

ATOM N1

MONOPOLE	5.184999	0.030343
DIPOL-X	0.051000	0.014055
DIPOL-Y	-0.189001	0.013568
DIPOL-Z	-0.118000	0.013857
4-POL-ZZ	-0.109000	0.013742
4-POL-ZX	0.045000	0.013308
4-POL-ZY	0.057001	0.012528
4-PXX-YY	0.111001	0.013108
4-POL-XY	0.007000	0.012977
8-POLZZZ	0.117000	0.014446
8-POLXZZ	0.002000	0.014049
8-POLYZZ	-0.001000	0.014228
8-PXX-YY	0.046000	0.013497
8-POLXYZ	-0.002000	0.013763
8-POLXXX	0.000000	0.013410
8-POLYYY	0.043000	0.012609

ATOM N2

MONOPOLE	5.212007	0.029707
DIPOL-X	-0.013000	0.017134
DIPOL-Y	0.064999	0.018359
DIPOL-Z	-0.039000	0.018376
4-POL-ZZ	0.087000	0.017596
4-POL-ZX	0.012000	0.015297
4-POL-ZY	-0.043000	0.016585
4-PXX-YY	-0.163001	0.016007
4-POL-XY	0.027000	0.015562
8-POLZZZ	0.447001	0.021626
8-POLXZZ	-0.031000	0.018235
8-POLYZZ	0.001000	0.021183
8-PXX-YY	0.301001	0.018640
8-POLXYZ	-0.006000	0.019091
8-POLXXX	0.046000	0.017765
8-POLYYY	0.034000	0.017374

ATOM N3

MONOPOLE	4.967001	0.027933
DIPOL-X	-0.047001	0.015941
DIPOL-Y	-0.000999	0.015908
DIPOL-Z	-0.011000	0.016367
4-POL-ZZ	0.091999	0.015567
4-POL-ZX	0.025000	0.013921
4-POL-ZY	0.015999	0.014899
4-PXX-YY	-0.150999	0.015130
4-POL-XY	-0.028000	0.014498
8-POLZZZ	0.386998	0.019651
8-POLXZZ	-0.068000	0.016863
8-POLYZZ	-0.007000	0.018001

8-PXX-YY	0.263999	0.017392
8-POLXYZ	0.002000	0.016924
8-POLXXX	0.060000	0.016088
8-POLYYY	0.021001	0.016211

ATOM N4

MONOPOLE	5.169995	0.048745
DIPOL-X	0.040001	0.021208
DIPOL-Y	-0.084999	0.030910
DIPOL-Z	0.025000	0.027832
4-POL-ZZ	0.008000	0.020966
4-POL-ZX	-0.011000	0.019491
4-POL-ZY	0.056000	0.022361
4-PXX-YY	0.021000	0.019657
4-POL-XY	-0.030001	0.017238
8-POLZZZ	0.357000	0.024519
8-POLXZZ	-0.010000	0.022452
8-POLYZZ	-0.040000	0.021630
8-PXX-YY	0.288002	0.023834
8-POLXYZ	0.042000	0.020786
8-POLXXX	-0.022000	0.019274
8-POLYYY	-0.028000	0.020624

ATOM N5

MONOPOLE	5.144985	0.048586
DIPOL-X	0.068001	0.017272
DIPOL-Y	-0.066000	0.023071
DIPOL-Z	-0.025998	0.021501
4-POL-ZZ	-0.064000	0.017025
4-POL-ZX	0.036000	0.015825
4-POL-ZY	0.054000	0.017408
4-PXX-YY	-0.012998	0.015442
4-POL-XY	0.052001	0.014173
8-POLZZZ	0.247000	0.019600
8-POLXZZ	0.031000	0.017574
8-POLYZZ	0.031000	0.016987
8-PXX-YY	0.231999	0.018352
8-POLXYZ	0.010000	0.016703
8-POLXXX	0.005000	0.015169
8-POLYYY	-0.021000	0.016579

ATOM N6

MONOPOLE	5.324003	0.033275
DIPOL-X	0.021000	0.014186
DIPOL-Y	-0.124000	0.013818
DIPOL-Z	-0.073000	0.014049
4-POL-ZZ	0.044000	0.013595
4-POL-ZX	-0.057000	0.013490
4-POL-ZY	-0.005000	0.012849
4-PXX-YY	-0.038000	0.013306
4-POL-XY	-0.025000	0.012794
8-POLZZZ	0.104000	0.014252
8-POLXZZ	0.026000	0.013614
8-POLYZZ	0.015000	0.013671
8-PXX-YY	0.085000	0.013365
8-POLXYZ	-0.001000	0.013409

8-POLXXX	-0.024000	0.012986
8-POLYYY	0.055000	0.012667

ATOM N7

MONOPOLE	5.207011	0.052065
DIPOL-X	0.011999	0.020189
DIPOL-Y	-0.001000	0.027914
DIPOL-Z	0.002997	0.023857
4-POL-ZZ	0.018999	0.018802
4-POL-ZX	-0.046000	0.018420
4-POL-ZY	-0.015000	0.020256
4-PXX-YY	-0.015002	0.018994
4-POL-XY	-0.041000	0.016229
8-POLZZZ	0.324000	0.021349
8-POLXZZ	0.037000	0.020617
8-POLYZZ	0.022000	0.018895
8-PXX-YY	0.195003	0.020158
8-POLXYZ	0.056001	0.018588
8-POLXXX	0.007000	0.018384
8-POLYYY	-0.004999	0.019244

ATOM N8

MONOPOLE	5.074986	0.049814
DIPOL-X	-0.018001	0.016119
DIPOL-Y	-0.091998	0.022192
DIPOL-Z	-0.009000	0.018675
4-POL-ZZ	0.017999	0.015773
4-POL-ZX	-0.049000	0.014807
4-POL-ZY	0.041999	0.016461
4-PXX-YY	0.011001	0.015538
4-POL-XY	-0.001000	0.014284
8-POLZZZ	0.221999	0.016767
8-POLXZZ	0.010000	0.015794
8-POLYZZ	-0.002000	0.015231
8-PXX-YY	0.159000	0.016245
8-POLXYZ	0.051999	0.014924
8-POLXXX	-0.042000	0.014934
8-POLYYY	0.022000	0.014807

ATOM C1

MONOPOLE	3.914001	0.051921
DIPOL-X	0.020000	0.018241
DIPOL-Y	-0.024000	0.020315
DIPOL-Z	-0.048999	0.022119
4-POL-ZZ	0.073000	0.019493
4-POL-ZX	0.012000	0.017171
4-POL-ZY	0.023999	0.018523
4-PXX-YY	-0.250000	0.017222
4-POL-XY	-0.002000	0.016385
8-POLZZZ	0.321001	0.022002
8-POLXZZ	-0.018000	0.020101
8-POLYZZ	-0.001999	0.023463
8-PXX-YY	0.220000	0.020408
8-POLXYZ	0.020000	0.020136
8-POLXXX	0.013000	0.018553
8-POLYYY	-0.009999	0.018459

ATOM C2		
MONOPOLE	4.022006	0.048216
DIPOL-X	0.042000	0.019162
DIPOL-Y	-0.023998	0.020984
DIPOL-Z	-0.048999	0.021651
4-POL-ZZ	0.125001	0.019842
4-POL-ZX	0.027001	0.017587
4-POL-ZY	0.018999	0.018994
4-PXX-YY	-0.262001	0.018330
4-POL-XY	0.063000	0.016911
8-POLZZZ	0.351001	0.023227
8-POLXZZ	0.010000	0.020445
8-POLYZZ	-0.019000	0.023848
8-PXX-YY	0.199000	0.021171
8-POLXYZ	0.007000	0.020454
8-POLXXX	0.005000	0.019482
8-POLYYY	0.010001	0.019795

ATOM H1		
MONOPOLE	0.661998	0.032651
DIPOL-Z	0.268003	0.030517
4-POL-ZZ	-0.010999	0.034686

ATOM H2		
MONOPOLE	0.829997	0.035514
DIPOL-Z	0.372002	0.031970
4-POL-ZZ	0.165000	0.037211

ATOM H3		
MONOPOLE	0.796002	0.032220
DIPOL-Z	0.364006	0.031211
4-POL-ZZ	0.172007	0.037283

ATOM H4		
MONOPOLE	0.661000	0.027165
DIPOL-Z	0.201004	0.030830
4-POL-ZZ	0.110006	0.038177

ATOM H5		
MONOPOLE	0.789995	0.035117
DIPOL-Z	0.370999	0.035902
4-POL-ZZ	0.094997	0.042400

ATOM H6		
MONOPOLE	0.647995	0.030701
DIPOL-Z	0.277998	0.030741
4-POL-ZZ	0.065996	0.035650

ATOM H7		
MONOPOLE	0.683002	0.027656
DIPOL-Z	0.124007	0.032043
4-POL-ZZ	0.056007	0.037250

ATOM H8		
MONOPOLE	0.857998	0.030294

DIPOL-Z	0.399002	0.034250
4-POL-ZZ	0.261003	0.040639

Contract No. N00014-95-1-0013 and N00014-97-1-0409

Program Officer: R. Miller/J. Goldwasser

**Title: Experimental Charge Densities and Electrostatic Potentials in Energetic
Materials and Infrastructure Upgrade for an X-ray Crystallography
Laboratory**

PI: A. Alan Pinkerton

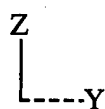
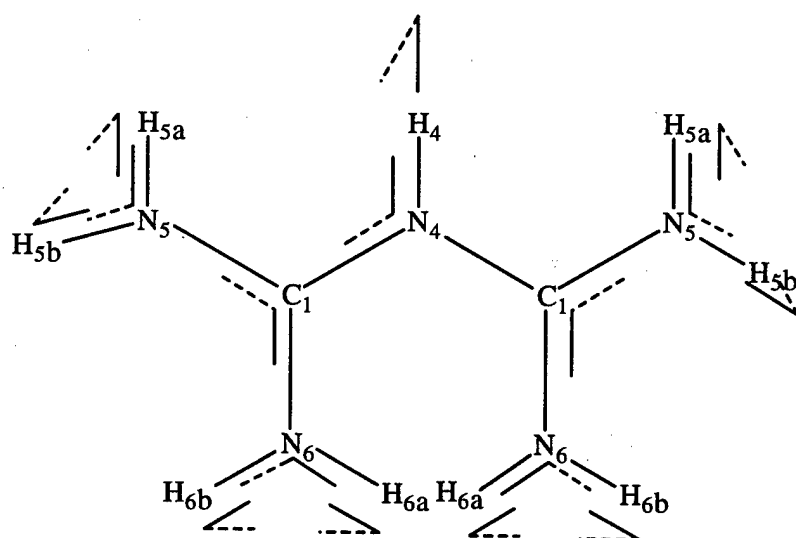
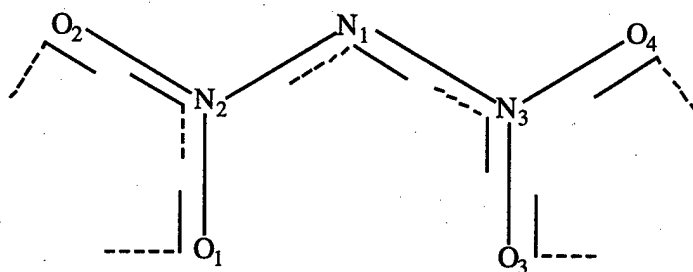
Department of Chemistry, University of Toledo, Toledo, OH 43606

tel. (419) 530-4580, FAX (419) 530-4033, email apinker@uoft02.utoledo.edu

APPENDIX 2c

Electron density and electrostatic potential for $\text{BiH}_2(\text{DN})_2$

Local coordinate system for $(\text{BIGH}_2)(\text{DN})_2$



The lines indicate the positive direction of the axis vectors.
The X axis is perpendicular to the Z and Y axis in the usual way

Summary of crystallographic details of (BIGH₂)(DN)₂ from multipole refinement

Empirical formula	C ₂ H ₉ N ₁₁ O ₈	Density (calc) (Mg/m ³)	1.84 (293K)
Formula weight	315.20	Absorption coeff. (mm ⁻¹)	0.172
Wavelength (Å)	0.71073Å	θ max (°)	73
Crystal system	Monoclinic	Reflections collected	21625
Space group	C2/c (#15)	Independent reflections	9455
Crystal size	0.32 x 0.23 x 0.13 mm	R _{int}	0.0287
Z	4	Data/parameters	9455/303
F(000)	688	Goodness-of-fit on F	1.13
Temperature (K)	90±1	R(F)	0.0255
a (Å)	11.667(2)	Rw(F)	0.0223
b (Å)	8.131(1)	R(F ²)	0.0297
c (Å)	12.973(1)	Rw(F ²)	0.0463
β (°)	117.41(1)		
Volume (Å ³)	1096.8		

Fractional coordinates for (BIGH₂)(DN)₂

ATOM	X	Y	Z
O1	0.09073(3)	-0.73507(3)	0.95846(3)
O2	0.14235(3)	-0.70278(3)	0.81892(3)
O3	0.15533(4)	-0.48728(4)	1.09578(3)
O4	0.12896(3)	-0.26188(3)	0.99932(2)
N1	0.14497(2)	-0.48334(3)	0.91353(2)
N2	0.12539(2)	-0.64771(2)	0.90062(2)
N3	0.14118(2)	-0.41224(2)	1.00933(2)
N4	0.00000	-0.02383(3)	0.75000
N5	0.11008(2)	-0.00107(2)	0.64402(2)
N6	0.11710(2)	-0.24808(2)	0.73280(2)
C1	0.07660(2)	-0.09565(2)	0.70836(2)
H4	0.00000	0.10262	0.75000
H5B	0.17799	-0.04105	0.62002
H5A	0.06710	0.11133	0.61411
H6A	0.11095	-0.31780	0.79618
H6B	0.16461	-0.29682	0.68987

Numbers in parentheses are estimated standard deviations in the least significant digits.

Anisotropic means-square atomic displacement parameters (1.0×10^5) for $(\text{BIGH}_2)(\text{DN})_2$

ATOM	U(1,1)	U(2,2)	U(3,3)	U(1,2)	U(1,3)	U(2,3)
O1	1779(9)	959(7)	1586(9)	-224(3)	482(4)	20(3)
O2	1844(9)	1161(7)	1650(9)	-113(4)	564(4)	-199(4)
O3	2682(13)	1345(10)	999(8)	-127(5)	457(5)	28(4)
O4	1466(8)	827(6)	1495(8)	-40(3)	413(4)	-73(3)
N1	1463(8)	732(6)	1036(7)	-100(3)	375(3)	-8(3)
N2	955(6)	735(5)	1057(6)	-75(2)	263(3)	-13(2)
N3	1094(6)	827(6)	893(6)	-72(2)	252(3)	-18(2)
N4	2305(13)	559(7)	2230(13)		980(6)	
N5	1305(7)	878(6)	1240(6)	55(3)	463(3)	119(3)
N6	1232(7)	856(6)	1429(7)	163(3)	424(3)	191(3)
C1	956(6)	653(6)	893(6)	4(3)	295(3)	21(3)
H4	3991					
H5A	2394					
H5B	2393					
H6A	3050					
H6B	2927					

Numbers in parentheses are estimated standard deviations in the least significant digits.

Bond Distances (Å) for (BIGH₂)(DN)₂

Atom 1	Atom 2	Distance
O1	N2	1.2289(4)
N1	N3	1.3897(4)
O2	N2	1.2475(3)
N4	C1	1.3697(2)
O3	N3	1.2194(3)
N4	C1	1.3697(2)
O4	N3	1.2309(3)
N5	C1	1.3194(3)
N1	N2	1.3533(3)
N6	C1	1.3123(3)

Numbers in parentheses are estimated standard deviations in the least significant digits.

Bond Angles in Degrees (°) for (BIGH₂)(DN)₂

Atom 1	Atom 2	Atom 3	Angle
N2	N1	N3	116.64(3)
O4	N3	N1	111.64(2)
O1	N2	O2	122.46(2)
C1	N4	C1	129.53(1)
O1	N2	N1	125.42(3)
N4	C1	N5	115.97(2)
O2	N2	N1	112.07(3)
N4	C1	N6	122.35(2)
O3	N3	O4	123.65(2)
N5	C1	N6	121.66(2)
O3	N3	N1	124.60(2)

Numbers in parentheses are estimated standard deviations in the least significant digits.

Torsion Angles (°) for (BIGH₂)(DN)₂

Atom 1	Atom 2	Atom 3	Atom 4	Angle
N3	N1	N2	O1	8.56(0.04)
N3	N1	N2	O2	-173.77(0.02)
N2	N1	N3	O3	20.01(0.05)
N2	N1	N3	O4	-163.81(0.03)
O1	N2	N3	O3	23.40(0.03)

Numbers in parentheses are estimated standard deviations in the least significant digits

Partial charges for the dinitramide anion from the kappa refinement

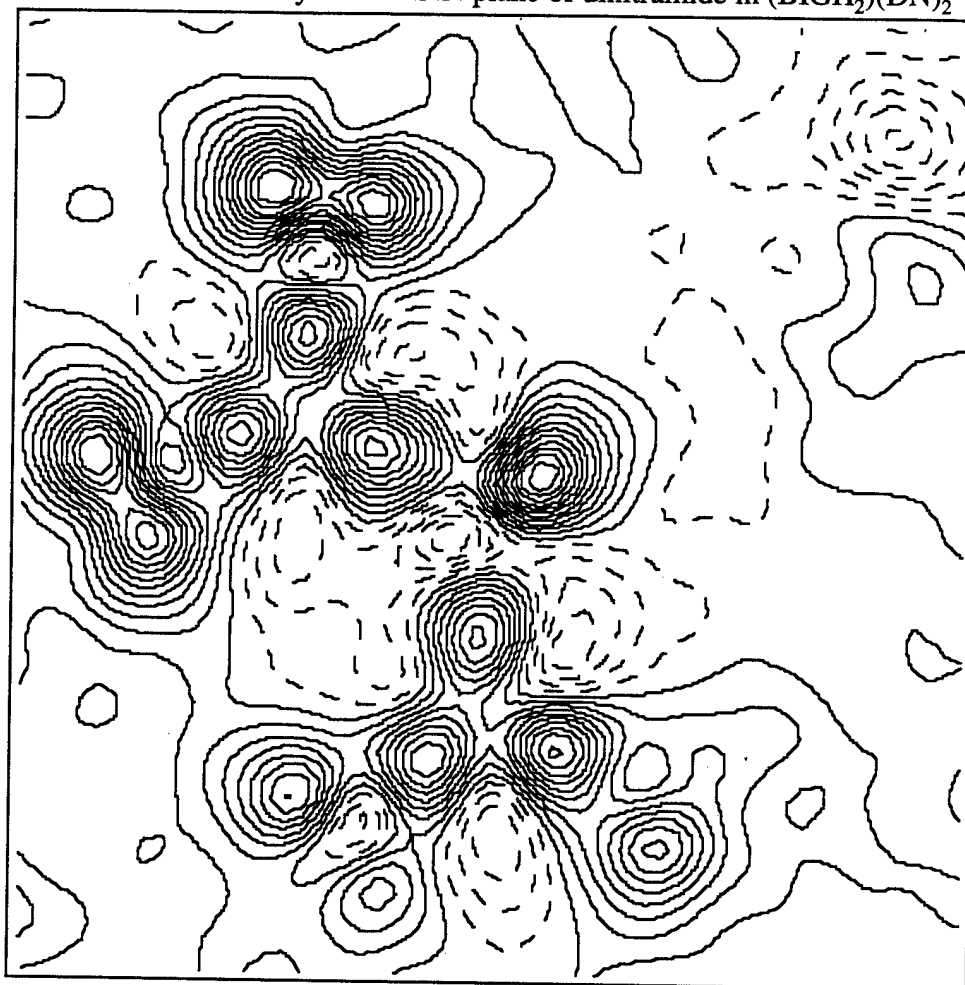
Atom	P _V (I=0)	N	-(P _V -N)	Theoretical
O1	6.41(3)	6	-0.41(3)	-0.221
O2	5.41(3)	6	-0.41(3)	-0.229
O3	6.21(4)	6	-0.21(4)	-0.220
O4	6.26(3)	6	-0.26(3)	-0.231
N1	5.35(4)	5	-0.35(4)	-0.184
N2	4.39(4)	5	+0.61(4)	+0.296
N3	4.44(4)	5	+0.56(4)	+0.299
TOTAL			-0.47	-0.490

Partial charges for the diprotonated biguanidinium cation from the kappa refinement

Atom	P _V (I=0)	N	-(P _V -N)	Theoretical
N4	2.68(3)	2.5*	-0.18	-0.110
N5	5.59(5)	5	-0.59	-0.232
N6	5.63(5)	5	-0.63	-0.214
C1	3.76(6)	4	+0.24	+0.440
H4	0.31(2)	0.5*	+0.19	+0.055
H5A	0.64(3)	1	+0.36	+0.136
H5B	0.65(2)	1	+0.35	+0.152
H6A	0.63(3)	1	+0.37	+0.106
H6B	0.63(3)	1	+0.37	+0.159
1/2 molecule			+0.48	+0.495
TOTAL			+0.96	+0.986

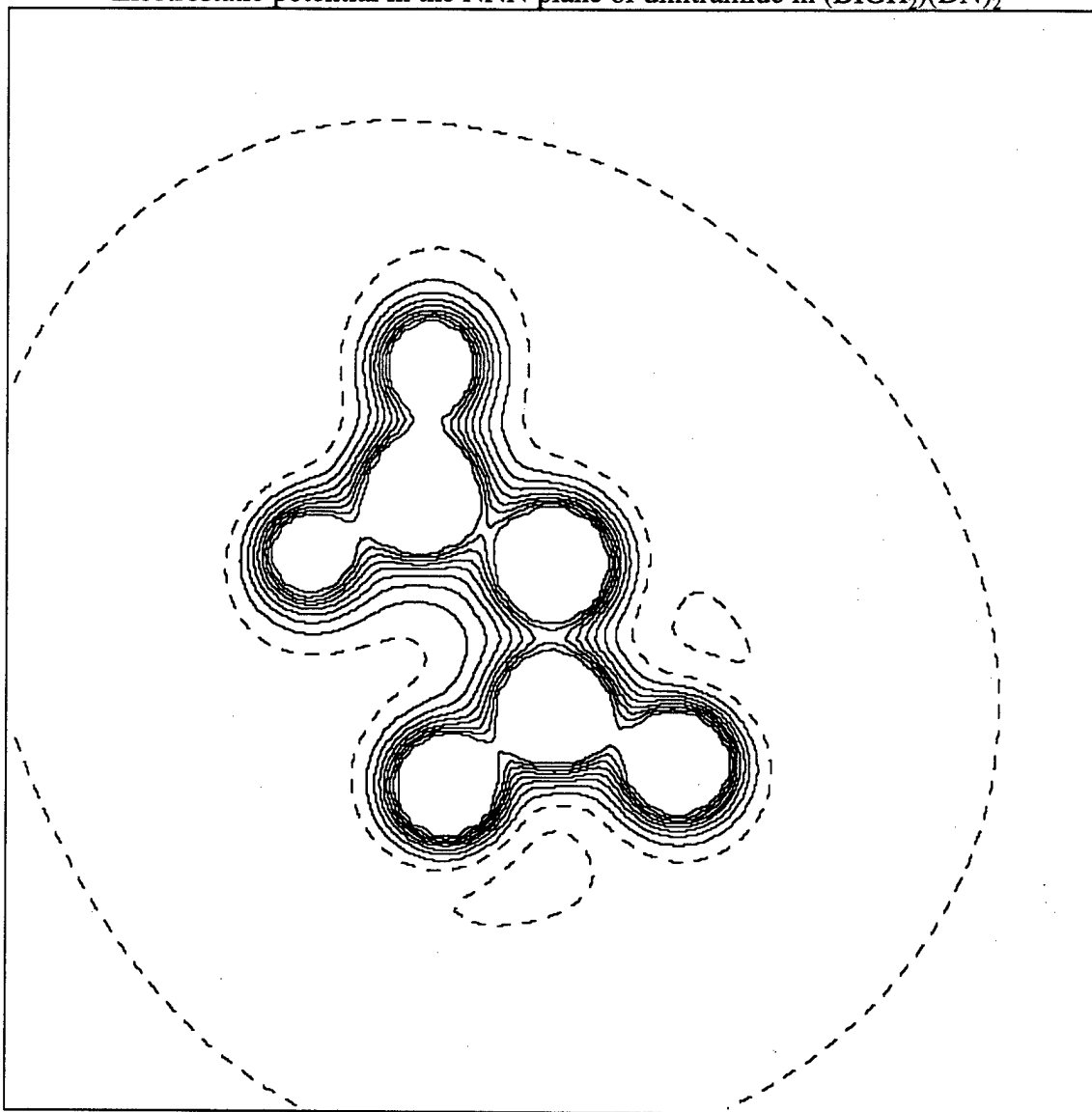
* Atoms on 2-fold axis

Deformation Density in the NNN plane of dinitramide in $(\text{BIGH}_2)(\text{DN})_2$



$0.05\text{e}/\text{\AA}^3$ Contour levels. Negative contours dashed

Electrostatic potential in the NNN plane of dinitramide in (BIGH₂)(DN)₂



0.25 e/Å Contour levels. Negative contours dashed

Value of multipole and associated error for each atom in (BIGH₂)(DN)₂

	ATOM O1	
MONOPOLE	6.313000	0.011195
DIPOL-X	-0.025000	0.007692
DIPOL-Y	0.001000	0.007007
DIPOL-Z	-0.116000	0.007437
4-POL-ZZ	-0.141000	0.007451
4-POL-ZX	-0.018000	0.007232
4-POL-ZY	-0.032000	0.006696

4-PXX-YY	-0.094000	0.007111
4-POL-XY	-0.001000	0.007187
8-POLZZZ	0.015000	0.006649
8-POLXZZ	0.016000	0.006383
8-POLYZZ	0.002000	0.006497
8-PXX-YY	0.009000	0.006275
8-POLXYZ	0.001000	0.006202
8-POLXXX	-0.004000	0.006015
8-POLYYY	0.019000	0.005959

ATOM O2

MONOPOLE	6.284000	0.011693
DIPOL-X	-0.018000	0.007474
DIPOL-Y	0.014000	0.007028
DIPOL-Z	-0.115000	0.007464
4-POL-ZZ	-0.171000	0.007928
4-POL-ZX	-0.012000	0.007390
4-POL-ZY	-0.029000	0.007148
4-PXX-YY	-0.090000	0.007241
4-POL-XY	-0.008000	0.007134
8-POLZZZ	0.004000	0.006920
8-POLXZZ	-0.005000	0.006582
8-POLYZZ	0.013000	0.006213
8-PXX-YY	0.020000	0.006245
8-POLXYZ	-0.012000	0.006437
8-POLXXX	0.013000	0.005938
8-POLYYY	-0.019000	0.006066

ATOM O3

MONOPOLE	6.236000	0.012979
DIPOL-X	-0.043000	0.008312
DIPOL-Y	-0.062000	0.006911
DIPOL-Z	-0.121000	0.007121
4-POL-ZZ	-0.110000	0.007628
4-POL-ZX	0.002000	0.007752
4-POL-ZY	0.028000	0.006878
4-PXX-YY	-0.133000	0.007844
4-POL-XY	-0.020000	0.007717
8-POLZZZ	0.022000	0.006351
8-POLXZZ	0.013000	0.006206
8-POLYZZ	0.027000	0.005793
8-PXX-YY	0.011000	0.005873
8-POLXYZ	0.002000	0.005962
8-POLXXX	0.010000	0.005923
8-POLYYY	0.050000	0.005973

ATOM O4

MONOPOLE	6.201000	0.011855
DIPOL-X	-0.018000	0.006800
DIPOL-Y	0.000000	0.006963
DIPOL-Z	-0.087000	0.007470
4-POL-ZZ	-0.079000	0.007536
4-POL-ZX	-0.011000	0.006403
4-POL-ZY	-0.003000	0.006549
4-PXX-YY	-0.101000	0.007020
4-POL-XY	0.026000	0.007187
8-POLZZZ	0.028000	0.006470

8-POLXZZ	0.002000	0.006091
8-POLYZZ	-0.010000	0.006194
8-PXX-YY	-0.002000	0.006010
8-POLXYZ	0.002000	0.006067
8-POLXXX	0.003000	0.005721
8-POLYYY	0.001000	0.005949

ATOM N1

MONOPOLE	5.015000	0.013913
DIPOL-X	-0.004000	0.006864
DIPOL-Y	-0.173000	0.006564
DIPOL-Z	-0.093000	0.006808
4-POL-ZZ	-0.029000	0.006776
4-POL-ZX	0.008000	0.006371
4-POL-ZY	0.062000	0.006011
4-PXX-YY	0.060000	0.006458
4-POL-XY	0.018000	0.006544
8-POLZZZ	0.103000	0.006685
8-POLXZZ	0.003000	0.006257
8-POLYZZ	-0.011000	0.006365
8-PXX-YY	0.059000	0.006295
8-POLXYZ	-0.012000	0.006247
8-POLXXX	-0.005000	0.006226
8-POLYYY	0.013000	0.006013

ATOM N2

MONOPOLE	5.117000	0.013554
DIPOL-X	0.001000	0.007736
DIPOL-Y	-0.058000	0.009082
DIPOL-Z	0.030000	0.009239
4-POL-ZZ	0.130000	0.008784
4-POL-ZX	0.011000	0.007662
4-POL-ZY	0.017000	0.008197
4-PXX-YY	-0.192000	0.008199
4-POL-XY	-0.004000	0.007293
8-POLZZZ	0.383000	0.010513
8-POLXZZ	0.002000	0.008918
8-POLYZZ	-0.037000	0.010233
8-PXX-YY	0.246000	0.009289
8-POLXYZ	0.014000	0.009148
8-POLXXX	-0.013000	0.008121
8-POLYYY	-0.009000	0.008475

ATOM N3

MONOPOLE	5.119000	0.014508
DIPOL-X	-0.013000	0.007982
DIPOL-Y	-0.055000	0.008842
DIPOL-Z	0.000000	0.009837
4-POL-ZZ	0.204000	0.009638
4-POL-ZX	-0.010000	0.007718
4-POL-ZY	0.048000	0.008734
4-PXX-YY	-0.169000	0.008540
4-POL-XY	-0.071000	0.008229
8-POLZZZ	0.388000	0.011444
8-POLXZZ	0.002000	0.009083
8-POLYZZ	-0.056000	0.010265

8-PXX-YY	0.286000	0.010385
8-POLXYZ	0.007000	0.009839
8-POLXXX	-0.007000	0.008289
8-POLYYY	0.021000	0.008626

ATOM N4

MONOPOLE	2.629000	0.015319
DIPOL-Z	0.020000	0.008812
4-POL-ZZ	0.053000	0.007507
4-PXX-YY	-0.010000	0.007285
4-POL-XY	-0.008000	0.006904
8-POLZZZ	0.169000	0.008098
8-PXX-YY	0.105000	0.007536
8-POLXYZ	0.002000	0.007222

ATOM N5

MONOPOLE	5.091000	0.023005
DIPOL-X	0.013000	0.008949
DIPOL-Y	-0.010000	0.012140
DIPOL-Z	-0.003000	0.012169
4-POL-ZZ	0.071000	0.009983
4-POL-ZX	0.017000	0.008214
4-POL-ZY	0.000000	0.009009
4-PXX-YY	-0.019000	0.009040
4-POL-XY	0.008000	0.008433
8-POLZZZ	0.283000	0.010881
8-POLXZZ	-0.004000	0.008021
8-POLYZZ	-0.001000	0.009080
8-PXX-YY	0.202000	0.009493
8-POLXYZ	-0.016000	0.009264
8-POLXXX	-0.033000	0.008928
8-POLYYY	0.038000	0.009216

ATOM N6

MONOPOLE	5.043000	0.023437
DIPOL-X	-0.038000	0.008325
DIPOL-Y	-0.053000	0.011497
DIPOL-Z	0.008000	0.012213
4-POL-ZZ	0.022000	0.009806
4-POL-ZX	0.001000	0.008678
4-POL-ZY	0.054000	0.009359
4-PXX-YY	-0.013000	0.009429
4-POL-XY	0.018000	0.008727
8-POLZZZ	0.262000	0.010245
8-POLXZZ	-0.003000	0.008056
8-POLYZZ	-0.042000	0.008671
8-PXX-YY	0.175000	0.008816
8-POLXYZ	-0.007000	0.008975
8-POLXXX	0.028000	0.008300
8-POLYYY	0.043000	0.008561

ATOM C1

MONOPOLE	3.756000	0.023252
DIPOL-X	0.004000	0.008654
DIPOL-Y	0.041000	0.010296
DIPOL-Z	0.007000	0.010339

4-POL-ZZ	0.187000	0.009459
4-POL-ZX	0.016000	0.008241
4-POL-ZY	-0.040000	0.009197
4-PXX-YY	-0.176000	0.008237
4-POL-XY	0.004000	0.007959
8-POLZZZ	0.220000	0.010858
8-POLXZZ	-0.005000	0.009280
8-POLYZZ	0.003000	0.011188
8-PXX-YY	0.191000	0.009665
8-POLXYZ	-0.010000	0.009738
8-POLXXX	-0.006000	0.009012
8-POLYYY	-0.011000	0.008709

ATOM H4

MONOPOLE	0.314000	0.011888
DIPOL-Z	0.098000	0.011684
4-POL-ZZ	0.051000	0.016049

ATOM H5B

MONOPOLE	0.709000	0.014969
DIPOL-Z	0.275000	0.016161
4-POL-ZZ	0.090000	0.019730

ATOM H5A

MONOPOLE	0.688000	0.015014
DIPOL-Z	0.289000	0.015205
4-POL-ZZ	0.160000	0.018238

ATOM H6A

MONOPOLE	0.736000	0.015484
DIPOL-Z	0.301000	0.016893
4-POL-ZZ	0.178000	0.019778

ATOM H6B

MONOPOLE	0.749000	0.014904
DIPOL-Z	0.347000	0.016374
4-POL-ZZ	0.150000	0.021031

Contract No. N00014-95-1-0013 and N00014-97-1-0409

Program Officer: R. Miller/J. Goldwasser

**Title: Experimental Charge Densities and Electrostatic Potentials in Energetic
Materials and Infrastructure Upgrade for an X-ray Crystallography
Laboratory**

PI: A. Alan Pinkerton

Department of Chemistry, University of Toledo, Toledo, OH 43606

tel. (419) 530-4580, FAX (419) 530-4033, email apinker@uoft02.utoledo.edu

APPENDIX 2d

Comparison of experimental and theoretical electron density for $\text{BiH}_2\cdot(\text{DN})_2$

An experimental data set of (BIGH₂)(DN)₂ was used to model the electron density using a multipole refinement model. The final coordinates were used as the input into CRYSTALS92. The electron density was modeled using a 6-21G basis set. While CRYSTALS92 produces extensive output, only the point charges and the structure factors are considered here as these are easily compared to the traditional multipole model and to the observed data.

The point charges from CRYSTALS92 are in qualitative agreement with the kappa refinement and in quantitative agreement for the overall charge on each of the ions in the crystal. However, the overall level of agreement with the multipole refinement is much poorer. Although the dinitramide oxygen atom partial charges appear to be in better agreement, the partial charges of the dinitramide nitrogen atoms have differing signs, and the overall charge for each ion is very different.

ATOM	Kappa	Multipole	Theoretical
O1	-0.41(3)	-0.31(1)	-0.220
O2	-0.41(3)	-0.28(1)	-0.231
O3	-0.21(4)	-0.24(1)	-0.221
O4	-0.26(3)	-0.20(1)	-0.229
N1	-0.35(4)	-0.01(1)	-0.184
N2	+0.61(4)	-0.12(1)	+0.299
N3	+0.56(4)	-0.12(1)	+0.296
TOTAL	-0.47	-1.28	-0.49

The structure factors from CRYSTALS92 are calculated with no thermal motion, therefore, they are not directly comparable to those from the multipole refinement. There are a number of possible solutions.

Initially, the thermal motion of the final multipole model is set to zero and the structure factors are recalculated. This allows the multipole structure factor to be directly compared to CRYSTALS92 structure factor. Only those structure factors that are calculated in CRYSTALS92 and were measured experimentally were compared. This gives an $R(F)$ value of 0.0229 (2.3%) for F_{calc} vs F_{theo} based on 1611 reflections, compared to an $R(F)$ for F_{obs} vs F_{calc} of 0.0210 (2.1%) and an $R_w(F)$ of 0.0180 (1.8%) for the same 1611 reflections. This initially suggested that the CRYSTALS92 structure factors are of the same quality as the multipole structure factors.

However, if the observed structure factors are adjusted by the ratio of the low temperature and high temperature calculated structure factors and the simulated 0K observed structure factor is compared to CRYSTALS92, then $R(F)$ is 4.1% and $R_w(F)$ is 4.9% suggesting that the CRYSTALS92 structure factors are significantly further away from the experimental data than the traditional multipole model. Furthermore, comparing the CRYSTALS92 structure factors to an isolated atom model refinement (i.e. a normal spherical atom refinement) with thermal parameters set to 0K produced an $R(F)$ of 1.7%. This result suggests that the theoretical structure factors are overly dominated by purely spherical atoms.

An alternative way of comparing the data is to model the CRYSTALS92 data as though it were experimental data set and look at difference maps. The thermal parameters are held to zero, and the scale factor is held at 1.0 since the data is perfectly scaled already. Anomalous scattering and extinction are also excluded as these are not found in the idealized CRYSTALS92 data. As all the data is equally well known, this allows unit weights to be used. None of the positional parameters are varied as the intention is to model the theoretical data as closely as possible. We can model the 1611 CRYSTALS92 structure factors to a high degree of accuracy, $R(F)=0.80\%$ and $R_w(F)=0.83\%$.

Using a larger basis set with a more limited set of structure factors gives an $R(F)$ value of 0.0247 (2.5%) for F_{calc} vs F_{theo} based on 523 reflections. Again this initially

suggested that the CRYSTALS 92 structure factors are of the same quality as the multipole structure factors, compared to an $R(F)$ of F_{obs} vs F_{calc} of 0.0142 (1.4%) on the same 523 reflections. Thus, the larger basis set CRYSTALS 92 structure factors appear to be of lower quality (!) than the multipole structure factors.

However, if the observed structure factors are adjusted by the ratio of the low temperature and high temperature calculated structure factors and the simulated 0 K observed structure factor is compared to CRYSTALS92, then $R(F)$ is 2.9% and $R_w(F)$ is 3.6% suggesting that the larger basis set of CRYSTALS92 structure factors are closer to the experimental data than the smaller basis set. Furthermore, comparing the CRYSTALS92 structure factors to an isolated atom model refinement (i.e. an ordinary refinement with thermal parameters set to 0K) produced an $R(F)$ of 4.5%. This result suggests that the theoretical structure factors are less dominated by isolated spherical atoms and may be closer to the multipole density.

The CRYSTALS92 data can now be plotted as deformation densities. Comparing the CRYSTALS92 data with two different methodologies means that there is some independent check on the results.

Contract No. N00014-95-1-0013 and N00014-97-1-0409

Program Officer: R. Miller/J. Goldwasser

**Title: Experimental Charge Densities and Electrostatic Potentials in Energetic
Materials and Infrastructure Upgrade for an X-ray Crystallography
Laboratory**

PI: A. Alan Pinkerton

Department of Chemistry, University of Toledo, Toledo, OH 43606

tel. (419) 530-4580, FAX (419) 530-4033, email apinker@uoft02.utoledo.edu

APPENDIX 2e

**Charge Densities and Electrostatic Potentials for Energetic Materials.
Pinkerton, A.A.; and Martin, A., *Mat. Res. Soc. Symp. Proc.*, 1996, 418, 49-53.**

CHARGE DENSITIES AND ELECTROSTATIC POTENTIALS FOR ENERGETIC MATERIALS

A.A. PINKERTON, A. MARTIN

Department of Chemistry, University of Toledo, Toledo, OH 43606

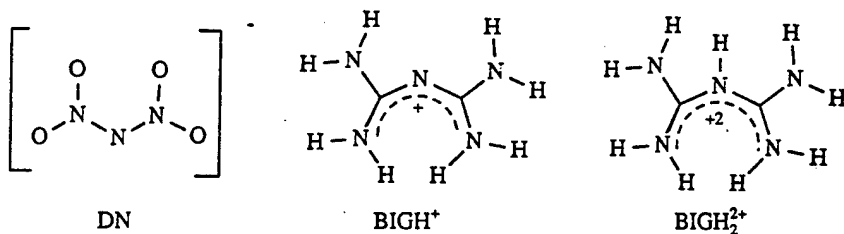
ABSTRACT

High resolution ($\sin\theta/\lambda < 1.34 \text{ \AA}^{-1}$), low temperature (85 K) X-ray diffraction data has been used to map the deformation density and the derived electrostatic potential for three dinitramide salts. The traditional presentation of contour maps has been replaced with 3D views of the molecule. A comparison of the dinitramide ions from each salt is presented.

INTRODUCTION

Charge density studies of energetic materials are not new. However, no intensive study on the effects of the geometry on the charge density and the derived electrostatic potential for any such material has been carried out. A recently reported class [1] of energetic materials is composed of the salts of the dinitramide anion, $\text{N}(\text{NO}_2)_2$, DN. A number of papers have described the characterization and thermal decomposition of the ammonium salt [2-5] and there have been reports of theoretical studies of the anion and the parent acid to gain insight into the possible mechanism of decomposition [6-8]. It is known from room temperature X-ray diffraction studies [9] on a variety of salts that the anion has much structural flexibility, in particular with respect to the amount of molecular twist (from 0 to 45°). At the same time, there are distinct differences in chemically equivalent bond lengths (up to 0.045 \AA for bonds to the bridging nitrogen).

In order to obtain further insight into the bonding and perhaps reactivity of these compounds, we have carried out more detailed X-ray diffraction studies on three such derivatives - the mono- and di-protonated biguanidinium (BIGH^+ and BIGH_2^{2+}) and ammonium salts which span the complete range of torsion angles (5.1 , 28.9 and 42.7° respectively). We have mapped the electron density distribution (reported as the deformation density, i.e. the difference between the total observed electron density and that obtained by the overlap of neutral spherical atoms) for all three compounds. We have also derived the electrostatic potentials for these systems to give insight into the solid state interactions and perhaps a starting point for molecular dynamics calculations



EXPERIMENT

X-ray diffraction data were obtained at 85 K for crystals of (BIGH)(DN), (BIGH₂)(DN)₂ and ADN using an Enraf-Nonius CAD4 automatic diffractometer and an Oxford Cryostream nitrogen gas cooling device. Data were obtained to the limits of the diffractometer ($\sin\theta/\lambda < 1.34 \text{ \AA}^{-1}$). The electron density was modeled using atom centered multipoles [10] and refined to conventional R values of 0.028, 0.026 and 0.022 respectively. The contribution from neutral spherical atoms was subtracted, resultant structure factors calculated and Fourier transformed to obtain deformation density maps. The results of the multipole refinements were also used to derive electrostatic potential maps. These numerical maps were used as input to obtain various 3D color coded maps, ray-traced maps and virtual reality representations of the results.

RESULTS

We now have the data to compare and contrast the deformation densities of the same ion in three different geometries. In order to compare and contrast these large amounts of data we use a combination of color coded 3D cutaway isosurfaces and virtual reality techniques. As this is only meaningful on a computer screen, for the purposes of this paper, we have prepared gray scale ray-traced images to prepare the reader for comparing the data across the experiments. Figures 1, 3 and 5 show the deformation density in the N-N-N plane of the dinitramide anion as a semi-transparent map, + signs indicating a build up of electron density and - signs indicating depletion. The white contour represents a deformation density of 0.0 e/\AA^3 . The atomic positions and bonds have been marked using 0.2 \AA spheres and 0.02 \AA cylinders respectively. Each image is centered in the same place with the longer N-N bond at the top.

In the three figures we see the expected build up of electron density in the bonding and lone pair regions, coupled with depleted regions necessary to obtain charge balance. Strain in the anion is indicated by the fact that the maximum bond density lies off the bond vector of the N-N-N bonds (bent bonds). The deformation density distribution between the 'equivalent' N-N bonds in dinitramide becomes more unsymmetrical as the torsion angle increases. The effect is small in the almost flat anion in (BIGH)(DN) but becomes more pronounced for the severely twisted anion in ADN. There is, however, no correlation with the difference in the two bond lengths ($\Delta \text{N-N}$ 0.023, 0.038 and 0.016 \AA respectively). We also note that the central lone pair in the N-N-N plane becomes more diffuse as the torsion angle increases.

Because of the different torsion angles, no meaningful comparison of the N-O bonding regions nor of the oxygen lone pair regions can be obtained from this representation, however, from the complete 3D maps we observe little difference across the series in these regions.

In figures 2, 4 and 6, we show gray scale cutaway isosurfaces representing the electrostatic potentials for (BIGH)(DN), (BIGH₂)(DN)₂ and ADN. In these figures the longer N-N bond is at the bottom. Although the isolated atom model that we have used should produce an electrostatic potential isolated from the crystal lattice, the influence of the lattice still resides in the electron density and is thus not completely removed from the

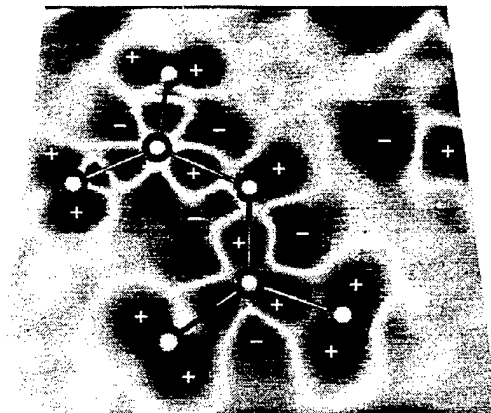
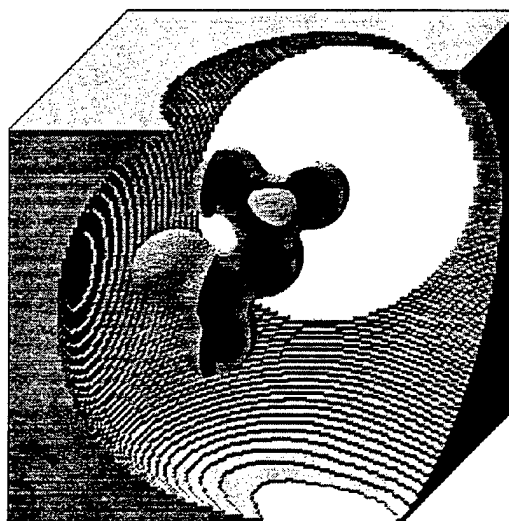


Figure 1: Deformation Density of Dinitramide in (BIGH)(DN)



Electrostatic Potential ($e/\text{\AA}$)
-1.12 2.0

Transparent from -1.02 to -0.48

Figure 2: Electrostatic Potential of Dinitramide from (BIGH)(DN)

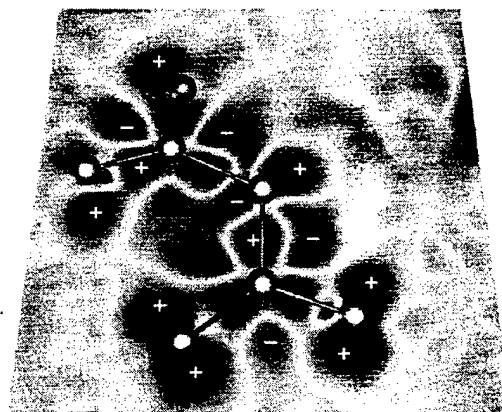
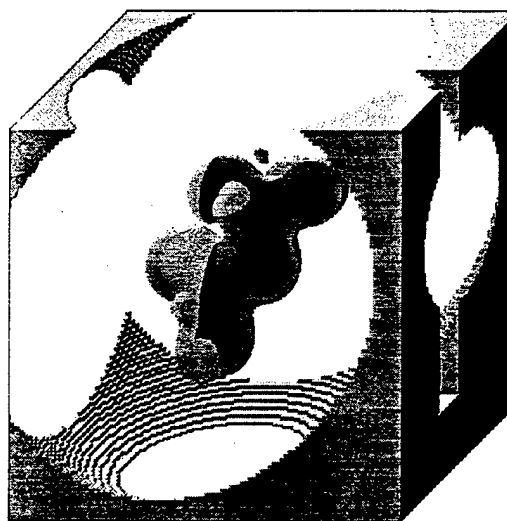


Figure 3: Deformation Density of Dinitramide in $(BIGH_2)(DN)_2$



Electrostatic Potential ($e/\text{\AA}$)
 -0.64 2.0
 Transparent from -0.55 to -0.20

Figure 4: Electrostatic Potential of Dinitramide from $(BIGH_2)(DN)_2$

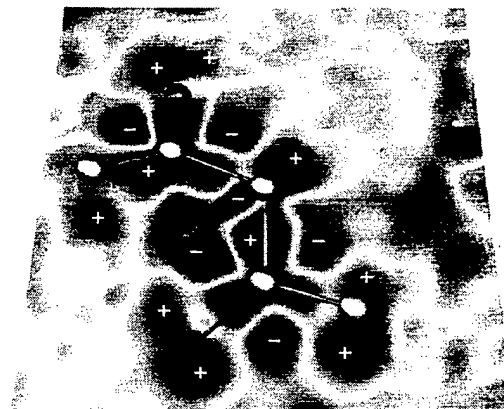
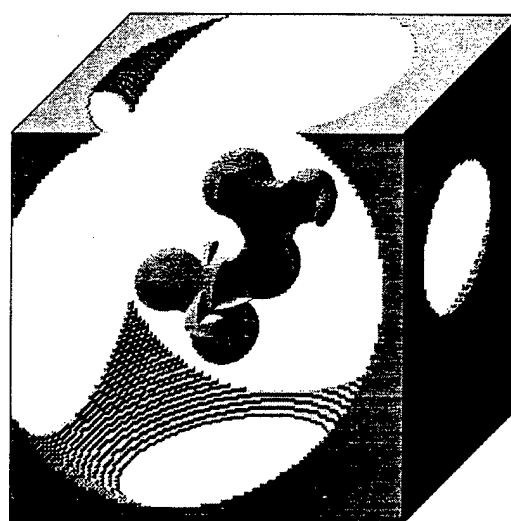


Figure 5: Deformation Density of Dinitramide in ADN



Electrostatic Potential ($e/\text{\AA}$)
-1.09 2.0

Transparent from -1.02 to -0.34

Figure 6: Electrostatic Potential of Dinitramide from ADN

computed potential. Again, we observe a trend with respect to the torsion angle of the anion. In (BIGH)(DN) which has the smallest torsion angle, the most negative region ($-1.12 \text{ e}/\text{\AA}$) lies above the N-N-N plane over a terminal nitrogen atom with another smaller negative region over the other terminal nitrogen atom. A similar situation is observed for (BIGH₂)(DN)₂ with a minimum value of $-0.636 \text{ e}/\text{\AA}$, however, the relationship between the magnitudes of the two minima is reversed with respect to the N-N bond asymmetry. Finally for ADN which has the largest torsion angle, we observe the same asymmetry in the potential with respect to the bond asymmetry as for (BIGH₂)(DN)₂ but now with a minimum value of $-1.09 \text{ e}/\text{\AA}$.

Interestingly, both *ab-initio* and semi-empirical calculations [9] produce electrostatic potentials for the gas phase ions that have the most negative region in the N-N-N plane near to the bridging nitrogen. Thus, we suggest that the use of experimental electrostatic potentials obtained from X-ray crystallography should give a more reliable starting point for understanding solid state reactivities, e.g. by the use of molecular dynamics calculations.

ACKNOWLEDGMENTS

The authors would like to thank the Office of Naval Research for financial support (Contract Nos. N00014-93-1-0597 and N00014-95-1-0013).

REFERENCES

1. J.C. Bottaro, R.J. Schmitt, P.E. Penwell and D.S. Ross, U.S. Pat. 5,198,204 and 5,254,324 (1991).
2. T.B. Brill, P.J. Brush and D.G. Patil, Combust. Flame, 92, 7788 (1991).
3. R.J. Doyle, Org. Mass Spectrom. 28, 83 (1993).
4. M.J. Rossi, J.C. Bottaro and D.F. McMillen, Int. J. Chem. Kinet. 25, 549 (1993).
5. R.J. Schmitt, M. Krempp and V.M. Bierbaum, Int. J. Mass Spectrom. Ion Processes 117, 612 (1992).
6. H.H. Michels and J.A. Montgomery Jr., J. Phys. Chem., 97, 6602 (1993).
7. P. Politzer and J.M. Seminario, Chem. Phys. Lett., 216, 348 (1993).
8. P. Politzer, J.M. Seminario, M.C. Concha and P.C. Redfern, J. Mol. Struct. THEOCHEM, 287, 235 (1993).
9. A. Martin, A.A. Pinkerton, R.D. Gilardi and J.C. Bottaro, to be published.
10. N.K. Hansen and P. Coppens, Acta Cryst., A34, 909 (1978).

Contract No. N00014-95-1-0013 and N00014-97-1-0409

Program Officer: R. Miller/J. Goldwasser

**Title: Experimental Charge Densities and Electrostatic Potentials in Energetic
Materials and Infrastructure Upgrade for an X-ray Crystallography
Laboratory**

PI: A. Alan Pinkerton

Department of Chemistry, University of Toledo, Toledo, OH 43606

tel. (419) 530-4580, FAX (419) 530-4033, email apinker@uoft02.utoledo.edu

APPENDIX 3a

**Anisotropic Thermal Expansion of Potassium Dinitramide - A Variable
Temperature Crystallographic Study**

**Hardie, M.J.; Martin, A. and Pinkerton, A.A., *Chem. Mater.*, submitted for
publication.**

Anisotropic Thermal Expansion of Potassium Dinitramide - A Variable Temperature Crystallographic Study

Michaele J. Hardie,¹ Anthony Martin and A. Alan Pinkerton*

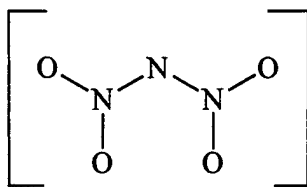
Department. of Chemistry, University of Toledo, Toledo, OH 43606, USA

Abstract

The single crystal X-ray structure of potassium dinitramide (KDN), has been determined at temperatures ranging from 85 - 298 K and the thermal expansion tensor calculated. The thermal expansion is strongly anisotropic and correlated to the atomic displacement parameters. A rigid body analysis of the dinitramide anion shows that the thermal motion is well represented by rigid body translations and librations. The curvature of the temperature dependence of the thermal motion is in agreement with an anharmonic contribution to the mean field potential. The Debye temperatures corresponding to the eigenvalues of the potassium thermal displacement tensor and to the dinitramide rigid body translation tensor have been estimated.

Introduction

The dinitramide ion $\text{N}(\text{NO}_2)_2$ (1) is an inorganic member of the nitramine class of compounds, which have been extensively studied due to their applications as explosives and low signature propellants.^{2,3} The first reported synthesis of a dinitramide compound was of the ammonium salt.⁴ Since that time there has been intense activity, a number of authors having reported syntheses of various dinitramide salts, their structural characterization, spectral properties, details of their thermal decomposition as well as theoretical studies of their structure, bonding and decomposition.⁵



1

There is current interest in the anisotropic properties of energetic materials, especially with respect to shock sensitivity.⁶ In this study we report the determination of the thermal expansion of potassium dinitramide (KDN) using single crystal X-ray diffraction techniques at temperatures ranging from 85 to 298 K, as well as the variation in the thermal displacement parameters with respect to temperature. The anisotropy of the thermal expansion is analyzed with respect to the thermal motion of the potassium cations and the rigid body motion of the dinitramide anions.

Experimental

A crystal of KDN suitable for single crystal diffraction studies, 0.34 x 0.14 x 0.08 mm, was mounted on a fine glass fiber with epoxy resin. Preliminary examination and data collection were carried out at ambient temperature with a Siemens SMART Platform diffractometer. In subsequent experiments, the crystal was cooled by nitrogen gas using an Oxford Cryostream system. Data collections were carried out at 298(1), 250(1), 200(1), 150(1), 100(1) and 85(1) K. 0.3° omega scans were performed at three different phi settings corresponding to a nominal hemisphere of data. The frame time was set at 20 seconds for all experiments. The unit cell parameters were determined at each temperature from the observed XYZ centroids for the complete data set. The intensities were corrected for absorption and decay using SADABS.⁷ The structures were solved by direct methods using SHELXS.⁸ Refinement for each structure was performed by full matrix least-squares on F^2 using SHELXL.⁹ All atoms were refined with anisotropic displacement parameters.

Details of the data collections and refinements at all six temperatures are given in Table 1. A rigid body analysis¹⁰ of the dinitramide anion was performed for each temperature using unit weights for each atom. Thermal expansion tensors were calculated from changes in the Bragg angle with temperature for all reflections across all six data sets with the program ALPHA.¹¹ The changes in d were constrained to be linear with respect to temperature (vide infra).

Results and Discussion

The single crystal X-ray structure of potassium dinitramide has been previously reported.¹² KDN crystallizes in space group $P2_1/n$ with $a = 6.6162(2)$, $b = 9.2831(2)$, $c = 7.2000(3)$ Å, $\beta = 97.583(1)^\circ$ at room temperature. The asymmetric unit consists of a single dinitramide anion and potassium cation shown, with room temperature atomic displacement parameters, in Figure 1.

The unit cell lengths and cell volume decrease on cooling with the b axis being the most sensitive to change of temperature. The β cell angle increases with decreasing temperature. The variation of unit cell parameters with temperature normalized to the room temperature cell are shown in Figure 2. The temperature dependence of all unit cell parameters are close to linear, with the worst correlation coefficient for the β parameter being 0.987. The calculated linear relationships between temperature and cell parameters are given in Table 2. It is because of this observed linearity that the variation in d with temperature was constrained to be linear for the determination of the thermal expansion tensor (vide infra).

The previously noted⁵ discrepancy between 'equivalent' bond lengths N1-N2 and N1-N3 is again apparent with an N1-N2 length of 1.388(2) Å and an N1-N3 length of 1.353(2) Å at room temperature. The contacts between the potassium cation and the oxygen atoms of the dinitramide anion decrease linearly with decreasing temperature as

expected from the unit cell variation. At room temperature the closest contacts between the potassium cation and nitro oxygens of the dinitramide anion range from 2.810(2) to 2.947(2) Å, at 85(1) K the contacts range from 2.7800(12) to 2.9159(12) Å. The libration corrected bond lengths within the dinitramide ion at all six of the temperatures show only minimal expansion (average 0.002 Å) with temperature, with a maximum value of 0.004 Å from 85 to 298 K.

Atomic displacement parameters decrease with lowered temperature. A representative plot of U_{eq} against temperature is shown in Figure 3. Fitting the U_{eq} 's to a straight line produces a good fit ($R = 0.990$ to 0.996), but with intercepts that have a high probability of being zero. This is physically unreasonable as, even at 0 K, there will be some displacement due to the zero point energy. Fitting the U_{eq} values to a quadratic polynomial produces a statistically better fit, showing a small but significant T^2 dependency (Table 3). The T^2 dependence of the U_{eq} values is due to the use of the harmonic oscillator approximation to model the anharmonic motion that must be present (in order for the crystal to expand).¹³

A rigid body analysis of the dinitramide ion using the TLS formalism was performed. The S matrix was small enough to be neglected in all cases. The eigenvalues of the libration tensor show significant librational motion (largest value, 0.0235 rad² at 298 K) with a small T^2 dependence (Figure 4), typical of an anharmonic mean field potential. The largest of the translational eigenvalues is 0.0339 Å² at 298 K. The translational eigenvalues also have a non-negligible T^2 dependence (Figure 5), however, the T_{ij} values also contain the systematic errors of the anisotropic thermal parameters.¹⁴

Thermal expansion is represented by a symmetrical second-rank tensor $[\alpha_{ij}]$. The tensor components, α_{ij} , were calculated from a least-squares fit to changes in d values with respect to temperature.¹¹

KDN has a monoclinic unit cell, so that two of the off-diagonal terms of the tensor must be zero and one axis of the tensor must be parallel to the crystallographic b

axis. The α_{ij} values are presented in Table 4 for each temperature range followed by the average for the whole temperature range. The corresponding eigenvalues and eigenvectors of the thermal expansion tensor are presented in Table 5. A representation of the thermal expansion tensor and the principal axes given by their eigenvalues and vectors visualized as an ellipsoid in a unit cell is shown (Figure 6). The ellipsoid has been scaled such that the largest principal axis is identical to the b axial length. KDN expands along the b -axis $[0\ 1\ 0]$ more than three times as much as any other direction. α_1 and α_2 lie approximately along $[1\ 0\ -1]$ and $[1\ 0\ 1]$ respectively. We note that the direction of greatest expansion coincides with the largest components of the displacement tensor of the potassium ions and the translation tensor of the dinitramide anions averaged over all positions in the unit cell.

Thermal expansion cannot occur unless the potential in which the atoms vibrate is anharmonic. The potential becomes less anharmonic as the temperature decreases. Therefore, if the atoms appear to move as the crystal is cooled they move toward positions that are better described by the harmonic oscillator model. Based on the hypothesis¹³ that the displacements of highest amplitude will correspond to those of highest anharmonicity, the direction of maximum thermal expansion should indeed correlate with the largest components of the displacement tensors averaged over the equivalent positions in the unit cell as observed. In addition, the other eigenvectors of the symmetry averaged potassium displacement tensor and dinitramide translation tensor are also approximately along $[1\ 0\ -1]$ and $[1\ 0\ 1]$ in close correspondence with α_1 and α_2 of the thermal expansion tensor.

Although not rigorously appropriate, we have used a modification of the Debye theory to estimate the Debye temperature, θ_D , corresponding to the eigenvalues of the potassium displacement tensor and dinitramide translation tensor. By evaluation of

$$\frac{4\pi^2 m v \langle u_i \rangle^2}{h} = \frac{1}{2} + \frac{1}{e^{\hbar\nu/k_B T} - 1}$$

for each eigenvalue u_i , where m is the mass of the vibrating ion, a numerical solution was obtained for the characteristic frequency, ν . This frequency was then used to obtain θ_D from the relationship¹⁵

$$\theta_D = \frac{h\nu}{k_B}$$

The results are reported in Table 6.

Acknowledgments

We thank the College of Arts and Sciences of the University of Toledo and the Ohio Board of Regents for generous financial support of the X-ray diffraction facility and thank the Office of Naval Research for funding this work. (Contract No. N00014-95-1-0013).

Supporting Information Available

Tables S1 - S13 with complete crystallographic details, refined atomic coordinates, bond distances and angles, anisotropic displacement parameters for all six temperatures. Ordering information is given on any current masthead page.

References

1. Present address: Department of Chemistry, Monash University, Clayton, Victoria 3168, Australia.
2. Yinon, J.; Zitrin, S. *The Analysis of Explosives*, Pergamon Press, Oxford, 1981.
3. Olah, G.A.; Squire, R.D. (editors) *Chemistry of Energetic Materials*, Academic Press, San Diego, 1991.
4. Bottaro, J.C.; Schmitt, R.J.; Penwell, P.E.; Ross, D.S. **1993** US patents 5,198,204 and 5,254,324; Bottaro, J.C.; Penwell, P.E.; Schmitt, R.J. *J. Synth. Commun.* **1991**, *21*, 945.
5. Tanbug, R.; Kirschbaum, K.; Pinkerton, A.A.; *J. Chem. Crystallogr.* **1999**, in press, and references therein.
6. Jindal, V.K.; Dlott, D.D. *J. Appl. Phys.* **1998**, *83*, 5203.
7. Sheldrick, G.M. SADABS, Univ. Göttingen, 1996.
8. Sheldrick, G.M. SHELXS-86, Univ. Göttingen, 1986.
9. Sheldrick, G.M. SHELXL-93, Univ. Göttingen, 1993.
10. Schomaker, V.; Trueblood, K.N. (1968), *Acta Cryst.* **1968**, *B24*, 63.
11. Jessen, S.M.; Küppers, H. *J. Appl. Cryst.* **1991**, *24*, 239.
12. Gilardi, R.; Flippen-Anderson, J.; George, C.; Butcher, R.J. *J. Am. Chem. Soc.* **1997**, *119*, 9411; Gidaspov, B.V.; Tselinskii, I.V.; Mel'nikov, V.V.; Margolis, N.V.; Grigor'eva, N.V. *Russ. J. Gen. Chem.* **1995**, *65*, 906.
13. Chen, Y.-S.; Martin, A.; Pinkerton, A.A., to be published.
14. Chandrasekhar, K.; Bürgi, H.B. *Acta. Cryst.* **1984**, *B40*, 387.
15. Coppens, P. *X-Ray Charge Densities and Chemical Bonding*, Oxford University Press, 1997.

Figure Captions

1. Potassium dinitramide at 298 K (50% probability ellipsoids).
2. Variation of unit cell parameters (normalized to the room temperature cell) with temperature for KDN.
3. Variation of U_{eq} with temperature for KDN.
4. Variation of the eigenvalues of the librational tensor with temperature for the dinitramide anion.
5. Variation of the eigenvalues of the translation tensor with temperature for the dinitramide anion.
6. Representation of the thermal expansion tensor in the unit cell for KDN. The size of the ellipsoid is scaled such that the largest principal axis is identical to b .

Table 1: Summary of data collection and structure refinement of potassium dinitramide at variable temperatures.

Empirical formula	KN ₃ O ₄									
Formula weight	145.13									
Wavelength	0.71073 Å									
Crystal system	Monoclinic									
Space group	<i>P</i> 2 ₁ / <i>n</i>									
Crystal size	0.34 x 0.14 x 0.08 mm									
Z	4									
F(000)	288									
Temperature (K)	298(1)	250(1)	200(1)	150(1)	100(1)	85(1)				
<i>a</i> (Å)	6.6162(2)	6.61140(10)	6.6029(4)	6.6010(3)	6.5918(4)	6.5891(4)				
<i>b</i> (Å)	9.2831(2)	9.2299(2)	9.1694(5)	9.1253(5)	9.0778(5)	9.0653(5)				
<i>c</i> (Å)	7.2000(3)	7.1878(2)	7.1731(4)	7.1657(4)	7.1540(4)	7.1459(4)				
β (°)	97.583(1)	97.639(1)	97.805(1)	97.890(1)	97.946(2)	97.975(2)				
Volume (Å ³)	438.35(2)	434.73(2)	430.27(4)	427.55(4)	423.98(4)	422.71(4)				
Density (calc) (Mg/m ³)	2.199	2.217	2.240	2.255	2.274	2.280				
Absorption coeff. (mm ⁻¹)	1.130	1.140	1.152	1.159	1.169	1.172				
θ range (°)	3.60 to 28.29	3.61 to 28.33	3.63 to 28.30	3.64 to 28.28	3.65 to 28.36	3.65 to 28.33				
Reflections collected	3648	3613	3510	3517	3547	3515				
Independent reflections	1084	1073	1060	1046	1041	1034				
Reflections with I>2σ(I)	854	882	911	917	918	902				
R _{int}	0.0570	0.0499	0.0402	0.0402	0.0463	0.0484				
Data / restraints / parameters	1084 / 0 / 73	1073 / 0 / 73	1060 / 0 / 73	1046 / 0 / 73	1041 / 0 / 73	1034 / 0 / 73				
Goodness-of-fit on F ²	0.983	0.996	1.004	1.039	0.996	1.023				
R1 [I>2σ(I)]	0.0391	0.0330	0.0315	0.0302	0.0294	0.0311				
wR2 [I>2σ(I)]	0.0944	0.0768	0.0750	0.0697	0.0664	0.0717				
R1 (all data)	0.0507	0.0417	0.0372	0.0356	0.0361	0.0399				
wR2 (all data)	0.0996	0.0809	0.0773	0.0717	0.0683	0.0749				
Largest diff. peak (e Å ⁻³)	0.429	0.306	0.359	0.363	0.533	0.552				
Largest diff. hole (e Å ⁻³)	-0.378	-0.432	-0.351	-0.386	-0.595	-0.601				

Table 2: Linear regression results of the unit cell parameters vs temperature for potassium dinitramide.

Y	m	C	R	RMS
a (Å)	1.244×10^{-4}	6.580	0.989	0.002
b (Å)	1.01×10^{-3}	8.975	0.995	0.006
c (Å)	2.403×10^{-4}	7.128	0.995	0.002
β (°)	-1.907×10^{-3}	98.150	0.987	0.029
V (Å ³)	7.231×10^{-2}	416.54	0.996	0.391

All lines have the form $Y = mT + C$, where Y is the appropriate unit cell parameter, T the temperature, R the correlation coefficient, and RMS the root mean square residual.

Table 3: Linear regression results of the U_{eq} 's vs temperature for potassium dinitramide.

Y (\AA^2)	a (\AA^2)	b ($\text{\AA}^2 \text{K}^{-1}$)	c ($\text{\AA}^2 \text{K}^{-2}$)	R	RMS (\AA^2)
K1	7.32×10^{-3}	2.5×10^{-5}	2.15×10^{-7}	1.000	0.064×10^{-3}
O1	7.03×10^{-3}	6.4×10^{-5}	2.36×10^{-7}	1.000	0.26×10^{-3}
O2	7.48×10^{-3}	5.4×10^{-5}	2.42×10^{-7}	1.000	0.21×10^{-3}
O3	9.70×10^{-3}	1.1×10^{-5}	2.83×10^{-7}	0.999	0.45×10^{-3}
O4	8.95×10^{-3}	2.4×10^{-5}	2.79×10^{-7}	1.000	0.27×10^{-3}
N1	8.06×10^{-3}	2.4×10^{-5}	2.04×10^{-7}	0.999	0.44×10^{-3}
N2	5.28×10^{-3}	4.1×10^{-5}	1.65×10^{-7}	1.000	0.15×10^{-3}
N3	6.75×10^{-3}	1.1×10^{-5}	2.02×10^{-7}	1.000	0.14×10^{-3}
Average	7.57×10^{-3}	3.2×10^{-5}	2.28×10^{-7}	1.000	0.10×10^{-3}

All lines have the form $Y = cT^2 + bT + a$, where Y is the appropriate U_{eq} parameter, T the temperature, R the correlation coefficient, and RMS the root mean square residual.

Table 4: Tensor components of thermal expansion ($10^{-6} \text{\AA K}^{-1}$) for potassium dinitramide

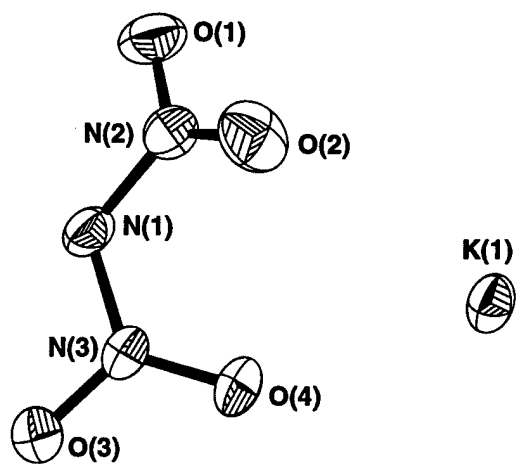
T(K)	α_{11}	α_{22}	α_{33}	α_{12}	α_{13}	α_{23}
85-100	23.8(2)	110.0(2)	34.5(2)	0.0	14.9(2)	0.0
100-150	23.8(2)	109.7(2)	34.5(2)	0.0	14.8(2)	0.0
150-200	23.9(2)	109.4(2)	34.5(2)	0.0	14.7(2)	0.0
200-250	23.9(2)	109.0(2)	34.5(2)	0.0	14.6(2)	0.0
250-298	23.9(2)	108.6(2)	34.6(2)	0.0	14.6(2)	0.0
85 - 298	23.86(5)	109.3(6)	34.52(4)	0.0	14.7(1)	0.0

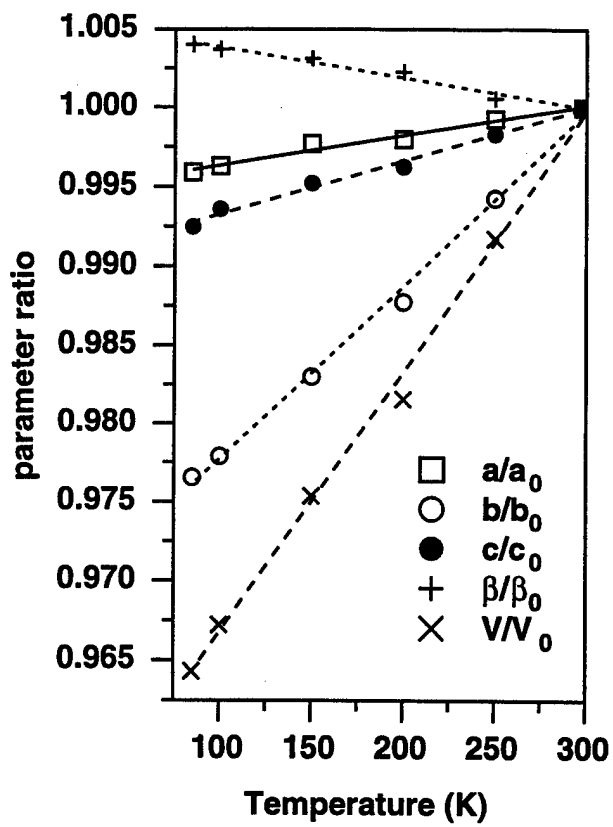
Table 5: Eigenvalues ($10^{-6} \text{ \AA K}^{-1}$) and Eigenvectors of the thermal expansion tensor.

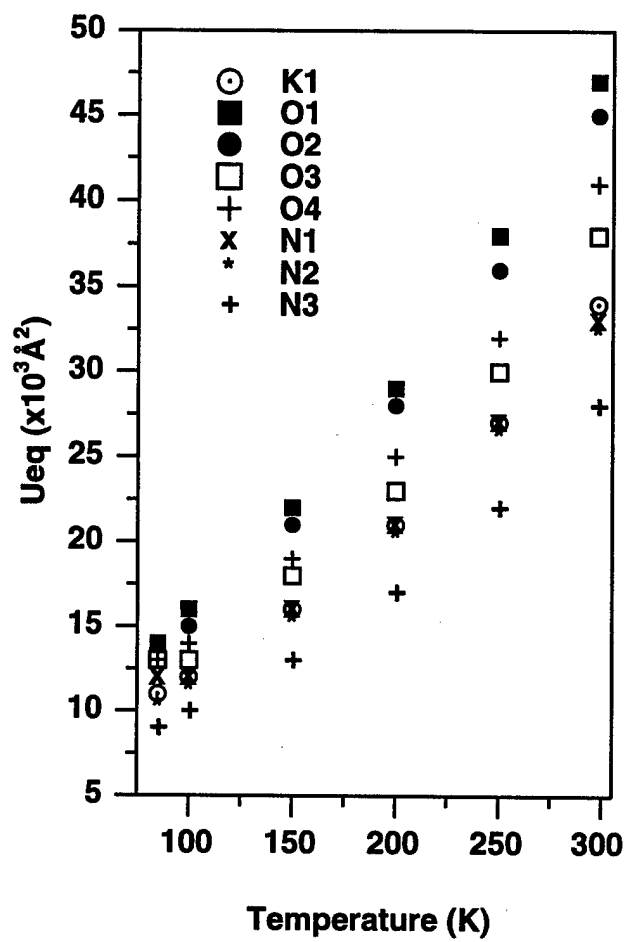
Temperature range (K)	Principal axes	Eigenvalue	Eigenvector		
85-100	α_1	13.3(2)	-0.818(3)	0.000	0.576(4)
	α_2	44.9(2)	0.576(4)	0.000	0.818(3)
	α_3	110.2(2)	0.000	-1.000	0.000
100-150	α_1	13.4(2)	-0.818(3)	0.000	0.576(4)
	α_2	44.9(2)	0.576(4)	0.000	0.818(3)
	α_3	109.7(2)	0.000	-1.000	0.000
150-200	α_1	13.5(2)	-0.818(3)	0.000	0.575(4)
	α_2	44.8(2)	0.575(4)	0.000	0.818(3)
	α_3	109.3(2)	0.000	-1.000	0.000
200-250	α_1	13.7(2)	-0.819(3)	0.000	0.574(4)
	α_2	44.8(2)	0.574(4)	0.000	0.819(3)
	α_3	109.0(2)	0.000	-1.000	0.000
250-298	α_1	13.8(2)	-0.819(3)	0.000	0.573(4)
	α_2	44.8(2)	0.573(4)	0.000	0.819(3)
	α_3	108.6(2)	0.000	-1.000	0.000
85-298	α_1	13.5(2)	-0.8184(5)	0.000	0.575(1)
	α_2	44.84(5)	0.575(1)	0.000	0.8184(5)
	α_3	109.4(6)	0.000	-1.000	0.000

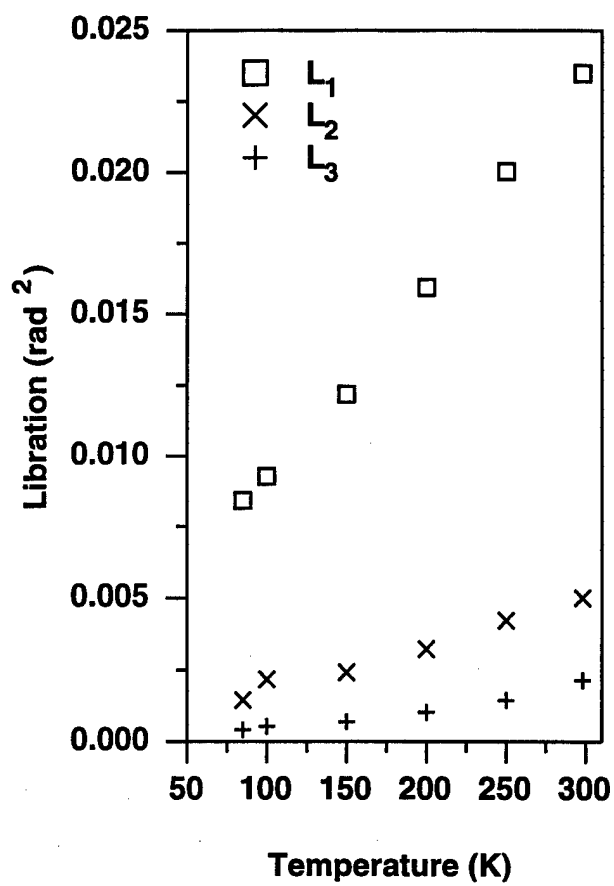
Table 6. Range of estimated Debye temperatures, θ_D , corresponding to the eigenvalues of the potassium displacement tensor and dinitramide translation tensor for six temperatures.

K^+	U_1	127.5 - 140.9 K
	U_2	98.4 - 109.5 K
	U_3	90.8 - 95.3 K
DN^-	U_1	62.5 - 68.5 K
	U_2	70.5 - 78.9 K
	U_3	77.3 - 85.0 K

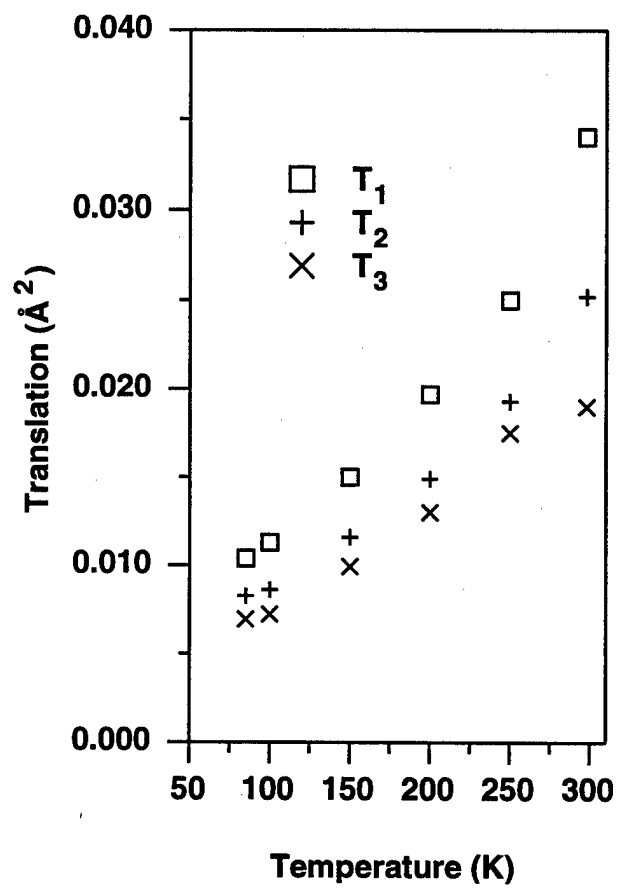




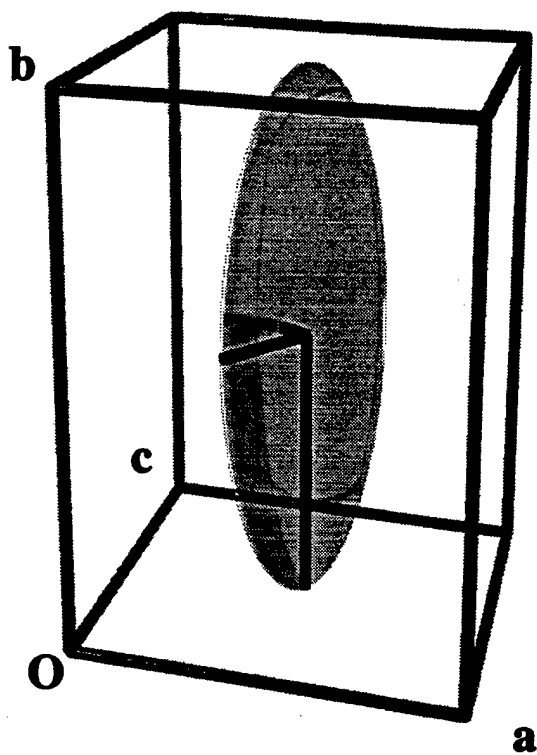




Häselke et al. Fig. 4



Herche et al. Fig 5



Huethe et al Fig 6

Table S1. Atomic coordinates and equivalent isotropic displacement parameters (\AA^2) for potassium dinitramide at room temperature (298 K). $U(\text{eq})$ is defined as one third of the trace of the orthogonalized U_{ij} tensor.

	x	y	z	$U(\text{eq})$
K1	0.85793(7)	0.34205(5)	0.82918(7)	0.0341(2)
N1	0.7576(3)	0.3765(2)	0.4044(3)	0.0328(4)
N2	0.6491(3)	0.4622(2)	0.2679(3)	0.0321(4)
N3	0.9470(3)	0.3414(2)	0.3683(2)	0.0279(4)
O1	0.4650(2)	0.4611(2)	0.2786(3)	0.0472(5)
O2	0.7282(3)	0.5379(2)	0.1588(3)	0.0455(4)
O3	0.0578(2)	0.2952(2)	0.5078(2)	0.0377(4)
O4	0.0067(3)	0.3452(2)	0.2134(2)	0.0409(4)

Table S2. Anisotropic displacement parameters (\AA^2) for potassium dinitramide at 298 K. The anisotropic displacement factor exponent takes the form:
 $-2\pi^2[(ha^*)^2U_{11} + \dots + 2hka^*b^*U_{12}]$

	U11	U22	U33	U23	U13	U12
K1	0.0340(3)	0.0406(3)	0.0296(3)	0.0006(2)	0.0113(2)	-0.0047(2)
N1	0.0330(10)	0.0364(10)	0.0316(10)	0.0047(7)	0.0146(8)	0.0073(7)
N2	0.0337(9)	0.0285(9)	0.0346(10)	-0.0033(7)	0.0065(8)	0.0009(7)
N3	0.0300(9)	0.0294(9)	0.0259(9)	-0.0021(6)	0.0102(7)	-0.0016(6)
O1	0.0327(9)	0.0525(10)	0.0575(12)	-0.0044(8)	0.0100(8)	0.0101(7)
O2	0.0484(11)	0.0407(9)	0.0472(11)	0.0145(7)	0.0053(8)	-0.0032(7)
O3	0.0388(9)	0.0458(9)	0.0285(8)	0.0022(7)	0.0042(7)	0.0076(7)
O4	0.0374(9)	0.0612(11)	0.0269(9)	0.0022(7)	0.0148(7)	0.0045(7)

Table S3. Atomic coordinates and equivalent isotropic displacement parameters (\AA^2) for potassium dinitramide at 250 K. $U(\text{eq})$ is defined as one third of the trace of the orthogonalized U_{ij} tensor.

	x	y	z	$U(\text{eq})$
K1	0.85870(6)	0.34234(4)	0.82994(5)	0.02730(15)
N1	0.7581(2)	0.3764(2)	0.4055(2)	0.0270(3)
N2	0.6491(2)	0.46221(15)	0.2686(2)	0.0259(3)
N3	0.9479(2)	0.34133(14)	0.3694(2)	0.0220(3)
O1	0.4645(2)	0.46136(15)	0.2790(2)	0.0377(3)
O2	0.7276(2)	0.53794(14)	0.1571(2)	0.0363(3)
O3	0.0592(2)	0.29509(14)	0.5097(2)	0.0302(3)
O4	0.0075(2)	0.34456(14)	0.2139(2)	0.0323(3)

Table S4. Anisotropic displacement parameters (\AA^2) for potassium dinitramide at 250 K. The anisotropic displacement factor exponent takes the form:
 $-2\pi^2[(ha^*)^2U_{11} + \dots + 2hka^*b^*U_{12}]$

	U_{11}	U_{22}	U_{33}	U_{23}	U_{13}	U_{12}
K1	0.0263(2)	0.0343(2)	0.0216(2)	0.00040(13)	0.00464(14)	-0.00368(13)
N1	0.0263(8)	0.0312(8)	0.0248(7)	0.0040(6)	0.0076(6)	0.0065(6)
N2	0.0276(7)	0.0244(7)	0.0252(7)	-0.0030(5)	0.0017(6)	0.0010(5)
N3	0.0236(7)	0.0238(7)	0.0188(7)	-0.0008(5)	0.0038(5)	-0.0017(5)
O1	0.0236(7)	0.0456(8)	0.0435(8)	-0.0045(6)	0.0035(6)	0.0074(5)
O2	0.0385(8)	0.0343(7)	0.0349(7)	0.0117(5)	0.0009(6)	-0.0024(5)
O3	0.0301(7)	0.0390(7)	0.0202(6)	0.0019(5)	-0.0015(5)	0.0061(5)
O4	0.0283(7)	0.0506(8)	0.0193(6)	0.0017(5)	0.0078(5)	0.0042(5)

Table S5. Atomic coordinates and equivalent isotropic displacement parameters (\AA^2) for potassium dinitramide at 200 K. $U(\text{eq})$ is defined as one third of the trace of the orthogonalized U_{ij} tensor.

	x	y	z	$U(\text{eq})$
K1	0.85932(5)	0.34264(4)	0.83074(5)	0.02090(14)
O4	0.0087(2)	0.34421(13)	0.2144(2)	0.0251(3)
O2	0.7270(2)	0.53812(13)	0.1565(2)	0.0277(3)
N2	0.6490(2)	0.46223(14)	0.2684(2)	0.0198(3)
O1	0.4642(2)	0.46145(14)	0.2792(2)	0.0287(3)
N1	0.7587(2)	0.3766(2)	0.4063(2)	0.0212(3)
N3	0.9489(2)	0.34099(13)	0.3703(2)	0.0170(3)
O3	0.0607(2)	0.29491(13)	0.5113(2)	0.0233(3)

Table S6. Anisotropic displacement parameters (\AA^2) for potassium dinitramide at 200 K. The anisotropic displacement factor exponent takes the form:
 $-2\pi^2[(ha^*)^2U_{11} + \dots + 2hka^*b^*U_{12}]$

	U11	U22	U33	U23	U13	U12
K1	0.0205(2)	0.0264(2)	0.0162(2)	0.00034(11)	0.00371(13)	-0.00291(12)
N1	0.0208(7)	0.0240(7)	0.0196(7)	0.0033(5)	0.0061(5)	0.0055(5)
N2	0.0218(7)	0.0182(6)	0.0189(6)	-0.0021(5)	0.0014(5)	0.0008(5)
N3	0.0192(7)	0.0180(6)	0.0140(6)	-0.0008(4)	0.0031(5)	-0.0015(4)
O1	0.0178(6)	0.0345(7)	0.0336(7)	-0.0029(5)	0.0030(5)	0.0055(5)
O2	0.0301(7)	0.0266(6)	0.0256(6)	0.0090(5)	0.0014(5)	-0.0020(5)
O3	0.0244(6)	0.0295(6)	0.0150(5)	0.0014(5)	-0.0012(4)	0.0043(5)
O4	0.0227(6)	0.0392(7)	0.0144(6)	0.0009(4)	0.0065(5)	0.0030(5)

Table S7. Atomic coordinates and equivalent isotropic displacement parameters (\AA^2) for potassium dinitramide at 150 K. $U(\text{eq})$ is defined as one third of the trace of the orthogonalized U_{ij} tensor.

	x	y	z	$U(\text{eq})$
K1	0.85986(5)	0.34296(3)	0.83151(4)	0.01590(13)
N1	0.7594(2)	0.37658(14)	0.4071(2)	0.0163(3)
N2	0.6489(2)	0.46223(13)	0.2683(2)	0.0152(3)
N3	0.9499(2)	0.34079(12)	0.3713(2)	0.0131(3)
O1	0.4639(2)	0.46152(13)	0.2799(2)	0.0219(3)
O2	0.7268(2)	0.53839(12)	0.1558(2)	0.0207(3)
O3	0.0620(2)	0.29468(12)	0.51298(14)	0.0178(2)
O4	0.0097(2)	0.34379(12)	0.2150(2)	0.0190(3)

Table S8. Anisotropic displacement parameters (\AA^2) for potassium dinitramide at 150 K. The anisotropic displacement factor exponent takes the form:
 $-2\pi^2[(ha^*)^2U_{11} + \dots + 2hka^*b^*U_{12}]$

	U_{11}	U_{22}	U_{33}	U_{23}	U_{13}	U_{12}
K1	0.0148(2)	0.0202(2)	0.0133(2)	0.00038(10)	0.00379(13)	-0.00209(11)
N1	0.0150(7)	0.0185(6)	0.0160(6)	0.0030(5)	0.0050(5)	0.0044(5)
N2	0.0160(6)	0.0147(6)	0.0149(6)	-0.0021(4)	0.0023(5)	0.0003(4)
N3	0.0136(6)	0.0138(6)	0.0124(6)	-0.0006(4)	0.0035(5)	-0.0014(4)
O1	0.0126(6)	0.0268(6)	0.0264(6)	-0.0024(4)	0.0029(5)	0.0039(4)
O2	0.0219(6)	0.0203(6)	0.0198(6)	0.0065(4)	0.0023(4)	-0.0019(4)
O3	0.0178(6)	0.0224(6)	0.0127(5)	0.0014(4)	0.0000(4)	0.0036(4)
O4	0.0172(6)	0.0290(6)	0.0120(5)	0.0011(4)	0.0058(4)	0.0023(4)

Table S9. Atomic coordinates and equivalent isotropic displacement parameters (\AA^2) for potassium dinitramide at 100 K. $U(\text{eq})$ is defined as one third of the trace of the orthogonalized U_{ij} tensor.

	x	y	z	$U(\text{eq})$
K1	0.86034(4)	0.34332(3)	0.83205(4)	0.01160(12)
N1	0.7599(2)	0.37665(14)	0.4081(2)	0.0122(3)
N2	0.6488(2)	0.46237(12)	0.2686(2)	0.0111(3)
N3	0.9506(2)	0.34062(12)	0.3721(2)	0.0100(3)
O1	0.4636(2)	0.46163(12)	0.2804(2)	0.0155(2)
O2	0.7262(2)	0.53844(11)	0.15502(15)	0.0148(2)
O3	0.06313(15)	0.29457(11)	0.51450(13)	0.0132(2)
O4	0.0104(2)	0.34353(11)	0.21534(15)	0.0139(2)

Table S10. Anisotropic displacement parameters (\AA^2) for potassium dinitramide at 100 K. The anisotropic displacement factor exponent takes the form:
 $-2\pi^2[(ha^*)^2U_{11} + \dots + 2hka^*b^*U_{12}]$

	U_{11}	U_{22}	U_{33}	U_{23}	U_{13}	U_{12}
K1	0.0107(2)	0.0152(2)	0.0092(2)	0.00025(10)	0.00223(12)	-0.00139(10)
N1	0.0113(6)	0.0150(6)	0.0108(6)	0.0022(4)	0.0031(5)	0.0033(4)
N2	0.0114(6)	0.0115(6)	0.0104(6)	-0.0018(4)	0.0013(4)	0.0004(4)
N3	0.0104(6)	0.0106(6)	0.0091(6)	-0.0006(4)	0.0022(4)	-0.0012(4)
O1	0.0081(5)	0.0196(6)	0.0188(5)	-0.0016(4)	0.0019(4)	0.0024(4)
O2	0.0158(6)	0.0154(5)	0.0133(5)	0.0043(4)	0.0019(4)	-0.0012(4)
O3	0.0131(5)	0.0167(5)	0.0090(5)	0.0009(4)	-0.0012(4)	0.0022(4)
O4	0.0130(5)	0.0215(6)	0.0080(5)	0.0008(4)	0.0041(4)	0.0017(4)

Table S11. Atomic coordinates and equivalent isotropic displacement parameters (\AA^2) for potassium dinitramide at 85 K. $U(\text{eq})$ is defined as one third of the trace of the orthogonalized U_{ij} tensor.

	x	y	z	$U(\text{eq})$
K1	0.86050(5)	0.34347(3)	0.83221(4)	0.01092(13)
N1	0.7602(2)	0.37658(15)	0.4085(2)	0.0117(3)
N2	0.6489(2)	0.46229(13)	0.2687(2)	0.0105(3)
N3	0.9507(2)	0.34065(13)	0.3723(2)	0.0090(3)
O1	0.4635(2)	0.46164(13)	0.2807(2)	0.0143(3)
O2	0.7261(2)	0.53857(12)	0.1548(2)	0.0141(3)
O3	0.0634(2)	0.29447(12)	0.51469(15)	0.0129(2)
O4	0.0107(2)	0.34344(12)	0.2155(2)	0.0126(3)

Table S12. Anisotropic displacement parameters (\AA^2) for potassium dinitramide at 85 K. The anisotropic displacement factor exponent takes the form:
 $-2\pi^2[(h a^*)^2 U_{11} + \dots + 2 h k a^* b^* U_{12}]$

	U_{11}	U_{22}	U_{33}	U_{23}	U_{13}	U_{12}
K1	0.0094(2)	0.0135(2)	0.0099(2)	0.00015(10)	0.00183(13)	-0.00124(10)
N1	0.0098(7)	0.0144(6)	0.0112(6)	0.0016(5)	0.0024(5)	0.0028(5)
N2	0.0104(6)	0.0107(6)	0.0105(6)	-0.0016(4)	0.0014(5)	0.0001(4)
N3	0.0086(6)	0.0095(6)	0.0092(6)	-0.0003(4)	0.0017(5)	-0.0014(4)
O1	0.0072(6)	0.0181(6)	0.0176(6)	-0.0016(4)	0.0020(4)	0.0021(4)
O2	0.0147(6)	0.0142(6)	0.0135(5)	0.0044(4)	0.0025(4)	-0.0008(4)
O3	0.0117(6)	0.0160(6)	0.0101(5)	0.0008(4)	-0.0011(4)	0.0018(4)
O4	0.0111(6)	0.0184(6)	0.0088(5)	0.0005(4)	0.0031(4)	0.0013(4)

Table S13. Bond lengths and shortest K..O contacts (Å) and angles (°) for potassium dinitramide.

At 298 K:

K1..O1	2.841(2)	O2-N2-O1	123.8(2)
K1..O2	2.947(2)	O2-N2-N1	124.0(2)
K1..O3	2.810(2)	O1-N2-N1	112.0(2)
K1..O4	2.812(2)	N3-N1-N2	114.1(2)
O4-N3	1.232(2)	O4-N3-O3	121.2(2)
O2-N2	1.222(3)	O4-N3-N1	125.6(2)
N2-O1	1.230(2)	O3-N3-N1	113.1(2)
N2-N1	1.388(2)		
N1-N3	1.353(2)		
N3-O3	1.239(2)		

At 250 K:

K1..O1	2.8313(13)	O2-N2-O1	123.39(14)
K1..O2	2.9399(14)	O2-N2-N1	124.24(14)
K1..O3	2.8070(13)	O1-N2-N1	112.22(14)
K1..O4	2.8043(14)	N3-N1-N2	114.05(13)
O4-N3	1.233(2)	O4-N3-O3	121.17(14)
O2-N2	1.229(2)	O4-N3-N1	125.71(13)
N2-O1	1.233(2)	O3-N3-N1	112.98(13)
N2-N1	1.387(2)		
N1-N3	1.354(2)		
N3-O3	1.242(2)		

At 200 K:

K1..O1	2.8206(13)	O2-N2-O1	123.48(13)
K1..O2	2.9318(13)	O2-N2-N1	124.19(14)
K1..O3	2.8020(12)	O1-N2-N1	112.15(13)
K1..O4	2.7945(13)	N3-N1-N2	114.07(12)
O4-N3	1.236(2)	O4-N3-O3	121.16(13)
O2-N2	1.227(2)	O4-N3-N1	125.77(12)
N2-O1	1.233(2)	O3-N3-N1	112.95(12)
N2-N1	1.388(2)		
N1-N3	1.356(2)		
N3-O3	1.242(2)		

At 150 K:

K1..O1	2.8139(12)	O2-N2-O1	123.59(12)
K1..O2	2.9250(12)	O2-N2-N1	124.15(13)
K1..O3	2.7991(11)	O1-N2-N1	112.06(12)
K1..O4	2.7900(12)	N3-N1-N2	114.12(11)
O4-N3	1.238(2)	O4-N3-O3	121.17(12)
O2-N2	1.230(2)	O4-N3-N1	125.77(12)
N2-O1	1.236(2)	O3-N3-N1	112.94(12)
N2-N1	1.390(2)		
N1-N3	1.357(2)		
N3-O3	1.245(2)		

At 100 K:

K1..O1	2.8049(11)	O2-N2-O1	123.51(12)
K1..O2	2.9188(11)	O2-N2-N1	124.26(12)
K1..O3	2.7957(11)	O1-N2-N1	112.05(11)
K1..O4	2.7834(11)	N3-N1-N2	114.09(11)
O4-N3	1.239(2)	O4-N3-O3	121.25(12)
O2-N2	1.230(2)	O4-N3-N1	125.82(11)
N2-O1	1.235(2)	O3-N3-N1	112.82(11)
N2-N1	1.391(2)		
N1-N3	1.357(2)		
N3-O3	1.2467(15)		

At 85 K:

K1..O1	2.8022(12)	O2-N2-O1	123.47(13)
K1..O2	2.9159(12)	O2-N2-N1	124.30(13)
K1..O3	2.7938(11)	O1-N2-N1	112.03(12)
K1..O4	2.7800(12)	N3-N1-N2	114.00(12)
O4-N3	1.239(2)	O4-N3-O3	121.10(13)
O2-N2	1.231(2)	O4-N3-N1	126.00(12)
N2-O1	1.236(2)	O3-N3-N1	112.78(12)
N2-N1	1.391(2)		
N1-N3	1.356(2)		
N3-O3	1.246(2)		

Contract No. N00014-95-1-0013 and N00014-97-1-0409

Program Officer: R. Miller/J. Goldwasser

**Title: Experimental Charge Densities and Electrostatic Potentials in Energetic
Materials and Infrastructure Upgrade for an X-ray Crystallography
Laboratory**

PI: A. Alan Pinkerton

Department of Chemistry, University of Toledo, Toledo, OH 43606

tel. (419) 530-4580, FAX (419) 530-4033, email apinker@uoft02.utoledo.edu

APPENDIX 3b

Variable temperature crystallographic study of BIGH.DN



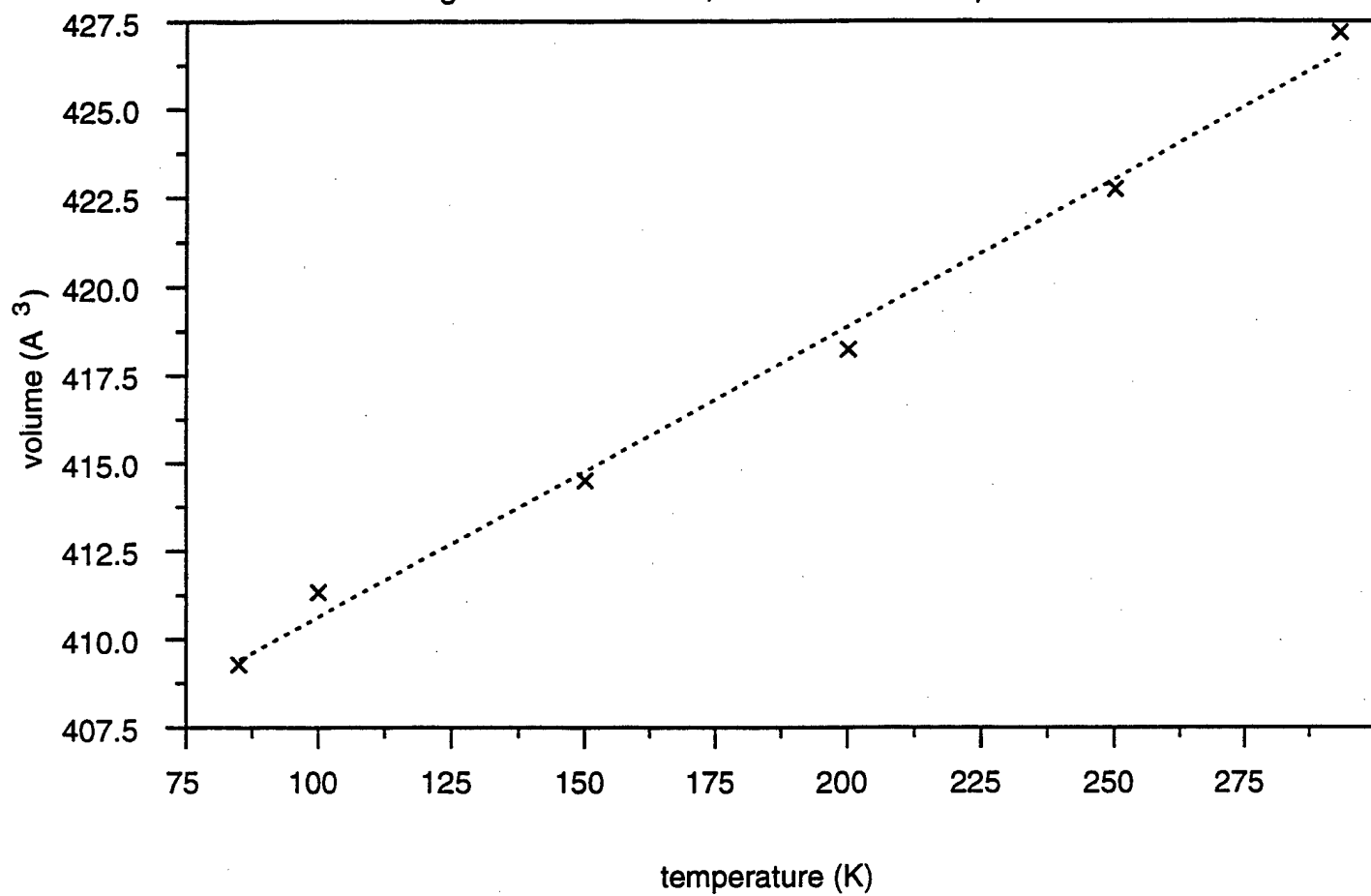
Table 1. Crystal data and structure refinement for biguanidinium dinitramide at various temperatures.

Empirical formula	$C_2H_8N_8O_4$									
Formula weight	208.14									
Wavelength	0.71073 Å									
Crystal system	Triclinic									
Space group	P-1									
F(000)	216									
Crystal size	0.23 x 0.15 x 0.06 mm									
Z	2									
Instrument	Siemens SMART CCD									
Detector distance	3.06 cm									
Scan width and axis	-0.3° in ω									
Refinement method	Full-matrix least-squares on F ²									
Temperature (K)	298(2)	250(2)	200(2)	150(2)	100(2)	85(2)				
a (Å)	4.3738(3)	4.35350(10)	4.3312(3)	4.3114(3)	4.29280(10)	4.28300(10)				
b (Å)	9.4027(5)	9.3742(4)	9.3456(5)	9.3227(5)	9.3043(2)	9.2887(3)				
c (Å)	10.7433(6)	10.6783(4)	10.6220(6)	10.5781(6)	10.5438(3)	10.5248(3)				
α (°)	83.518(2)	84.0720(10)	84.5410(10)	84.9180(10)	85.236(2)	85.407(2)				
β (°)	80.343(2)	80.834(2)	81.285(2)	81.686(2)	82.032(2)	82.196(2)&				
γ (°)	79.867(2)	80.273(2)	80.632(2)	80.928(2)	81.190(2)	81.278(2)				
Volume (Å ³)	427.18(4)	422.73(3)	418.23(4)	414.50(4)	411.33(2)	409.28(2)				
Density (calc) (Mg/m ³)	1.618	1.635	1.653	1.668	1.681	1.689				
Absorption coeff. (mm ⁻¹)	0.147	0.149	0.151	0.152	0.153	0.154				
θ range	1.93 to 28.28°	1.94 to 28.27°	1.94 to 28.32°	1.95 to 28.29°	1.95 to 28.29°	1.96 to 28.34&°				
Limiting indices	-5 < h < 5 -12 < k < 12 -14 < l < 14	-5 < h < 5 -12 < k < 12 -14 < l < 14	-5 < h < 5 -12 < k < 12 -14 < l < 14	-5 < h < 5 -12 < k < 12 -14 < l < 14	-5 < h < 5 -12 < k < 12 -14 < l < 14	-5 < h < 5 -12 < k < 12 -14 < l < 14				
Reflections collected	5746	5731	5689	5627	5628	5617				
Independent reflections	2111	2091	2076	2053	2046	2038				
R _{int}	0.0695	0.0598	0.0608	0.0535	0.0532	0.0569				
Data / restraints / parameters	2111 / 8 / 161	2091 / 8 / 160	2076 / 8 / 160	2053 / 8 / 160	2046 / 8 / 160	2038 / 8 / 160				
Goodness-of-fit on F ²	1.021	1.033	1.021	1.056	1.068	1.016				
R1 [I > 2 σ (I)]	0.0689	0.0591	0.0584	0.0560	0.0560	0.0552				
wR2 [I > 2 σ (I)]	0.1452	0.1249	0.1315	0.1266	0.1303	0.1363				
R1 (all data)	0.1484	0.1202	0.1095	0.0972	0.0903	0.0896				
wR2 (all data)	0.1825	0.1538	0.1578	0.1502	0.1497	0.1573				
Extinction coefficient	0.038(13)	0.028(10)	0.018(10)	0.027(11)	0.030(11)	0.037(13)				
Largest diff. peak (eÅ ⁻³)	0.265	0.231	0.283	0.331	0.362	0.410				
Largest diff. hole (eÅ ⁻³)	-0.308	-0.266	-0.344	-0.334	-0.406	-0.375				

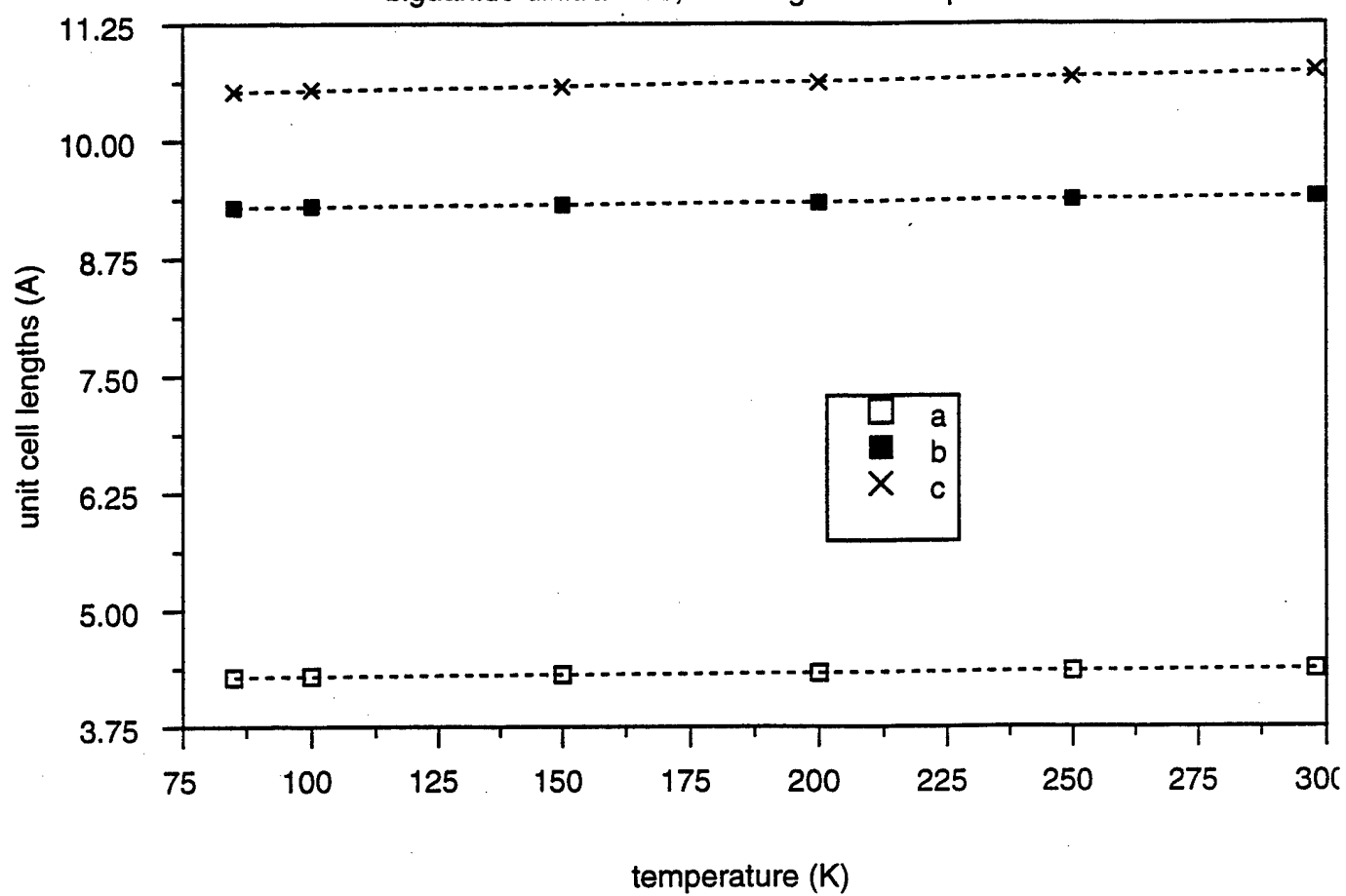
Table 15. Unit cell parameters for variable temperature structure determinations of biguanidinium dinitramide.

T (K)	<i>a</i> (Å)	<i>b</i> (Å)	<i>c</i> (Å)	α (°)	β (°)	γ (°)	volume (Å ³)
298	4.3738(3)	9.4027(5)	10.7433(6)	83.518(2)	80.343(2)	79.867(2)	427.18(4)
250	4.3535(1)	9.3742(4)	10.6783(4)	84.072(1)	80.834(2)	80.273(2)	422.73(3)
200	4.3312(3)	9.3456(5)	10.6220(6)	84.541(1)	81.285(2)	80.632(2)	418.23(4)
150	4.3114(3)	9.3227(5)	10.5781(6)	84.918(1)	81.686(2)	80.928(2)	414.50(4)
100	4.2928(1)	9.3043(2)	10.5438(3)	85.236(2)	82.032(2)	81.190(2)	411.33(2)
85	4.2830(1)	9.2887(3)	10.5248(3)	85.407(2)	82.196(2)	81.278(2)	409.28(2)

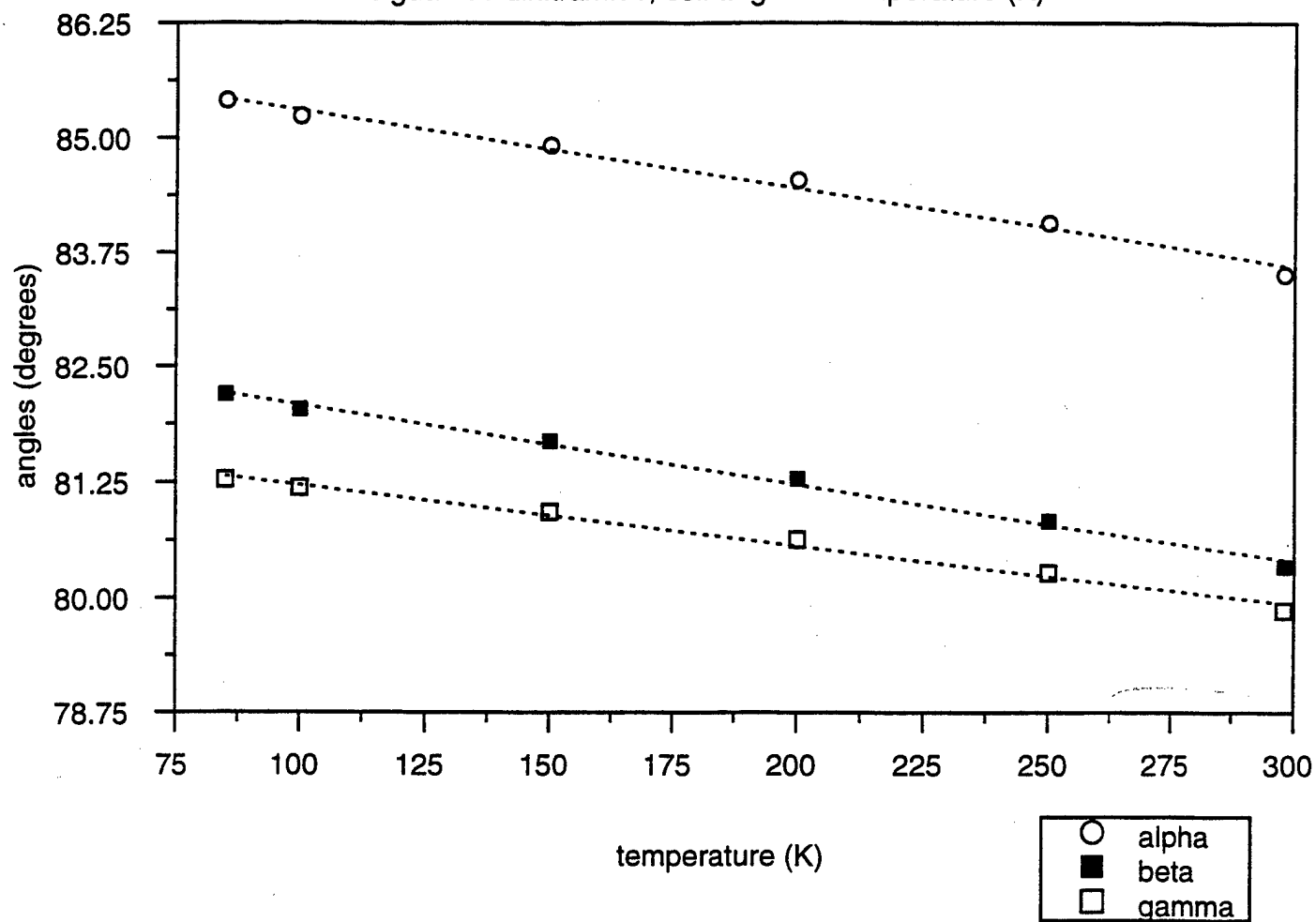
biguanide dinitramide, cell volume vs temperature



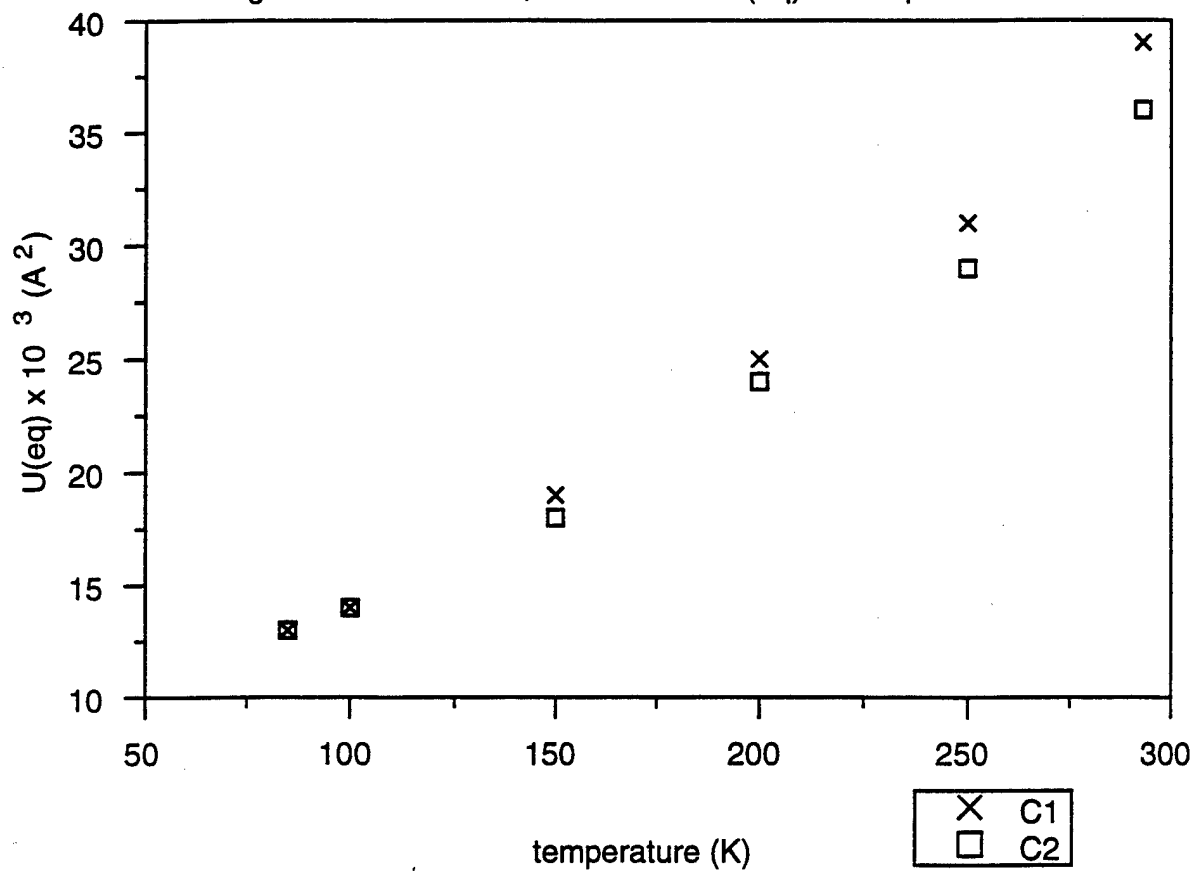
biguanide dinitramide, cell lengths vs temperature



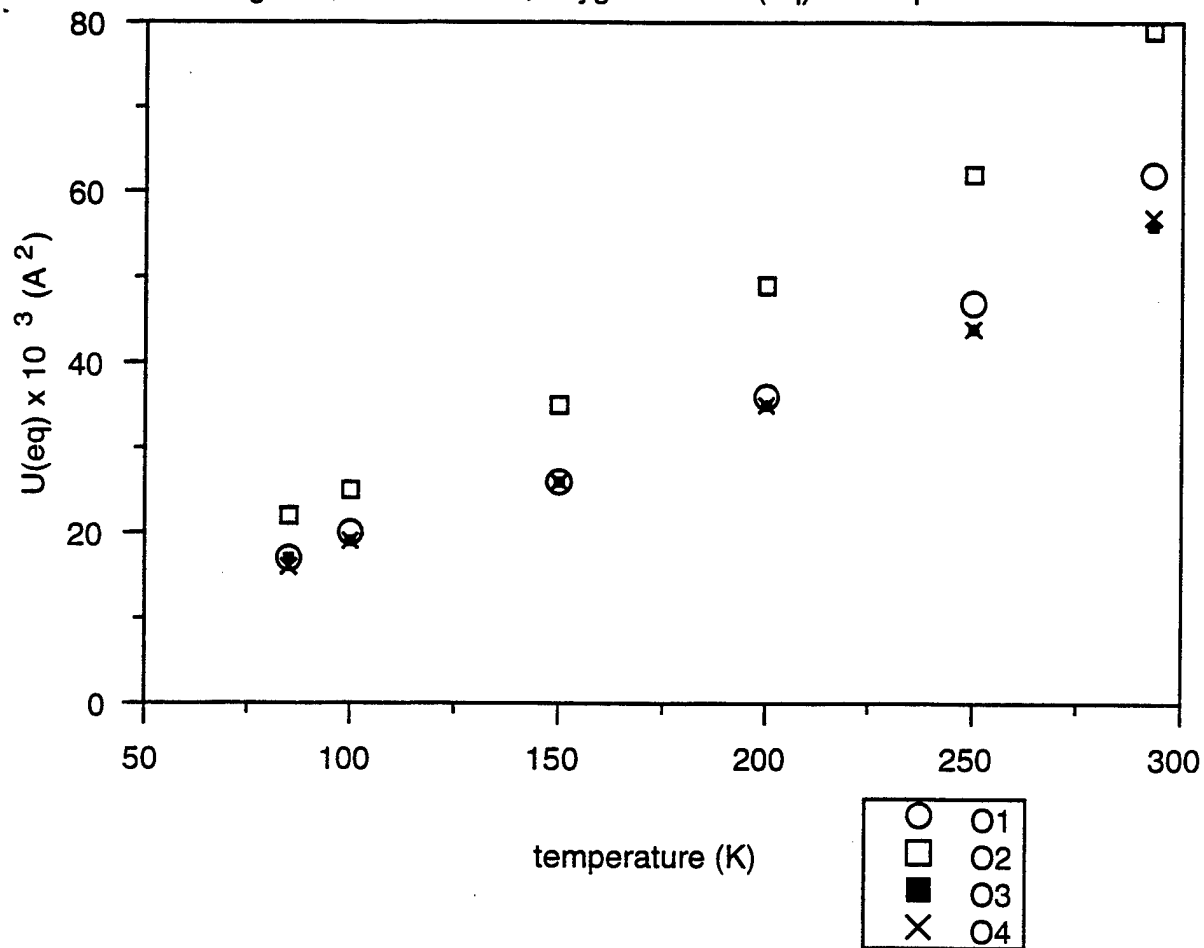
biguanide dinitramide, cell angles v temperature (K)



Biguanide dinitramide, carbon atom U(eq) vs temperature



Biguanide dinitramide, oxygen atom U(eq) vs temperature

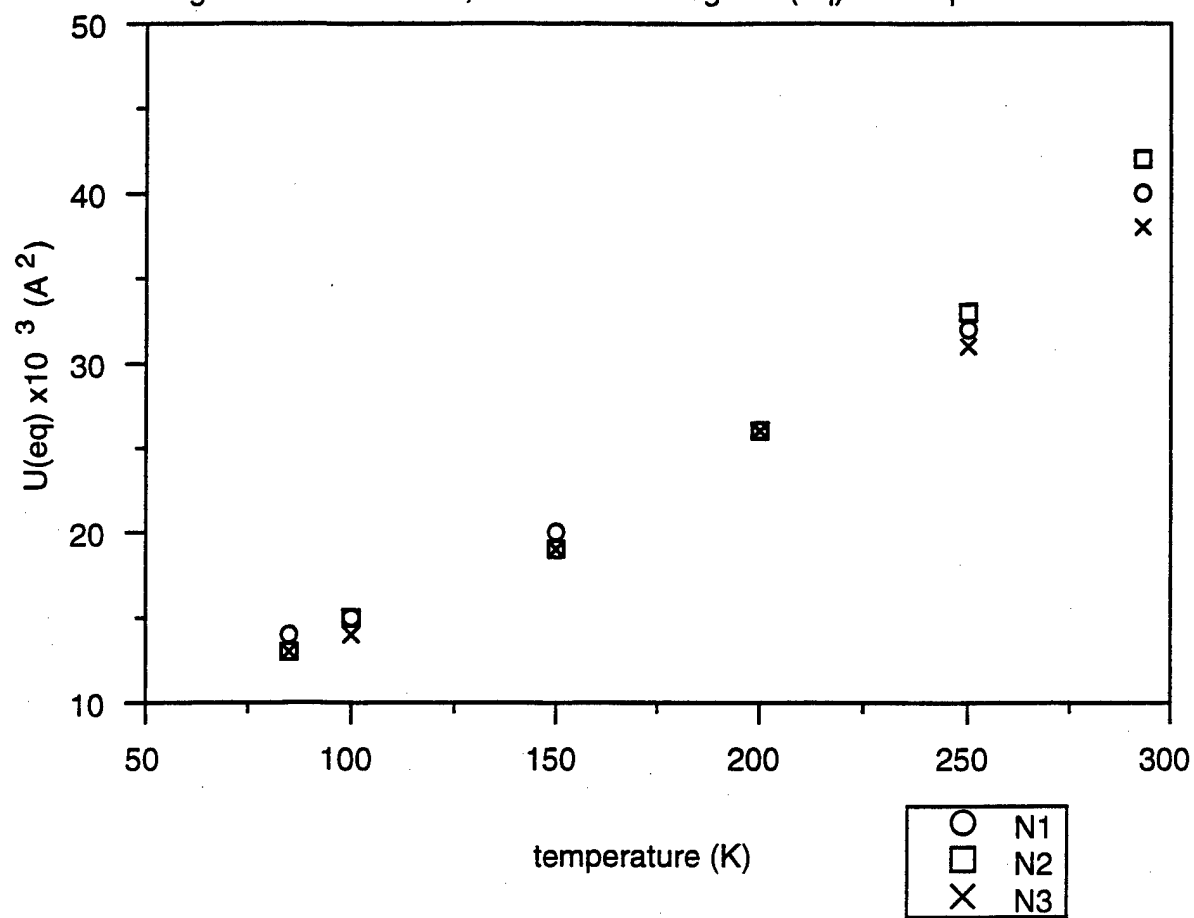


Eqs:

$$O1 = 0.188021 T - 0.947761 \quad r = 0.9923$$

$$O2 = 0.267426 T - 2.71418 \quad r = 0.994 ??$$

biguanide dinitramide, dinitramide nitrogen U(eq) vs temperature



biguanide dinitramide, biguanide nitrogen U(eq) vs temperature

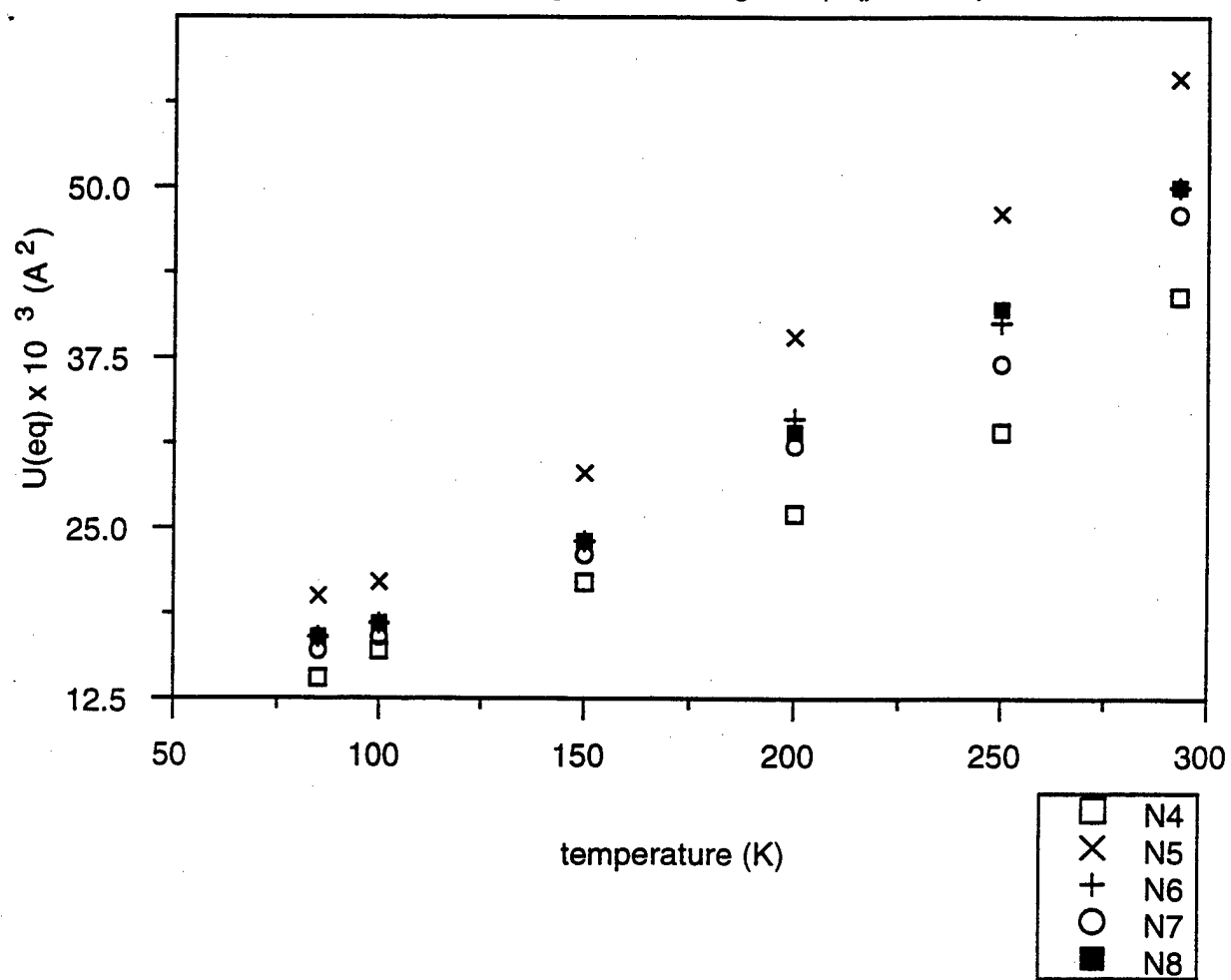


Table 2. Atomic coordinates and equivalent isotropic thermal parameters (\AA^2) for biguanidinium dinitramide at room temperature (298 K). $U(\text{eq})$ is defined as one third of the trace of the orthogonalized U_{ij} tensor.

	x	y	z	$U(\text{eq})/U(\text{iso})$
C1	-0.5133(7)	0.1754(3)	0.7406(3)	0.0387(8)
C2	-0.8268(7)	0.1924(3)	0.9394(3)	0.0357(7)
O1	-0.7715(6)	0.5993(2)	0.5562(2)	0.0615(8)
O2	-0.1286(7)	0.7857(3)	0.5608(3)	0.0793(10)
O3	-0.5488(6)	0.5768(2)	0.8586(2)	0.0560(7)
O4	-0.5569(6)	0.7818(2)	0.7474(2)	0.0572(7)
N1	-0.1589(6)	0.5880(2)	0.7081(2)	0.0395(7)
N2	-0.0219(6)	0.6663(3)	0.6041(2)	0.0415(7)
N3	-0.4303(6)	0.6567(3)	0.7706(2)	0.0375(6)
N4	-0.6121(6)	0.1190(2)	0.8559(2)	0.0416(7)
N5	-0.3767(8)	0.0829(3)	0.6553(3)	0.0581(9)
N6	-0.5230(7)	0.3160(3)	0.7035(3)	0.0500(8)
N7	-0.8503(7)	0.1384(3)	0.0589(2)	0.0475(8)
N8	-0.0253(7)	0.3121(3)	0.9111(3)	0.0497(8)
H5A	-0.2609(77)	0.1176(36)	0.5722(19)	0.071(11)
H5B	-0.3979(98)	0.9780(16)	0.6757(38)	0.088(13)
H6A	-0.5840(87)	0.3903(29)	0.7668(26)	0.069(11)
H6B	-0.4189(79)	0.3453(39)	0.6160(17)	0.074(12)
H7A	-0.6949(59)	0.0512(24)	0.0814(28)	0.055(10)
H7B	-0.0245(63)	0.1699(38)	0.1286(25)	0.071(11)
H8A	-0.0443(87)	0.3539(37)	0.8225(15)	0.070(11)
H8B	-0.1795(63)	0.3531(33)	0.9836(22)	0.061(10)

Table 3. Anisotropic displacement parameters (\AA^2) for biguanidinium dinitramide at room temperature (298 K).

The anisotropic displacement factor exponent takes the form: $-2\pi^2[(ha^*)^2U_{11} + \dots + 2hka^*b^*U_{12}]$

	U11	U22	U33	U23	U13	U12
C1	0.045(2)	0.0261(15)	0.040(2)	0.0010(12)	-0.0003(14)	0.0011(12)
C2	0.039(2)	0.0256(14)	0.040(2)	0.0009(12)	-0.0019(14)	-0.0061(12)
O1	0.059(2)	0.0507(14)	0.056(2)	0.0060(11)	0.0188(13)	0.0075(12)
O2	0.087(2)	0.0458(15)	0.075(2)	0.0288(13)	0.022(2)	0.0174(14)
O3	0.064(2)	0.0399(13)	0.0526(14)	0.0036(10)	0.0180(12)	-0.0074(11)
O4	0.0580(15)	0.0288(12)	0.073(2)	-0.0018(10)	0.0114(13)	0.0041(10)
N1	0.0395(15)	0.0303(13)	0.0411(14)	0.0025(10)	0.0058(12)	0.0003(11)
N2	0.046(2)	0.0318(14)	0.0404(15)	0.0019(11)	0.0037(13)	-0.0012(12)
N3	0.0412(15)	0.0284(13)	0.0396(14)	-0.0035(10)	0.0013(12)	-0.0034(11)
N4	0.053(2)	0.0252(12)	0.0369(14)	0.0051(10)	0.0069(12)	0.0017(11)
N5	0.088(2)	0.0286(15)	0.045(2)	-0.0002(12)	0.015(2)	-0.0021(14)
N6	0.074(2)	0.0234(13)	0.044(2)	0.0042(11)	0.0065(15)	-0.0045(13)
N7	0.055(2)	0.039(2)	0.037(2)	0.0020(12)	0.0056(13)	0.0063(13)
N8	0.051(2)	0.043(2)	0.045(2)	0.0019(12)	0.0005(14)	0.0123(13)

Table 4. Atomic coordinates and equivalent isotropic thermal parameters (\AA^2) for biguanidinium dinitramide at 250 K. $U(\text{eq})$ is defined as one third of the trace of the orthogonalized U_{ij} tensor.

	x	y	z	$U(\text{eq})/U(\text{iso})$
C1	-0.5107(6)	0.1744(3)	0.7394(2)	0.0306(6)
C2	-0.8277(6)	0.1921(3)	0.9396(2)	0.0286(6)
O1	-0.7693(5)	0.5976(2)	0.5561(2)	0.0474(6)
O2	-0.1274(6)	0.7850(2)	0.5598(2)	0.0623(8)
O3	-0.5482(5)	0.5760(2)	0.8589(2)	0.0436(6)
O4	-0.5591(5)	0.7813(2)	0.7467(2)	0.0440(6)
N1	-0.1575(5)	0.5879(2)	0.7080(2)	0.0323(5)
N2	-0.0202(5)	0.6651(2)	0.6032(2)	0.0330(5)
N3	-0.4307(5)	0.6564(2)	0.7703(2)	0.0309(5)
N4	-0.6117(5)	0.1180(2)	0.8555(2)	0.0324(6)
N5	-0.3773(7)	0.0812(3)	0.6537(2)	0.0480(7)
N6	-0.5241(6)	0.3153(2)	0.7035(2)	0.0404(6)
N7	-0.8495(6)	0.1377(2)	0.0596(2)	0.0371(6)
N8	-0.0251(6)	0.3123(3)	0.9110(2)	0.0407(6)
H5A	-0.2547(63)	0.1092(32)	0.5703(16)	0.049(9)
H5B	-0.3724(85)	0.9747(13)	0.6758(33)	0.070(11)
H6A	-0.5769(80)	0.3924(26)	0.7655(24)	0.064(10)
H6B	-0.4192(71)	0.3443(35)	0.6164(16)	0.060(10)
H7A	-0.6964(60)	0.0503(24)	0.0826(28)	0.061(10)
H7B	-0.0379(50)	0.1723(33)	0.1220(24)	0.054(9)
H8A	-0.0331(86)	0.3576(35)	0.8230(15)	0.072(11)
H8B	-0.1845(59)	0.3525(32)	0.9819(21)	0.057(9)

Table 5. Anisotropic displacement parameters (\AA^2) for biguanidinium dinitramide at 250 K. The anisotropic displacement factor exponent takes the form: $-2\pi^2[(h a^*)^2 U_{11} + \dots + 2h k a^* b^* U_{12}]$

	U11	U22	U33	U23	U13	U12
C1	0.0345(14)	0.0238(12)	0.0304(13)	-0.0002(10)	-0.0008(11)	-0.0011(11)
C2	0.0310(13)	0.0216(12)	0.0319(13)	0.0006(10)	-0.0019(10)	-0.0045(10)
O1	0.0437(12)	0.0424(12)	0.0430(11)	0.0031(9)	0.0147(9)	0.0065(10)
O2	0.069(2)	0.0378(12)	0.0575(14)	0.0214(11)	0.0192(12)	0.0145(11)
O3	0.0484(12)	0.0339(11)	0.0405(11)	0.0028(9)	0.0128(9)	-0.0055(9)
O4	0.0433(12)	0.0253(10)	0.0550(12)	-0.0024(9)	0.0069(10)	0.0050(9)
N1	0.0343(12)	0.0259(11)	0.0312(11)	0.0021(9)	0.0038(9)	-0.0003(9)
N2	0.0378(13)	0.0298(12)	0.0285(11)	0.0009(9)	0.0004(10)	-0.0037(10)
N3	0.0327(12)	0.0263(11)	0.0313(11)	-0.0045(9)	0.0023(9)	-0.0029(10)
N4	0.0395(13)	0.0215(10)	0.0310(12)	0.0019(9)	0.0045(10)	-0.0016(9)
N5	0.073(2)	0.0264(12)	0.0347(13)	-0.0003(10)	0.0128(12)	-0.0006(12)
N6	0.060(2)	0.0213(11)	0.0344(13)	0.0034(10)	0.0066(11)	-0.0054(11)
N7	0.0397(14)	0.0338(13)	0.0298(12)	0.0016(10)	0.0049(10)	0.0048(11)
N8	0.0395(14)	0.0370(13)	0.0375(13)	0.0009(11)	-0.0002(11)	0.0097(11)

Table 6. Atomic coordinates and equivalent isotropic thermal parameters (\AA^2) for biguanidinium dinitramide at 200 K. $U(\text{eq})$ is defined as one third of the trace of the orthogonalized U_{ij} tensor.

	x	y	z	$U(\text{eq})/U(\text{iso})$
C1	-0.5111(6)	0.1737(3)	0.7390(2)	0.0249(6)
C2	-0.8278(6)	0.1917(3)	0.9398(2)	0.0237(5)
O1	-0.7674(4)	0.5962(2)	0.5555(2)	0.0358(5)
O2	-0.1283(5)	0.7842(2)	0.5586(2)	0.0485(6)
O3	-0.5476(4)	0.5757(2)	0.8594(2)	0.0348(5)
O4	-0.5610(5)	0.7807(2)	0.7458(2)	0.0351(5)
N1	-0.1568(5)	0.5873(2)	0.7085(2)	0.0265(5)
N2	-0.0190(5)	0.6637(2)	0.6027(2)	0.0262(5)
N3	-0.4311(5)	0.6557(2)	0.7701(2)	0.0255(5)
N4	-0.6117(5)	0.1175(2)	0.8555(2)	0.0264(5)
N5	-0.3762(6)	0.0796(2)	0.6527(2)	0.0388(6)
N6	-0.5242(6)	0.3148(2)	0.7031(2)	0.0331(6)
N7	-0.8499(5)	0.1376(2)	0.0601(2)	0.0308(6)
N8	-0.0254(5)	0.3120(2)	0.9108(2)	0.0322(6)
H5A	-0.2395(67)	0.1146(35)	0.5747(21)	0.060(10)
H5B	-0.3752(83)	0.9733(14)	0.6759(31)	0.060(10)
H6A	-0.5791(84)	0.3922(26)	0.7659(24)	0.068(11)
H6B	-0.4343(68)	0.3478(32)	0.6154(15)	0.045(8)
H7A	-0.6968(49)	0.0508(20)	0.0825(23)	0.032(7)
H7B	-0.0340(49)	0.1729(31)	0.1240(22)	0.044(8)
H8A	-0.0448(87)	0.3599(36)	0.8237(17)	0.070(11)
H8B	-0.1758(55)	0.3521(29)	0.9842(18)	0.041(8)

Table 7. Anisotropic displacement parameters (\AA^2) for biguanidinium dinitramide at 200 K. The anisotropic displacement factor exponent takes the form: $-2\pi^2[(h a^*)^2 U_{11} + \dots + 2 h k a^* b^* U_{12}]$

	U11	U22	U33	U23	U13	U12
C1	0.0289(13)	0.0180(11)	0.0248(12)	0.0008(9)	-0.0004(10)	0.0009(10)
C2	0.0267(12)	0.0162(11)	0.0273(12)	0.0007(9)	-0.0017(10)	-0.0043(10)
O1	0.0331(10)	0.0308(10)	0.0339(10)	0.0013(8)	0.0111(8)	0.0071(8)
O2	0.0551(13)	0.0279(11)	0.0450(12)	0.0146(9)	0.0167(10)	0.0137(10)
O3	0.0387(11)	0.0256(10)	0.0336(10)	0.0018(8)	0.0112(8)	-0.0025(8)
O4	0.0361(11)	0.0182(9)	0.0445(11)	-0.0017(8)	0.0062(8)	0.0043(8)
N1	0.0277(11)	0.0179(10)	0.0285(11)	0.0013(8)	0.0044(9)	0.0029(9)
N2	0.0320(12)	0.0201(10)	0.0238(10)	0.0000(8)	0.0010(9)	-0.0014(9)
N3	0.0275(11)	0.0196(10)	0.0278(11)	-0.0033(9)	-0.0003(9)	-0.0017(9)
N4	0.0337(12)	0.0172(10)	0.0239(10)	0.0006(8)	0.0039(9)	0.0008(9)
N5	0.058(2)	0.0202(11)	0.0306(12)	-0.0008(9)	0.0115(11)	0.0001(11)
N6	0.0482(14)	0.0172(10)	0.0287(12)	0.0024(9)	0.0061(10)	-0.0030(10)
N7	0.0375(13)	0.0229(11)	0.0257(11)	-0.0008(9)	0.0044(9)	0.0051(10)
N8	0.0298(12)	0.0283(12)	0.0311(12)	0.0012(10)	0.0012(9)	0.0099(10)

Table 8. Atomic coordinates and equivalent isotropic thermal parameters (\AA^2) for biguanidinium dinitramide at 150 K. $U(\text{eq})$ is defined as one third of the trace of the orthogonalized U_{ij} tensor.

	x	y	z	$U(\text{eq})/U(\text{iso})$
C1	-0.5107(5)	0.1727(2)	0.7386(2)	0.0188(5)
C2	-0.8266(5)	0.1918(2)	0.9398(2)	0.0182(5)
O1	-0.7664(4)	0.5948(2)	0.5555(2)	0.0265(4)
O2	-0.1280(5)	0.7838(2)	0.5577(2)	0.0349(5)
O3	-0.5470(4)	0.5756(2)	0.8595(2)	0.0258(4)
O4	-0.5634(4)	0.7804(2)	0.7452(2)	0.0255(4)
N1	-0.1565(4)	0.5873(2)	0.7080(2)	0.0199(4)
N2	-0.0192(5)	0.6633(2)	0.6025(2)	0.0194(4)
N3	-0.4325(5)	0.6555(2)	0.7697(2)	0.0188(4)
N4	-0.6112(5)	0.1173(2)	0.8554(2)	0.0208(5)
N5	-0.3751(6)	0.0782(2)	0.6521(2)	0.0286(5)
N6	-0.5251(5)	0.3145(2)	0.7025(2)	0.0244(5)
N7	-0.8503(5)	0.1382(2)	0.0605(2)	0.0231(5)
N8	-0.0245(5)	0.3123(2)	0.9109(2)	0.0243(5)
H5A	-0.2475(61)	0.1135(30)	0.5725(18)	0.038(8)
H5B	-0.3822(80)	0.9718(13)	0.6712(30)	0.053(9)
H6A	-0.5684(78)	0.3916(25)	0.7658(23)	0.055(10)
H6B	-0.4449(67)	0.3421(32)	0.6116(13)	0.037(8)
H7A	-0.6939(47)	0.0546(20)	0.0863(22)	0.025(7)
H7B	-0.0430(51)	0.1687(34)	0.1223(25)	0.050(9)
H8A	-0.0354(74)	0.3534(32)	0.8210(14)	0.045(9)
H8B	-0.1858(59)	0.3538(31)	0.9807(21)	0.047(9)

Table 9. Anisotropic displacement parameters (\AA^2) for biguanidinium dinitramide at 150 K. The anisotropic displacement factor exponent takes the form: $-2\pi^2[(h a^*)^2 U_{11} + \dots + 2h k a^* b^* U_{12}]$

	U11	U22	U33	U23	U13	U12
C1	0.0217(11)	0.0132(10)	0.0191(11)	-0.0003(8)	-0.0002(9)	0.0024(9)
C2	0.0209(11)	0.0123(10)	0.0207(11)	-0.0011(8)	-0.0015(9)	-0.0013(9)
O1	0.0257(9)	0.0225(9)	0.0254(9)	-0.0015(7)	0.0061(7)	0.0053(7)
O2	0.0407(11)	0.0191(9)	0.0335(10)	0.0107(8)	0.0091(8)	0.0108(8)
O3	0.0303(9)	0.0171(8)	0.0250(9)	0.0007(7)	0.0088(7)	-0.0012(7)
O4	0.0277(9)	0.0118(8)	0.0328(9)	-0.0020(7)	0.0030(7)	0.0044(7)
N1	0.0209(10)	0.0142(9)	0.0214(10)	0.0010(7)	0.0021(8)	0.0021(8)
N2	0.0246(10)	0.0141(9)	0.0174(9)	-0.0010(7)	0.0001(8)	0.0009(8)
N3	0.0226(10)	0.0140(9)	0.0188(9)	-0.0041(7)	0.0003(8)	-0.0001(8)
N4	0.0252(10)	0.0126(9)	0.0207(10)	0.0005(7)	0.0035(8)	0.0023(8)
N5	0.0439(13)	0.0136(10)	0.0225(10)	-0.0020(8)	0.0084(9)	0.0021(9)
N6	0.0360(12)	0.0115(9)	0.0217(10)	0.0013(8)	0.0044(9)	-0.0004(8)
N7	0.0255(11)	0.0199(10)	0.0198(10)	-0.0014(8)	0.0020(8)	0.0042(9)
N8	0.0253(11)	0.0208(10)	0.0220(10)	-0.0005(8)	0.0000(8)	0.0079(9)

Table 10. Atomic coordinates and equivalent isotropic thermal parameters (\AA^2) for biguanidinium dinitramide at 100 K. $U(\text{eq})$ is defined as one third of the trace of the orthogonalized U_{ij} tensor.

	x	y	z	$U(\text{eq})/U(\text{iso})$
C1	-0.5118(5)	0.1720(2)	0.7385(2)	0.0142(5)
C2	-0.8257(6)	0.1917(2)	0.9398(2)	0.0139(5)
O1	-0.7652(4)	0.5940(2)	0.5549(2)	0.0195(4)
O2	-0.1286(4)	0.7833(2)	0.5562(2)	0.0250(5)
O3	-0.5460(4)	0.5754(2)	0.8597(2)	0.0192(4)
O4	-0.5645(4)	0.7799(2)	0.7444(2)	0.0188(4)
N1	-0.1560(5)	0.5867(2)	0.7079(2)	0.0150(4)
N2	-0.0196(5)	0.6627(2)	0.6019(2)	0.0146(4)
N3	-0.4326(5)	0.6549(2)	0.7695(2)	0.0141(4)
N4	-0.6120(5)	0.1165(2)	0.8550(2)	0.0155(4)
N5	-0.3742(5)	0.0770(2)	0.6518(2)	0.0214(5)
N6	-0.5253(5)	0.3140(2)	0.7020(2)	0.0182(5)
N7	-0.8490(5)	0.1378(2)	0.0607(2)	0.0174(5)
N8	-0.0239(5)	0.3129(2)	0.9107(2)	0.0183(5)
H5A	-0.2515(61)	0.1082(30)	0.5696(17)	0.025(7)
H5B	-0.3970(83)	0.9720(15)	0.6732(32)	0.046(10)
H6A	-0.5790(80)	0.3872(27)	0.7687(23)	0.043(9)
H6B	-0.4484(68)	0.3388(32)	0.6100(13)	0.026(7)
H7A	-0.6949(65)	0.0518(26)	0.0855(31)	0.050(10)
H7B	-0.0399(48)	0.1712(32)	0.1220(23)	0.029(8)
H8A	-0.0381(77)	0.3586(32)	0.8224(15)	0.037(9)
H8B	-0.1801(58)	0.3516(31)	0.9837(20)	0.032(8)

Table 11. Anisotropic displacement parameters (\AA^2) for biguanidinium dinitramide at 100 K. The anisotropic displacement factor exponent takes the form: $-2\pi^2[(h a^*)^2 U_{11} + \dots + 2 h k a^* b^* U_{12}]$

	U11	U22	U33	U23	U13	U12
C1	0.0161(11)	0.0080(10)	0.0171(11)	-0.0006(8)	-0.0012(9)	0.0022(8)
C2	0.0156(11)	0.0084(10)	0.0176(11)	-0.0026(8)	-0.0010(8)	-0.0009(8)
O1	0.0175(9)	0.0146(8)	0.0220(9)	-0.0016(7)	0.0048(7)	0.0053(7)
O2	0.0291(10)	0.0122(9)	0.0262(9)	0.0068(7)	0.0056(8)	0.0083(7)
O3	0.0214(9)	0.0127(8)	0.0207(9)	-0.0011(7)	0.0047(7)	-0.0004(7)
O4	0.0201(9)	0.0070(8)	0.0257(9)	-0.0016(6)	0.0012(7)	0.0059(6)
N1	0.0150(10)	0.0090(9)	0.0179(10)	-0.0004(7)	0.0024(8)	0.0036(7)
N2	0.0173(10)	0.0111(9)	0.0138(9)	-0.0013(7)	-0.0005(7)	0.0014(8)
N3	0.0159(10)	0.0097(9)	0.0149(9)	-0.0023(7)	0.0001(7)	0.0023(7)
N4	0.0189(10)	0.0086(9)	0.0163(10)	0.0002(7)	0.0015(8)	0.0026(8)
N5	0.0319(12)	0.0095(9)	0.0184(10)	-0.0004(8)	0.0046(9)	0.0029(8)
N6	0.0253(11)	0.0095(9)	0.0168(10)	-0.0008(8)	0.0037(8)	0.0014(8)
N7	0.0197(11)	0.0129(10)	0.0163(10)	-0.0021(8)	0.0023(8)	0.0049(8)
N8	0.0192(11)	0.0130(10)	0.0188(10)	0.0010(8)	0.0004(8)	0.0063(8)

Table 12. Atomic coordinates and equivalent isotropic thermal parameters (\AA^2) for biguanidinium dinitramide at 85 K. $U(\text{eq})$ is defined as one third of the trace of the orthogonalized U_{ij} tensor.

	x	y	z	$U(\text{eq})/U(\text{iso})$
C1	-0.5115(5)	0.1722(2)	0.7381(2)	0.0128(5)
C2	-0.8265(5)	0.1915(2)	0.9397(2)	0.0133(5)
O1	-0.7654(4)	0.5938(2)	0.55519(15)	0.0170(4)
O2	-0.1287(4)	0.7830(2)	0.5561(2)	0.0217(4)
O3	-0.5458(4)	0.5750(2)	0.85950(15)	0.0169(4)
O4	-0.5648(4)	0.7799(2)	0.7442(2)	0.0165(4)
N1	-0.1566(4)	0.5867(2)	0.7081(2)	0.0139(4)
N2	-0.0189(5)	0.6625(2)	0.6018(2)	0.0134(4)
N3	-0.4328(5)	0.6549(2)	0.7694(2)	0.0129(4)
N4	-0.6122(5)	0.1164(2)	0.8553(2)	0.0141(4)
N5	-0.3747(5)	0.0768(2)	0.6515(2)	0.0196(5)
N6	-0.5255(5)	0.3139(2)	0.7021(2)	0.0167(5)
N7	-0.8496(5)	0.1379(2)	0.0605(2)	0.0160(5)
N8	-0.0242(5)	0.3128(2)	0.9108(2)	0.0172(5)
H5A	-0.2537(66)	0.1071(32)	0.5683(17)	0.029(8)
H5B	-0.3896(77)	0.9700(13)	0.6660(29)	0.035(8)
H6A	-0.5622(76)	0.3854(26)	0.7705(21)	0.037(9)
H6B	-0.4541(72)	0.3431(33)	0.6108(13)	0.028(8)
H7A	-0.7002(50)	0.0504(20)	0.0855(23)	0.017(7)
H7B	-0.0303(50)	0.1748(30)	0.1243(22)	0.025(7)
H8A	-0.0438(75)	0.3586(31)	0.8229(15)	0.034(8)
H8B	-0.1748(65)	0.3517(34)	0.9852(21)	0.040(9)

Table 13. Anisotropic displacement parameters (\AA^2) for biguanidinium dinitramide at 85 K. The anisotropic displacement factor exponent takes the form: $-2\pi^2[(h a^*)^2 U_{11} + \dots + 2 h k a^* b^* U_{12}]$

	U11	U22	U33	U23	U13	U12
C1	0.0118(11)	0.0085(10)	0.0170(11)	0.0002(8)	-0.0023(8)	0.0023(8)
C2	0.0127(11)	0.0069(10)	0.0198(11)	-0.0018(8)	-0.0007(8)	0.0000(8)
O1	0.0145(8)	0.0126(8)	0.0202(8)	-0.0027(6)	0.0028(6)	0.0065(6)
O2	0.0248(9)	0.0098(8)	0.0244(9)	0.0052(7)	0.0037(7)	0.0077(7)
O3	0.0187(8)	0.0100(8)	0.0190(9)	-0.0005(6)	0.0043(7)	0.0012(7)
O4	0.0178(8)	0.0050(7)	0.0237(9)	-0.0014(6)	0.0011(7)	0.0054(6)
N1	0.0133(9)	0.0078(9)	0.0179(9)	0.0004(7)	0.0021(7)	0.0025(7)
N2	0.0149(10)	0.0082(9)	0.0158(9)	-0.0014(7)	-0.0001(7)	0.0019(7)
N3	0.0145(9)	0.0081(9)	0.0149(9)	-0.0034(7)	-0.0006(7)	0.0023(7)
N4	0.0155(10)	0.0081(9)	0.0165(10)	-0.0013(7)	0.0009(7)	0.0032(7)
N5	0.0277(11)	0.0088(9)	0.0182(10)	-0.0001(7)	0.0052(8)	0.0035(8)
N6	0.0225(11)	0.0075(9)	0.0175(10)	-0.0002(7)	0.0030(8)	0.0007(8)
N7	0.0172(10)	0.0120(10)	0.0155(10)	-0.0019(7)	0.0019(8)	0.0054(8)
N8	0.0165(10)	0.0123(10)	0.0190(10)	0.0005(8)	0.0002(8)	0.0074(8)

Table 14. Bond lengths (Å) and angles (°) of biguanidinium dinitramide at various temperatures.

At 298 K:

O4-N3 1.226(3)	N3-N1-N2	115.7(2)
N1-N3 1.356(3)	O4-N3-O3	121.1(2)
N1-N2 1.376(3)	O4-N3-N1	126.9(2)
O3-N3 1.240(3)	O3-N3-N1	112.0(2)
O1-N2 1.226(3)	O2-N2-O1	122.1(2)
O2-N2 1.210(3)	O2-N2-N1	126.2(2)
N6-C1 1.333(4)	O1-N2-N1	111.7(2)
N8-C2 1.334(4)	C1-N4-C2	123.1(2)
N4-C1 1.325(3)	N4-C1-N5	117.0(3)
N4-C2 1.338(4)	N4-C1-N6	126.3(3)
C1-N5 1.330(4)	N5-C1-N6	116.6(3)
C2-N7 1.321(4)	N7-C2-N8	117.6(3)
	N7-C2-N4	116.9(3)
	N8-C2-N4	125.5(3)

At 250 K:

O4-N3 1.228(3)	N3-N1-N2	116.0(2)
N1-N3 1.360(3)	O4-N3-O3	121.3(2)
N1-N2 1.377(3)	O4-N3-N1	127.0(2)
O3-N3 1.246(3)	O3-N3-N1	111.7(2)
O1-N2 1.226(3)	O2-N2-O1	122.5(2)
O2-N2 1.217(3)	O2-N2-N1	125.9(2)
N6-C1 1.331(3)	O1-N2-N1	111.6(2)
N8-C2 1.337(3)	C1-N4-C2	123.2(2)
N4-C1 1.334(3)	N5-C1-N6	117.5(2)
N4-C2 1.346(3)	N5-C1-N4	116.8(2)
C1-N5 1.327(3)	N6-C1-N4	125.6(2)
C2-N7 1.324(3)	N7-C2-N8	118.1(2)
	N7-C2-N4	116.5(2)
	N8-C2-N4	125.4(2)

At 200 K:

O4-N3 1.233(3)	N3-N1-N2	116.1(2)
N1-N3 1.358(3)	O4-N3-O3	121.3(2)
N1-N2 1.383(3)	O4-N3-N1	127.0(2)
O3-N3 1.247(2)	O3-N3-N1	111.7(2)
O1-N2 1.228(3)	O2-N2-O1	122.5(2)
O2-N2 1.227(3)	O2-N2-N1	125.6(2)
N6-C1 1.332(3)	O1-N2-N1	111.8(2)
N8-C2 1.338(3)	C1-N4-C2	123.2(2)
N4-C1 1.335(3)	N6-C1-N5	117.4(2)
N4-C2 1.346(3)	N6-C1-N4	125.8(2)
C1-N5 1.334(3)	N5-C1-N4	116.8(2)
C2-N7 1.325(3)	N7-C2-N8	118.1(2)
	N7-C2-N4	116.5(2)
	N8-C2-N4	125.3(2)

At 150 K:

O4-N3 1.234(2)	N3-N1-N2 116.2(2)
N1-N3 1.363(2)	O4-N3-O3 121.4(2)
N1-N2 1.378(2)	O4-N3-N1 127.0(2)
O3-N3 1.247(2)	O3-N3-N1 111.5(2)
O1-N2 1.234(2)	O2-N2-O1 122.6(2)
O2-N2 1.228(2)	O2-N2-N1 125.9(2)
N6-C1 1.338(3)	O1-N2-N1 111.5(2)
N8-C2 1.340(3)	C1-N4-C2 123.4(2)
N4-C1 1.336(3)	N5-C1-N4 117.0(2)
N4-C2 1.345(3)	N5-C1-N6 117.4(2)
C1-N5 1.334(3)	N4-C1-N6 125.5(2)
C2-N7 1.325(3)	N7-C2-N8 117.8(2)
	N7-C2-N4 116.8(2)
	N8-C2-N4 125.4(2)

At 100 K:

O4-N3 1.238(2)	N3-N1-N2 116.1(2)
N1-N3 1.363(2)	O4-N3-O3 121.6(2)
N1-N2 1.381(3)	O4-N3-N1 127.0(2)
O3-N3 1.247(2)	O3-N3-N1 111.5(2)
O1-N2 1.239(2)	O2-N2-O1 122.4(2)
O2-N2 1.233(3)	O2-N2-N1 126.3(2)
N6-C1 1.340(3)	O1-N2-N1 111.3(2)
N8-C2 1.345(3)	C1-N4-C2 123.2(2)
N4-C1 1.333(3)	N4-C1-N5 116.8(2)
N4-C2 1.346(3)	N4-C1-N6 126.0(2)
C1-N5 1.338(3)	N5-C1-N6 117.2(2)
C2-N7 1.326(3)	N7-C2-N8 117.9(2)
	N7-C2-N4 116.7(2)
	N8-C2-N4 125.3(2)

At 85 K:

O4-N3 1.237(2)	N3-N1-N2 116.3(2)
N1-N3 1.359(2)	O4-N3-O3 121.8(2)
N1-N2 1.385(3)	O4-N3-N1 126.9(2)
O3-N3 1.247(2)	O3-N3-N1 111.3(2)
O1-N2 1.234(2)	O2-N2-O1 122.6(2)
O2-N2 1.233(2)	O2-N2-N1 126.0(2)
N6-C1 1.335(3)	O1-N2-N1 111.4(2)
N8-C2 1.344(3)	C1-N4-C2 123.1(2)
N4-C1 1.341(3)	N6-C1-N5 117.5(2)
N4-C2 1.342(3)	N6-C1-N4 125.8(2)
C1-N5 1.336(3)	N5-C1-N4 116.6(2)
C2-N7 1.324(3)	N7-C2-N4 116.6(2)
	N7-C2-N8 117.9(2)
	N4-C2-N8 125.4(2)

Contract No. N00014-95-1-0013 and N00014-97-1-0409

Program Officer: R. Miller/J. Goldwasser

**Title: Experimental Charge Densities and Electrostatic Potentials in Energetic
Materials and Infrastructure Upgrade for an X-ray Crystallography
Laboratory**

PI: A. Alan Pinkerton

Department of Chemistry, University of Toledo, Toledo, OH 43606

tel. (419) 530-4580, FAX (419) 530-4033, email apinker@uoft02.utoledo.edu

APPENDIX 3c

Variable temperature crystallographic study of $\text{BiGH}_2(\text{DN})_2$

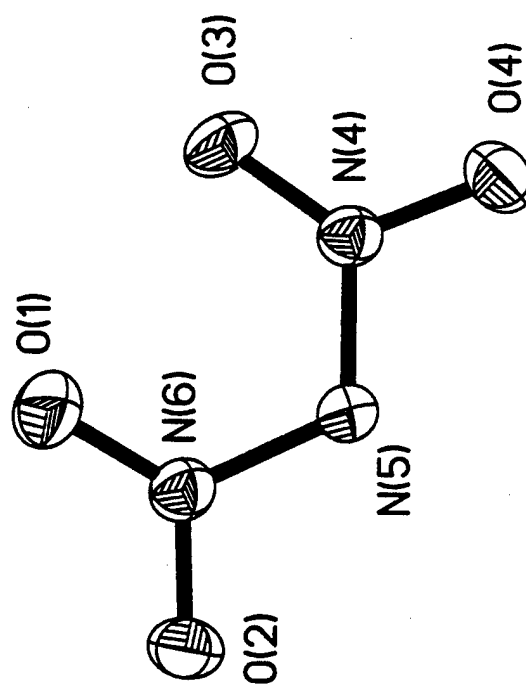
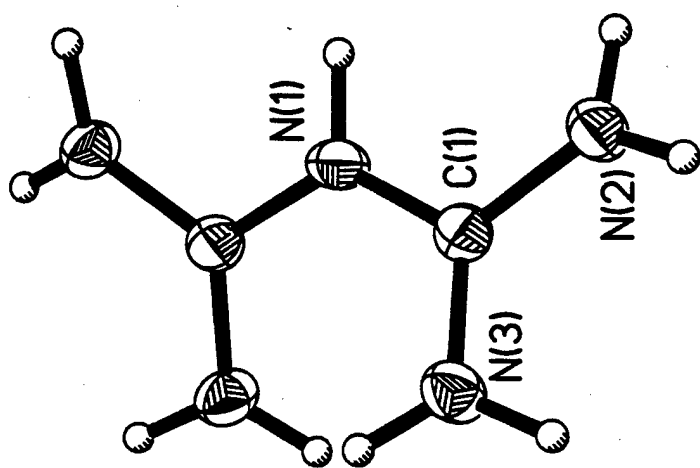


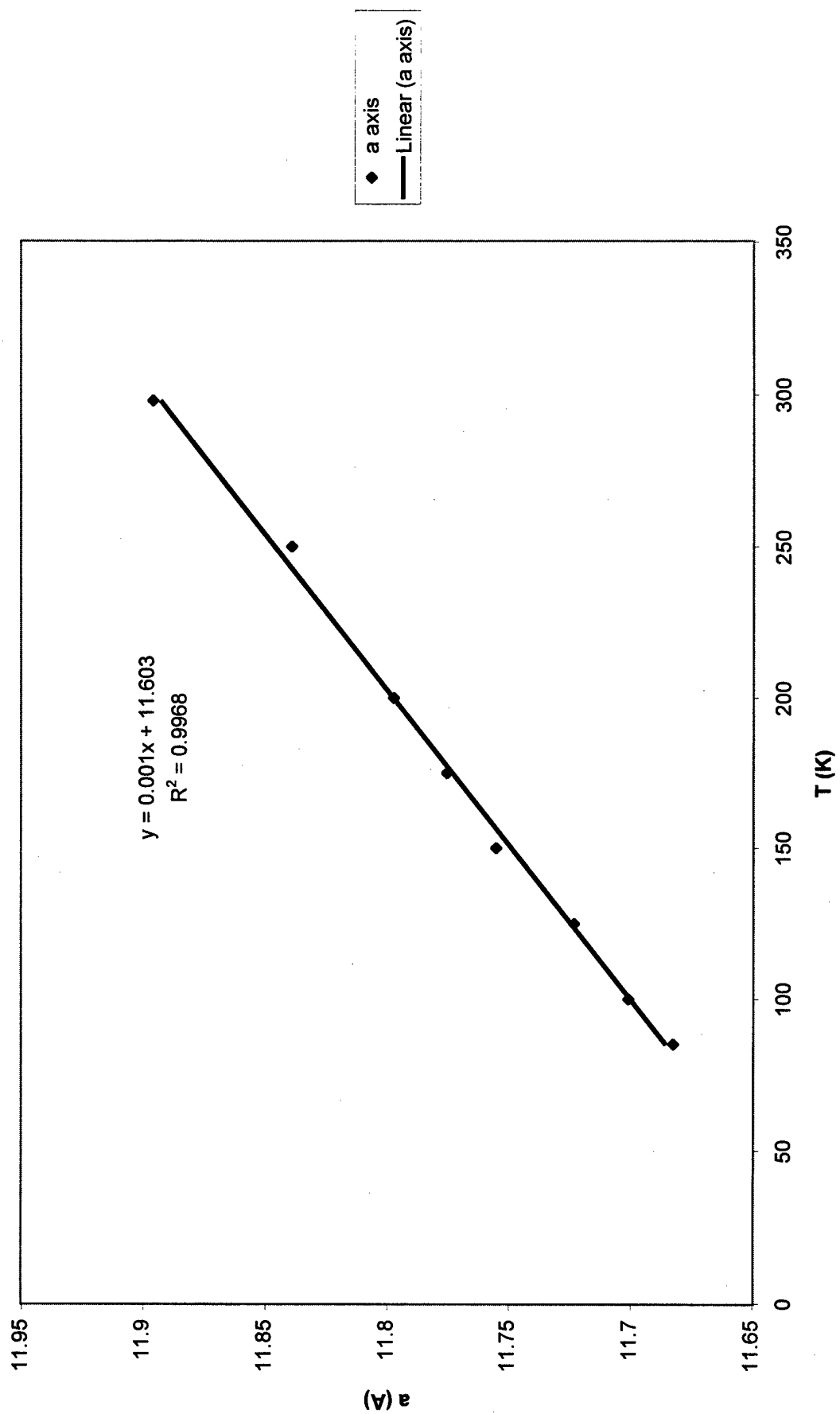
Table 1. Crystal data and structure refinement for biguanidinium bisdinitramide at various temperatures.

Empirical formula	$C_2H_9N_8O_4$									
Formula weight	209.07									
Wavelength	0.71073 Å									
Crystal system	Monoclinic									
Space group	C2/c									
F(000)	648									
Crystal size	0.22 x 0.21 x 0.20 mm									
Z	4									
Instrument	Siemens SMART CCD									
Detector distance	4.99 cm									
Scan width and axis	-0.3° in ω									
Refinement method	Full-matrix least-squares on F ²									
Temperature (K)	293(2)	250(2)	200(2)	150(2)	100(2)	85(2)				
a (Å)	11.8959(6)	11.8391(9)	11.7973(4)	11.7551(5)	11.7008(8)	11.6824(3)				
b (Å)	8.1349(4)	8.1392(6)	8.1492(3)	8.1557(3)	8.1485(5)	8.1450(1)				
c (Å)	13.0359(5)	3.0265(10)	13.0286(3)	13.0302(4)	13.0111(9)	13.0023(3)				
β (°)	115.8060(10)	116.2250(10)	116.6390(10)	117.0050(10)	117.3370(10)	117.4070(10)				
Volume (Å ³)	1135.70(9)	1126.0(2)	1119.59(6)	1113.01(7)	1101.99(13)	1098.33(4)				
Density (calc) (Mg/m ³)	1.843	1.859	1.870	1.881	1.900	1.906				
Absorption coeff. (mm ⁻¹)	0.178	0.179	0.180	0.181	0.183	0.184				
θ range	3.14 to 28.28°	3.15 to 28.31°	3.16 to 28.26°	3.16 to 28.26°	3.17 to 28.28°	3.17 to 28.29°				
Limiting indices	-15 < h < 15	-15 < h < 15	-15 < h < 15	-14 < h < 15	-14 < h < 15	-14 < h < 15				
	-10 < k < 8	-10 < k < 8	-10 < k < 8	-10 < k < 8	-10 < k < 8	-10 < k < 8				
	-17 < l < 17	-17 < l < 17	-17 < l < 17	-17 < l < 17	-17 < l < 17	-17 < l < 17				
Reflections collected	3838	3810	3797	3723	3674	3661				
Independent reflections	1410	1402	1396	1382	1366	1364				
R _{int}	0.0342	0.0327	0.0310	0.0289	0.0306	0.0330				
Data / restraints / parameters	1410 / 5 / 115	1402 / 5 / 115	1396 / 5 / 115	1382 / 5 / 115	1366 / 5 / 115	1364 / 5 / 115				
Goodness-of-fit on F ²	1.040	1.067	1.084	1.051	1.101	1.075				
R1 [I > 2 σ (I)]	0.0467	0.0456	0.0421	0.0371	0.0373	0.0365				
wR2 [I > 2 σ (I)]	0.1302	0.1287	0.1190	0.0995	0.1045	0.1053				
R1 (all data)	0.0641	0.0582	0.0535	0.0455	0.0441	0.0435				
wR2 (all data)	0.1428	0.1384	0.1267	0.1054	0.1101	0.1100				
Extinction coefficient	0.006(2)	0.005(2)	0.005(2)	0.0052(13)	0.0034(13)	0.0028(13)				
Largest diff. peak (eÅ ⁻³)	0.243	0.317	0.279	0.277	0.296	0.305				
Largest diff. hole (eÅ ⁻³)	-0.257	-0.318	-0.294	-0.304	-0.359	-0.354				

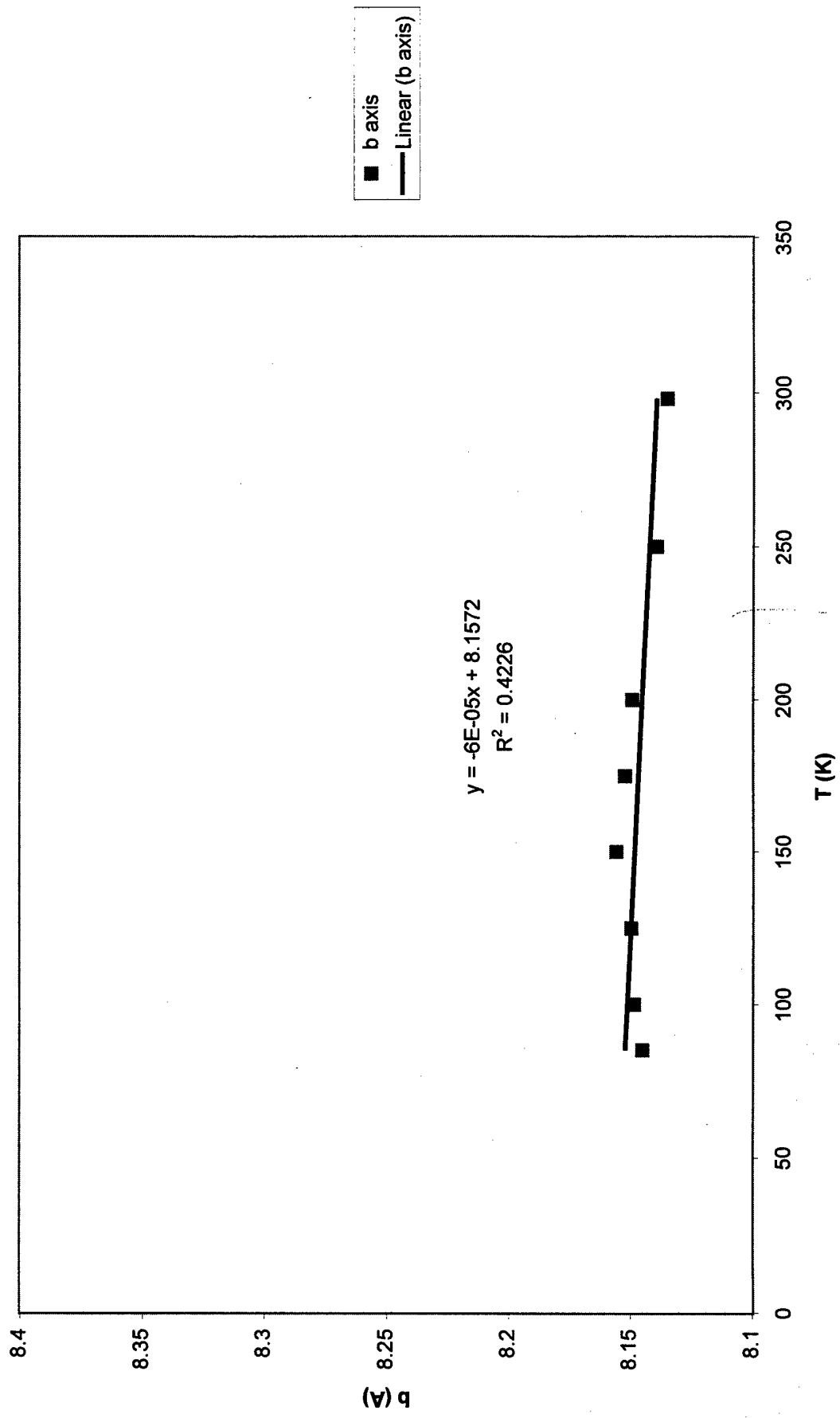
Table. Unit cell parameters for biguanidinium bisdinitramide at various temperatures.

T (K)	<i>a</i> (Å)	<i>b</i> (Å)	<i>c</i> (Å)	β (°)	volume (Å ³)
298	11.8959(6)	8.1349(4)	13.0359(5)	115.806(1)	1135.70(9)
250	11.8391(9)	8.1392(6)	13.0265(10)	116.225(1)	1126.04(15)
200	11.7973(4)	8.1492(3)	13.0286(3)	116.639(1)	1119.59(6)
175	11.7754(4)	8.1522(3)	13.0292(4)	116.824(1)	1116.16(7)
150	11.7551(5)	8.1557(3)	13.0302(4)	117.005(1)	1113.01(7)
125	11.7232(3)	8.1495(2)	13.0160(1)	117.171(1)	1106.32(4)
100	11.7008(8)	8.1485(5)	13.0111(9)	117.337(1)	1101.99(13)
85	11.6824(3)	8.1450(1)	13.0023(3)	117.401(1)	1098.33(4)

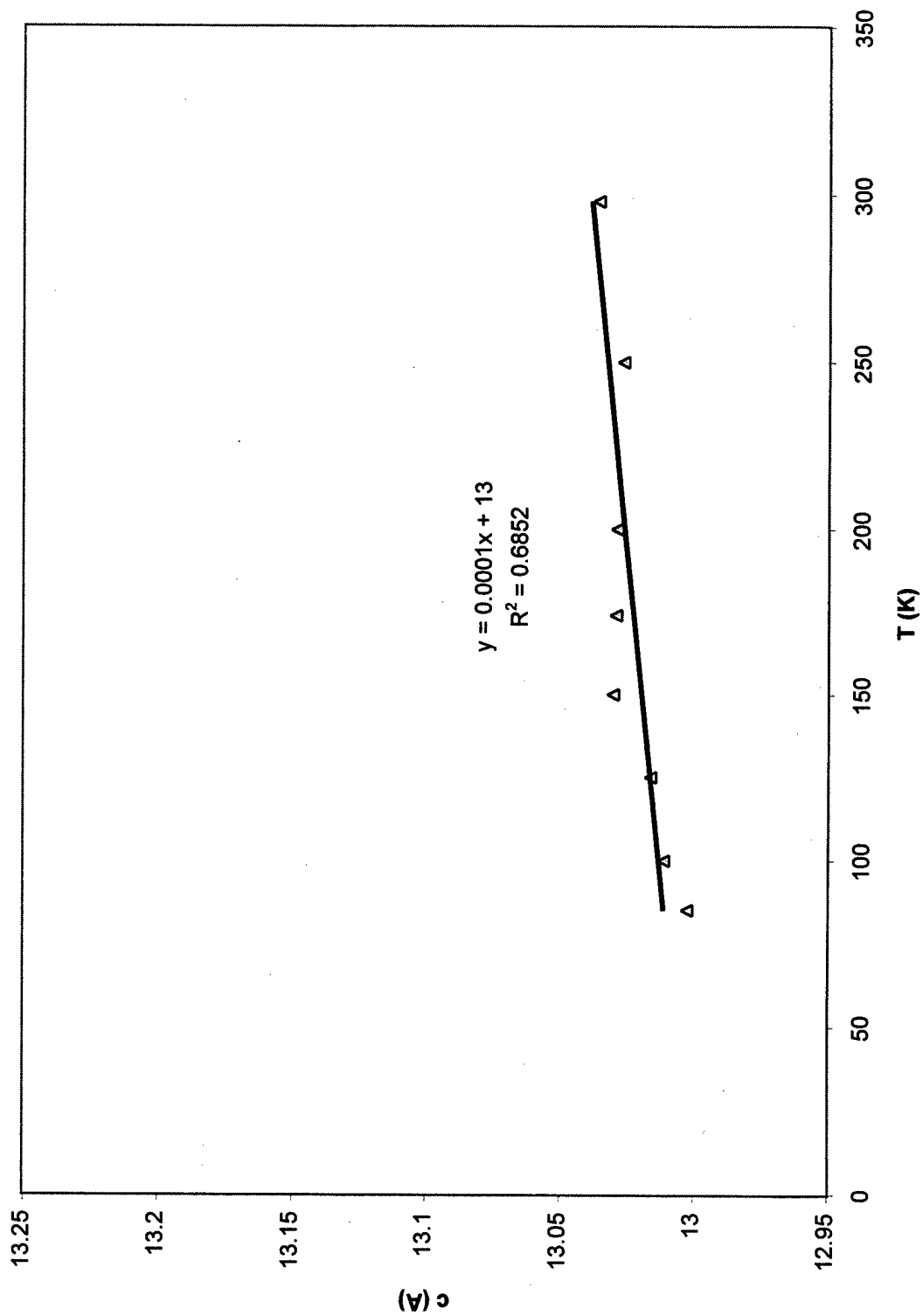
a vs T



b vs T

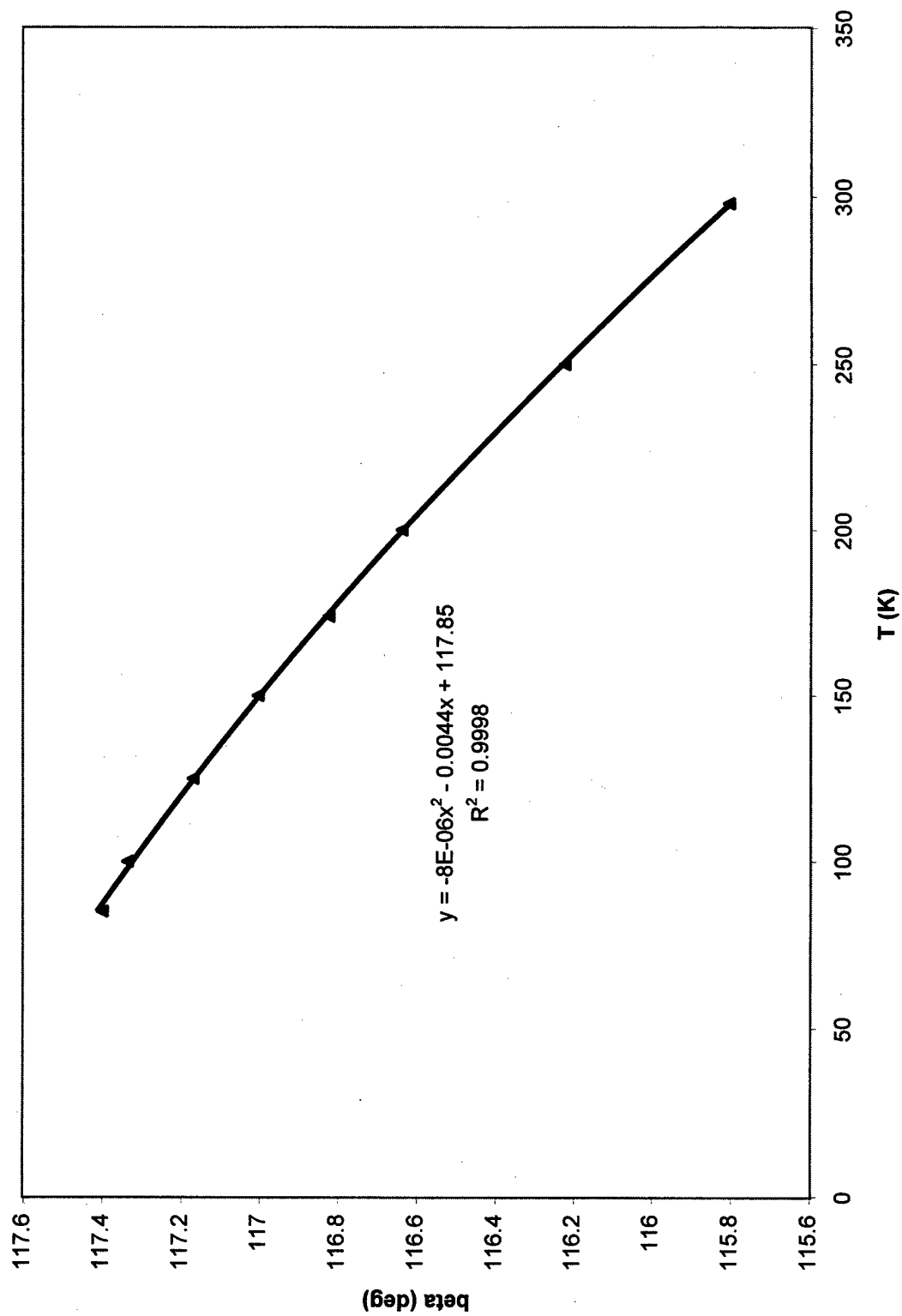


c vs T



Δ c axis
— Linear (c axis)

beta vs T



▲ beta
— Poly. (beta)

vol vs T

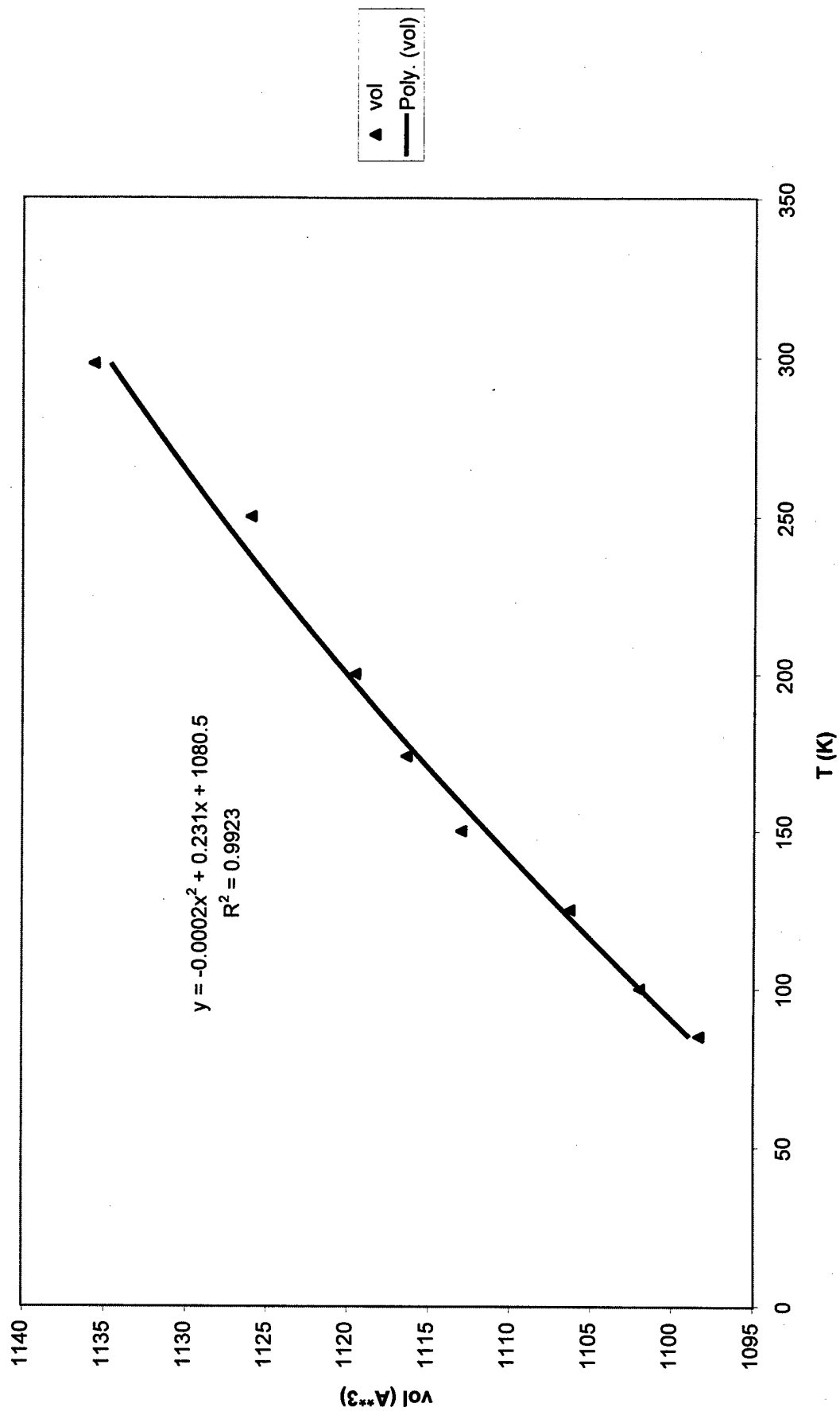


Table 1. Atomic coordinates and equivalent isotropic or isotropic displacement parameters for biguanidinium bisdinitramide at room temperature (298 K). U(eq) is defined as one third of the trace of the orthogonalized Uij tensor.

	x	y	z	U(eq)/U(iso)
C1	0.42495(15)	0.4037(2)	0.29248(12)	0.0251(4)
N1	0.5000	0.4746(3)	0.2500	0.0365(6)
N2	0.3928(2)	0.4983(2)	0.35728(13)	0.0327(4)
N3	0.38594(15)	0.2529(2)	0.26921(14)	0.0338(4)
N4	0.37447(13)	0.1479(2)	0.59989(12)	0.0320(4)
N5	0.3530(2)	-0.0154(2)	0.58705(13)	0.0341(4)
N6	0.35560(13)	-0.0860(2)	0.49066(12)	0.0331(4)
O1	0.3375(2)	-0.0107(2)	0.40456(12)	0.0612(5)
O2	0.37002(13)	-0.2353(2)	0.50034(12)	0.0433(4)
O3	0.41015(15)	0.2337(2)	0.54254(13)	0.0482(4)
O4	0.3586(2)	0.2042(2)	0.68133(13)	0.0521(5)
H1	0.5000	0.5725(43)	0.2500	0.057(10)
H2A	0.4242(22)	0.5958(30)	0.3775(19)	0.048(6)
H2B	0.3316(22)	0.4623(26)	0.3747(18)	0.044(6)
H3A	0.3462(25)	0.2133(32)	0.3102(22)	0.067(8)
H3B	0.3922(22)	0.2049(29)	0.2185(22)	0.050(7)

Table2. Anisotropic displacement parameters (\AA^2) for biguanidinium bisdinitramide at 298 K. The anisotropic displacement factor exponent takes the form:

$$-2\pi^2[(ha^*)^2U_{11} + \dots + 2hka^*b^*U_{12}]$$

	U11	U22	U33	U23	U13	U12
C1	0.0273(8)	0.0274(8)	0.0220(7)	0.0024(6)	0.0120(6)	0.0034(6)
N1	0.0569(15)	0.0202(10)	0.0522(14)	0.000	0.0421(12)	0.000
N2	0.0418(9)	0.0301(8)	0.0365(8)	-0.0055(6)	0.0265(7)	-0.0044(7)
N3	0.0383(9)	0.0324(9)	0.0377(9)	-0.0097(6)	0.0231(7)	-0.0089(6)
N4	0.0296(8)	0.0300(8)	0.0359(8)	-0.0001(6)	0.0138(6)	-0.0044(6)
N5	0.0475(9)	0.0271(8)	0.0318(8)	-0.0004(6)	0.0211(7)	-0.0065(6)
N6	0.0336(8)	0.0371(9)	0.0289(8)	-0.0022(6)	0.0139(6)	-0.0079(6)
O1	0.0968(14)	0.0566(10)	0.0279(7)	0.0014(6)	0.0251(8)	-0.0141(9)
O2	0.0472(9)	0.0330(8)	0.0536(9)	-0.0073(6)	0.0254(7)	-0.0028(6)
O3	0.0611(10)	0.0378(8)	0.0516(9)	0.0020(6)	0.0302(8)	-0.0181(7)
O4	0.0667(10)	0.0467(9)	0.0561(9)	-0.0175(7)	0.0389(8)	-0.0091(7)

Table 3. Atomic coordinates and equivalent isotropic or isotropic displacement parameters for biguanidinium bisdinitramide at 250 K. U(eq) is defined as one third of the trace of the orthogonalized Uij tensor.

	x	y	z	U(eq)/U(iso)
C1	0.42452(13)	0.4040(2)	0.29227(11)	0.0210(3)
N1	0.5000	0.4748(2)	0.2500	0.0307(5)
N2	0.39208(14)	0.4985(2)	0.35683(11)	0.0267(3)
N3	0.38503(13)	0.2530(2)	0.26855(12)	0.0276(4)
N4	0.37440(11)	0.1478(2)	0.59970(11)	0.0257(3)
N5	0.35366(13)	-0.0158(2)	0.58715(11)	0.0280(3)
N6	0.35633(12)	-0.0865(2)	0.49075(10)	0.0268(3)
O1	0.3393(2)	-0.0109(2)	0.40425(10)	0.0485(4)
O2	0.37028(11)	-0.23612(14)	0.50033(11)	0.0347(3)
O3	0.41007(13)	0.23414(14)	0.54233(11)	0.0389(4)
O4	0.35841(13)	0.2041(2)	0.68125(11)	0.0415(4)
H1	0.5000	0.5757(39)	0.2500	0.051(9)
H2A	0.4248(19)	0.5970(26)	0.3781(17)	0.038(5)
H2B	0.3319(20)	0.4653(23)	0.3763(16)	0.038(5)
H3A	0.3469(21)	0.2106(26)	0.3093(18)	0.049(6)
H3B	0.3930(21)	0.1993(27)	0.2184(21)	0.050(6)

Table 4. Anisotropic displacement parameters (\AA^2) for biguanidinium bisdinitramide at 250 K. The anisotropic displacement factor exponent takes the form:

$$-2\pi^2[(ha^*)^2U_{11} + \dots + 2hka^*b^*U_{12}]$$

	U11	U22	U33	U23	U13	U12
C1	0.0243(7)	0.0213(7)	0.0188(7)	0.0024(5)	0.0108(5)	0.0028(6)
N1	0.0507(12)	0.0144(9)	0.0458(12)	0.000	0.0384(11)	0.000
N2	0.0353(7)	0.0228(7)	0.0307(7)	-0.0052(5)	0.0226(6)	-0.0032(6)
N3	0.0327(7)	0.0242(7)	0.0326(8)	-0.0083(5)	0.0207(6)	-0.0073(5)
N4	0.0259(6)	0.0225(7)	0.0291(7)	-0.0004(5)	0.0126(5)	-0.0040(5)
N5	0.0401(8)	0.0210(7)	0.0269(7)	-0.0012(5)	0.0184(6)	-0.0063(5)
N6	0.0292(7)	0.0283(7)	0.0238(7)	-0.0016(5)	0.0126(5)	-0.0065(5)
O1	0.0778(11)	0.0433(8)	0.0241(7)	0.0016(5)	0.0221(7)	-0.0098(7)
O2	0.0394(7)	0.0246(6)	0.0431(7)	-0.0050(5)	0.0210(6)	-0.0020(5)
O3	0.0511(8)	0.0290(7)	0.0422(7)	0.0025(5)	0.0256(6)	-0.0144(6)
O4	0.0532(8)	0.0361(7)	0.0457(8)	-0.0139(6)	0.0314(7)	-0.0070(6)

Table 5. Atomic coordinates and equivalent isotropic or isotropic displacement parameters for biguanidinium bisdinitramide at 200 K. U(eq) is defined as one third of the trace of the orthogonalized Uij tensor.

	x	y	z	U(eq)/Uiso
C1	0.42411(13)	0.4041(2)	0.29204(11)	0.0169(3)
N1	0.5000	0.4751(2)	0.2500	0.0251(4)
N2	0.39133(13)	0.4984(2)	0.35645(11)	0.0210(3)
N3	0.38440(12)	0.2526(2)	0.26822(12)	0.0221(3)
N4	0.37456(11)	0.1479(2)	0.59968(11)	0.0202(3)
N5	0.35412(13)	-0.0162(2)	0.58712(11)	0.0217(3)
N6	0.35701(12)	-0.0869(2)	0.49051(10)	0.0211(3)
O1	0.34095(14)	-0.0114(2)	0.40415(10)	0.0377(4)
O2	0.37062(11)	-0.23684(14)	0.50052(10)	0.0268(3)
O3	0.41002(12)	0.23445(14)	0.54204(10)	0.0304(3)
O4	0.35826(12)	0.20366(15)	0.68124(10)	0.0320(3)
H1	0.5000	0.5765(41)	0.2500	0.042(8)
H2A	0.4264(21)	0.5960(28)	0.3812(18)	0.039(6)
H2B	0.3300(22)	0.4655(25)	0.3747(18)	0.039(6)
H3A	0.3446(22)	0.2117(28)	0.3070(19)	0.043(6)
H3B	0.3913(19)	0.1997(25)	0.2166(18)	0.031(5)

Table 6. Anisotropic displacement parameters (\AA^2) for biguanidinium bisdinitramide at 200 K. The anisotropic displacement factor exponent takes the form:

$$-2\pi^2[(ha^*)^2U_{11} + \dots + 2hka^*b^*U_{12}]$$

	U11	U22	U33	U23	U13	U12
C1	0.0186(6)	0.0164(7)	0.0165(6)	0.0018(5)	0.0083(5)	0.0015(5)
N1	0.0430(12)	0.0104(9)	0.0370(11)	0.000	0.0315(10)	0.000
N2	0.0275(7)	0.0166(7)	0.0254(7)	-0.0046(5)	0.0177(6)	-0.0029(5)
N3	0.0258(7)	0.0190(7)	0.0266(7)	-0.0066(5)	0.0163(6)	-0.0056(5)
N4	0.0197(6)	0.0174(6)	0.0230(6)	0.0003(5)	0.0091(5)	-0.0029(5)
N5	0.0305(7)	0.0153(7)	0.0220(6)	-0.0007(5)	0.0142(5)	-0.0044(5)
N6	0.0223(6)	0.0207(7)	0.0206(6)	-0.0008(5)	0.0098(5)	-0.0046(5)
O1	0.0607(9)	0.0325(7)	0.0202(6)	0.0014(5)	0.0185(6)	-0.0067(6)
O2	0.0305(6)	0.0177(6)	0.0347(7)	-0.0035(4)	0.0169(5)	-0.0017(4)
O3	0.0398(7)	0.0219(6)	0.0335(6)	0.0023(4)	0.0198(6)	-0.0109(5)
O4	0.0409(7)	0.0267(6)	0.0360(7)	-0.0101(5)	0.0241(6)	-0.0047(5)

Table 7. Atomic coordinates and equivalent isotropic or isotropic displacement parameters for biguanidinium bisdinitramide at 175 K. U(eq) is defined as one third of the trace of the orthogonalized Uij tensor.

	x	y	z	U(eq)/U(iso)
C1	0.42381(14)	0.4042(2)	0.29179(13)	0.0216(4)
N1	0.5000	0.4751(2)	0.2500	0.0300(5)
N2	0.39086(15)	0.4986(2)	0.35612(13)	0.0260(4)
N3	0.38409(14)	0.2526(2)	0.26804(14)	0.0265(4)
N4	0.37448(13)	0.1477(2)	0.59972(12)	0.0247(4)
N5	0.35394(15)	-0.0164(2)	0.58668(13)	0.0261(4)
N6	0.35763(13)	-0.0873(2)	0.49068(12)	0.0255(4)
O1	0.3418(2)	-0.0118(2)	0.40418(11)	0.0393(4)
O2	0.37047(12)	-0.2374(2)	0.50041(12)	0.0304(4)
O3	0.40974(14)	0.2347(2)	0.54185(12)	0.0337(4)
O4	0.35786(13)	0.2036(2)	0.68109(12)	0.0348(4)
H1	0.5000	0.5810(54)	0.2500	0.069(13)
H2A	0.4284(23)	0.5970(30)	0.3850(20)	0.042(6)
H2B	0.3303(24)	0.4670(28)	0.3754(20)	0.040(6)
H3A	0.3437(23)	0.2121(30)	0.3068(21)	0.042(6)
H3B	0.3891(21)	0.1981(29)	0.2142(21)	0.037(6)

Table 8. Anisotropic displacement parameters (\AA^2) for biguanidinium bisdinitramide at 175 K. The anisotropic displacement factor exponent takes the form:

$$-2\pi^2[(ha^*)^2U_{11} + \dots + 2hka^*b^*U_{12}]$$

	U11	U22	U33	U23	U13	U12
C1	0.0224(7)	0.0208(7)	0.0228(8)	0.0005(6)	0.0112(6)	0.0015(6)
N1	0.0459(12)	0.0154(9)	0.0443(13)	0.000	0.0340(11)	0.000
N2	0.0304(7)	0.0225(7)	0.0318(8)	-0.0043(6)	0.0200(6)	-0.0023(6)
N3	0.0286(8)	0.0234(8)	0.0327(8)	-0.0064(6)	0.0185(7)	-0.0054(6)
N4	0.0235(6)	0.0223(7)	0.0282(8)	-0.0008(5)	0.0117(6)	-0.0020(5)
N5	0.0343(8)	0.0204(7)	0.0271(8)	-0.0010(5)	0.0170(6)	-0.0031(5)
N6	0.0261(7)	0.0247(7)	0.0260(7)	-0.0006(5)	0.0121(6)	-0.0037(5)
O1	0.0579(9)	0.0356(8)	0.0249(7)	0.0018(5)	0.0191(6)	-0.0055(6)
O2	0.0329(7)	0.0224(6)	0.0382(8)	-0.0030(5)	0.0181(6)	-0.0010(5)
O3	0.0406(7)	0.0262(7)	0.0386(8)	0.0022(5)	0.0217(6)	-0.0097(5)
O4	0.0410(7)	0.0308(7)	0.0394(8)	-0.0091(6)	0.0241(6)	-0.0038(6)

Table 9. Atomic coordinates and equivalent isotropic or isotropic displacement parameters for biguanidinium bisdinitramide at 150 K. $U(eq)$ is defined as one third of the trace of the orthogonalized U_{ij} tensor

	x	y	z	$U(eq)/U(iso)$
C1	0.42358(11)	0.40429(15)	0.29176(10)	0.0139(3)
N1	0.5000	0.4752(2)	0.2500	0.0206(4)
N2	0.39055(11)	0.49860(13)	0.35608(9)	0.0167(3)
N3	0.38366(10)	0.25252(13)	0.26773(10)	0.0176(3)
N4	0.37456(10)	0.14796(14)	0.59952(9)	0.0161(3)
N5	0.35449(11)	-0.01665(13)	0.58703(9)	0.0176(3)
N6	0.35797(10)	-0.08732(14)	0.49062(9)	0.0166(3)
O1	0.34252(11)	-0.01167(12)	0.40403(8)	0.0285(3)
O2	0.37082(9)	-0.23747(11)	0.50055(8)	0.0208(2)
O3	0.40981(10)	0.23487(12)	0.54177(9)	0.0237(3)
O4	0.35781(10)	0.20331(12)	0.68104(8)	0.0248(3)
H1	0.5000	0.5756(34)	0.2500	0.035(7)
H2A	0.4235(17)	0.5941(23)	0.3795(15)	0.030(4)
H2B	0.3293(18)	0.4650(21)	0.3753(15)	0.032(5)
H3A	0.3424(17)	0.2126(22)	0.3047(16)	0.032(5)
H3B	0.3900(16)	0.1981(21)	0.2150(15)	0.025(4)

Table 10. Anisotropic displacement parameters (\AA^2) for biguanidinium bisdinitramide at 150 K. The anisotropic displacement factor exponent takes the form:
 $-2\pi^2[(ha^*)^2U_{11} + \dots + 2hka^*b^*U_{12}]$

	U11	U22	U33	U23	U13	U12
C1	0.0152(6)	0.0136(6)	0.0129(5)	0.0022(4)	0.0064(4)	0.0021(5)
N1	0.0357(9)	0.0081(7)	0.0310(9)	0.000	0.0265(8)	0.000
N2	0.0220(6)	0.0130(5)	0.0201(5)	-0.0031(4)	0.0140(5)	-0.0024(4)
N3	0.0211(6)	0.0149(6)	0.0208(5)	-0.0051(4)	0.0131(5)	-0.0040(4)
N4	0.0162(5)	0.0146(5)	0.0171(5)	0.0006(4)	0.0072(4)	-0.0016(4)
N5	0.0258(6)	0.0119(5)	0.0182(5)	-0.0006(4)	0.0127(5)	-0.0033(4)
N6	0.0180(5)	0.0160(5)	0.0161(5)	-0.0007(4)	0.0078(4)	-0.0032(4)
O1	0.0452(7)	0.0256(6)	0.0156(5)	0.0021(4)	0.0145(5)	-0.0045(5)
O2	0.0249(5)	0.0134(5)	0.0262(5)	-0.0023(3)	0.0133(4)	-0.0014(4)
O3	0.0311(5)	0.0171(5)	0.0259(5)	0.0018(4)	0.0156(4)	-0.0080(4)
O4	0.0323(6)	0.0212(5)	0.0268(5)	-0.0074(4)	0.0187(5)	-0.0029(4)

Table 11. Atomic coordinates and equivalent isotropic or isotropic displacement parameters for biguanidinium bisdinitramide at 125 K. U(eq) is defined as one third of the trace of the orthogonalized Uij tensor

	x	y	z	U(eq)/U(iso)
C1	0.42336(14)	0.4043(2)	0.29169(13)	0.0175(4)
N1	0.5000	0.4755(3)	0.2500	0.0241(5)
N2	0.39032(14)	0.4986(2)	0.35591(13)	0.0205(4)
N3	0.38327(14)	0.2527(2)	0.26750(13)	0.0209(4)
N4	0.37449(13)	0.1475(2)	0.59954(12)	0.0193(4)
N5	0.35442(14)	-0.0167(2)	0.58663(12)	0.0206(4)
N6	0.35834(12)	-0.0877(2)	0.49066(12)	0.0199(4)
O1	0.34324(14)	-0.0120(2)	0.40398(11)	0.0297(4)
O2	0.37088(12)	-0.2381(2)	0.50051(11)	0.0235(3)
O3	0.40950(13)	0.2352(2)	0.54166(12)	0.0260(3)
O4	0.35770(13)	0.2033(2)	0.68107(11)	0.0266(4)
H1	0.5000	0.5787(50)	0.2500	0.046(10)
H2A	0.4276(23)	0.5972(31)	0.3851(21)	0.035(6)
H2B	0.3298(26)	0.4652(30)	0.3745(21)	0.038(7)
H3A	0.3432(22)	0.2123(29)	0.3054(20)	0.030(6)
H3B	0.3892(22)	0.1961(30)	0.2129(21)	0.033(6)

Table 12. Anisotropic displacement parameters (\AA^2) for biguanidinium bisdinitramide at 125 K. The anisotropic displacement factor exponent takes the form:

$$-2\pi^2[(ha^*)^2U_{11} + \dots + 2hka^*b^*U_{12}]$$

	U11	U22	U33	U23	U13	U12
C1	0.0168(7)	0.0194(8)	0.0164(7)	0.0005(6)	0.0076(6)	0.0011(6)
N1	0.0370(12)	0.0144(10)	0.0335(12)	0.000	0.0270(10)	0.000
N2	0.0234(7)	0.0196(7)	0.0228(7)	-0.0031(6)	0.0143(6)	-0.0019(5)
N3	0.0221(7)	0.0205(8)	0.0242(7)	-0.0044(6)	0.0140(6)	-0.0034(5)
N4	0.0178(6)	0.0189(7)	0.0203(7)	-0.0007(5)	0.0081(5)	-0.0018(5)
N5	0.0262(7)	0.0176(7)	0.0204(7)	-0.0011(5)	0.0127(6)	-0.0029(5)
N6	0.0193(6)	0.0207(7)	0.0192(7)	-0.0003(5)	0.0084(5)	-0.0033(5)
O1	0.0418(8)	0.0292(7)	0.0185(6)	0.0017(5)	0.0139(6)	-0.0037(6)
O2	0.0249(6)	0.0188(6)	0.0276(7)	-0.0018(5)	0.0127(5)	-0.0008(5)
O3	0.0308(7)	0.0221(7)	0.0276(7)	0.0018(5)	0.0155(6)	-0.0073(5)
O4	0.0308(7)	0.0260(7)	0.0276(7)	-0.0068(5)	0.0173(6)	-0.0028(5)

Table 13. Atomic coordinates and equivalent isotropic or isotropic displacement parameters for biguanidinium bisdinitramide at 100 K. U(eq) is defined as one third of the trace of the orthogonalized Uij tensor

	x	y	z	U(eq)/U(iso)
C1	0.42318(12)	0.40433(15)	0.29165(10)	0.0106(3)
N1	0.5000	0.4757(2)	0.2500	0.0157(4)
N2	0.38999(11)	0.49881(13)	0.35581(9)	0.0124(3)
N3	0.38294(11)	0.25259(13)	0.26734(10)	0.0132(3)
N4	0.37457(10)	0.14783(14)	0.59948(9)	0.0118(3)
N5	0.35490(11)	-0.01702(13)	0.58694(9)	0.0127(3)
N6	0.35873(10)	-0.08791(14)	0.49068(9)	0.0123(3)
O1	0.34418(11)	-0.01197(12)	0.40400(8)	0.0200(3)
O2	0.37112(9)	-0.23814(11)	0.50059(8)	0.0148(2)
O3	0.40945(10)	0.23542(11)	0.54148(9)	0.0168(3)
O4	0.35770(9)	0.20309(12)	0.68123(8)	0.0173(3)
H1	0.5000	0.5781(35)	0.2500	0.031(7)
H2A	0.4250(18)	0.5957(23)	0.3806(16)	0.025(5)
H2B	0.3292(19)	0.4675(21)	0.3713(15)	0.022(4)
H3A	0.3436(18)	0.2116(22)	0.3041(16)	0.024(5)
H3B	0.3876(17)	0.1993(22)	0.2147(17)	0.022(4)

Table 14. Anisotropic displacement parameters (\AA^2) for biguanidinium bisdinitramide at 100 K. The anisotropic displacement factor exponent takes the form:

$$-2\pi^2[(ha^*)^2U_{11} + \dots + 2hka^*b^*U_{12}]$$

	U11	U22	U33	U23	U13	U12
C1	0.0104(6)	0.0127(6)	0.0076(5)	0.0019(4)	0.0033(4)	0.0021(4)
N1	0.0270(9)	0.0069(7)	0.0224(8)	0.000	0.0192(7)	0.000
N2	0.0158(5)	0.0110(5)	0.0135(5)	-0.0022(4)	0.0094(5)	-0.0017(4)
N3	0.0154(6)	0.0126(6)	0.0136(6)	-0.0034(4)	0.0084(5)	-0.0023(4)
N4	0.0116(5)	0.0116(5)	0.0109(5)	0.0007(4)	0.0041(4)	-0.0006(4)
N5	0.0184(6)	0.0100(5)	0.0115(5)	-0.0012(4)	0.0084(4)	-0.0021(4)
N6	0.0122(5)	0.0133(5)	0.0105(5)	-0.0001(4)	0.0046(4)	-0.0022(4)
O1	0.0303(6)	0.0192(5)	0.0097(5)	0.0013(4)	0.0085(4)	-0.0030(4)
O2	0.0175(5)	0.0097(5)	0.0179(5)	-0.0017(3)	0.0087(4)	-0.0011(3)
O3	0.0217(5)	0.0134(5)	0.0171(5)	0.0015(3)	0.0105(4)	-0.0054(4)
O4	0.0213(5)	0.0166(5)	0.0171(5)	-0.0052(4)	0.0115(4)	-0.0017(4)

Table 15. Atomic coordinates and equivalent isotropic or isotropic displacement parameters for biguanidinium bisdinitramide at 85 K. $U(eq)$ is defined as one third of the trace of the orthogonalized U_{ij} tensor

	x	y	z	$U(eq)/U(iso)$
C1	0.42316(12)	0.40426(15)	0.29161(10)	0.0097(3)
N1	0.5000	0.4757(2)	0.2500	0.0144(4)
N2	0.38981(11)	0.49884(13)	0.35571(9)	0.0112(3)
N3	0.38274(10)	0.25250(13)	0.26705(9)	0.0121(3)
N4	0.37461(10)	0.14776(13)	0.59950(9)	0.0107(3)
N5	0.35512(11)	-0.01703(13)	0.58689(9)	0.0115(3)
N6	0.35897(10)	-0.08805(13)	0.49059(8)	0.0110(3)
O1	0.34446(10)	-0.01206(11)	0.40402(8)	0.0174(3)
O2	0.37123(9)	-0.23823(11)	0.50064(8)	0.0132(2)
O3	0.40943(9)	0.23547(11)	0.54152(8)	0.0149(2)
O4	0.35754(9)	0.20277(11)	0.68120(8)	0.0157(3)
H1	0.5000	0.5814(32)	0.2500	0.026(6)
H2A	0.4249(18)	0.5981(23)	0.3814(16)	0.029(5)
H2B	0.3294(18)	0.4674(20)	0.3732(15)	0.021(4)
H3A	0.3436(18)	0.2094(22)	0.3058(16)	0.026(5)
H3B	0.3882(16)	0.1970(21)	0.2134(16)	0.021(4)

Table 16. Anisotropic displacement parameters (\AA^2) for biguanidinium bisdinitramide at 85 K. The anisotropic displacement factor exponent takes the form:

$$-2\pi^2[(ha^*)^2U_{11} + \dots + 2hka^*b^*U_{12}]$$

	U11	U22	U33	U23	U13	U12
C1	0.0104(6)	0.0119(6)	0.0050(5)	0.0021(4)	0.0021(4)	0.0021(4)
N1	0.0245(9)	0.0075(7)	0.0187(8)	0.000	0.0166(7)	0.000
N2	0.0146(5)	0.0102(5)	0.0113(5)	-0.0021(4)	0.0080(4)	-0.0014(4)
N3	0.0147(6)	0.0115(6)	0.0114(5)	-0.0031(4)	0.0072(5)	-0.0020(4)
N4	0.0103(5)	0.0112(5)	0.0088(5)	0.0004(4)	0.0030(4)	-0.0007(4)
N5	0.0174(6)	0.0090(5)	0.0092(5)	-0.0011(4)	0.0071(4)	-0.0017(4)
N6	0.0116(5)	0.0121(5)	0.0082(5)	-0.0008(4)	0.0036(4)	-0.0020(4)
O1	0.0270(5)	0.0173(5)	0.0075(5)	0.0018(3)	0.0075(4)	-0.0024(4)
O2	0.0160(5)	0.0087(5)	0.0147(5)	-0.0011(3)	0.0068(4)	-0.0007(3)
O3	0.0199(5)	0.0121(5)	0.0131(5)	0.0023(3)	0.0080(4)	-0.0044(4)
O4	0.0207(5)	0.0155(5)	0.0131(5)	-0.0044(4)	0.0096(4)	-0.0010(4)

Table 17. Bond lengths (Å) and angles (°) for biguanidinium bisdinitramide.

At 298 K:

C1-N1 1.366(2)	N3-C1-N2	121.8(2)
C1-N2 1.316(2)	N3-C1-N1	122.3(2)
C1-N3 1.300(2)	N2-C1-N1	115.9(2)
N4-O3 1.226(2)	N4-N5-N6	116.11(13)
N4-O4 1.244(2)	O3-N4-O4	122.2(2)
N5-N4 1.349(2)	O3-N4-N5	125.6(2)
N6-O1 1.213(2)	O4-N4-N5	112.20(14)
N6-O2 1.226(2)	O1-N6-O2	123.8(2)
N6-N5 1.394(2)	O1-N6-N5	124.2(2)
	O2-N6-N5	111.86(14)

At 250 K:

N6-O1 1.220(2)	O1-N6-O2	123.64(14)
N6-O2 1.228(2)	O1-N6-N5	124.29(14)
N6-N5 1.394(2)	O2-N6-N5	111.92(12)
N5-N4 1.351(2)	N4-N5-N6	116.15(12)
N4-O3 1.229(2)	O3-N4-O4	122.06(14)
N4-O4 1.246(2)	O3-N4-N5	125.68(13)
C1-N3 1.303(2)	O4-N4-N5	112.19(12)
C1-N2 1.316(2)	N3-C1-N2	121.83(14)
C1-N1 1.367(2)	N3-C1-N1	122.14(14)
	N2-C1-N1	116.01(14)

At 200 K:

N6-O1 1.220(2)	O1-N6-O2	123.82(13)
N6-O2 1.232(2)	O1-N6-N5	124.50(13)
N6-N5 1.398(2)	O2-N6-N5	111.57(12)
N5-N4 1.356(2)	N4-N5-N6	116.09(12)
N4-O3 1.232(2)	O3-N4-O4	122.33(13)
N4-O4 1.247(2)	O3-N4-N5	125.58(13)
C1-N3 1.308(2)	O4-N4-N5	112.03(12)
C1-N2 1.318(2)	N3-C1-N2	121.74(14)
C1-N1 1.370(2)	N3-C1-N1	122.20(14)
	N2-C1-N1	116.05(14)
	C1-N1-C1	130.0(2)

At 175 K:

N6-O1 1.222(2)	O1-N6-O2	123.7(2)
N6-O2 1.233(2)	O1-N6-N5	124.3(2)
N6-N5 1.396(2)	O2-N6-N5	111.76(13)
N5-N4 1.356(2)	N4-N5-N6	116.39(13)
N4-O3 1.236(2)	O3-N4-O4	122.22(15)
N4-O4 1.248(2)	O3-N4-N5	125.45(15)
C1-N3 1.308(2)	O4-N4-N5	112.29(14)
C1-N2 1.319(2)	N3-C1-N2	121.7(2)
C1-N1 1.370(2)	N3-C1-N1	122.2(2)
	N2-C1-N1	116.05(15)
	C1-N1-C1	130.0(2)

At 150 K:

N6-O1 1.2251(14)	O1-N6-O2	123.82(11)
N6-O2 1.2334(14)	O1-N6-N5	124.53(11)
N6-N5 1.3995(14)	O2-N6-N5	111.52(10)
N5-N4 1.3600(15)	N4-N5-N6	116.09(10)
N4-O3 1.2343(14)	O3-N4-O4	122.47(11)
N4-O4 1.2494(14)	O3-N4-N5	125.59(11)
C1-N3 1.310(2)	O4-N4-N5	111.88(10)
C1-N2 1.319(2)	N3-C1-N2	121.72(12)
C1-N1 1.3716(13)	N3-C1-N1	122.10(12)
	N2-C1-N1	116.17(12)
	C1-N1-C1	130.1(2)

At 125 K:

N6-O1 1.225(2)	O1-N6-O2	123.74(15)
N6-O2 1.235(2)	O1-N6-N5	124.42(15)
N6-N5 1.396(2)	O2-N6-N5	111.69(13)
N5-N4 1.355(2)	N4-N5-N6	116.43(13)
N4-O3 1.237(2)	O3-N4-O4	122.14(15)
N4-O4 1.250(2)	O3-N4-N5	125.60(14)
C1-N3 1.309(2)	O4-N4-N5	112.22(14)
C1-N2 1.317(2)	N3-C1-N2	121.7(2)
C1-N1 1.372(2)	N3-C1-N1	122.2(2)
	N2-C1-N1	116.1(2)
	C1-N1-C1	130.0(2)

At 100 K:

N6-O1 1.2278(14)	O1-N6-O2	123.83(11)
N6-O2 1.2325(14)	O1-N6-N5	124.50(11)
N6-N5 1.3985(14)	O2-N6-N5	111.54(10)
N5-N4 1.3599(15)	N4-N5-N6	116.25(10)
N4-O3 1.2363(14)	O3-N4-O4	122.43(11)
N4-O4 1.2513(14)	O3-N4-N5	125.60(11)
C1-N3 1.309(2)	O4-N4-N5	111.93(10)
C1-N2 1.318(2)	N3-C1-N2	121.78(12)
C1-N1 1.3736(14)	N3-C1-N1	122.16(12)
	N2-C1-N1	116.05(12)
	C1-N1-C1	129.9(2)

At 85 K:

N6-O1 1.2260(13)	O1-N6-O2	123.99(11)
N6-O2 1.2315(14)	O1-N6-N5	124.42(11)
N6-N5 1.3986(14)	O2-N6-N5	111.46(9)
N5-N4 1.3586(15)	N4-N5-N6	116.36(10)
N4-O3 1.2355(14)	O3-N4-O4	122.49(11)
N4-O4 1.2506(13)	O3-N4-N5	125.55(10)
C1-N3 1.309(2)	O4-N4-N5	111.91(10)
C1-N2 1.319(2)	N3-C1-N2	121.83(12)
C1-N1 1.3726(14)	N3-C1-N1	122.13(12)
	N2-C1-N1	116.02(11)
	C1-N1-C1	129.9(2)

Contract No. N00014-95-1-0013 and N00014-97-1-0409

Program Officer: R. Miller/J. Goldwasser

**Title: Experimental Charge Densities and Electrostatic Potentials in Energetic
Materials and Infrastructure Upgrade for an X-ray Crystallography
Laboratory**

PI: A. Alan Pinkerton

Department of Chemistry, University of Toledo, Toledo, OH 43606

tel. (419) 530-4580, FAX (419) 530-4033, email apinker@uoft02.utoledo.edu

APPENDIX 3d

Variable temperature crystallographic study of ϵ -CL20

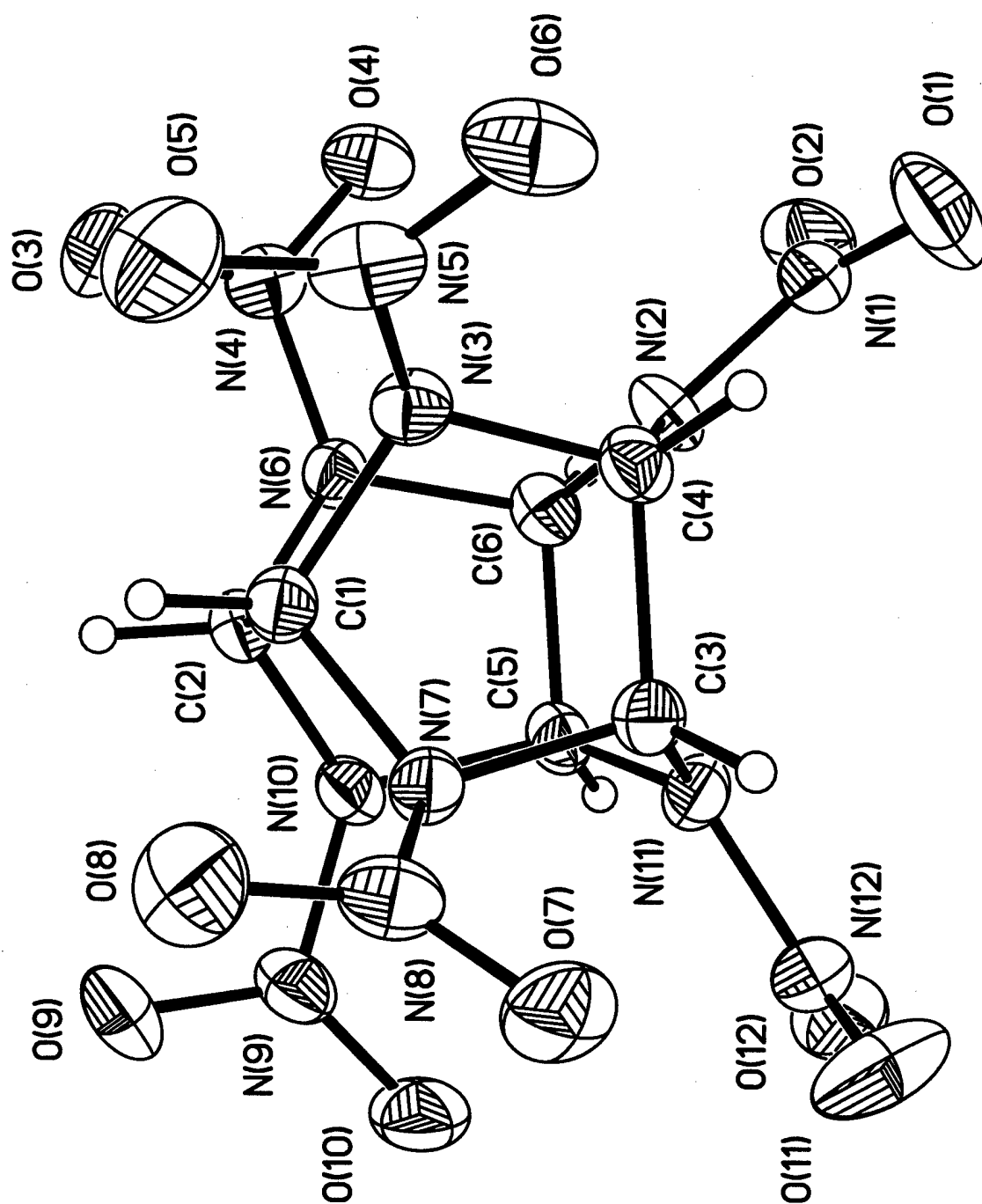
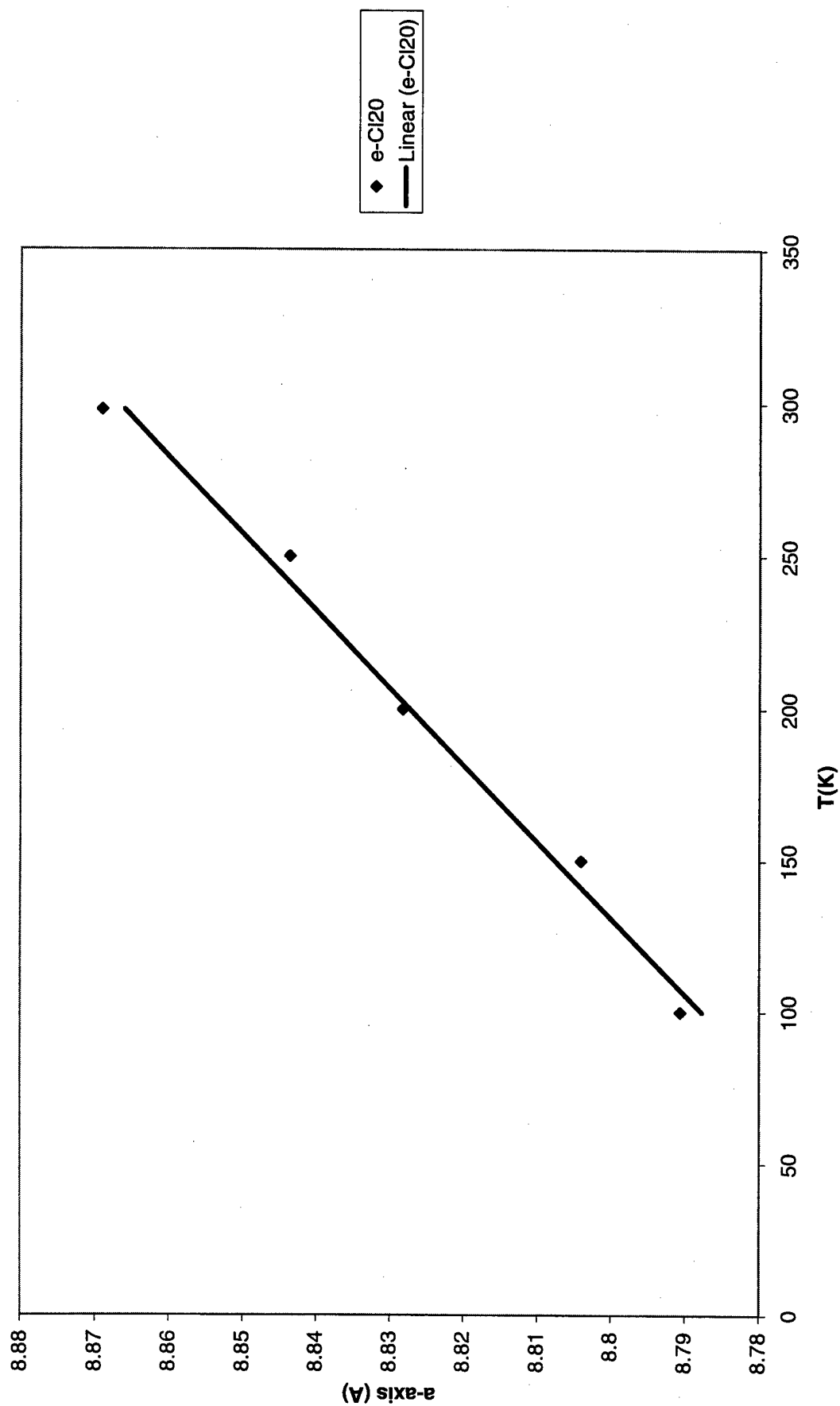


Table 1. Crystal data and structure refinement for ϵ -Cl20 at various temperatures.

Empirical formula	$C_6H_6N_{12}O_{12}$		
Formula weight	438.23		
Wavelength	0.71073 Å		
Crystal system	Monoclinic		
Space group	$P2_1/n$		
$F(000)$	888		
Crystal size	0.3 x 0.2 x 0.2 mm		
Z	4		
Instrument	Siemens SMART CCD		
Detector distance	5 cm		
Scan width and axis	-0.3° in ω		
Refinement method	Full-matrix least-squares on F^2		
Temperature (K)	298(1)	250(1)	200(1)
a (Å)	8.8690(3)	8.8436(2)	8.8282(2)
b (Å)	12.6023(4)	12.5638(2)	12.5364(1)
c (Å)	13.4070(4)	13.3622(4)	13.3455(3)
β ($^\circ$)	106.932(1)	106.821(1)	106.751(1)
Volume (Å ³)	1433.54(8)	1421.14(2)	1414.32(2)
Density (calc) (Mg/m ³)	2.030	2.048	2.058
Absorption coeff. (mm ⁻¹)	0.195	0.196	0.197
θ range	2.27 to 28.25 $^\circ$	2.27 to 28.26 $^\circ$	2.28 to 28.28 $^\circ$
Limiting indices	-10 < h < 11 -15 < k < 16 -15 < l < 17	-10 < h < 11 -15 < k < 16 -15 < l < 17	-10 < h < 11 -15 < k < 16 -15 < l < 17
Reflections collected	9481	9531	9483
Independent reflections	3521	3492	3473
R_{int}	0.0470	0.0457	0.0441
Data / restraints / parameters	3521 / 0 / 295	3492 / 0 / 295	3473 / 0 / 295
Goodness-of-fit on F^2	1.057	1.026	1.011
$R1 [I > 2\sigma(I)]$	0.0522	0.0479	0.0445
$wR2 [I > 2\sigma(I)]$	0.0977	0.0930	0.0879
$R1$ (all data)	0.0999	0.0920	0.0853
$wR2$ (all data)	0.1187	0.1107	0.1037
Largest diff. peak (eÅ ⁻³)	0.250	0.313	0.259
Largest diff. hole (eÅ ⁻³)	-0.290	-0.333	-0.317
			150(1)
			8.8040(3)
			12.5058(4)
			13.3050(5)
			106.615(1)
			1403.73(2)
			2.074
			0.199
			2.28 to 28.28 $^\circ$
			-10 < h < 11
			-15 < k < 16
			-15 < l < 17
			9412
			3437
			0.0419
			3437 / 0 / 295
			1.013
			0.0437
			0.0901
			0.0743
			0.1030
			0.315
			-0.383

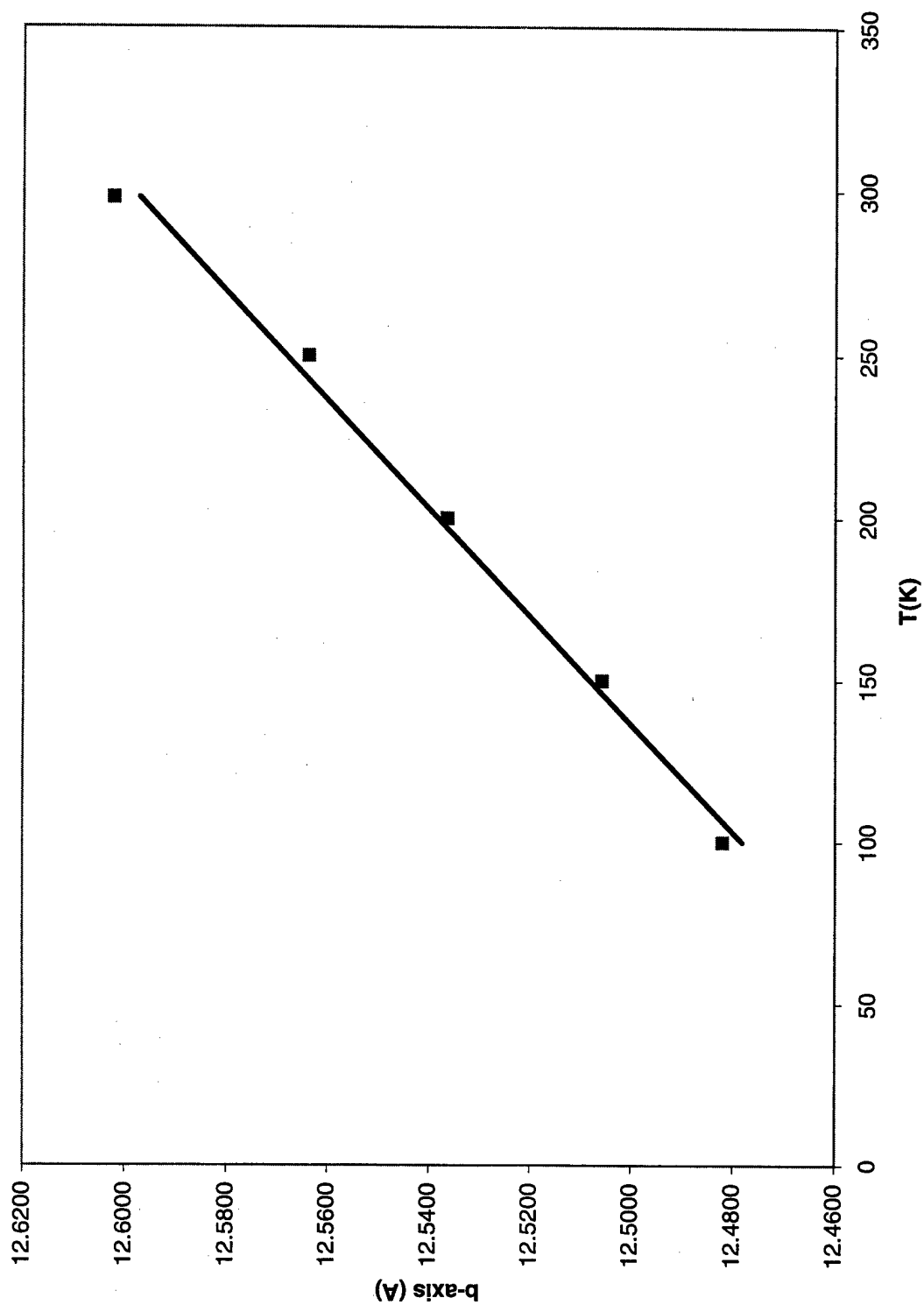
e-Cl2O: Temperature Dependence of the a-axis

$$y = 0.0004x + 8.7481$$
$$R^2 = 0.9892$$



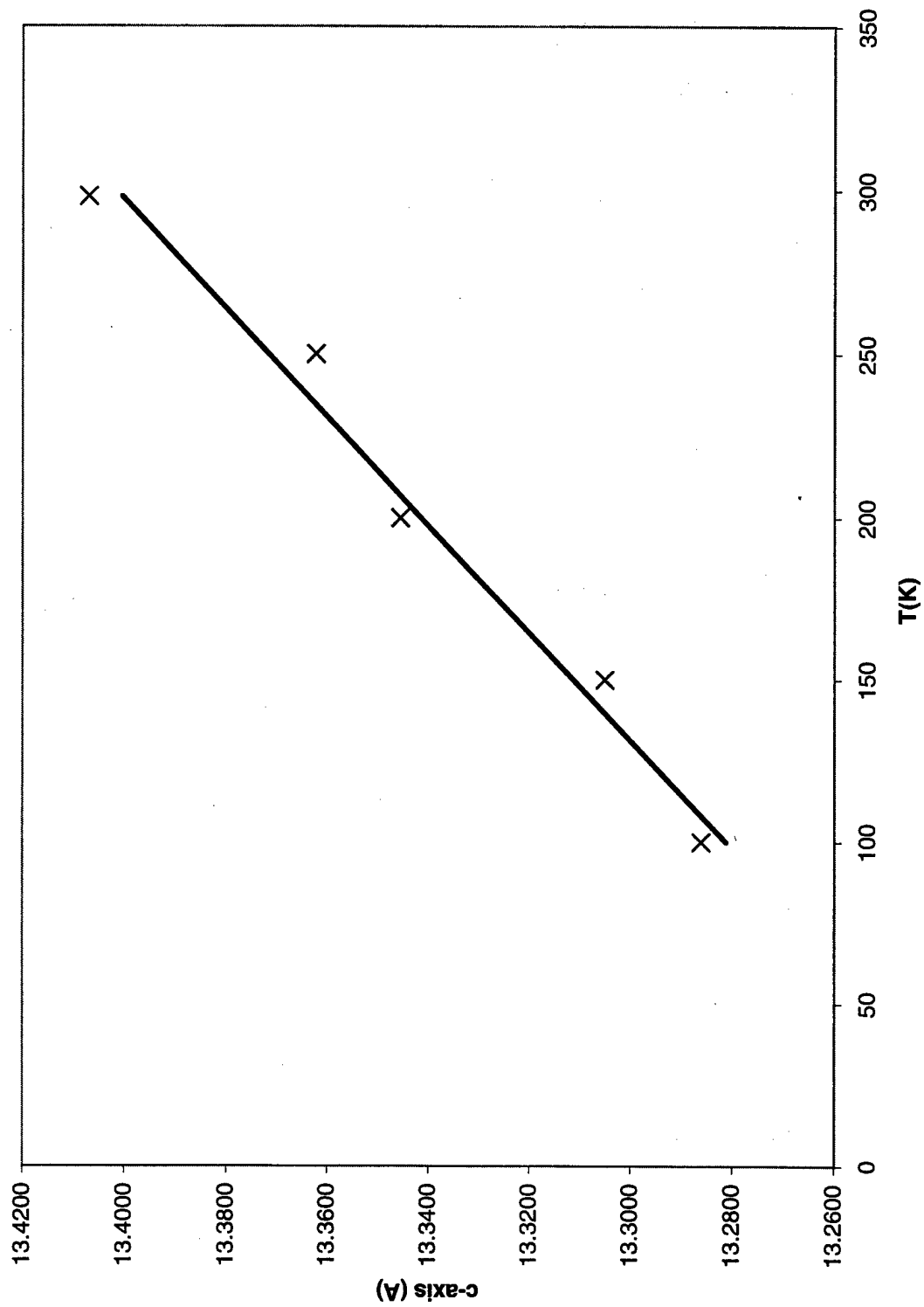
e-Cl20: Temperature Dependence of the b-axis

$$y = 0.0006x + 12.418$$
$$R^2 = 0.9921$$



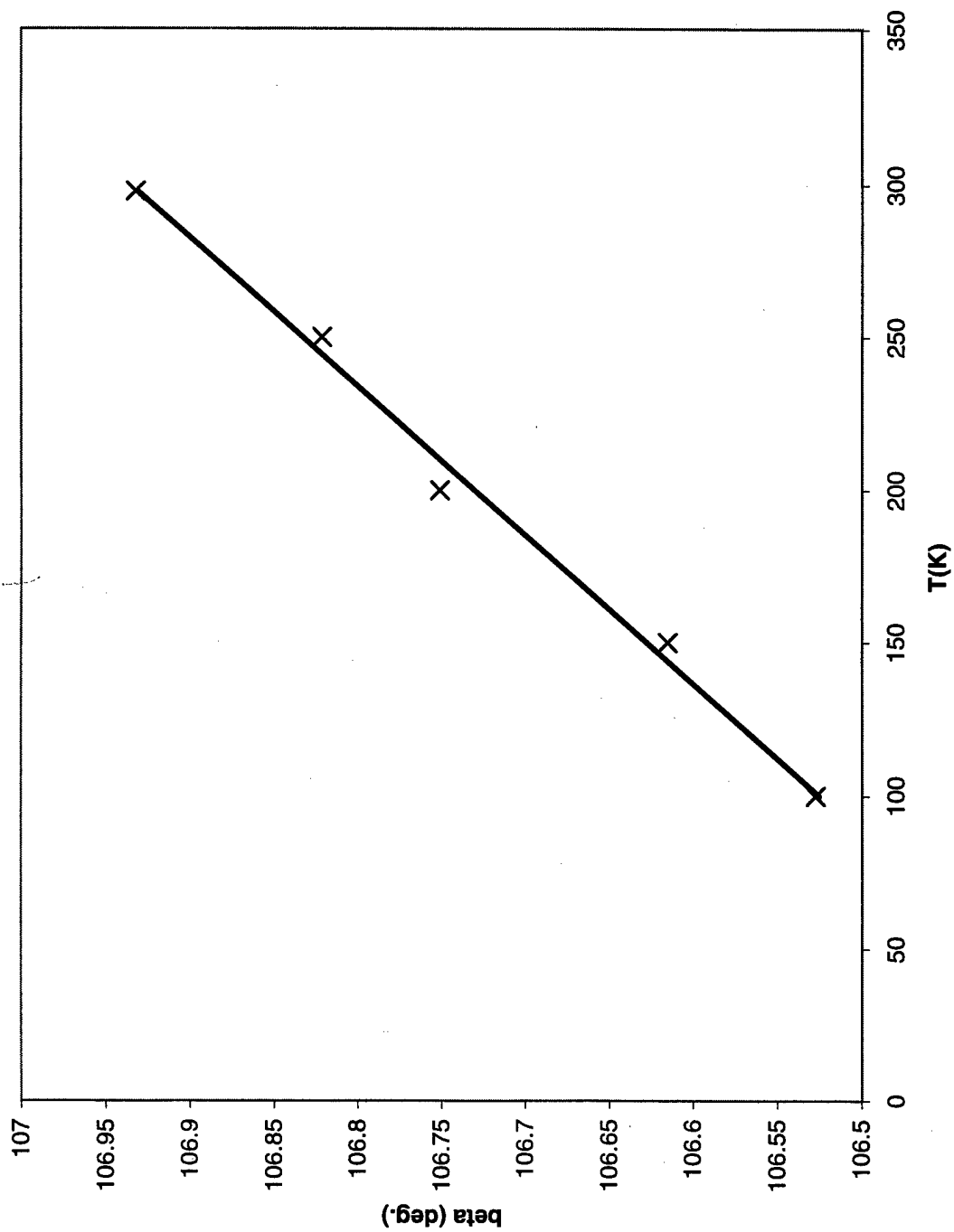
e-Cl20: Temperature Dependence of the c-axis

$$y = 0.0006x + 13.221$$
$$R^2 = 0.9771$$



e-Cl2O: Temperature Dependence of the beta-angle

$$y = 0.002x + 106.32$$
$$R^2 = 0.9929$$



X beta-angle (deg.)
— Linear (beta-angle (deg.))

e-Cl2O: Temperature Dependence of the Volume

$$y = 0.22x + 1372.1$$
$$R^2 = 0.9318$$

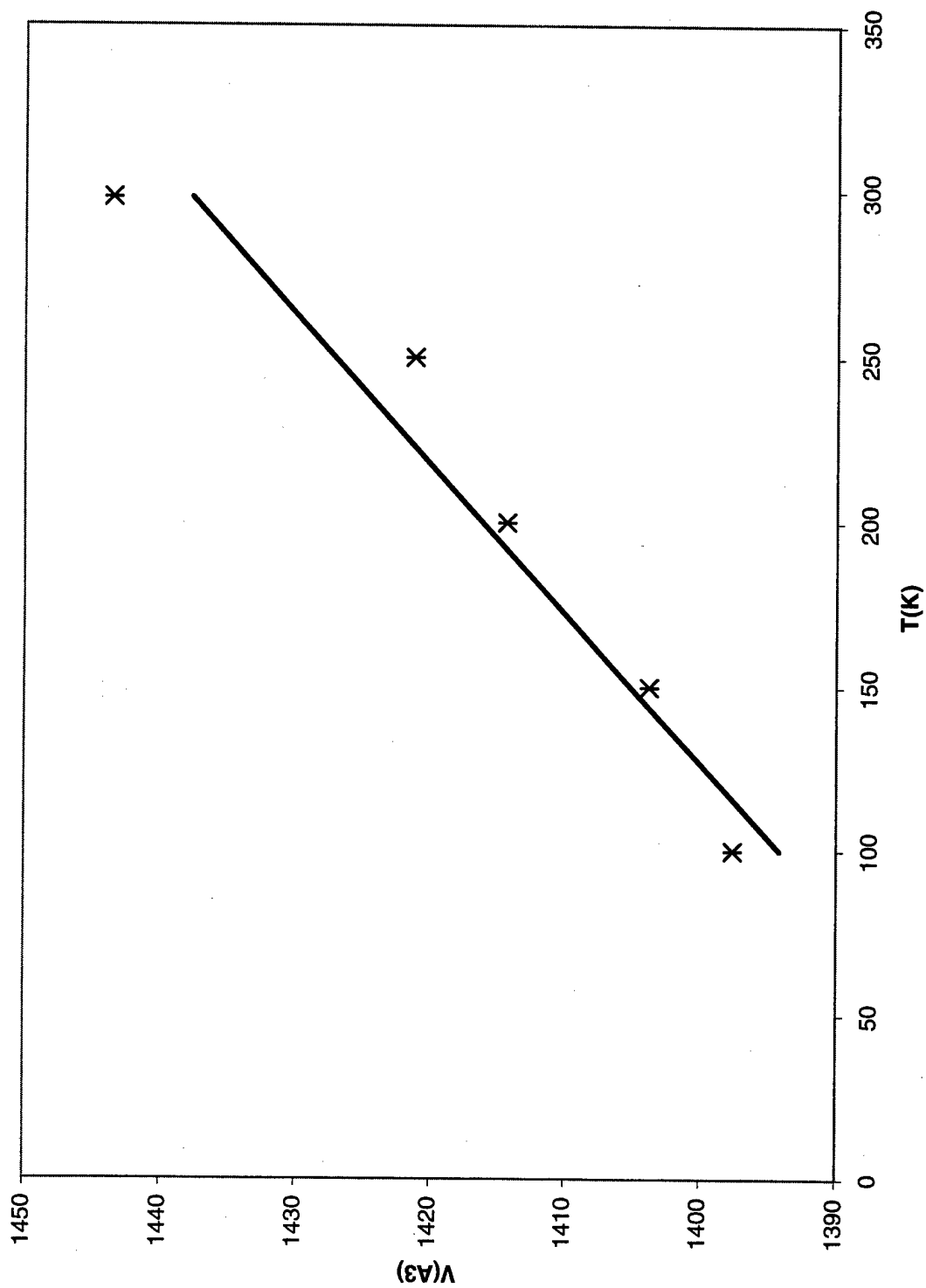


Table 3. Crystal data and structure refinement for e-Cl20. 298K

Identification code	ras
Empirical formula	C6 H6 N12 O12
Formula weight	438.23
Temperature	298(1) K
Wavelength	0.71073 Å
Crystal system, space group	Monoclinic, P2(1)/n
Unit cell dimensions	a = 8.8690(3) Å alpha = 90 deg. b = 12.6023(4) Å beta = 106.932(1) deg. c = 13.4070(4) Å gamma = 90 deg.
Volume	1433.54(8) Å ³
Z, Calculated density	4, 2.030 Mg/m ³
Absorption coefficient	0.195 mm ⁻¹
F(000)	888
Crystal size	0.3 x 0.2 x 0.2 mm
Theta range for data collection	2.27 to 28.25 deg.
Limiting indices	-10<=h<=11, -15<=k<=16, -15<=l<=17
Reflections collected / unique	9481 / 3521 [R(int) = 0.0470]
Absorption correction	Empirical :Multipole Expansion (Blessing, 19
Max. and min. transmission	0.990286 and 0.835534
Refinement method	Full-matrix least-squares on F ²
Data / restraints / parameters	3521 / 0 / 295
Goodness-of-fit on F ²	1.057
Final R indices [I>2sigma(I)]	R1 = 0.0522, wR2 = 0.0977
R indices (all data)	R1 = 0.0999, wR2 = 0.1187
Largest diff. peak and hole	0.250 and -0.290 e.Å ⁻³

Table 4. Atomic coordinates ($\times 10^4$) and equivalent isotropic displacement parameters ($\text{\AA}^2 \times 10^3$) for e-Cl20.
 $U(\text{eq})$ is defined as one third of the trace of the orthogonalized U_{ij} tensor.

298K

	x	y	z	U(eq)
O(1)	1911(3)	10554(2)	-81(2)	55(1)
O(2)	3753(2)	9376(2)	100(1)	38(1)
O(3)	4236(2)	8880(1)	3885(1)	36(1)
O(4)	4057(2)	8396(1)	2290(1)	33(1)
O(5)	1524(3)	10958(2)	3920(2)	53(1)
O(6)	395(2)	11152(2)	2255(2)	41(1)
O(7)	4020(2)	14115(1)	3214(2)	39(1)
O(8)	4016(3)	13187(2)	4581(2)	45(1)
O(9)	7891(3)	11990(2)	4871(1)	45(1)
O(10)	8490(2)	12602(2)	3512(2)	42(1)
O(11)	5893(3)	13851(2)	1484(2)	58(1)
O(12)	7600(2)	12751(2)	1191(2)	42(1)
N(1)	3128(3)	10126(2)	390(2)	31(1)
N(2)	3895(2)	10543(2)	1369(2)	26(1)
N(3)	3029(2)	10968(2)	2835(2)	23(1)
N(4)	4523(2)	8967(2)	3047(2)	26(1)
N(5)	1523(3)	11054(2)	3015(2)	33(1)
N(6)	5519(2)	9778(2)	2966(1)	22(1)
N(7)	4722(2)	12402(1)	3284(2)	22(1)
N(8)	4182(3)	13304(2)	3722(2)	29(1)
N(9)	7864(3)	11973(2)	3958(2)	30(1)
N(10)	7064(2)	11133(2)	3370(2)	24(1)
N(11)	5678(2)	12121(2)	1794(2)	25(1)
N(12)	6462(3)	12977(2)	1475(2)	33(1)
C(1)	4379(3)	11370(2)	3663(2)	22(1)
C(2)	5850(3)	10617(2)	3738(2)	23(1)
C(3)	4312(3)	12343(2)	2135(2)	23(1)
C(4)	3174(3)	11361(2)	1837(2)	23(1)
C(5)	6578(3)	11186(2)	2219(2)	23(1)
C(6)	5456(3)	10195(2)	1930(2)	24(1)

Table 5. Bond lengths [Å] and angles [deg] for e-Cl20.

298 K

O(1)-N(1)	1.208(3)
O(2)-N(1)	1.215(3)
O(3)-N(4)	1.226(3)
O(4)-N(4)	1.214(3)
O(5)-N(5)	1.218(3)
O(6)-N(5)	1.209(3)
O(7)-N(8)	1.214(3)
O(8)-N(8)	1.212(3)
O(9)-N(9)	1.218(3)
O(10)-N(9)	1.220(3)
O(11)-N(12)	1.213(3)
O(12)-N(12)	1.211(3)
N(2)-N(1)	1.393(3)
N(2)-C(4)	1.449(3)
N(2)-C(6)	1.438(3)
N(3)-N(5)	1.429(3)
N(3)-C(1)	1.466(3)
N(3)-C(4)	1.467(3)
N(4)-N(6)	1.376(3)
N(6)-C(2)	1.449(3)
N(6)-C(6)	1.471(3)
N(7)-N(8)	1.424(3)
N(7)-C(1)	1.461(3)
N(7)-C(3)	1.478(3)
N(9)-N(10)	1.385(3)
N(10)-C(2)	1.461(3)
N(10)-C(5)	1.479(3)
N(11)-N(12)	1.415(3)
N(11)-C(3)	1.442(3)
N(11)-C(5)	1.443(3)
C(1)-C(2)	1.592(3)
C(3)-C(4)	1.573(3)
C(5)-C(6)	1.573(3)

O(1)-N(1)-N(2)	116.2(2)
O(2)-N(1)-O(1)	127.0(2)
O(2)-N(1)-N(2)	116.9(2)
N(1)-N(2)-C(4)	121.4(2)
N(1)-N(2)-C(6)	120.6(2)
C(4)-N(2)-C(6)	118.0(2)
N(5)-N(3)-C(1)	116.3(2)
N(5)-N(3)-C(4)	117.6(2)
C(1)-N(3)-C(4)	107.7(2)
O(3)-N(4)-O(4)	127.0(2)
O(3)-N(4)-N(6)	116.6(2)
O(4)-N(4)-N(6)	116.4(2)
O(5)-N(5)-O(6)	127.6(2)
O(5)-N(5)-N(3)	115.5(2)
O(6)-N(5)-N(3)	116.7(2)
N(4)-N(6)-C(2)	119.1(2)
N(4)-N(6)-C(6)	119.5(2)
C(2)-N(6)-C(6)	111.0(2)
N(8)-N(7)-C(1)	115.9(2)
N(8)-N(7)-C(3)	117.4(2)
C(1)-N(7)-C(3)	107.8(2)
O(7)-N(8)-O(8)	127.5(2)
O(7)-N(8)-N(7)	116.0(2)
O(8)-N(8)-N(7)	116.3(2)
O(9)-N(9)-O(10)	127.0(2)
O(9)-N(9)-N(10)	116.2(2)
O(10)-N(9)-N(10)	116.7(2)
N(9)-N(10)-C(2)	117.0(2)

N(9)-N(10)-C(5)	120.3(2)
C(2)-N(10)-C(5)	110.7(2)
N(12)-N(11)-C(3)	118.6(2)
N(12)-N(11)-C(5)	118.5(2)
C(3)-N(11)-C(5)	116.9(2)
O(11)-N(12)-O(12)	127.1(2)
O(11)-N(12)-N(11)	116.6(2)
O(12)-N(12)-N(11)	116.3(2)
N(3)-C(1)-N(7)	104.5(2)
N(3)-C(1)-C(2)	108.4(2)
N(7)-C(1)-C(2)	107.6(2)
N(6)-C(2)-N(10)	95.7(2)
N(6)-C(2)-C(1)	113.5(2)
N(10)-C(2)-C(1)	112.6(2)
N(7)-C(3)-N(11)	111.5(2)
N(7)-C(3)-C(4)	104.4(2)
N(11)-C(3)-C(4)	107.6(2)
N(2)-C(4)-N(3)	108.8(2)
N(2)-C(4)-C(3)	109.7(2)
N(3)-C(4)-C(3)	104.8(2)
N(10)-C(5)-N(11)	114.2(2)
N(10)-C(5)-C(6)	101.1(2)
N(11)-C(5)-C(6)	108.3(2)
N(2)-C(6)-N(6)	111.7(2)
N(2)-C(6)-C(5)	109.3(2)
N(6)-C(6)-C(5)	101.7(2)

Symmetry transformations used to generate equivalent atoms:

Table 6. Anisotropic displacement parameters ($\text{\AA}^2 \times 10^3$) for e-Cl20.

298K

The anisotropic displacement factor exponent takes the form:

$$-2 \pi^2 [h^2 a^{*2} U_{11} + \dots + 2 h k a^* b^* U_{12}]$$

	U11	U22	U33	U23	U13	U12
O(1)	48(1)	61(2)	36(1)	-2(1)	-16(1)	5(1)
O(2)	43(1)	43(1)	31(1)	-16(1)	16(1)	-11(1)
O(3)	43(1)	38(1)	31(1)	8(1)	16(1)	-2(1)
O(4)	34(1)	25(1)	39(1)	-8(1)	9(1)	-3(1)
O(5)	47(1)	73(2)	52(1)	-3(1)	33(1)	-8(1)
O(6)	21(1)	39(1)	59(1)	-7(1)	6(1)	2(1)
O(7)	42(1)	22(1)	49(1)	3(1)	8(1)	4(1)
O(8)	61(2)	40(1)	43(1)	-9(1)	30(1)	2(1)
O(9)	52(1)	57(1)	21(1)	-9(1)	3(1)	-13(1)
O(10)	38(1)	46(1)	44(1)	-8(1)	15(1)	-20(1)
O(11)	54(2)	28(1)	98(2)	14(1)	32(1)	-3(1)
O(12)	39(1)	51(1)	43(1)	-1(1)	23(1)	-13(1)
N(1)	33(1)	34(1)	22(1)	0(1)	5(1)	-10(1)
N(2)	23(1)	31(1)	18(1)	-7(1)	-1(1)	0(1)
N(3)	17(1)	27(1)	26(1)	0(1)	9(1)	0(1)
N(4)	22(1)	23(1)	32(1)	2(1)	7(1)	3(1)
N(5)	30(1)	26(1)	47(2)	-7(1)	18(1)	-2(1)
N(6)	26(1)	20(1)	21(1)	1(1)	6(1)	0(1)
N(7)	28(1)	18(1)	21(1)	-1(1)	7(1)	1(1)
N(8)	26(1)	25(1)	36(1)	-6(1)	8(1)	0(1)
N(9)	25(1)	35(1)	27(1)	-4(1)	2(1)	-4(1)
N(10)	21(1)	28(1)	20(1)	-2(1)	2(1)	-2(1)
N(11)	24(1)	26(1)	24(1)	6(1)	7(1)	-1(1)
N(12)	34(1)	33(1)	32(1)	3(1)	9(1)	-10(1)
C(1)	25(1)	22(1)	21(1)	1(1)	6(1)	0(1)
C(2)	24(1)	25(1)	18(1)	1(1)	3(1)	0(1)
C(3)	22(1)	22(1)	23(1)	2(1)	4(1)	1(1)
C(4)	21(1)	25(1)	22(1)	1(1)	2(1)	2(1)
C(5)	21(1)	30(1)	18(1)	-2(1)	6(1)	-1(1)
C(6)	22(1)	27(1)	22(1)	-3(1)	7(1)	2(1)

298°K

Table 7. Hydrogen coordinates ($\times 10^4$) and isotropic displacement parameters ($\text{\AA}^2 \times 10^3$) for e-Cl20.

	x	y	z	U(eq)
H(1)	4188(31)	11380(20)	4310(20)	32(7)
H(2)	6269(32)	10347(21)	4436(21)	33(7)
H(3)	3875(30)	12977(21)	1833(20)	27(7)
H(4)	2202(33)	11543(20)	1349(20)	29(7)
H(5)	7470(29)	11130(18)	1972(18)	19(6)
H(6)	5798(28)	9697(19)	1543(18)	23(6)

Table 1. Crystal data and structure refinement for e-Cl20.

250K

Identification code	kk
Empirical formula	C6 H6 N12 O12
Formula weight	438.23
Temperature	250(1) K
Wavelength	0.71073 Å
Crystal system, space group	Monoclinic, P2(1)/n
Unit cell dimensions	a = 8.8436(2) Å alpha = 90 deg. b = 12.5638(2) Å beta = 106.821(1) deg. c = 13.3622(4) Å gamma = 90 deg.
Volume	1421.14(6) Å ³
Z, Calculated density	4, 2.048 Mg/m ³
Absorption coefficient	0.196 mm ⁻¹
F(000)	888
Crystal size	0.3 x 0.2 x 0.2 mm
Theta range for data collection	2.27 to 28.26 deg.
Limiting indices	-10<=h<=11, -15<=k<=16, -15<=l<=17
Reflections collected / unique	9531 / 3492 [R(int) = 0.0457]
Completeness to theta = 28.26	99.1 %
Refinement method	Full-matrix least-squares on F ²
Data / restraints / parameters	3492 / 0 / 295
Goodness-of-fit on F ²	1.026
Final R indices [I>2sigma(I)]	R1 = 0.0479, wR2 = 0.0930
R indices (all data)	R1 = 0.0920, wR2 = 0.1107
Largest diff. peak and hole	0.313 and -0.333 e.Å ⁻³

Table 2. Atomic coordinates ($\times 10^4$) and equivalent isotropic displacement parameters ($\text{\AA}^2 \times 10^3$) for e-Cl20. U(eq) is defined as one third of the trace of the orthogonalized U_{ij} tensor.

250K

	x	y	z	U(eq)
O(1)	1909(2)	10551(2)	-90(1)	45(1)
O(2)	3758(2)	9369(1)	98(1)	33(1)
O(3)	4226(2)	8877(1)	3889(1)	30(1)
O(4)	4047(2)	8393(1)	2287(1)	28(1)
O(5)	1517(2)	10959(2)	3925(2)	45(1)
O(6)	387(2)	11158(1)	2255(2)	35(1)
O(7)	4019(2)	14123(1)	3213(1)	33(1)
O(8)	4014(2)	13193(1)	4585(1)	38(1)
O(9)	7893(2)	11996(2)	4873(1)	37(1)
O(10)	8487(2)	12612(1)	3511(1)	35(1)
O(11)	5895(2)	13858(1)	1477(2)	47(1)
O(12)	7608(2)	12752(1)	1183(1)	35(1)
N(1)	3133(2)	10121(2)	387(1)	26(1)
N(2)	3894(2)	10543(1)	1365(1)	22(1)
N(3)	3027(2)	10969(1)	2837(1)	20(1)
N(4)	4519(2)	8966(1)	3048(2)	22(1)
N(5)	1511(2)	11058(2)	3017(2)	27(1)
N(6)	5520(2)	9777(1)	2965(1)	19(1)
N(7)	4724(2)	12406(1)	3287(1)	19(1)
N(8)	4183(2)	13311(2)	3724(2)	24(1)
N(9)	7863(2)	11979(2)	3955(2)	25(1)
N(10)	7066(2)	11135(1)	3371(1)	19(1)
N(11)	5682(2)	12124(1)	1791(1)	21(1)
N(12)	6466(2)	12980(2)	1468(2)	28(1)
C(1)	4380(3)	11368(2)	3664(2)	19(1)
C(2)	5856(3)	10616(2)	3743(2)	20(1)
C(3)	4316(3)	12348(2)	2137(2)	19(1)
C(4)	3173(3)	11364(2)	1833(2)	20(1)
C(5)	6588(3)	11186(2)	2220(2)	20(1)
C(6)	5463(3)	10194(2)	1928(2)	20(1)

Table 3. Bond lengths [Å] and angles [deg] for e-Cl20.

25015

O(1)-N(1)	1.213(3)
O(2)-N(1)	1.213(2)
O(3)-N(4)	1.229(2)
O(4)-N(4)	1.217(2)
O(5)-N(5)	1.218(3)
O(6)-N(5)	1.207(3)
O(7)-N(8)	1.213(2)
O(8)-N(8)	1.211(2)
O(9)-N(9)	1.220(2)
O(10)-N(9)	1.215(2)
O(11)-N(12)	1.215(3)
O(12)-N(12)	1.212(3)
N(1)-N(2)	1.390(3)
N(2)-C(6)	1.441(3)
N(2)-C(4)	1.446(3)
N(3)-N(5)	1.433(3)
N(3)-C(1)	1.462(3)
N(3)-C(4)	1.470(3)
N(4)-N(6)	1.375(2)
N(6)-C(2)	1.450(3)
N(6)-C(6)	1.469(3)
N(7)-N(8)	1.422(2)
N(7)-C(1)	1.461(3)
N(7)-C(3)	1.476(3)
N(9)-N(10)	1.382(2)
N(10)-C(2)	1.458(3)
N(10)-C(5)	1.473(3)
N(11)-N(12)	1.414(3)
N(11)-C(3)	1.441(3)
N(11)-C(5)	1.446(3)
C(1)-C(2)	1.590(3)
C(3)-C(4)	1.574(3)
C(5)-C(6)	1.572(3)
O(1)-N(1)-O(2)	126.8(2)
O(1)-N(1)-N(2)	116.1(2)
O(2)-N(1)-N(2)	117.1(2)
N(1)-N(2)-C(6)	120.38(18)
N(1)-N(2)-C(4)	121.57(18)
C(6)-N(2)-C(4)	118.02(18)
N(5)-N(3)-C(1)	116.54(17)
N(5)-N(3)-C(4)	117.39(18)
C(1)-N(3)-C(4)	107.80(16)
O(4)-N(4)-O(3)	126.76(19)
O(4)-N(4)-N(6)	116.37(18)
O(3)-N(4)-N(6)	116.84(18)
O(6)-N(5)-O(5)	128.0(2)
O(6)-N(5)-N(3)	116.68(19)
O(5)-N(5)-N(3)	115.1(2)
N(4)-N(6)-C(2)	118.98(17)
N(4)-N(6)-C(6)	119.55(17)
C(2)-N(6)-C(6)	111.11(16)
N(8)-N(7)-C(1)	116.30(17)
N(8)-N(7)-C(3)	117.23(17)
C(1)-N(7)-C(3)	107.55(17)
O(8)-N(8)-O(7)	127.58(19)
O(8)-N(8)-N(7)	116.16(18)
O(7)-N(8)-N(7)	116.16(19)
O(10)-N(9)-O(9)	126.8(2)
O(10)-N(9)-N(10)	117.08(18)
O(9)-N(9)-N(10)	116.11(18)
N(9)-N(10)-C(2)	117.08(17)

N(9)-N(10)-C(5)	120.09(17)
C(2)-N(10)-C(5)	110.96(17)
N(12)-N(11)-C(3)	118.71(18)
N(12)-N(11)-C(5)	118.45(17)
C(3)-N(11)-C(5)	116.84(17)
O(12)-N(12)-O(11)	127.2(2)
O(12)-N(12)-N(11)	116.30(19)
O(11)-N(12)-N(11)	116.48(19)
N(7)-C(1)-N(3)	104.61(17)
N(7)-C(1)-C(2)	107.69(17)
N(3)-C(1)-C(2)	108.82(17)
N(6)-C(2)-N(10)	95.72(16)
N(6)-C(2)-C(1)	113.01(18)
N(10)-C(2)-C(1)	112.42(17)
N(11)-C(3)-N(7)	111.62(18)
N(11)-C(3)-C(4)	107.43(17)
N(7)-C(3)-C(4)	104.67(17)
N(2)-C(4)-N(3)	108.67(18)
N(2)-C(4)-C(3)	109.93(17)
N(3)-C(4)-C(3)	104.38(17)
N(11)-C(5)-N(10)	114.10(17)
N(11)-C(5)-C(6)	107.98(17)
N(10)-C(5)-C(6)	101.26(16)
N(2)-C(6)-N(6)	111.45(18)
N(2)-C(6)-C(5)	109.47(18)
N(6)-C(6)-C(5)	101.64(16)

250K

Symmetry transformations used to generate equivalent atoms:

Table 4. Anisotropic displacement parameters ($\text{\AA}^2 \times 10^3$) for e-Cl20. The anisotropic displacement factor exponent takes the form:
 $-2 \pi^2 [h^2 a^{*2} U_{11} + \dots + 2 h k a^* b^* U_{12}]$

250K

	U11	U22	U33	U23	U13	U12
O(1)	42(1)	49(1)	31(1)	-2(1)	-13(1)	4(1)
O(2)	39(1)	35(1)	26(1)	-13(1)	14(1)	-8(1)
O(3)	36(1)	33(1)	24(1)	7(1)	14(1)	-2(1)
O(4)	29(1)	22(1)	33(1)	-8(1)	8(1)	-2(1)
O(5)	41(1)	63(1)	41(1)	-3(1)	27(1)	-7(1)
O(6)	19(1)	33(1)	49(1)	-6(1)	6(1)	2(1)
O(7)	36(1)	19(1)	40(1)	1(1)	7(1)	2(1)
O(8)	53(1)	34(1)	34(1)	-7(1)	25(1)	2(1)
O(9)	44(1)	46(1)	18(1)	-7(1)	4(1)	-12(1)
O(10)	33(1)	38(1)	35(1)	-6(1)	12(1)	-16(1)
O(11)	45(1)	23(1)	79(2)	11(1)	27(1)	-1(1)
O(12)	34(1)	41(1)	36(1)	-2(1)	20(1)	-10(1)
N(1)	28(1)	29(1)	18(1)	0(1)	4(1)	-10(1)
N(2)	21(1)	26(1)	16(1)	-5(1)	1(1)	0(1)
N(3)	17(1)	23(1)	22(1)	-1(1)	8(1)	-1(1)
N(4)	21(1)	17(1)	27(1)	3(1)	7(1)	4(1)
N(5)	24(1)	22(1)	40(1)	-4(1)	16(1)	-3(1)
N(6)	20(1)	18(1)	18(1)	-1(1)	6(1)	0(1)
N(7)	23(1)	15(1)	21(1)	-1(1)	8(1)	1(1)
N(8)	21(1)	22(1)	30(1)	-5(1)	6(1)	0(1)
N(9)	22(1)	30(1)	22(1)	-3(1)	4(1)	-3(1)
N(10)	17(1)	21(1)	17(1)	-2(1)	3(1)	-3(1)
N(11)	21(1)	22(1)	20(1)	4(1)	7(1)	-2(1)
N(12)	28(1)	29(1)	27(1)	2(1)	9(1)	-10(1)
C(1)	22(1)	19(1)	16(1)	-1(1)	7(1)	0(1)
C(2)	21(1)	21(1)	15(1)	2(1)	4(1)	2(1)
C(3)	20(1)	20(1)	18(1)	3(1)	4(1)	2(1)
C(4)	14(1)	24(1)	21(1)	1(1)	3(1)	0(1)
C(5)	18(1)	23(1)	18(1)	-1(1)	6(1)	-2(1)
C(6)	20(1)	22(1)	17(1)	-2(1)	5(1)	3(1)

Table 5. Hydrogen coordinates ($\times 10^4$) and isotropic displacement parameters ($\text{\AA}^2 \times 10^3$) for e-Cl20.

250K

	x	y	z	U(eq)
H(1)	4120(30)	11420(18)	4281(18)	22(6)
H(2)	6280(30)	10349(18)	4445(19)	23(6)
H(3)	3880(30)	12962(19)	1852(18)	20(6)
H(4)	2180(30)	11533(17)	1392(17)	15(6)
H(5)	7480(30)	11164(18)	1976(18)	25(6)
H(6)	5790(20)	9676(17)	1530(16)	12(5)

Table 1. Crystal data and structure refinement for e-Cl20.

200K

Identification code	kk
Empirical formula	C6 H6 N12 O12
Formula weight	438.23
Temperature	200(1) K
Wavelength	0.71073 Å
Crystal system, space group	Monoclinic, P2(1)/n
Unit cell dimensions	a = 8.8282(2) Å alpha = 90 deg. b = 12.5364(1) Å beta = 106.751(1) deg. c = 13.3455(3) Å gamma = 90 deg.
Volume	1414.32(5) Å ³
Z, Calculated density	4, 2.058 Mg/m ³
Absorption coefficient	0.197 mm ⁻¹
F(000)	888
Crystal size	0.3 x 0.2 x 0.2 mm
Theta range for data collection	2.28 to 28.26 deg.
Limiting indices	-10<=h<=11, -15<=k<=16, -15<=l<=17
Reflections collected / unique	9483 / 3473 [R(int) = 0.0441]
Completeness to theta = 28.26	99.3 %
Refinement method	Full-matrix least-squares on F ²
Data / restraints / parameters	3473 / 0 / 295
Goodness-of-fit on F ²	1.011
Final R indices [I>2sigma(I)]	R1 = 0.0445, wR2 = 0.0879
R indices (all data)	R1 = 0.0853, wR2 = 0.1037
Largest diff. peak and hole	0.259 and -0.317 e.Å ⁻³

Table 2. Atomic coordinates ($\times 10^4$) and equivalent isotropic displacement parameters ($\text{\AA}^2 \times 10^3$) for e-Cl20. 200K
 $U(\text{eq})$ is defined as one third of the trace of the orthogonalized U_{ij} tensor.

	x	y	z	$U(\text{eq})$
O(1)	1907(2)	10550(1)	-98(1)	36(1)
O(2)	3762(2)	9362(1)	94(1)	25(1)
O(3)	4218(2)	8876(1)	3890(1)	24(1)
O(4)	4040(2)	8390(1)	2283(1)	22(1)
O(5)	1512(2)	10964(1)	3929(1)	36(1)
O(6)	379(2)	11162(1)	2254(1)	27(1)
O(7)	4019(2)	14131(1)	3212(1)	26(1)
O(8)	4016(2)	13200(1)	4591(1)	30(1)
O(9)	7899(2)	12002(1)	4876(1)	29(1)
O(10)	8486(2)	12620(1)	3504(1)	28(1)
O(11)	7616(2)	12754(1)	1178(1)	27(1)
O(12)	5897(2)	13865(1)	1470(2)	38(1)
N(1)	3130(2)	10121(2)	385(1)	20(1)
N(2)	3898(2)	10541(1)	1365(1)	17(1)
N(3)	3024(2)	10966(1)	2836(1)	16(1)
N(4)	4514(2)	8962(1)	3048(1)	18(1)
N(5)	1508(2)	11061(1)	3020(2)	21(1)
N(6)	5523(2)	9773(1)	2968(1)	14(1)
N(7)	4727(2)	12409(1)	3287(1)	15(1)
N(8)	4184(2)	13316(1)	3726(2)	20(1)
N(9)	7870(2)	11983(1)	3958(1)	20(1)
N(10)	7074(2)	11135(1)	3372(1)	16(1)
N(11)	5686(2)	12126(1)	1787(1)	17(1)
N(12)	6470(2)	12985(2)	1464(1)	22(1)
C(1)	4379(2)	11370(2)	3665(2)	15(1)
C(2)	5859(2)	10615(2)	3745(2)	15(1)
C(3)	4316(2)	12348(2)	2133(2)	15(1)
C(4)	3169(3)	11364(2)	1831(2)	16(1)
C(5)	6593(2)	11187(2)	2215(2)	16(1)
C(6)	5465(2)	10191(2)	1926(2)	15(1)

Table 3. Bond lengths [Å] and angles [deg] for e-Cl20.

200K

O(1)-N(1)	1.212(2)
O(2)-N(1)	1.222(2)
O(3)-N(4)	1.230(2)
O(4)-N(4)	1.219(2)
O(5)-N(5)	1.218(2)
O(6)-N(5)	1.212(2)
O(7)-N(8)	1.216(2)
O(8)-N(8)	1.213(2)
O(9)-N(9)	1.218(2)
O(10)-N(9)	1.221(2)
O(11)-N(12)	1.215(2)
O(12)-N(12)	1.215(2)
N(1)-N(2)	1.392(2)
N(2)-C(6)	1.439(3)
N(2)-C(4)	1.448(3)
N(3)-N(5)	1.434(2)
N(3)-C(1)	1.465(3)
N(3)-C(4)	1.471(3)
N(4)-N(6)	1.376(2)
N(6)-C(2)	1.450(3)
N(6)-C(6)	1.472(2)
N(7)-N(8)	1.425(2)
N(7)-C(1)	1.461(3)
N(7)-C(3)	1.478(3)
N(9)-N(10)	1.385(2)
N(10)-C(2)	1.460(3)
N(10)-C(5)	1.480(3)
N(11)-N(12)	1.413(2)
N(11)-C(3)	1.441(3)
N(11)-C(5)	1.446(3)
C(1)-C(2)	1.592(3)
C(3)-C(4)	1.573(3)
C(5)-C(6)	1.574(3)

O(1)-N(1)-O(2)	126.60(19)
O(1)-N(1)-N(2)	116.72(18)
O(2)-N(1)-N(2)	116.68(18)
N(1)-N(2)-C(6)	120.60(17)
N(1)-N(2)-C(4)	121.13(17)
C(6)-N(2)-C(4)	118.23(17)
N(5)-N(3)-C(1)	116.21(15)
N(5)-N(3)-C(4)	117.32(16)
C(1)-N(3)-C(4)	107.74(15)
O(4)-N(4)-O(3)	127.01(18)
O(4)-N(4)-N(6)	116.26(16)
O(3)-N(4)-N(6)	116.70(17)
O(6)-N(5)-O(5)	128.09(19)
O(6)-N(5)-N(3)	116.46(17)
O(5)-N(5)-N(3)	115.29(18)
N(4)-N(6)-C(2)	119.04(16)
N(4)-N(6)-C(6)	119.30(16)
C(2)-N(6)-C(6)	111.15(15)
N(8)-N(7)-C(1)	116.13(16)
N(8)-N(7)-C(3)	117.34(16)
C(1)-N(7)-C(3)	107.51(16)
O(8)-N(8)-O(7)	127.59(18)
O(8)-N(8)-N(7)	116.30(17)
O(7)-N(8)-N(7)	115.99(17)
O(9)-N(9)-O(10)	127.11(19)
O(9)-N(9)-N(10)	116.29(17)
O(10)-N(9)-N(10)	116.59(17)
N(9)-N(10)-C(2)	116.94(16)

200K

N(9)-N(10)-C(5)	120.11(15)
C(2)-N(10)-C(5)	110.94(16)
N(12)-N(11)-C(3)	118.72(16)
N(12)-N(11)-C(5)	118.48(16)
C(3)-N(11)-C(5)	116.82(16)
O(12)-N(12)-O(11)	127.20(18)
O(12)-N(12)-N(11)	116.68(18)
O(11)-N(12)-N(11)	116.08(18)
N(7)-C(1)-N(3)	104.72(16)
N(7)-C(1)-C(2)	107.64(16)
N(3)-C(1)-C(2)	108.73(16)
N(6)-C(2)-N(10)	95.73(15)
N(6)-C(2)-C(1)	112.97(17)
N(10)-C(2)-C(1)	112.41(16)
N(11)-C(3)-N(7)	111.56(17)
N(11)-C(3)-C(4)	107.71(16)
N(7)-C(3)-C(4)	104.71(16)
N(2)-C(4)-N(3)	108.46(17)
N(2)-C(4)-C(3)	109.63(16)
N(3)-C(4)-C(3)	104.53(16)
N(11)-C(5)-N(10)	114.05(16)
N(11)-C(5)-C(6)	108.02(16)
N(10)-C(5)-C(6)	101.05(15)
N(2)-C(6)-N(6)	111.51(16)
N(2)-C(6)-C(5)	109.36(16)
N(6)-C(6)-C(5)	101.75(15)

Symmetry transformations used to generate equivalent atoms:

Table 4. Anisotropic displacement parameters ($\text{\AA}^2 \times 10^3$) for e-Cl20.
The anisotropic displacement factor exponent takes the form:
 $-2 \pi^2 [h^2 a^{*2} U_{11} + \dots + 2 h k a^* b^* U_{12}]$

200K

	U11	U22	U33	U23	U13	U12
O(1)	32(1)	40(1)	25(1)	0(1)	-10(1)	4(1)
O(2)	28(1)	28(1)	21(1)	-10(1)	10(1)	-6(1)
O(3)	27(1)	26(1)	20(1)	6(1)	11(1)	-1(1)
O(4)	21(1)	18(1)	28(1)	-6(1)	7(1)	-2(1)
O(5)	31(1)	50(1)	33(1)	-3(1)	21(1)	-8(1)
O(6)	14(1)	26(1)	41(1)	-6(1)	5(1)	1(1)
O(7)	27(1)	14(1)	34(1)	2(1)	5(1)	3(1)
O(8)	41(1)	27(1)	27(1)	-5(1)	19(1)	2(1)
O(9)	34(1)	36(1)	15(1)	-6(1)	2(1)	-8(1)
O(10)	24(1)	30(1)	30(1)	-4(1)	10(1)	-13(1)
O(11)	25(1)	32(1)	29(1)	-2(1)	15(1)	-8(1)
O(12)	36(1)	18(1)	64(1)	9(1)	22(1)	-1(1)
N(1)	21(1)	24(1)	14(1)	-1(1)	3(1)	-7(1)
N(2)	14(1)	21(1)	14(1)	-3(1)	1(1)	1(1)
N(3)	11(1)	18(1)	18(1)	0(1)	5(1)	-1(1)
N(4)	14(1)	16(1)	22(1)	2(1)	5(1)	2(1)
N(5)	20(1)	16(1)	32(1)	-4(1)	13(1)	-3(1)
N(6)	16(1)	12(1)	15(1)	1(1)	5(1)	0(1)
N(7)	17(1)	12(1)	16(1)	0(1)	6(1)	1(1)
N(8)	16(1)	17(1)	27(1)	-4(1)	6(1)	1(1)
N(9)	16(1)	24(1)	18(1)	-2(1)	1(1)	-2(1)
N(10)	14(1)	18(1)	15(1)	-1(1)	2(1)	-2(1)
N(11)	16(1)	16(1)	19(1)	4(1)	7(1)	0(1)
N(12)	21(1)	22(1)	23(1)	2(1)	6(1)	-7(1)
C(1)	16(1)	17(1)	12(1)	-1(1)	4(1)	-1(1)
C(2)	16(1)	16(1)	12(1)	1(1)	3(1)	-1(1)
C(3)	15(1)	15(1)	15(1)	2(1)	3(1)	2(1)
C(4)	14(1)	17(1)	17(1)	0(1)	2(1)	0(1)
C(5)	14(1)	18(1)	15(1)	0(1)	4(1)	2(1)
C(6)	14(1)	17(1)	14(1)	-1(1)	4(1)	1(1)

Table 5. Hydrogen coordinates ($\times 10^4$) and isotropic displacement parameters ($\text{\AA}^2 \times 10^3$) for e-Cl20.

200K

	x	y	z	U(eq)
H(1)	4190(30)	11409(17)	4278(17)	17(6)
H(2)	6270(30)	10351(18)	4426(19)	25(6)
H(3)	3860(30)	12950(19)	1846(17)	19(6)
H(4)	2150(30)	11544(17)	1338(17)	18(6)
H(5)	7540(30)	11140(16)	1960(16)	14(5)
H(6)	5800(30)	9686(18)	1514(17)	18(6)

Table 1. Crystal data and structure refinement for e-Cl20.

150K

Identification code	kk
Empirical formula	C6 H6 N12 O12
Formula weight	438.23
Temperature	150(1) K
Wavelength	0.71073 Å
Crystal system, space group	Monoclinic, P2(1)/n
Unit cell dimensions	a = 8.8040(3) Å alpha = 90 deg. b = 12.5058(4) Å beta = 106.615(1) deg. c = 13.3050(5) Å gamma = 90 deg.
Volume	1403.73(8) Å ³
Z, Calculated density	4, 2.074 Mg/m ³
Absorption coefficient	0.199 mm ⁻¹
F(000)	888
Crystal size	0.3 x 0.2 x 0.2 mm
Theta range for data collection	2.28 to 28.28 deg.
Limiting indices	-10<=h<=11, -15<=k<=16, -15<=l<=17
Reflections collected / unique	9412 / 3457 [R(int) = 0.0423]
Completeness to theta = 28.28	99.3 %
Refinement method	Full-matrix least-squares on F ²
Data / restraints / parameters	3457 / 0 / 295
Goodness-of-fit on F ²	0.995
Final R indices [I>2sigma(I)]	R1 = 0.0441, wR2 = 0.0920
R indices (all data)	R1 = 0.0776, wR2 = 0.1059
Largest diff. peak and hole	0.289 and -0.331 e.Å ⁻³

Table 2. Atomic coordinates ($\times 10^4$) and equivalent isotropic displacement parameters ($\text{\AA}^2 \times 10^3$) for e-Cl20. U(eq) is defined as one third of the trace of the orthogonalized U_{ij} tensor.

150K

	x	y	z	U(eq)
O(1)	1906(2)	10548(1)	-107(1)	28(1)
O(2)	3763(2)	9356(1)	90(1)	20(1)
O(3)	4213(2)	8874(1)	3890(1)	19(1)
O(4)	4032(2)	8389(1)	2281(1)	18(1)
O(5)	1504(2)	10970(1)	3934(1)	28(1)
O(6)	373(2)	11167(1)	2255(1)	22(1)
O(7)	4021(2)	14140(1)	3212(1)	21(1)
O(8)	4016(2)	13208(1)	4595(1)	24(1)
O(9)	7903(2)	12010(1)	4879(1)	23(1)
O(10)	8486(2)	12630(1)	3499(1)	22(1)
O(11)	7629(2)	12757(1)	1174(1)	22(1)
O(12)	5898(2)	13873(1)	1462(1)	29(1)
N(1)	3133(2)	10118(1)	383(1)	17(1)
N(2)	3896(2)	10541(1)	1361(1)	14(1)
N(3)	3025(2)	10970(1)	2839(1)	13(1)
N(4)	4506(2)	8965(1)	3047(1)	14(1)
N(5)	1503(2)	11064(1)	3024(2)	18(1)
N(6)	5526(2)	9772(1)	2964(1)	12(1)
N(7)	4730(2)	12413(1)	3288(1)	13(1)
N(8)	4181(2)	13323(1)	3728(1)	16(1)
N(9)	7868(2)	11990(1)	3954(1)	16(1)
N(10)	7081(2)	11139(1)	3372(1)	13(1)
N(11)	5687(2)	12129(1)	1783(1)	13(1)
N(12)	6474(2)	12987(1)	1458(1)	17(1)
C(1)	4380(2)	11370(2)	3670(2)	12(1)
C(2)	5863(2)	10617(2)	3747(2)	14(1)
C(3)	4317(2)	12356(2)	2131(2)	13(1)
C(4)	3166(2)	11368(2)	1830(2)	13(1)
C(5)	6596(2)	11188(2)	2213(2)	13(1)
C(6)	5468(2)	10191(2)	1926(2)	13(1)

Table 3. Bond lengths [Å] and angles [deg] for e-Cl20.

150 K

O(1)-N(1)	1.217(2)
O(2)-N(1)	1.222(2)
O(3)-N(4)	1.227(2)
O(4)-N(4)	1.220(2)
O(5)-N(5)	1.218(2)
O(6)-N(5)	1.212(2)
O(7)-N(8)	1.217(2)
O(8)-N(8)	1.212(2)
O(9)-N(9)	1.222(2)
O(10)-N(9)	1.221(2)
O(11)-N(12)	1.216(2)
O(12)-N(12)	1.220(2)
N(1)-N(2)	1.387(2)
N(2)-C(6)	1.441(3)
N(2)-C(4)	1.449(3)
N(3)-N(5)	1.435(2)
N(3)-C(1)	1.464(3)
N(3)-C(4)	1.470(3)
N(4)-N(6)	1.376(2)
N(6)-C(2)	1.453(3)
N(6)-C(6)	1.465(2)
N(7)-N(8)	1.426(2)
N(7)-C(1)	1.464(3)
N(7)-C(3)	1.478(3)
N(9)-N(10)	1.380(2)
N(10)-C(2)	1.460(2)
N(10)-C(5)	1.480(3)
N(11)-N(12)	1.411(2)
N(11)-C(3)	1.439(2)
N(11)-C(5)	1.445(3)
C(1)-C(2)	1.589(3)
C(3)-C(4)	1.576(3)
C(5)-C(6)	1.572(3)

O(1)-N(1)-O(2)	126.09(18)
O(1)-N(1)-N(2)	116.84(17)
O(2)-N(1)-N(2)	117.06(17)
N(1)-N(2)-C(6)	120.57(16)
N(1)-N(2)-C(4)	121.34(17)
C(6)-N(2)-C(4)	118.06(16)
N(5)-N(3)-C(1)	116.23(15)
N(5)-N(3)-C(4)	117.10(16)
C(1)-N(3)-C(4)	108.09(15)
O(4)-N(4)-O(3)	126.72(17)
O(4)-N(4)-N(6)	116.23(16)
O(3)-N(4)-N(6)	116.99(16)
O(6)-N(5)-O(5)	128.05(18)
O(6)-N(5)-N(3)	116.48(16)
O(5)-N(5)-N(3)	115.33(17)
N(4)-N(6)-C(2)	118.66(16)
N(4)-N(6)-C(6)	119.32(16)
C(2)-N(6)-C(6)	111.17(15)
N(8)-N(7)-C(1)	116.05(15)
N(8)-N(7)-C(3)	117.03(16)
C(1)-N(7)-C(3)	107.74(15)
O(8)-N(8)-O(7)	127.67(17)
O(8)-N(8)-N(7)	116.27(16)
O(7)-N(8)-N(7)	115.92(16)
O(10)-N(9)-O(9)	126.79(18)
O(10)-N(9)-N(10)	116.81(16)
O(9)-N(9)-N(10)	116.37(16)
N(9)-N(10)-C(2)	116.96(15)

N(9)-N(10)-C(5)	120.10(15)
C(2)-N(10)-C(5)	110.71(16)
N(12)-N(11)-C(3)	118.62(16)
N(12)-N(11)-C(5)	118.39(16)
C(3)-N(11)-C(5)	116.97(15)
O(11)-N(12)-O(12)	127.02(18)
O(11)-N(12)-N(11)	116.29(17)
O(12)-N(12)-N(11)	116.65(17)
N(3)-C(1)-N(7)	104.46(16)
N(3)-C(1)-C(2)	108.83(16)
N(7)-C(1)-C(2)	107.50(16)
N(6)-C(2)-N(10)	95.70(15)
N(6)-C(2)-C(1)	112.93(17)
N(10)-C(2)-C(1)	112.47(16)
N(11)-C(3)-N(7)	111.44(16)
N(11)-C(3)-C(4)	107.46(16)
N(7)-C(3)-C(4)	104.60(15)
N(2)-C(4)-N(3)	108.38(16)
N(2)-C(4)-C(3)	109.72(16)
N(3)-C(4)-C(3)	104.40(15)
N(11)-C(5)-N(10)	114.10(16)
N(11)-C(5)-C(6)	108.06(16)
N(10)-C(5)-C(6)	101.19(15)
N(2)-C(6)-N(6)	111.71(16)
N(2)-C(6)-C(5)	109.34(16)
N(6)-C(6)-C(5)	101.85(15)

150 K

Symmetry transformations used to generate equivalent atoms:

Table 4. Anisotropic displacement parameters ($\text{\AA}^2 \times 10^3$) for e-Cl20.
The anisotropic displacement factor exponent takes the form:
 $-2 \pi^2 [h^2 a^{*2} U_{11} + \dots + 2 h k a^* b^* U_{12}]$

150 K

	U11	U22	U33	U23	U13	U12
O(1)	24(1)	33(1)	19(1)	0(1)	-7(1)	3(1)
O(2)	23(1)	21(1)	17(1)	-8(1)	9(1)	-4(1)
O(3)	22(1)	23(1)	16(1)	5(1)	9(1)	-1(1)
O(4)	18(1)	15(1)	22(1)	-4(1)	7(1)	-1(1)
O(5)	25(1)	41(1)	24(1)	-2(1)	17(1)	-5(1)
O(6)	11(1)	22(1)	33(1)	-3(1)	5(1)	2(1)
O(7)	21(1)	13(1)	26(1)	2(1)	4(1)	2(1)
O(8)	32(1)	23(1)	22(1)	-4(1)	16(1)	0(1)
O(9)	26(1)	30(1)	12(1)	-4(1)	3(1)	-6(1)
O(10)	21(1)	24(1)	23(1)	-2(1)	10(1)	-9(1)
O(11)	19(1)	28(1)	24(1)	-1(1)	13(1)	-6(1)
O(12)	26(1)	16(1)	49(1)	7(1)	17(1)	0(1)
N(1)	17(1)	20(1)	12(1)	-1(1)	4(1)	-7(1)
N(2)	12(1)	19(1)	10(1)	-4(1)	1(1)	1(1)
N(3)	9(1)	17(1)	14(1)	-1(1)	5(1)	0(1)
N(4)	13(1)	14(1)	17(1)	2(1)	5(1)	3(1)
N(5)	14(1)	15(1)	26(1)	-5(1)	10(1)	-2(1)
N(6)	13(1)	10(1)	13(1)	1(1)	5(1)	-1(1)
N(7)	15(1)	12(1)	13(1)	0(1)	6(1)	1(1)
N(8)	13(1)	16(1)	20(1)	-2(1)	5(1)	1(1)
N(9)	12(1)	19(1)	16(1)	-1(1)	2(1)	-1(1)
N(10)	11(1)	15(1)	13(1)	-1(1)	3(1)	-2(1)
N(11)	12(1)	14(1)	14(1)	4(1)	6(1)	1(1)
N(12)	18(1)	18(1)	17(1)	2(1)	6(1)	-6(1)
C(1)	12(1)	14(1)	11(1)	-1(1)	3(1)	-1(1)
C(2)	14(1)	16(1)	12(1)	1(1)	4(1)	0(1)
C(3)	13(1)	14(1)	13(1)	2(1)	4(1)	1(1)
C(4)	11(1)	15(1)	12(1)	0(1)	2(1)	1(1)
C(5)	12(1)	16(1)	12(1)	-1(1)	2(1)	0(1)
C(6)	12(1)	15(1)	13(1)	-1(1)	4(1)	2(1)

Table 5. Hydrogen coordinates ($\times 10^4$) and isotropic displacement parameters ($\text{\AA}^2 \times 10^3$) for e-Cl20.

150 K

	x	y	z	U(eq)
H(1)	4140(30)	11417(17)	4290(17)	15(6)
H(2)	6280(30)	10337(19)	4460(20)	24(6)
H(3)	3910(30)	12983(19)	1850(17)	14(6)
H(4)	2170(30)	11539(17)	1359(16)	11(5)
H(5)	7500(30)	11175(16)	1957(16)	13(6)
H(6)	5800(30)	9664(18)	1542(17)	16(6)

Table 1. Crystal data and structure refinement for e-Cl20.

100 K

Identification code	kk
Empirical formula	C6 H6 N12 O12
Formula weight	438.23
Temperature	100(1) K
Wavelength	0.71073 Å
Crystal system, space group	Monoclinic, P2(1)/n
Unit cell dimensions	a = 8.7906(2) Å alpha = 90 deg. b = 12.4820(1) Å beta = 106.527(1) deg. c = 13.2860(3) Å gamma = 90 deg.
Volume	1397.57(5) Å ³
Z, Calculated density	4, 2.083 Mg/m ³
Absorption coefficient	0.200 mm ⁻¹
F(000)	888
Crystal size	0.3 x 0.2 x 0.2 mm
Theta range for data collection	2.28 to 28.31 deg.
Limiting indices	-10<=h<=11, -15<=k<=16, -15<=l<=17
Reflections collected / unique	9312 / 3437 [R(int) = 0.0419]
Completeness to theta = 28.31	98.8 %
Refinement method	Full-matrix least-squares on F ²
Data / restraints / parameters	3437 / 0 / 295
Goodness-of-fit on F ²	1.013
Final R indices [I>2sigma(I)]	R1 = 0.0437, wR2 = 0.0901
R indices (all data)	R1 = 0.0743, wR2 = 0.1030
Largest diff. peak and hole	0.315 and -0.383 e.Å ⁻³

Table 2. Atomic coordinates ($\times 10^4$) and equivalent isotropic displacement parameters ($\text{\AA}^2 \times 10^3$) for e-Cl20.

100K

U(eq) is defined as one third of the trace of the orthogonalized U_{ij} tensor.

	x	y	z	U(eq)
O(1)	1908(2)	10548(1)	-113(1)	21(1)
O(2)	3773(2)	9350(1)	91(1)	15(1)
O(3)	4203(2)	8873(1)	3892(1)	15(1)
O(4)	4026(2)	8390(1)	2280(1)	13(1)
O(5)	1495(2)	10976(1)	3938(1)	21(1)
O(6)	368(2)	11174(1)	2256(1)	17(1)
O(7)	4021(2)	14148(1)	3210(1)	16(1)
O(8)	4014(2)	13213(1)	4599(1)	17(1)
O(9)	7904(2)	12016(1)	4881(1)	17(1)
O(10)	8487(2)	12638(1)	3495(1)	16(1)
O(11)	5902(2)	13881(1)	1454(1)	21(1)
O(12)	7636(2)	12760(1)	1167(1)	16(1)
N(1)	3134(2)	10114(1)	378(1)	12(1)
N(2)	3899(2)	10542(1)	1359(1)	11(1)
N(3)	3024(2)	10970(1)	2840(1)	10(1)
N(4)	4505(2)	8962(1)	3044(1)	11(1)
N(5)	1498(2)	11069(1)	3023(1)	13(1)
N(6)	5527(2)	9770(1)	2967(1)	10(1)
N(7)	4732(2)	12418(1)	3289(1)	10(1)
N(8)	4185(2)	13329(1)	3729(1)	12(1)
N(9)	7870(2)	11996(1)	3953(1)	12(1)
N(10)	7084(2)	11140(1)	3372(1)	10(1)
N(11)	5695(2)	12131(1)	1781(1)	10(1)
N(12)	6482(2)	12991(1)	1454(1)	13(1)
C(1)	4381(2)	11373(2)	3670(2)	10(1)
C(2)	5864(2)	10617(2)	3750(2)	10(1)
C(3)	4318(2)	12362(2)	2131(2)	10(1)
C(4)	3169(3)	11368(2)	1828(2)	10(1)
C(5)	6603(2)	11188(2)	2210(2)	10(1)
C(6)	5474(2)	10189(2)	1923(2)	10(1)

Table 3. Bond lengths [Å] and angles [deg] for e-Cl20.

100 K

O(1)-N(1)	1.217(2)
O(2)-N(1)	1.222(2)
O(3)-N(4)	1.234(2)
O(4)-N(4)	1.215(2)
O(5)-N(5)	1.222(2)
O(6)-N(5)	1.212(2)
O(7)-N(8)	1.218(2)
O(8)-N(8)	1.216(2)
O(9)-N(9)	1.226(2)
O(10)-N(9)	1.222(2)
O(11)-N(12)	1.221(2)
O(12)-N(12)	1.216(2)
N(1)-N(2)	1.392(2)
N(2)-C(6)	1.443(3)
N(2)-C(4)	1.446(3)
N(3)-N(5)	1.435(2)
N(3)-C(1)	1.464(3)
N(3)-C(4)	1.473(2)
N(4)-N(6)	1.373(2)
N(6)-C(2)	1.453(2)
N(6)-C(6)	1.471(2)
N(7)-N(8)	1.424(2)
N(7)-C(1)	1.463(2)
N(7)-C(3)	1.479(2)
N(9)-N(10)	1.382(2)
N(10)-C(2)	1.461(3)
N(10)-C(5)	1.481(3)
N(11)-N(12)	1.411(2)
N(11)-C(3)	1.444(2)
N(11)-C(5)	1.445(3)
C(1)-C(2)	1.588(3)
C(3)-C(4)	1.577(3)
C(5)-C(6)	1.573(3)

O(1)-N(1)-O(2)	126.53(18)
O(1)-N(1)-N(2)	116.75(16)
O(2)-N(1)-N(2)	116.71(17)
N(1)-N(2)-C(6)	120.35(16)
N(1)-N(2)-C(4)	121.46(17)
C(6)-N(2)-C(4)	118.16(16)
N(5)-N(3)-C(1)	116.30(15)
N(5)-N(3)-C(4)	116.95(16)
C(1)-N(3)-C(4)	107.93(15)
O(4)-N(4)-O(3)	126.67(17)
O(4)-N(4)-N(6)	116.62(16)
O(3)-N(4)-N(6)	116.67(16)
O(6)-N(5)-O(5)	127.89(18)
O(6)-N(5)-N(3)	116.70(16)
O(5)-N(5)-N(3)	115.27(17)
N(4)-N(6)-C(2)	119.06(15)
N(4)-N(6)-C(6)	119.03(16)
C(2)-N(6)-C(6)	111.18(15)
N(8)-N(7)-C(1)	116.17(15)
N(8)-N(7)-C(3)	116.95(15)
C(1)-N(7)-C(3)	107.69(15)
O(8)-N(8)-O(7)	127.70(17)
O(8)-N(8)-N(7)	116.25(16)
O(7)-N(8)-N(7)	115.94(16)
O(10)-N(9)-O(9)	126.86(17)
O(10)-N(9)-N(10)	116.82(16)
O(9)-N(9)-N(10)	116.30(16)
N(9)-N(10)-C(2)	116.96(15)

N(9)-N(10)-C(5)	119.98(15)
C(2)-N(10)-C(5)	110.87(16)
N(12)-N(11)-C(3)	118.46(16)
N(12)-N(11)-C(5)	118.50(16)
C(3)-N(11)-C(5)	117.04(15)
O(12)-N(12)-O(11)	126.97(17)
O(12)-N(12)-N(11)	116.18(16)
O(11)-N(12)-N(11)	116.80(17)
N(7)-C(1)-N(3)	104.65(16)
N(7)-C(1)-C(2)	107.63(16)
N(3)-C(1)-C(2)	108.85(16)
N(6)-C(2)-N(10)	95.73(14)
N(6)-C(2)-C(1)	112.85(17)
N(10)-C(2)-C(1)	112.34(16)
N(11)-C(3)-N(7)	111.35(16)
N(11)-C(3)-C(4)	107.20(15)
N(7)-C(3)-C(4)	104.67(15)
N(2)-C(4)-N(3)	108.46(16)
N(2)-C(4)-C(3)	109.89(16)
N(3)-C(4)-C(3)	104.35(15)
N(11)-C(5)-N(10)	113.97(16)
N(11)-C(5)-C(6)	108.07(16)
N(10)-C(5)-C(6)	101.21(15)
N(2)-C(6)-N(6)	111.51(16)
N(2)-C(6)-C(5)	109.27(16)
N(6)-C(6)-C(5)	101.81(15)

100K

Symmetry transformations used to generate equivalent atoms:

Table 4. Anisotropic displacement parameters ($\text{\AA}^2 \times 10^3$) for e-Cl20.
The anisotropic displacement factor exponent takes the form:
 $-2 \pi^2 [h^2 a^{*2} U_{11} + \dots + 2 h k a^* b^* U_{12}]$

100K

	U11	U22	U33	U23	U13	U12
O(1)	19(1)	23(1)	15(1)	1(1)	-4(1)	3(1)
O(2)	20(1)	14(1)	12(1)	-5(1)	8(1)	-2(1)
O(3)	19(1)	16(1)	11(1)	4(1)	7(1)	-2(1)
O(4)	15(1)	11(1)	14(1)	-4(1)	4(1)	-1(1)
O(5)	22(1)	28(1)	17(1)	-2(1)	12(1)	-4(1)
O(6)	12(1)	16(1)	22(1)	-2(1)	4(1)	2(1)
O(7)	18(1)	9(1)	19(1)	1(1)	3(1)	1(1)
O(8)	24(1)	17(1)	14(1)	-3(1)	11(1)	0(1)
O(9)	21(1)	21(1)	9(1)	-2(1)	2(1)	-4(1)
O(10)	17(1)	17(1)	16(1)	-1(1)	7(1)	-6(1)
O(11)	21(1)	11(1)	33(1)	4(1)	11(1)	1(1)
O(12)	16(1)	19(1)	17(1)	-1(1)	9(1)	-4(1)
N(1)	16(1)	13(1)	8(1)	2(1)	2(1)	-3(1)
N(2)	10(1)	13(1)	8(1)	-2(1)	1(1)	1(1)
N(3)	9(1)	12(1)	9(1)	-1(1)	4(1)	-1(1)
N(4)	12(1)	9(1)	11(1)	1(1)	3(1)	2(1)
N(5)	13(1)	11(1)	18(1)	-2(1)	8(1)	0(1)
N(6)	12(1)	8(1)	9(1)	1(1)	4(1)	-2(1)
N(7)	13(1)	7(1)	10(1)	-2(1)	5(1)	1(1)
N(8)	11(1)	12(1)	14(1)	-2(1)	4(1)	-1(1)
N(9)	11(1)	14(1)	10(1)	-1(1)	1(1)	-1(1)
N(10)	11(1)	10(1)	9(1)	-1(1)	2(1)	-2(1)
N(11)	10(1)	10(1)	11(1)	3(1)	4(1)	0(1)
N(12)	15(1)	14(1)	10(1)	2(1)	4(1)	-4(1)
C(1)	12(1)	9(1)	8(1)	0(1)	3(1)	-1(1)
C(2)	12(1)	10(1)	8(1)	-1(1)	2(1)	-1(1)
C(3)	11(1)	11(1)	9(1)	0(1)	3(1)	0(1)
C(4)	10(1)	12(1)	7(1)	0(1)	1(1)	1(1)
C(5)	10(1)	11(1)	8(1)	-1(1)	2(1)	0(1)
C(6)	11(1)	11(1)	7(1)	0(1)	2(1)	0(1)

Table 5. Hydrogen coordinates ($\times 10^4$) and isotropic displacement parameters ($\text{\AA}^2 \times 10^3$) for e-Cl20.

100K

	x	y	z	U(eq)
H(1)	4150(30)	11428(17)	4313(17)	11(6)
H(2)	6270(30)	10342(17)	4447(18)	10(5)
H(3)	3840(30)	12994(19)	1815(17)	10(6)
H(4)	2200(30)	11538(17)	1345(17)	7(5)
H(5)	7540(30)	11162(15)	1975(15)	2(5)
H(6)	5810(20)	9671(17)	1543(16)	3(5)

Contract No. N00014-95-1-0013 and N00014-97-1-0409

Program Officer: R. Miller/J. Goldwasser

**Title: Experimental Charge Densities and Electrostatic Potentials in Energetic
Materials and Infrastructure Upgrade for an X-ray Crystallography
Laboratory**

PI: A. Alan Pinkerton

Department of Chemistry, University of Toledo, Toledo, OH 43606

tel. (419) 530-4580, FAX (419) 530-4033, email apinker@uoft02.utoledo.edu

APPENDIX 3e

Variable temperature crystallographic study of γ -CL20

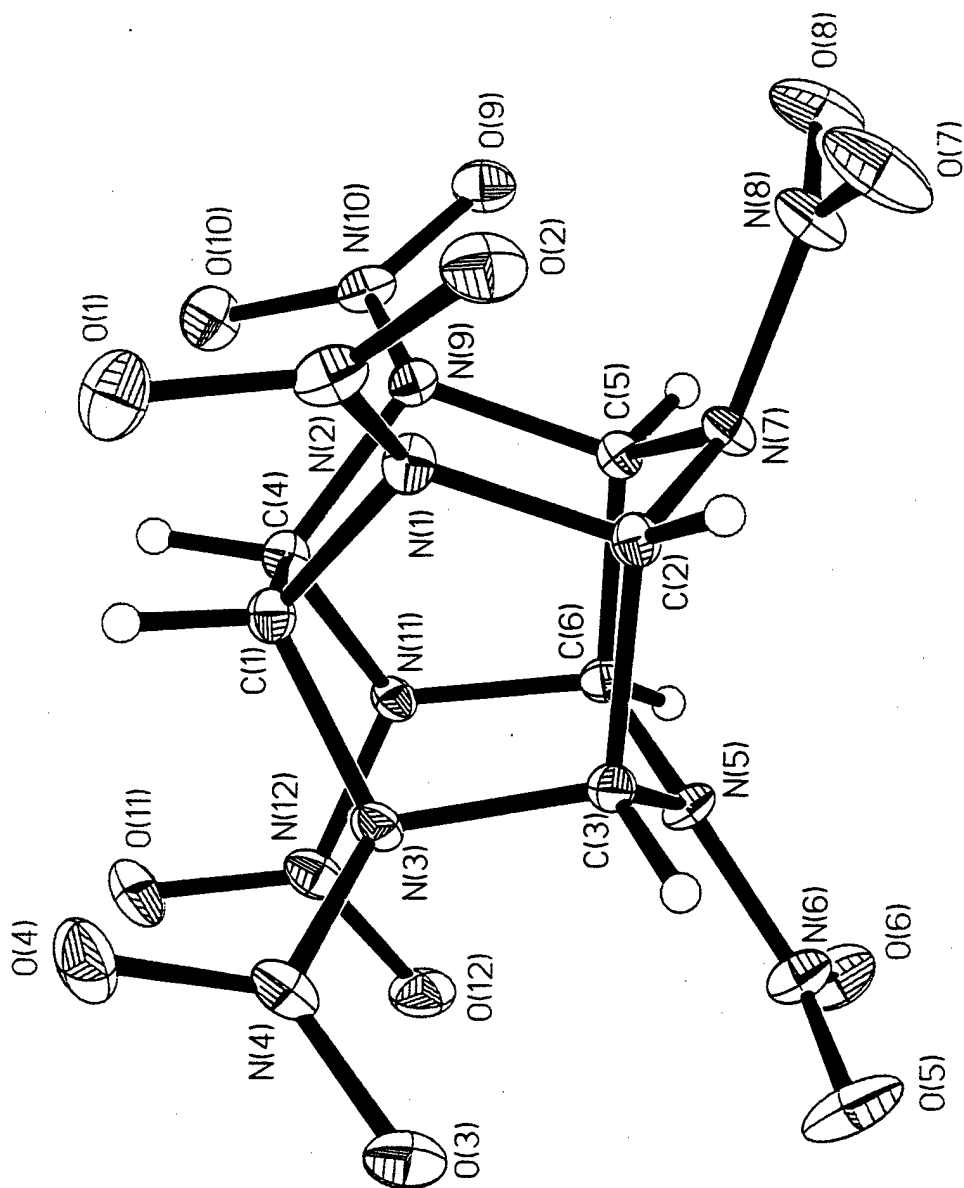


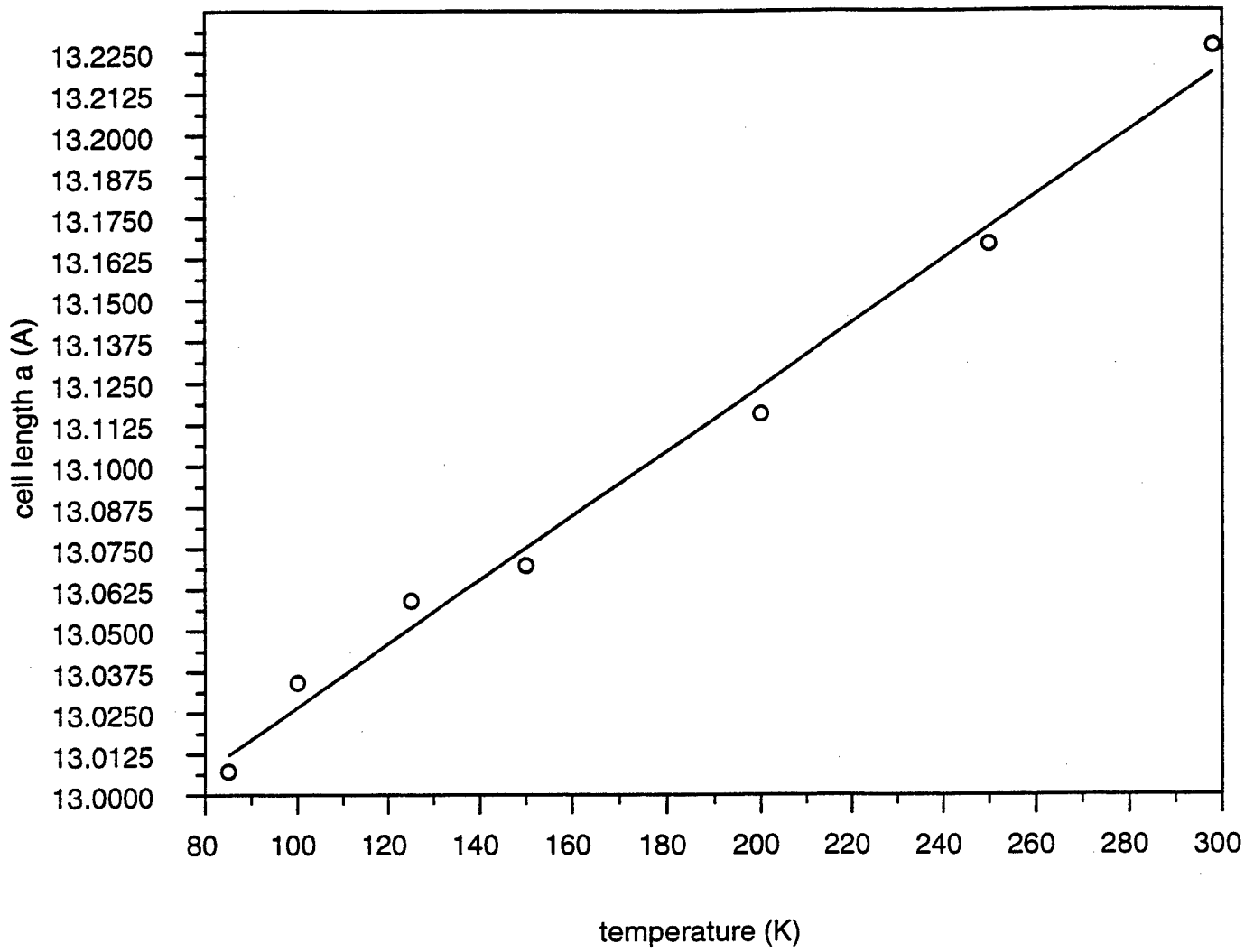
Table 1. Crystal data and structure refinement for hexanitrohexaazaisowurtzitane at various temperatures.

Empirical formula	$C_6H_6N_{12}O_{12}$									
Formula weight	438.02									
Wavelength	0.71073 Å									
Crystal system	Monoclinic									
Space group	$P2(1)/n$									
F(000)	888									
Crystal size	0.37 x 0.33 x 0.18 mm									
Z	4									
Instrument	Siemens SMART CCD									
Detector distance	4.99 cm									
Scan width and axis	-0.3° in ω									
Refinement method	Full-matrix least-squares on F ²									
Temperature (K)	293(2)	250(2)	200(2)	150(2)	125(2)	100(2)	85(2)			
a (Å)	13.2268(8)	13.1670(3)	13.1156(7)	13.0698(4)	13.0590(4)	13.0342(3)	13.0072(4)			
b (Å)	8.1695(5)	8.16760(10)	8.1713(4)	8.1737(3)	8.1810(3)	8.1773(2)	8.1684(2)			
c (Å)	14.8922(8)	14.84360(10)	14.8059(8)	14.7718(5)	14.7695(5)	14.7465(2)	14.7216(4)			
β (°)	109.1630(10)	109.0010(10)	108.8410(10)	108.6960(10)	108.6418(2)	108.5660(10)	108.5247(9)			
Volume (Å ³)	1520.0(2)	1509.34(4)	1501.75(14)	1494.78(9)	1495.12(9)	1489.95(5)	1483.10(7)			
Density (calc) (Mg/m ³)	1.915	1.929	1.938	1.947	1.947	1.954	1.963			
Absorption coeff. (mm ⁻¹)	0.184	0.185	0.186	0.187	0.187	0.187	0.188			
θ range	2.51 to 28.30°	2.52 to 28.30°	2.52 to 28.25°	2.52 to 28.29°	2.52 to 28.28°	2.52 to 28.26°	2.89 to 28.32°			
Limiting indices	-17 < h < 7	-17 < h < 7	-17 < h < 7	-17 < h < 7	-17 < h < 7	-17 < h < 7	-17 < h < 7			
	-10 < k < 10	-10 < k < 10	-10 < k < 10	-10 < k < 10	-10 < k < 10	-10 < k < 10	-10 < k < 10			
	-19 < l < 19	-19 < l < 19	-19 < l < 19	-19 < l < 19	-19 < l < 19	-19 < l < 19	-19 < l < 19			
Reflections collected	10300	10203	10149	10088	10026	9973	9964			
Independent reflections	3746	3714	3686	3678	3673	3658	3660			
R _{int}	0.0394	0.0366	0.0361	0.0340	0.0331	0.0360	0.0517			
Data / restraints / parameters	3746 / 0 / 296	3714 / 0 / 296	3686 / 0 / 296	3678 / 0 / 296	3673 / 0 / 296	3658 / 0 / 296	3660 / 0 / 296			
Goodness-of-fit on F ²	1.020	1.032	1.036	1.042	1.044	1.038	0.968			
R1 [$I > 2\sigma(I)$]	0.0411	0.0387	0.0369	0.0351	0.0348	0.0340	0.0399			
wR2 [$I > 2\sigma(I)$]	0.1047	0.0985	0.0932	0.0894	0.0890	0.0880	0.1000			
R1 (all data)	0.0632	0.0581	0.0516	0.0469	0.0454	0.0440	0.0507			
wR2 (all data)	0.1150	0.1090	0.1006	0.0949	0.0943	0.0926	0.1044			
Extinction coefficient	0.013(2)	0.0096(13)	0.0078(11)	0.0074(11)	0.0068(10)	0.0083(11)	0.0142(14)			
Largest diff. peak (eÅ ⁻³)	0.269	0.314	0.341	0.324	0.350	0.376	0.434			
Largest diff. hole (eÅ ⁻³)	-0.215	-0.223	-0.241	-0.262	-0.309	-0.280	-0.402			

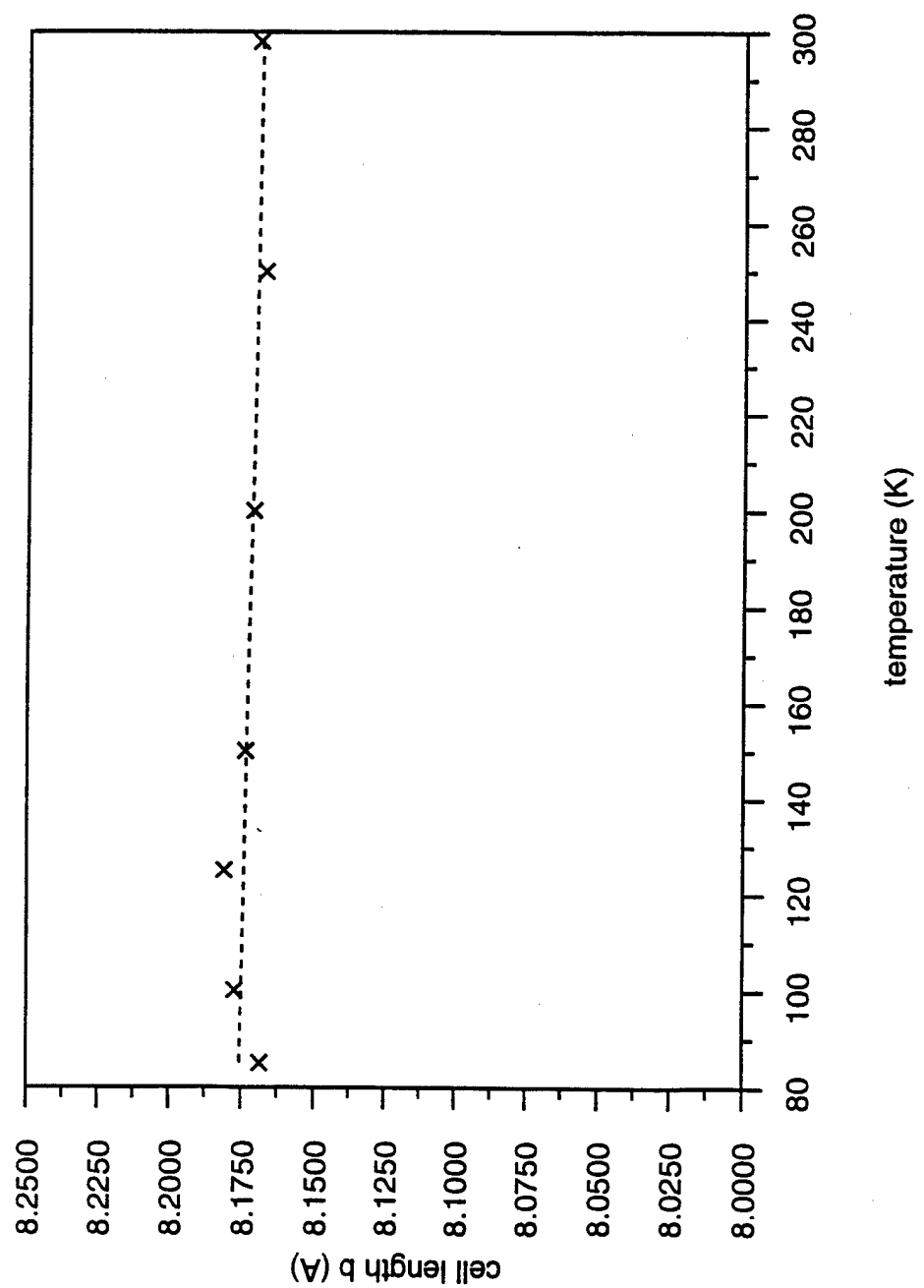
Table 16. Unit cell parameters for variable temperature structure determinations of hexanitrohexaazaisowurtzitane.

T (K)	<i>a</i> (Å)	<i>b</i> (Å)	<i>c</i> (Å)	β (°)	volume (Å ³)	ρ_{calc} (g/cm ³)
298	13.2268(8)	8.1695(5)	14.8922(8)	109.1630(10)	1520.0(2)	1.915
250	13.1670(3)	8.16760(10)	14.84360(10)	109.0010(10)	1509.34(4)	1.929
200	13.1156(7)	8.1713(4)	14.8059(8)	108.8410(10)	1501.75(14)	1.938
150	13.0698(4)	8.1737(3)	14.7718(5)	108.6960(10)	1494.78(9)	1.947
125	13.0590(4)	8.1810(3)	14.7695(5)	108.6418(2)	1495.12(9)	1.947
100	13.0342(3)	8.1773(2)	14.7465(2)	108.5660(10)	1489.95(5)	1.954
85	13.0072(4)	8.1684(2)	14.7216(4)	108.5247(9)	1483.10(7)	1.963

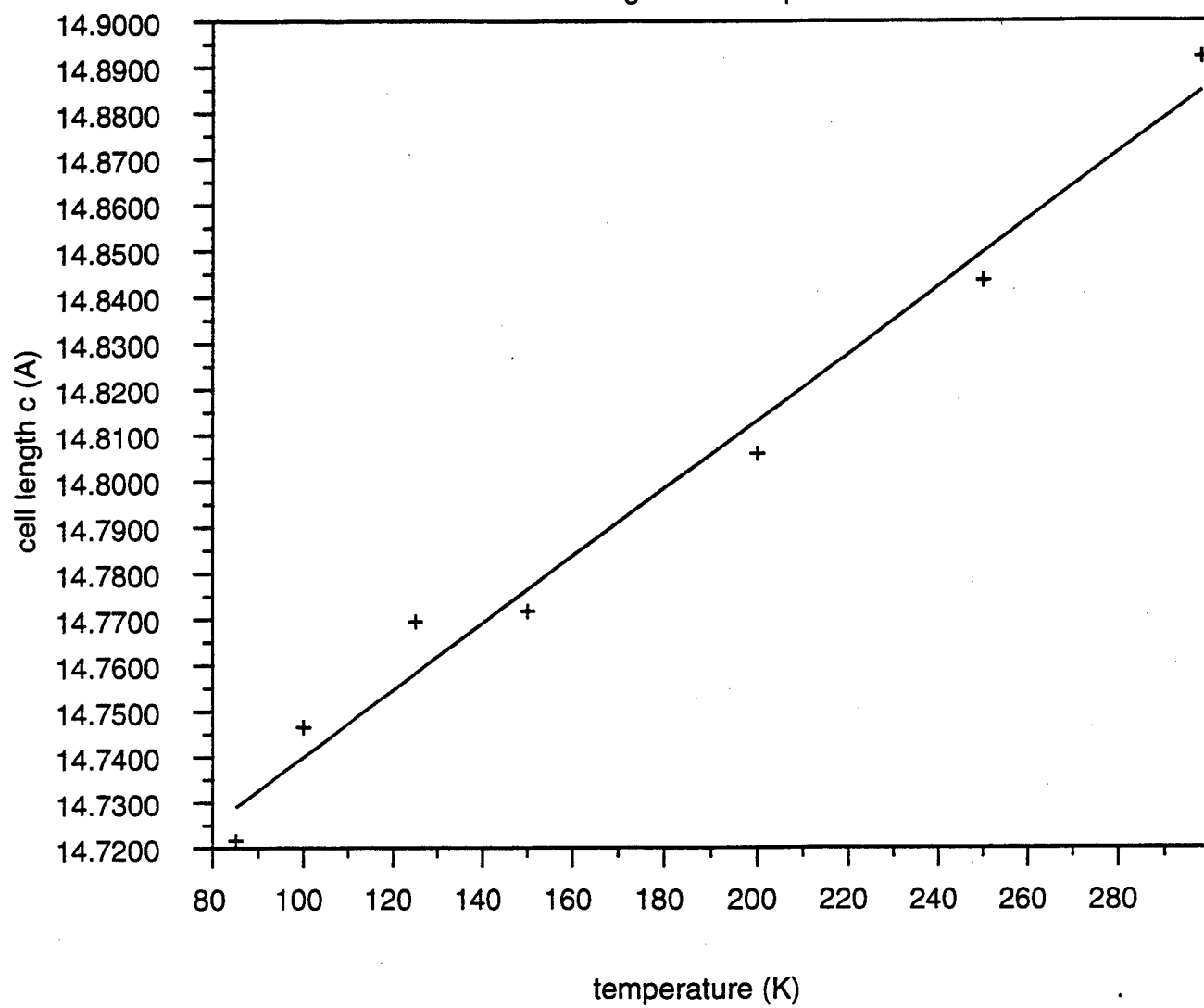
cl20 cell length a vs temperature



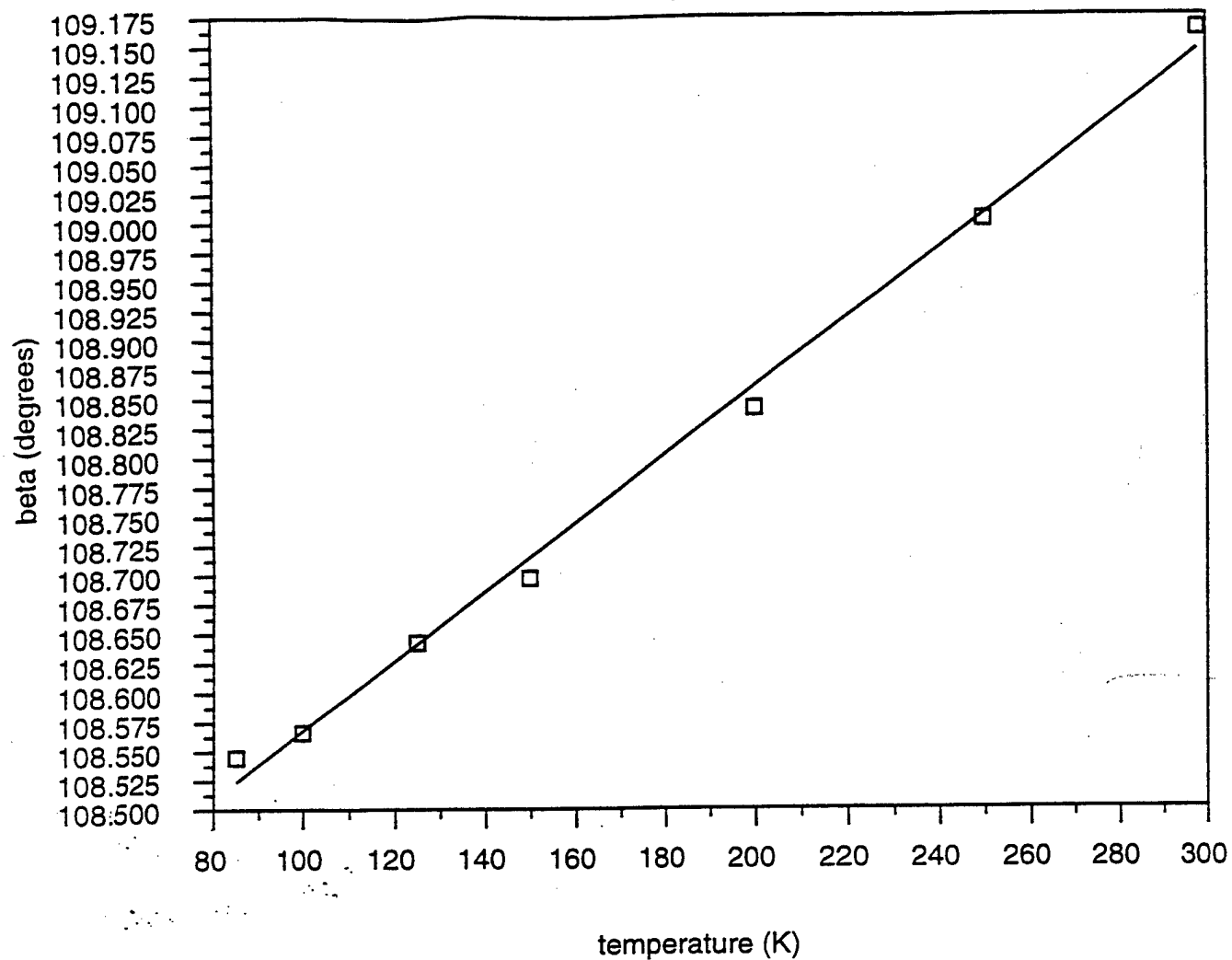
hexanitrohexaazaisowurtzitane
cell length b vs temperature



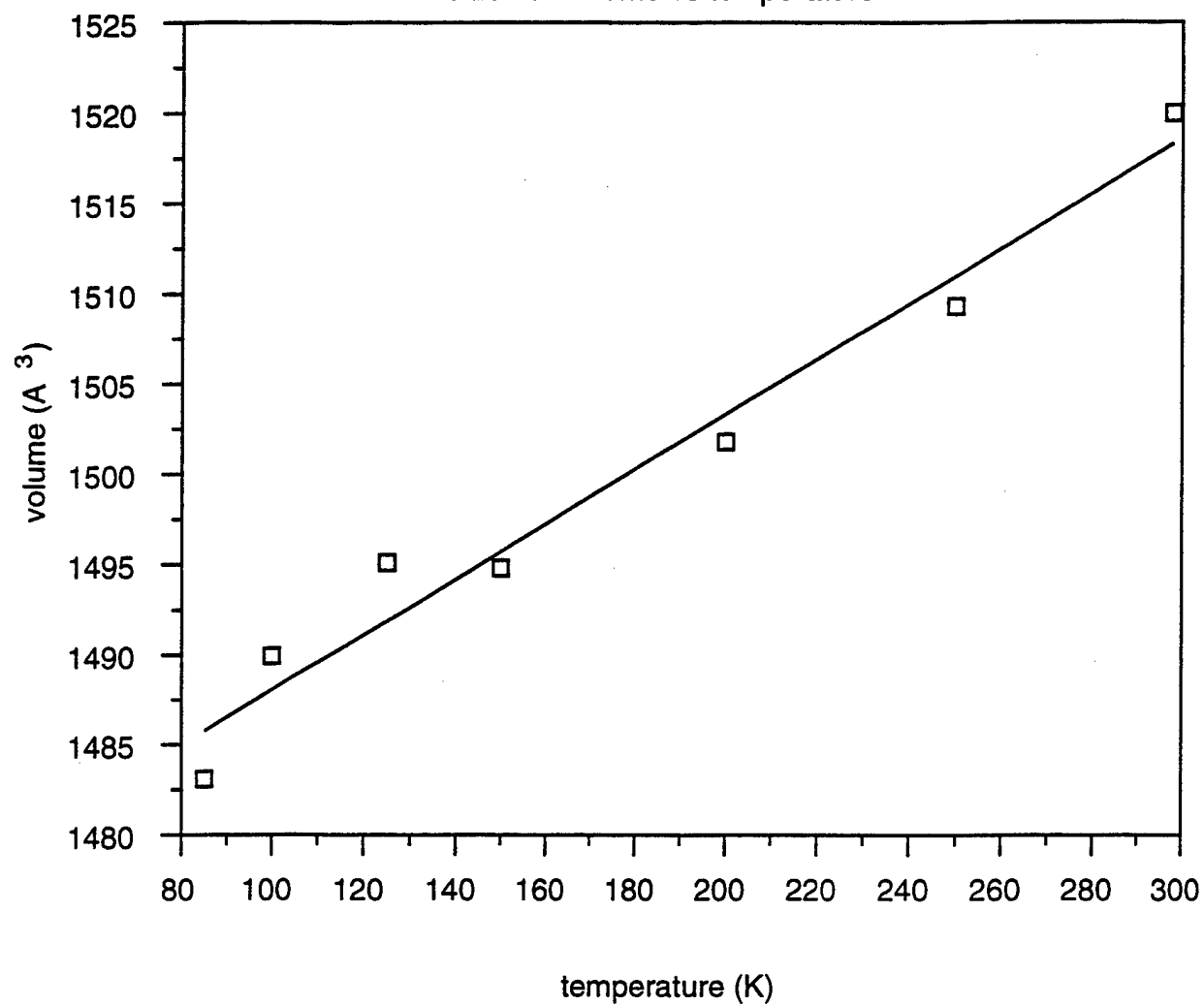
cl20 cell length c vs temperature



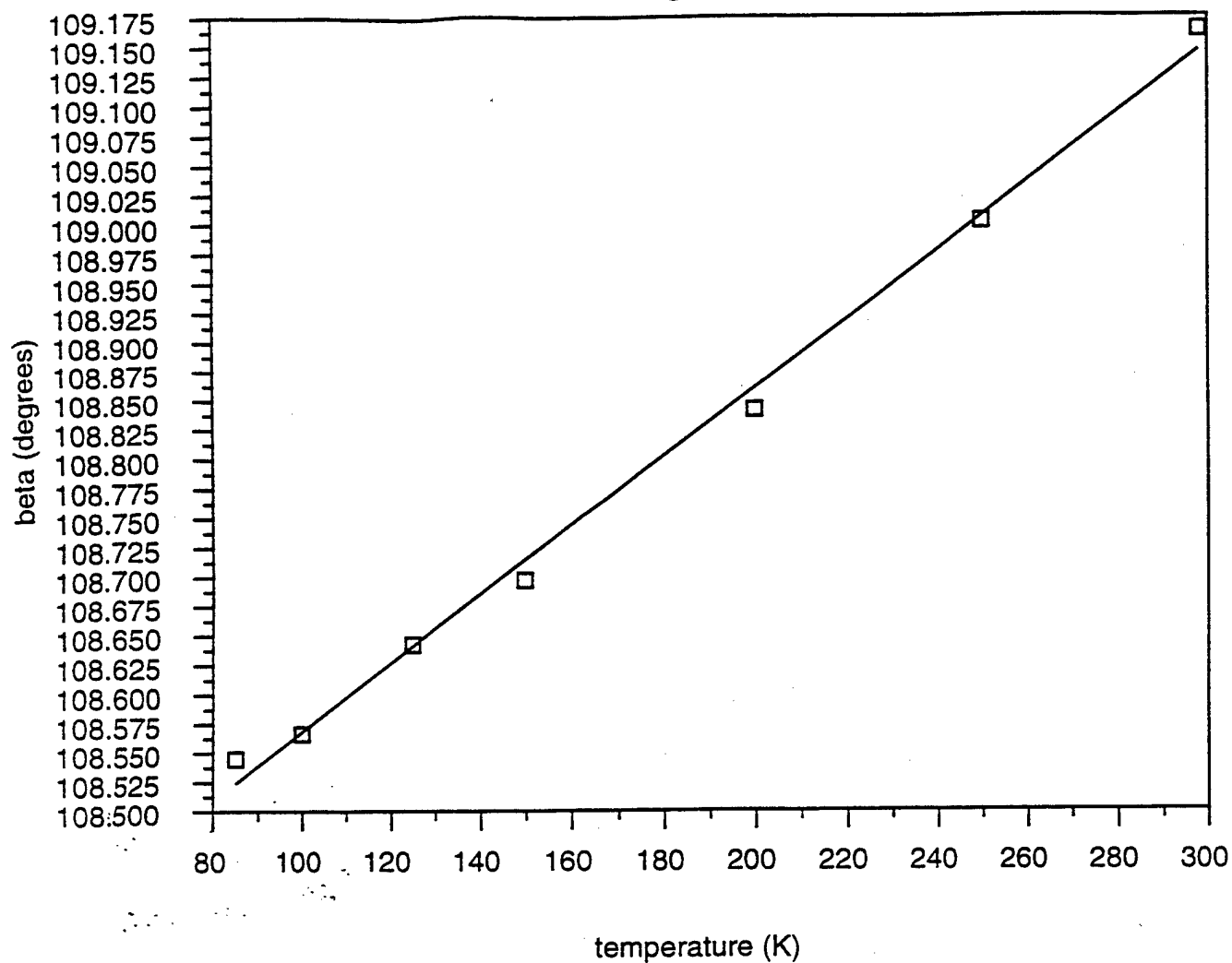
cl20 beta cell angle vs temperature



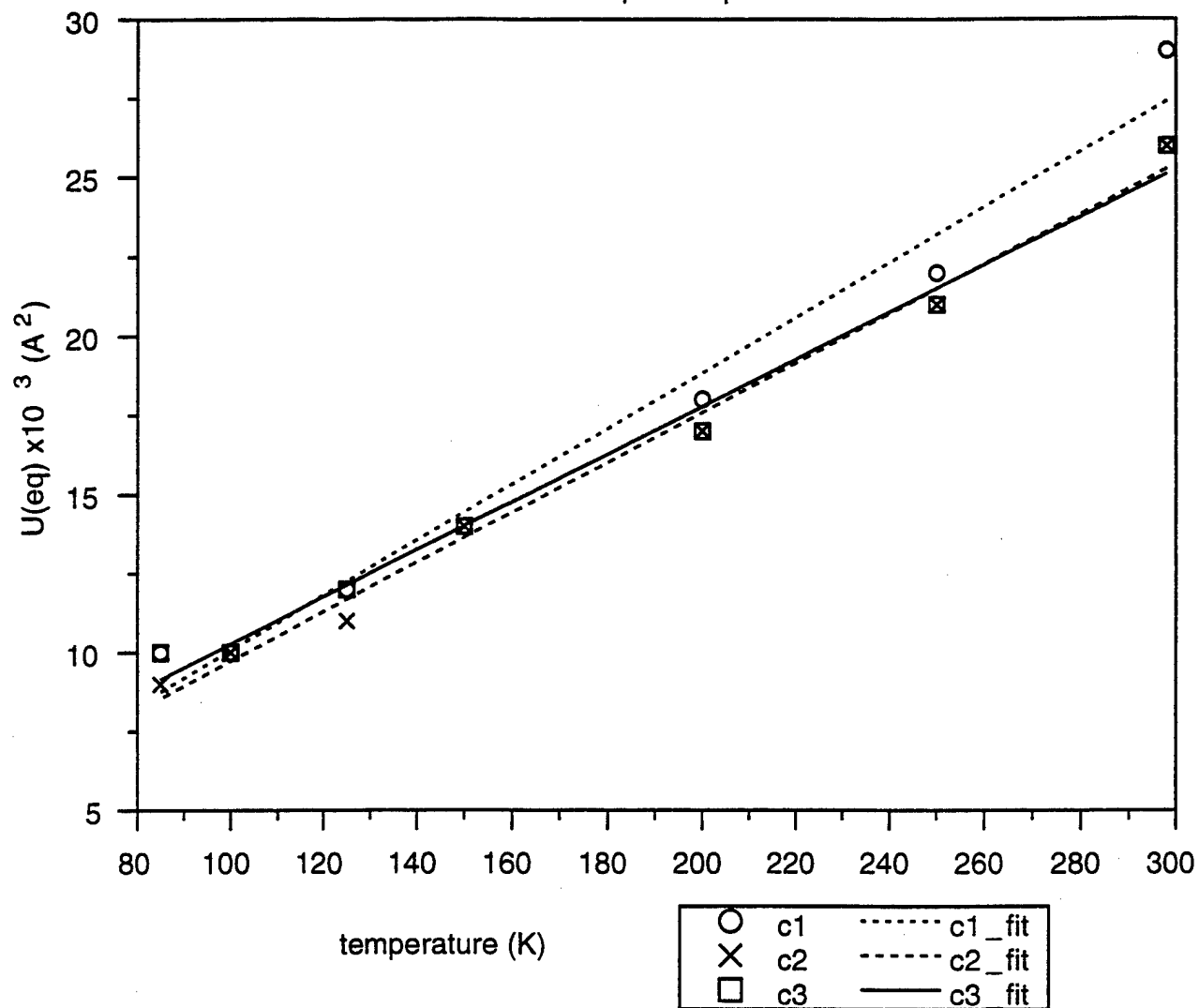
cl20 cell volume vs temperature



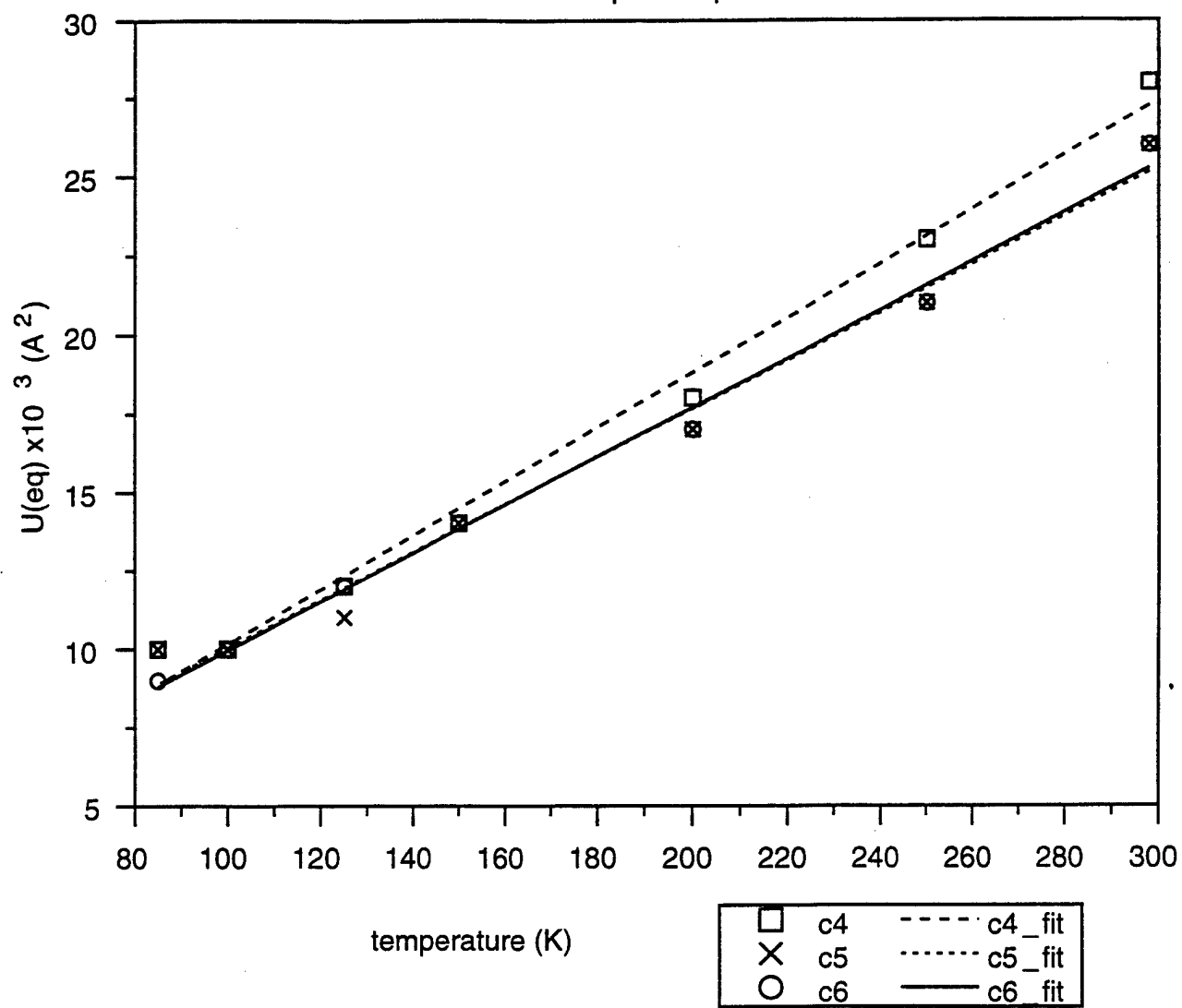
cl20 beta cell angle vs temperature



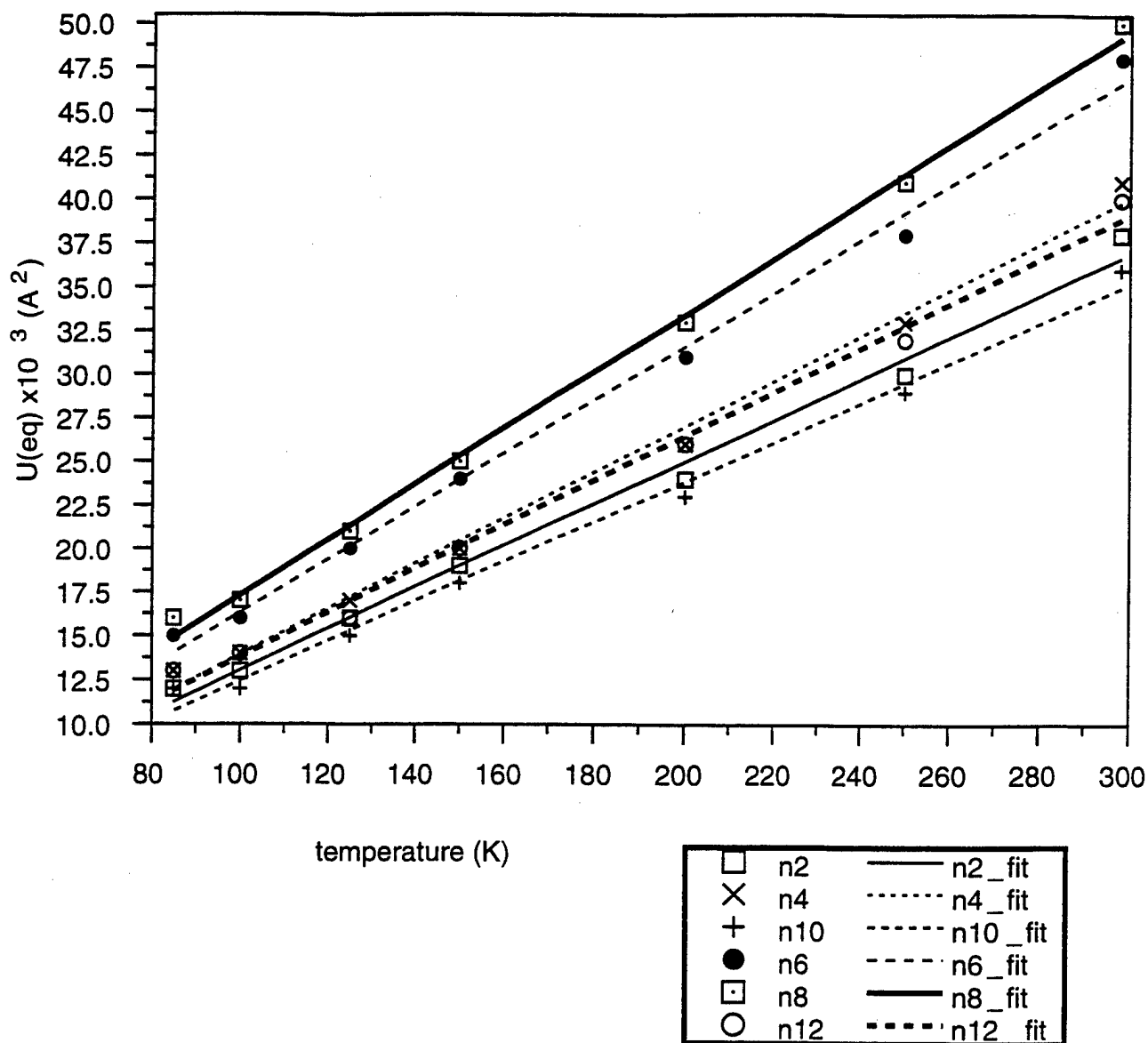
cl20 c1-c3 Ueq vs temperature



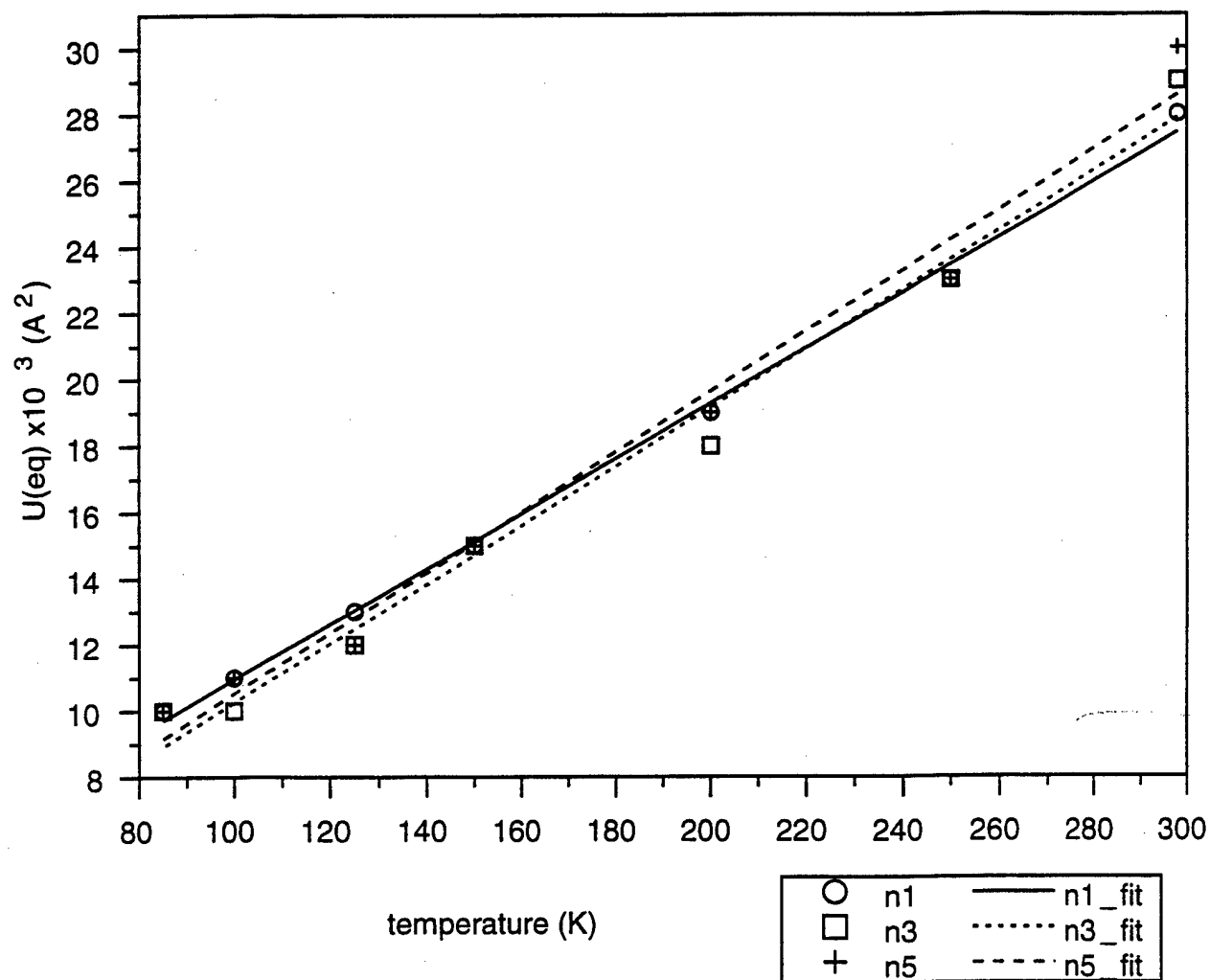
cl20 c4-c6 Ueq vs temperature



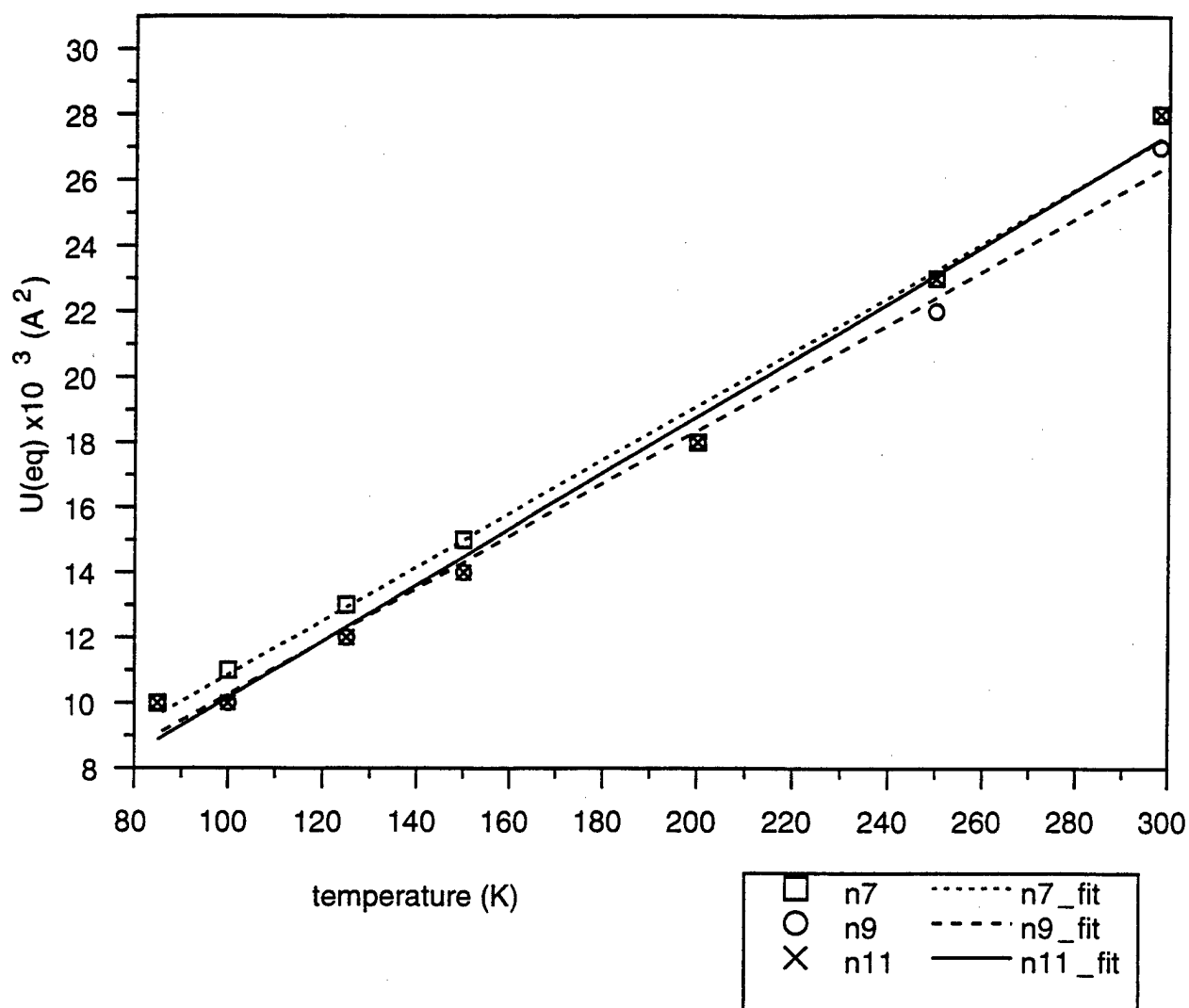
cl20 nitro N atom Ueq vs temperature



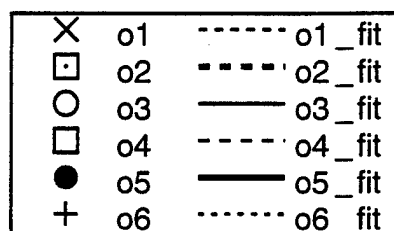
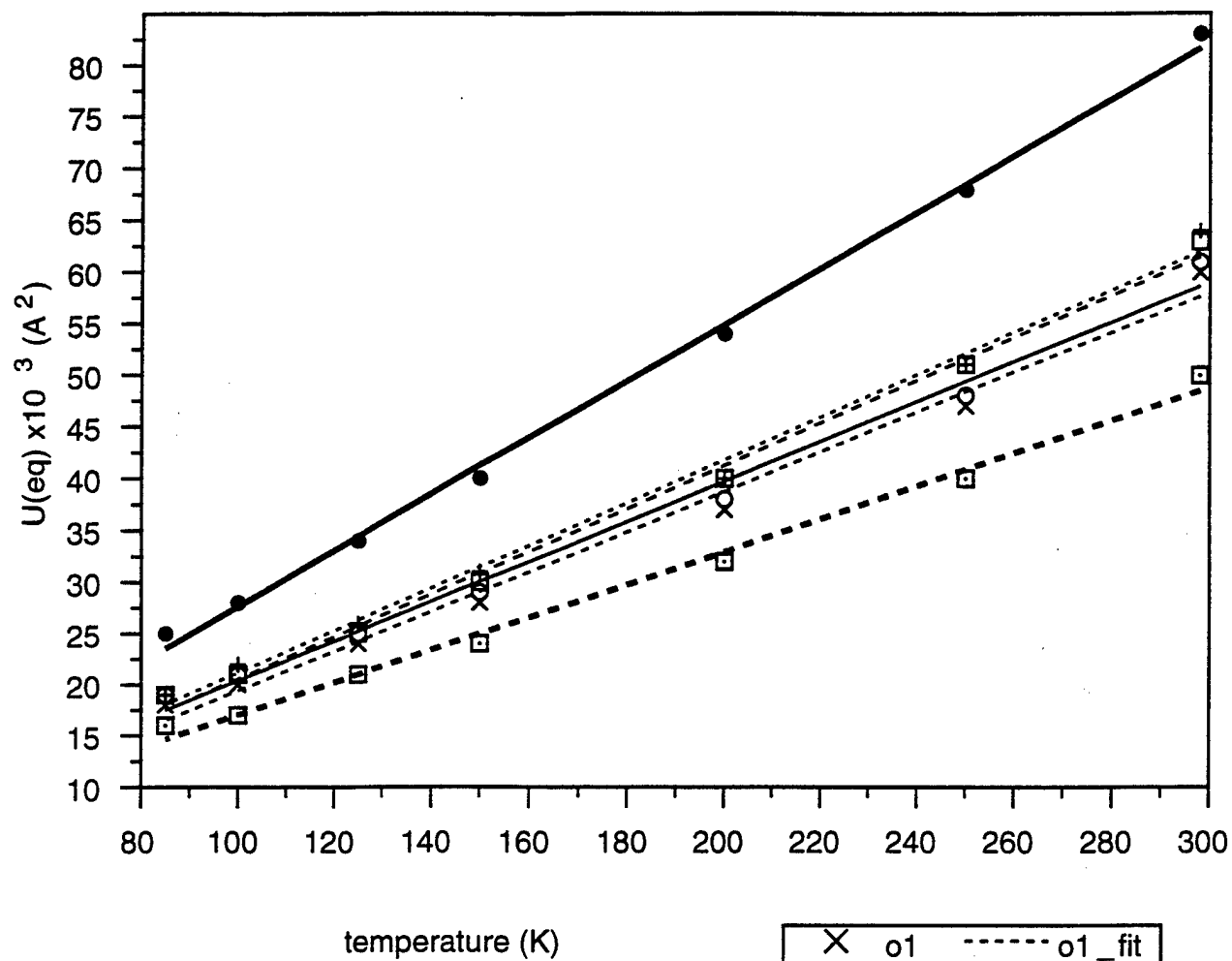
cl20 cage N Ueq vs temperature



cl20 cage N Ueq vs temperature



cl20 o1-o6 Ueq vs temperature



cl20 O7-O12 Ueq vs temperature

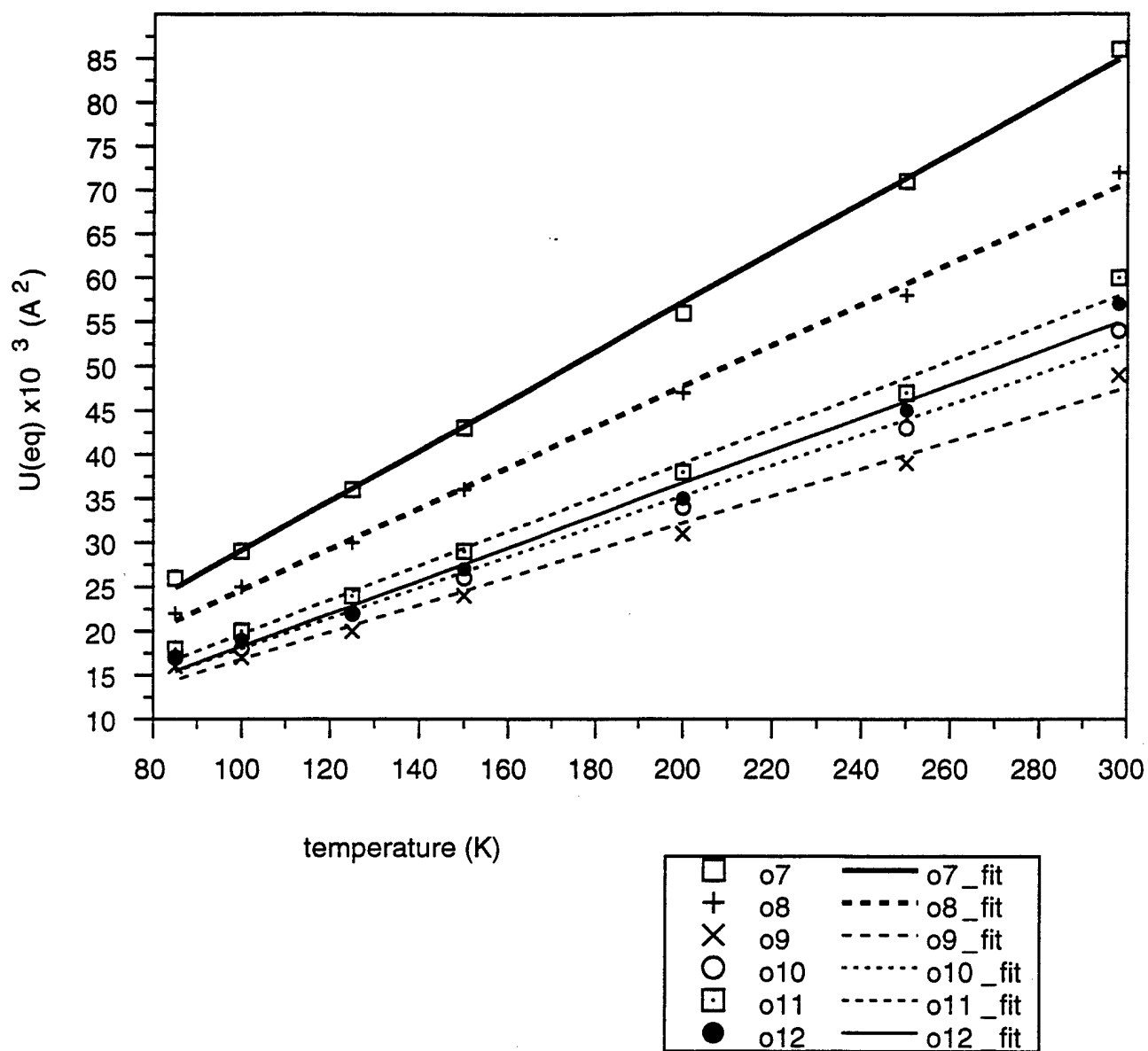


Table 2. Atomic coordinates and equivalent isotropic thermal parameters (\AA^2) for hexanitrohexaazaisowurtzitane at room temperature (298 K). $U(\text{eq})$ is defined as one third of the orthogonalized U_{ij} tensor.

	x	y	z	$U(\text{eq})/U_{\text{iso}}$
C1	0.10707(13)	0.5134(2)	0.32341(10)	0.0286(3)
C2	0.93689(12)	0.5926(2)	0.32615(10)	0.0260(3)
C3	0.00665(12)	0.7500(2)	0.32963(10)	0.0261(3)
C4	0.08410(12)	0.5012(2)	0.21178(10)	0.0278(3)
C5	0.90143(13)	0.5741(2)	0.15363(10)	0.0257(3)
C6	0.96894(13)	0.7334(2)	0.15718(10)	0.0265(3)
N1	0.01349(11)	0.4574(2)	0.34558(8)	0.0285(3)
N2	0.03025(14)	0.3637(2)	0.42837(9)	0.0380(4)
N3	0.11598(10)	0.6861(2)	0.34891(8)	0.0286(3)
N4	0.19287(12)	0.7302(2)	0.43760(10)	0.0412(4)
N5	0.97052(11)	0.82907(14)	0.23881(8)	0.0295(3)
N6	0.96633(14)	0.9988(2)	0.23263(11)	0.0480(4)
N7	0.85936(10)	0.5784(2)	0.23148(8)	0.0283(3)
N8	0.77517(13)	0.4669(2)	0.22496(11)	0.0496(4)
N9	0.97772(11)	0.43594(14)	0.16436(8)	0.0272(3)
N10	0.96690(13)	0.3580(2)	0.07474(9)	0.0365(3)
N11	0.07285(11)	0.66059(15)	0.16574(8)	0.0281(3)
N12	0.16158(12)	0.7583(2)	0.17901(10)	0.0404(4)
O1	0.11604(13)	0.2992(2)	0.46269(9)	0.0597(4)
O2	0.95367(12)	0.3504(2)	0.45602(8)	0.0495(4)
O3	0.18378(13)	0.8665(2)	0.46544(10)	0.0611(4)
O4	0.26246(12)	0.6317(2)	0.47409(10)	0.0634(4)
O5	0.9853(2)	0.0716(2)	0.30754(11)	0.0832(6)
O6	0.93915(14)	0.0574(2)	0.15360(9)	0.0641(5)
O7	0.75611(14)	0.4420(3)	0.29756(11)	0.0865(6)
O8	0.72838(13)	0.4108(2)	0.14741(10)	0.0717(5)
O9	0.87675(12)	0.3432(2)	0.02050(8)	0.0488(4)
O10	0.04827(12)	0.3081(2)	0.06365(9)	0.0538(4)
O11	0.24831(11)	0.6909(2)	0.20907(11)	0.0597(4)
O12	0.14506(12)	0.9007(2)	0.15740(10)	0.0567(4)
H1	0.1698(15)	0.4553(21)	0.3558(12)	0.034(4)
H2	0.9006(15)	0.5929(19)	0.3688(12)	0.031(4)
H3	0.0065(14)	0.8248(20)	0.3780(12)	0.031(4)
H4	0.1372(15)	0.4374(21)	0.2000(11)	0.033(4)
H5	0.8471(14)	0.5608(18)	0.0980(11)	0.023(4)
H6	0.9407(13)	0.7961(20)	0.1022(12)	0.028(4)

Table 3. Anisotropic displacement parameters (\AA^2) for hexanitrohexaazaisowurtzitane at room temperature (298 K). The anisotropic displacement factor exponent takes the form: $-2\pi^2[(ha^*)^2U_{11} + \dots + 2hka^*b^*U_{12}]$

	U11	U22	U33	U23	U13	U12
C1	0.0261(8)	0.0355(8)	0.0235(7)	0.0018(6)	0.0073(6)	0.0054(7)
C2	0.0256(8)	0.0313(8)	0.0234(7)	-0.0009(5)	0.0111(6)	-0.0013(6)
C3	0.0280(8)	0.0266(7)	0.0241(7)	-0.0042(5)	0.0089(6)	-0.0011(6)
C4	0.0280(8)	0.0342(8)	0.0230(7)	0.0002(6)	0.0106(6)	0.0037(7)
C5	0.0256(8)	0.0272(7)	0.0216(7)	0.0006(5)	0.0041(6)	-0.0031(6)
C6	0.0305(8)	0.0251(7)	0.0227(7)	0.0016(5)	0.0072(6)	-0.0029(6)
N1	0.0341(7)	0.0303(7)	0.0225(6)	0.0049(5)	0.0111(5)	0.0030(5)
N2	0.0606(11)	0.0301(7)	0.0228(6)	0.0011(5)	0.0132(7)	-0.0030(7)
N3	0.0231(7)	0.0382(7)	0.0215(6)	-0.0044(5)	0.0032(5)	-0.0040(5)
N4	0.0310(8)	0.0612(10)	0.0270(7)	-0.0069(6)	0.0038(6)	-0.0136(7)
N5	0.0376(8)	0.0206(6)	0.0292(6)	0.0005(4)	0.0094(6)	-0.0001(5)
N6	0.0676(11)	0.0239(7)	0.0500(9)	-0.0003(6)	0.0158(8)	-0.0011(7)
N7	0.0202(6)	0.0370(7)	0.0276(6)	-0.0015(5)	0.0079(5)	-0.0063(5)
N8	0.0351(9)	0.0717(11)	0.0422(9)	-0.0040(7)	0.0129(7)	-0.0248(8)
N9	0.0349(7)	0.0277(6)	0.0190(6)	-0.0031(4)	0.0090(5)	-0.0015(5)
N10	0.0565(10)	0.0305(7)	0.0258(7)	-0.0028(5)	0.0182(7)	-0.0054(6)
N11	0.0270(7)	0.0338(7)	0.0250(6)	0.0010(5)	0.0105(5)	-0.0051(5)
N12	0.0366(9)	0.0537(10)	0.0343(8)	-0.0040(6)	0.0160(7)	-0.0162(7)
O1	0.0704(11)	0.0606(9)	0.0406(7)	0.0218(6)	0.0079(7)	0.0185(8)
O2	0.0736(10)	0.0457(7)	0.0390(7)	0.0031(5)	0.0320(7)	-0.0129(6)
O3	0.0622(10)	0.0599(9)	0.0489(8)	-0.0224(6)	0.0017(7)	-0.0188(7)
O4	0.0368(8)	0.0915(11)	0.0440(8)	-0.0067(7)	-0.0108(6)	0.0089(8)
O5	0.155(2)	0.0293(7)	0.0565(9)	-0.0145(6)	0.0228(10)	-0.0053(9)
O6	0.1053(14)	0.0298(7)	0.0538(8)	0.0143(6)	0.0217(9)	0.0049(7)
O7	0.0648(11)	0.148(2)	0.0541(9)	-0.0068(10)	0.0301(8)	-0.0623(11)
O8	0.0593(10)	0.1030(13)	0.0484(8)	-0.0152(8)	0.0118(7)	-0.0524(9)
O9	0.0596(9)	0.0513(8)	0.0287(6)	-0.0113(5)	0.0052(6)	-0.0102(6)
O10	0.0632(10)	0.0624(9)	0.0457(7)	-0.0181(6)	0.0315(7)	0.0010(7)
O11	0.0289(8)	0.0847(11)	0.0660(9)	0.0029(8)	0.0161(7)	-0.0088(7)
O12	0.0601(10)	0.0457(8)	0.0701(9)	-0.0008(6)	0.0293(8)	-0.0222(7)

Table 4. Atomic coordinates and equivalent isotropic thermal parameters (\AA^2) for hexanitrohexaazaisowurtzitane at 250 K. $U(\text{eq})$ is defined as one third of the orthogonalized U_{ij} tensor.

	x	y	z	$U(\text{eq})/U_{\text{iso}}$
C1	0.10712(12)	0.5120(2)	0.32352(10)	0.0224(3)
C2	0.93654(12)	0.5942(2)	0.32656(10)	0.0208(3)
C3	0.00748(12)	0.7505(2)	0.32999(10)	0.0211(3)
C4	0.08408(12)	0.4996(2)	0.21162(10)	0.0226(3)
C5	0.90099(12)	0.5748(2)	0.15356(10)	0.0205(3)
C6	0.96961(12)	0.7335(2)	0.15709(10)	0.0214(3)
N1	0.01287(10)	0.45789(14)	0.34580(8)	0.0231(3)
N2	0.02870(13)	0.3641(2)	0.42844(9)	0.0301(3)
N3	0.11678(10)	0.68546(15)	0.34901(8)	0.0228(3)
N4	0.19387(11)	0.7288(2)	0.43789(9)	0.0329(3)
N5	0.97169(11)	0.82949(14)	0.23886(8)	0.0233(3)
N6	0.96819(13)	0.9995(2)	0.23260(10)	0.0383(4)
N7	0.85886(10)	0.58036(15)	0.23191(8)	0.0227(3)
N8	0.77392(12)	0.4701(2)	0.22545(11)	0.0406(4)
N9	0.97693(11)	0.43579(14)	0.16438(8)	0.0218(3)
N10	0.96593(12)	0.3580(2)	0.07439(9)	0.0287(3)
N11	0.07362(10)	0.65945(15)	0.16537(8)	0.0228(3)
N12	0.16289(11)	0.7559(2)	0.17898(9)	0.0325(3)
O1	0.11490(12)	0.2990(2)	0.46309(9)	0.0473(4)
O2	0.95137(11)	0.35137(15)	0.45605(8)	0.0398(3)
O3	0.18566(12)	0.8657(2)	0.46546(9)	0.0481(4)
O4	0.26315(11)	0.6294(2)	0.47468(9)	0.0510(4)
O5	0.9872(2)	0.0726(2)	0.30750(10)	0.0685(6)
O6	0.94194(14)	0.05779(14)	0.15356(9)	0.0515(4)
O7	0.75388(13)	0.4468(2)	0.29855(10)	0.0707(5)
O8	0.72656(13)	0.4137(2)	0.14787(10)	0.0584(5)
O9	0.87529(11)	0.34288(15)	0.02060(8)	0.0387(3)
O10	0.04726(11)	0.3087(2)	0.06240(9)	0.0429(3)
O11	0.24989(10)	0.6878(2)	0.20908(10)	0.0474(4)
O12	0.14703(12)	0.8992(2)	0.15747(10)	0.0455(3)
H1	0.1707(15)	0.4521(20)	0.3554(12)	0.027(4)
H2	0.9007(14)	0.5964(19)	0.3689(12)	0.022(4)
H3	0.0077(14)	0.8239(19)	0.3789(12)	0.022(4)
H4	0.1382(15)	0.4326(21)	0.1986(12)	0.027(4)
H5	0.8463(14)	0.5621(18)	0.0976(11)	0.018(4)
H6	0.9414(13)	0.7959(19)	0.1018(12)	0.021(4)

Table 5. Anisotropic displacement parameters (\AA^2) for hexanitrohexaazaisowurtzitane at 250 K. The anisotropic displacement factor exponent takes the form:

$$-2\pi^2[(ha^*)^2U_{11} + \dots + 2hka^*b^*U_{12}]$$

	U11	U22	U33	U23	U13	U12
C1	0.0207(7)	0.0270(7)	0.0196(7)	0.0012(5)	0.0067(6)	0.0043(6)
C2	0.0196(7)	0.0247(7)	0.0200(7)	-0.0009(5)	0.0090(6)	-0.0016(6)
C3	0.0221(7)	0.0217(7)	0.0199(7)	-0.0023(5)	0.0074(6)	-0.0010(6)
C4	0.0238(8)	0.0255(7)	0.0193(7)	-0.0003(5)	0.0082(6)	0.0019(6)
C5	0.0191(7)	0.0220(7)	0.0185(7)	-0.0002(5)	0.0034(6)	-0.0018(6)
C6	0.0239(8)	0.0206(7)	0.0187(7)	0.0014(5)	0.0057(6)	-0.0015(6)
N1	0.0291(7)	0.0232(6)	0.0184(6)	0.0044(4)	0.0097(5)	0.0017(5)
N2	0.0468(9)	0.0240(6)	0.0192(6)	0.0008(5)	0.0103(6)	-0.0022(6)
N3	0.0190(6)	0.0304(7)	0.0167(6)	-0.0033(4)	0.0027(5)	-0.0036(5)
N4	0.0244(7)	0.0479(9)	0.0236(7)	-0.0054(6)	0.0038(6)	-0.0101(6)
N5	0.0297(7)	0.0148(6)	0.0244(6)	0.0003(4)	0.0076(5)	0.0002(5)
N6	0.0540(10)	0.0186(6)	0.0407(8)	-0.0004(5)	0.0131(7)	-0.0001(6)
N7	0.0159(6)	0.0282(6)	0.0240(6)	-0.0014(5)	0.0067(5)	-0.0040(5)
N8	0.0268(8)	0.0602(10)	0.0354(8)	-0.0026(7)	0.0109(6)	-0.0201(7)
N9	0.0280(7)	0.0211(6)	0.0166(6)	-0.0027(4)	0.0078(5)	-0.0012(5)
N10	0.0447(9)	0.0230(6)	0.0216(6)	-0.0026(5)	0.0153(6)	-0.0036(6)
N11	0.0214(6)	0.0267(6)	0.0215(6)	0.0010(4)	0.0088(5)	-0.0045(5)
N12	0.0288(8)	0.0439(9)	0.0279(7)	-0.0037(6)	0.0134(6)	-0.0124(6)
O1	0.0564(9)	0.0472(8)	0.0330(7)	0.0165(5)	0.0070(6)	0.0149(7)
O2	0.0580(9)	0.0362(7)	0.0330(6)	0.0024(5)	0.0256(6)	-0.0117(6)
O3	0.0492(9)	0.0452(8)	0.0405(7)	-0.0175(6)	0.0017(6)	-0.0148(6)
O4	0.0311(7)	0.0718(10)	0.0366(7)	-0.0051(6)	-0.0074(6)	0.0080(7)
O5	0.129(2)	0.0233(7)	0.0452(8)	-0.0117(5)	0.0181(9)	-0.0028(8)
O6	0.0844(12)	0.0237(6)	0.0441(7)	0.0119(5)	0.0177(8)	0.0046(6)
O7	0.0521(10)	0.1225(15)	0.0440(8)	-0.0065(8)	0.0245(7)	-0.0516(10)
O8	0.0481(9)	0.0840(11)	0.0400(8)	-0.0127(7)	0.0103(7)	-0.0436(8)
O9	0.0467(8)	0.0402(7)	0.0242(6)	-0.0098(5)	0.0046(6)	-0.0085(6)
O10	0.0505(9)	0.0483(8)	0.0375(7)	-0.0142(5)	0.0249(6)	0.0012(6)
O11	0.0228(7)	0.0661(9)	0.0534(8)	0.0025(7)	0.0123(6)	-0.0077(6)
O12	0.0481(9)	0.0355(7)	0.0578(8)	-0.0008(5)	0.0240(7)	-0.0175(6)

Table 6. Atomic coordinates and equivalent isotropic thermal parameters (\AA^2) for hexanitrohexaazaisowurtzitane at 200 K. $U(\text{eq})$ is defined as one third of the orthogonalized U_{ij} tensor.

	x	y	z	$U(\text{eq})/U_{\text{iso}}$
C1	0.10720(11)	0.5111(2)	0.32365(9)	0.0179(3)
C2	0.93625(11)	0.5956(2)	0.32705(9)	0.0168(3)
C3	0.00836(11)	0.7511(2)	0.33030(9)	0.0173(3)
C4	0.08410(12)	0.4987(2)	0.21157(9)	0.0178(3)
C5	0.90077(11)	0.5757(2)	0.15365(9)	0.0166(3)
C6	0.97020(11)	0.7335(2)	0.15690(9)	0.0171(3)
N1	0.01222(10)	0.45845(14)	0.34615(8)	0.0186(3)
N2	0.02746(11)	0.36460(14)	0.42874(8)	0.0238(3)
N3	0.11783(9)	0.68472(14)	0.34902(8)	0.0185(2)
N4	0.19506(10)	0.7277(2)	0.43801(8)	0.0255(3)
N5	0.97287(10)	0.83010(13)	0.23890(8)	0.0188(3)
N6	0.96981(12)	0.99998(15)	0.23253(9)	0.0308(3)
N7	0.85806(9)	0.58261(13)	0.23218(8)	0.0182(2)
N8	0.77247(11)	0.4731(2)	0.22624(10)	0.0326(3)
N9	0.97620(10)	0.43585(13)	0.16435(7)	0.0177(2)
N10	0.96495(11)	0.35815(14)	0.07412(8)	0.0228(3)
N11	0.07432(10)	0.65821(14)	0.16502(8)	0.0183(2)
N12	0.16436(10)	0.7536(2)	0.17904(8)	0.0257(3)
O1	0.11373(11)	0.29824(15)	0.46342(8)	0.0371(3)
O2	0.94947(10)	0.35243(13)	0.45625(7)	0.0315(3)
O3	0.18758(11)	0.86525(15)	0.46553(8)	0.0384(3)
O4	0.26401(10)	0.6273(2)	0.47512(8)	0.0400(3)
O5	0.98885(15)	0.07368(14)	0.30776(9)	0.0535(4)
O6	0.94454(12)	0.05803(13)	0.15316(8)	0.0405(3)
O7	0.75175(11)	0.4517(2)	0.29931(9)	0.0561(4)
O8	0.72508(11)	0.4161(2)	0.14838(9)	0.0468(4)
O9	0.87372(10)	0.34231(13)	0.02086(7)	0.0306(3)
O10	0.04669(10)	0.30949(14)	0.06142(8)	0.0339(3)
O11	0.25148(9)	0.6851(2)	0.20917(9)	0.0377(3)
O12	0.14891(10)	0.89760(14)	0.15769(8)	0.0352(3)
H1	0.1713(14)	0.4526(19)	0.3563(11)	0.018(4)
H2	0.8996(14)	0.6011(18)	0.3708(11)	0.019(4)
H3	0.0088(14)	0.8265(20)	0.3782(12)	0.026(4)
H4	0.1379(14)	0.4329(19)	0.2004(11)	0.018(4)
H5	0.8437(14)	0.5633(18)	0.0976(11)	0.017(4)
H6	0.9434(12)	0.7964(18)	0.1026(11)	0.015(4)

Table 7. Anisotropic displacement parameters (\AA^2) for hexanitrohexaazaisowurtzitane at 200 K. The anisotropic displacement factor exponent takes the form:

$$-2\pi^2[(ha^*)^2U_{11} + \dots + 2hka^*b^*U_{12}]$$

	U11	U22	U33	U23	U13	U12
C1	0.0166(7)	0.0207(7)	0.0165(6)	0.0007(5)	0.0055(5)	0.0031(5)
C2	0.0157(7)	0.0201(6)	0.0159(6)	-0.0007(4)	0.0069(5)	-0.0014(5)
C3	0.0177(7)	0.0170(6)	0.0178(6)	-0.0020(5)	0.0064(5)	-0.0005(5)
C4	0.0183(7)	0.0209(7)	0.0149(6)	-0.0002(5)	0.0065(5)	0.0019(5)
C5	0.0150(7)	0.0187(6)	0.0151(6)	0.0001(4)	0.0036(5)	-0.0017(5)
C6	0.0190(7)	0.0164(6)	0.0153(6)	0.0011(5)	0.0046(5)	-0.0013(5)
N1	0.0229(6)	0.0191(6)	0.0157(5)	0.0034(4)	0.0088(5)	0.0017(5)
N2	0.0371(8)	0.0188(6)	0.0153(6)	0.0003(4)	0.0082(5)	-0.0019(5)
N3	0.0151(6)	0.0240(6)	0.0146(5)	-0.0033(4)	0.0022(4)	-0.0025(5)
N4	0.0180(6)	0.0369(7)	0.0193(6)	-0.0036(5)	0.0029(5)	-0.0066(5)
N5	0.0244(6)	0.0126(5)	0.0189(6)	0.0004(4)	0.0060(5)	0.0005(4)
N6	0.0426(8)	0.0152(6)	0.0333(7)	-0.0003(5)	0.0103(6)	0.0001(6)
N7	0.0128(6)	0.0236(6)	0.0188(6)	-0.0013(4)	0.0058(5)	-0.0036(4)
N8	0.0223(7)	0.0475(8)	0.0286(7)	-0.0019(6)	0.0088(6)	-0.0155(6)
N9	0.0230(6)	0.0174(5)	0.0137(5)	-0.0027(4)	0.0072(5)	-0.0004(5)
N10	0.0353(8)	0.0187(6)	0.0166(6)	-0.0016(4)	0.0115(5)	-0.0034(5)
N11	0.0167(6)	0.0222(6)	0.0171(5)	0.0009(4)	0.0072(4)	-0.0033(5)
N12	0.0227(7)	0.0343(7)	0.0223(6)	-0.0028(5)	0.0101(5)	-0.0094(5)
O1	0.0453(8)	0.0366(6)	0.0257(6)	0.0120(5)	0.0064(5)	0.0112(6)
O2	0.0448(8)	0.0297(6)	0.0263(6)	0.0015(4)	0.0201(5)	-0.0089(5)
O3	0.0386(8)	0.0362(7)	0.0330(6)	-0.0132(5)	0.0013(5)	-0.0105(5)
O4	0.0245(6)	0.0557(8)	0.0299(6)	-0.0033(5)	-0.0049(5)	0.0066(6)
O5	0.1003(13)	0.0196(6)	0.0352(7)	-0.0087(5)	0.0143(7)	-0.0021(6)
O6	0.0652(10)	0.0207(6)	0.0340(6)	0.0094(4)	0.0136(6)	0.0027(6)
O7	0.0398(8)	0.0994(12)	0.0343(7)	-0.0051(7)	0.0190(6)	-0.0389(8)
O8	0.0387(8)	0.0665(9)	0.0325(7)	-0.0108(6)	0.0077(6)	-0.0342(7)
O9	0.0364(7)	0.0314(6)	0.0198(5)	-0.0074(4)	0.0031(5)	-0.0067(5)
O10	0.0391(7)	0.0383(6)	0.0303(6)	-0.0106(5)	0.0194(5)	0.0010(5)
O11	0.0183(6)	0.0515(8)	0.0434(7)	0.0022(5)	0.0104(5)	-0.0048(5)
O12	0.0375(7)	0.0281(6)	0.0439(7)	-0.0003(5)	0.0184(6)	-0.0129(5)

Table 8. Atomic coordinates and equivalent isotropic thermal parameters (\AA^2) for hexanitrohexaazaisowurtzitane at 150 K. $U(\text{eq})$ is defined as one third of the orthogonalized U_{ij} tensor.

	x	y	z	Uiso
C1	0.10726(11)	0.5103(2)	0.32378(9)	0.0142(3)
C2	0.93615(11)	0.59724(15)	0.32746(9)	0.0136(3)
C3	0.00915(11)	0.75182(15)	0.33048(9)	0.0139(3)
C4	0.08430(11)	0.49759(15)	0.21156(9)	0.0143(3)
C5	0.90041(11)	0.57671(15)	0.15361(9)	0.0136(3)
C6	0.97084(11)	0.73366(15)	0.15673(9)	0.0139(3)
N1	0.01165(9)	0.45888(13)	0.34637(7)	0.0148(2)
N2	0.02649(10)	0.36479(13)	0.42896(8)	0.0187(3)
N3	0.11873(9)	0.68410(13)	0.34911(7)	0.0149(2)
N4	0.19613(9)	0.72646(15)	0.43823(8)	0.0197(3)
N5	0.97397(9)	0.83042(12)	0.23902(7)	0.0150(2)
N6	0.97140(11)	0.00083(14)	0.23260(9)	0.0235(3)
N7	0.85770(9)	0.58446(13)	0.23261(7)	0.0146(2)
N8	0.77116(10)	0.4758(2)	0.22663(9)	0.0250(3)
N9	0.97559(9)	0.43555(13)	0.16437(7)	0.0142(2)
N10	0.96409(10)	0.35832(13)	0.07394(7)	0.0178(2)
N11	0.07511(9)	0.65711(13)	0.16477(7)	0.0145(2)
N12	0.16552(10)	0.75212(14)	0.17898(8)	0.0196(3)
O1	0.11291(9)	0.29777(13)	0.46367(7)	0.0280(3)
O2	0.94769(9)	0.35343(12)	0.45644(7)	0.0241(2)
O3	0.18930(9)	0.86484(13)	0.46548(7)	0.0294(3)
O4	0.26482(9)	0.62540(14)	0.47553(7)	0.0300(3)
O5	0.99010(13)	0.07447(13)	0.30782(8)	0.0405(3)
O6	0.94683(10)	0.05842(12)	0.15298(7)	0.0307(3)
O7	0.75003(10)	0.4560(2)	0.30015(8)	0.0428(3)
O8	0.72381(10)	0.41806(15)	0.14881(8)	0.0355(3)
O9	0.87237(9)	0.34196(12)	0.02101(7)	0.0239(2)
O10	0.04614(9)	0.31042(13)	0.06036(7)	0.0258(2)
O11	0.25286(8)	0.68271(14)	0.20910(8)	0.0288(3)
O12	0.15046(9)	0.89649(12)	0.15786(8)	0.0270(3)
H1	0.1714(13)	0.4487(18)	0.3565(11)	0.016(4)
H2	0.8981(13)	0.6033(18)	0.3717(11)	0.016(4)
H3	0.0101(13)	0.8252(18)	0.3785(11)	0.016(4)
H4	0.1383(13)	0.4288(18)	0.1998(10)	0.015(4)
H5	0.8442(13)	0.5661(17)	0.0961(11)	0.012(4)
H6	0.9455(12)	0.7951(18)	0.1022(11)	0.013(4)

Table 9. Anisotropic displacement parameters (\AA^2) for hexanitrohexaazaisowurtzitane at 150 K. The anisotropic displacement factor exponent takes the form:

$$-2\pi^2[(ha^*)^2U_{11} + \dots + 2hka^*b^*U_{12}]$$

	U11	U22	U33	U23	U13	U12
C1	0.0137(6)	0.0167(6)	0.0126(6)	0.0009(4)	0.0048(5)	0.0022(5)
C2	0.0131(6)	0.0152(6)	0.0133(6)	-0.0005(4)	0.0053(5)	-0.0005(5)
C3	0.0141(6)	0.0142(6)	0.0138(6)	-0.0010(4)	0.0051(5)	-0.0007(5)
C4	0.0152(6)	0.0158(6)	0.0125(6)	0.0001(4)	0.0055(5)	0.0010(5)
C5	0.0135(6)	0.0151(6)	0.0118(6)	-0.0002(4)	0.0034(5)	-0.0011(5)
C6	0.0148(6)	0.0144(6)	0.0122(6)	0.0008(4)	0.0040(5)	-0.0011(5)
N1	0.0171(6)	0.0154(5)	0.0130(5)	0.0029(4)	0.0063(4)	0.0014(4)
N2	0.0284(7)	0.0152(5)	0.0125(5)	-0.0002(4)	0.0068(5)	-0.0016(5)
N3	0.0122(5)	0.0187(5)	0.0120(5)	-0.0024(4)	0.0015(4)	-0.0019(4)
N4	0.0146(6)	0.0283(6)	0.0151(5)	-0.0021(4)	0.0030(4)	-0.0054(5)
N5	0.0202(6)	0.0096(5)	0.0149(5)	0.0004(4)	0.0053(4)	0.0001(4)
N6	0.0323(7)	0.0118(5)	0.0254(6)	-0.0003(4)	0.0078(5)	-0.0003(5)
N7	0.0106(5)	0.0188(5)	0.0149(5)	-0.0012(4)	0.0049(4)	-0.0037(4)
N8	0.0173(6)	0.0359(7)	0.0220(6)	-0.0015(5)	0.0064(5)	-0.0109(5)
N9	0.0178(6)	0.0148(5)	0.0105(5)	-0.0018(4)	0.0053(4)	0.0002(4)
N10	0.0277(7)	0.0150(5)	0.0123(5)	-0.0012(4)	0.0085(5)	-0.0028(5)
N11	0.0140(5)	0.0167(5)	0.0134(5)	0.0006(4)	0.0052(4)	-0.0026(4)
N12	0.0176(6)	0.0266(6)	0.0164(5)	-0.0018(4)	0.0077(5)	-0.0069(5)
O1	0.0340(6)	0.0273(5)	0.0201(5)	0.0083(4)	0.0049(5)	0.0086(5)
O2	0.0335(6)	0.0236(5)	0.0202(5)	0.0009(4)	0.0154(5)	-0.0071(4)
O3	0.0295(6)	0.0280(6)	0.0258(5)	-0.0097(4)	0.0022(5)	-0.0081(5)
O4	0.0196(6)	0.0414(6)	0.0223(5)	-0.0017(4)	-0.0029(4)	0.0049(5)
O5	0.0740(10)	0.0160(5)	0.0273(6)	-0.0078(4)	0.0102(6)	-0.0016(5)
O6	0.0488(8)	0.0164(5)	0.0257(6)	0.0072(4)	0.0104(5)	0.0022(5)
O7	0.0321(7)	0.0741(9)	0.0265(6)	-0.0038(6)	0.0156(5)	-0.0284(7)
O8	0.0292(6)	0.0503(7)	0.0251(6)	-0.0077(5)	0.0061(5)	-0.0244(5)
O9	0.0280(6)	0.0247(5)	0.0161(5)	-0.0050(4)	0.0031(4)	-0.0053(4)
O10	0.0294(6)	0.0300(6)	0.0227(5)	-0.0076(4)	0.0151(5)	0.0009(5)
O11	0.0152(5)	0.0385(6)	0.0326(6)	0.0022(5)	0.0075(4)	-0.0020(5)
O12	0.0286(6)	0.0217(5)	0.0334(6)	-0.0002(4)	0.0137(5)	-0.0093(4)

Table 10. Atomic coordinates and equivalent isotropic thermal parameters (\AA^2) for hexanitrohexaazaisowurtzitane at 125 K. $U(\text{eq})$ is defined as one third of the orthogonalized U_{ij} tensor.

	x	y	z	Uiso
C1	0.10723(11)	0.5100(2)	0.32375(9)	0.0122(3)
C2	0.93600(11)	0.59774(15)	0.32773(9)	0.0112(2)
C3	0.00946(10)	0.75220(15)	0.33057(9)	0.0117(3)
C4	0.08424(11)	0.4972(2)	0.21147(9)	0.0120(3)
C5	0.90033(11)	0.57707(15)	0.15372(9)	0.0111(2)
C6	0.97103(11)	0.73394(15)	0.15670(9)	0.0117(3)
N1	0.01152(9)	0.45921(13)	0.34656(7)	0.0126(2)
N2	0.02591(10)	0.36501(13)	0.42895(8)	0.0156(2)
N3	0.11916(9)	0.68380(13)	0.34909(7)	0.0124(2)
N4	0.19660(9)	0.72615(15)	0.43828(8)	0.0166(2)
N5	0.97437(9)	0.83064(12)	0.23901(7)	0.0124(2)
N6	0.97201(11)	0.00113(14)	0.23257(8)	0.0195(3)
N7	0.85764(9)	0.58521(13)	0.23276(7)	0.0127(2)
N8	0.77054(10)	0.4769(2)	0.22687(9)	0.0209(3)
N9	0.97538(9)	0.43574(13)	0.16438(7)	0.0118(2)
N10	0.96366(10)	0.35859(13)	0.07375(8)	0.0148(2)
N11	0.07534(9)	0.65678(13)	0.16468(7)	0.0123(2)
N12	0.16608(10)	0.75133(14)	0.17886(8)	0.0165(2)
O1	0.11238(9)	0.29743(13)	0.46372(7)	0.0235(2)
O2	0.94688(9)	0.35380(12)	0.45643(7)	0.0206(2)
O3	0.18994(9)	0.86482(13)	0.46546(7)	0.0247(3)
O4	0.26516(9)	0.62485(14)	0.47583(7)	0.0253(2)
O5	0.99041(12)	0.07510(13)	0.30781(8)	0.0340(3)
O6	0.94777(10)	0.05858(12)	0.15283(7)	0.0257(3)
O7	0.74931(10)	0.4578(2)	0.30057(8)	0.0358(3)
O8	0.72323(10)	0.41870(15)	0.14904(8)	0.0297(3)
O9	0.87168(9)	0.34188(12)	0.02104(7)	0.0201(2)
O10	0.04594(9)	0.31067(13)	0.05990(7)	0.0216(2)
O11	0.25351(8)	0.68168(13)	0.20913(8)	0.0240(2)
O12	0.15119(9)	0.89602(12)	0.15792(7)	0.0224(2)
H1	0.1709(14)	0.4496(19)	0.3561(11)	0.015(4)
H2	0.8995(13)	0.6034(18)	0.3717(11)	0.011(4)
H3	0.0107(13)	0.8270(18)	0.3803(11)	0.011(4)
H4	0.1384(13)	0.4307(18)	0.1989(10)	0.010(4)
H5	0.8461(14)	0.5688(18)	0.0970(11)	0.011(4)
H6	0.9436(13)	0.7967(18)	0.1019(11)	0.010(4)

Table 11. Anisotropic displacement parameters (\AA^2) for hexanitrohexaazaisowurtzitane at 125 K. The anisotropic displacement factor exponent takes the form:

$$-2\pi^2[(ha^*)^2U_{11} + \dots + 2hka^*b^*U_{12}]$$

	U11	U22	U33	U23	U13	U12
C1	0.0126(6)	0.0127(6)	0.0117(6)	0.0005(4)	0.0047(5)	0.0013(5)
C2	0.0108(6)	0.0122(6)	0.0112(6)	-0.0004(4)	0.0045(5)	0.0001(5)
C3	0.0119(6)	0.0116(6)	0.0117(6)	-0.0010(4)	0.0040(5)	-0.0006(5)
C4	0.0128(6)	0.0130(6)	0.0111(6)	0.0001(4)	0.0050(5)	0.0006(5)
C5	0.0110(6)	0.0113(6)	0.0106(6)	0.0001(4)	0.0027(5)	-0.0004(5)
C6	0.0130(6)	0.0114(6)	0.0108(6)	0.0003(4)	0.0040(5)	-0.0004(5)
N1	0.0146(6)	0.0133(5)	0.0108(5)	0.0028(4)	0.0055(4)	0.0020(4)
N2	0.0233(6)	0.0122(5)	0.0111(5)	-0.0006(4)	0.0053(5)	-0.0016(5)
N3	0.0098(5)	0.0151(5)	0.0105(5)	-0.0017(4)	0.0007(4)	-0.0010(4)
N4	0.0124(6)	0.0238(6)	0.0127(5)	-0.0024(4)	0.0026(4)	-0.0045(5)
N5	0.0169(6)	0.0070(5)	0.0131(5)	0.0003(4)	0.0044(4)	-0.0001(4)
N6	0.0267(7)	0.0096(5)	0.0216(6)	-0.0002(4)	0.0070(5)	0.0000(5)
N7	0.0090(5)	0.0161(5)	0.0133(5)	-0.0008(4)	0.0040(4)	-0.0030(4)
N8	0.0143(6)	0.0294(7)	0.0192(6)	-0.0006(5)	0.0058(5)	-0.0084(5)
N9	0.0140(6)	0.0121(5)	0.0095(5)	-0.0021(4)	0.0042(4)	0.0005(4)
N10	0.0225(6)	0.0116(5)	0.0114(5)	-0.0007(4)	0.0070(5)	-0.0022(4)
N11	0.0112(5)	0.0137(5)	0.0127(5)	0.0011(4)	0.0047(4)	-0.0022(4)
N12	0.0153(6)	0.0216(6)	0.0142(5)	-0.0016(4)	0.0068(5)	-0.0060(5)
O1	0.0282(6)	0.0229(5)	0.0173(5)	0.0062(4)	0.0042(4)	0.0067(5)
O2	0.0279(6)	0.0197(5)	0.0182(5)	0.0006(4)	0.0131(4)	-0.0059(4)
O3	0.0245(6)	0.0232(5)	0.0222(5)	-0.0088(4)	0.0018(4)	-0.0068(4)
O4	0.0162(5)	0.0344(6)	0.0195(5)	-0.0014(4)	-0.0025(4)	0.0048(5)
O5	0.0619(9)	0.0137(5)	0.0226(6)	-0.0065(4)	0.0081(6)	-0.0005(5)
O6	0.0404(7)	0.0142(5)	0.0216(5)	0.0061(4)	0.0083(5)	0.0020(5)
O7	0.0262(6)	0.0624(8)	0.0224(6)	-0.0025(5)	0.0130(5)	-0.0235(6)
O8	0.0246(6)	0.0419(7)	0.0212(6)	-0.0068(5)	0.0052(5)	-0.0204(5)
O9	0.0232(6)	0.0207(5)	0.0137(5)	-0.0043(4)	0.0024(4)	-0.0046(4)
O10	0.0245(6)	0.0244(5)	0.0202(5)	-0.0066(4)	0.0131(4)	0.0007(4)
O11	0.0120(5)	0.0324(6)	0.0277(6)	0.0021(4)	0.0063(4)	-0.0011(4)
O12	0.0237(6)	0.0177(5)	0.0282(6)	-0.0003(4)	0.0116(5)	-0.0078(4)

Table 12. Atomic coordinates and equivalent isotropic thermal parameters (\AA^2) for hexanitrohexaazaisowurtzitane at 100 K. $U(\text{eq})$ is defined as one third of the orthogonalized U_{ij} tensor.

	x	y	z	Uiso
C1	0.10727(11)	0.50974(14)	0.32381(8)	0.0105(2)
C2	0.93592(10)	0.59834(14)	0.32778(8)	0.0100(2)
C3	0.00962(10)	0.75247(14)	0.33073(8)	0.0099(2)
C4	0.08423(11)	0.49692(14)	0.21143(8)	0.0104(2)
C5	0.90035(11)	0.57728(14)	0.15385(9)	0.0100(2)
C6	0.97135(10)	0.73394(14)	0.15666(8)	0.0100(2)
N1	0.01135(9)	0.45952(12)	0.34664(7)	0.0111(2)
N2	0.02541(10)	0.36499(13)	0.42906(7)	0.0133(2)
N3	0.11940(9)	0.68354(12)	0.34915(7)	0.0105(2)
N4	0.19704(9)	0.72571(13)	0.43841(7)	0.0138(2)
N5	0.97493(9)	0.83092(12)	0.23918(7)	0.0107(2)
N6	0.97257(10)	0.00135(13)	0.23254(8)	0.0165(2)
N7	0.85735(9)	0.58604(12)	0.23289(7)	0.0110(2)
N8	0.77013(9)	0.47805(14)	0.22725(8)	0.0171(2)
N9	0.97526(9)	0.43563(12)	0.16447(7)	0.0102(2)
N10	0.96331(9)	0.35854(12)	0.07362(7)	0.0125(2)
N11	0.07558(9)	0.65640(12)	0.16451(7)	0.0105(2)
N12	0.16654(9)	0.75069(13)	0.17876(7)	0.0138(2)
O1	0.11202(9)	0.29716(12)	0.46395(7)	0.0198(2)
O2	0.94622(8)	0.35409(11)	0.45655(6)	0.0171(2)
O3	0.19055(9)	0.86472(12)	0.46543(7)	0.0206(2)
O4	0.26541(8)	0.62406(12)	0.47593(7)	0.0212(2)
O5	0.99071(11)	0.07556(12)	0.30786(7)	0.0282(3)
O6	0.94865(9)	0.05874(11)	0.15268(7)	0.0215(2)
O7	0.74863(9)	0.45946(15)	0.30095(7)	0.0294(3)
O8	0.72269(9)	0.41955(13)	0.14925(7)	0.0247(2)
O9	0.87133(8)	0.34172(11)	0.02114(6)	0.0168(2)
O10	0.04581(8)	0.31104(12)	0.05955(6)	0.0182(2)
O11	0.25407(8)	0.68108(12)	0.20910(7)	0.0202(2)
O12	0.15173(8)	0.89558(11)	0.15797(7)	0.0188(2)
H1	0.1707(13)	0.4509(18)	0.3561(10)	0.012(4)
H2	0.9008(13)	0.6025(17)	0.3731(11)	0.012(4)
H3	0.0112(12)	0.8277(18)	0.3802(11)	0.012(4)
H4	0.1377(13)	0.4298(18)	0.1997(10)	0.011(4)
H5	0.8460(13)	0.5697(17)	0.0968(10)	0.008(3)
H6	0.9426(12)	0.7980(17)	0.1008(10)	0.007(3)

Table 13. Anisotropic displacement parameters (\AA^2) for hexanitrohexaazaisowurtzitane at 100 K. The anisotropic displacement factor exponent takes the form:

$$-2\pi^2[(ha^*)^2U_{11} + \dots + 2hka^*b^*U_{12}]$$

	U11	U22	U33	U23	U13	U12
C1	0.0101(6)	0.0116(6)	0.0106(6)	0.0004(4)	0.0042(5)	0.0009(5)
C2	0.0096(6)	0.0113(6)	0.0097(6)	0.0003(4)	0.0041(5)	0.0004(4)
C3	0.0098(6)	0.0096(5)	0.0105(6)	-0.0005(4)	0.0036(5)	-0.0004(4)
C4	0.0112(6)	0.0114(6)	0.0097(6)	0.0005(4)	0.0046(5)	0.0008(5)
C5	0.0096(6)	0.0112(5)	0.0090(6)	0.0004(4)	0.0027(5)	0.0000(4)
C6	0.0107(6)	0.0098(5)	0.0094(5)	-0.0003(4)	0.0030(5)	-0.0006(4)
N1	0.0124(6)	0.0121(5)	0.0100(5)	0.0025(4)	0.0051(4)	0.0014(4)
N2	0.0198(6)	0.0112(5)	0.0091(5)	-0.0009(4)	0.0048(4)	-0.0014(4)
N3	0.0085(5)	0.0126(5)	0.0087(5)	-0.0015(3)	0.0006(4)	-0.0012(4)
N4	0.0100(5)	0.0198(5)	0.0111(5)	-0.0018(4)	0.0025(4)	-0.0039(4)
N5	0.0152(6)	0.0062(5)	0.0108(5)	0.0006(3)	0.0041(4)	0.0007(4)
N6	0.0218(6)	0.0093(5)	0.0182(6)	-0.0004(4)	0.0061(5)	0.0000(4)
N7	0.0081(5)	0.0142(5)	0.0110(5)	-0.0009(4)	0.0037(4)	-0.0028(4)
N8	0.0113(6)	0.0241(6)	0.0162(5)	-0.0004(4)	0.0047(4)	-0.0061(5)
N9	0.0122(6)	0.0104(5)	0.0085(5)	-0.0019(3)	0.0039(4)	-0.0001(4)
N10	0.0187(6)	0.0101(5)	0.0097(5)	-0.0007(4)	0.0060(4)	-0.0020(4)
N11	0.0087(5)	0.0118(5)	0.0115(5)	0.0009(4)	0.0040(4)	-0.0012(4)
N12	0.0122(6)	0.0188(5)	0.0115(5)	-0.0018(4)	0.0054(4)	-0.0043(4)
O1	0.0227(6)	0.0203(5)	0.0146(5)	0.0049(4)	0.0035(4)	0.0058(4)
O2	0.0219(6)	0.0175(5)	0.0153(5)	0.0002(3)	0.0108(4)	-0.0047(4)
O3	0.0204(6)	0.0190(5)	0.0192(5)	-0.0068(4)	0.0020(4)	-0.0055(4)
O4	0.0135(5)	0.0284(5)	0.0170(5)	-0.0002(4)	-0.0017(4)	0.0040(4)
O5	0.0502(8)	0.0119(5)	0.0194(5)	-0.0054(3)	0.0069(5)	-0.0012(5)
O6	0.0333(6)	0.0126(5)	0.0182(5)	0.0055(3)	0.0075(4)	0.0018(4)
O7	0.0215(6)	0.0515(7)	0.0184(5)	-0.0021(5)	0.0108(4)	-0.0178(5)
O8	0.0207(6)	0.0345(6)	0.0173(5)	-0.0055(4)	0.0037(4)	-0.0161(5)
O9	0.0188(5)	0.0173(5)	0.0123(4)	-0.0032(3)	0.0021(4)	-0.0040(4)
O10	0.0202(6)	0.0209(5)	0.0169(5)	-0.0047(3)	0.0105(4)	0.0012(4)
O11	0.0099(5)	0.0273(5)	0.0234(5)	0.0020(4)	0.0054(4)	-0.0006(4)
O12	0.0206(6)	0.0141(5)	0.0236(5)	0.0000(3)	0.0096(4)	-0.0060(4)

Table 14. Atomic coordinates and equivalent isotropic thermal parameters (\AA^2) for hexanitrohexaazaisowurtzitane at 85 K. $U(\text{eq})$ is defined as one third of the orthogonalized U_{ij} tensor.

	x	y	z	Uiso
C1	0.10726(12)	0.5098(2)	0.32371(10)	0.0102(3)
C2	0.93605(12)	0.5991(2)	0.32818(10)	0.0095(3)
C3	0.00990(12)	0.7526(2)	0.33090(10)	0.0095(3)
C4	0.08423(12)	0.4965(2)	0.21161(10)	0.0101(3)
C5	0.90017(12)	0.5776(2)	0.15380(10)	0.0096(3)
C6	0.97145(12)	0.7340(2)	0.15668(10)	0.0095(3)
N1	0.01116(10)	0.45969(14)	0.34676(8)	0.0104(3)
N2	0.02507(11)	0.36522(15)	0.42905(8)	0.0124(3)
N3	0.11946(10)	0.68353(14)	0.34909(8)	0.0099(3)
N4	0.19740(10)	0.7255(2)	0.43859(9)	0.0130(3)
N5	0.97509(10)	0.83098(14)	0.23920(8)	0.0097(3)
N6	0.97291(11)	0.00153(15)	0.23257(9)	0.0148(3)
N7	0.85737(10)	0.58653(14)	0.23303(8)	0.0104(3)
N8	0.76991(11)	0.4786(2)	0.22744(9)	0.0157(3)
N9	0.97506(10)	0.43576(14)	0.16438(8)	0.0097(3)
N10	0.96318(11)	0.35854(14)	0.07351(8)	0.0117(3)
N11	0.07579(10)	0.65610(14)	0.16449(8)	0.0096(2)
N12	0.16697(11)	0.75056(15)	0.17878(8)	0.0129(3)
O1	0.11182(10)	0.29714(13)	0.46404(8)	0.0181(3)
O2	0.94598(9)	0.35416(13)	0.45670(7)	0.0157(2)
O3	0.19082(10)	0.86468(13)	0.46536(8)	0.0188(3)
O4	0.26562(9)	0.62365(14)	0.47607(8)	0.0191(3)
O5	0.99090(12)	0.07584(13)	0.30787(8)	0.0250(3)
O6	0.94916(10)	0.05890(13)	0.15257(7)	0.0193(3)
O7	0.74812(10)	0.4605(2)	0.30112(8)	0.0262(3)
O8	0.72251(10)	0.41999(15)	0.14946(8)	0.0224(3)
O9	0.87105(9)	0.34163(13)	0.02120(7)	0.0156(2)
O10	0.04561(9)	0.31122(13)	0.05925(7)	0.0166(2)
O11	0.25448(9)	0.68054(14)	0.20906(8)	0.0183(3)
O12	0.15208(10)	0.89530(13)	0.15801(8)	0.0174(3)
H1	0.1718(16)	0.4495(22)	0.3568(12)	0.017(4)
H2	0.9018(15)	0.6060(19)	0.3716(12)	0.008(4)
H3	0.0096(15)	0.8282(21)	0.3801(12)	0.013(4)
H4	0.1369(15)	0.4264(20)	0.1989(11)	0.008(4)
H5	0.8455(14)	0.5695(18)	0.0972(11)	0.004(4)
H6	0.9428(15)	0.7970(20)	0.1009(12)	0.010(4)

Table 15. Anisotropic displacement parameters (\AA^2) for hexanitrohexaazaisowurtzitane at 85 K. The anisotropic displacement factor exponent takes the form:

$$-2\pi^2[(ha^*)^2U_{11} + \dots + 2hka^*b^*U_{12}]$$

	U11	U22	U33	U23	U13	U12
C1	0.0107(7)	0.0104(7)	0.0098(7)	0.0002(5)	0.0038(6)	0.0003(5)
C2	0.0101(7)	0.0094(7)	0.0094(7)	-0.0002(4)	0.0038(6)	0.0004(5)
C3	0.0102(7)	0.0086(6)	0.0096(7)	0.0000(5)	0.0029(5)	0.0001(5)
C4	0.0115(7)	0.0097(7)	0.0095(7)	0.0007(5)	0.0042(6)	0.0000(5)
C5	0.0105(7)	0.0085(6)	0.0089(7)	0.0002(4)	0.0018(6)	0.0006(5)
C6	0.0111(7)	0.0080(6)	0.0092(6)	-0.0011(5)	0.0031(5)	-0.0001(5)
N1	0.0134(6)	0.0095(6)	0.0091(6)	0.0025(4)	0.0047(5)	0.0012(5)
N2	0.0191(7)	0.0091(6)	0.0090(6)	-0.0003(4)	0.0043(5)	-0.0008(5)
N3	0.0092(6)	0.0103(6)	0.0088(6)	-0.0020(4)	0.0009(5)	-0.0012(5)
N4	0.0106(6)	0.0171(6)	0.0109(6)	-0.0008(4)	0.0029(5)	-0.0036(5)
N5	0.0150(6)	0.0040(6)	0.0097(6)	0.0000(4)	0.0034(5)	0.0001(4)
N6	0.0194(7)	0.0083(6)	0.0161(6)	-0.0009(4)	0.0046(5)	-0.0003(5)
N7	0.0083(6)	0.0121(6)	0.0111(6)	-0.0006(4)	0.0034(5)	-0.0025(4)
N8	0.0118(6)	0.0196(7)	0.0157(6)	-0.0005(5)	0.0043(5)	-0.0055(5)
N9	0.0125(6)	0.0086(6)	0.0082(5)	-0.0015(4)	0.0034(5)	0.0009(5)
N10	0.0194(7)	0.0075(6)	0.0090(6)	-0.0007(4)	0.0054(5)	-0.0020(5)
N11	0.0091(6)	0.0093(6)	0.0107(6)	0.0010(4)	0.0033(5)	-0.0014(4)
N12	0.0134(6)	0.0158(6)	0.0103(6)	-0.0014(4)	0.0048(5)	-0.0042(5)
O1	0.0220(6)	0.0162(5)	0.0141(5)	0.0043(4)	0.0029(5)	0.0049(5)
O2	0.0211(6)	0.0142(5)	0.0146(5)	-0.0001(4)	0.0099(5)	-0.0040(4)
O3	0.0203(6)	0.0152(6)	0.0181(6)	-0.0055(4)	0.0022(5)	-0.0041(4)
O4	0.0139(6)	0.0235(6)	0.0160(5)	0.0007(4)	-0.0006(5)	0.0043(5)
O5	0.0454(8)	0.0097(5)	0.0171(6)	-0.0051(4)	0.0060(6)	-0.0012(5)
O6	0.0300(7)	0.0106(5)	0.0162(5)	0.0047(4)	0.0059(5)	0.0010(5)
O7	0.0205(6)	0.0443(8)	0.0168(6)	-0.0023(5)	0.0101(5)	-0.0159(6)
O8	0.0197(6)	0.0296(7)	0.0164(6)	-0.0051(4)	0.0034(5)	-0.0136(5)
O9	0.0181(6)	0.0149(5)	0.0115(5)	-0.0028(4)	0.0014(4)	-0.0035(4)
O10	0.0186(6)	0.0182(6)	0.0158(5)	-0.0042(4)	0.0096(5)	0.0009(4)
O11	0.0108(6)	0.0227(6)	0.0208(6)	0.0014(4)	0.0042(5)	-0.0004(5)
O12	0.0201(6)	0.0123(6)	0.0216(6)	-0.0002(4)	0.0091(5)	-0.0052(4)

Table 16. Bond lengths (Å) and angles (°) for hexanitrohexaazaisowurtzitane at various temperatures.

At 298 K:

N1-N2	1.405(2)	N1-C1	1.456(2)
N1-C2	1.462(2)	C1-N3	1.456(2)
C1-C4	1.592(2)	O1-N2	1.202(2)
O2-N2	1.217(2)	C2-N7	1.450(2)
C2-C3	1.573(2)	N3-N4	1.424(2)
N3-C3	1.474(2)	C3-N5	1.432(2)
O3-N4	1.208(2)	C4-N9	1.453(2)
C4-N11	1.457(2)	O4-N4	1.209(2)
N5-N6	1.390(2)	N5-C6	1.440(2)
C5-N7	1.442(2)	C5-N9	1.487(2)
C5-C6	1.569(2)	O5-N6	1.215(2)
C6-N11	1.464(2)	O6-N6	1.211(2)
N7-N8	1.417(2)	O7-N8	1.205(2)
O8-N8	1.207(2)	O9-N10	1.207(2)
N9-N10	1.443(2)	N10-O10	1.212(2)
N11-N12	1.379(2)	O11-N12	1.218(2)
N12-O12	1.208(2)		
N2-N1-C1	117.97(13)	N2-N1-C2	118.98(12)
C1-N1-C2	107.65(11)	N1-C1-N3	104.32(12)
N1-C1-C4	109.40(12)	N3-C1-C4	107.72(11)
N7-C2-N1	110.78(11)	N7-C2-C3	108.50(11)
N1-C2-C3	104.49(12)	O1-N2-O2	126.23(14)
O1-N2-N1	117.82(15)	O2-N2-N1	115.86(15)
N4-N3-C1	117.34(12)	N4-N3-C3	116.58(12)
C1-N3-C3	107.59(11)	N5-C3-N3	110.21(12)
N5-C3-C2	109.10(12)	N3-C3-C2	104.13(11)
N9-C4-N11	99.57(11)	N9-C4-C1	110.67(12)
N11-C4-C1	112.99(12)	O3-N4-O4	127.3(2)
O3-N4-N3	115.50(15)	O4-N4-N3	117.07(15)
N6-N5-C3	120.42(12)	N6-N5-C6	119.79(12)
C3-N5-C6	117.42(11)	N7-C5-N9	111.08(11)
N7-C5-C6	108.55(11)	N9-C5-C6	105.50(12)
N5-C6-N11	113.20(12)	N5-C6-C5	109.22(12)
N11-C6-C5	100.00(11)	O6-N6-O5	127.3(2)
O6-N6-N5	116.82(14)	O5-N6-N5	115.82(14)
N8-N7-C5	115.55(12)	N8-N7-C2	114.02(12)
C5-N7-C2	116.57(12)	O7-N8-O8	127.0(2)
O7-N8-N7	115.99(14)	O8-N8-N7	117.00(14)
N10-N9-C4	113.43(12)	N10-N9-C5	112.20(11)
C4-N9-C5	106.78(11)	O9-N10-O10	126.99(14)
O9-N10-N9	116.08(14)	O10-N10-N9	116.85(14)
N12-N11-C4	119.97(13)	N12-N11-C6	120.52(12)
C4-N11-C6	110.61(11)	O12-N12-O11	126.9(2)
O12-N12-N11	116.65(15)	O11-N12-N11	116.46(15)

At 250 K:

C1-N1	1.453(2)	C1-N3	1.461(2)
C1-C4	1.592(2)	C2-N7	1.448(2)
C2-N1	1.464(2)	C2-C3	1.573(2)
C3-N5	1.433(2)	C3-N3	1.473(2)
C4-N9	1.453(2)	C4-N11	1.460(2)
C5-N7	1.443(2)	C5-N9	1.486(2)
C5-C6	1.571(2)	C6-N5	1.438(2)
C6-N11	1.465(2)	N1-N2	1.403(2)
N2-O1	1.206(2)	N2-O2	1.220(2)
N3-N4	1.423(2)	N4-O3	1.207(2)
N4-O4	1.211(2)	N5-N6	1.392(2)
N6-O6	1.208(2)	N6-O5	1.214(2)
N7-N8	1.415(2)	N8-O8	1.208(2)
N8-O7	1.212(2)	N9-N10	1.443(2)
N10-O9	1.207(2)	N10-O10	1.210(2)
N11-N12	1.374(2)	N12-O12	1.213(2)
N12-O11	1.219(2)		

N1-C1-N3	104.16(11)	N1-C1-C4	109.36(12)
N3-C1-C4	107.61(11)	N7-C2-N1	110.66(11)
N7-C2-C3	108.61(11)	N1-C2-C3	104.38(12)
N5-C3-N3	110.12(11)	N5-C3-C2	109.00(11)
N3-C3-C2	104.25(11)	N9-C4-N11	99.54(11)
N9-C4-C1	110.59(11)	N11-C4-C1	113.00(11)
N7-C5-N9	111.02(11)	N7-C5-C6	108.34(11)
N9-C5-C6	105.50(12)	N5-C6-N11	113.20(12)
N5-C6-C5	109.31(11)	N11-C6-C5	100.00(11)
N2-N1-C1	118.04(12)	N2-N1-C2	118.87(12)
C1-N1-C2	107.89(11)	O1-N2-O2	126.28(14)
O1-N2-N1	117.70(14)	O2-N2-N1	115.95(14)
N4-N3-C1	117.20(12)	N4-N3-C3	116.46(12)
C1-N3-C3	107.64(11)	O3-N4-O4	127.28(15)
O3-N4-N3	115.42(14)	O4-N4-N3	117.16(14)
N6-N5-C3	120.38(11)	N6-N5-C6	119.78(11)
C3-N5-C6	117.50(11)	O6-N6-O5	127.18(15)
O6-N6-N5	116.81(13)	O5-N6-N5	115.92(13)
N8-N7-C5	115.34(11)	N8-N7-C2	114.12(12)
C5-N7-C2	116.68(12)	O8-N8-O7	126.73(15)
O8-N8-N7	117.31(13)	O7-N8-N7	115.90(14)
N10-N9-C4	113.20(12)	N10-N9-C5	112.02(11)
C4-N9-C5	106.95(11)	O9-N10-O10	126.90(13)
O9-N10-N9	115.91(13)	O10-N10-N9	117.10(14)
N12-N11-C4	119.86(12)	N12-N11-C6	120.48(12)
C4-N11-C6	110.55(11)	O12-N12-O11	126.61(15)
O12-N12-N11	116.65(14)	O11-N12-N11	116.71(14)

At 200 K:

C1-N1	1.455(2)	C1-N3	1.462(2)
C1-C4	1.591(2)	C2-N7	1.451(2)
C2-N1	1.465(2)	C2-C3	1.576(2)

C3-N5	1.434(2)	C3-N3	1.475(2)
C4-N9	1.455(2)	C4-N11	1.460(2)
C5-N7	1.446(2)	C5-N9	1.486(2)
C5-C6	1.570(2)	C6-N5	1.439(2)
C6-N11	1.467(2)	N1-N2	1.402(2)
N2-O1	1.209(2)	N2-O2	1.221(2)
N3-N4	1.422(2)	N4-O3	1.211(2)
N4-O4	1.213(2)	N5-N6	1.391(2)
N6-O6	1.210(2)	N6-O5	1.219(2)
N7-N8	1.416(2)	N8-O7	1.210(2)
N8-O8	1.212(2)	N9-N10	1.4431(15)
N10-O9	1.209(2)	N10-O10	1.214(2)
N11-N12	1.373(2)	N12-O12	1.218(2)
N12-O11	1.220(2)		

N1-C1-N3	104.23(10)	N1-C1-C4	109.35(11)
N3-C1-C4	107.45(10)	N7-C2-N1	110.77(10)
N7-C2-C3	108.56(10)	N1-C2-C3	104.30(11)
N5-C3-N3	110.02(11)	N5-C3-C2	108.98(11)
N3-C3-C2	104.31(10)	N9-C4-N11	99.49(10)
N9-C4-C1	110.60(11)	N11-C4-C1	113.18(10)
N7-C5-N9	111.22(10)	N7-C5-C6	108.35(10)
N9-C5-C6	105.58(11)	N5-C6-N11	113.11(11)
N5-C6-C5	109.39(11)	N11-C6-C5	99.99(10)
N2-N1-C1	118.05(11)	N2-N1-C2	118.90(11)
C1-N1-C2	107.98(10)	O1-N2-O2	126.26(12)
O1-N2-N1	117.77(12)	O2-N2-N1	115.89(13)
N4-N3-C1	117.22(11)	N4-N3-C3	116.23(11)
C1-N3-C3	107.60(10)	O3-N4-O4	127.24(13)
O3-N4-N3	115.46(12)	O4-N4-N3	117.16(12)
N6-N5-C3	120.41(11)	N6-N5-C6	119.86(10)
C3-N5-C6	117.47(10)	O6-N6-O5	127.21(13)
O6-N6-N5	116.74(12)	O5-N6-N5	115.99(12)
N8-N7-C5	115.51(11)	N8-N7-C2	113.88(11)
C5-N7-C2	116.43(11)	O7-N8-O8	126.89(14)
O7-N8-N7	115.99(12)	O8-N8-N7	117.05(12)
N10-N9-C4	113.14(11)	N10-N9-C5	111.97(10)
C4-N9-C5	106.87(10)	O9-N10-O10	126.99(12)
O9-N10-N9	115.77(12)	O10-N10-N9	117.15(12)
N12-N11-C4	119.66(11)	N12-N11-C6	120.44(11)
C4-N11-C6	110.52(10)	O12-N12-O11	126.54(13)
O12-N12-N11	116.48(13)	O11-N12-N11	116.94(12)

At 150 K:

C1-N1	1.455(2)	C1-N3	1.464(2)
C1-C4	1.591(2)	C2-N7	1.451(2)
C2-N1	1.468(2)	C2-C3	1.575(2)
C3-N5	1.432(2)	C3-N3	1.477(2)
C4-N9	1.458(2)	C4-N11	1.463(2)
C5-N7	1.447(2)	C5-N9	1.491(2)
C5-C6	1.571(2)	C6-N5	1.440(2)
C6-N11	1.469(2)	N1-N2	1.4021(14)

N2-O1	1.211(2)	N2-O2	1.226(2)
N3-N4	1.422(2)	N4-O3	1.213(2)
N4-O4	1.214(2)	N5-N6	1.3958(15)
N6-O6	1.211(2)	N6-O5	1.218(2)
N7-N8	1.419(2)	N8-O8	1.213(2)
N8-O7	1.214(2)	N9-N10	1.4411(14)
N10-O9	1.210(2)	N10-O10	1.217(2)
N11-N12	1.373(2)	N12-O12	1.220(2)
N12-O11	1.224(2)		

N1-C1-N3	104.28(10)	N1-C1-C4	109.34(10)
N3-C1-C4	107.42(9)	N7-C2-N1	110.62(10)
N7-C2-C3	108.61(10)	N1-C2-C3	104.38(10)
N5-C3-N3	110.06(10)	N5-C3-C2	108.95(10)
N3-C3-C2	104.31(10)	N9-C4-N11	99.46(10)
N9-C4-C1	110.51(10)	N11-C4-C1	113.19(10)
N7-C5-N9	111.06(10)	N7-C5-C6	108.32(10)
N9-C5-C6	105.60(10)	N5-C6-N11	113.02(10)
N5-C6-C5	109.34(10)	N11-C6-C5	100.03(9)
N2-N1-C1	117.94(11)	N2-N1-C2	119.04(10)
C1-N1-C2	107.96(10)	O1-N2-O2	126.45(11)
O1-N2-N1	117.81(11)	O2-N2-N1	115.66(11)
N4-N3-C1	117.18(10)	N4-N3-C3	116.16(10)
C1-N3-C3	107.60(10)	O3-N4-O4	127.29(12)
O3-N4-N3	115.34(11)	O4-N4-N3	117.22(11)
N6-N5-C3	120.35(10)	N6-N5-C6	119.82(10)
C3-N5-C6	117.62(10)	O6-N6-O5	127.41(12)
O6-N6-N5	116.56(11)	O5-N6-N5	115.97(11)
N8-N7-C5	115.36(10)	N8-N7-C2	114.06(10)
C5-N7-C2	116.50(10)	O8-N8-O7	127.07(13)
O8-N8-N7	117.19(11)	O7-N8-N7	115.67(11)
N10-N9-C4	113.05(10)	N10-N9-C5	111.77(10)
C4-N9-C5	106.84(10)	O9-N10-O10	126.91(11)
O9-N10-N9	115.75(11)	O10-N10-N9	117.25(11)
N12-N11-C4	119.73(11)	N12-N11-C6	120.14(10)
C4-N11-C6	110.57(10)	O12-N12-O11	126.62(12)
O12-N12-N11	116.59(12)	O11-N12-N11	116.76(11)

At 125 K.

C1-N1	1.455(2)	C1-N3	1.466(2)
C1-C4	1.591(2)	C2-N7	1.452(2)
C2-N1	1.469(2)	C2-C3	1.579(2)
C3-N5	1.433(2)	C3-N3	1.480(2)
C4-N9	1.458(2)	C4-N11	1.464(2)
C5-N7	1.447(2)	C5-N9	1.491(2)
C5-C6	1.573(2)	C6-N5	1.439(2)
C6-N11	1.471(2)	N1-N2	1.4013(15)
N2-O1	1.214(2)	N2-O2	1.227(2)
N3-N4	1.4235(15)	N4-O3	1.216(2)
N4-O4	1.216(2)	N5-N6	1.3977(15)
N6-O6	1.2123(15)	N6-O5	1.220(2)
N7-N8	1.422(2)	N8-O8	1.215(2)

N8-O7	1.216(2)	N9-N10	1.4431(14)
N10-O9	1.212(2)	N10-O10	1.221(2)
N11-N12	1.374(2)	N12-O12	1.223(2)
N12-O11	1.225(2)		
N1-C1-N3	104.31(10)	N1-C1-C4	109.41(10)
N3-C1-C4	107.43(10)	N7-C2-N1	110.58(10)
N7-C2-C3	108.47(10)	N1-C2-C3	104.30(10)
N5-C3-N3	110.02(10)	N5-C3-C2	108.96(10)
N3-C3-C2	104.26(10)	N9-C4-N11	99.44(10)
N9-C4-C1	110.51(10)	N11-C4-C1	113.13(10)
N7-C5-N9	111.12(10)	N7-C5-C6	108.29(10)
N9-C5-C6	105.64(10)	N5-C6-N11	113.00(10)
N5-C6-C5	109.33(10)	N11-C6-C5	99.92(9)
N2-N1-C1	118.13(10)	N2-N1-C2	118.95(10)
C1-N1-C2	108.05(10)	O1-N2-O2	126.36(11)
O1-N2-N1	117.79(11)	O2-N2-N1	115.77(11)
N4-N3-C1	117.30(10)	N4-N3-C3	116.00(10)
C1-N3-C3	107.57(10)	O3-N4-O4	127.25(12)
O3-N4-N3	115.35(11)	O4-N4-N3	117.25(11)
N6-N5-C3	120.29(10)	N6-N5-C6	119.80(10)
C3-N5-C6	117.71(10)	O6-N6-O5	127.36(12)
O6-N6-N5	116.50(11)	O5-N6-N5	116.07(11)
N8-N7-C5	115.38(10)	N8-N7-C2	113.96(10)
C5-N7-C2	116.64(10)	O8-N8-O7	127.17(12)
O8-N8-N7	117.19(11)	O7-N8-N7	115.58(11)
N10-N9-C4	113.05(10)	N10-N9-C5	111.72(9)
C4-N9-C5	106.90(10)	O9-N10-O10	126.91(11)
O9-N10-N9	115.76(11)	O10-N10-N9	117.24(11)
N12-N11-C4	119.70(11)	N12-N11-C6	120.13(10)
C4-N11-C6	110.62(10)	O12-N12-O11	126.62(12)
O12-N12-N11	116.52(11)	O11-N12-N11	116.84(11)

At 100 K:

C1-N1	1.454(2)	C1-N3	1.4652(15)
C1-C4	1.591(2)	C2-N7	1.451(2)
C2-N1	1.469(2)	C2-C3	1.577(2)
C3-N5	1.4318(15)	C3-N3	1.480(2)
C4-N9	1.457(2)	C4-N11	1.4638(15)
C5-N7	1.447(2)	C5-N9	1.491(2)
C5-C6	1.573(2)	C6-N5	1.4407(14)
C6-N11	1.470(2)	N1-N2	1.4024(14)
N2-O1	1.2153(15)	N2-O2	1.2264(15)
N3-N4	1.4239(14)	N4-O4	1.2154(15)
N4-O3	1.2164(14)	N5-N6	1.3968(14)
N6-O6	1.2126(14)	N6-O5	1.2208(14)
N7-N8	1.4210(15)	N8-O7	1.2151(14)
N8-O8	1.2170(15)	N9-N10	1.4434(13)
N10-O9	1.2101(15)	N10-O10	1.2217(15)
N11-N12	1.3732(15)	N12-O12	1.2236(14)
N12-O11	1.2251(15)		

N1-C1-N3	104.23(9)	N1-C1-C4	109.37(10)
N3-C1-C4	107.39(9)	N7-C2-N1	110.69(9)
N7-C2-C3	108.59(9)	N1-C2-C3	104.32(10)
N5-C3-N3	109.89(10)	N5-C3-C2	108.99(10)
N3-C3-C2	104.21(9)	N9-C4-N11	99.50(9)
N9-C4-C1	110.49(10)	N11-C4-C1	113.22(9)
N7-C5-N9	111.26(9)	N7-C5-C6	108.30(9)
N9-C5-C6	105.66(10)	N5-C6-N11	112.98(10)
N5-C6-C5	109.33(9)	N11-C6-C5	99.90(9)
N2-N1-C1	118.15(10)	N2-N1-C2	119.00(10)
C1-N1-C2	108.12(9)	O1-N2-O2	126.36(11)
O1-N2-N1	117.77(10)	O2-N2-N1	115.79(11)
N4-N3-C1	117.25(10)	N4-N3-C3	116.00(9)
C1-N3-C3	107.64(10)	O4-N4-O3	127.40(11)
O4-N4-N3	117.22(10)	O3-N4-N3	115.22(10)
N6-N5-C3	120.43(9)	N6-N5-C6	119.73(9)
C3-N5-C6	117.73(9)	O6-N6-O5	127.34(11)
O6-N6-N5	116.57(10)	O5-N6-N5	116.02(10)
N8-N7-C5	115.47(9)	N8-N7-C2	113.92(9)
C5-N7-C2	116.42(10)	O7-N8-O8	127.13(12)
O7-N8-N7	115.69(10)	O8-N8-N7	117.12(10)
N10-N9-C4	113.10(9)	N10-N9-C5	111.62(9)
C4-N9-C5	106.82(9)	O9-N10-O10	126.99(10)
O9-N10-N9	115.81(10)	O10-N10-N9	117.12(10)
N12-N11-C4	119.68(10)	N12-N11-C6	120.07(10)
C4-N11-C6	110.59(9)	O12-N12-O11	126.56(11)
O12-N12-N11	116.47(11)	O11-N12-N11	116.95(10)

At 85 K:

C1-N1	1.454(2)	C1-N3	1.463(2)
C1-C4	1.585(2)	C2-N7	1.452(2)
C2-N1	1.468(2)	C2-C3	1.573(2)
C3-N5	1.431(2)	C3-N3	1.476(2)
C4-N9	1.456(2)	C4-N11	1.464(2)
C5-N7	1.445(2)	C5-N9	1.490(2)
C5-C6	1.571(2)	C6-N5	1.438(2)
C6-N11	1.470(2)	N1-N2	1.399(2)
N2-O1	1.216(2)	N2-O2	1.224(2)
N3-N4	1.426(2)	N4-O4	1.214(2)
N4-O3	1.215(2)	N5-N6	1.396(2)
N6-O6	1.213(2)	N6-O5	1.220(2)
N7-N8	1.421(2)	N8-O7	1.214(2)
N8-O8	1.215(2)	N9-N10	1.442(2)
N10-O9	1.209(2)	N10-O10	1.219(2)
N11-N12	1.374(2)	N12-O12	1.221(2)
N12-O11	1.224(2)		
N1-C1-N3	104.19(11)	N1-C1-C4	109.36(12)
N3-C1-C4	107.56(11)	N7-C2-N1	110.38(11)
N7-C2-C3	108.57(11)	N1-C2-C3	104.41(11)
N5-C3-N3	109.88(11)	N5-C3-C2	108.96(11)
N3-C3-C2	104.26(11)	N9-C4-N11	99.35(11)

N9-C4-C1	110.72(11)	N11-C4-C1	113.16(11)
N7-C5-N9	111.21(11)	N7-C5-C6	108.20(11)
N9-C5-C6	105.60(11)	N5-C6-N11	112.99(11)
N5-C6-C5	109.36(11)	N11-C6-C5	99.93(10)
N2-N1-C1	118.24(12)	N2-N1-C2	118.97(11)
C1-N1-C2	107.97(11)	O1-N2-O2	126.17(12)
O1-N2-N1	117.81(12)	O2-N2-N1	115.95(12)
N4-N3-C1	117.18(11)	N4-N3-C3	115.96(11)
C1-N3-C3	107.73(11)	O4-N4-O3	127.62(13)
O4-N4-N3	117.25(12)	O3-N4-N3	114.96(12)
N6-N5-C3	120.36(11)	N6-N5-C6	119.74(11)
C3-N5-C6	117.77(11)	O6-N6-O5	127.34(13)
O6-N6-N5	116.53(11)	O5-N6-N5	116.06(11)
N8-N7-C5	115.37(11)	N8-N7-C2	113.93(11)
C5-N7-C2	116.61(12)	O7-N8-O8	127.11(13)
O7-N8-N7	115.70(12)	O8-N8-N7	117.12(12)
N10-N9-C4	113.13(11)	N10-N9-C5	111.67(10)
C4-N9-C5	106.92(11)	O9-N10-O10	127.03(12)
O9-N10-N9	115.66(12)	O10-N10-N9	117.23(12)
N12-N11-C4	119.75(12)	N12-N11-C6	119.97(11)
C4-N11-C6	110.53(11)	O12-N12-O11	126.77(13)
O12-N12-N11	116.42(12)	O11-N12-N11	116.80(12)

Contract No. N00014-95-1-0013 and N00014-97-1-0409

Program Officer: R. Miller/J. Goldwasser

**Title: Experimental Charge Densities and Electrostatic Potentials in Energetic
Materials and Infrastructure Upgrade for an X-ray Crystallography
Laboratory**

PI: A. Alan Pinkerton

Department of Chemistry, University of Toledo, Toledo, OH 43606

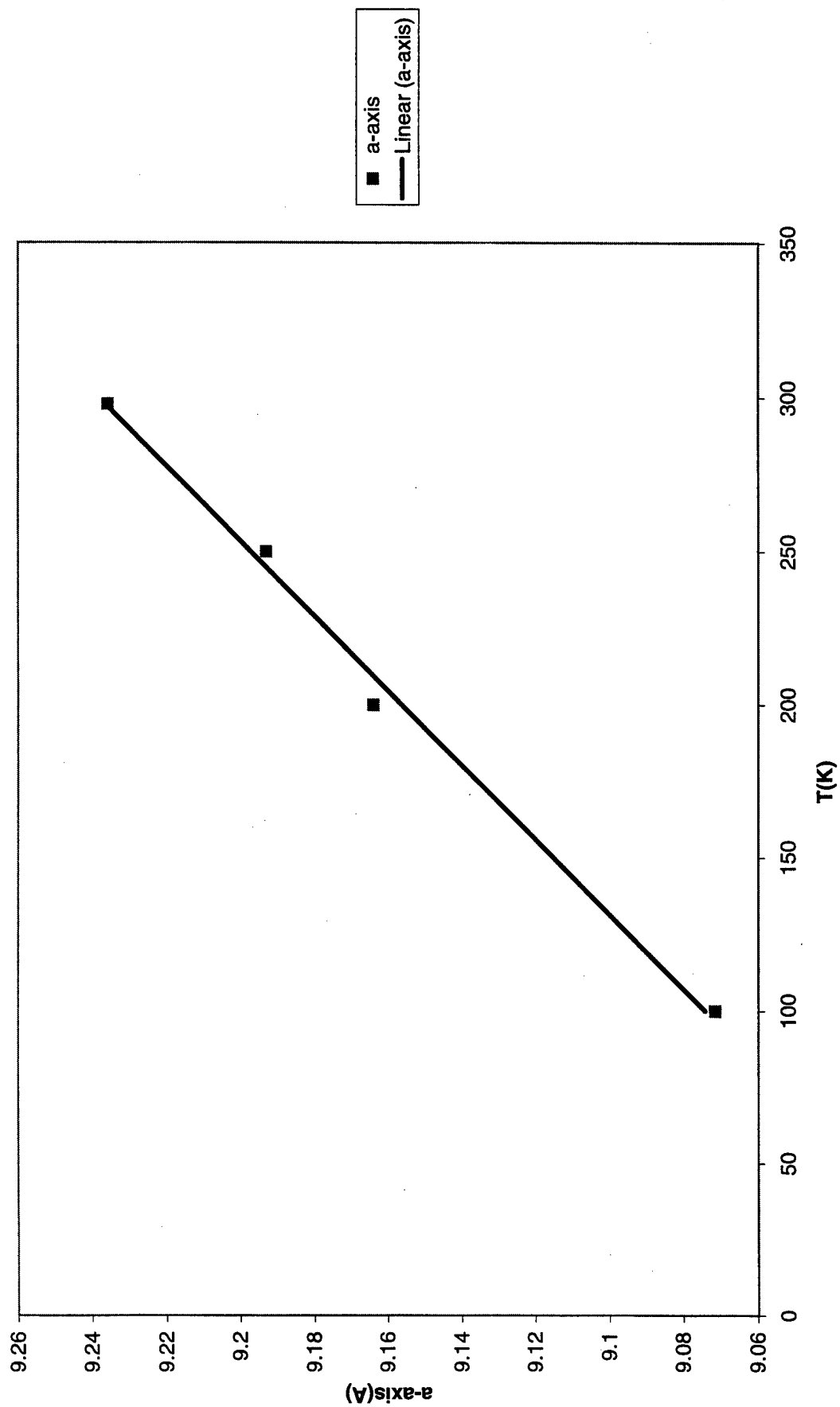
tel. (419) 530-4580, FAX (419) 530-4033, email apinker@uoft02.utoledo.edu

APPENDIX 3f

Variable temperature crystallographic study of AP

AP: a-axis

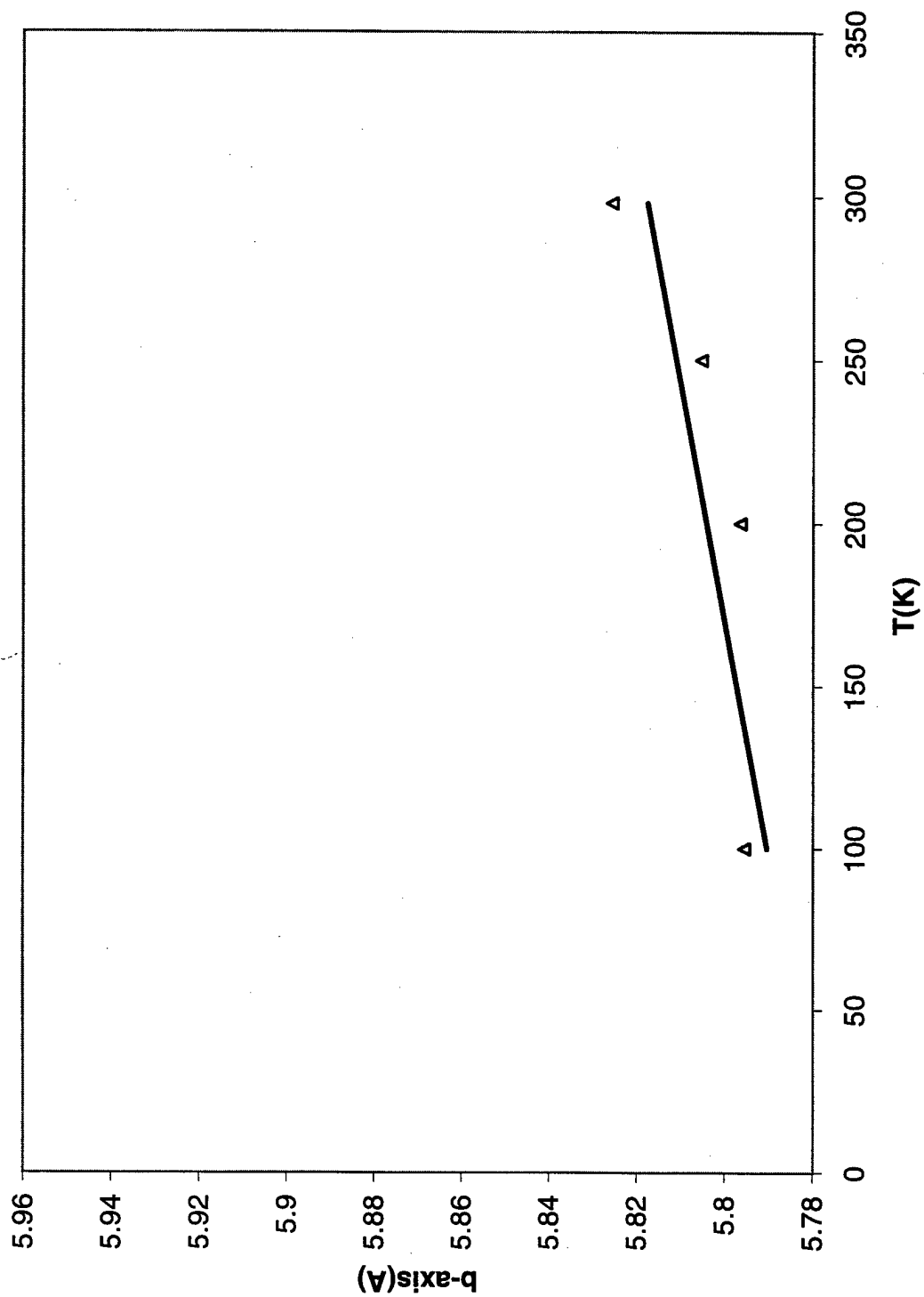
$$y = 0.0008x + 8.9923$$
$$R^2 = 0.9941$$



AP: b-axis

$$y = 0.0001x + 5.7766$$

$$R^2 = 0.6884$$

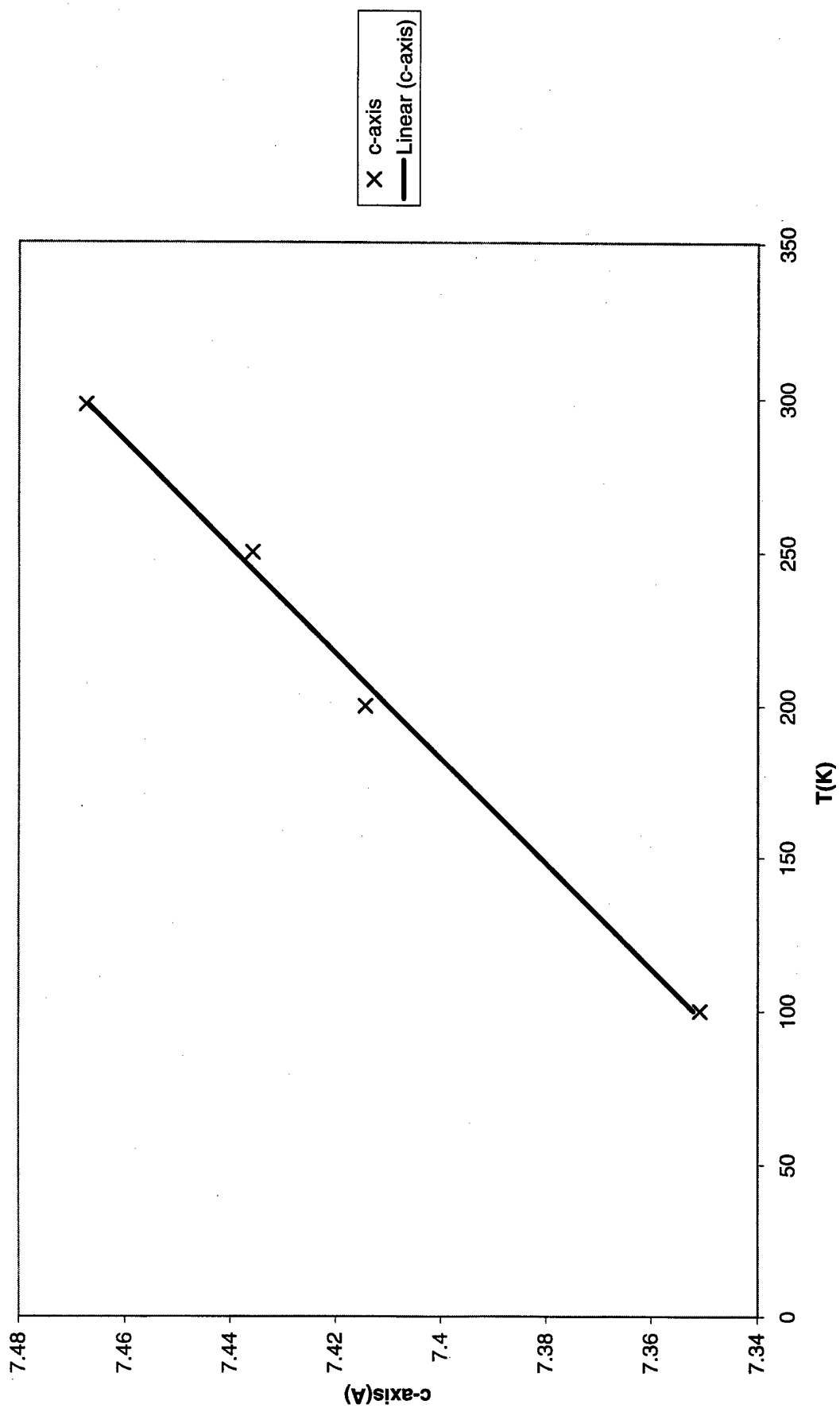


Δ b-axis

— Linear (b-axis)

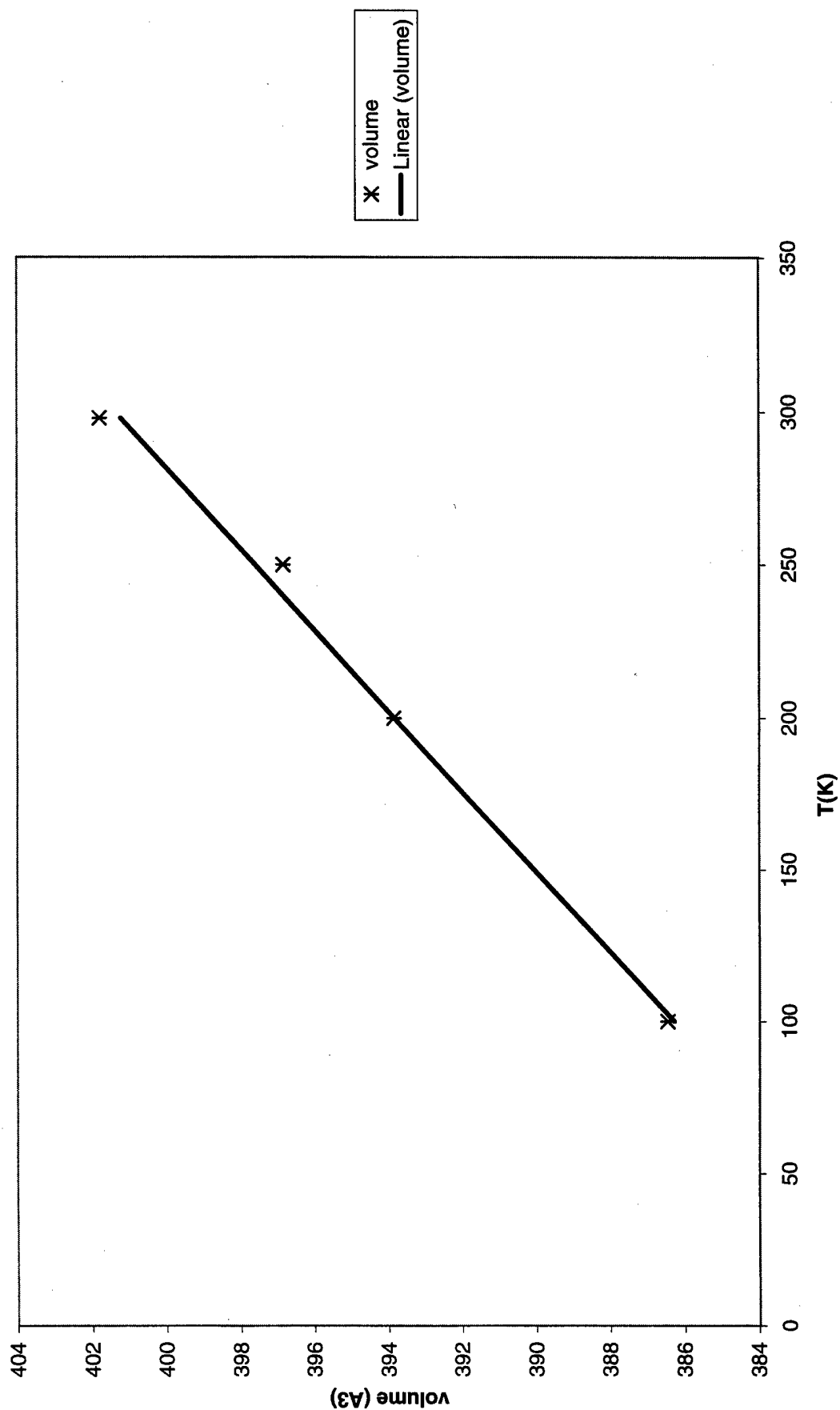
AP: c-axis

$$y = 0.0006x + 7.2941$$
$$R^2 = 0.9958$$



AP: Volume

$$y = 0.0754x + 378.74$$
$$R^2 = 0.9924$$



Contract No. N00014-95-1-0013 and N00014-97-1-0409

Program Officer: R. Miller/J. Goldwasser

**Title: Experimental Charge Densities and Electrostatic Potentials in Energetic
Materials and Infrastructure Upgrade for an X-ray Crystallography
Laboratory**

PI: A. Alan Pinkerton

Department of Chemistry, University of Toledo, Toledo, OH 43606

tel. (419) 530-4580, FAX (419) 530-4033, email apinker@uoft02.utoledo.edu

APPENDIX 3g

Variable temperature crystallographic study of RDX

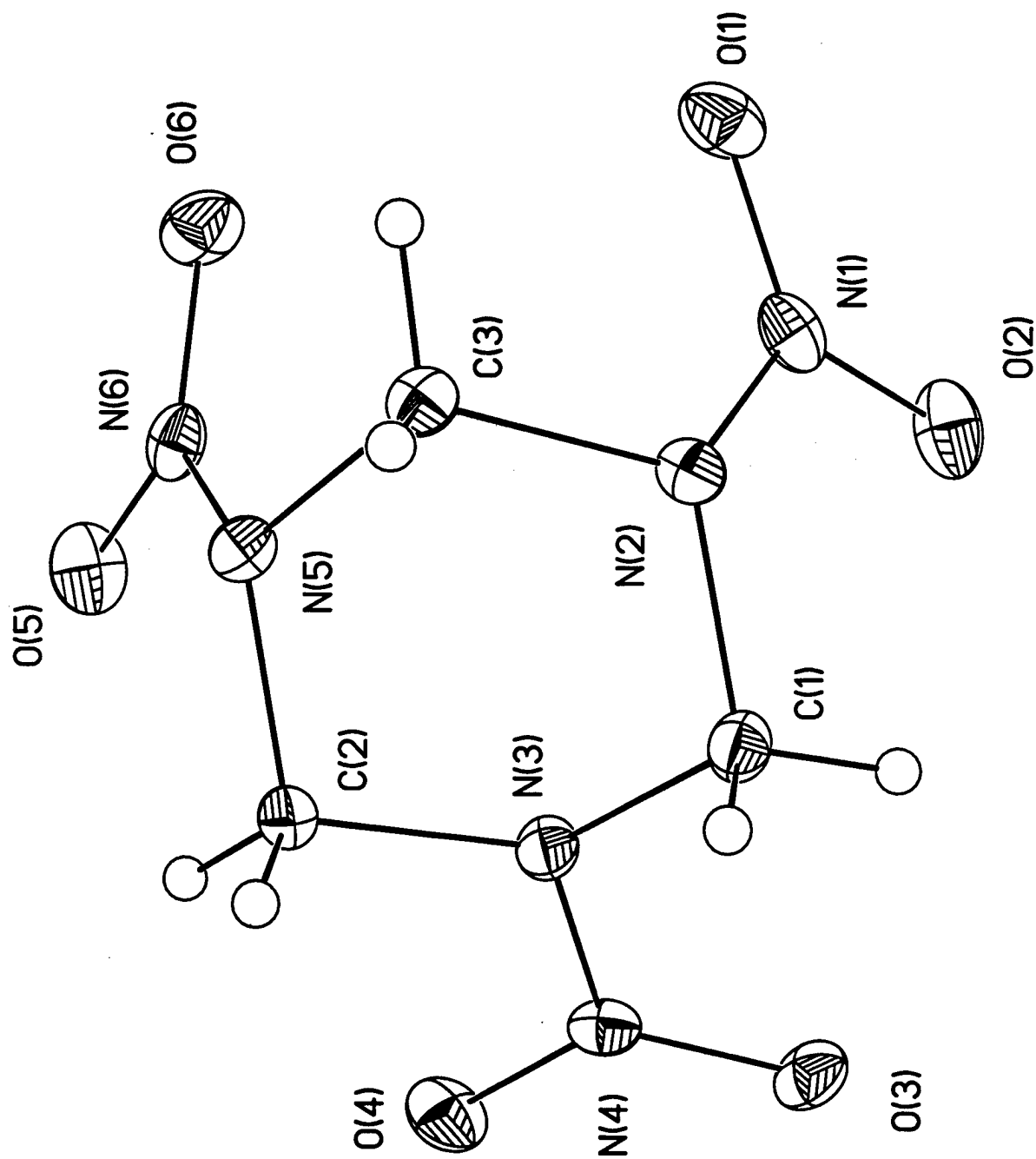


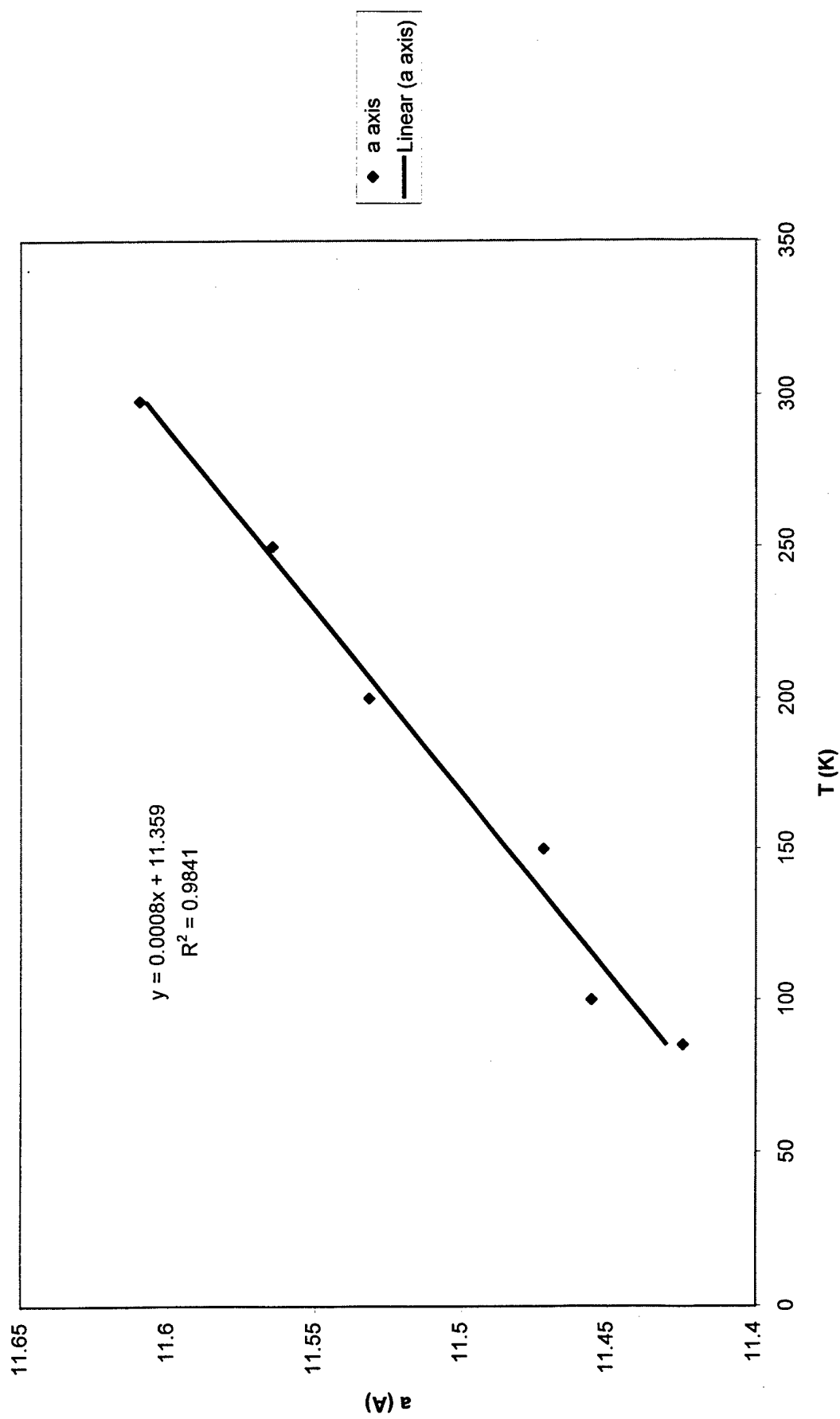
Table 1. Crystal data and structure refinement for RDX at various temperatures.

Empirical formula	$C_3H_6N_6O_6$				
Formula weight	222.14				
Wavelength	0.71073 Å				
Crystal system	Orthorhombic				
Space group	Pbca				
F(000)	912				
Crystal size	0.20 x 0.10 x 0.10 mm				
Z	8				
Instrument	Siemens SMART CCD				
Detector distance	4.9920 cm				
Scan width and axis	-0.3° in ω				
Refinement method	Full-matrix least-squares on F ²				
Temperature (K)	298(2)	250(2)	200(2)	150(2)	100(2)
a (Å)	11.6096(3)	11.56460(10)	11.5317(4)	11.47180(10)	11.4555(2)
b (Å)	10.7255(3)	10.6895(2)	10.6702(3)	10.6264(2)	10.6204(2)
c (Å)	13.20100(10)	13.1901(3)	13.1879(3)	13.1666(2)	13.1781(2)
α (°)	90.00	90.00	90.00	90.00	90.00
β (°)	90.00	90.00	90.00	90.00	90.00
γ (°)	90.00	90.00	90.00	90.00	90.00
Volume (Å ³)	1643.77(6)	1630.56(5)	1622.71(8)	1605.06(4)	1603.27(5)
Density (calc) (Mg/m ³)	1.795	1.810	1.819	1.839	1.853
Absorption coeff. (mm ⁻¹)	0.171	0.172	0.173	0.175	0.176
θ range	3.01–28.27	3.02–28.27	3.03–28.25	3.04–28.28	3.04–28.25
Limiting indices	-15–15 -14–10 -13–17	-15–15 -10–14 -17–13	-15–15 -14–10 -17–13	-15–15 -14–10 -17–13	-15–15 -14–10 -13–17
Reflections collected	10486	10358	10199	10110	10079
Independent reflections	2039	2018	2011	1989	1980
R _{int}	0.0452	0.0435	0.0444	0.0423	0.0410
Data / restraints / parameters	2039/1/160	2018/1/160	2011/1/160	1989/1/160	1980/1/160
Goodness-of-fit on F ²	1.021	1.041	1.008	1.037	1.065
R1[I>2 σ (I)]	0.0432	0.0399	0.0358	0.0336	0.0312
wR2 [I>2 σ (I)]	0.1086	0.1021	0.0908	0.0881	0.0789
R1(all data)	0.0657	0.0565	0.0510	0.0439	0.0312
wR2 (all data)	0.1218	0.1116	0.0992	0.0932	0.0838
Largest diff. peak (eÅ ⁻³)	0.187	0.201	0.224	0.229	0.247
Largest diff. hole (eÅ ⁻³)	-0.267	-0.262	-0.280	-0.273	-0.280
					85(2)
					11.42440(10)
					10.5940(2)
					13.1559(2)
					90.00
					90.00
					90.00
					1592.26(4)
					1.853
					0.176
					3.0–28.31
					-15–14
					-10–14
					-13–17
					1975
					0.0407
					1975/1/160
					1.072
					0.0308
					0.0800
					0.0390
					0.0838
					0.235
					-0.296

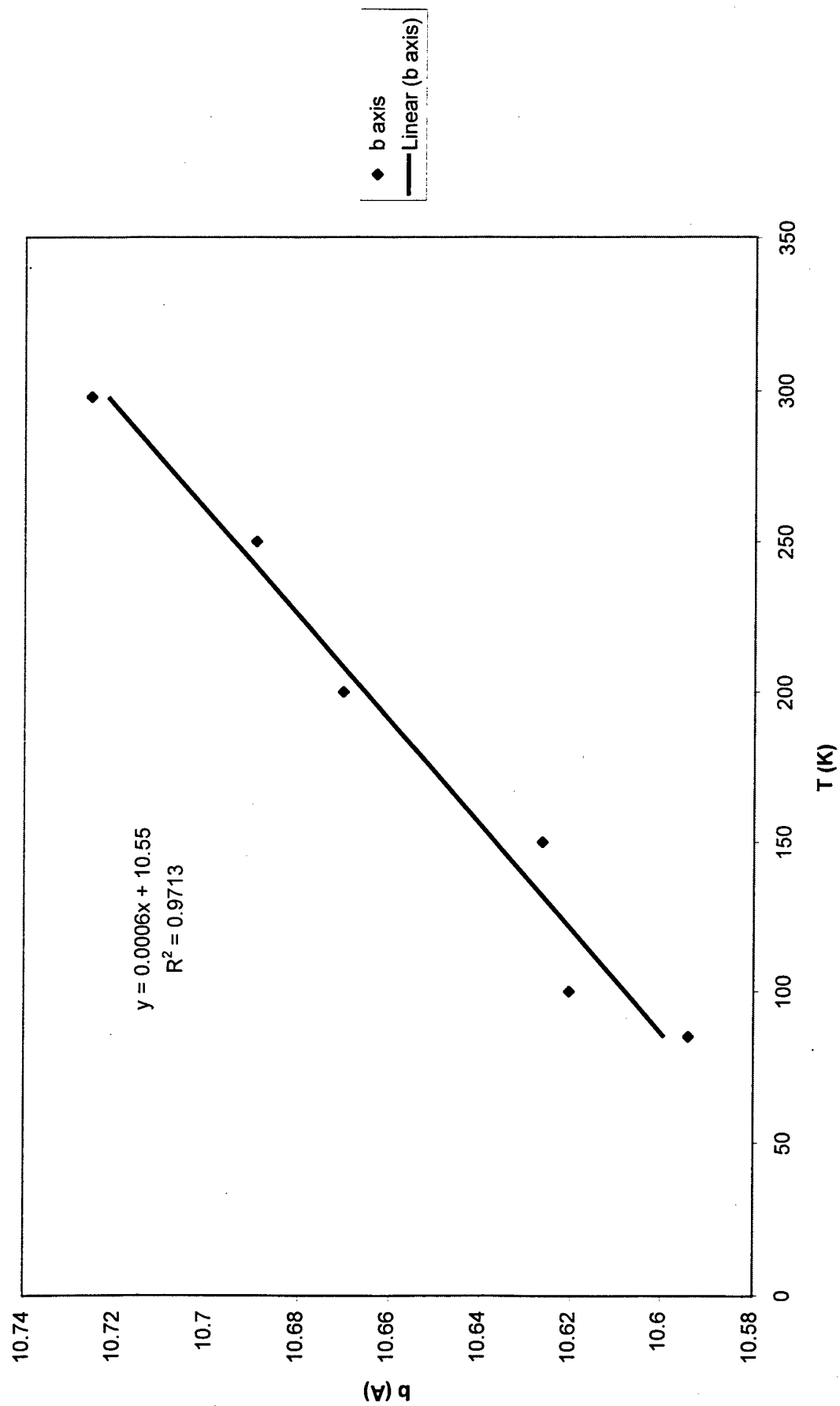
Table 15. Unit cell parameters for variable temperature structure determinations of RDX.

T (K)	<i>a</i> (Å)	<i>b</i> (Å)	<i>c</i> (Å)	volume (Å ³)
298	11.6096(3)	10.7255(3)	13.20100(10)	1643.77(6)
250	11.56460(10)	10.6895(2)	13.1901(3)	1630.56(5)
200	11.5317(4)	10.6702(3)	13.1879(3)	1622.71(8)
150	11.47180(10)	10.6264(2)	13.1666(2)	1605.06(4)
100	11.4555(2)	10.6204(2)	13.1781(2)	1603.27(5)
85	11.42440(10)	10.5940(2)	13.1559(2)	1592.26(4)

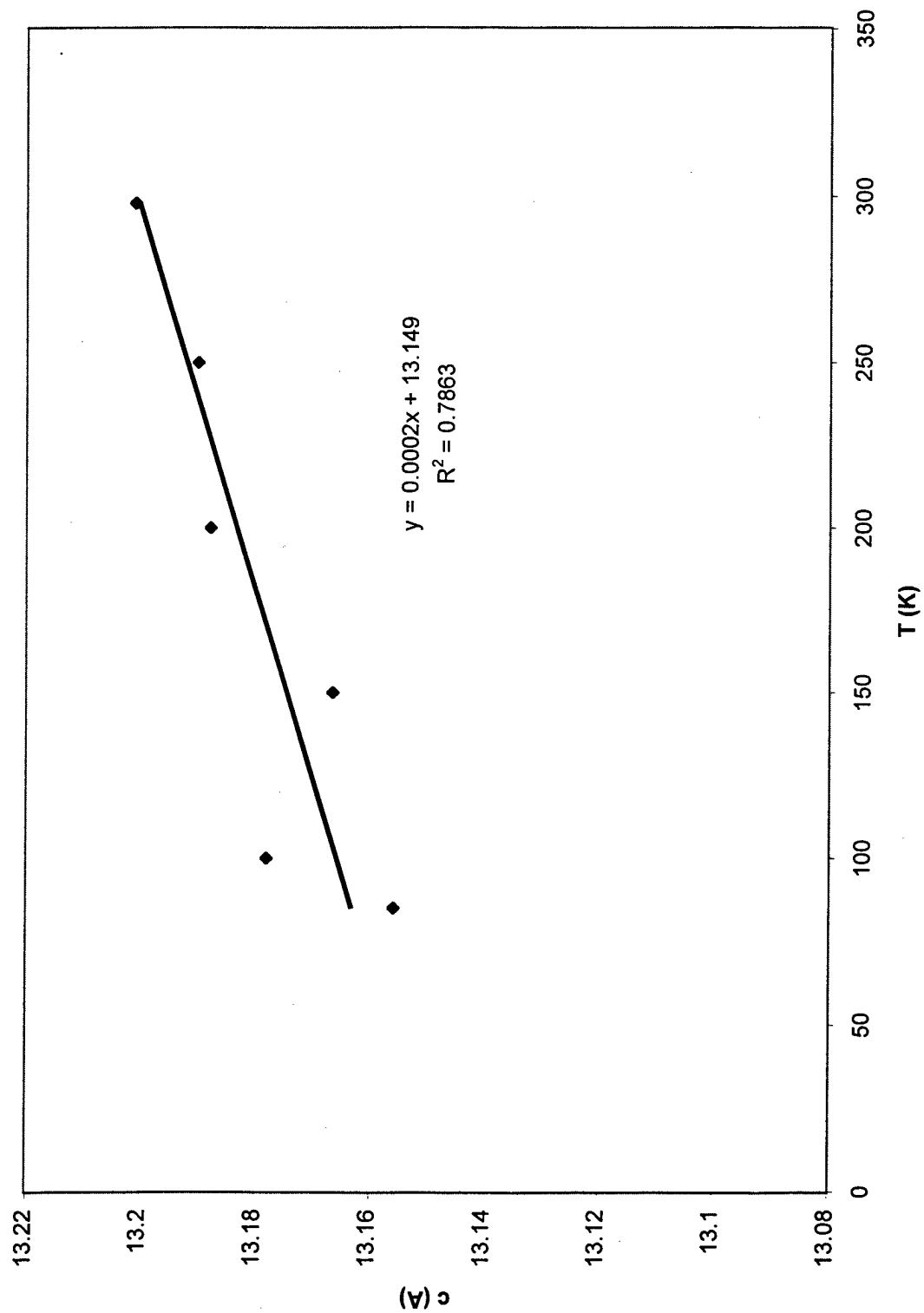
a vs T



b vs T



c vs T



c (Å)

T (K)

$$y = 0.0002x + 13.149$$
$$R^2 = 0.7863$$

◆ c axis
— Linear (c axis)

vol vs T

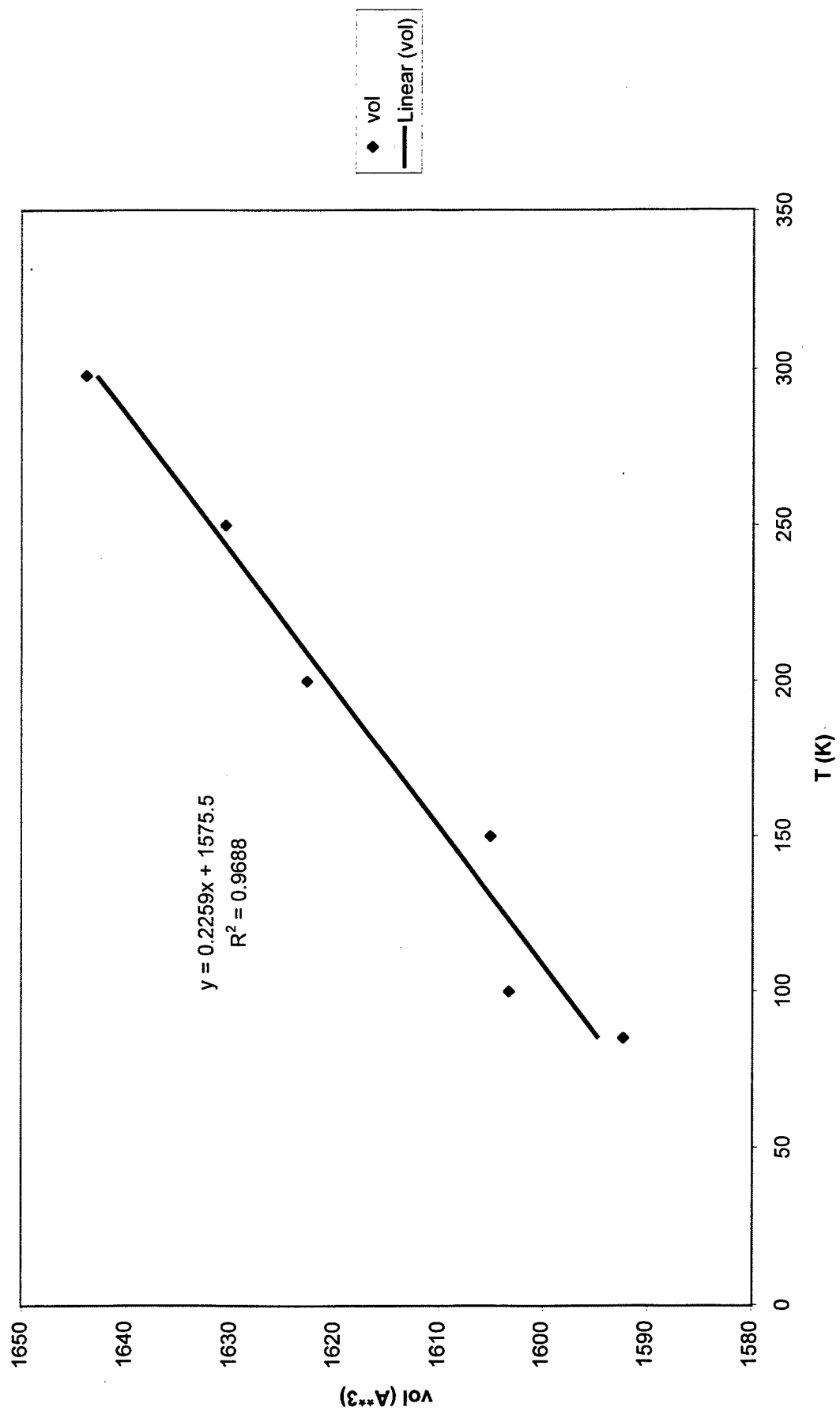


Table 2. Atomic coordinates and equivalent isotropic thermal parameters (\AA^2) for RDX at room temperature (298 K). $U(\text{eq})$ is defined as one third of the trace of the orthogonalized U_{ij} tensor.

	x	y	z	$U(\text{eq})/U(\text{iso})$
O6	0.64625(12)	0.25136(15)	0.61222(10)	0.0636(4)
O5	0.53038(13)	0.13855(14)	0.52362(12)	0.0680(4)
O4	0.40657(11)	0.23816(13)	0.27215(11)	0.0592(4)
O3	0.43157(10)	0.43316(13)	0.23596(9)	0.0516(4)
O2	0.57225(13)	0.59947(13)	0.45388(13)	0.0696(5)
O1	0.68522(15)	0.52596(15)	0.56929(12)	0.0699(5)
N6	0.61206(12)	0.20799(14)	0.53327(11)	0.0428(4)
N5	0.67782(10)	0.23222(13)	0.44621(10)	0.0338(3)
N4	0.46188(11)	0.33475(14)	0.27390(10)	0.0387(3)
N3	0.56404(11)	0.33319(12)	0.32411(10)	0.0380(3)
N2	0.70095(10)	0.45300(12)	0.41202(10)	0.0360(3)
N1	0.64689(13)	0.52975(14)	0.48393(13)	0.0474(4)
H3B	0.8156(16)	0.3212(17)	0.4037(15)	0.042(5)
H3A	0.7827(17)	0.3530(17)	0.5128(15)	0.044(5)
H2B	0.5635(16)	0.1519(18)	0.3553(14)	0.048(5)
H2A	0.6772(17)	0.1938(18)	0.3009(16)	0.047(5)
H1B	0.6985(16)	0.4208(17)	0.2626(15)	0.049(5)
H1A	0.6005(17)	0.5139(19)	0.3033(15)	0.049(5)
C3	0.75527(13)	0.3394(2)	0.44967(13)	0.0360(4)
C2	0.61855(15)	0.2152(2)	0.35058(13)	0.0371(4)
C1	0.64176(15)	0.4397(2)	0.31592(14)	0.0403(4)

Table 3. Anisotropic displacement parameters (\AA^2) for RDX at room temperature (298 K). The anisotropic displacement factor exponent takes the form: $-2\pi^2[(ha^*)^2U_{11} + \dots + 2hka^*b^*U_{12}]$

	U11	U22	U33	U23	U13	U12
O6	0.0772(9)	0.0837(11)	0.0299(7)	0.0047(7)	0.0078(6)	0.0056(8)
O5	0.0585(8)	0.0630(9)	0.0823(11)	0.0115(8)	0.0236(7)	-0.0138(7)
O4	0.0442(6)	0.0628(9)	0.0707(10)	-0.0121(7)	-0.0144(6)	-0.0099(6)
O3	0.0466(6)	0.0637(8)	0.0446(7)	0.0036(6)	-0.0110(5)	0.0191(6)
O2	0.0537(8)	0.0407(7)	0.1145(13)	-0.0041(8)	0.0280(8)	0.0087(7)
O1	0.0903(11)	0.0709(10)	0.0485(9)	-0.0234(7)	0.0180(8)	-0.0202(8)
N6	0.0423(7)	0.0462(8)	0.0398(9)	0.0102(6)	0.0113(6)	0.0113(6)
N5	0.0313(6)	0.0422(7)	0.0278(7)	0.0046(5)	0.0029(5)	0.0054(5)
N4	0.0326(6)	0.0531(9)	0.0303(7)	-0.0091(6)	-0.0045(5)	0.0039(6)
N3	0.0361(6)	0.0365(7)	0.0415(8)	0.0002(6)	-0.0143(6)	0.0010(5)
N2	0.0304(6)	0.0391(7)	0.0384(8)	-0.0075(5)	0.0011(5)	-0.0013(5)
N1	0.0425(7)	0.0379(8)	0.0619(11)	-0.0114(7)	0.0192(7)	-0.0128(7)
C3	0.0259(6)	0.0500(9)	0.0323(8)	-0.0002(7)	-0.0009(6)	0.0023(6)
C2	0.0437(8)	0.0325(8)	0.0349(9)	-0.0032(7)	-0.0052(7)	0.0042(7)
C1	0.0405(8)	0.0382(9)	0.0422(10)	0.0068(7)	-0.0069(7)	0.0003(7)

Table 4. Atomic coordinates and equivalent isotropic thermal parameters (\AA^2) for RDX at 250 K. $U(\text{eq})$ is defined as one third of the trace of the orthogonalized U_{ij} tensor.

	x	y	z	$U(\text{eq})/U(\text{iso})$
O6	0.64717(11)	0.25217(12)	0.61359(9)	0.0508(3)
O5	0.53187(11)	0.13741(12)	0.52466(10)	0.0542(4)
O4	0.40664(9)	0.23740(11)	0.27185(10)	0.0475(3)
O3	0.43178(9)	0.43345(11)	0.23502(8)	0.0411(3)
O2	0.57065(10)	0.60065(11)	0.45364(11)	0.0545(4)
O1	0.68410(12)	0.52790(12)	0.57016(10)	0.0545(4)
N6	0.61306(10)	0.20819(12)	0.53442(10)	0.0338(3)
N5	0.67906(9)	0.23300(11)	0.44704(9)	0.0272(3)
N4	0.46228(10)	0.33478(12)	0.27361(9)	0.0310(3)
N3	0.56446(10)	0.33372(11)	0.32456(9)	0.0308(3)
N2	0.70161(9)	0.45491(11)	0.41235(9)	0.0288(3)
N1	0.64632(11)	0.53111(12)	0.48429(11)	0.0372(3)
H3B	0.8170(15)	0.3221(15)	0.4066(13)	0.035(4)
H3A	0.7830(14)	0.3561(14)	0.5146(13)	0.032(4)
H2B	0.5643(14)	0.1508(16)	0.3570(12)	0.039(4)
H2A	0.6790(15)	0.1951(16)	0.3016(14)	0.039(4)
H1B	0.7000(14)	0.4179(16)	0.2622(13)	0.039(4)
H1A	0.5995(16)	0.5132(18)	0.3033(14)	0.046(5)
C3	0.75649(11)	0.34112(14)	0.45062(11)	0.0289(3)
C2	0.61971(13)	0.21556(13)	0.35120(11)	0.0303(3)
C1	0.64251(13)	0.44066(14)	0.31603(12)	0.0323(3)

Table 5. Anisotropic displacement parameters (\AA^2) for RDX at 250 K.

The anisotropic displacement factor exponent takes the form: $-2\pi^2[(ha^*)^2U_{11} + \dots + 2hka^*b^*U_{12}]$

	U11	U22	U33	U23	U13	U12
O6	0.0627(7)	0.0656(8)	0.0242(6)	0.0033(5)	0.0056(5)	0.0049(7)
O5	0.0477(7)	0.0501(7)	0.0650(9)	0.0092(6)	0.0183(6)	-0.0116(6)
O4	0.0360(5)	0.0496(7)	0.0569(8)	-0.0103(6)	-0.0114(5)	-0.0082(5)
O3	0.0380(5)	0.0500(7)	0.0355(6)	0.0027(5)	-0.0093(4)	0.0144(5)
O2	0.0420(6)	0.0330(6)	0.0884(10)	-0.0023(6)	0.0205(6)	0.0069(5)
O1	0.0704(8)	0.0547(8)	0.0386(7)	-0.0169(6)	0.0138(6)	-0.0151(7)
N6	0.0347(6)	0.0349(6)	0.0318(7)	0.0080(5)	0.0084(5)	0.0091(5)
N5	0.0266(5)	0.0330(6)	0.0222(6)	0.0031(4)	0.0027(4)	0.0031(5)
N4	0.0266(5)	0.0420(7)	0.0245(6)	-0.0076(5)	-0.0033(5)	0.0041(5)
N3	0.0300(6)	0.0298(6)	0.0326(7)	0.0006(5)	-0.0112(5)	0.0007(5)
N2	0.0259(5)	0.0297(6)	0.0308(7)	-0.0052(5)	0.0011(5)	-0.0009(5)
N1	0.0349(6)	0.0293(6)	0.0472(8)	-0.0073(5)	0.0152(6)	-0.0088(5)
C3	0.0213(6)	0.0396(8)	0.0260(7)	-0.0002(6)	-0.0008(5)	0.0023(5)
C2	0.0368(7)	0.0253(7)	0.0288(8)	-0.0018(6)	-0.0036(6)	0.0026(6)
C1	0.0331(6)	0.0300(7)	0.0339(8)	0.0061(6)	-0.0050(6)	-0.0006(6)

Table 6. Atomic coordinates and equivalent isotropic thermal parameters (\AA^2) for RDX at 200 K. $U(\text{eq})$ is defined as one third of the trace of the orthogonalized U_{ij} tensor.

	x	y	z	$U(\text{eq})/U(\text{iso})$
O6	0.64781(10)	0.25313(11)	0.61485(8)	0.0398(3)
O5	0.53312(10)	0.13608(11)	0.52549(9)	0.0430(3)
O4	0.40677(9)	0.23685(10)	0.27148(9)	0.0380(3)
O3	0.43195(8)	0.43389(10)	0.23434(8)	0.0329(3)
O2	0.56929(9)	0.60192(10)	0.45346(10)	0.0421(3)
O1	0.68317(11)	0.52970(11)	0.57094(8)	0.0419(3)
N6	0.61405(10)	0.20819(11)	0.53530(9)	0.0273(3)
N5	0.68017(9)	0.23375(10)	0.44784(8)	0.0221(2)
N4	0.46259(9)	0.33478(11)	0.27319(8)	0.0251(3)
N3	0.56480(9)	0.33446(10)	0.32494(8)	0.0247(3)
N2	0.70236(9)	0.45672(10)	0.41286(8)	0.0231(2)
N1	0.64582(10)	0.53268(11)	0.48459(10)	0.0293(3)
H3B	0.8198(14)	0.3236(15)	0.4063(13)	0.029(4)
H3A	0.7843(14)	0.3582(14)	0.5168(13)	0.030(4)
H2B	0.5662(13)	0.1506(15)	0.3581(12)	0.031(4)
H2A	0.6780(13)	0.1967(15)	0.3014(13)	0.027(4)
H1B	0.6998(14)	0.4206(16)	0.2646(13)	0.036(4)
H1A	0.5987(14)	0.5153(16)	0.3025(12)	0.030(4)
C3	0.75770(11)	0.34248(13)	0.45143(10)	0.0234(3)
C2	0.62042(12)	0.21588(12)	0.35174(10)	0.0246(3)
C1	0.64293(12)	0.44191(13)	0.31625(11)	0.0257(3)

Table 7. Anisotropic displacement parameters (\AA^2) for RDX at 200 K.

The anisotropic displacement factor exponent takes the form: $-2\pi^2[(ha^*)^2U_{11} + \dots + 2hka^*b^*U_{12}]$

	U11	U22	U33	U23	U13	U12
O6	0.0504(6)	0.0497(6)	0.0193(5)	0.0023(5)	0.0043(5)	0.0038(5)
O5	0.0391(6)	0.0388(6)	0.0510(7)	0.0069(5)	0.0136(5)	-0.0092(5)
O4	0.0314(5)	0.0381(6)	0.0445(7)	-0.0081(5)	-0.0090(5)	-0.0063(5)
O3	0.0321(5)	0.0390(6)	0.0275(6)	0.0024(4)	-0.0070(4)	0.0112(5)
O2	0.0338(5)	0.0261(5)	0.0662(8)	-0.0003(5)	0.0141(5)	0.0063(4)
O1	0.0554(7)	0.0409(6)	0.0294(6)	-0.0120(5)	0.0097(5)	-0.0104(5)
N6	0.0287(6)	0.0264(6)	0.0266(6)	0.0059(5)	0.0065(5)	0.0065(5)
N5	0.0232(5)	0.0257(5)	0.0175(5)	0.0018(4)	0.0022(4)	0.0019(4)
N4	0.0231(5)	0.0329(6)	0.0194(6)	-0.0062(4)	-0.0022(4)	0.0032(5)
N3	0.0245(5)	0.0226(6)	0.0270(6)	0.0004(4)	-0.0086(4)	0.0005(4)
N2	0.0223(5)	0.0231(5)	0.0237(6)	-0.0038(4)	0.0006(4)	-0.0008(4)
N1	0.0286(6)	0.0226(6)	0.0367(7)	-0.0052(5)	0.0111(5)	-0.0073(5)
C3	0.0192(6)	0.0294(7)	0.0216(7)	0.0001(5)	-0.0009(5)	0.0016(5)
C2	0.0313(6)	0.0199(6)	0.0226(7)	-0.0016(5)	-0.0031(5)	0.0020(5)
C1	0.0282(6)	0.0227(7)	0.0261(7)	0.0038(5)	-0.0036(6)	-0.0001(5)

Table 8. Atomic coordinates and equivalent isotropic thermal parameters (\AA^2) for RDX at 150 K. $U(\text{eq})$ is defined as one third of the trace of the orthogonalized U_{ij} tensor.

	x	y	z	$U(\text{eq})/U(\text{iso})$
O6	0.64839(8)	0.25381(9)	0.61587(7)	0.0290(2)
O5	0.53420(8)	0.13484(9)	0.52639(8)	0.0311(2)
O4	0.40681(7)	0.23645(9)	0.27108(7)	0.0280(2)
O3	0.43216(7)	0.43432(9)	0.23360(7)	0.0243(2)
O2	0.56810(8)	0.60308(8)	0.45342(8)	0.0303(2)
O1	0.68221(9)	0.53132(9)	0.57172(7)	0.0298(2)
N6	0.61490(8)	0.20811(10)	0.53610(8)	0.0201(2)
N5	0.68105(8)	0.23454(9)	0.44857(7)	0.0164(2)
N4	0.46279(8)	0.33498(10)	0.27296(7)	0.0185(2)
N3	0.56508(8)	0.33501(9)	0.32524(7)	0.0179(2)
N2	0.70293(7)	0.45824(9)	0.41312(7)	0.0170(2)
N1	0.64521(8)	0.53395(9)	0.48492(8)	0.0213(2)
H3B	0.8212(12)	0.3263(13)	0.4087(11)	0.022(4)
H3A	0.7840(12)	0.3596(12)	0.5182(11)	0.019(3)
H2B	0.5669(12)	0.1509(13)	0.3600(11)	0.023(4)
H2A	0.6787(12)	0.1974(13)	0.3003(11)	0.017(3)
H1B	0.7017(13)	0.4213(14)	0.2637(11)	0.027(4)
H1A	0.5994(12)	0.5160(14)	0.3023(11)	0.020(3)
C3	0.75882(9)	0.34412(11)	0.45217(9)	0.0171(2)
C2	0.62127(10)	0.21617(11)	0.35231(9)	0.0182(3)
C1	0.64367(10)	0.44289(11)	0.31632(9)	0.0189(3)

Table 9. Anisotropic displacement parameters (\AA^2) for RDX at 150 K.

The anisotropic displacement factor exponent takes the form: $-2\pi^2[(ha^*)^2U_{11} + \dots + 2hka^*b^*U_{12}]$

	U11	U22	U33	U23	U13	U12
O6	0.0354(5)	0.0367(5)	0.0148(5)	0.0010(4)	0.0027(4)	0.0037(4)
O5	0.0263(4)	0.0283(5)	0.0388(6)	0.0047(4)	0.0089(4)	-0.0068(4)
O4	0.0212(4)	0.0280(5)	0.0348(6)	-0.0061(4)	-0.0061(4)	-0.0053(4)
O3	0.0223(4)	0.0295(5)	0.0211(5)	0.0020(4)	-0.0049(3)	0.0081(4)
O2	0.0225(4)	0.0200(5)	0.0484(6)	0.0006(4)	0.0090(4)	0.0049(4)
O1	0.0367(5)	0.0306(5)	0.0222(5)	-0.0081(4)	0.0062(4)	-0.0070(4)
N6	0.0196(5)	0.0204(5)	0.0203(5)	0.0041(4)	0.0051(4)	0.0060(4)
N5	0.0158(4)	0.0191(5)	0.0142(5)	0.0018(4)	0.0021(4)	0.0006(4)
N4	0.0154(4)	0.0245(5)	0.0157(5)	-0.0045(4)	-0.0011(4)	0.0018(4)
N3	0.0158(4)	0.0178(5)	0.0202(5)	0.0007(4)	-0.0064(4)	0.0002(4)
N2	0.0150(4)	0.0175(5)	0.0186(5)	-0.0029(4)	0.0002(4)	-0.0003(4)
N1	0.0188(4)	0.0167(5)	0.0284(6)	-0.0031(4)	0.0075(4)	-0.0050(4)
C3	0.0126(5)	0.0214(6)	0.0174(6)	0.0002(4)	-0.0004(4)	0.0010(4)
C2	0.0216(5)	0.0150(5)	0.0181(6)	-0.0014(4)	-0.0019(5)	0.0022(4)
C1	0.0194(5)	0.0175(6)	0.0198(6)	0.0035(4)	-0.0028(5)	-0.0015(5)

Table 10. Atomic coordinates and equivalent isotropic thermal parameters (\AA^2) for RDX at 100 K. $U(\text{eq})$ is defined as one third of the trace of the orthogonalized U_{ij} tensor.

	x	y	z	$U(\text{eq})/U(\text{iso})$
O6	0.64894(8)	0.25427(9)	0.61682(6)	0.0204(2)
O5	0.53524(7)	0.13362(8)	0.52700(7)	0.0220(2)
O4	0.40670(7)	0.23627(8)	0.27064(7)	0.0202(2)
O3	0.43224(7)	0.43472(8)	0.23280(6)	0.0173(2)
O2	0.56702(7)	0.60407(8)	0.45339(7)	0.0209(2)
O1	0.68150(8)	0.53259(8)	0.57230(7)	0.0204(2)
N6	0.61559(8)	0.20832(9)	0.53689(8)	0.0143(2)
N5	0.68190(8)	0.23516(9)	0.44909(7)	0.0121(2)
N4	0.46298(8)	0.33514(9)	0.27250(7)	0.0134(2)
N3	0.56528(8)	0.33571(9)	0.32563(7)	0.0131(2)
N2	0.70341(8)	0.45968(9)	0.41350(7)	0.0125(2)
N1	0.64472(8)	0.53514(9)	0.48526(8)	0.0148(2)
H3B	0.8235(12)	0.3275(13)	0.4092(11)	0.014(3)
H3A	0.7842(12)	0.3594(13)	0.5189(11)	0.015(3)
H2B	0.5682(12)	0.1502(13)	0.3594(11)	0.014(3)
H2A	0.6803(12)	0.1974(13)	0.3015(11)	0.015(3)
H1B	0.7022(12)	0.4243(14)	0.2662(11)	0.016(3)
H1A	0.6000(12)	0.5176(14)	0.3009(11)	0.015(3)
C3	0.75955(9)	0.34504(11)	0.45289(9)	0.0125(2)
C2	0.62186(10)	0.21633(10)	0.35275(9)	0.0133(2)
C1	0.64417(10)	0.44387(11)	0.31645(9)	0.0137(2)

Table 11. Anisotropic displacement parameters (\AA^2) for RDX at 100 K.

The anisotropic displacement factor exponent takes the form: $-2\pi^2[(ha^*)^2U_{11} + \dots + 2hka^*b^*U_{12}]$

	U11	U22	U33	U23	U13	U12
O6	0.0240(4)	0.0253(5)	0.0120(4)	0.0004(3)	0.0018(3)	0.0026(4)
O5	0.0176(4)	0.0201(5)	0.0284(5)	0.0033(4)	0.0059(4)	-0.0049(3)
O4	0.0149(4)	0.0196(4)	0.0260(5)	-0.0045(4)	-0.0038(3)	-0.0043(3)
O3	0.0156(4)	0.0206(4)	0.0157(4)	0.0018(3)	-0.0031(3)	0.0055(3)
O2	0.0147(4)	0.0147(4)	0.0332(5)	0.0011(4)	0.0050(4)	0.0032(3)
O1	0.0239(4)	0.0212(5)	0.0161(4)	-0.0047(3)	0.0034(4)	-0.0045(4)
N6	0.0131(4)	0.0144(5)	0.0154(5)	0.0029(4)	0.0035(4)	0.0044(4)
N5	0.0112(4)	0.0144(5)	0.0106(5)	0.0013(3)	0.0016(3)	0.0001(4)
N4	0.0104(4)	0.0179(5)	0.0119(5)	-0.0030(4)	-0.0007(3)	0.0015(4)
N3	0.0108(4)	0.0126(5)	0.0160(5)	0.0006(4)	-0.0043(4)	0.0001(3)
N2	0.0105(4)	0.0131(4)	0.0140(5)	-0.0021(3)	-0.0002(3)	0.0008(3)
N1	0.0126(4)	0.0123(5)	0.0196(5)	-0.0016(4)	0.0048(4)	-0.0033(4)
C3	0.0085(5)	0.0147(5)	0.0143(5)	0.0006(4)	-0.0004(4)	0.0006(4)
C2	0.0151(5)	0.0111(5)	0.0135(6)	-0.0006(4)	-0.0024(4)	0.0013(4)
C1	0.0134(5)	0.0130(5)	0.0147(6)	0.0025(4)	-0.0016(4)	-0.0012(4)

Table 12. Atomic coordinates and equivalent isotropic thermal parameters (\AA^2) for RDX at 85 K. $U(\text{eq})$ is defined as one third of the trace of the orthogonalized U_{ij} tensor.

	x	y	z	$U(\text{eq})/U(\text{iso})$
O6	0.64908(7)	0.25434(8)	0.61708(6)	0.0182(2)
O5	0.53551(7)	0.13334(8)	0.52719(7)	0.0195(2)
O4	0.40666(7)	0.23622(8)	0.27047(7)	0.0179(2)
O3	0.43235(6)	0.43483(8)	0.23268(6)	0.0156(2)
O2	0.56670(7)	0.60427(8)	0.45339(7)	0.0184(2)
O1	0.68129(7)	0.53302(8)	0.57249(6)	0.0179(2)
N6	0.61581(8)	0.20810(9)	0.53705(7)	0.0128(2)
N5	0.68218(7)	0.23536(9)	0.44921(7)	0.0110(2)
N4	0.46296(8)	0.33528(9)	0.27245(7)	0.0121(2)
N3	0.56529(7)	0.33588(8)	0.32579(7)	0.0118(2)
N2	0.70353(7)	0.46001(8)	0.41357(7)	0.0111(2)
N1	0.64452(8)	0.53546(9)	0.48533(7)	0.0131(2)
H3B	0.8242(11)	0.3276(12)	0.4102(10)	0.012(3)
H3A	0.7846(11)	0.3610(12)	0.5188(10)	0.011(3)
H2B	0.5679(11)	0.1507(13)	0.3595(10)	0.012(3)
H2A	0.6801(11)	0.1981(12)	0.3019(10)	0.010(3)
H1B	0.7035(12)	0.4235(14)	0.2651(11)	0.018(3)
H1A	0.6005(12)	0.5176(14)	0.3015(11)	0.015(3)
C3	0.75982(9)	0.34545(10)	0.45307(8)	0.0114(2)
C2	0.62208(9)	0.21648(10)	0.35289(9)	0.0120(2)
C1	0.64434(9)	0.44404(10)	0.31644(8)	0.0126(2)

Table 13. Anisotropic displacement parameters (\AA^2) for RDX at 85 K.

The anisotropic displacement factor exponent takes the form: $-2\pi^2[(h a^*)^2 U_{11} + \dots + 2 h k a^* b^* U_{12}]$

	U11	U22	U33	U23	U13	U12
O6	0.0210(4)	0.0228(4)	0.0109(4)	0.0000(3)	0.0009(3)	0.0023(3)
O5	0.0156(4)	0.0177(4)	0.0252(5)	0.0025(3)	0.0048(3)	-0.0044(3)
O4	0.0136(4)	0.0175(4)	0.0226(5)	-0.0037(3)	-0.0031(3)	-0.0038(3)
O3	0.0142(4)	0.0185(4)	0.0142(4)	0.0021(3)	-0.0025(3)	0.0049(3)
O2	0.0127(4)	0.0136(4)	0.0288(5)	0.0012(3)	0.0042(3)	0.0027(3)
O1	0.0209(4)	0.0191(4)	0.0138(4)	-0.0039(3)	0.0025(3)	-0.0038(3)
N6	0.0117(4)	0.0131(4)	0.0135(5)	0.0023(3)	0.0027(3)	0.0039(3)
N5	0.0103(4)	0.0133(4)	0.0094(4)	0.0011(3)	0.0015(3)	-0.0003(3)
N4	0.0093(4)	0.0167(5)	0.0104(5)	-0.0025(3)	-0.0002(3)	0.0011(3)
N3	0.0093(4)	0.0117(4)	0.0143(5)	0.0006(3)	-0.0039(3)	0.0001(3)
N2	0.0096(4)	0.0121(4)	0.0117(5)	-0.0019(3)	0.0003(3)	0.0008(3)
N1	0.0107(4)	0.0108(4)	0.0177(5)	-0.0015(3)	0.0044(4)	-0.0031(3)
C3	0.0078(4)	0.0133(5)	0.0131(5)	0.0005(4)	-0.0007(4)	0.0002(4)
C2	0.0132(5)	0.0108(5)	0.0121(5)	-0.0004(4)	-0.0013(4)	0.0013(4)
C1	0.0123(4)	0.0125(5)	0.0129(5)	0.0019(4)	-0.0015(4)	-0.0013(4)

Table 14. Bond lengths (Å) and angles (°) of RDX at various temperatures.

At 298 K:

N6	O6	1.208(2)	
N6	O5	1.212(2)	
N5	N6	1.404(2)	
N5	C2	1.449(2)	
N5	C3	1.460(2)	
N4	O4	1.219(2)	
N4	O3	1.220(2)	
N4	N3	1.359(2)	
N3	C2	1.458(2)	
N3	C1	1.460(2)	
N2	N1	1.405(2)	
N2	C1	1.450(2)	
N2	C3	1.459(2)	
N1	O2	1.211(2)	
N1	O1	1.212(2)	
C3	H3B	0.95(2)	
C3	H3A	0.90(2)	
C2	H2B	0.93(2)	
C2	H2A	0.97(2)	
C1	H1B	0.99(2)	
C1	H1A	0.94(2)	
O6	N6	O5	125.7(2)
O6	N6	N5	117.13(15)
O5	N6	N5	116.93(15)
N6	N5	C3	117.06(13)
N6	N5	C2	115.57(13)
C2	N5	C3	114.76(13)
O4	N4	O3	125.13(13)
O4	N4	N3	117.30(14)
O3	N4	N3	117.55(14)
N4	N3	C2	120.44(13)
N4	N3	C1	119.60(13)
C2	N3	C1	115.39(13)
N1	N2	C1	115.94(14)
N1	N2	C3	116.89(13)
C1	N2	C3	114.87(13)
O2	N1	O1	126.0(2)
O2	N1	N2	117.4(2)
O1	N1	N2	116.4(2)
N5	C3	H3B	105.8(11)
N5	C3	H3A	111.9(12)
N2	C3	N5	112.37(12)
N2	C3	H3B	105.9(11)
N2	C3	H3A	109.4(12)
H3B	C3	H3A	111.3(17)
N5	C2	N3	107.80(12)
N5	C2	H2B	111.0(11)
N5	C2	H2A	106.5(11)
N3	C2	H2B	110.4(11)
N3	C2	H2A	110.3(12)
H2B	C2	H2A	110.7(15)

N3	C1	H1B	107.8(11)
N3	C1	H1A	111.0(12)
N2	C1	N3	107.77(13)
N2	C1	H1B	109.2(11)
N2	C1	H1A	108.2(12)
H1B	C1	H1A	112.7(16)

At 250 K:

N6	O6	1.211(2)	
N6	O5	1.213(2)	
N5	N6	1.408(2)	
N5	C2	1.450(2)	
N5	C3	1.463(2)	
N4	O3	1.223(2)	
N4	O4	1.224(2)	
N4	N3	1.359(2)	
N3	C2	1.458(2)	
N3	C1	1.461(2)	
N2	N1	1.405(2)	
N2	C1	1.451(2)	
N2	C3	1.462(2)	
N1	O1	1.214(2)	
N1	O2	1.217(2)	
C3	H3B	0.93(2)	
C3	H3A	0.91(2)	
C2	H2B	0.95(2)	
C2	H2A	0.97(2)	
C1	H1B	1.00(2)	
C1	H1A	0.94(2)	
O6	N6	O5	125.87(13)
O6	N6	N5	117.15(12)
O5	N6	N5	116.77(13)
N6	N5	C2	115.65(11)
N6	N5	C3	117.02(12)
C2	N5	C3	114.79(11)
O3	N4	O4	125.02(12)
O3	N4	N3	117.62(12)
O4	N4	N3	117.34(12)
N4	N3	C2	120.48(11)
N4	N3	C1	119.50(11)
C2	N3	C1	115.18(11)
N1	N2	C1	115.98(12)
N1	N2	C3	116.55(12)
C1	N2	C3	114.81(11)
O1	N1	O2	125.85(14)
O1	N1	N2	116.73(13)
O2	N1	N2	117.20(14)
N2	C3	N5	112.36(10)
N2	C3	H3B	107.0(11)
N5	C3	H3B	105.5(10)
N2	C3	H3A	108.6(10)
N5	C3	H3A	112.0(10)
H3B	C3	H3A	111.2(15)
N5	C2	N3	107.82(11)
N5	C2	H2B	110.1(10)

N3	C2	H2B	110.9(10)
N5	C2	H2A	106.3(10)
N3	C2	H2A	110.0(11)
H2B	C2	H2A	111.5(14)
N2	C1	N3	107.80(11)
N2	C1	H1B	109.5(9)
N3	C1	H1B	105.9(10)
N2	C1	H1A	108.7(11)
N3	C1	H1A	109.5(11)
H1B	C1	H1A	115.2(15)

At 200 K:

N6	O5	1.216(2)	
N6	O6	1.217(2)	
N5	N6	1.409(2)	
N5	C2	1.455(2)	
N5	C3	1.465(2)	
N4	O3	1.227(2)	
N4	O4	1.227(2)	
N4	N3	1.3620(15)	
N3	C2	1.462(2)	
N3	C1	1.463(2)	
N2	N1	1.406(2)	
N2	C1	1.455(2)	
N2	C3	1.467(2)	
N1	O1	1.218(2)	
N1	O2	1.222(2)	
C3	H3B	0.95(2)	
C3	H3A	0.93(2)	
C2	H2B	0.94(2)	
C2	H2A	0.96(2)	
C1	H1B	0.97(2)	
C1	H1A	0.95(2)	
O5	N6	O6	125.88(12)
O5	N6	N5	116.78(12)
O6	N6	N5	117.13(11)
N6	N5	C2	115.55(10)
N6	N5	C3	117.19(11)
C2	N5	C3	114.88(10)
O3	N4	O4	125.10(11)
O3	N4	N3	117.42(11)
O4	N4	N3	117.44(11)
N4	N3	C2	120.20(11)
N4	N3	C1	119.47(10)
C2	N3	C1	115.28(10)
N1	N2	C1	115.67(11)
N1	N2	C3	116.58(11)
C1	N2	C3	114.72(10)
O1	N1	O2	125.82(13)
O1	N1	N2	116.75(12)
O2	N1	N2	117.22(12)
N5	C3	N2	112.41(10)
N5	C3	H3B	105.7(9)
N2	C3	H3B	106.6(10)

N5	C3	H3A	111.9(10)
N2	C3	H3A	108.3(10)
H3B	C3	H3A	111.7(14)
N5	C2	N3	107.75(10)
N5	C2	H2B	109.5(10)
N3	C2	H2B	111.8(9)
N5	C2	H2A	107.6(9)
N3	C2	H2A	108.7(10)
H2B	C2	H2A	111.3(13)
N2	C1	N3	107.86(10)
N2	C1	H1B	108.7(10)
N3	C1	H1B	106.7(10)
N2	C1	H1A	109.2(10)
N3	C1	H1A	109.2(10)
H1B	C1	H1A	114.9(14)

At 150 K:

N6	O5	1.2164(13)	
N6	O6	1.2194(14)	
N5	N6	1.4081(13)	
N5	C2	1.4542(15)	
N5	C3	1.4678(15)	
N4	O3	1.2273(13)	
N4	O4	1.2285(13)	
N4	N3	1.3605(13)	
N3	C2	1.4620(14)	
N3	C1	1.4632(14)	
N2	N1	1.4069(13)	
N2	C1	1.4537(14)	
N2	C3	1.4649(14)	
N1	O1	1.2195(14)	
N1	O2	1.2223(14)	
C3	H3B	0.936(15)	
C3	H3A	0.930(14)	
C2	H2B	0.938(14)	
C2	H2A	0.971(14)	
C1	H1B	0.988(15)	
C1	H1A	0.947(14)	
O5	N6	O6	125.82(11)
O5	N6	N5	116.86(10)
O6	N6	N5	117.12(10)
N6	N5	C2	115.62(9)
N6	N5	C3	117.35(9)
C2	N5	C3	114.92(9)
O3	N4	O4	125.09(10)
O3	N4	N3	117.41(10)
O4	N4	N3	117.47(10)
N4	N3	C2	120.23(9)
N4	N3	C1	119.41(9)
C2	N3	C1	115.13(9)
N1	N2	C1	115.67(9)
N1	N2	C3	116.33(9)
C1	N2	C3	114.81(9)
O1	N1	O2	125.71(11)
O1	N1	N2	116.92(10)

O2	N1	N2	117.15(10)
N2	C3	N5	112.29(9)
N2	C3	H3B	106.7(9)
N5	C3	H3B	106.5(9)
N2	C3	H3A	108.5(8)
N5	C3	H3A	111.1(8)
H3B	C3	H3A	111.7(12)
N5	C2	N3	107.73(9)
N5	C2	H2B	108.6(9)
N3	C2	H2B	111.8(8)
N5	C2	H2A	108.8(8)
N3	C2	H2A	107.7(8)
H2B	C2	H2A	112.0(11)
N2	C1	N3	107.80(9)
N2	C1	H1B	109.0(8)
N3	C1	H1B	106.8(9)
N2	C1	H1A	109.3(9)
N3	C1	H1A	109.2(8)
H1B	C1	H1A	114.5(12)

At 100 K:

N6	O6	1.2221(13)	
N6	O5	1.2221(13)	
N5	N6	1.4132(13)	
N5	C2	1.4577(15)	
N5	C3	1.4682(14)	
N4	O3	1.2313(13)	
N4	O4	1.2324(13)	
N4	N3	1.3651(13)	
N3	C1	1.4666(14)	
N3	C2	1.4681(14)	
N2	N1	1.4101(13)	
N2	C1	1.4576(14)	
N2	C3	1.4716(14)	
N1	O1	1.2223(14)	
N1	O2	1.2266(13)	
C3	H3B	0.951(14)	
C3	H3A	0.927(15)	
C2	H2B	0.937(14)	
C2	H2A	0.972(15)	
C1	H1B	0.961(14)	
C1	H1A	0.954(14)	
O6	N6	O5	125.91(10)
O6	N6	N5	117.20(9)
O5	N6	N5	116.65(10)
N6	N5	C2	115.58(9)
N6	N5	C3	117.26(9)
C2	N5	C3	115.13(9)
O3	N4	O4	125.01(9)
O3	N4	N3	117.36(9)
O4	N4	N3	117.58(9)
N4	N3	C1	119.35(9)
N4	N3	C2	120.01(9)
C1	N3	C2	115.11(9)
N1	N2	C1	115.59(9)

N1	N2	C3	116.23(9)
C1	N2	C3	114.69(9)
O1	N1	O2	125.77(10)
O1	N1	N2	116.90(9)
O2	N1	N2	117.10(10)
N5	C3	N2	112.38(9)
N5	C3	H3B	106.9(8)
N2	C3	H3B	106.6(9)
N5	C3	H3A	110.4(8)
N2	C3	H3A	109.1(9)
H3B	C3	H3A	111.5(12)
N5	C2	N3	107.57(9)
N5	C2	H2B	109.3(9)
N3	C2	H2B	112.3(8)
N5	C2	H2A	108.0(8)
N3	C2	H2A	108.3(8)
H2B	C2	H2A	111.2(12)
N2	C1	N3	107.74(9)
N2	C1	H1B	107.9(8)
N3	C1	H1B	108.3(9)
N2	C1	H1A	109.9(9)
N3	C1	H1A	109.5(8)
H1B	C1	H1A	113.4(12)

At 85 K:

N6	O5	1.2189(12)	
N6	O6	1.2218(13)	
N5	N6	1.4120(13)	
N5	C2	1.4550(14)	
N5	C3	1.4661(13)	
N4	O3	1.2281(12)	
N4	O4	1.2312(12)	
N4	N3	1.3634(12)	
N3	C1	1.4642(13)	
N3	C2	1.4657(13)	
N2	N1	1.4088(12)	
N2	C1	1.4555(13)	
N2	C3	1.4686(13)	
N1	O1	1.2215(13)	
N1	O2	1.2241(12)	
C3	H3B	0.946(13)	
C3	H3A	0.925(13)	
C2	H2B	0.936(13)	
C2	H2A	0.963(13)	
C1	H1B	0.980(14)	
C1	H1A	0.947(14)	
O5	N6	O6	125.90(10)
O5	N6	N5	116.74(9)
O6	N6	N5	117.14(9)
N6	N5	C2	115.55(8)
N6	N5	C3	117.34(9)
C2	N5	C3	115.15(8)
O3	N4	O4	125.04(9)
O3	N4	N3	117.35(9)

O4	N4	N3	117.57(9)
N4	N3	C1	119.29(9)
N4	N3	C2	120.05(9)
C1	N3	C2	115.01(8)
N1	N2	C1	115.60(8)
N1	N2	C3	116.18(9)
C1	N2	C3	114.71(8)
O1	N1	O2	125.78(10)
O1	N1	N2	116.91(9)
O2	N1	N2	117.09(9)
N5	C3	N2	112.35(8)
N5	C3	H3B	106.9(8)
N2	C3	H3B	107.1(8)
N5	C3	H3A	111.1(8)
N2	C3	H3A	108.5(8)
H3B	C3	H3A	110.7(12)
N5	C2	N3	107.58(8)
N5	C2	H2B	109.5(8)
N3	C2	H2B	111.9(8)
N5	C2	H2A	108.1(8)
N3	C2	H2A	108.0(8)
H2B	C2	H2A	111.6(11)
N2	C1	N3	107.68(8)
N2	C1	H1B	108.1(8)
N3	C1	H1B	108.0(8)
N2	C1	H1A	109.4(8)
N3	C1	H1A	109.5(8)
H1B	C1	H1A	113.9(12)

Contract No. N00014-95-1-0013 and N00014-97-1-0409

Program Officer: R. Miller/J. Goldwasser

**Title: Experimental Charge Densities and Electrostatic Potentials in Energetic
Materials and Infrastructure Upgrade for an X-ray Crystallography
Laboratory**

PI: A. Alan Pinkerton

Department of Chemistry, University of Toledo, Toledo, OH 43606

tel. (419) 530-4580, FAX (419) 530-4033, email apinker@uoft02.utoledo.edu

APPENDIX 3h

Variable temperature crystallographic study of TNAZ

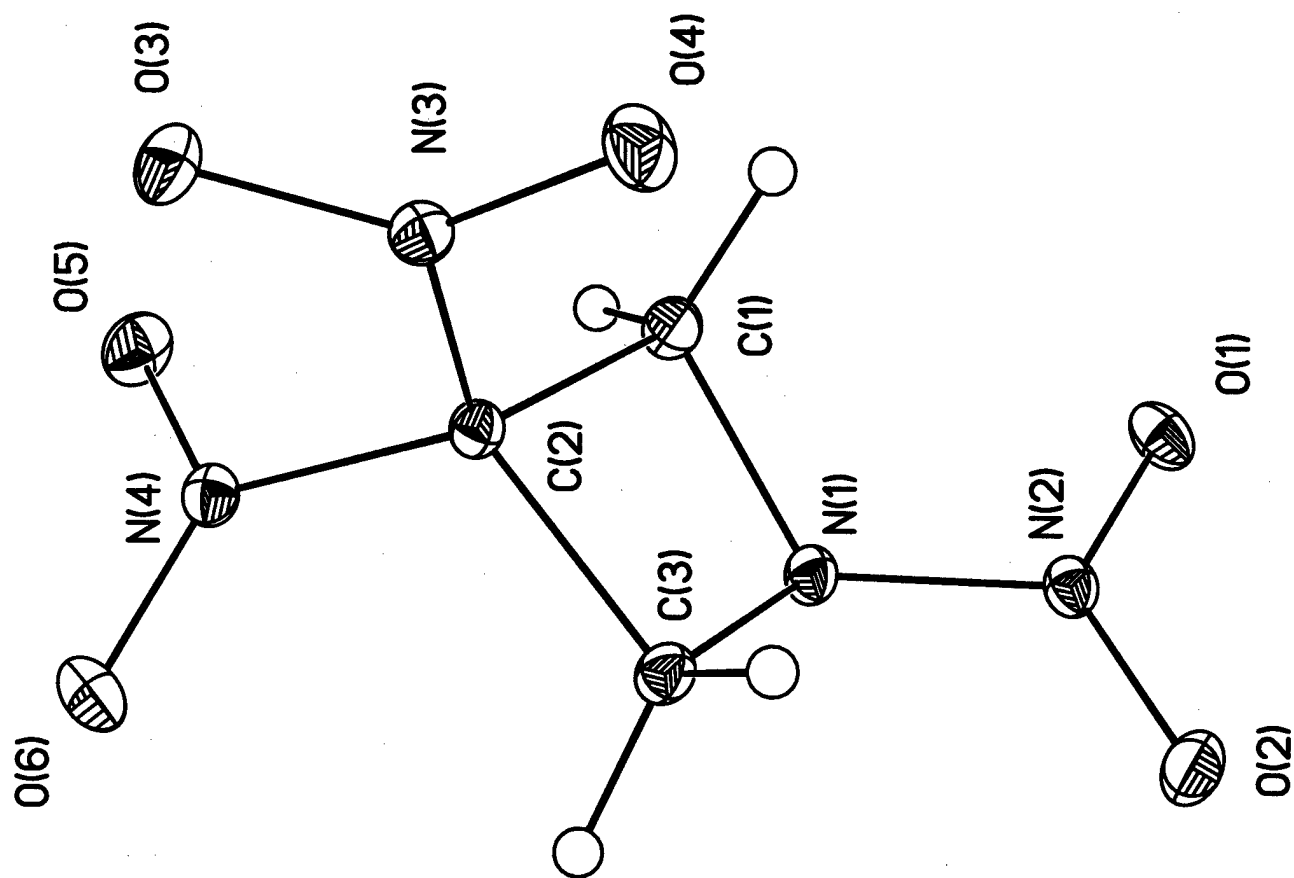
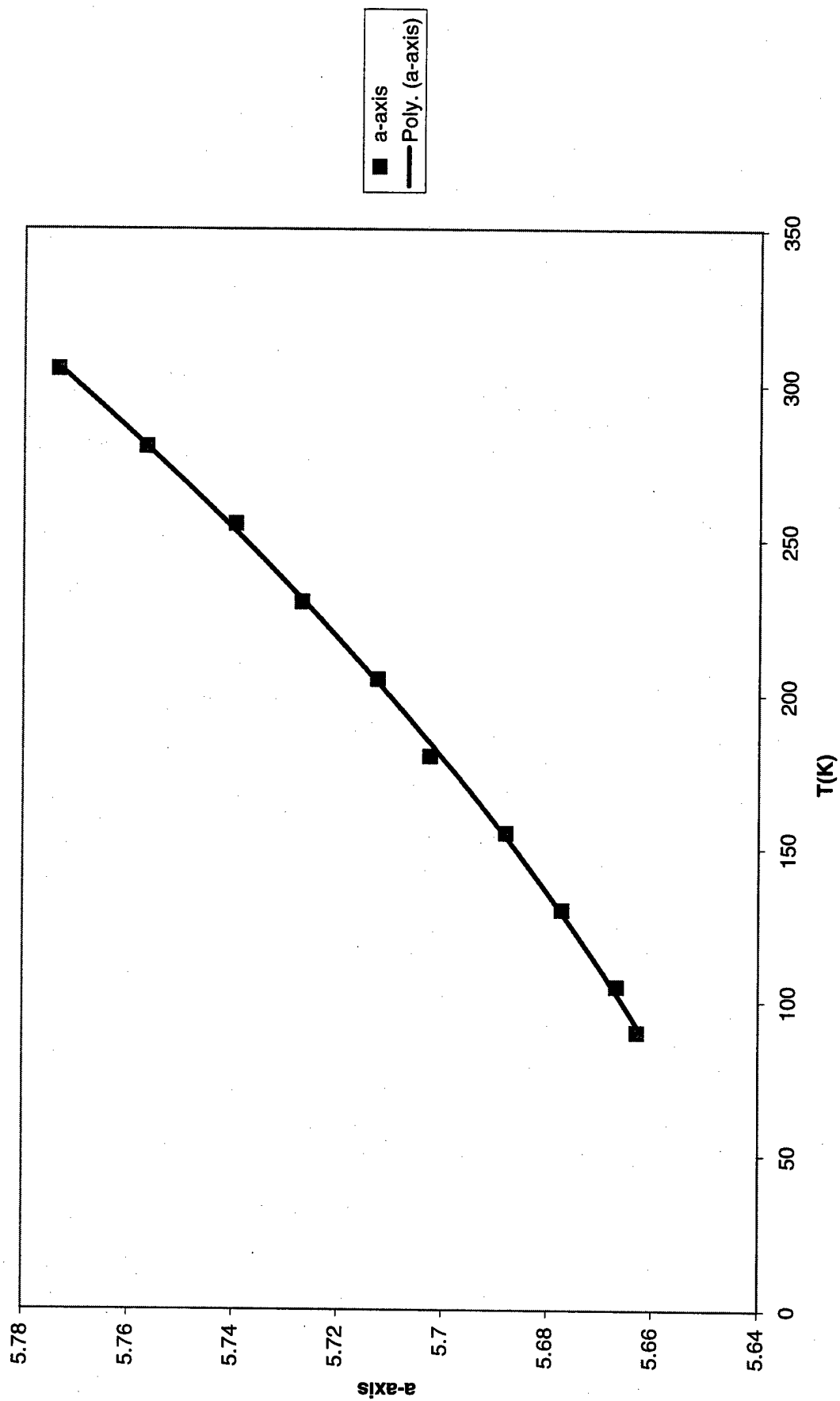


Table 15. Unit cell parameters for variable temperature structure determinations of 1,3,3-Trinitroazetidine.

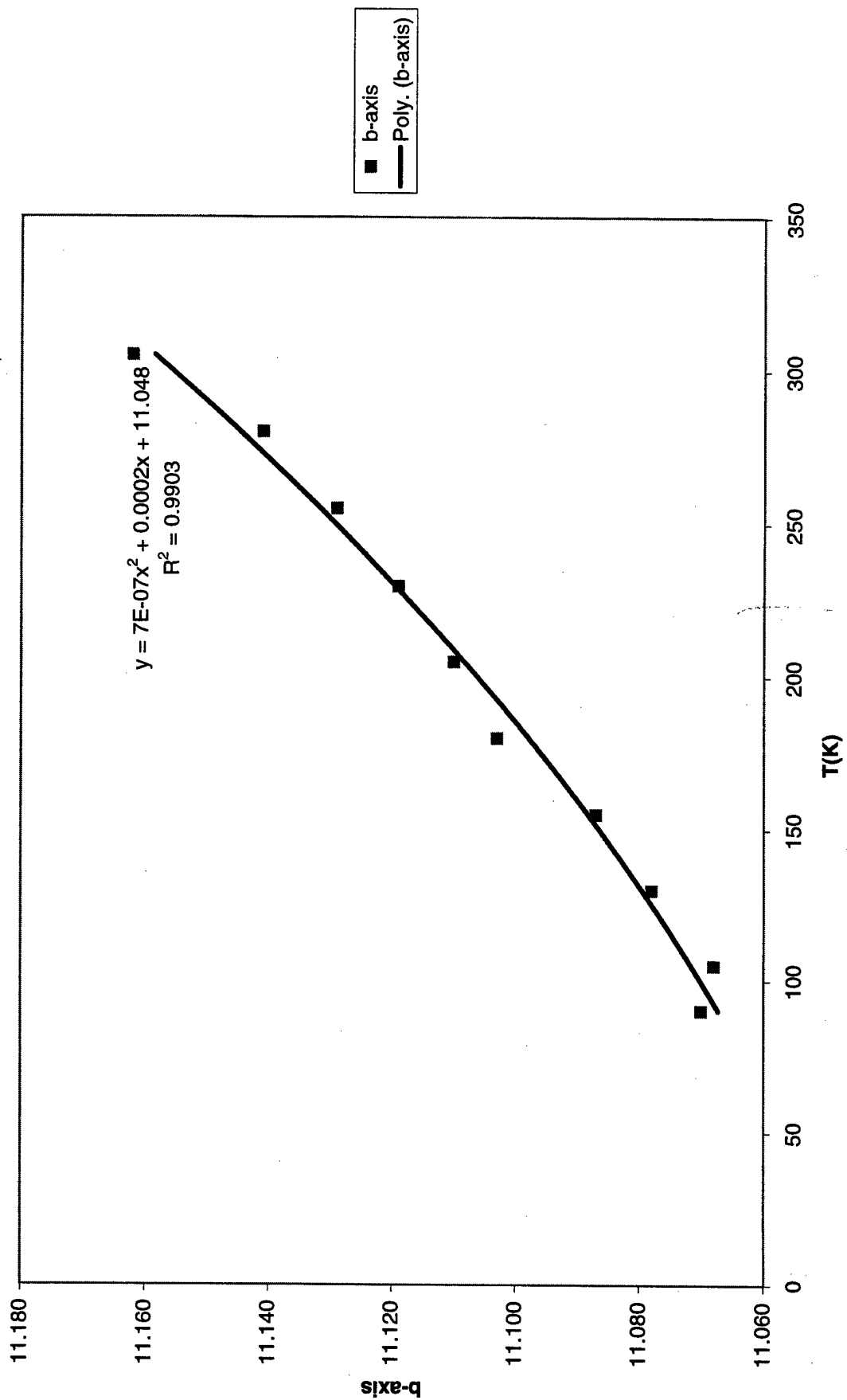
T (K)	a (Å)	b (Å)	c (Å)	volume (Å ³)
305	5.7735(12)	11.162(2)	21.569(4)	1390.0(5)
280	5.7567(12)	11.141(2)	21.537(4)	1381.2(5)
255	5.7398(11)	11.129(2)	21.499(4)	1373.3(5)
230	5.7270(11)	11.119(2)	21.469(4)	1367.1(5)
205	5.7125(11)	11.110(2)	21.435(4)	1360.4(5)
180	5.7025(11)	11.103(2)	21.415(4)	1355.8(5)
155	5.6879(11)	11.087(2)	21.376(4)	1348.0(5)
130	5.6772(11)	11.078(2)	21.354(4)	1343.0(5)
105	5.6668(11)	11.068(2)	21.320(4)	1337.2(5)
90	5.6629(11)	11.070(2)	21.323(4)	1336.5(5)

TNAX: a-axis vs T

$$y = 7E-07x^2 + 0.0002x + 5.6359$$
$$R^2 = 0.9993$$

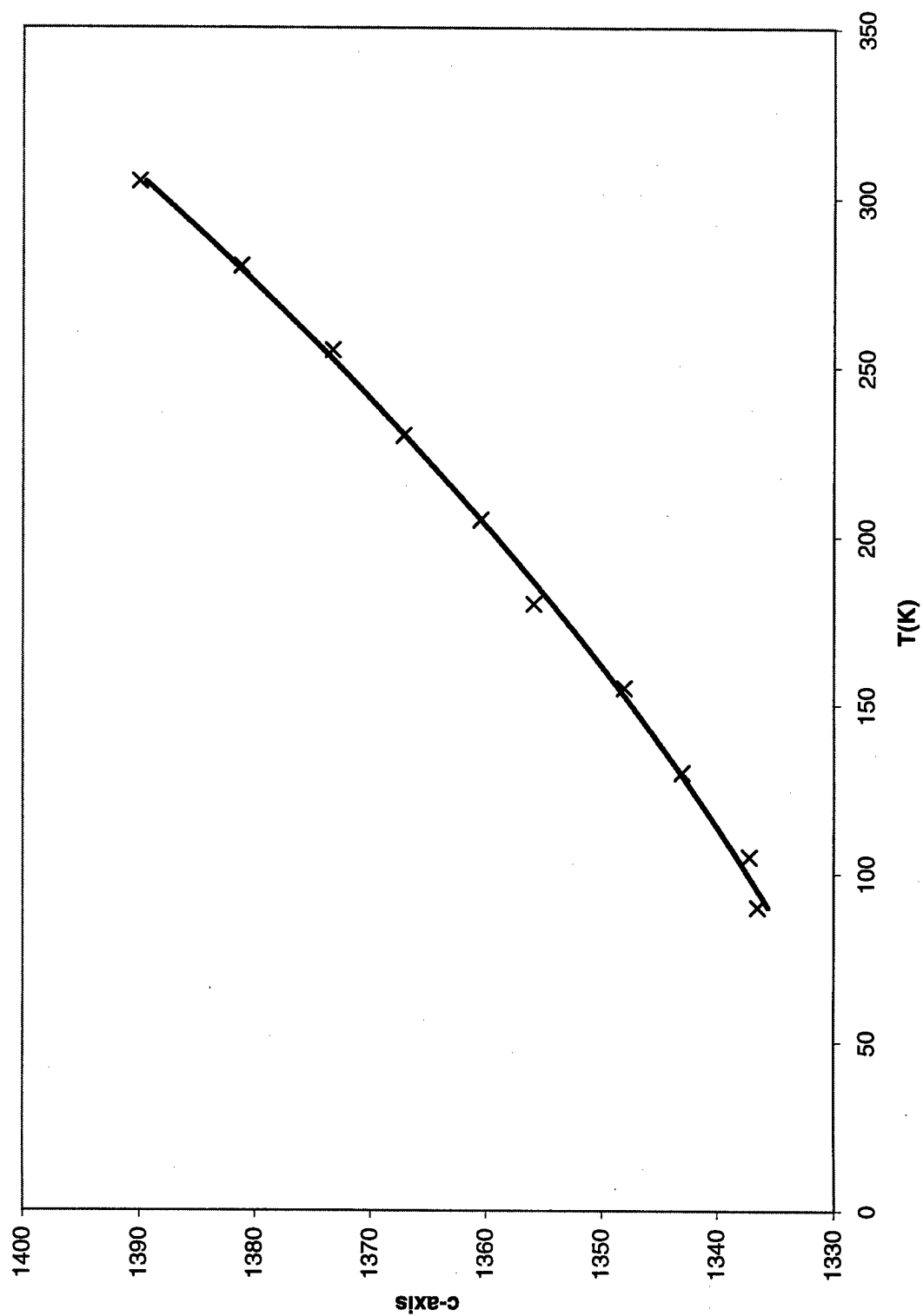


TNAZ: b-axis vs T



TNAZ: c-axis vs T

$$y = 0.0003x^2 + 0.1127x + 1322.7$$
$$R^2 = 0.9981$$



TNAZ: volume vs T

$$y = 0.0003x^2 + 0.1127x + 1322.7$$
$$R^2 = 0.9981$$

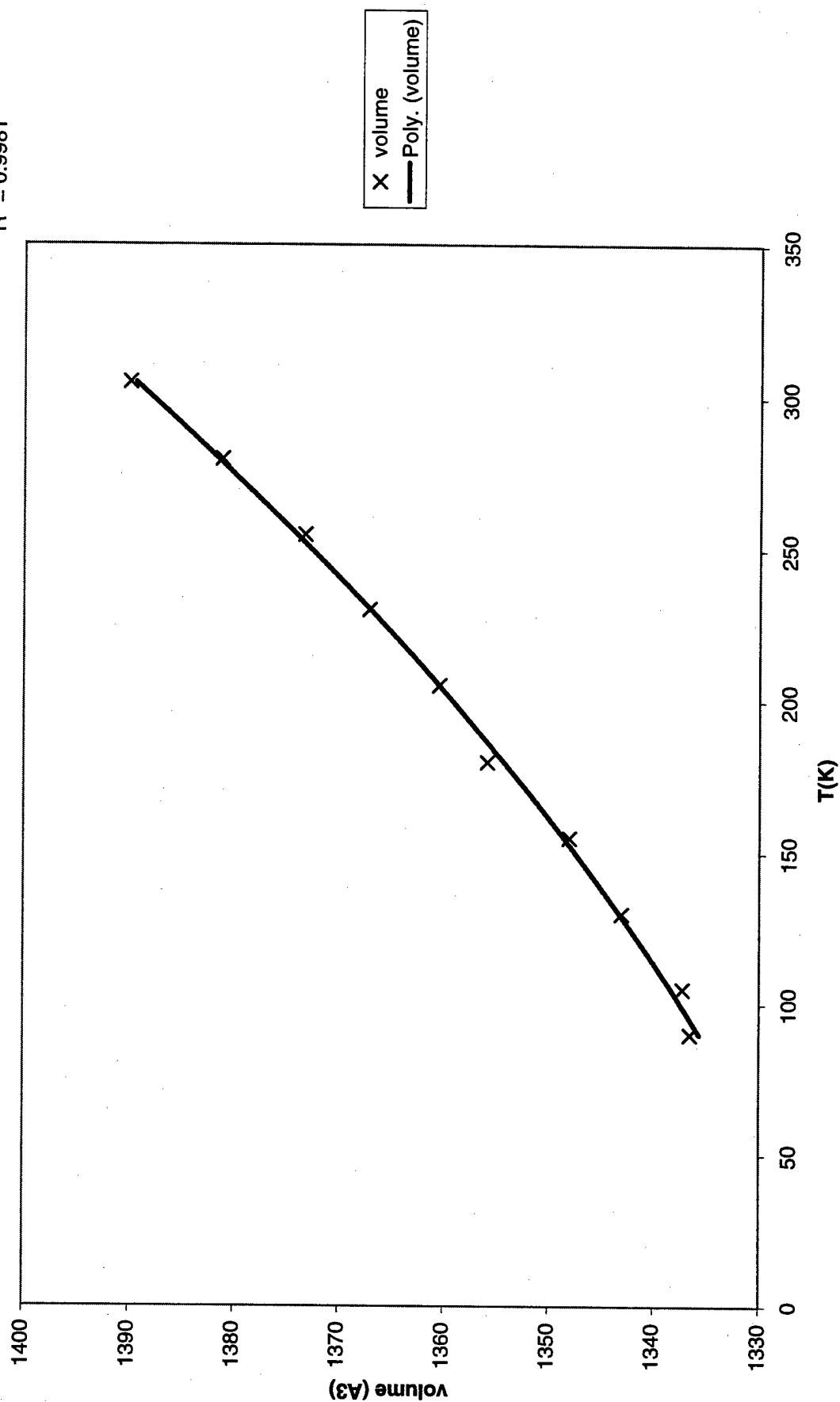


Table 1. Crystal data and structure refinement for 1,3,3-Trinitroazetidine at various temperatures.

Empirical formula	$C_3H_4N_4O_6$														
Formula weight	192.10														
Wavelength	0.71073 Å														
Crystal system	Orthorhombic														
Space group	Pbca														
F(000)	784														
Crystal size	0.31 x 0.26 x 0.21 mm														
Z	8														
Instrument	Siemens SMART CCD														
Detector distance	2.58 cm														
Scan width and axis	-0.3° in ω														
Refinement method	Full-matrix least-squares on F ²														
Temperature (K)	305(1)	280(1)	255(1)	230(1)	205(1)	180(1)	155(1)	130(1)	105(1)	90(1)					
a (Å)	5.7735(12)	5.7567(12)	5.7398(11)	5.7270(11)	5.7125(11)	5.7025(11)	5.6879(11)	5.6772(11)	5.6668(11)	5.6629(11)					
b (Å)	11.162(2)	11.141(2)	11.129(2)	11.119(2)	11.110(2)	11.103(2)	11.087(2)	11.078(2)	11.068(2)	11.070(2)					
c (Å)	21.569(4)	21.537(4)	21.499(4)	21.469(4)	21.435(4)	21.415(4)	21.376(4)	21.354(4)	21.320(4)	21.323(4)					
α (°)	90.00	90.00	90.00	90.00	90.00	90.00	90.00	90.00	90.00	90.00					
β (°)	90.00	90.00	90.00	90.00	90.00	90.00	90.00	90.00	90.00	90.00					
γ (°)	90.00	90.00	90.00	90.00	90.00	90.00	90.00	90.00	90.00	90.00					
Volume (Å ³)	1390.0(5)	1381.2(5)	1373.3(5)	1367.1(5)	1360.4(5)	1355.8(5)	1348.0(5)	1343.0(5)	1337.2(5)	1336.5(5)					
Density (calc) (Mg/m ³)	1.836	1.848	1.858	1.867	1.876	1.882	1.893	1.900	1.908	1.909					
Absorption coeff. (mm ⁻¹)	0.179	0.180	0.181	0.182	0.183	0.183	0.184	0.185	0.186	0.186					
θ range	1.89 – 45.00	1.89 – 45.00	1.89 – 45.00	1.90 – 44.99	1.90 – 45.00	1.90 – 45.00	1.91 – 45.00	1.91 – 45.00	1.91 – 45.00	1.91 – 45.00					
Limiting indices	-11 – 6	-11 – 6	-6 – 11	-6 – 11	-11 – 6	-11 – 6	-11 – 6	-6 – 11	-11 – 6	-11 – 6					
	-22 – 16	-24 – 16	-24 – 16	-24 – 16	-16 – 24	-24 – 16	-24 – 16	-16 – 24	-16 – 24	-16 – 24					
	-39 – 27	-41 – 33	-33 – 41	-33 – 41	-33 – 41	-41 – 33	-40 – 33	-40 – 33	-33 – 40	-37 – 42					
Reflections collected	18576	18465	18345	18624	18065	18111	18005	17943	17868	59115					
Independent reflections	5438	5408	5370	5333	5314	5286	5252	5212	5208	5512					
R _{int}	0.1809	0.1597	0.1233	0.1007	0.1049	0.1010	0.0880	0.0845	0.0780	0.0436					
Data/restraints/parameters	4176/1/118	5408/1/118	5370/1/118	5333/1/118	5314/1/118	5286/1/118	5252/1/118	5212/1/118	5208/1/118	59155/1/118					
Goodness-of-fit on F ²	0.949	0.895	0.960	0.963	0.963	0.959	0.987	0.977	0.971	1.0512					
R _I [$>2\sigma(I)$]	0.0760	0.0578	0.0568	0.0572	0.0591	0.0591	0.0543	0.0545	0.0506	0.0326					
wR ₂ [$I > 2\sigma(I)$]	0.1643	0.1320	0.1201	0.1237	0.1308	0.1256	0.1158	0.1116	0.1076	0.0853					
R _I (all data)	0.3154	0.2587	0.2372	0.2082	0.1949	0.1887	0.1652	0.1478	0.1278	0.0442					
wR ₂ (all data)	0.2879	0.2087	0.1911	0.1814	0.1828	0.1756	0.1619	0.1458	0.1344	0.0899					
Largest diff. peak (eÅ ⁻³)	0.292	0.391	0.323	0.381	0.455	0.422	0.479	0.519	0.503	0.50					
Largest diff. hole (eÅ ⁻³)	-0.459	-0.334	-0.349	-0.429	-0.503	-0.559	-0.498	-0.448	-0.501	-0.403					

Table 1. Atomic coordinates and equivalent isotropic thermal parameters (\AA^2) for 1,3,3-Trinitroazetidine at room temperature (305 K). $U(\text{eq})$ is defined as one third of the trace of the orthogonalized U_{ij} tensor.

	x	y	z	$U(\text{eq})/U(\text{iso})$
O6	0.5972(3)	0.34510(19)	0.01448(9)	0.0514(5)
O5	0.5836(4)	0.47985(16)	0.08622(10)	0.0508(5)
O4	0.0004(3)	0.26721(19)	0.11432(10)	0.0509(6)
O3	0.1075(3)	0.40462(16)	0.04954(9)	0.0442(5)
O2	0.4912(4)	-0.00966(17)	0.19135(9)	0.0507(5)
O1	0.5034(3)	0.12721(18)	0.26381(8)	0.0452(5)
N4	0.5395(4)	0.38199(17)	0.06504(11)	0.0354(5)
N3	0.1447(3)	0.32753(17)	0.08760(9)	0.0332(5)
N2	0.5054(4)	0.09410(19)	0.20972(10)	0.0353(5)
N1	0.5407(4)	0.18039(17)	0.16616(9)	0.0336(5)
H4	0.5747	0.1459	0.0722	0.042
H3	0.5638	0.3617	0.1863	0.045
H2	0.3125	0.3074	0.2006	0.045
H1	0.3223	0.1136	0.0982	0.042
C3	0.4554(5)	0.1661(2)	0.10210(11)	0.0347(5)
C2	0.3947(4)	0.30038(19)	0.10452(11)	0.0293(5)
C1	0.4484(5)	0.3028(2)	0.17432(12)	0.0377(6)

Table 2. Anisotropic displacement parameters (\AA^2) for 1,3,3-Trinitroazetidine at room temperature (305 K). The anisotropic displacement factor exponent takes the form: $-2\pi^2[(h a^*)^2 U_{11} + \dots + 2 h k a^* b^* U_{12}]$

	U11	U22	U33	U23	U13	U12
O6	0.0544(13)	0.0611(12)	0.0386(11)	0.0042(10)	0.0110(9)	-0.0005(10)
O5	0.0513(13)	0.0357(9)	0.0653(14)	0.0024(9)	-0.0004(10)	-0.0122(9)
O4	0.0367(11)	0.0563(12)	0.0599(13)	0.0097(10)	0.0067(10)	-0.0106(9)
O3	0.0398(11)	0.0399(8)	0.0530(11)	0.0099(9)	-0.0088(9)	0.0039(8)
O2	0.0644(14)	0.0352(9)	0.0525(12)	0.0084(9)	0.0003(10)	0.0013(9)
O1	0.0416(11)	0.0628(13)	0.0312(10)	0.0059(9)	-0.0009(8)	-0.0004(9)
N4	0.0310(11)	0.0345(9)	0.0408(12)	0.0054(10)	-0.0035(9)	0.0000(8)
N3	0.0314(11)	0.0337(9)	0.0345(11)	-0.0012(9)	-0.0008(8)	-0.0007(8)
N2	0.0308(11)	0.0403(10)	0.0349(11)	0.0068(10)	-0.0009(8)	0.0005(9)
N1	0.0368(12)	0.0339(9)	0.0300(10)	0.0032(8)	-0.0024(9)	0.0012(8)
C3	0.0443(15)	0.0301(10)	0.0298(12)	-0.0008(9)	-0.0032(10)	0.0057(10)
C2	0.0281(11)	0.0294(9)	0.0304(11)	0.0010(9)	-0.0009(9)	-0.0010(9)
C1	0.0502(16)	0.0308(10)	0.0323(12)	-0.0022(10)	-0.0060(11)	-0.0005(10)

Table 3. Atomic coordinates and equivalent isotropic thermal parameters (\AA^2) for 1,3,3-Trinitroazetidine at room temperature (280 K). $U(\text{eq})$ is defined as one third of the trace of the orthogonalized U_{ij} tensor.

	x	y	z	$U(\text{eq})/U(\text{iso})$
O6	0.5964(3)	0.34477(14)	0.01424(7)	0.0426(4)
O5	0.5838(3)	0.47996(12)	0.08643(7)	0.0426(4)
O4	-0.0012(2)	0.26710(14)	0.11442(8)	0.0429(4)
O3	0.1059(2)	0.40499(12)	0.04929(6)	0.0368(3)
O2	0.4912(3)	-0.01037(13)	0.19155(7)	0.0432(4)
O1	0.5036(2)	0.12698(13)	0.26406(6)	0.0375(4)
N4	0.5390(3)	0.38198(13)	0.06490(8)	0.0290(3)
N3	0.1432(3)	0.32754(13)	0.08747(7)	0.0273(3)
N2	0.5057(3)	0.09385(14)	0.21001(7)	0.0284(3)
N1	0.5408(3)	0.17976(13)	0.16623(7)	0.0261(3)
H4	0.5743(3)	0.14590(15)	0.07190(8)	0.034
H3	0.5645(3)	0.3615(2)	0.18614(8)	0.036
H2	0.3127(3)	0.3073(2)	0.20095(8)	0.036
H1	0.3216(3)	0.11300(15)	0.09798(8)	0.034
C3	0.4547(3)	0.16580(15)	0.10191(8)	0.0280(4)
C2	0.3929(3)	0.30006(14)	0.10445(8)	0.0233(3)
C1	0.4485(3)	0.3026(2)	0.17440(8)	0.0302(4)

Table 4. Anisotropic displacement parameters (\AA^2) for 1,3,3-Trinitroazetidine at room temperature (275 K). The anisotropic displacement factor exponent takes the form: $-2\pi^2[(h a^*)^2 U_{11} + \dots + 2 h k a^* b^* U_{12}]$

	U11	U22	U33	U23	U13	U12
O6	0.0473(9)	0.0503(9)	0.0304(8)	0.0040(7)	0.0087(6)	-0.0012(7)
O5	0.0438(8)	0.0259(6)	0.0580(10)	0.0027(6)	-0.0003(7)	-0.0098(6)
O4	0.0320(8)	0.0462(9)	0.0505(10)	0.0096(7)	0.0059(7)	-0.0085(6)
O3	0.0354(7)	0.0312(7)	0.0438(8)	0.0074(6)	-0.0083(6)	0.0035(6)
O2	0.0557(9)	0.0280(7)	0.0461(9)	0.0075(6)	0.0012(7)	0.0013(6)
O1	0.0349(8)	0.0533(9)	0.0243(7)	0.0069(6)	0.0005(6)	-0.0009(6)
N4	0.0249(7)	0.0274(7)	0.0346(9)	0.0057(7)	-0.0023(6)	0.0001(6)
N3	0.0292(8)	0.0239(7)	0.0288(8)	-0.0020(6)	0.0002(6)	-0.0016(6)
N2	0.0262(7)	0.0303(8)	0.0287(8)	0.0062(6)	0.0002(6)	0.0013(6)
N1	0.0304(7)	0.0245(6)	0.0234(7)	0.0040(6)	-0.0015(6)	0.0009(6)
C3	0.0383(10)	0.0199(7)	0.0258(9)	-0.0010(6)	-0.0030(7)	0.0053(7)
C2	0.0259(8)	0.0187(6)	0.0252(8)	0.0001(6)	-0.0006(6)	0.0002(6)
C1	0.0417(10)	0.0234(8)	0.0254(9)	-0.0019(7)	-0.0047(8)	0.0001(7)

Table 5. Atomic coordinates and equivalent isotropic thermal parameters (\AA^2) for 1,3,3-Trinitroazetidine at room temperature (255 K). $U(\text{eq})$ is defined as one third of the trace of the orthogonalized U_{ij} tensor.

	x	y	z	$U(\text{eq})/U(\text{iso})$
O6	0.5958(2)	0.34471(12)	0.01394(6)	0.0392(3)
O5	0.5840(2)	0.47993(11)	0.08638(7)	0.0391(3)
O4	-0.0037(2)	0.26718(12)	0.11443(7)	0.0394(3)
O3	0.1042(2)	0.40531(10)	0.04928(6)	0.0339(3)
O2	0.4913(3)	-0.01092(11)	0.19166(6)	0.0392(3)
O1	0.5047(2)	0.12626(12)	0.26438(5)	0.0346(3)
N4	0.5388(2)	0.38194(12)	0.06486(7)	0.0267(3)
N3	0.1419(2)	0.32740(12)	0.08764(6)	0.0250(3)
N2	0.5060(2)	0.09329(12)	0.21007(7)	0.0266(3)
N1	0.5406(2)	0.17958(12)	0.16627(6)	0.0247(3)
H4	0.5738(3)	0.14570(14)	0.07188(7)	0.031
H3	0.5645(3)	0.36136(14)	0.18612(8)	0.034
H2	0.3121(3)	0.30706(14)	0.20109(8)	0.034
H1	0.3205(3)	0.11276(14)	0.09811(7)	0.031
C3	0.4540(3)	0.16567(14)	0.10197(7)	0.0256(3)
C2	0.3920(3)	0.29971(13)	0.10438(7)	0.0217(3)
C1	0.4481(3)	0.30232(14)	0.17443(8)	0.0280(3)

Table 6. Anisotropic displacement parameters (\AA^2) for 1,3,3-Trinitroazetidine at room temperature (255 K). The anisotropic displacement factor exponent takes the form: $-2\pi^2[(h a^*)^2 U_{11} + \dots + 2 h k a^* b^* U_{12}]$

	U11	U22	U33	U23	U13	U12
O6	0.0434(8)	0.0476(8)	0.0265(6)	0.0049(6)	0.0076(6)	-0.0014(6)
O5	0.0397(7)	0.0260(6)	0.0515(8)	0.0018(6)	-0.0003(6)	-0.0094(5)
O4	0.0289(7)	0.0428(8)	0.0465(8)	0.0079(6)	0.0049(6)	-0.0075(5)
O3	0.0330(7)	0.0296(6)	0.0390(7)	0.0078(5)	-0.0063(5)	0.0042(5)
O2	0.0512(8)	0.0260(6)	0.0403(8)	0.0066(5)	0.0024(7)	0.0009(5)
O1	0.0332(7)	0.0503(8)	0.0204(6)	0.0056(5)	-0.0004(5)	-0.0012(6)
N4	0.0234(7)	0.0267(6)	0.0299(7)	0.0048(6)	-0.0026(5)	-0.0002(5)
N3	0.0251(7)	0.0245(6)	0.0254(7)	-0.0014(5)	-0.0001(5)	-0.0004(5)
N2	0.0229(7)	0.0304(7)	0.0265(7)	0.0058(6)	-0.0003(5)	0.0010(5)
N1	0.0295(7)	0.0243(6)	0.0204(6)	0.0032(5)	-0.0016(5)	0.0006(5)
C3	0.0339(9)	0.0211(6)	0.0218(7)	-0.0006(6)	-0.0028(6)	0.0045(6)
C2	0.0231(7)	0.0193(6)	0.0228(7)	0.0005(5)	-0.0009(6)	0.0006(5)
C1	0.0384(9)	0.0223(6)	0.0232(8)	-0.0007(6)	-0.0046(7)	0.0001(6)

Table 7. Atomic coordinates and equivalent isotropic thermal parameters (\AA^2) for 1,3,3-Trinitroazetidine at room temperature (230 K). $U(\text{eq})$ is defined as one third of the trace of the orthogonalized U_{ij} tensor.

	x	y	z	$U(\text{eq})/U(\text{iso})$
O6	0.5954(2)	0.34425(11)	0.01375(5)	0.0351(3)
O5	0.5840(2)	0.47999(9)	0.08639(6)	0.0350(3)
O4	-0.0050(2)	0.26686(11)	0.11452(6)	0.0354(3)
O3	0.1031(2)	0.40553(9)	0.04919(5)	0.0301(3)
O2	0.4913(2)	-0.01170(10)	0.19164(6)	0.0348(3)
O1	0.5052(2)	0.12572(10)	0.26462(5)	0.0309(3)
N4	0.5383(2)	0.38174(10)	0.06497(6)	0.0241(2)
N3	0.1404(2)	0.32730(10)	0.08757(6)	0.0228(2)
N2	0.5059(2)	0.09277(10)	0.21015(6)	0.0236(2)
N1	0.5401(2)	0.17908(10)	0.16634(6)	0.0222(2)
H4	0.5743(3)	0.14468(11)	0.07147(7)	0.028
H3	0.5655(3)	0.36177(12)	0.18649(7)	0.03
H2	0.3098(3)	0.30696(12)	0.20158(7)	0.03
H1	0.3177(3)	0.11162(11)	0.09807(7)	0.028
C3	0.4531(3)	0.16498(11)	0.10194(7)	0.0230(3)
C2	0.3915(2)	0.29959(11)	0.10447(7)	0.0199(2)
C1	0.4476(3)	0.30215(12)	0.17463(7)	0.0252(3)

Table 8. Anisotropic displacement parameters (\AA^2) for 1,3,3-Trinitroazetidine at room temperature (230 K). The anisotropic displacement factor exponent takes the form: $-2\pi^2[(ha^*)^2U_{11} + \dots + 2hka^*b^*U_{12}]$

	U11	U22	U33	U23	U13	U12
O6	0.0362(6)	0.0440(6)	0.0250(6)	0.0037(5)	0.0066(5)	-0.0022(5)
O5	0.0372(7)	0.0223(4)	0.0455(7)	0.0018(5)	-0.0006(6)	-0.0079(4)
O4	0.0259(6)	0.0397(6)	0.0405(7)	0.0068(5)	0.0041(5)	-0.0074(5)
O3	0.0283(6)	0.0266(4)	0.0353(6)	0.0069(4)	-0.0054(5)	0.0024(4)
O2	0.0452(7)	0.0242(4)	0.0351(7)	0.0050(4)	0.0004(6)	0.0004(4)
O1	0.0287(6)	0.0442(6)	0.0198(5)	0.0049(5)	0.0001(4)	0.0004(5)
N4	0.0208(6)	0.0246(5)	0.0269(6)	0.0045(5)	-0.0023(5)	0.0003(4)
N3	0.0218(6)	0.0229(4)	0.0236(6)	-0.0017(4)	-0.0004(4)	-0.0001(4)
N2	0.0207(6)	0.0278(5)	0.0224(6)	0.0055(5)	0.0002(4)	0.0010(4)
N1	0.0260(6)	0.0217(4)	0.0189(5)	0.0032(4)	-0.0020(4)	0.0008(4)
C3	0.0311(7)	0.0190(5)	0.0187(6)	-0.0010(5)	-0.0027(5)	0.0044(5)
C2	0.0206(6)	0.0176(4)	0.0215(6)	0.0008(5)	0.0000(5)	-0.0001(4)
C1	0.0339(8)	0.0219(5)	0.0199(7)	-0.0008(5)	-0.0036(6)	-0.0001(5)

Table 9. Atomic coordinates and equivalent isotropic thermal parameters (\AA^2) for 1,3,3-Trinitroazetidine at room temperature (205 K). $U(\text{eq})$ is defined as one third of the trace of the orthogonalized U_{ij} tensor.

	x	y	z	$U(\text{eq})/U(\text{iso})$
O6	0.5949(2)	0.34413(10)	0.01345(5)	0.0309(3)
O5	0.5838(2)	0.48014(9)	0.08633(6)	0.0308(3)
O4	-0.0070(2)	0.26665(11)	0.11441(6)	0.0309(3)
O3	0.1018(2)	0.40566(9)	0.04921(5)	0.0263(2)
O2	0.4912(2)	-0.01244(9)	0.19169(6)	0.0302(3)
O1	0.5057(2)	0.12533(10)	0.26482(5)	0.0267(2)
N4	0.5382(2)	0.38156(10)	0.06482(6)	0.0209(2)
N3	0.1396(2)	0.32738(10)	0.08762(6)	0.0194(2)
N2	0.5064(2)	0.09221(10)	0.21030(6)	0.0203(2)
N1	0.5401(2)	0.17843(10)	0.16640(6)	0.0190(2)
H4	0.5740(3)	0.14442(11)	0.07143(6)	0.024
H3	0.5662(3)	0.36142(11)	0.18640(7)	0.026
H2	0.3098(3)	0.30690(11)	0.20167(7)	0.026
H1	0.3168(3)	0.11140(11)	0.09810(6)	0.024
C3	0.4526(3)	0.16477(11)	0.10197(6)	0.0197(3)
C2	0.3907(2)	0.29957(11)	0.10438(6)	0.0169(2)
C1	0.4477(3)	0.30188(11)	0.17460(7)	0.0214(3)

Table 10. Anisotropic displacement parameters (\AA^2) for 1,3,3-Trinitroazetidine at room temperature (205 K). The anisotropic displacement factor exponent takes the form: $-2\pi^2[(ha^*)^2U_{11} + \dots + 2hka^*b^*U_{12}]$

	U11	U22	U33	U23	U13	U12
O6	0.0330(6)	0.0367(6)	0.0229(5)	0.0033(5)	0.0065(5)	-0.0020(5)
O5	0.0319(6)	0.0191(4)	0.0413(7)	0.0021(4)	-0.0004(5)	-0.0071(4)
O4	0.0244(5)	0.0326(6)	0.0358(7)	0.0058(5)	0.0040(5)	-0.0066(4)
O3	0.0247(5)	0.0225(4)	0.0318(6)	0.0059(4)	-0.0050(4)	0.0032(4)
O2	0.0403(7)	0.0190(4)	0.0315(6)	0.0044(4)	0.0008(5)	0.0001(4)
O1	0.0253(5)	0.0368(6)	0.0181(5)	0.0042(4)	-0.0001(4)	-0.0002(5)
N4	0.0191(5)	0.0198(4)	0.0237(6)	0.0042(4)	-0.0018(4)	0.0005(4)
N3	0.0187(5)	0.0182(4)	0.0213(6)	-0.0015(4)	-0.0005(4)	0.0001(4)
N2	0.0182(5)	0.0211(5)	0.0216(6)	0.0052(4)	-0.0007(4)	0.0005(4)
N1	0.0225(6)	0.0175(4)	0.0169(5)	0.0027(4)	-0.0014(4)	0.0008(4)
C3	0.0269(7)	0.0155(5)	0.0166(6)	0.0000(4)	-0.0013(5)	0.0033(5)
C2	0.0185(6)	0.0146(4)	0.0175(6)	0.0009(4)	0.0000(5)	0.0000(4)
C1	0.0302(7)	0.0165(5)	0.0176(6)	-0.0012(4)	-0.0034(5)	0.0009(5)

Table 11. Atomic coordinates and equivalent isotropic thermal parameters (\AA^2) for 1,3,3-Trinitroazetidine at room temperature (180 K). $U(\text{eq})$ is defined as one third of the trace of the orthogonalized U_{ij} tensor.

	x	y	z	$U(\text{eq})/U(\text{iso})$
O6	0.5948(2)	0.34395(10)	0.01336(5)	0.0264(2)
O5	0.5838(2)	0.48007(9)	0.08638(6)	0.0264(2)
O4	-0.0085(2)	0.26673(10)	0.11454(6)	0.0259(2)
O3	0.1007(2)	0.40581(9)	0.04908(5)	0.0227(2)
O2	0.4917(2)	-0.01310(9)	0.19180(6)	0.0259(2)
O1	0.5063(2)	0.12472(10)	0.26516(5)	0.0228(2)
N4	0.5377(2)	0.38153(10)	0.06472(6)	0.0173(2)
N3	0.1379(2)	0.32740(10)	0.08757(6)	0.0172(2)
N2	0.5066(2)	0.09177(10)	0.21036(6)	0.0177(2)
N1	0.5399(2)	0.17838(10)	0.16641(5)	0.0164(2)
H4	0.5747(3)	0.14363(11)	0.07112(6)	0.021
H3	0.5664(3)	0.36197(11)	0.18687(7)	0.023
H2	0.3069(3)	0.30644(11)	0.20210(7)	0.023
H1	0.3145(3)	0.11048(11)	0.09820(6)	0.021
C3	0.4521(3)	0.16437(11)	0.10202(6)	0.0176(2)
C2	0.3904(2)	0.29929(11)	0.10438(6)	0.0144(2)
C1	0.4468(3)	0.30167(11)	0.17481(7)	0.0188(3)

Table 12. Anisotropic displacement parameters (\AA^2) for 1,3,3-Trinitroazetidine at room temperature (180 K). The anisotropic displacement factor exponent takes the form: $-2\pi^2[(h a^*)^2 U_{11} + \dots + 2 h k a^* b^* U_{12}]$

	U11	U22	U33	U23	U13	U12
O6	0.0277(6)	0.0313(5)	0.0203(5)	0.0022(4)	0.0049(4)	-0.0016(5)
O5	0.0273(6)	0.0158(4)	0.0361(6)	0.0010(4)	-0.0006(5)	-0.0062(4)
O4	0.0200(5)	0.0273(5)	0.0303(6)	0.0050(4)	0.0039(5)	-0.0050(4)
O3	0.0213(5)	0.0188(4)	0.0278(5)	0.0053(4)	-0.0042(4)	0.0026(4)
O2	0.0345(6)	0.0161(4)	0.0271(6)	0.0037(4)	0.0009(5)	-0.0003(4)
O1	0.0210(5)	0.0319(5)	0.0156(5)	0.0026(4)	-0.0003(4)	0.0002(4)
N4	0.0153(5)	0.0164(4)	0.0202(6)	0.0027(4)	-0.0014(4)	0.0003(4)
N3	0.0164(5)	0.0155(4)	0.0198(5)	-0.0012(4)	0.0000(4)	-0.0005(4)
N2	0.0164(5)	0.0181(4)	0.0184(5)	0.0039(4)	-0.0001(4)	0.0004(4)
N1	0.0195(5)	0.0152(4)	0.0145(5)	0.0011(4)	-0.0017(4)	0.0007(4)
C3	0.0241(6)	0.0128(4)	0.0158(6)	-0.0001(4)	-0.0025(5)	0.0032(4)
C2	0.0150(5)	0.0122(4)	0.0161(6)	0.0012(4)	-0.0002(4)	0.0000(4)
C1	0.0253(7)	0.0145(5)	0.0167(6)	-0.0011(4)	-0.0027(5)	-0.0001(5)

Table 13. Atomic coordinates and equivalent isotropic thermal parameters (\AA^2) for 1,3,3-Trinitroazetidine at room temperature (155 K). $U(\text{eq})$ is defined as one third of the trace of the orthogonalized U_{ij} tensor.

	x	y	z	$U(\text{eq})/U(\text{iso})$
O6	0.5942(2)	0.34386(9)	0.01310(5)	0.0229(2)
O5	0.5835(2)	0.48025(8)	0.08640(5)	0.0227(2)
O4	-0.0103(2)	0.26663(9)	0.11456(5)	0.0222(2)
O3	0.0999(2)	0.40601(8)	0.04900(5)	0.0197(2)
O2	0.4922(2)	-0.01363(8)	0.19188(5)	0.0228(2)
O1	0.5069(2)	0.12426(9)	0.26534(4)	0.0197(2)
N4	0.5374(2)	0.38142(9)	0.06462(5)	0.0150(2)
N3	0.1373(2)	0.32733(9)	0.08762(5)	0.0144(2)
N2	0.5071(2)	0.09128(9)	0.21053(5)	0.0155(2)
N1	0.5399(2)	0.17807(8)	0.16644(5)	0.0141(2)
H4	0.5735(2)	0.14322(10)	0.07083(6)	0.018
H3	0.5661(2)	0.36188(10)	0.18705(6)	0.019
H2	0.3062(2)	0.30605(10)	0.20235(6)	0.019
H1	0.3129(2)	0.11017(10)	0.09819(6)	0.018
C3	0.4509(2)	0.16406(10)	0.10189(6)	0.0149(2)
C2	0.3894(2)	0.29915(9)	0.10431(6)	0.0126(2)
C1	0.4463(2)	0.30144(10)	0.17496(6)	0.0162(2)

Table 14. Anisotropic displacement parameters (\AA^2) for 1,3,3-Trinitroazetidine at room temperature (155 K). The anisotropic displacement factor exponent takes the form: $-2\pi^2[(h a^*)^2 U_{11} + \dots + 2 h k a^* b^* U_{12}]$

	U11	U22	U33	U23	U13	U12
O6	0.0241(5)	0.0291(4)	0.0155(5)	0.0023(4)	0.0042(4)	-0.0006(4)
O5	0.0230(5)	0.0149(3)	0.0304(6)	0.0012(3)	0.0000(4)	-0.0050(3)
O4	0.0157(5)	0.0249(4)	0.0261(6)	0.0042(4)	0.0036(4)	-0.0041(3)
O3	0.0184(5)	0.0183(3)	0.0223(5)	0.0047(3)	-0.0038(4)	0.0019(3)
O2	0.0294(6)	0.0157(3)	0.0232(5)	0.0024(3)	0.0000(4)	-0.0007(3)
O1	0.0184(5)	0.0292(4)	0.0117(4)	0.0018(3)	0.0005(4)	0.0001(4)
N4	0.0119(5)	0.0158(3)	0.0174(5)	0.0030(3)	-0.0012(4)	0.0005(3)
N3	0.0132(5)	0.0146(3)	0.0154(5)	-0.0013(3)	0.0001(4)	0.0001(3)
N2	0.0130(5)	0.0181(4)	0.0155(5)	0.0035(4)	-0.0006(4)	0.0006(3)
N1	0.0162(5)	0.0142(3)	0.0120(4)	0.0023(3)	-0.0007(4)	0.0009(3)
C3	0.0192(6)	0.0130(4)	0.0124(5)	-0.0003(3)	-0.0027(4)	0.0019(4)
C2	0.0120(5)	0.0133(3)	0.0126(5)	0.0003(3)	-0.0005(4)	-0.0003(3)
C1	0.0210(6)	0.0139(4)	0.0137(5)	-0.0007(4)	-0.0021(4)	0.0002(4)

Table 15. Atomic coordinates and equivalent isotropic thermal parameters (\AA^2) for 1,3,3-Trinitroazetidine at room temperature (130 K). $U(\text{eq})$ is defined as one third of the trace of the orthogonalized U_{ij} tensor.

	x	y	z	$U(\text{eq})/U(\text{iso})$
O6	0.5941(2)	0.34364(8)	0.01291(4)	0.0192(2)
O5	0.5840(2)	0.48021(7)	0.08648(5)	0.0192(2)
O4	-0.0116(2)	0.26658(8)	0.11456(5)	0.0194(2)
O3	0.0988(2)	0.40613(7)	0.04902(4)	0.0164(2)
O2	0.4925(2)	-0.01409(7)	0.19187(5)	0.0190(2)
O1	0.5075(2)	0.12373(8)	0.26549(4)	0.0165(2)
N4	0.5374(2)	0.38128(8)	0.06453(5)	0.0130(2)
N3	0.1359(2)	0.32724(8)	0.08756(5)	0.0123(2)
N2	0.5072(2)	0.09079(8)	0.21063(5)	0.0128(2)
N1	0.5396(2)	0.17771(8)	0.16647(5)	0.0117(2)
H4	0.5737(2)	0.14287(9)	0.07093(5)	0.016
H3	0.5665(2)	0.36179(9)	0.18708(6)	0.017
H2	0.3061(2)	0.30614(9)	0.20253(6)	0.017
H1	0.3126(2)	0.10964(9)	0.09830(5)	0.016
C3	0.4508(2)	0.16365(9)	0.10202(5)	0.0132(2)
C2	0.3888(2)	0.29914(9)	0.10448(5)	0.0110(2)
C1	0.4462(2)	0.30140(9)	0.17505(6)	0.0139(2)

Table 16. Anisotropic displacement parameters (\AA^2) for 1,3,3-Trinitroazetidine at room temperature (130 K). The anisotropic displacement factor exponent takes the form: $-2\pi^2[(h a^*)^2 U_{11} + \dots + 2 h k a^* b^* U_{12}]$

	U11	U22	U33	U23	U13	U12
O6	0.0207(4)	0.0234(4)	0.0135(4)	0.0010(3)	0.0025(3)	-0.0008(3)
O5	0.0200(4)	0.0110(3)	0.0267(5)	-0.0003(3)	-0.0008(4)	-0.0040(3)
O4	0.0147(4)	0.0199(4)	0.0235(5)	0.0038(3)	0.0033(3)	-0.0043(3)
O3	0.0161(4)	0.0134(3)	0.0198(4)	0.0047(3)	-0.0032(3)	0.0020(3)
O2	0.0249(5)	0.0112(3)	0.0210(5)	0.0019(3)	0.0004(4)	0.0000(3)
O1	0.0151(4)	0.0231(4)	0.0115(4)	0.0015(3)	0.0001(3)	0.0004(3)
N4	0.0112(4)	0.0125(3)	0.0152(4)	0.0023(3)	-0.0007(3)	0.0003(3)
N3	0.0117(4)	0.0113(3)	0.0138(4)	-0.0008(3)	-0.0002(3)	0.0002(3)
N2	0.0106(4)	0.0134(3)	0.0143(4)	0.0030(3)	-0.0003(3)	0.0008(3)
N1	0.0139(4)	0.0107(3)	0.0106(4)	0.0015(3)	-0.0010(3)	0.0002(3)
C3	0.0181(5)	0.0095(3)	0.0119(5)	-0.0009(3)	-0.0019(4)	0.0022(3)
C2	0.0115(4)	0.0094(3)	0.0121(4)	0.0009(3)	0.0002(4)	-0.0004(3)
C1	0.0173(5)	0.0110(3)	0.0132(5)	-0.0009(3)	-0.0022(4)	0.0010(3)

Table 17. Atomic coordinates and equivalent isotropic thermal parameters (\AA^2) for 1,3,3-Trinitroazetidine at room temperature (105 K). $U(\text{eq})$ is defined as one third of the trace of the orthogonalized U_{ij} tensor.

	x	y	z	$U(\text{eq})/U(\text{iso})$
O6	0.59385(15)	0.34350(7)	0.01276(4)	0.0163(2)
O5	0.5837(2)	0.48025(6)	0.08648(4)	0.0163(2)
O4	-0.01295(15)	0.26639(7)	0.11452(4)	0.0162(2)
O3	0.09801(15)	0.40636(6)	0.04892(4)	0.01405(15)
O2	0.4931(2)	-0.01470(7)	0.19196(4)	0.0159(2)
O1	0.50767(14)	0.12334(7)	0.26579(4)	0.01409(14)
N4	0.5375(2)	0.38113(7)	0.06451(4)	0.01119(15)
N3	0.1353(2)	0.32724(7)	0.08752(4)	0.01084(14)
N2	0.5077(2)	0.09041(7)	0.21062(4)	0.01095(14)
N1	0.5400(2)	0.17738(7)	0.16653(4)	0.01052(14)
H4	0.5734(2)	0.14268(8)	0.07069(5)	0.014
H3	0.5660(2)	0.36168(8)	0.18728(5)	0.015
H2	0.3054(2)	0.30565(8)	0.20268(5)	0.015
H1	0.3120(2)	0.10938(8)	0.09819(5)	0.014
C3	0.4505(2)	0.16344(8)	0.10188(5)	0.0113(2)
C2	0.3884(2)	0.29897(8)	0.10438(5)	0.0096(2)
C1	0.4458(2)	0.30112(8)	0.17517(5)	0.0123(2)

Table 18. Anisotropic displacement parameters (\AA^2) for 1,3,3-Trinitroazetidine at room temperature (105 K). The anisotropic displacement factor exponent takes the form: $-2\pi^2[(h a^*)^2 U_{11} + \dots + 2 h k a^* b^* U_{12}]$

	U11	U22	U33	U23	U13	U12
O6	0.0175(4)	0.0200(3)	0.0114(4)	0.0006(3)	0.0026(3)	-0.0005(3)
O5	0.0163(4)	0.0099(2)	0.0229(4)	-0.0003(3)	-0.0004(3)	-0.0030(3)
O4	0.0129(4)	0.0175(3)	0.0184(4)	0.0029(3)	0.0028(3)	-0.0036(3)
O3	0.0144(4)	0.0116(3)	0.0162(4)	0.0034(3)	-0.0027(3)	0.0014(2)
O2	0.0209(4)	0.0095(2)	0.0174(4)	0.0009(3)	0.0002(3)	-0.0001(3)
O1	0.0131(3)	0.0200(3)	0.0091(3)	0.0010(3)	0.0004(3)	0.0001(3)
N4	0.0100(3)	0.0109(3)	0.0127(4)	0.0019(3)	-0.0008(3)	0.0001(3)
N3	0.0107(3)	0.0099(3)	0.0119(4)	-0.0009(3)	0.0002(3)	-0.0004(3)
N2	0.0091(3)	0.0117(3)	0.0120(4)	0.0022(3)	-0.0004(3)	0.0000(3)
N1	0.0127(4)	0.0099(3)	0.0089(4)	0.0011(2)	-0.0010(3)	0.0007(3)
C3	0.0147(4)	0.0091(3)	0.0101(4)	-0.0005(3)	-0.0017(3)	0.0018(3)
C2	0.0102(4)	0.0086(3)	0.0102(4)	0.0008(3)	0.0003(3)	-0.0005(3)
C1	0.0162(4)	0.0097(3)	0.0109(4)	-0.0008(3)	-0.0019(3)	0.0007(3)

Table 19. Atomic coordinates and equivalent isotropic thermal parameters (\AA^2) for 1,3,3-Trinitroazetidine at room temperature (90 K). $U(\text{eq})$ is defined as one third of the trace of the orthogonalized U_{ij} tensor.

	x	y	z	$U(\text{eq})/U(\text{iso})$
O6	0.59371(8)	0.34347(4)	0.012725(18)	0.01416(6)
O5	0.58391(8)	0.48025(3)	0.08647(2)	0.01399(6)
O4	-0.01380(7)	0.26636(4)	0.11460(2)	0.01385(6)
O3	0.09734(7)	0.40639(3)	0.048905(18)	0.01225(6)
O2	0.49316(8)	-0.01500(3)	0.191984(19)	0.01411(7)
O1	0.50817(7)	0.12307(4)	0.265819(16)	0.01232(6)
N4	0.53733(7)	0.38110(3)	0.064446(19)	0.00952(6)
N3	0.13437(7)	0.32727(3)	0.087585(18)	0.00914(6)
N2	0.50772(7)	0.09021(3)	0.210729(18)	0.00936(6)
N1	0.53938(8)	0.17724(3)	0.166618(17)	0.00916(6)
H4	0.5734	0.1425	0.0708	0.012
H3	0.5663	0.3614	0.1873	0.013
H2	0.3052	0.3057	0.2027	0.013
H1	0.3116	0.1093	0.0982	0.012
C3	0.45021(9)	0.16328(4)	0.10193(2)	0.00979(6)
C2	0.38817(8)	0.29884(3)	0.10443(2)	0.00818(6)
C1	0.44571(9)	0.30097(4)	0.17519(2)	0.01045(7)

Table 20. Anisotropic displacement parameters (\AA^2) for 1,3,3-Trinitroazetidine at room temperature (90 K). The anisotropic displacement factor exponent takes the form: $-2\pi^2[(h a^*)^2 U_{11} + \dots + 2 h k a^* b^* U_{12}]$

	U11	U22	U33	U23	U13	U12
O6	0.01517(16)	0.01781(14)	0.00951(12)	0.00063(10)	0.00242(11)	-0.00044(12)
O5	0.01436(16)	0.00936(11)	0.01825(15)	-0.00002(10)	-0.00001(12)	-0.00264(10)
O4	0.01053(14)	0.01539(13)	0.01562(15)	0.00278(11)	0.00222(11)	-0.00279(10)
O3	0.01247(15)	0.01110(11)	0.01318(13)	0.00314(10)	-0.00217(11)	0.00136(10)
O2	0.01878(17)	0.00932(11)	0.01422(14)	0.00138(10)	-0.00007(12)	-0.00030(11)
O1	0.01149(14)	0.01795(14)	0.00752(11)	0.00092(10)	0.00025(10)	0.00010(11)
N4	0.00844(14)	0.00977(11)	0.01035(13)	0.00146(9)	-0.00034(10)	-0.00019(10)
N3	0.00862(14)	0.00926(11)	0.00954(12)	-0.00010(9)	-0.00025(10)	0.00003(10)
N2	0.00828(13)	0.01081(11)	0.00900(12)	0.00189(9)	-0.00010(10)	0.00027(10)
N1	0.01085(14)	0.00912(11)	0.00751(11)	0.00110(9)	-0.00069(10)	0.00049(10)
C3	0.01278(17)	0.00835(12)	0.00824(13)	-0.00018(10)	-0.00119(12)	0.00130(11)
C2	0.00859(15)	0.00805(12)	0.00789(12)	0.00036(9)	-0.00051(11)	0.00005(10)
C1	0.01366(18)	0.00938(13)	0.00830(13)	-0.00069(10)	-0.00133(12)	0.00052(11)

Table 21. Bond lengths (Å) and angles (°) of 1,3,3-Trinitroazetidine at various temperatures.

At 305 K:

N1	N2	1.361(3)	
N1	C3	1.475(3)	
N1	C1	1.477(3)	
N2	O1	1.224(3)	
N2	O2	1.227(3)	
N3	O3	1.208(3)	
N3	O4	1.216(3)	
N4	O5	1.211(3)	
N4	O6	1.212(3)	
C1	C2	1.537(3)	
C2	N4	1.501(3)	
C2	N3	1.520(3)	
C2	C3	1.540(3)	
N2	N1	C3	121.32(19)
N2	N1	C1	121.2(2)
C3	N1	C1	95.23(17)
O1	N2	O2	126.3(2)
O1	N2	N1	116.5(2)
O2	N2	N1	117.1(2)
O3	N3	O4	126.5(2)
O3	N3	C2	118.28(19)
O4	N3	C2	115.2(2)
O5	N4	O6	126.0(2)
O5	N4	C2	116.8(2)
O6	N4	C2	117.2(2)
N1	C1	C2	86.54(16)
N3	C2	C1	115.0(2)
N3	C2	C3	113.70(18)
N4	C2	N3	105.76(17)
N4	C2	C1	115.62(19)
N4	C2	C3	116.4(2)
C1	C2	C3	90.26(16)
N1	C3	C2	86.50(16)

At 280 K:

N1	N2	1.359(2)	
N1	C1	1.478(2)	
N1	C3	1.479(2)	
N2	O1	1.221(2)	
N2	O2	1.230(2)	
N3	O3	1.211(2)	
N3	O4	1.217(2)	
N4	O6	1.213(2)	
N4	O5	1.214(2)	
C1	C2	1.540(2)	
C2	N4	1.505(2)	
C2	N3	1.514(2)	
C2	C3	1.538(2)	
N2	N1	C1	121.06(14)
N2	N1	C3	121.74(14)
C1	N1	C3	95.08(12)
O1	N2	O2	126.3(2)
O1	N2	N1	116.7(2)
O2	N2	N1	116.8(2)
O3	N3	O4	126.6(2)
O3	N3	C2	118.45(14)
O4	N3	C2	114.94(14)
O6	N4	O5	126.4(2)
O6	N4	C2	117.00(15)
O5	N4	C2	116.6(2)
N1	C1	C2	86.64(12)
N4	C2	N3	105.73(13)
N4	C2	C3	116.12(14)
N3	C2	C3	114.04(13)
N4	C2	C1	115.24(14)
N3	C2	C1	115.44(14)
C3	C2	C1	90.25(13)
N1	C3	C2	86.67(12)

At 255K:

N1	N2	1.360(2)	
N1	C1	1.476(2)	
N1	C3	1.477(2)	
N2	O1	1.224(2)	
N2	O2	1.228(2)	
N3	O3	1.216(2)	
N3	O4	1.216(2)	
N4	O5	1.213(2)	
N4	O6	1.215(2)	
C1	C2	1.540(2)	
C2	N4	1.507(2)	
C2	N3	1.512(2)	
C2	C3	1.534(2)	
N2	N1	C1	121.25(13)
N2	N1	C3	121.66(13)
C1	N1	C3	95.01(11)
O1	N2	O2	126.16(15)
O1	N2	N1	116.73(14)
O2	N2	N1	116.99(14)
O3	N3	O4	126.30(15)
O3	N3	C2	118.40(13)
O4	N3	C2	115.30(13)
O5	N4	O6	126.35(15)
O5	N4	C2	116.79(14)
O6	N4	C2	116.84(13)
N1	C1	C2	86.65(11)
N4	C2	N3	105.85(12)
N4	C2	C3	116.21(13)
N3	C2	C3	114.23(12)
N4	C2	C1	115.02(13)
N3	C2	C1	115.32(13)
C3	C2	C1	90.16(11)
N1	C3	C2	86.83(11)

At 230 K:

N1	N2	1.358(2)	
N1	C3	1.478(2)	
N1	C1	1.478(2)	
N2	O1	1.225(2)	
N2	O2	1.231(2)	
N3	O4	1.216(2)	
N3	O3	1.217(2)	
N4	O5	1.2139(15)	
N4	O6	1.221(2)	
C1	C2	1.541(2)	
C2	N4	1.503(2)	
C2	N3	1.514(2)	
C2	C3	1.539(2)	
N2	N1	C3	121.62(11)
N2	N1	C1	121.27(12)
C3	N1	C1	95.16(10)
O1	N2	O2	126.17(13)
O1	N2	N1	116.74(12)
O2	N2	N1	116.96(13)
O4	N3	O3	126.62(13)
O4	N3	C2	115.06(11)
O3	N3	C2	118.32(11)
O5	N4	O6	126.20(13)
O5	N4	C2	116.99(13)
O6	N4	C2	116.78(12)
N1	C1	C2	86.56(10)
N4	C2	N3	105.80(10)
N4	C2	C3	116.27(11)
N3	C2	C3	114.04(11)
N4	C2	C1	115.06(11)
N3	C2	C1	115.37(12)
C3	C2	C1	90.26(10)
N1	C3	C2	86.63(9)

At 205K:

N1	N2	1.356(2)	
N1	C3	1.476(2)	
N1	C1	1.480(2)	
N2	O1	1.225(2)	
N2	O2	1.232(2)	
N3	O3	1.217(2)	
N3	O4	1.219(2)	
N4	O5	1.2165(15)	
N4	O6	1.221(2)	
C1	C2	1.540(2)	
C2	N4	1.503(2)	
C2	N3	1.511(2)	
C2	C3	1.540(2)	
N2	N1	C3	121.89(11)
N2	N1	C1	121.43(12)
C3	N1	C1	94.91(10)
O1	N2	O2	126.30(13)
O1	N2	N1	116.75(12)
O2	N2	N1	116.85(12)
O3	N3	O4	126.33(13)
O3	N3	C2	118.39(11)
O4	N3	C2	115.28(11)
O5	N4	O6	126.27(13)
O5	N4	C2	116.87(12)
O6	N4	C2	116.82(11)
N1	C1	C2	86.79(9)
N4	C2	N3	105.91(10)
N4	C2	C3	116.21(11)
N3	C2	C3	114.16(11)
N4	C2	C1	115.01(11)
N3	C2	C1	115.46(11)
C3	C2	C1	90.02(10)
N1	C3	C2	86.93(9)

At 180 K:

N1	N2	1.359(2)	
N1	C3	1.475(2)	
N1	C1	1.479(2)	
N2	O1	1.229(2)	
N2	O2	1.233(2)	
N3	O3	1.218(2)	
N3	O4	1.218(2)	
N4	O5	1.2170(15)	
N4	O6	1.221(2)	
C1	C2	1.542(2)	
C2	N4	1.503(2)	
C2	N3	1.517(2)	
C2	C3	1.539(2)	
N2	N1	C3	121.70(11)
N2	N1	C1	121.38(11)
C3	N1	C1	95.13(10)
O1	N2	O2	126.06(13)
O1	N2	N1	116.80(11)
O2	N2	N1	117.03(12)
O3	N3	O4	126.63(13)
O3	N3	C2	118.27(11)
O4	N3	C2	115.10(11)
O5	N4	O6	126.37(13)
O5	N4	C2	116.84(12)
O6	N4	C2	116.76(11)
N1	C1	C2	86.56(9)
N4	C2	N3	105.74(10)
N4	C2	C3	116.41(11)
N3	C2	C3	114.17(10)
N4	C2	C1	115.18(11)
N3	C2	C1	115.24(11)
C3	C2	C1	90.07(9)
N1	C3	C2	86.80(9)

At 155K:

N1	N2	1.3599(14)	
N1	C3	1.478(2)	
N1	C1	1.4791(15)	
N2	O1	1.227(2)	
N2	O2	1.2324(13)	
N3	O3	1.2198(14)	
N3	O4	1.2204(14)	
N4	O5	1.2190(13)	
N4	O6	1.221(2)	
C1	C2	1.545(2)	
C2	N4	1.504(2)	
C2	N3	1.510(2)	
C2	C3	1.539(2)	
N2	N1	C3	121.72(10)
N2	N1	C1	121.30(10)
C3	N1	C1	95.11(9)
O1	N2	O2	126.15(11)
O1	N2	N1	116.80(10)
O2	N2	N1	116.93(11)
O3	N3	O4	126.42(12)
O3	N3	C2	118.26(10)
O4	N3	C2	115.31(10)
O5	N4	O6	126.47(11)
O5	N4	C2	116.75(11)
O6	N4	C2	116.75(10)
N1	C1	C2	86.54(8)
N4	C2	N3	105.84(9)
N4	C2	C3	116.37(10)
N3	C2	C3	114.16(9)
N4	C2	C1	115.12(10)
N3	C2	C1	115.24(10)
C3	C2	C1	90.07(8)
N1	C3	C2	86.80(8)

At 130 K:

N1	N2	1.3603(13)	
N1	C3	1.474(2)	
N1	C1	1.4806(14)	
N2	O1	1.2270(14)	
N2	O2	1.2318(12)	
N3	O4	1.2186(13)	
N3	O3	1.2189(13)	
N4	O5	1.2209(12)	
N4	O6	1.2217(14)	
C1	C2	1.542(2)	
C2	N4	1.5057(14)	
C2	N3	1.5128(15)	
C2	C3	1.5427(14)	
N2	N1	C3	121.75(9)
N2	N1	C1	121.38(9)
C3	N1	C1	95.21(8)
O1	N2	O2	126.23(10)
O1	N2	N1	116.82(9)
O2	N2	N1	116.83(10)
O4	N3	O3	126.58(10)
O4	N3	C2	115.20(9)
O3	N3	C2	118.23(9)
O5	N4	O6	126.56(10)
O5	N4	C2	116.51(10)
O6	N4	C2	116.90(9)
N1	C1	C2	86.55(8)
N4	C2	N3	105.80(8)
N4	C2	C1	115.18(9)
N3	C2	C1	115.50(9)
N4	C2	C3	116.15(9)
N3	C2	C3	114.12(8)
C1	C2	C3	90.05(8)
N1	C3	C2	86.76(8)

At 105K:

N1	N2	1.3579(12)
N1	C3	1.4768(14)
N1	C1	1.4814(13)
N2	O1	1.2313(12)
N2	O2	1.2322(11)
N3	O3	1.2202(11)
N3	O4	1.2210(12)
N4	O5	1.2213(11)
N4	O6	1.2219(13)
C1	C2	1.5443(15)
C2	N4	1.5042(13)
C2	N3	1.5113(14)
C2	C3	1.5416(13)

N2	N1	C3	121.72(8)
N2	N1	C1	121.38(9)
C3	N1	C1	95.10(7)
O1	N2	O2	126.00(9)
O1	N2	N1	116.84(8)
O2	N2	N1	117.05(9)
O3	N3	O4	126.50(10)
O3	N3	C2	118.25(8)
O4	N3	C2	115.25(8)
O5	N4	O6	126.60(9)
O5	N4	C2	116.55(9)
O6	N4	C2	116.81(8)
N1	C1	C2	86.57(7)
N4	C2	N3	105.87(7)
N4	C2	C3	116.13(8)
N3	C2	C3	114.21(8)
N4	C2	C1	115.12(8)
N3	C2	C1	115.42(8)
C3	C2	C1	90.03(7)
N1	C3	C2	86.83(7)

At 90K:

N1	N2	1.3583(6)	
N1	C3	1.4770(6)	
N1	C1	1.4801(6)	
N2	O1	1.2297(6)	
N2	O2	1.2341(6)	
N3	O4	1.2208(6)	
N3	O3	1.2212(5)	
N4	O6	1.2214(6)	
N4	O5	1.2226(6)	
C1	C2	1.5439(7)	
C2	N4	1.5064(6)	
C2	N3	1.5145(7)	
C2	C3	1.5422(6)	
N2	N1	C3	121.82(4)
N2	N1	C1	121.57(4)
C3	N1	C1	95.15(3)
O1	N2	O2	126.06(4)
O1	N2	N1	116.83(4)
O2	N2	N1	117.00(4)
O4	N3	O3	126.64(5)
O4	N3	C2	115.19(4)
O3	N3	C2	118.17(4)
O6	N4	O5	126.63(4)
O6	N4	C2	116.83(4)
O5	N4	C2	116.51(4)
N1	C1	C2	86.61(3)
N4	C2	N3	105.80(3)
N4	C2	C3	116.16(4)
N3	C2	C3	114.22(3)
N4	C2	C1	115.18(4)
N3	C2	C1	115.39(4)
C3	C2	C1	90.03(3)
N1	C3	C2	86.78(3)

Contract No. N00014-95-1-0013 and N00014-97-1-0409

Program Officer: R. Miller/J. Goldwasser

**Title: Experimental Charge Densities and Electrostatic Potentials in Energetic
Materials and Infrastructure Upgrade for an X-ray Crystallography
Laboratory**

PI: A. Alan Pinkerton

Department of Chemistry, University of Toledo, Toledo, OH 43606

tel. (419) 530-4580, FAX (419) 530-4033, email apinker@uoft02.utoledo.edu

APPENDIX 3i

Variable temperature crystallographic study of TDAP

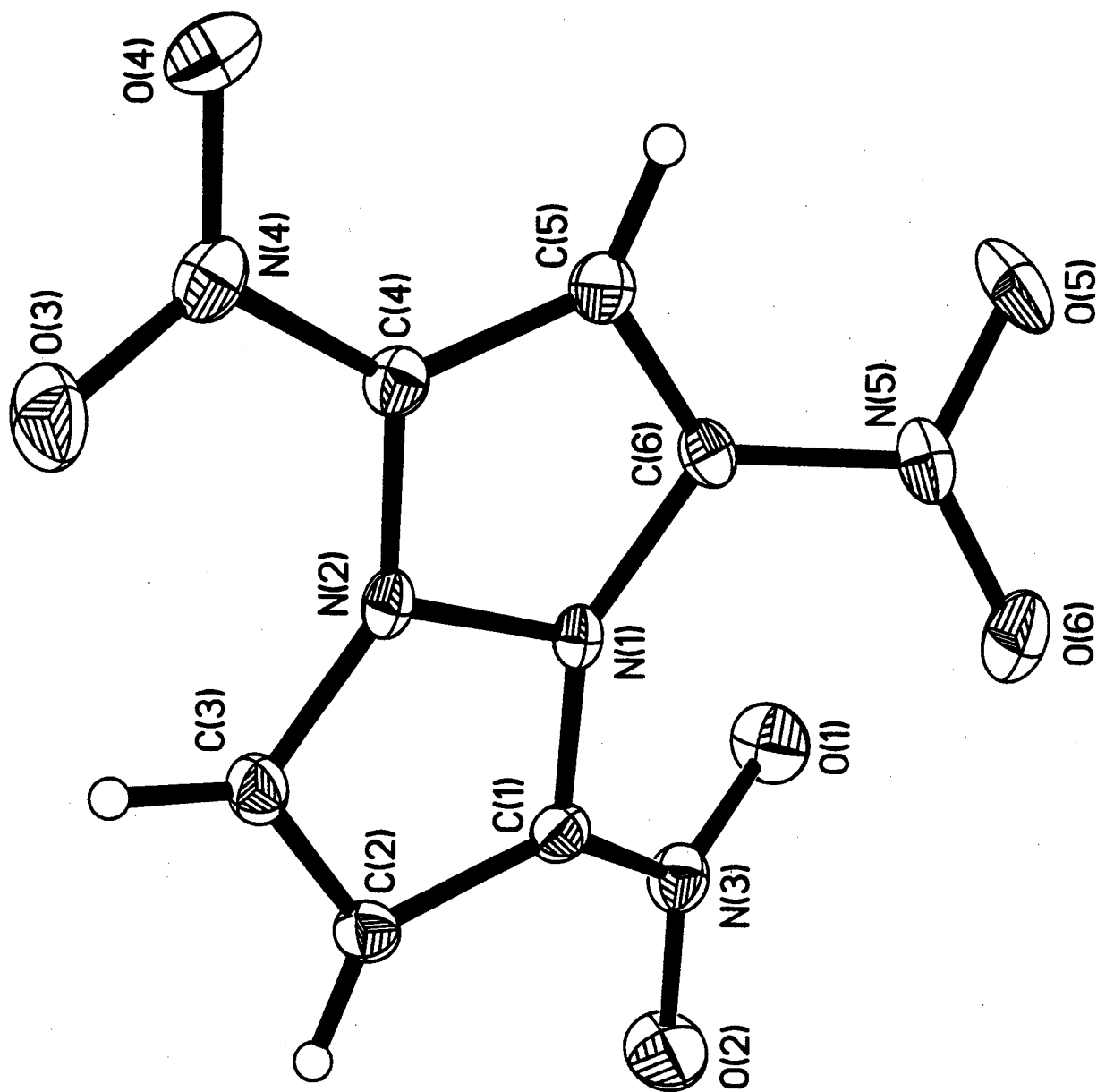


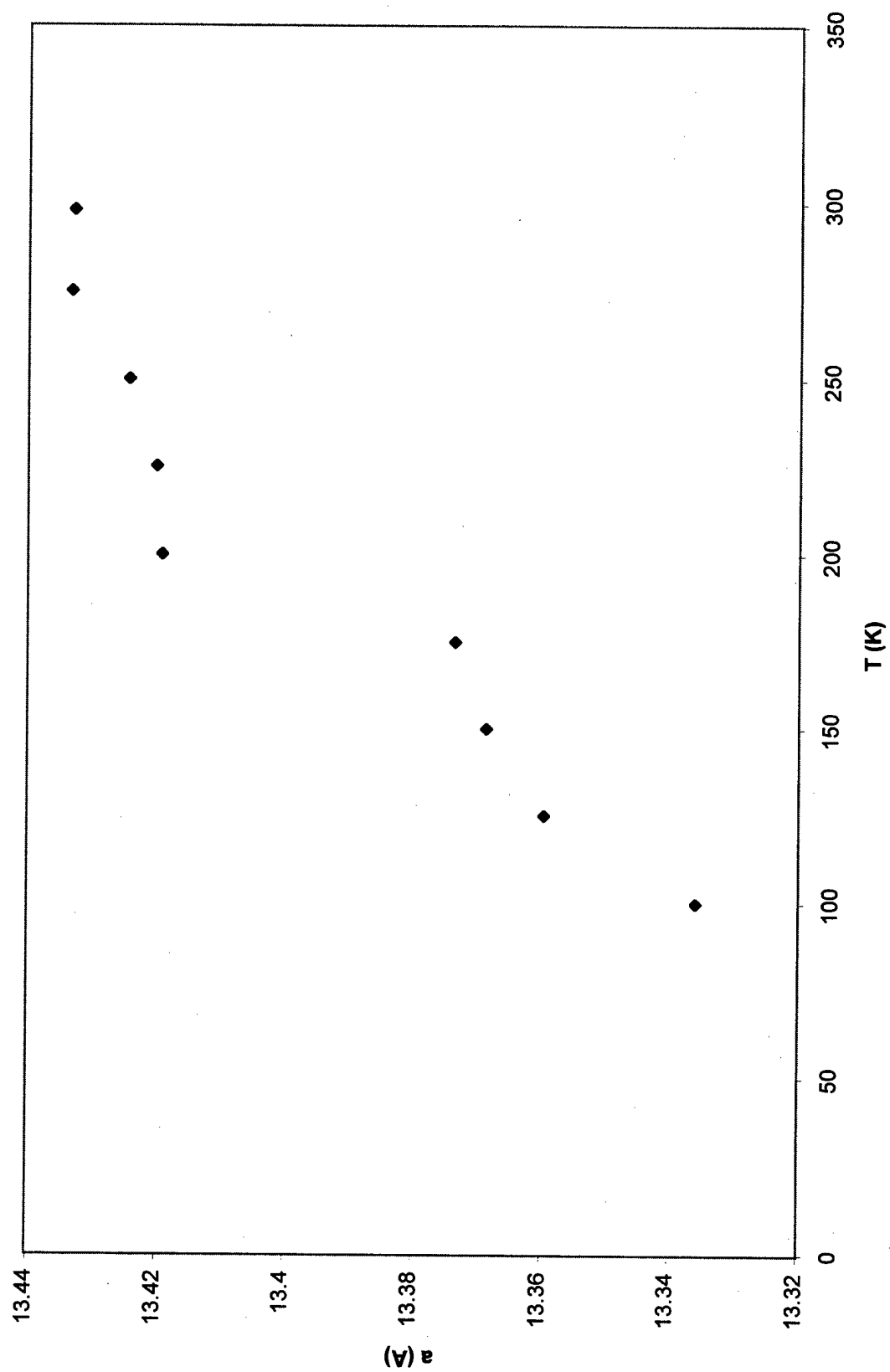
Table 1. Crystal data and structure refinement for trinitrodiazapentalene at various temperatures.

Empirical formula	$C_6H_3N_5O_6$									
Formula weight	241.13									
Wavelength	0.71073 Å									
Crystal system	Orthorhombic									
Space group	Pca2(1)									
F(000)	488									
Crystal size	0.25 x 0.20 x 0.15 mm									
Z	4									
Instrument	Siemens SMART CCD									
Detector distance	4.9640 cm									
Scan width and axis	-0.3° in ω									
Refinement method	Full-matrix least-squares on F ²									
Temperature (K)	298(1)	275(1)	250(1)	225(1)	200(1)	175(1)	150(1)	125(1)	100(1)	
a (Å)	13.4330(2)	13.4334(4)	13.4244(7)	13.4201(3)	13.4192(4)	13.3735(1)	13.3686(1)	13.3596(6)	13.3358(7)	
b (Å)	7.0275(2)	7.02620(10)	7.0266(4)	7.0274(3)	7.0299(2)	7.01030(1)	7.0100(2)	7.0106(3)	7.0022(4)	
c (Å)	9.4914(3)	9.4823(3)	9.4665(5)	9.4559(4)	9.4452(3)	9.4062(2)	9.3941(2)	9.3820(5)	9.3589(5)	
α (°)	90.00	90.00	90.00	90.00	90.00	90.00	90.00	90.00	90.00	
β (°)	90.00	90.00	90.00	90.00	90.00	90.00	90.00	90.00	90.00	
γ (°)	90.00	90.00	90.00	90.00	90.00	90.00	90.00	90.00	90.00	
Volume (Å ³)	895.99(4)	894.99(4)	892.95(8)	891.77(6)	891.02(5)	881.85(2)	880.36(3)	878.71(7)	873.93(8)	
Density (calc) (Mg/m ³)	1.788	1.790	1.794	1.796	1.798	1.816	1.819	1.823	1.833	
Absorption coeff. (mm ⁻¹)	0.162	0.163	0.163	0.163	0.163	0.165	0.165	0.166	0.167	
θ range	2.90–29.67	2.90–29.68	2.90–29.68	2.90–29.68	2.90–29.68	2.91–29.78	2.91–29.79	2.91–29.83	2.91–29.83	
Limiting indices	-18–16	-18–16	-18–16	-18–16	-18–16	-18–16	-18–16	-18–16	-18–16	
	-9–7	-9–7	-9–7	-9–7	-9–7	-9–7	-9–7	-9–7	-9–7	
	-12–12	-12–12	-12–12	-12–12	-12–12	-12–12	-12–12	-12–12	-12–12	
Reflections collected	5947	5956	5966	5953	5930	5903	5876	5840	5971	
Independent reflections	2292	2294	2293	2280	2271	2275	2263	2250	2245	
R _{int}	0.0370	0.0364	0.0305	0.0309	0.0330	0.0283	0.0292	0.0275	0.0333	
Data/restraints/parameters	2292/1/166	2294/1/166	2293/1/166	2280/1/166	2271/1/166	2275/1/166	2263/1/166	2250/1/166	2245/1/166	
Goodness-of-fit on F ²	1.186	1.032	1.039	1.047	1.037	1.056	1.052	1.067	1.044	
R1 [I>2 σ (I)]	0.0481	0.0417	0.0398	0.0381	0.0381	0.0367	0.0337	0.0333	0.0355	
wR2 [I>2 σ (I)]	0.1027	0.0892	0.0851	0.0818	0.0849	0.0834	0.0787	0.0794	0.0864	
R1 (all data)	0.0656	0.0633	0.0568	0.0526	0.0470	0.0442	0.0398	0.0385	0.0396	
wR2 (all data)	0.1145	0.0997	0.0931	0.0892	0.0903	0.0879	0.0826	0.0824	0.0896	
Largest diff. peak (eÅ ⁻³)	0.284	0.222	0.168	0.211	0.245	0.189	0.240	0.229	0.273	
Largest diff. hole (eÅ ⁻³)	-0.266	-0.215	-0.227	-0.239	-0.182	-0.270	-0.251	-0.275	-0.309	

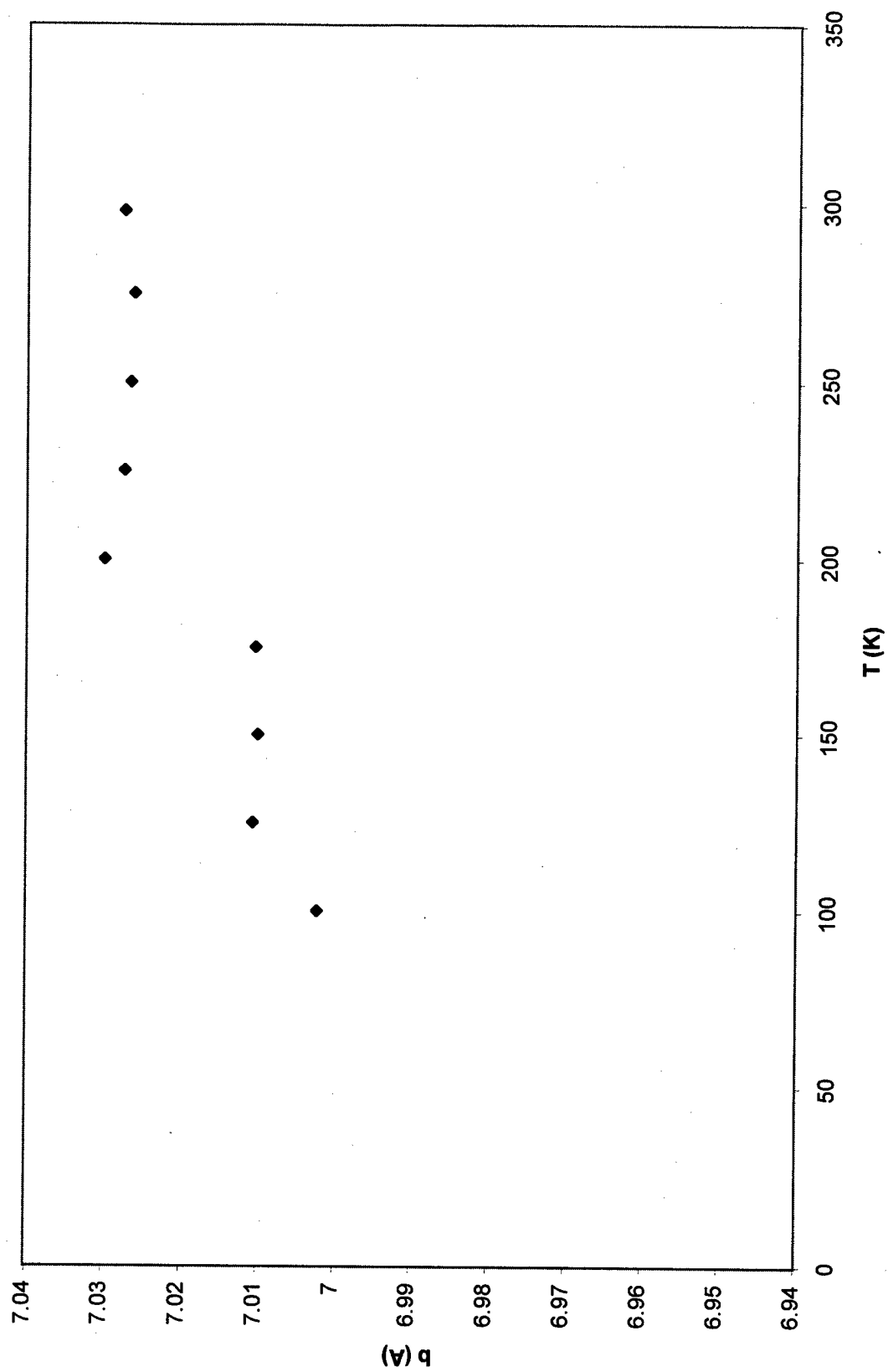
Table 15. Unit cell parameters for variable temperature structure determinations of trinitrodiazapentalene .

T (K)	<i>a</i> (Å)	<i>b</i> (Å)	<i>c</i> (Å)	volume (Å ³)
298	13.4330(2)	7.0275(2)	9.4914(3)	895.99(4)
275	13.4334(4)	7.02620(10)	9.4823(3)	894.99(4)
250	13.4244(7)	7.0266(4)	9.4665(5)	892.95(8)
225	13.4201(3)	7.0274(3)	9.4559(4)	891.77(6)
200	13.4192(4)	7.0299(2)	9.4452(3)	891.02(5)
175	13.3735(1)	7.01030(1)	9.4062(2)	881.85(2)
150	13.3686(1)	7.0100(2)	9.3941(2)	880.36(3)
125	13.3596(6)	7.0106(3)	9.3820(5)	878.71(7)
100	13.3358(7)	7.0022(4)	9.3589(5)	873.93(8)

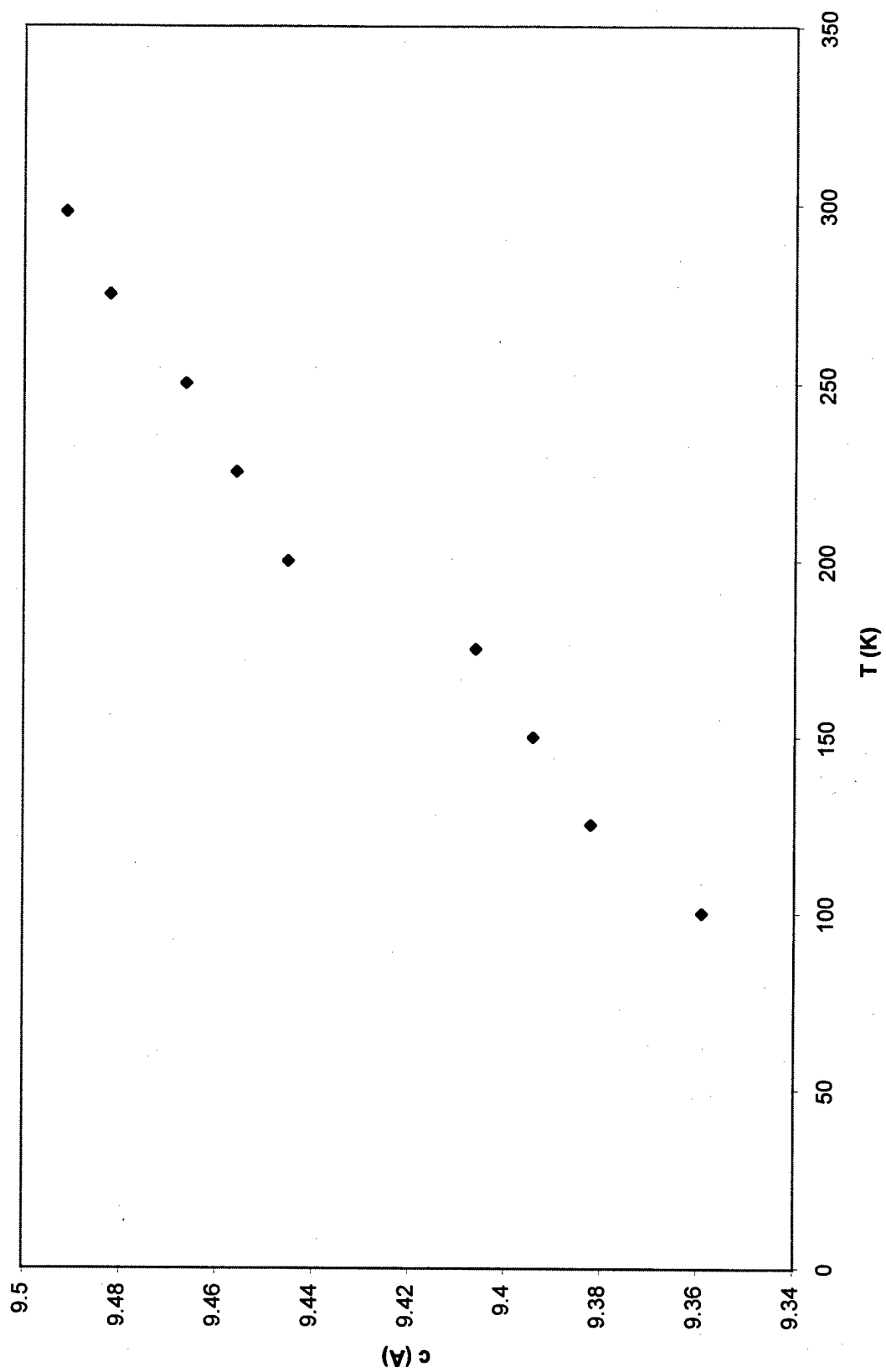
a vs T



b vs T

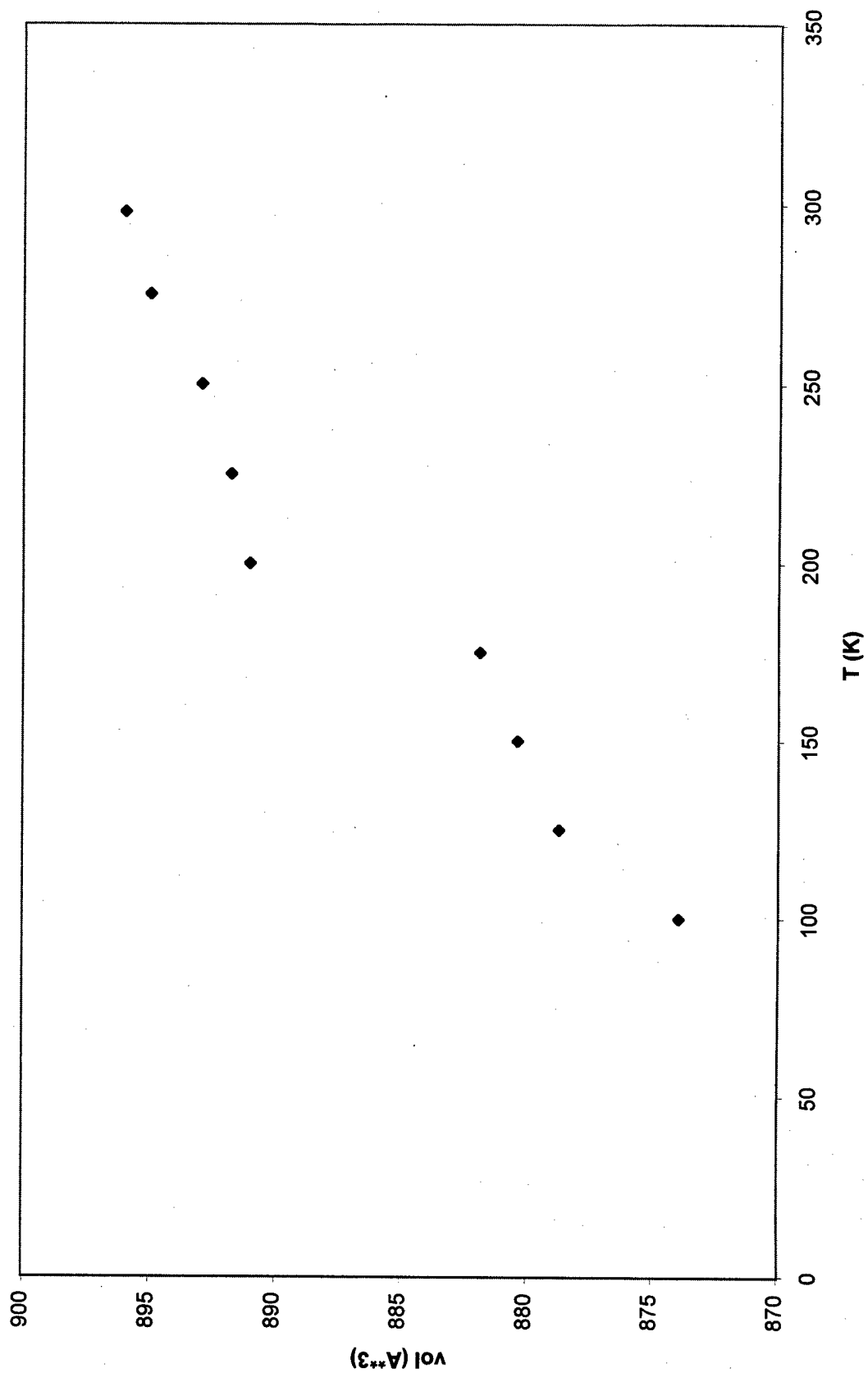


c vs T



◆ c axis

vol vs T



◆ vol

Table 1. Atomic coordinates and equivalent isotropic thermal parameters (\AA^2) for trinitrodiazapentalene at room temperature (298 K). $U(\text{eq})$ is defined as one third of the trace of the orthogonalized U_{ij} tensor.

	x	y	z	$U(\text{eq})/U(\text{iso})$
O6	0.36089(15)	0.2696(4)	0.5859(3)	0.0671(7)
O5	0.36010(17)	0.5784(4)	0.5844(3)	0.0696(8)
O4	0.00444(19)	0.7160(3)	0.8626(3)	0.0594(6)
O3	-0.05929(17)	0.4312(4)	0.8806(3)	0.0627(7)
O2	0.2061(2)	-0.1297(4)	0.3997(4)	0.0809(9)
O1	0.2551(2)	0.1623(3)	0.3764(3)	0.0618(6)
N5	0.31874(16)	0.4236(4)	0.5951(2)	0.0453(6)
N4	0.0022(2)	0.5448(4)	0.8357(2)	0.0443(6)
N3	0.20893(17)	0.0382(4)	0.4377(3)	0.0429(6)
N2	0.07355(14)	0.2917(3)	0.6932(2)	0.0298(4)
N1	0.15776(13)	0.2651(3)	0.6141(2)	0.0272(4)
H3	0.193(2)	0.667(4)	0.734(3)	0.034(8)
H2	-0.046(2)	0.132(4)	0.729(3)	0.033(7)
H1	0.040(3)	-0.108(5)	0.572(4)	0.055(10)
C6	0.21593(17)	0.4267(4)	0.6263(3)	0.0320(5)
C5	0.1662(2)	0.5572(4)	0.7069(3)	0.0362(6)
C4	0.07861(19)	0.4744(4)	0.7474(3)	0.0345(6)
C3	0.01538(19)	0.1330(4)	0.6861(3)	0.0378(6)
C2	0.06265(18)	0.0050(4)	0.6013(3)	0.0386(6)
C1	0.15038(18)	0.0892(4)	0.5549(3)	0.0322(5)

Table 2. Anisotropic displacement parameters (\AA^2) for trinitrodiazapentalene at room temperature (298 K). The anisotropic displacement factor exponent takes the form: $-2\pi^2[(h a^*)^2 U_{11} + \dots + 2 h k a^* b^* U_{12}]$

	U11	U22	U33	U23	U13	U12
O6	0.0330(10)	0.0806(18)	0.0876(19)	-0.0044(15)	0.0105(11)	0.0102(11)
O5	0.0513(12)	0.0830(17)	0.0746(17)	-0.0148(14)	0.0136(12)	-0.0375(12)
O4	0.0706(14)	0.0539(14)	0.0537(14)	-0.0116(12)	0.0048(12)	0.0206(12)
O3	0.0463(13)	0.0815(18)	0.0602(15)	-0.0096(13)	0.0231(12)	-0.0016(12)
O2	0.0761(17)	0.0586(16)	0.108(2)	-0.0421(16)	0.0302(16)	-0.0046(14)
O1	0.0699(14)	0.0713(15)	0.0441(12)	0.0034(12)	0.0248(12)	-0.0035(14)
N5	0.0291(10)	0.0691(17)	0.0378(13)	-0.0071(11)	0.0019(10)	-0.0107(12)
N4	0.0399(12)	0.0584(17)	0.0344(12)	-0.0034(12)	0.0010(10)	0.0103(13)
N3	0.0383(12)	0.0503(15)	0.0401(12)	-0.0085(11)	0.0041(11)	0.0017(11)
N2	0.0230(9)	0.0391(11)	0.0274(10)	0.0030(9)	0.0033(8)	0.0023(8)
N1	0.0216(8)	0.0339(10)	0.0262(9)	0.0020(9)	0.0012(8)	0.0016(7)
C6	0.0263(11)	0.0398(13)	0.0301(12)	-0.0002(11)	-0.0014(10)	-0.0055(9)
C5	0.0352(12)	0.0380(15)	0.0356(13)	-0.0019(11)	-0.0045(11)	-0.0019(12)
C4	0.0347(13)	0.0382(14)	0.0306(12)	-0.0034(11)	0.0007(10)	0.0054(11)
C3	0.0282(11)	0.0435(15)	0.0418(14)	0.0087(12)	0.0060(11)	-0.0026(11)
C2	0.0374(12)	0.0326(13)	0.0457(15)	0.0069(12)	-0.0026(13)	-0.0047(11)
C1	0.0300(11)	0.0343(13)	0.0322(12)	0.0005(10)	0.0000(10)	0.0029(10)

Table 3. Atomic coordinates and equivalent isotropic thermal parameters (\AA^2) for trinitrodiazapentalene at room temperature (275 K). $U(\text{eq})$ is defined as one third of the trace of the orthogonalized U_{ij} tensor.

	x	y	z	$U(\text{eq})/U(\text{iso})$
O6	0.36119(11)	0.2697(3)	0.5858(2)	0.0616(6)
O5	0.36013(13)	0.5789(3)	0.5836(2)	0.0639(6)
O4	0.00426(15)	0.7171(2)	0.8626(2)	0.0554(5)
O3	-0.05969(14)	0.4324(3)	0.8806(2)	0.0573(5)
O2	0.20592(16)	-0.1297(3)	0.3996(3)	0.0744(7)
O1	0.25562(15)	0.1620(3)	0.3766(2)	0.0568(5)
N5	0.31865(13)	0.4240(3)	0.5951(2)	0.0416(5)
N4	0.00239(16)	0.5461(3)	0.8357(2)	0.0404(5)
N3	0.20935(13)	0.0381(3)	0.4374(2)	0.0387(5)
N2	0.07350(11)	0.2917(2)	0.69301(17)	0.0280(4)
N1	0.15764(10)	0.2650(2)	0.61436(18)	0.0256(3)
H3	0.1951(16)	0.668(3)	0.732(3)	0.036(6)
H2	-0.0469(17)	0.129(3)	0.726(2)	0.031(6)
H1	0.041(2)	-0.107(4)	0.577(3)	0.053(8)
C6	0.21604(14)	0.4266(3)	0.6265(2)	0.0303(4)
C5	0.16648(16)	0.5578(3)	0.7069(2)	0.0333(5)
C4	0.07873(15)	0.4750(3)	0.7475(2)	0.0319(5)
C3	0.01526(15)	0.1332(3)	0.6869(2)	0.0348(5)
C2	0.06263(15)	0.0057(3)	0.6016(2)	0.0356(5)
C1	0.15037(14)	0.0890(3)	0.5546(2)	0.0296(4)

Table 4. Anisotropic displacement parameters (\AA^2) for trinitrodiazapentalene at room temperature (275 K). The anisotropic displacement factor exponent takes the form: $-2\pi^2[(h a^*)^2 U_{11} + \dots + 2 h k a^* b^* U_{12}]$

	U11	U22	U33	U23	U13	U12
O6	0.0329(8)	0.0744(13)	0.0777(14)	-0.0034(11)	0.0088(8)	0.0111(8)
O5	0.0504(10)	0.0747(12)	0.0665(13)	-0.0112(10)	0.0115(10)	-0.0367(9)
O4	0.0689(11)	0.0483(11)	0.0489(11)	-0.0124(9)	0.0032(9)	0.0193(9)
O3	0.0431(10)	0.0735(13)	0.0552(12)	-0.0092(10)	0.0187(9)	-0.0030(9)
O2	0.0736(13)	0.0551(13)	0.0946(18)	-0.0394(12)	0.0276(12)	-0.0053(10)
O1	0.0666(11)	0.0645(11)	0.0392(9)	0.0018(9)	0.0222(9)	-0.0025(11)
N5	0.0297(8)	0.0615(12)	0.0336(10)	-0.0046(9)	0.0020(8)	-0.0081(9)
N4	0.0395(10)	0.0519(13)	0.0298(9)	-0.0049(9)	0.0015(8)	0.0104(10)
N3	0.0377(10)	0.0409(11)	0.0375(10)	-0.0079(9)	0.0037(9)	0.0014(8)
N2	0.0220(7)	0.0361(9)	0.0258(9)	0.0028(7)	0.0027(6)	0.0029(6)
N1	0.0212(7)	0.0314(8)	0.0242(8)	0.0032(7)	0.0004(6)	0.0007(6)
C6	0.0278(9)	0.0370(11)	0.0262(10)	0.0012(9)	-0.0030(8)	-0.0041(8)
C5	0.0362(10)	0.0324(12)	0.0312(11)	-0.0012(9)	-0.0031(9)	-0.0020(9)
C4	0.0333(10)	0.0353(11)	0.0270(11)	-0.0033(8)	0.0003(8)	0.0045(9)
C3	0.0268(10)	0.0379(12)	0.0396(12)	0.0078(10)	0.0050(9)	-0.0012(9)
C2	0.0379(10)	0.0300(11)	0.0388(12)	0.0051(10)	-0.0028(10)	-0.0037(9)
C1	0.0313(10)	0.0279(10)	0.0295(10)	0.0006(8)	-0.0010(8)	0.0026(8)

Table 5. Atomic coordinates and equivalent isotropic thermal parameters (\AA^2) for trinitrodiazapentalene at room temperature (250 K). $U(\text{eq})$ is defined as one third of the trace of the orthogonalized U_{ij} tensor.

	x	y	z	$U(\text{eq})/U(\text{iso})$
O6	0.36165(11)	0.2693(3)	0.5862(2)	0.0566(5)
O5	0.36051(12)	0.5795(3)	0.5833(2)	0.0581(5)
O4	0.00425(14)	0.7183(2)	0.86256(19)	0.0489(4)
O3	-0.06001(13)	0.4330(3)	0.88099(19)	0.0529(5)
O2	0.20588(15)	-0.1303(3)	0.3999(3)	0.0670(6)
O1	0.25595(14)	0.1620(2)	0.3761(2)	0.0516(4)
N5	0.31899(12)	0.4237(3)	0.59497(19)	0.0378(4)
N4	0.00247(15)	0.5467(3)	0.83576(19)	0.0373(4)
N3	0.20918(12)	0.0380(3)	0.43729(19)	0.0352(4)
N2	0.07340(11)	0.2924(2)	0.69322(17)	0.0254(3)
N1	0.15766(10)	0.2655(2)	0.61406(17)	0.0236(3)
H3	0.1931(14)	0.675(3)	0.732(2)	0.025(5)
H2	-0.0485(16)	0.130(3)	0.729(2)	0.028(5)
H1	0.040(2)	-0.108(4)	0.575(3)	0.058(8)
C6	0.21622(13)	0.4271(3)	0.6265(2)	0.0272(4)
C5	0.16664(15)	0.5584(3)	0.7067(2)	0.0301(4)
C4	0.07851(14)	0.4758(3)	0.7473(2)	0.0292(4)
C3	0.01504(14)	0.1336(3)	0.6871(2)	0.0321(4)
C2	0.06277(14)	0.0053(3)	0.6019(2)	0.0327(4)
C1	0.15042(13)	0.0893(3)	0.5547(2)	0.0269(4)

Table 6. Anisotropic displacement parameters (\AA^2) for trinitrodiazapentalene at room temperature (250 K). The anisotropic displacement factor exponent takes the form: $-2\pi^2[(h a^*)^2 U_{11} + \dots + 2 h k a^* b^* U_{12}]$

	U11	U22	U33	U23	U13	U12
O6	0.0298(8)	0.0683(12)	0.0718(13)	-0.0027(10)	0.0078(8)	0.0103(8)
O5	0.0426(9)	0.0695(11)	0.0621(12)	-0.0118(9)	0.0107(9)	-0.0317(8)
O4	0.0589(10)	0.0425(10)	0.0453(10)	-0.0105(8)	0.0028(8)	0.0165(8)
O3	0.0378(9)	0.0721(12)	0.0487(11)	-0.0091(9)	0.0187(8)	-0.0021(9)
O2	0.0621(12)	0.0498(11)	0.0890(16)	-0.0347(11)	0.0235(11)	-0.0053(9)
O1	0.0588(10)	0.0594(10)	0.0365(9)	0.0016(8)	0.0216(8)	-0.0023(9)
N5	0.0258(8)	0.0557(11)	0.0319(10)	-0.0031(8)	0.0011(7)	-0.0082(8)
N4	0.0354(9)	0.0484(12)	0.0279(9)	-0.0031(8)	0.0009(8)	0.0086(9)
N3	0.0319(9)	0.0396(10)	0.0341(10)	-0.0050(8)	0.0033(8)	0.0011(8)
N2	0.0190(7)	0.0329(9)	0.0241(8)	0.0020(7)	0.0029(6)	0.0028(6)
N1	0.0190(6)	0.0288(8)	0.0230(7)	0.0016(7)	0.0014(6)	0.0015(6)
C6	0.0242(9)	0.0319(10)	0.0255(10)	0.0013(9)	-0.0026(7)	-0.0034(7)
C5	0.0297(9)	0.0324(11)	0.0283(10)	-0.0013(8)	-0.0035(8)	-0.0012(8)
C4	0.0285(10)	0.0334(11)	0.0257(10)	-0.0024(8)	0.0001(8)	0.0039(8)
C3	0.0251(9)	0.0354(11)	0.0357(11)	0.0069(9)	0.0036(9)	-0.0026(8)
C2	0.0333(9)	0.0279(10)	0.0367(11)	0.0052(9)	-0.0009(9)	-0.0022(8)
C1	0.0265(9)	0.0261(10)	0.0282(10)	0.0002(8)	-0.0015(7)	0.0030(7)

Table 7. Atomic coordinates and equivalent isotropic thermal parameters (\AA^2) for trinitrodiazapentalene at room temperature (225 K). $U(\text{eq})$ is defined as one third of the trace of the orthogonalized U_{ij} tensor.

	x	y	z	$U(\text{eq})/U(\text{iso})$
O6	0.36191(10)	0.2694(2)	0.5864(2)	0.0503(5)
O5	0.36085(11)	0.5795(2)	0.5830(2)	0.0524(5)
O4	0.00392(13)	0.7193(2)	0.86245(17)	0.0442(4)
O3	-0.06028(12)	0.4342(3)	0.88113(18)	0.0474(4)
O2	0.20568(13)	-0.1308(2)	0.3991(2)	0.0593(6)
O1	0.25619(13)	0.1620(2)	0.37587(19)	0.0467(4)
N5	0.31912(11)	0.4242(3)	0.59487(18)	0.0336(4)
N4	0.00219(14)	0.5476(2)	0.83571(18)	0.0326(4)
N3	0.20903(12)	0.0376(2)	0.43719(19)	0.0320(4)
N2	0.07353(10)	0.2929(2)	0.69347(16)	0.0228(3)
N1	0.15785(10)	0.26558(19)	0.61428(16)	0.0209(3)
H3	0.1933(14)	0.674(3)	0.735(2)	0.023(5)
H2	-0.0492(17)	0.132(3)	0.731(2)	0.031(6)
H1	0.0388(18)	-0.107(3)	0.574(3)	0.041(7)
C6	0.21625(12)	0.4274(3)	0.6259(2)	0.0244(4)
C5	0.16650(14)	0.5592(3)	0.7067(2)	0.0272(4)
C4	0.07842(14)	0.4764(3)	0.7477(2)	0.0264(4)
C3	0.01492(13)	0.1337(3)	0.6876(2)	0.0282(4)
C2	0.06252(13)	0.0056(3)	0.6022(2)	0.0293(4)
C1	0.15039(13)	0.0892(2)	0.5549(2)	0.0243(4)

Table 8. Anisotropic displacement parameters (\AA^2) for trinitrodiazapentalene at room temperature (225 K). The anisotropic displacement factor exponent takes the form: $-2\pi^2[(h a^*)^2 U_{11} + \dots + 2 h k a^* b^* U_{12}]$

	U11	U22	U33	U23	U13	U12
O6	0.0263(7)	0.0592(11)	0.0654(12)	-0.0027(9)	0.0059(7)	0.0090(7)
O5	0.0385(8)	0.0628(10)	0.0560(11)	-0.0104(8)	0.0090(8)	-0.0286(8)
O4	0.0538(9)	0.0380(9)	0.0408(9)	-0.0084(7)	0.0048(8)	0.0140(8)
O3	0.0338(8)	0.0625(11)	0.0460(10)	-0.0080(8)	0.0172(7)	-0.0039(8)
O2	0.0566(11)	0.0436(10)	0.0778(14)	-0.0324(10)	0.0206(10)	-0.0040(8)
O1	0.0537(9)	0.0515(9)	0.0349(8)	0.0018(8)	0.0188(8)	-0.0022(9)
N5	0.0227(7)	0.0491(10)	0.0289(9)	-0.0045(7)	-0.0003(7)	-0.0081(7)
N4	0.0305(8)	0.0407(11)	0.0268(8)	-0.0035(8)	0.0007(7)	0.0073(9)
N3	0.0286(8)	0.0346(10)	0.0326(9)	-0.0050(8)	0.0021(7)	0.0013(7)
N2	0.0165(6)	0.0276(8)	0.0242(8)	0.0013(6)	0.0024(6)	0.0021(6)
N1	0.0155(6)	0.0254(7)	0.0217(7)	0.0012(6)	0.0010(6)	0.0007(5)
C6	0.0211(8)	0.0288(9)	0.0234(9)	0.0002(8)	-0.0015(7)	-0.0038(6)
C5	0.0279(9)	0.0267(10)	0.0271(10)	-0.0017(8)	-0.0036(7)	-0.0013(8)
C4	0.0261(9)	0.0272(10)	0.0259(9)	-0.0021(8)	-0.0001(7)	0.0020(8)
C3	0.0216(8)	0.0308(10)	0.0322(10)	0.0056(8)	0.0029(8)	-0.0022(8)
C2	0.0283(8)	0.0251(9)	0.0344(11)	0.0059(8)	-0.0012(8)	-0.0029(7)
C1	0.0249(9)	0.0223(9)	0.0256(9)	0.0002(7)	-0.0009(7)	0.0037(7)

Table 9. Atomic coordinates and equivalent isotropic thermal parameters (\AA^2) for trinitrodiazapentalene at room temperature (200 K). $U(\text{eq})$ is defined as one third of the trace of the orthogonalized U_{ij} tensor.

	x	y	z	$U(\text{eq})/U(\text{iso})$
O6	0.36218(11)	0.2694(2)	0.5868(2)	0.0460(4)
O5	0.36113(12)	0.5801(2)	0.5823(2)	0.0471(4)
O4	0.00380(13)	0.7208(2)	0.86225(18)	0.0400(4)
O3	-0.06056(12)	0.4355(3)	0.88114(19)	0.0434(4)
O2	0.20542(14)	-0.1311(2)	0.3990(2)	0.0532(5)
O1	0.25648(13)	0.1619(2)	0.37561(19)	0.0420(4)
N5	0.31947(12)	0.4240(3)	0.59502(18)	0.0300(4)
N4	0.00219(14)	0.5485(3)	0.83557(18)	0.0302(4)
N3	0.20908(12)	0.0375(3)	0.43694(19)	0.0291(4)
N2	0.07348(11)	0.2934(2)	0.69366(17)	0.0210(3)
N1	0.15760(10)	0.2659(2)	0.61433(17)	0.0191(3)
H3	0.1936(16)	0.670(3)	0.736(2)	0.024(6)
H2	-0.0484(19)	0.130(3)	0.732(3)	0.032(6)
H1	0.037(2)	-0.116(4)	0.572(3)	0.045(7)
C6	0.21659(13)	0.4276(3)	0.6258(2)	0.0229(4)
C5	0.16660(14)	0.5604(3)	0.7063(2)	0.0250(4)
C4	0.07843(14)	0.4772(3)	0.7477(2)	0.0245(4)
C3	0.01468(14)	0.1339(3)	0.6885(2)	0.0266(4)
C2	0.06235(14)	0.0052(3)	0.6028(2)	0.0275(4)
C1	0.15060(13)	0.0889(3)	0.5550(2)	0.0223(4)

Table 10. Anisotropic displacement parameters (\AA^2) for trinitrodiazapentalene at room temperature (200 K). The anisotropic displacement factor exponent takes the form: $-2\pi^2[(h a^*)^2 U_{11} + \dots + 2 h k a^* b^* U_{12}]$

	U11	U22	U33	U23	U13	U12
O6	0.0251(7)	0.0529(10)	0.0601(11)	-0.0032(9)	0.0056(7)	0.0085(7)
O5	0.0361(8)	0.0540(10)	0.0512(10)	-0.0092(8)	0.0076(8)	-0.0250(7)
O4	0.0500(9)	0.0335(9)	0.0364(9)	-0.0091(7)	0.0033(7)	0.0131(7)
O3	0.0324(8)	0.0551(11)	0.0425(10)	-0.0072(8)	0.0147(7)	-0.0026(8)
O2	0.0522(10)	0.0362(10)	0.0711(14)	-0.0288(9)	0.0180(9)	-0.0033(8)
O1	0.0481(9)	0.0448(9)	0.0331(8)	0.0016(8)	0.0165(8)	-0.0028(8)
N5	0.0209(7)	0.0418(10)	0.0274(9)	-0.0037(7)	0.0008(7)	-0.0061(7)
N4	0.0276(8)	0.0377(11)	0.0252(8)	-0.0033(8)	0.0003(7)	0.0066(8)
N3	0.0280(8)	0.0305(9)	0.0289(9)	-0.0058(7)	0.0017(7)	0.0007(7)
N2	0.0164(7)	0.0252(8)	0.0215(8)	0.0012(6)	0.0021(6)	0.0015(6)
N1	0.0165(6)	0.0214(7)	0.0195(7)	0.0010(6)	0.0005(6)	-0.0005(5)
C6	0.0213(8)	0.0240(9)	0.0234(9)	-0.0002(8)	-0.0016(7)	-0.0038(6)
C5	0.0254(9)	0.0242(10)	0.0255(10)	-0.0017(8)	-0.0018(7)	-0.0005(7)
C4	0.0242(9)	0.0249(10)	0.0244(9)	-0.0014(7)	-0.0003(7)	0.0030(8)
C3	0.0204(8)	0.0284(10)	0.0308(10)	0.0060(8)	0.0032(8)	-0.0016(8)
C2	0.0284(9)	0.0220(9)	0.0323(10)	0.0047(8)	-0.0011(9)	-0.0014(7)
C1	0.0231(8)	0.0198(8)	0.0239(9)	0.0003(7)	-0.0007(7)	0.0033(7)

Table 11. Atomic coordinates and equivalent isotropic thermal parameters (\AA^2) for trinitrodiazapentalene at room temperature (175 K). $U(\text{eq})$ is defined as one third of the trace of the orthogonalized U_{ij} tensor.

	x	y	z	$U(\text{eq})/U(\text{iso})$
O6	0.36255(10)	0.2695(2)	0.5869(2)	0.0398(4)
O5	0.36140(11)	0.5803(2)	0.58180(19)	0.0405(4)
O4	0.00363(12)	0.7217(2)	0.86207(16)	0.0342(3)
O3	-0.06112(11)	0.4365(2)	0.88139(17)	0.0372(4)
O2	0.20503(13)	-0.1312(2)	0.3986(2)	0.0454(5)
O1	0.25690(12)	0.1621(2)	0.37550(17)	0.0361(3)
N5	0.31948(11)	0.4245(2)	0.59455(17)	0.0266(3)
N4	0.00181(13)	0.5494(2)	0.83595(17)	0.0258(4)
N3	0.20910(11)	0.0372(2)	0.43701(17)	0.0250(3)
N2	0.07320(10)	0.2939(2)	0.69362(15)	0.0181(3)
N1	0.15784(10)	0.26630(19)	0.61442(16)	0.0170(3)
H3	0.1927(16)	0.671(3)	0.733(3)	0.029(6)
H2	-0.0492(16)	0.132(3)	0.732(2)	0.020(5)
H1	0.0382(18)	-0.114(3)	0.574(3)	0.033(6)
C6	0.21667(12)	0.4282(2)	0.62568(18)	0.0194(3)
C5	0.16689(13)	0.5609(3)	0.7064(2)	0.0218(4)
C4	0.07823(13)	0.4778(3)	0.74768(19)	0.0205(4)
C3	0.01446(13)	0.1346(3)	0.6889(2)	0.0229(4)
C2	0.06224(13)	0.0053(3)	0.6030(2)	0.0230(4)
C1	0.15030(13)	0.0889(2)	0.55504(18)	0.0192(3)

Table 12. Anisotropic displacement parameters (\AA^2) for trinitrodiazapentalene at room temperature (175 K). The anisotropic displacement factor exponent takes the form: $-2\pi^2[(h a^*)^2 U_{11} + \dots + 2 h k a^* b^* U_{12}]$

	U11	U22	U33	U23	U13	U12
O6	0.0218(6)	0.0474(9)	0.0503(10)	-0.0029(8)	0.0043(7)	0.0084(6)
O5	0.0310(7)	0.0481(9)	0.0424(9)	-0.0078(7)	0.0064(7)	-0.0230(7)
O4	0.0413(8)	0.0311(8)	0.0301(8)	-0.0075(6)	0.0038(6)	0.0110(7)
O3	0.0256(7)	0.0488(9)	0.0373(9)	-0.0066(7)	0.0129(6)	-0.0037(7)
O2	0.0432(9)	0.0335(9)	0.0595(12)	-0.0249(8)	0.0141(8)	-0.0035(7)
O1	0.0412(8)	0.0408(8)	0.0263(7)	0.0027(7)	0.0143(7)	-0.0013(7)
N5	0.0185(7)	0.0392(9)	0.0221(8)	-0.0036(7)	0.0005(6)	-0.0056(6)
N4	0.0248(7)	0.0321(9)	0.0205(8)	-0.0041(7)	0.0007(6)	0.0065(7)
N3	0.0229(7)	0.0283(8)	0.0238(8)	-0.0051(6)	0.0026(6)	0.0014(6)
N2	0.0140(6)	0.0229(7)	0.0175(7)	0.0022(6)	0.0028(5)	0.0018(5)
N1	0.0130(6)	0.0208(7)	0.0172(7)	0.0011(6)	0.0014(5)	0.0012(5)
C6	0.0181(8)	0.0224(8)	0.0178(8)	0.0005(7)	-0.0018(6)	-0.0031(6)
C5	0.0213(8)	0.0227(9)	0.0215(9)	-0.0004(7)	-0.0025(7)	0.0002(7)
C4	0.0220(8)	0.0215(8)	0.0180(8)	-0.0027(7)	0.0000(6)	0.0025(7)
C3	0.0180(8)	0.0243(9)	0.0264(9)	0.0040(7)	0.0016(7)	-0.0014(7)
C2	0.0241(8)	0.0194(8)	0.0255(9)	0.0032(7)	-0.0020(7)	-0.0016(7)
C1	0.0200(8)	0.0184(8)	0.0191(8)	0.0000(6)	-0.0008(6)	0.0021(6)

Table 13. Atomic coordinates and equivalent isotropic thermal parameters (\AA^2) for trinitrodiazapentalene at room temperature (150 K). $U(\text{eq})$ is defined as one third of the trace of the orthogonalized U_{ij} tensor.

	x	y	z	$U(\text{eq})/U(\text{iso})$
O6	0.36284(9)	0.2694(2)	0.58730(18)	0.0343(3)
O5	0.36162(10)	0.5809(2)	0.58126(17)	0.0351(3)
O4	0.00351(11)	0.72297(19)	0.86191(15)	0.0293(3)
O3	-0.06123(11)	0.4375(2)	0.88152(15)	0.0329(3)
O2	0.20474(11)	-0.1317(2)	0.39849(19)	0.0389(4)
O1	0.25698(11)	0.1620(2)	0.37525(16)	0.0314(3)
N5	0.31981(10)	0.4245(2)	0.59436(16)	0.0229(3)
N4	0.00160(12)	0.5507(2)	0.83602(16)	0.0225(3)
N3	0.20894(10)	0.0372(2)	0.43672(16)	0.0213(3)
N2	0.07327(9)	0.29453(19)	0.69374(14)	0.0157(3)
N1	0.15782(9)	0.26662(18)	0.61449(15)	0.0144(3)
H3	0.1924(14)	0.669(3)	0.731(2)	0.018(5)
H2	-0.0491(16)	0.128(3)	0.731(2)	0.019(5)
H1	0.0371(18)	-0.117(3)	0.575(3)	0.035(6)
C6	0.21676(11)	0.4281(2)	0.62589(17)	0.0174(3)
C5	0.16698(12)	0.5614(2)	0.70615(18)	0.0186(3)
C4	0.07829(12)	0.4784(2)	0.74766(18)	0.0179(3)
C3	0.01444(12)	0.1351(3)	0.68919(19)	0.0196(3)
C2	0.06207(12)	0.0050(3)	0.60333(19)	0.0204(3)
C1	0.15028(12)	0.0890(2)	0.55541(17)	0.0170(3)

Table 14. Anisotropic displacement parameters (\AA^2) for trinitrodiazapentalene at room temperature (150 K). The anisotropic displacement factor exponent takes the form: $-2\pi^2[(h a^*)^2 U_{11} + \dots + 2 h k a^* b^* U_{12}]$

	U11	U22	U33	U23	U13	U12
O6	0.0179(6)	0.0418(8)	0.0432(8)	-0.0015(7)	0.0034(6)	0.0062(5)
O5	0.0261(6)	0.0426(8)	0.0367(8)	-0.0071(6)	0.0056(6)	-0.0187(6)
O4	0.0355(7)	0.0262(7)	0.0263(7)	-0.0059(6)	0.0023(6)	0.0092(6)
O3	0.0239(7)	0.0439(8)	0.0309(8)	-0.0060(6)	0.0107(6)	-0.0030(6)
O2	0.0374(8)	0.0296(8)	0.0497(10)	-0.0204(7)	0.0109(7)	-0.0025(6)
O1	0.0345(7)	0.0359(7)	0.0237(7)	0.0028(6)	0.0124(6)	-0.0019(7)
N5	0.0147(6)	0.0345(8)	0.0195(7)	-0.0029(6)	0.0002(6)	-0.0044(6)
N4	0.0213(7)	0.0290(8)	0.0170(7)	-0.0022(6)	0.0011(6)	0.0047(7)
N3	0.0191(7)	0.0253(8)	0.0197(7)	-0.0036(6)	0.0019(6)	0.0009(6)
N2	0.0115(6)	0.0207(6)	0.0147(6)	0.0012(5)	0.0021(5)	0.0016(5)
N1	0.0103(5)	0.0190(6)	0.0138(6)	0.0013(5)	0.0008(5)	0.0005(5)
C6	0.0143(7)	0.0216(8)	0.0163(8)	0.0005(7)	-0.0021(6)	-0.0031(6)
C5	0.0191(7)	0.0202(8)	0.0166(8)	-0.0008(6)	-0.0019(6)	-0.0007(6)
C4	0.0172(7)	0.0207(8)	0.0157(7)	-0.0015(6)	-0.0003(6)	0.0028(6)
C3	0.0161(7)	0.0225(8)	0.0203(8)	0.0041(6)	0.0016(6)	-0.0013(6)
C2	0.0195(7)	0.0183(7)	0.0233(8)	0.0044(7)	-0.0011(7)	-0.0019(6)
C1	0.0182(7)	0.0173(7)	0.0154(7)	0.0002(6)	-0.0010(6)	0.0015(6)

Table 15. Atomic coordinates and equivalent isotropic thermal parameters (\AA^2) for trinitrodiazapentalene at room temperature (125 K). $U(\text{eq})$ is defined as one third of the trace of the orthogonalized U_{ij} tensor.

	x	y	z	$U(\text{eq})/U(\text{iso})$
O6	0.36307(9)	0.26957(19)	0.58760(17)	0.0296(3)
O5	0.36186(10)	0.5812(2)	0.58100(17)	0.0302(3)
O4	0.00339(11)	0.72410(19)	0.86177(15)	0.0253(3)
O3	-0.06169(10)	0.4385(2)	0.88156(15)	0.0287(3)
O2	0.20450(11)	-0.1318(2)	0.39839(18)	0.0332(4)
O1	0.25722(11)	0.16157(19)	0.37519(15)	0.0267(3)
N5	0.32021(10)	0.4247(2)	0.59413(16)	0.0196(3)
N4	0.00162(12)	0.5516(2)	0.83583(16)	0.0190(3)
N3	0.20903(10)	0.0371(2)	0.43660(16)	0.0189(3)
N2	0.07319(9)	0.29495(19)	0.69407(14)	0.0136(3)
N1	0.15777(9)	0.26673(18)	0.61450(15)	0.0126(3)
H3	0.1936(15)	0.677(3)	0.733(2)	0.018(5)
H2	-0.0489(16)	0.130(3)	0.733(2)	0.017(5)
H1	0.0358(17)	-0.114(3)	0.576(3)	0.027(6)
C6	0.21683(11)	0.4284(2)	0.62555(17)	0.0151(3)
C5	0.16702(12)	0.5626(2)	0.70591(18)	0.0163(3)
C4	0.07803(12)	0.4791(2)	0.74783(18)	0.0157(3)
C3	0.01421(12)	0.1355(2)	0.68948(19)	0.0176(3)
C2	0.06181(11)	0.0051(3)	0.60371(19)	0.0173(3)
C1	0.15049(12)	0.0893(2)	0.55565(17)	0.0147(3)

Table 16. Anisotropic displacement parameters (\AA^2) for trinitrodiazapentalene at room temperature (125 K). The anisotropic displacement factor exponent takes the form: $-2\pi^2[(h a^*)^2 U_{11} + \dots + 2 h k a^* b^* U_{12}]$

	U11	U22	U33	U23	U13	U12
O6	0.0172(6)	0.0347(7)	0.0368(8)	-0.0010(6)	0.0024(5)	0.0063(5)
O5	0.0226(6)	0.0359(7)	0.0322(8)	-0.0060(6)	0.0043(6)	-0.0167(6)
O4	0.0308(7)	0.0216(6)	0.0236(7)	-0.0041(5)	0.0016(5)	0.0080(6)
O3	0.0206(6)	0.0372(8)	0.0283(7)	-0.0045(6)	0.0089(6)	-0.0030(6)
O2	0.0318(7)	0.0243(7)	0.0436(9)	-0.0179(7)	0.0094(6)	-0.0014(6)
O1	0.0294(7)	0.0308(7)	0.0199(6)	0.0012(6)	0.0103(5)	-0.0022(6)
N5	0.0129(6)	0.0295(7)	0.0163(7)	-0.0025(6)	0.0011(6)	-0.0042(5)
N4	0.0187(6)	0.0241(8)	0.0142(7)	-0.0023(6)	0.0008(6)	0.0044(6)
N3	0.0171(6)	0.0214(7)	0.0181(7)	-0.0026(6)	0.0009(6)	0.0013(6)
N2	0.0104(6)	0.0178(6)	0.0126(6)	0.0014(5)	0.0019(5)	0.0018(5)
N1	0.0095(5)	0.0165(6)	0.0118(6)	0.0009(5)	0.0008(5)	0.0006(5)
C6	0.0137(7)	0.0185(7)	0.0131(8)	-0.0001(6)	-0.0021(6)	-0.0028(5)
C5	0.0157(7)	0.0181(8)	0.0151(8)	0.0002(6)	-0.0019(6)	0.0002(6)
C4	0.0151(7)	0.0177(8)	0.0142(7)	-0.0016(6)	-0.0001(6)	0.0012(6)
C3	0.0149(7)	0.0190(8)	0.0189(8)	0.0048(6)	0.0013(6)	-0.0008(6)
C2	0.0178(7)	0.0156(7)	0.0185(8)	0.0034(6)	-0.0005(6)	-0.0007(6)
C1	0.0143(7)	0.0142(7)	0.0156(7)	-0.0001(6)	-0.0012(6)	0.0017(6)

Table 17. Atomic coordinates and equivalent isotropic thermal parameters (\AA^2) for trinitrodiazapentalene at room temperature (100 K). $U(\text{eq})$ is defined as one third of the trace of the orthogonalized U_{ij} tensor.

	x	y	z	$U(\text{eq})/U(\text{iso})$
O6	0.36340(10)	0.2695(2)	0.58765(18)	0.0249(3)
O5	0.36218(10)	0.5815(2)	0.58037(18)	0.0258(3)
O4	0.00340(11)	0.72524(19)	0.86152(16)	0.0215(3)
O3	-0.06207(11)	0.4397(2)	0.88160(16)	0.0241(3)
O2	0.20438(11)	-0.1321(2)	0.39836(19)	0.0279(3)
O1	0.25743(11)	0.1615(2)	0.37528(16)	0.0231(3)
N5	0.32031(11)	0.4250(2)	0.59421(17)	0.0169(3)
N4	0.00145(12)	0.5526(2)	0.83567(17)	0.0166(3)
N3	0.20903(11)	0.0372(2)	0.43695(17)	0.0163(3)
N2	0.07307(10)	0.2956(2)	0.69394(15)	0.0122(3)
N1	0.15769(10)	0.26702(19)	0.61443(16)	0.0113(3)
H3	0.1941(16)	0.679(3)	0.733(3)	0.015(5)
H2	-0.0483(17)	0.133(3)	0.736(3)	0.013(5)
H1	0.0376(19)	-0.117(4)	0.577(3)	0.026(6)
C6	0.21698(12)	0.4288(2)	0.62531(18)	0.0126(3)
C5	0.16708(13)	0.5632(2)	0.7059(2)	0.0141(3)
C4	0.07809(13)	0.4798(3)	0.74817(19)	0.0139(3)
C3	0.01388(13)	0.1356(3)	0.6899(2)	0.0153(3)
C2	0.06181(12)	0.0053(3)	0.6041(2)	0.0154(3)
C1	0.15043(13)	0.0892(2)	0.55568(19)	0.0130(3)

Table 18. Anisotropic displacement parameters (\AA^2) for trinitrodiazapentalene at room temperature (100 K). The anisotropic displacement factor exponent takes the form: $-2\pi^2[(h a^*)^2 U_{11} + \dots + 2 h k a^* b^* U_{12}]$

	U11	U22	U33	U23	U13	U12
O6	0.0130(6)	0.0284(7)	0.0333(8)	-0.0019(6)	0.0014(6)	0.0051(5)
O5	0.0186(6)	0.0298(7)	0.0289(8)	-0.0038(6)	0.0044(6)	-0.0134(6)
O4	0.0254(7)	0.0174(6)	0.0216(7)	-0.0044(5)	0.0022(5)	0.0062(5)
O3	0.0158(6)	0.0309(7)	0.0255(8)	-0.0039(6)	0.0077(6)	-0.0032(5)
O2	0.0245(7)	0.0212(7)	0.0379(9)	-0.0142(7)	0.0073(6)	-0.0011(6)
O1	0.0237(7)	0.0257(7)	0.0199(7)	0.0022(6)	0.0094(6)	-0.0016(6)
N5	0.0100(6)	0.0251(7)	0.0156(7)	-0.0015(6)	-0.0001(6)	-0.0031(5)
N4	0.0140(7)	0.0210(8)	0.0148(7)	-0.0013(6)	-0.0001(6)	0.0038(6)
N3	0.0140(7)	0.0185(7)	0.0164(7)	-0.0025(6)	0.0007(6)	0.0000(6)
N2	0.0077(6)	0.0155(6)	0.0134(7)	0.0014(5)	0.0018(5)	0.0011(5)
N1	0.0075(6)	0.0135(6)	0.0129(6)	0.0001(5)	0.0014(5)	-0.0003(5)
C6	0.0099(7)	0.0157(7)	0.0120(8)	-0.0003(6)	-0.0010(6)	-0.0025(5)
C5	0.0130(7)	0.0149(8)	0.0144(8)	0.0000(6)	-0.0002(6)	-0.0003(6)
C4	0.0131(8)	0.0142(8)	0.0143(8)	-0.0008(6)	-0.0002(6)	0.0013(6)
C3	0.0114(7)	0.0170(8)	0.0175(8)	0.0037(6)	0.0004(6)	-0.0020(6)
C2	0.0135(7)	0.0149(7)	0.0177(8)	0.0030(7)	-0.0004(7)	-0.0011(6)
C1	0.0119(7)	0.0117(7)	0.0154(8)	0.0002(6)	-0.0005(6)	0.0014(6)

Table 19. Bond lengths (Å) and angles (°) of trinitrodiazapentalene at various temperatures.

At 298 K:

N5	O6	1.224(3)	
N5	O5	1.226(3)	
N4	O4	1.230(3)	
N3	O2	1.235(3)	
N3	O1	1.218(3)	
O3	N4	1.226(3)	
C1	N3	1.409(3)	
N2	N1	1.370(3)	
N5	C6	1.413(3)	
N1	C6	1.383(3)	
C5	C6	1.368(4)	
N4	C4	1.414(4)	
N2	C4	1.384(3)	
C5	C4	1.368(4)	
N2	C3	1.364(3)	
C3	C2	1.364(4)	
C1	C2	1.390(3)	
N1	C1	1.362(3)	
O6	N5	O5	124.7(2)
O6	N5	C6	118.8(2)
O5	N5	C6	116.5(3)
O3	N4	O4	125.5(3)
O3	N4	C4	117.9(2)
O4	N4	C4	116.6(3)
O1	N3	O2	124.1(3)
O1	N3	C1	118.7(2)
O2	N3	C1	117.2(2)
C3	N2	N1	109.5(2)
C3	N2	C4	143.6(2)
N1	N2	C4	106.81(19)
C1	N1	N2	106.84(18)
C1	N1	C6	145.2(2)
N2	N1	C6	107.97(18)
C5	C6	N1	108.7(2)
C5	C6	N5	127.2(2)
N1	C6	N5	121.4(2)
C4	C5	C6	107.0(2)
C5	C4	N2	109.4(2)
C5	C4	N4	129.9(3)
N2	C4	N4	120.6(2)
N2	C3	C2	107.6(2)
C3	C2	C1	107.5(3)
N1	C1	C2	108.5(2)
N1	C1	N3	121.1(2)
C2	C1	N3	128.0(3)

At 275 K:

N5	O6	1.229(3)	
N5	O5	1.227(2)	
N4	O4	1.228(2)	
N3	O2	1.233(2)	
N3	O1	1.216(3)	
O3	N4	1.231(3)	
C1	N3	1.411(3)	
N2	N1	1.367(2)	
N1	C6	1.385(2)	
N5	C6	1.410(3)	
C5	C6	1.369(3)	
N2	C4	1.389(3)	
C5	C4	1.370(3)	
N4	C4	1.415(3)	
N2	C3	1.362(3)	
C1	C2	1.390(3)	
C3	C2	1.364(3)	
N1	C1	1.363(2)	
O6	N5	O5	124.37(18)
O6	N5	C6	118.76(18)
O5	N5	C6	116.82(19)
O3	N4	O4	125.2(2)
O3	N4	C4	117.79(19)
O4	N4	C4	117.0(2)
O1	N3	O2	124.5(2)
O1	N3	C1	118.62(18)
O2	N3	C1	116.80(19)
C3	N2	N1	109.84(16)
C3	N2	C4	143.39(17)
N1	N2	C4	106.75(15)
C1	N1	N2	106.98(14)
C1	N1	C6	144.95(16)
N2	N1	C6	108.07(14)
C5	C6	N1	108.85(17)
C5	C6	N5	126.99(18)
N1	C6	N5	121.69(17)
C6	C5	C4	106.80(19)
C5	C4	N2	109.44(18)
C5	C4	N4	129.8(2)
N2	C4	N4	120.70(18)
C2	C3	N2	107.10(18)
C3	C2	C1	108.0(2)
N1	C1	C2	108.00(18)
N1	C1	N3	121.16(17)
C2	C1	N3	128.5(2)

At 250 K:

N5	O6	1.230(2)	
N5	O5	1.233(2)	
N4	O4	1.232(2)	
N3	O2	1.235(2)	
N3	O1	1.221(2)	
O3	N4	1.235(3)	
C1	N3	1.410(3)	
N2	N1	1.370(2)	
N1	C6	1.386(2)	
N5	C6	1.412(2)	
C5	C6	1.368(3)	
N2	C4	1.388(2)	
C5	C4	1.373(3)	
N4	C4	1.411(3)	
N2	C3	1.365(3)	
C1	C2	1.390(3)	
C3	C2	1.369(3)	
N1	C1	1.363(2)	
O6	N5	O5	124.51(17)
O6	N5	C6	118.97(17)
O5	N5	C6	116.47(17)
O4	N4	O3	125.1(2)
O4	N4	C4	116.97(19)
O3	N4	C4	117.96(18)
O1	N3	O2	124.48(19)
O1	N3	C1	118.64(17)
O2	N3	C1	116.80(18)
C3	N2	N1	109.75(15)
C3	N2	C4	143.41(17)
N1	N2	C4	106.81(14)
C1	N1	N2	106.97(14)
C1	N1	C6	145.04(15)
N2	N1	C6	107.99(14)
C5	C6	N1	108.88(16)
C5	C6	N5	127.18(17)
N1	C6	N5	121.50(16)
C6	C5	C4	106.83(18)
C5	C4	N2	109.38(17)
C5	C4	N4	129.81(19)
N2	C4	N4	120.72(17)
N2	C3	C2	107.14(17)
C3	C2	C1	107.81(19)
N1	C1	C2	108.28(17)
N1	C1	N3	121.15(16)
C2	C1	N3	128.19(19)

At 225 K:

N5	O6	1.233(2)	
N5	O5	1.232(2)	
N4	O4	1.233(2)	
N3	O2	1.238(2)	
N3	O1	1.225(2)	
O3	N4	1.234(2)	
C1	N3	1.410(2)	
N2	N1	1.3705(19)	
N1	C6	1.385(2)	
N5	C6	1.411(2)	
C5	C6	1.374(3)	
N2	C4	1.389(2)	
C5	C4	1.373(3)	
N4	C4	1.411(3)	
N2	C3	1.369(2)	
C1	C2	1.391(3)	
C3	C2	1.368(3)	
N1	C1	1.365(2)	
O5	N5	O6	124.34(16)
O5	N5	C6	116.73(17)
O6	N5	C6	118.88(16)
O4	N4	O3	124.99(19)
O4	N4	C4	117.02(18)
O3	N4	C4	117.99(17)
O1	N3	O2	124.29(19)
O1	N3	C1	118.56(17)
O2	N3	C1	117.07(17)
C3	N2	N1	109.75(14)
C3	N2	C4	143.21(16)
N1	N2	C4	107.02(13)
C1	N1	N2	106.95(13)
C1	N1	C6	145.06(15)
N2	N1	C6	107.99(13)
C5	C6	N1	108.81(15)
C5	C6	N5	126.97(16)
N1	C6	N5	121.60(16)
C4	C5	C6	106.85(17)
C5	C4	N2	109.25(16)
N1	C1	C2	108.26(16)
N1	C1	N3	121.15(15)
C2	C1	N3	128.18(18)

At 200 K:

N5	O6	1.231(2)
N5	O5	1.237(2)
N4	O4	1.237(2)
N3	O2	1.239(2)
N3	O1	1.227(2)
O3	N4	1.235(3)
C1	N3	1.410(2)
N2	N1	1.368(2)
N1	C6	1.389(2)
N5	C6	1.411(2)
C5	C6	1.379(3)
N2	C4	1.391(2)
C5	C4	1.377(3)
N4	C4	1.410(3)
N2	C3	1.372(2)
C1	C2	1.397(3)
C3	C2	1.372(3)
N1	C1	1.368(2)

O6	N5	O5	124.49(16)
O6	N5	C6	118.96(16)
O5	N5	C6	116.51(17)
O3	N4	O4	124.80(19)
O3	N4	C4	118.11(18)
O4	N4	C4	117.09(18)
O1	N3	O2	124.45(19)
O1	N3	C1	118.64(17)
O2	N3	C1	116.84(17)
N1	N2	C3	109.85(15)
N1	N2	C4	107.01(14)
C3	N2	C4	143.11(16)
C1	N1	N2	107.23(13)
C1	N1	C6	144.60(15)
N2	N1	C6	108.17(14)
C5	C6	N1	108.66(16)
C5	C6	N5	127.00(17)
N1	C6	N5	121.80(16)
C4	C5	C6	106.66(17)
C5	C4	N2	109.39(16)
C5	C4	N4	129.76(19)
N2	C4	N4	120.79(17)
C2	C3	N2	106.95(17)
C3	C2	C1	107.97(19)
N1	C1	C2	107.97(17)
N1	C1	N3	121.24(16)
C2	C1	N3	128.27(18)

At 175 K:

N5	O6	1.232(2)	
N5	O5	1.233(2)	
N4	O4	1.233(2)	
N3	O2	1.235(2)	
N3	O1	1.229(2)	
O3	N4	1.232(2)	
C1	N3	1.408(2)	
N2	N1	1.3688(18)	
N1	C6	1.385(2)	
N5	C6	1.406(2)	
C5	C6	1.373(2)	
N2	C4	1.387(2)	
C5	C4	1.377(2)	
N4	C4	1.409(2)	
N2	C3	1.366(2)	
C1	C2	1.391(2)	
C3	C2	1.372(3)	
N1	C1	1.367(2)	
O6	N5	O5	124.25(15)
O6	N5	C6	119.03(15)
O5	N5	C6	116.67(16)
O3	N4	O4	125.02(17)
O3	N4	C4	118.11(16)
O4	N4	C4	116.87(17)
O1	N3	O2	124.48(17)
O1	N3	C1	118.58(16)
O2	N3	C1	116.85(16)
C3	N2	N1	110.00(14)
C3	N2	C4	143.08(15)
N1	N2	C4	106.91(13)
C1	N1	N2	106.86(13)
C1	N1	C6	144.94(14)
N2	N1	C6	108.19(13)
C5	C6	N1	108.79(15)
C5	C6	N5	126.98(16)
N1	C6	N5	121.66(15)
C6	C5	C4	106.67(16)
C5	C4	N2	109.35(15)
C5	C4	N4	129.80(17)
N2	C4	N4	120.77(16)
N2	C3	C2	106.95(16)
C3	C2	C1	107.88(17)
N1	C1	C2	108.26(15)
N1	C1	N3	121.01(15)
C2	C1	N3	128.34(17)

At 150 K:

N5	O6	1.232(2)	
N5	O5	1.2366(19)	
N4	O4	1.232(2)	
N3	O2	1.238(2)	
N3	O1	1.229(2)	
O3	N4	1.232(2)	
C1	N3	1.411(2)	
N2	N1	1.3676(17)	
N1	C6	1.3836(19)	
N5	C6	1.409(2)	
C5	C6	1.372(2)	
N2	C4	1.386(2)	
C5	C4	1.377(2)	
N4	C4	1.413(2)	
N2	C3	1.367(2)	
C1	C2	1.393(2)	
C3	C2	1.374(3)	
N1	C1	1.367(2)	
O6	N5	O5	124.46(14)
O6	N5	C6	118.93(14)
O5	N5	C6	116.54(14)
O4	N4	O3	125.24(16)
O4	N4	C4	116.91(15)
O3	N4	C4	117.85(15)
O1	N3	O2	124.60(16)
O1	N3	C1	118.58(15)
O2	N3	C1	116.75(15)
C3	N2	N1	109.97(13)
C3	N2	C4	143.05(14)
N1	N2	C4	106.97(12)
C1	N1	N2	106.88(12)
C1	N1	C6	144.97(13)
N2	N1	C6	108.15(12)
C5	C6	N1	108.86(14)
C5	C6	N5	126.99(15)
N1	C6	N5	121.71(14)
C6	C5	C4	106.60(15)
C5	C4	N2	109.32(14)
C5	C4	N4	129.74(16)
N2	C4	N4	120.87(15)
N2	C3	C2	107.12(14)
C3	C2	C1	107.56(16)
N1	C1	C2	108.43(14)
N1	C1	N3	120.96(14)
C2	C1	N3	128.12(16)

At 125 K:

N5	O6	1.231(2)	
N5	O5	1.2367(19)	
N4	O4	1.234(2)	
N3	O2	1.239(2)	
N3	O1	1.228(2)	
O3	N4	1.236(2)	
C1	N3	1.412(2)	
N2	N1	1.3687(17)	
N1	C6	1.3846(19)	
N5	C6	1.4125(19)	
C5	C6	1.377(2)	
N2	C4	1.387(2)	
C5	C4	1.382(2)	
N4	C4	1.408(2)	
N2	C3	1.368(2)	
C1	C2	1.398(2)	
C3	C2	1.374(2)	
N1	C1	1.364(2)	
O6	N5	O5	124.75(13)
O6	N5	C6	118.78(14)
O5	N5	C6	116.40(14)
O4	N4	O3	124.99(16)
O4	N4	C4	117.12(15)
O3	N4	C4	117.89(14)
O1	N3	O2	124.68(15)
O1	N3	C1	118.54(14)
O2	N3	C1	116.71(14)
C3	N2	N1	109.89(13)
C3	N2	C4	142.98(14)
N1	N2	C4	107.11(12)
C1	N1	N2	107.08(12)
C1	N1	C6	144.79(13)
N2	N1	C6	108.14(12)
C5	C6	N1	108.95(14)
C5	C6	N5	126.81(14)
N1	C6	N5	121.78(14)
C6	C5	C4	106.38(15)
C5	C4	N2	109.31(14)
C5	C4	N4	129.60(16)
N2	C4	N4	121.03(14)
N2	C3	C2	107.18(14)
C3	C2	C1	107.48(16)
N1	C1	C2	108.34(14)
N1	C1	N3	121.12(14)
C2	C1	N3	127.97(16)

At 100 K:

N5	O6	1.233(2)	
N5	O5	1.237(2)	
N4	O4	1.233(2)	
N3	O2	1.240(2)	
N3	O1	1.228(2)	
O3	N4	1.236(2)	
C1	N3	1.406(2)	
N2	N1	1.3664(19)	
N1	C6	1.386(2)	
N5	C6	1.409(2)	
C5	C6	1.377(2)	
N2	C4	1.388(2)	
C5	C4	1.380(2)	
N4	C4	1.406(2)	
N2	C3	1.371(2)	
C1	C2	1.395(2)	
C3	C2	1.373(3)	
N1	C1	1.365(2)	
O6	N5	O5	124.54(14)
O6	N5	C6	118.88(14)
O5	N5	C6	116.53(15)
O4	N4	O3	125.01(17)
O4	N4	C4	117.06(16)
O3	N4	C4	117.93(15)
O1	N3	O2	124.53(16)
O1	N3	C1	118.68(15)
O2	N3	C1	116.72(15)
N1	N2	C3	109.93(13)
N1	N2	C4	107.18(13)
C3	N2	C4	142.88(15)
C1	N1	N2	107.12(13)
C1	N1	C6	144.72(14)
N2	N1	C6	108.16(13)
C5	C6	N1	108.84(14)
C5	C6	N5	126.79(15)
N1	C6	N5	121.85(15)
C6	C5	C4	106.47(15)
C5	C4	N2	109.26(15)
C5	C4	N4	129.68(16)
N2	C4	N4	121.03(15)
N2	C3	C2	106.92(15)
C3	C2	C1	107.73(16)
N1	C1	C2	108.26(15)
N1	C1	N3	121.01(15)
C2	C1	N3	128.19(16)

Contract No. N00014-95-1-0013 and N00014-97-1-0409

Program Officer: R. Miller/J. Goldwasser

**Title: Experimental Charge Densities and Electrostatic Potentials in Energetic
Materials and Infrastructure Upgrade for an X-ray Crystallography
Laboratory**

PI: A. Alan Pinkerton

Department of Chemistry, University of Toledo, Toledo, OH 43606

tel. (419) 530-4580, FAX (419) 530-4033, email apinker@uoft02.utoledo.edu

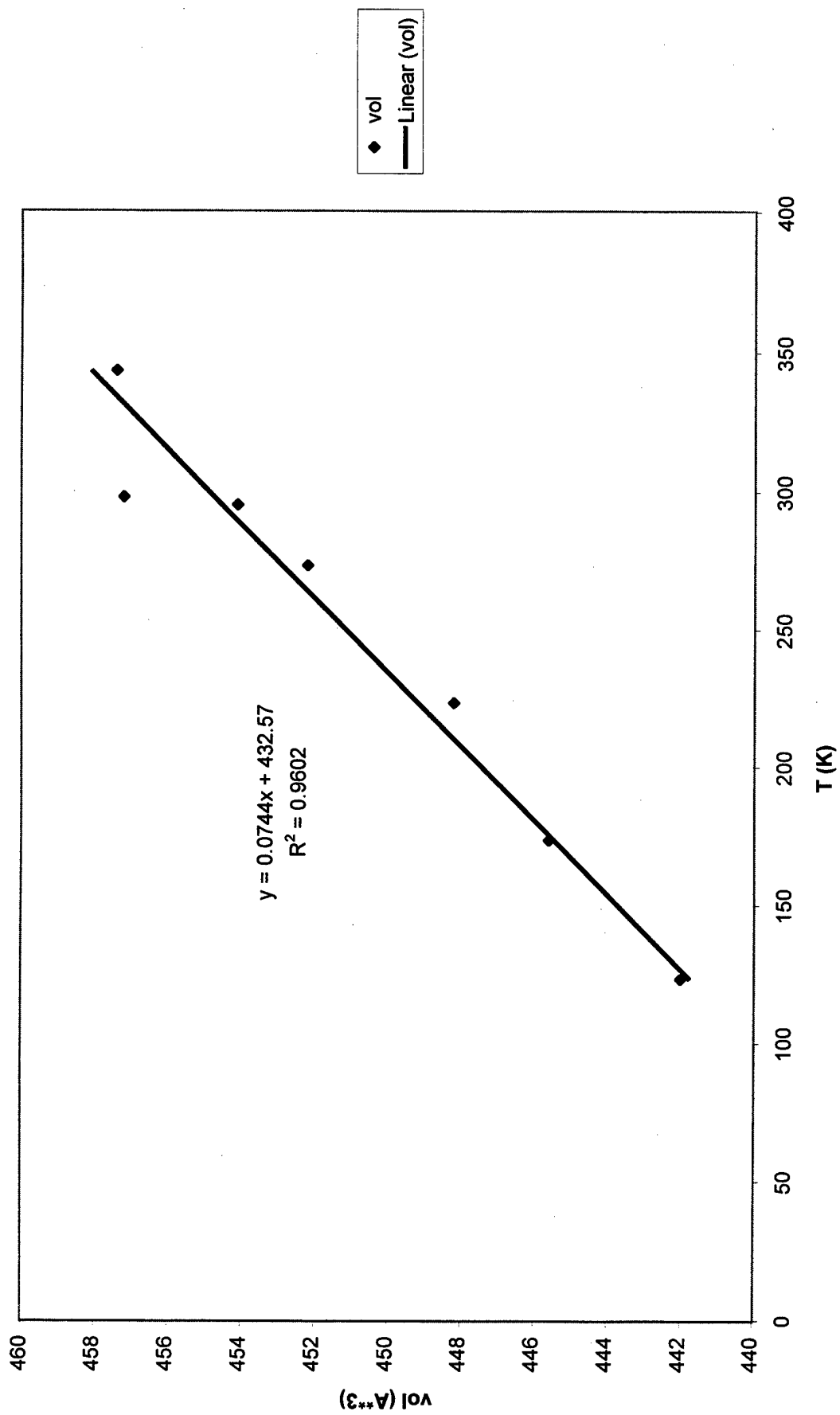
APPENDIX 3j

Variable temperature crystallographic study of ADN

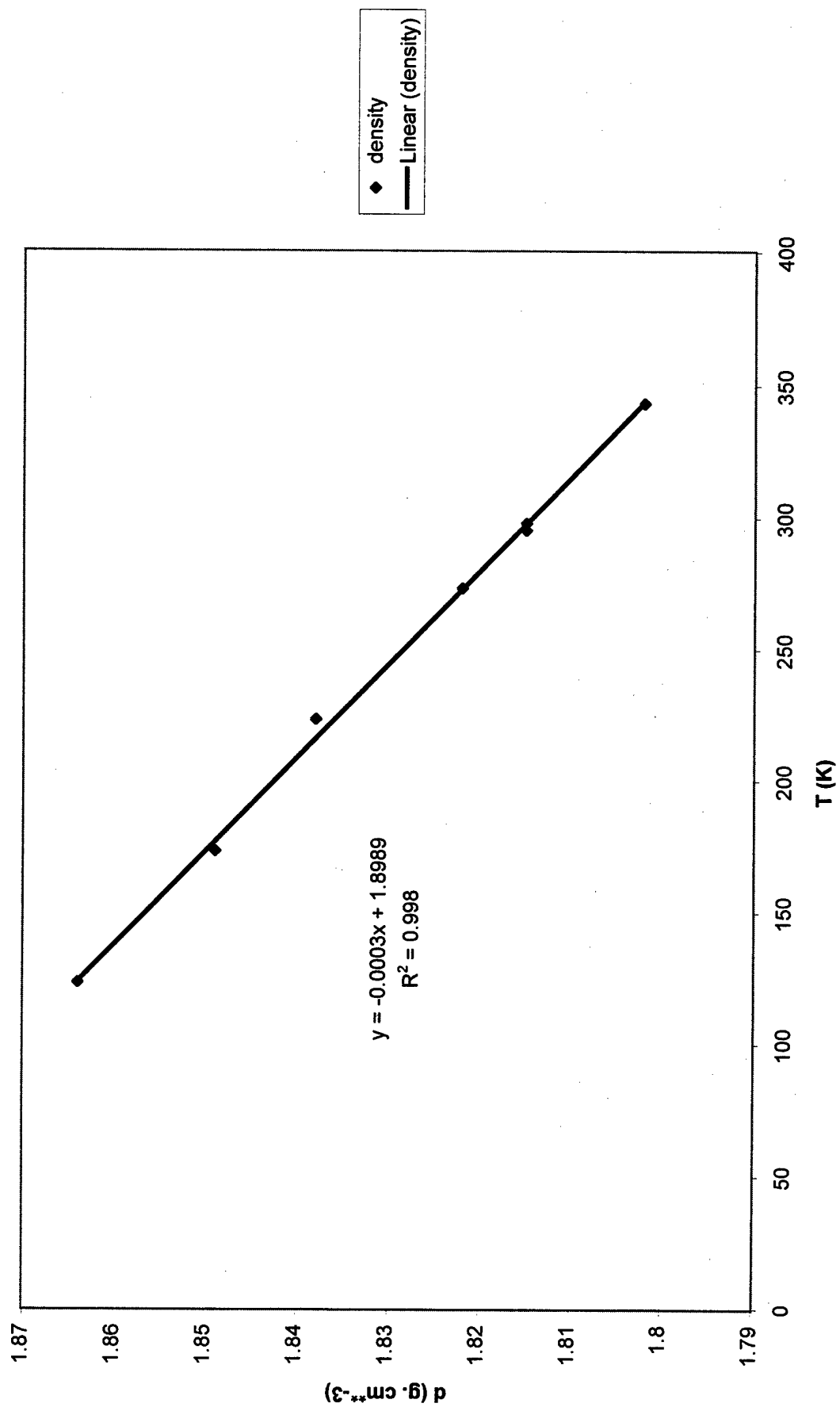
Variation of unit cell volume and density with temperature for ADN

T (K)	Vol (\AA^3)	d (g cm^{-3})
123.4	442.0	1.864
173.4	445.6	1.849
223.4	448.2	1.838
273.4	452.2	1.822
295.4	454.1	1.815
298.1	457.2	1.815
343.4	457.4	1.802

vol vs T



d vs T



Contract No. N00014-95-1-0013 and N00014-97-1-0409

Program Officer: R. Miller/J. Goldwasser

**Title: Experimental Charge Densities and Electrostatic Potentials in Energetic
Materials and Infrastructure Upgrade for an X-ray Crystallography
Laboratory**

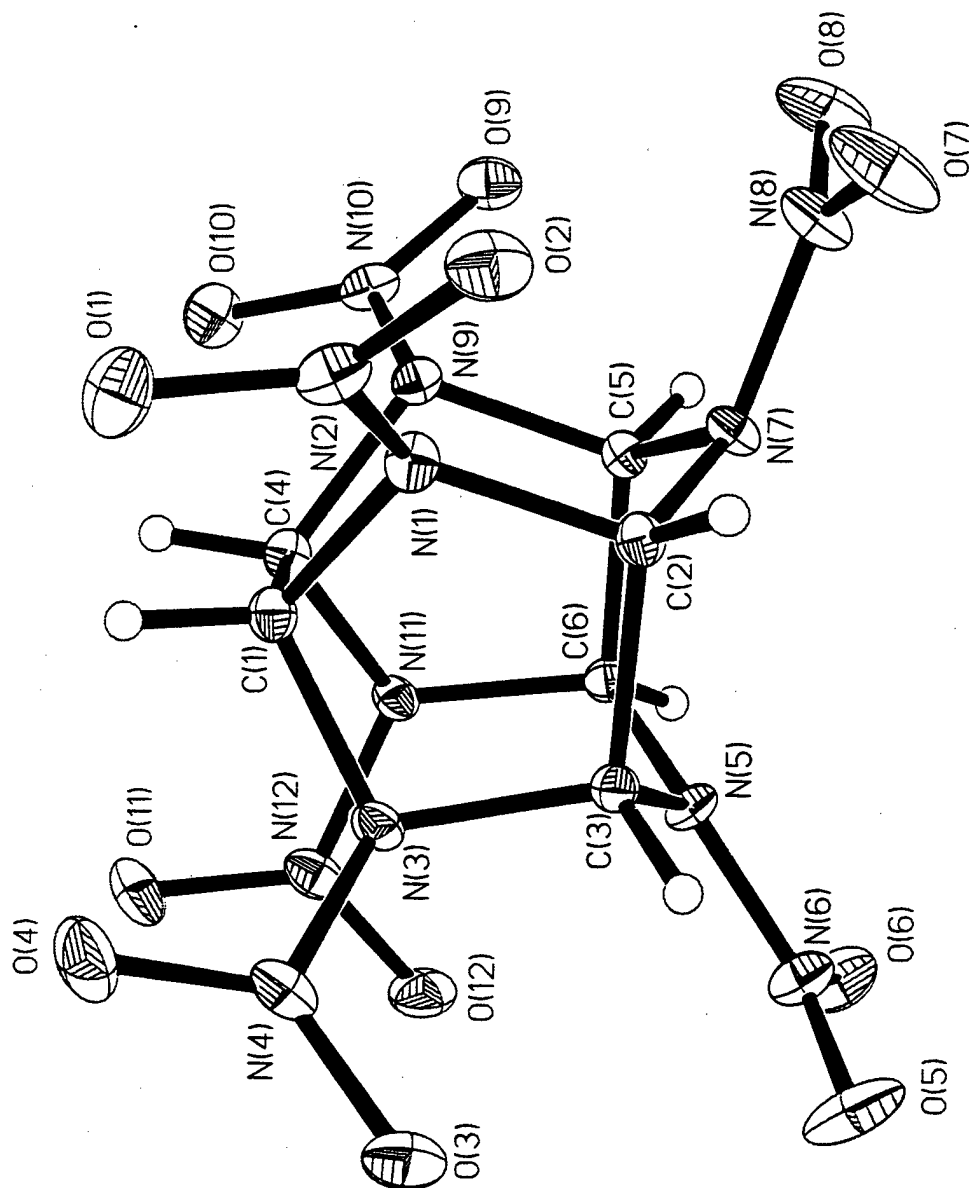
PI: A. Alan Pinkerton

Department of Chemistry, University of Toledo, Toledo, OH 43606

tel. (419) 530-4580, FAX (419) 530-4033, email apinker@uoft02.utoledo.edu

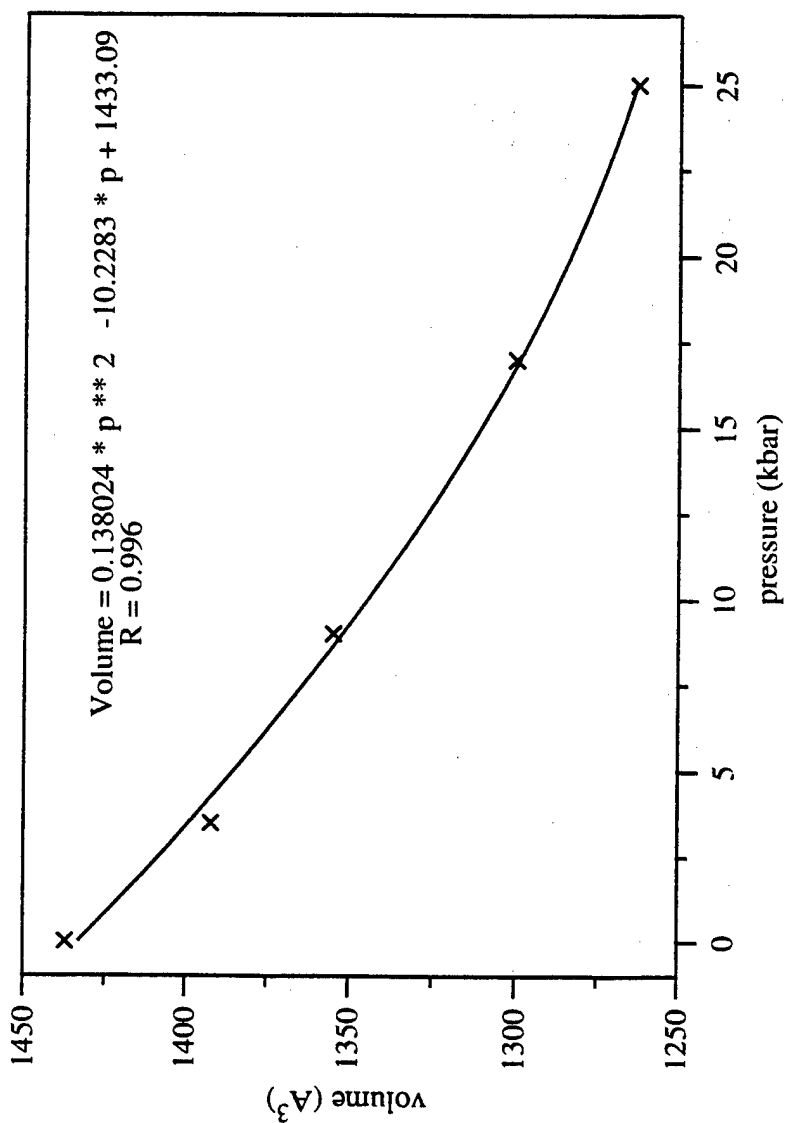
APPENDIX 4a

Variable pressure crystallographic study of ϵ -CL20



Pressure(Kbar)	a	b	c	beta
1	8.878	12.6108	13.4178	106.9187
3.5	8.783	12.453	13.281	106.61
9	8.7285	12.3091	13.1514	106.261
17	8.5999	12.1114	12.9745	106.006
25	8.544	11.937	12.839	105.28

epsilon-hexanitrohexaazaisowurtzitane
unit cell volume vs pressure



Contract No. N00014-95-1-0013 and N00014-97-1-0409

Program Officer: R. Miller/J. Goldwasser

**Title: Experimental Charge Densities and Electrostatic Potentials in Energetic
Materials and Infrastructure Upgrade for an X-ray Crystallography
Laboratory**

PI: A. Alan Pinkerton

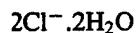
Department of Chemistry, University of Toledo, Toledo, OH 43606

tel. (419) 530-4580, FAX (419) 530-4033, email apinker@uoft02.utoledo.edu

APPENDIX 5a

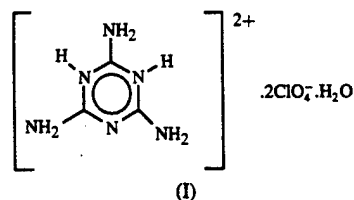
Melaminium Diperchlorate Hydrate.

Martin, A.; and Pinkerton, A.A., *Acta Crystallogr.*, 1995, C51, 2174-2177.



Comment

The asymmetric unit of melaminium diperchlorate, (I), consists of two well defined perchlorate anions, a well defined aromatic ring protonated at two of the three ring N atoms and a partially disordered water molecule.



There is an extensive hydrogen-bonding network throughout the lattice (Fig. 1). Both perchlorate anions have the expected tetrahedral geometry, with bond lengths ranging from 1.430 (2) (Cl1—O1) to 1.458 (1) Å (Cl1—O4). The bond angles range from 108.78 (7) (O3—Cl1—O4) to 110.86 (8)° (O6—Cl2—O7). Protonation of the ring N atoms distorts the bond lengths in the aromatic ring. The two shortest bonds [N3—C3 1.320 (2) and N3—C1 1.333 (2) Å] are those furthest from the protonated ring N atoms. The two longest bonds [N2—C3 1.378 (2) and N1—C1 1.376 (2) Å] are those connected to the shortest bonds. This has the effect of opening up the ring bond angles at atoms C1 and C3, thus creating the largest bond angles in the ring [N2—C3—N3 122.2 (2) and N1—C1—N3 122.1 (1)°]. The amine groups do not appear to be affected in any systematic way by the distortion of the ring.

The bond length most likely to be affected, N5—C2 [1.304 (2) Å], lies midway between N4—

Acta Cryst. (1995). C51, 2174–2177

Melaminium Diperchlorate Hydrate

ANTHONY MARTIN AND A. ALAN PINKERTON

Department of Chemistry, University of Toledo, Toledo, OH 43606, USA

(Received 28 September 1994; accepted 16 March 1995)

Abstract

The structure of the new melaminium salt, 2,4,6-triamino-1,3,5-triazine-1,3-dium diperchlorate hydrate, $\text{C}_3\text{H}_8\text{N}_6^{2+} \cdot 2\text{ClO}_4^- \cdot \text{H}_2\text{O}$, has been characterized using low-temperature X-ray diffraction data (100 K). Melaminium diperchlorate has a high density ($\rho_c = 1.94 \text{ Mg m}^{-3}$), is extensively hydrogen bonded and contains a water dimer.

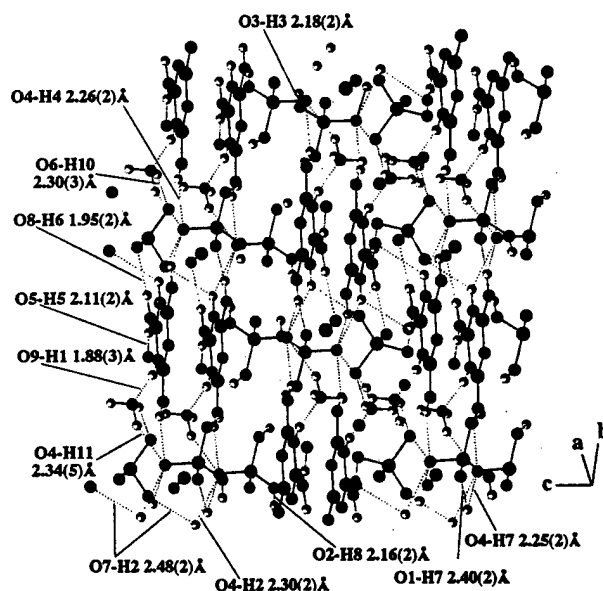


Fig. 1. Packing diagram for melaminium diperchlorate showing three unit cells in the *a* direction and two unit cells in the *b* and *c* directions, with hydrogen bonds ($\text{O} \cdots \text{H} < 2.5 \text{ Å}$) shown.

C1 [1.301(2) Å] and N6—C3 [1.309(2) Å]. A semi-empirical calculation, with the AM1 parameter set (Dewar, Zoebisch, Healy & Stewart, 1985), on the protonated melaminium dication results in the same geometrical features. Thus, the ring distortion is a result of protonation and not hydrogen bonding or crystal packing. The distortion of the aromatic ring is quite similar to that reported for the melamine-cyanuric acid complex hydrochloride (Wang, Wei & Wang, 1990), the only other simple salt of diprotonated melamine that has been structurally determined.

For the purposes of this discussion a hydrogen bond has been defined as having an O...H contact of less than 2.5 Å.

One perchlorate anion (Fig. 2) is involved in seven or eight hydrogen bonds, depending on the orientation of the disordered water molecule. These bonds come from four different melaminium moieties. Atom O4 is the most interesting as it accepts three hydrogen bonds. These are O4...H4 [2.26(2) Å], O4...H7 [2.25(2) Å] and O4...H2 [2.30(2) Å]. It also forms a hydrogen bond with a half-occupied H atom on the water molecule, O4...H11 [2.34(5) Å]. Each of the other O atoms has one H atom bonded to it. The shortest of all the hydrogen bonds to this perchlorate anion is O2...H8 [2.16(2) Å], which is almost linear [O2...H8—N6 168(2)°]. The longest is O1...H7 [2.40(2) Å], which is substantially bent [O1...H7—N6 110(2)°].

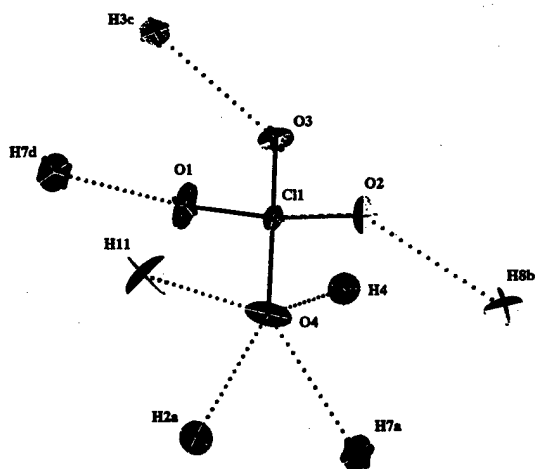


Fig. 2. Diagram with 50% displacement ellipsoids showing the hydrogen bonds to perchlorate (1) [symmetry codes: (a) $x, y+1, z$; (b) $-x+2, -y+1, -z+1$; (c) $x-1, y, z$; (d) $x-1, y+1, z$].

The other perchlorate anion (Fig. 3) forms four hydrogen bonds with two different melaminium moieties. There is one hydrogen bond to each O atom. The shortest is O8...H6 [1.95(2) Å], which is essentially linear [O8...H6—N5 173(2)°], while the longest is O7...H2 [2.48(2) Å], which is very bent [O7...H2—N2 114(2)°].

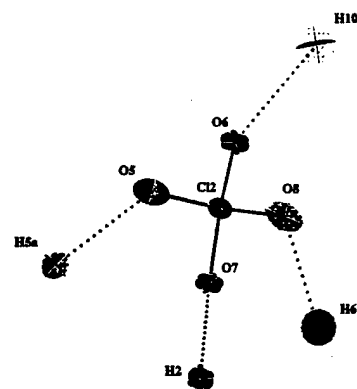


Fig. 3. Diagram with 50% displacement ellipsoids showing the hydrogen bonds to perchlorate (2) [symmetry codes: (a) $-x, -y, -z$; (b) $x, y-1, z$].

The melaminium moiety (Fig. 4) has 11 O atoms bonded to it from both perchlorate anions, related by one of six different symmetry operations. The most noticeable feature is that there are two bifurcated hydrogen bonds (involving atoms H2 and H7) and that they share a common O atom (O4). Both H2 and H7 have the shorter of their bifurcated bonds to O4 [O4...H2 2.30(2) and O4...H7 2.25(2) Å], with very similar bond angles [O4...H2—N2 142(2) and O4...H7—N6 143(2)°]. The second bond from each H atom is longer [O7...H2 2.48(2) and O1...H7 2.40(2) Å] and is bent even more [O7...H2—N2 114(2) and O1...H7—N6 110(2)°]. These bonds are clearly of a weaker nature. The remainder of the hydrogen bonding involving the melaminium cation is quite ordinary.

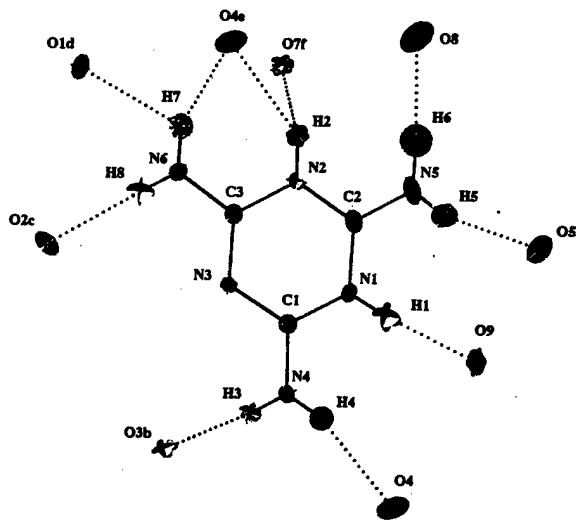
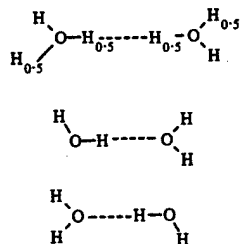


Fig. 4. Diagram with 50% displacement ellipsoids showing the hydrogen bonds from the melaminium cation [symmetry codes: (a) $-x, -y, -z$; (b) $x+1, y, z$; (c) $-x+2, -y+1, -z+1$; (d) $x+1, y-1, z$; (e) $x, y-1, z$; (f) $x+1, y, z$].

The disordered water molecule (Fig. 5) forms a hydrogen-bonded dimeric structure with itself across a center of symmetry and has the shortest hydrogen bonds in the crystal structure associated with it.



One orientation is H9—O9—H10 which forms a 'dimer' with the other orientation H10—O9—H11. The hydrogen bond H10—O9...H9 is 2.01 (4) Å long and has a bond angle of 108 (4)°. The shortest hydrogen bond in the crystal [O9...H1 1.88 (3) Å], between the water O atom and a melaminium H atom, is the same regardless of the orientation of the water molecule and is almost linear [O9...H1—N1 170 (2)°].

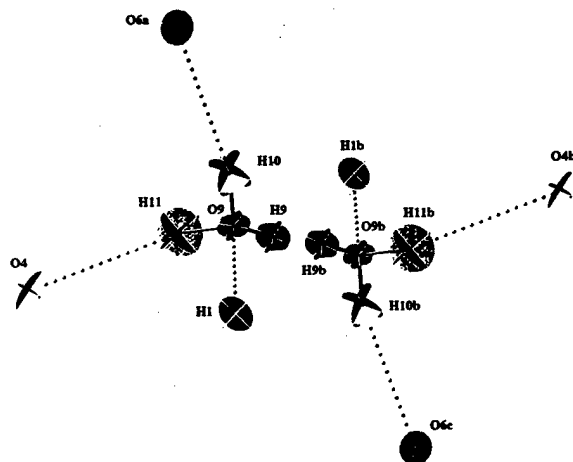


Fig. 5. Diagram with 50% displacement ellipsoids showing the hydrogen bonds to and from the water dimer [symmetry codes: (a) $x, y+1, z$; (b) $-x+1, -y+1, -z$; (c) $-x+1, -y+2, -z$]. Atoms H9 and H11 are disordered with occupancies of 0.5.

Experimental

Melamine was dissolved in perchloric acid (60%) and the resulting solution was slowly evaporated. After several days, colorless crystals of the title salt appeared.

Crystal data

$C_3H_8N_6^{2+} \cdot 2ClO_4^- \cdot H_2O$
 $M_r = 345.06$

Mo $K\alpha$ radiation
 $\lambda = 0.71073$ Å

Triclinic

$P\bar{1}$

$a = 5.8981$ (6) Å

$b = 9.235$ (1) Å

$c = 11.101$ (2) Å

$\alpha = 97.85$ (1)°

$\beta = 90.38$ (1)°

$\gamma = 98.87$ (1)°

$V = 591.6$ (3) Å³

$Z = 2$

$D_x = 1.94$ Mg m⁻³

Data collection

Enraf-Nonius CAD-4
 diffractometer

$\theta/2\theta$ scans

Absorption correction:

ψ scans (North, Phillips
 & Mathews, 1968)

$T_{\min} = 0.929$, $T_{\max} =$
 0.999

2624 measured reflections

2316 independent reflections

Refinement

Refinement on F

$R = 0.026$

$wR = 0.035$

$S = 3.350$

2180 reflections

226 parameters

All H-atom parameters
 refined

$w = 1/\sigma^2(F_o)$

$(\Delta/\sigma)_{\max} = 0.002$

Cell parameters from 25

reflections

$\theta = 10-14^\circ$

$\mu = 0.606$ mm⁻¹

$T = 100$ K

Parallelepiped

$0.31 \times 0.24 \times 0.20$ mm

Colorless

2180 observed reflections

$[I > 3\sigma(I)]$

$R_{\text{int}} = 0.019$

$\theta_{\max} = 25.99^\circ$

$h = 0 \rightarrow 7$

$k = -11 \rightarrow 11$

$l = -13 \rightarrow 13$

3 standard reflections

frequency: 50 min

intensity decay: 3.11%

$\Delta\rho_{\max} = 0.28$ e Å⁻³
 $\Delta\rho_{\min} = -0.51$ e Å⁻³

Extinction correction:

isotropic (Zachariasen,
 1963)

Extinction coefficient:

0.13 (1) $\times 10^{-4}$

Atomic scattering factors

from *International Tables*
 for X-ray Crystallography
 (1974, Vol. IV)

Table 1. Fractional atomic coordinates and isotropic or equivalent isotropic displacement parameters (Å²)

U_{iso} for H atoms; $U_{\text{eq}} = (1/3)\sum_i \sum_j U_{ij} a_i^* a_j^* a_i \cdot a_j$ for others.

	x	y	z	$U_{\text{iso}}/U_{\text{eq}}$
C11	0.46207 (6)	0.75853 (4)	0.40263 (3)	0.01158 (8)
C12	0.04855 (7)	-0.23629 (4)	0.04972 (3)	0.01499 (8)
O1	0.2716 (2)	0.8215 (1)	0.3642 (1)	0.0258 (3)
O2	0.5504 (2)	0.8351 (1)	0.5184 (1)	0.0225 (3)
O3	0.3927 (2)	0.6041 (1)	0.4101 (1)	0.0193 (3)
O4	0.6417 (2)	0.7739 (1)	0.3136 (1)	0.0240 (3)
O5	-0.0103 (3)	-0.2759 (2)	-0.0787 (1)	0.0342 (4)
O6	-0.0048 (2)	-0.3643 (1)	0.1097 (1)	0.0215 (3)
O7	-0.0784 (2)	-0.1222 (1)	0.0993 (1)	0.0201 (3)
O8	0.2909 (2)	-0.1812 (2)	0.0634 (2)	0.0360 (4)
O9	0.4262 (2)	0.5030 (1)	0.1226 (1)	0.0257 (3)
N1	0.6257 (2)	0.3266 (1)	0.2522 (1)	0.0140 (3)
N2	0.6880 (2)	0.0872 (1)	0.2558 (1)	0.0139 (3)
N3	0.9526 (2)	0.2837 (1)	0.3590 (1)	0.0123 (3)
N4	0.8955 (2)	0.5183 (1)	0.3420 (1)	0.0155 (3)
N5	0.3698 (3)	0.1308 (2)	0.1540 (1)	0.0214 (4)
N6	0.9965 (2)	0.0436 (1)	0.3649 (1)	0.0164 (3)
C1	0.8273 (3)	0.3763 (2)	0.3184 (1)	0.0117 (3)
C2	0.5570 (3)	0.1812 (2)	0.2192 (1)	0.0141 (4)
C3	0.8817 (3)	0.1407 (2)	0.3279 (1)	0.0123 (3)
H1	0.558 (4)	0.386 (2)	0.220 (2)	0.031 (6)
H2	0.650 (4)	-0.006 (2)	0.237 (2)	0.021 (5)
H3	1.022 (3)	0.548 (2)	0.377 (2)	0.018 (5)
H4	0.824 (4)	0.576 (2)	0.317 (2)	0.022 (5)
H5	0.297 (4)	0.189 (2)	0.136 (2)	0.026 (6)

H6	0.330 (4)	0.029 (3)	0.125 (2)	0.040 (7)
H7	0.954 (4)	-0.050 (2)	0.344 (2)	0.025 (6)
H8	1.111 (4)	0.075 (2)	0.406 (2)	0.027 (6)
H9†	0.474 (8)	0.498 (5)	0.050 (4)	0.03 (1)
H10	0.299 (4)	0.509 (3)	0.120 (2)	0.048 (8)
H11†	0.47 (1)	0.595 (6)	0.156 (5)	0.06 (2)

† Occupancy = 0.5.

Table 2. Selected geometric parameters (Å, °)

Cl1—O1	1.430 (1)	N1—C2	1.341 (2)
Cl1—O2	1.433 (1)	N2—C2	1.347 (2)
Cl1—O3	1.436 (1)	N2—C3	1.378 (2)
Cl1—O4	1.458 (1)	N3—C1	1.333 (2)
Cl2—O5	1.449 (1)	N3—C3	1.320 (2)
Cl2—O6	1.430 (1)	N4—C1	1.301 (2)
Cl2—O7	1.437 (1)	N5—C2	1.304 (2)
Cl2—O8	1.441 (1)	N6—C3	1.309 (2)
N1—C1	1.376 (2)		
O1—Cl1—O2	109.89 (8)	C1—N1—C2	120.3 (1)
O1—Cl1—O3	110.11 (7)	C2—N2—C3	120.2 (1)
O1—Cl1—O4	108.85 (8)	C1—N3—C3	117.2 (1)
O2—Cl1—O3	110.19 (8)	N1—C1—N3	122.1 (1)
O2—Cl1—O4	109.00 (7)	N1—C1—N4	118.4 (2)
O3—Cl1—O4	108.78 (7)	N3—C1—N4	119.5 (1)
O5—Cl2—O6	109.36 (8)	N1—C2—N2	117.9 (1)
O5—Cl2—O7	108.77 (9)	N1—C2—N5	121.7 (2)
O5—Cl2—O8	108.7 (1)	N2—C2—N5	120.4 (2)
O6—Cl2—O7	110.86 (8)	N2—C3—N3	122.2 (2)
O6—Cl2—O8	109.64 (9)	N2—C3—N6	117.4 (1)
O7—Cl2—O8	109.43 (8)	N3—C3—N6	120.4 (1)

Table 3. Hydrogen-bonding geometry (Å, °)

D—H...A	D—H	H...A	D...A	D—H...A
N1—H1...O9	0.84 (3)	1.88 (3)	2.705 (2)	170 (2)
N2—H2...O4 ⁱ	0.85 (2)	2.30 (2)	3.021 (2)	142 (2)
N2—H2...O7 ⁱⁱ	0.85 (2)	2.48 (2)	2.931 (2)	114 (2)
N4—H3...O3 ⁱⁱ	0.83 (2)	2.18 (2)	2.982 (2)	162 (2)
N4—H4...O4	0.80 (2)	2.26 (2)	3.033 (2)	161 (2)
N5—H5...O5 ⁱⁱⁱ	0.78 (2)	2.11 (2)	2.854 (2)	159 (2)
N5—H6...O8	0.94 (2)	1.95 (2)	2.884 (2)	173 (2)
N6—H7...O1 ^{iv}	0.86 (2)	2.40 (2)	2.804 (2)	110 (2)
N6—H7...O4 ⁱ	0.86 (2)	2.25 (2)	2.983 (2)	143 (2)
N6—H8...O2 ^v	0.81 (2)	2.16 (2)	2.951 (2)	168 (2)
O9—H9...O9 ^{vi}	0.85 (4)	2.01 (4)	2.860 (2)	176 (5)
O9—H10...O6 ^{vii}	0.76 (3)	2.30 (3)	2.998 (2)	153 (3)
O9—H11...O4	0.88 (5)	2.34 (5)	3.146 (2)	152 (5)

Symmetry codes: (i) $x, y - 1, z$; (ii) $1 + x, y, z$; (iii) $-x, -y, -z$; (iv) $1 + x, y - 1, z$; (v) $2 - x, 1 - y, 1 - z$; (vi) $1 - x, 1 - y, -z$; (vii) $x, 1 + y, z$.

Backgrounds were obtained from analysis of the scan profile (Blessing, Coppens & Becker, 1974). The structure was solved by Patterson and Fourier methods.

Data collection: CAD-4 diffractometer software (Enraf-Nonius, 1977). Cell refinement: CAD-4 diffractometer software. Data reduction: *MolEN PROCESS* (Fair, 1990) and *SORTAV* (Blessing, 1987). Program(s) used to refine structure: *MolEN LSFM*. Molecular graphics: *CACHE WORKSYSTEM* (Cache Scientific, 1993). Software used to prepare material for publication: *MolEN CIF VAX*.

We thank the Office of Naval Research (Contract No. 000149310597) and the College of Arts and Sciences of the University of Toledo for generous financial support.

Lists of structure factors, anisotropic displacement parameters, H-atom coordinates and complete geometry have been deposited with the IUCr (Reference: BK1103). Copies may be obtained through The Managing Editor, International Union of Crystallography, 5 Abbey Square, Chester CH1 2HU, England.

References

- Blessing, R. H. (1987). *Cryst. Rev.* **1**, 3–57.
 Blessing, R. H., Coppens, P. & Becker, P. (1974). *J. Appl. Cryst.* **7**, 488–492.
 Cache Scientific (1993). *CACHE Reference Manual*. Cache Scientific, Beaverton, Oregon, USA.
 Dewar, M. J. S., Zebisch, E. G., Healy, E. F. & Stewart, J. J. P. (1985). *J. Am. Chem. Soc.* **107**, 3902–3909.
 Enraf-Nonius (1977). *CAD-4 Operations Manual*. Enraf-Nonius, Delft, The Netherlands.
 Fair, C. K. (1990). *MolEN. An Interactive Intelligent System for Crystal Structure Analysis*. Enraf-Nonius, Delft, The Netherlands.
 North, A. C. T., Phillips, D. C. & Mathews, F. S. (1968). *Acta Cryst.* **A24**, 351–359.
 Wang, Y., Wei, B. & Wang, Q. (1990). *J. Crystallogr. Spectrosc. Res.* **20**, 79–84.
 Zachariasen, W. H. (1963). *Acta Cryst.* **16**, 1139–1144.

Contract No. N00014-95-1-0013 and N00014-97-1-0409

Program Officer: R. Miller/J. Goldwasser

**Title: Experimental Charge Densities and Electrostatic Potentials in Energetic
Materials and Infrastructure Upgrade for an X-ray Crystallography
Laboratory**

PI: A. Alan Pinkerton

Department of Chemistry, University of Toledo, Toledo, OH 43606

tel. (419) 530-4580, FAX (419) 530-4033, email apinker@uoft02.utoledo.edu

APPENDIX 5b

**Energetic Materials: The Preparation and Structural Characterization of
Melaminium Dinitramide and Melaminium Nitrate.**

**Tanbug, R; Kirschbaum, K.; and Pinkerton, A.A.; *J. Chem. Crystallogr.*, in
press.**

**Energetic materials: the preparation and structural characterization of melaminium
dinitramide and melaminium nitrate**

Rasim Tanbug, Kristin Kirschbaum and A. Alan Pinkerton*,

Department of Chemistry, University of Toledo

Toledo, OH, 43606

USA

Energetic materials: melaminium salts

Abstract

Two energetic salts of the melaminium cation have been prepared and structurally characterized from room temperature X-ray single crystal diffraction data. Melaminium dinitramide (**I**), triclinic, $P\bar{1}$, $a = 6.6861(11)$, $b = 6.9638(16)$, $c = 10.447(2)$ Å, $\alpha = 99.07(3)$, $\beta = 98.30(3)$, $\gamma = 108.50(3)^\circ$, $V = 445.6(2)$ Å³, $Z = 2$. Melaminium nitrate (**II**), monoclinic, $P2_1/c$, $a = 3.5789(7)$, $b = 20.466(4)$, $c = 10.060(2)$ Å, $\beta = 94.01(2)^\circ$, $V = 735.0(3)$ Å³, $Z = 4$.

The crystal structures of both salts show distinct monoprotonated melaminium cations and dinitramide- or nitrate anions, respectively. Efficient packing in the solid state is achieved by extensive hydrogen bonding between two-dimensional zigzag ribbons of the melaminium cations and the respective anions resulting in high densities of the solid state structures of 1.74 (**I**) and 1.71 g/cm³ (**II**).

Key Words

Melaminium dinitramide and melaminium nitrate, melaminium salts, dinitramide salt, hydrogen bonding, X-ray structure, energetic materials

Introduction

In recent years there has been great interest in the development of new solid energetic materials, especially propellants with low signatures. Desired properties for this class of

compounds are a halogen-free, nitrogen and oxygen-rich molecular composition, high densities and a high heat of formation. A break-through in this area of chemistry came in 1991 with the first reports on dinitraminic acid, $\text{NH}(\text{NO}_2)_2$ and its dinitramide salts.¹ The ability of the dinitramide anion, N_3O_4^- , to form stable oxygen rich salts with high densities with a variety of cations makes it a promising candidate in the development of energetic oxidizers for solid propellants.²

Ammonium dinitramide was among the first salts synthesized.³ Its spectroscopic^{2,4} and other properties,^{5,6} in particular its photo-^{7,8} or thermal decomposition,⁹⁻¹⁷ and theoretical studies on the thermochemistry,¹⁸⁻²⁰ as well as its photographic²¹ and medical²²⁻²⁴ applications have been extensively investigated. Numerous other salts of dinitraminic acid and the acid itself have since been prepared and characterized in great detail.^{2-4, 25-54} An interesting feature of the dinitramide anion is its amazing variety of conformations in the solid state. While ab initio calculations on the dinitramide anion determined the 'ideal' minimum energy conformation to be of C_2 geometry, structural characterizations have revealed a diversity of conformations with no (C_1) symmetry, C_s symmetry and also with the predicted C_2 geometry. With a barrier to rotation about the N-N bonds of <3 kcal/mol,⁵⁵ the conformation of the dinitramide anion in a crystal lattice is considerably influenced by packing effects and interionic interactions such as hydrogen bonds.

Melamine, 2,4,6-triamino-1,3,5-triazine, is a nitrogen-rich, 'planar' compound with the potential to form both mono- and diprotonated cations and to participate in extensive hydrogen bonding. Even though its use in the design of hydrogen-bonded supramolecular aggregates is well known,⁵⁶⁻⁶⁴ surprisingly few structural studies have been carried out on compounds containing the mono-⁶⁵⁻⁶⁷ or diprotonated melaminium cations.⁶⁸⁻⁷¹

As an extension of our investigation of nitrogen-rich and energetic materials such as biguanidinium carbonate, –sulfates,⁷² –nitrates,⁷³ –perchlorates,⁷⁴ and –dinitramides,⁷⁵ as well as melaminium diperchlorate hydrate,⁶⁸ we have synthesized two new energetic melaminium salts. The present paper describes the preparation and single crystal X-ray structures of melaminium dinitramide (**I**) and melaminium nitrate (**II**).

Experimental

Colorless crystals of the new melaminium salt, 2,4,6-triamino-1,3,5-triazinium dinitramide (melaminium dinitramide, **I**) were isolated by slow evaporation of an aqueous solution containing melaminium perchlorate and potassium dinitramide.⁷⁶ A crystal of **I** of approximate dimensions 0.15 x 0.15 x 0.10 mm was mounted on a thin glass fiber and X-ray diffraction data were collected at 293(1) K on an Enraf-Nonius CAD-4 diffractometer. The unit cell was determined to be triclinic with $a = 6.6861(11)$, $b = 6.9638(16)$, $c = 10.447(2)$ Å, $\alpha = 99.07(3)$, $\beta = 98.30(3)$ and $\gamma = 108.50(3)^\circ$. Intensities were corrected for absorption (ψ -scan)⁷⁷ and decay. The structure was solved by direct methods in space group $P\bar{1}$ and refined by full matrix least squares on F.

Colorless crystals of the new melaminium salt, 2,4,6-triamino-1,3,5-triazinium nitrate (melaminium nitrate, **II**) were obtained from slow evaporation of a solution of melamine in concentrated nitric acid. A crystal of **II** of approximate dimensions 0.20 x 0.15 x 0.10 mm was mounted on a thin glass fiber and X-ray diffraction data were collected at 293(1) K on a Siemens SMART platform diffractometer. The intensities were corrected for absorption and decay using SADABS⁷⁸. Melaminium nitrate crystallizes in a monoclinic unit cell with $a = 3.5789(7)$, $b = 20.466(4)$, $c = 10.060(2)$ Å and $\beta = 94.01(2)^\circ$. The structure was solved in the

space group $P2_1/c$ by direct methods and refined by full matrix least squares on F^2 using SHELXTL⁷⁹.

For both structures, neutral atom scattering factors were used with the corrections for real and imaginary anomalous dispersion. All non-hydrogen atoms were refined with anisotropic atomic displacement parameters. The hydrogen atoms were located from difference Fourier maps and included in the refinement with isotropic displacement parameters. Further details of data collection and refinement are given in table 1, fractional coordinates and equivalent isotropic atomic displacement factors for **I** and **II** are given in tables 2 and 4, respectively. Selected bond distances and angles are listed in tables 3 and 5.

Results and Discussion

Crystals of **I** contain one monoprotonated melaminium cation and one dinitramide anion in the asymmetric unit. Efficient packing of the ions is obtained through a complex hydrogen-bonding network (vide infra) resulting in a high density of the solid state structure of 1.74 g/cm³. The solid state structure of **II** consists of one monoprotonated melaminium cation and one nitrate anion in the asymmetric unit, which are also connected through hydrogen bonds to build a three dimensional network. However, the packing of these ions is not quite as efficient, leading to a density of 1.71 g/cm³ (vide infra).

Melaminium cations

The melaminium cations in **I** and **II** are essentially planar. However, considering the ideal plane through the ring atoms C(1),C(2),C(3),N(2),N(4),N(6), significant differences concerning the deviation from planarity are observed. The central ring in **I** is planar within

$\pm 0.007(2)$ Å and the amine N-atoms also deviate no more than $0.023(5)$ Å from the ideal plane. In contrast, a slight boat configuration - similar to the one observed in melamine itself⁸⁰ - with deviations of up to $0.020(1)$ Å from the central plane is adopted by the melaminium cation in **II**. In this case, the amine groups deviate by as much as $0.075(3)$ Å from the mean aromatic plane. From these observations, it is clear that neither the planarity nor the slight boat configuration are intrinsic to melamine or the protonated melaminium cation, but rather are due to the chemical environment in the solid state (i.e. hydrogen bonding or packing effects). The melaminium cation in its respective chemical environment is shown in figure 1 for **I** and figure 2 for **II**.

Protonation of the aromatic ring in the melamine molecule results in a redistribution of the π -electrons. The exocyclic NH_2 -C bonds { $1.310(4)$ - $1.321(4)$ Å in **I** and $1.311(3)$ - $1.319(3)$ Å in **II**} are significantly shorter than the comparable ones in the parent neutral base { $1.337(1)$ - $1.362(4)$ Å}⁸⁰⁻⁸³ indicating an increase in bond order of the C-amine bonds on protonation. Three resonance forms containing an $\text{NH}_2^+=\text{C}$ bond are possible, which cause the C-N bonds in the triazine ring to fall into three groups.⁶⁵ This is clearly reflected in the C-N bond lengths in **II**, the two C-atoms bonded to the N-H functional group being the longest {C(2)-N(4), $1.370(3)$; C(1)-N(4), $1.374(3)$ Å}, the C-N bonds connected to these long bonds the shortest {C(2)-N(6), $1.326(3)$; C(1)-N(2), $1.327(3)$ Å}, and the C-N bond located furthest away from the imino-group being of intermediate length {C(3)-N(2), $1.349(3)$; C(3)-N(6), $1.354(3)$ Å}. Similar - but not quite as distinct - differences are observed in the crystal structure of **I**. Longer C-N bonds of $1.354(4)$ {C(1)-N(4)} and $1.358(4)$ Å {C(2)-N(4)} can be found for the two C-atoms bonded to the N-H functional group. The shortest ones are the C-N bonds connected to these longer bonds: C(2)-N(6) with $1.317(4)$ and C(1)-N(2) with $1.325(4)$

Å. The C-N bonds located furthest away from the imino-group are only on average of medium length: 1.349(4) {C(3)-N(2)} and 1.361(4) Å {C(3)-N(6)}.

To the best of our knowledge,⁸⁴ only three other compounds containing a monoprotonated melaminium cation have been structurally characterized. Melaminium bromide hemihydrate, (HMel)Br,⁶⁵ and barbituric acid melamine, (HMel)(BarH),⁶⁶ revealed similar differences in the C-N-ring bond distances. Both structures show the longest C-N bonds with distances between 1.354(5) and 1.376(5) Å connected to the respective imino-group, the adjacent ones are short with 1.316(5) to 1.327(5) Å, while the ones furthest away from the imino-group are of medium length {1.352(5) to 1.357[#] Å}.

It is interesting to compare these results to the melaminium cation in the solid state structure of the heavy metal salt melaminium β-octamolybdate, (HMel)₄Mo₈O₂₆.⁶⁷ The cation exhibits a similar distribution in C-N bond length within the six-membered ring {long: 1.360(7)-1.380(10), medium: 1.347(9)-1.353(7), short: 1.303(9)-1.326(9) Å}. However, there is no significant shortening for the exocyclic C-NH₂ bonds {averaged: 1.347 in melamine,⁸⁰ 1.341 Å in (HMel)₄Mo₈O₂₆ compared to 1.309 Å in (HMel)Br, 1.322 in (HMel)(BarH), and 1.316 Å in **I** and **II**}.

Besides introducing a deviation from ideal D_{3h}-symmetry in the bond lengths, protonation of melamine causes the angles within the 6-membered ring to become highly asymmetric.

Endocyclic angles at the N-atoms range from 115.2(3) to 119.5(3)° in **I** and 115.96(18) to 119.53(18)° in **II**, the largest angle being associated with the imino group in both cases. In contrast, the comparable angles in melamine⁸⁰ are essentially equal {114.3(2) – 114.7(1)°}.

The angles at the C-atoms within the aromatic rings, range from 121.8(3) to 126.2(3)° in **I** and 120.94(19) to 126.13(19)° in **II** with the largest N-C-N angle opposite the largest C-N-C angle. By comparison, the analogous angles in melamine only range from 124.9(1) to 125.9(6)°.

The introduction of asymmetric features into the aromatic ring – such as the angle opening at the protonated sites – is observed not only in the other monoprotonated melaminium compounds (HMel)₄Mo₈O₂₆, (HMel)Br and (HMel)(BarH) but also in the diprotonated melaminium salts: melaminium diperchlorate hydrate⁶⁸ and melamine-cyanuric acid hydrochloride⁶⁹. All of these compounds show an opening of ca. 3° in the C-N(H)-C bond angles compared to the C-N-C angle. We therefore believe it is possible to identify the protonated N-atoms in the isomorphous melaminium hexahalogenodicuprates(II) (H₂Mel)Cu₂Br₆⁷⁰ and (H₂Mel)Cu₂Cl₆⁷¹ as the ones associated with the bond angles 120.13 and 120.55° (compared to 116.92°)* in (H₂Mel)Cu₂Cl₆ and 123.08 and 119.59° (compared to 116.43°) in (H₂Mel)Cu₂Br₆. (Note: the hydrogen positions were not available from the crystal structures.) In contrast, hydrogen bonds in the solid state structure of melamine itself only cause minor differentiation of the bond angles of the aromatic ring.⁸⁰

Dinitramide anion

The dinitramide anion consists of a central N-atom bonded to two trigonal planar NO₂-groups. The two halves of the molecule (N-NO₂ planes) are twisted with respect to each other by an angle of 11.8(2)°, probably in order to counteract repulsion between the 'inner'

* The distance was taken from CSD, esds are therefore not available.

O-atoms O(2)/O(4). As discussed later, this effect can be easily overcome by environmental influences like hydrogen bonding leading to the known rich diversity of conformations for this ion. This twist is commonly described by the pseudotorsion angle, defined in the structure of **I** as the torsion angle O(2)-N(7)···N(9)-O(4) {11.6(3)°} (see fig. 1), which has been found to range from 0.0 to 43.4^{54,75, 85-88} or even 59.9° for dinitramide coordinated to the metal ion in Re(bipy)(CO)₃(N₃O₄)⁸⁹.

Extensive π -delocalization throughout the anion causes bond orders greater than 1 as suggested by the short bond lengths {N-N_{ave.}: 1.362 compared to 1.425 Å for N-N and 1.240 Å for N=N;⁹⁰ N-O_{ave.}: 1.218 compared to NO₂ groups (1.218) and the NO₃⁻ ion (1.239 Å). While this is expected for the dinitramide anion, the equivalence in the N-N bond length (Δ =0.005 Å) is rather unusual. Out of the 16 published dinitramide structures, only lithium dinitramide⁸⁷ and 3,3-dinitroazetidinium dinitramide⁸⁶ contain dinitramide ions with equivalent N-N bonds. In both cases the dinitramide ion is situated on a crystallographic special position and the equivalency of the N-N bonds is crystallographically required. All other structure show differences in the N-N bond lengths from 0.011 (cubane-1,2,4,7-tetraammonium dinitramide⁸⁵, hexaaquozinc(II) dihydrate dinitramide⁸⁸) to 0.045 (biguanidinium bis-dinitramide monohydrate⁷⁵) or even 0.076 Å for the coordinated dinitramide ligand in Re(bipy)(CO)₃(N₃O₄)⁸⁹.

Another interesting feature of the dinitramide anion is the large value of the NNN bond angle {116.9(3)°}, which is only surpassed by that of the 3,3-dinitroazetidinium salt⁸⁶ {118.1(4)°}. In other known structures this angle ranges from 112.5(2) {1-*i*-propyl-3,3-dinitroazetidinium

dinitramide,⁸⁶ $\text{Re}(\text{bipy})(\text{CO})_3(\text{N}_3\text{O}_4)^{89}$ to $116.2(2)^\circ$ (cubane-1,2,4,7-tetraammonium dinitramide⁸⁵), but is most commonly found between 114.5 and 115.5° . This is indicative of a hybridization of the central N-atom intermediate between sp^2 and sp^3 . Several theoretical papers on the structure of the dinitramide anion have been published.^{19,55,91} A central sp^2 -hybridized N-atom would allow a complete delocalization of π -electrons over the whole planar anion, whereas sp^3 -hybridization causes two independent conjugated halves of the molecule in which each of the NO_2 -groups can twist out of the NNN-plane, but still remain conjugated to one of the lone pairs of the central N-atom. Calculations suggested a 27° twist of the NO_2 -group out of the NNN-plane as the best geometry for a conjugated system with a central sp^3 -hybridized N-atom and a 0° twist for a central sp^2 -hybridized N-atom.⁹¹

In the present structure of **I**, a relatively small twist of the NO_2 -groups of $5.0(5)^\circ$ and $8.5(5)^\circ$ accompanied by a small pseudo-torsion angle of $11.8(2)^\circ$ indicate more sp^2 -character of the central N-atom as expected from the relatively large NNN-bond angle. It is important to note that ab initio calculations on the independent dinitramide ion determined the rotational barrier for the NO_2 -group around the N-N-bond to be less than 3 kcal/mol ⁵⁵ emphasizing the importance of the local environment in determining the geometry of the anion.

Hydrogen bonding

Melaminium dinitramide (I)

The hydrogen bonded network in **I** can be described as a two dimensional step-system connected through hydrogen bonds (fig. 3). Infinite zigzag ribbons of planar hydrogen bonded melaminium cations form parallel horizontal steps, which are connected through

additional hydrogen bonds to the dinitramide anions. The dinitramide ion is twisted in such a way that its 'inner' O-atoms and one 'outer' O-atom hydrogen bond to an 'upper' step, while the other 'outer' O-atom and the central N-atom hydrogen bond a melaminium cation of the 'lower' step (see also the figure in the index). The neighboring dinitramide anion is connected vice versa. There is no additional hydrogen bonding in the third dimension between the individual staircases.

In detail, every melaminium cation contains seven H-atoms and two unprotonated N-atoms, each of which is involved in at least one hydrogen bond. The two nitrogen atoms accept hydrogen bonds from two other melaminium cations creating the zigzag ribbon, while nine hydrogen bonds are donated to the same two melaminium cations and to four dinitramide ions. All hydrogen bond angles within the melaminium ribbons are close to 180° {N(5)-H(5)···N(6B): $174(3)^\circ$ (2x); N(3)-H(3)···N(2A): $175(3)^\circ$ (2x)} keeping this ribbon almost planar.

Especially interesting are the hydrogen bonds donated by H(6) to the inner O-atoms of one dinitramide anion. As a requirement for the step-bridging function of the dinitramide ion, these hydrogen bonds are severely bent with angles of $130(3)^\circ$ {N(5)-H(6)···O(4)} and $136(3)^\circ$ {N(5)-H(6)···O(2)}. The smaller angle of these two correlates with the smaller H···acceptor distance {H(6)···O(4): $2.16(4) \text{ \AA}$ compared to H(6)···O(2): $2.41(4) \text{ \AA}$ }. The same type of hydrogen bond has been observed in other dinitramide salts, e.g. for one of the two independent dinitramide ions in biguanidinium bis-dinitramide monohydrate,⁷⁵ a bifurcated hydrogen bond is formed between a hydrogen atom of a primary amine group and the inner oxygen atoms of the dinitramide ion. In that case the reported H···acceptor bonds were

almost equal (2.19 and 2.22 Å) and again strongly bent (N-H...O: 128 and 144°).^{**} The inner O-atom O(4) in **I** accepts an additional hydrogen bond from a neighboring melaminium cation {O(4)...H(4B): 2.28(4) Å} possibly explaining the longer N(9)-O(4) bond of 1.217(3) Å in comparison to 1.209(3) Å for N(7)-O(2). However, this trend is not statistically significant.

Considering the 'opposing' side of the dinitramide ion, we observe a bifurcated hydrogen bond between O(1C) and N(8C) and the acidic H-atom of the melaminium moiety, H(7), with distances of 2.19(4) {O(1C)...H(7) Å} and 2.34(4) {N(8C)...H(7) Å}. The atom N(8C) is also involved in a hydrogen bond to H(1) {2.31(4) Å} of same melaminium cation. All of these bonds deviate strongly from linearity; O(1C)...H(7)-N(4): 145(4)°, N(8C)...H(7)-N(4): 149(4)°, N(8C)...H(1)-N(1): 157(3)°.

Melaminium nitrate (II)

The packing in the solid state structure of **II** is characterized by a three dimensional network of hydrogen bonded ions. The melaminium cations form infinite almost planar zigzag ribbons similar to those in **I**. However, nitrate ions link these ribbons via hydrogen bonds to a herringbone like network in contrast to the parallel steps in **I** (figs. 3 and 4).

Each melaminium cation forms nine hydrogen bonds, seven of which are donated by the seven H-atoms and two are accepted by the two unprotonated N-atoms. The bonds within the melaminium zigzag ribbons in **I** and **II** are very similar. In both cases central melaminium cations form two parallel hydrogen bonds to each of two neighboring cations thus forming

^{**} The discussion of the hydrogen bonds in this structure were based on calculated positions of the H-atoms

six-membered N \cdots NCN \cdots NC rings (a motif reminiscent of that observed in carboxylic acid dimers). The hydrogen bond angles are all close to linear { 170(2) $^\circ$, N(3)-H(3) \cdots N(2A) and 180(3) $^\circ$, N(5)-H(5) \cdots N(6B) in **II** } and the bond lengths of 2.13(3) Å { N(2A) \cdots H(3), N(6B) \cdots H(5) } indicate slightly stronger interactions in **II** compared to **I**.

Five hydrogen bonds accepted by the nitrate ion from different melaminium cations dominate the interaction between the cation ribbons and the anions (see also the figure in the index). A nitrate ion within the plane described by the melaminium cations (+/- 0.31 Å) binds one of the 'in-plane' melaminium cations with two of its O-atoms { O(1) \cdots H(7): 1.98(3), O(2) \cdots H(2): 1.97(3) Å } again forming a six membered ring (O \cdots NCN \cdots ON). Connection to the next ribbon is made through three hydrogen bonds: one additional bond to O(2) and two bonds to O(3). These three bonds bind the NO $_3^-$ anion to three different, neighboring melaminium cations of the next inclined ribbon { O(2C) \cdots H(6): 2.08(3); O(3D) \cdots H(4): 2.16(2); O(3E) \cdots H(1): 2.09(3) Å }. Most of these bonds are close to linearity { 164(3)-174(2) $^\circ$ } with the notable exception of the longest hydrogen bond in this structure, O(3D) \cdots H(4): 2.16(3) Å and O(3D) \cdots H(4)-N(3): 137(2) $^\circ$.

Even though an approach of the small anion is not sterically hindered allowing relatively short hydrogen bonds { 1.97(3) – 2.16(3) Å }, the packing in the crystal structure of **II** is not as efficient as in **I**, as indicated by a density of 1.71 g/cm 3 compared to 1.74 g/cm 3 .

Acknowledgement

We thank the College of Arts and Sciences of the University of Toledo and the Ohio Board of Regents for generous financial support of the X-ray diffraction facility and thank the

Table 1. Crystal data and structure refinement of melaminium dinitramide (I) and melaminium nitrate (II)

	I	II
Formula	$C_3H_7N_6^+ N_3O_4^-$	$C_3H_7N_6^+ NO_3^-$
Color/shape	colorless/parallelepiped	colorless/parallelepiped
Empirical formula	$C_3H_7N_9O_4$	$C_3H_7N_7O_3$
Formula weight	233.18	189.16
Temperature	293(1) K	293(1) K
Crystal system	triclinic	monoclinic
Space group	$P\bar{1}$	$P2_1/c$
Unit cell dimensions	$a = 6.6861(11) \text{ \AA}$ $b = 6.9638(16) \text{ \AA}$ $c = 10.447(2) \text{ \AA}$ $\alpha = 99.07(3)^\circ$ $\beta = 98.30(3)^\circ$ $\gamma = 108.50(3)^\circ$	$a = 3.5789(7) \text{ \AA}$ $b = 20.466(4) \text{ \AA}$ $c = 10.060(2) \text{ \AA}$ $\beta = 94.01(2)^\circ$
Volume	$445.6(2) \text{ \AA}^3$	$735.0(3) \text{ \AA}^3$
Z	2	4
Density (calc.)	1.74 g cm^{-3}	1.71 g cm^{-3}
Diffractionmeter/scan	Enraf-Nonius CAD-4/ ω -2 θ scans	Siemens SMART / ω -scans
Radiation/wavelength	Mo K α (graphite monochromated)/ 0.71073 \AA	Mo K α (graphite monochromated)/ 0.71073 \AA
F(000)	240	392
Crystal size	$0.15 \times 0.15 \times 0.10 \text{ mm}$	$0.20 \times 0.15 \times 0.10 \text{ mm}$
Θ -range for data collection	$2.02 - 25.96^\circ$	$1.99 - 27.60$
Index range	$h = -8 \rightarrow 8, k = -8 \rightarrow 8, l = -12 \rightarrow 12$	$h = -4 \rightarrow 4, k = -25 \rightarrow 14, l = -12 \rightarrow 13$
Reflections collected	3476	4055
Independent/observed reflections	1738/785 [$I > 2\sigma(I)$]	1552 /1078 [$I > 2\sigma(I)$]
R(int)	0.060	0.034
Absorption correction	ψ -scans	SADABS
Relat. Transm. factor range	0.924 – 0.999	0.635 - 0.989
Refinement method	Full-matrix least-squares on F	Full-matrix least-squares on F^2
Computing	MolEN ⁹²	SHELXTL, Vers. 5 ⁷⁹
Data/restraints/parameters	1355/0/173	1552/0/146
R_1 -indices [$I > 2\sigma(I)$] (F)	0.0479	0.0497
R_1 -indices (F, all data)	0.0950	0.0797
wR_2 -indices [$F^2, I > 2\sigma(I)$]	N/A	0.1114

Office of Naval Research for funding this work (Contract Nos. N00014-95-1-0013 and N00014-95-1-1252).

wR₂-indices (F², all data)
Max., min. peak

N/A
0.255, -0.328 e/Å³

0.1282
0.192, -0.273 e/Å³

Table 2. Atomic coordinates and isotropic (H) or equivalent isotropic (O,N,C) displacement parameters [\AA^2] for melaminium dinitramide (I).

	x	y	z	U(eq)/U(is)
O(1)	0.8558(5)	0.9959(4)	0.6419(3)	0.071(1)
O(2)	0.7141(5)	0.8134(4)	0.4459(3)	0.070(1)
O(3)	0.6340(5)	1.3188(4)	0.3661(3)	0.073(1)
O(4)	0.6440(5)	1.0246(5)	0.2802(3)	0.075(1)
N(1)	1.2580(6)	0.4573(6)	0.2995(3)	0.060(1)
N(2)	1.0081(4)	0.2492(4)	0.1146(3)	0.034(1)
N(3)	0.7481(6)	0.0583(5)	-0.0646(3)	0.042(1)
N(4)	0.9803(5)	0.5592(4)	0.2207(3)	0.037(1)
N(5)	0.7068(6)	0.6691(5)	0.1461(3)	0.048(1)
N(7)	0.7723(5)	0.9771(4)	0.5249(3)	0.043(1)
N(6)	0.7148(4)	0.3603(4)	0.0339(2)	0.032(1)
N(8)	0.7516(5)	1.1587(5)	0.5030(3)	0.050(1)
N(9)	0.6740(5)	1.1625(5)	0.3761(3)	0.043(1)
C(1)	1.0807(5)	0.4181(5)	0.2109(3)	0.036(1)
C(2)	0.7971(5)	0.5257(5)	0.1315(3)	0.033(1)
C(3)	0.8260(5)	0.2268(5)	0.0295(3)	0.031(1)
H(1)	1.287(6)	0.559(6)	0.369(4)	0.049(11)
H(2)	1.316(7)	0.380(7)	0.303(4)	0.064(15)
H(3)	0.815(6)	-0.033(6)	-0.075(4)	0.046(11)
H(4)	0.646(6)	0.031(5)	-0.116(4)	0.039(11)
H(5)	0.584(7)	0.654(5)	0.099(4)	0.048(12)
H(6)	0.757(7)	0.773(6)	0.220(4)	0.069(13)
H(7)	1.022(7)	0.665(6)	0.291(4)	0.070(13)

U(eq) is defined as one third of the trace of the orthogonalized U_{ij} tensor

Table 3. Selected distances (Å) and angles (°) for melaminium dinitramide (I)Bond lengths

O(1)-N(7)	1.237(4)	N(1)-C(1)	1.317(4)
O(2)-N(7)	1.209(3)	N(2)-C(1)	1.325(4)
O(3)-N(9)	1.217(4)	N(2)-C(3)	1.349(4)
O(4)-N(9)	1.217(3)	N(3)-C(3)	1.310(4)
N(7)-N(8)	1.365(4)	N(4)-C(1)	1.354(4)
N(8)-N(9)	1.360(4)	N(4)-C(2)	1.358(4)
		N(5)-C(2)	1.321(4)
		N(6)-C(2)	1.317(4)
		N(6)-C(3)	1.361(4)

Bond angles

O(2)-N(7)-O(1)	121.7(3)	C(1)-N(2)-C(3)	115.2(3)
O(2)-N(7)-N(8)	127.3(3)	C(1)-N(4)-C(2)	119.5(3)
O(1)-N(7)-N(8)	111.0(3)	C(2)-N(6)-C(3)	115.3(3)
N(9)-N(8)-N(7)	116.9(3)	N(1)-C(1)-N(2)	120.7(3)
O(3)-N(9)-O(4)	122.0(3)	N(1)-C(1)-N(4)	117.4(3)
O(3)-N(9)-N(8)	113.3(3)	N(2)-C(1)-N(4)	121.9(3)
O(4)-N(9)-N(8)	124.6(3)	N(6)-C(2)-N(5)	121.5(3)
		N(6)-C(2)-N(4)	121.8(3)
		N(5)-C(2)-N(4)	116.7(3)
		N(3)-C(3)-N(2)	116.3(3)
		N(3)-C(3)-N(6)	117.5(3)
		N(2)-C(3)-N(6)	126.2(3)

Torsion angle

O(2)-N(7)...N(9)-O(4)	-11.6(3)
-----------------------	----------

Deviation from best plane through C(1)C(2)C(3)N(2)N(4)N(6)

C(1)	-0.007(2)
C(2)	-0.001(2)
C(3)	0.001(2)
N(2)	0.004(2)
N(4)	0.006(2)
N(6)	-0.002(2)
N(1)	0.002(6)
N(3)	-0.023(5)
N(5)	0.014(5)

Hydrogen bonds

D-H...A	d(D-H)	d(H...A)	d(D...A)	<(DHA)
N(1)-H(1)...N(8C)	0.88(4)	2.31(4)	3.133(5)	157(3)
N(1)-H(2)...O(3D)	0.76(4)	2.32(4)	2.996(5)	148(4)
N(3)-H(3)...N(2A)	0.89(4)	2.22(4)	3.102(4)	175(3)
N(3)-H(4)...O(4B)	0.76(4)	2.28(4)	3.034(4)	174(4)
N(5)-H(5)...N(6B)	0.86(4)	2.23(4)	3.083(4)	174(3)
N(4)-H(7)...O(1C)	0.90(4)	2.19(4)	2.975(4)	145(4)
N(4)-H(7)...N(8C)	0.90(4)	2.34(4)	3.145(4)	149(4)
N(5)-H(6)...O(4)	0.91(4)	2.16(4)	2.829(4)	130(3)
N(5)-H(6)...O(2)	0.91(4)	2.41(4)	3.123(4)	136(3)

Symmetry transformations used to generate equivalent atoms:

(A) $-x+2, -y, -z$ (B) $-x+1, -y+1, -z$ (C) $-x+2, -y+2, -z+1$ (D) $x+1, y-1, z$

Table 4. Atomic coordinates and isotropic (H) or equivalent isotropic (C,N,O) displacement parameters [\AA^2] for melaminium nitrate (**II**).

	x	y	z	U(eq)/U(is)
O(1)	1.0596(6)	0.7430(1)	0.8108(2)	0.052(1)
O(2)	0.8838(5)	0.7857(1)	0.6203(2)	0.046(1)
O(3)	1.2101(5)	0.8424(1)	0.7676(2)	0.043(1)
N(1)	0.5160(6)	0.6651(1)	0.5519(2)	0.036(1)
N(2)	0.3065(5)	0.5624(1)	0.6010(2)	0.027(1)
N(3)	0.1311(6)	0.4604(1)	0.6606(2)	0.032(1)
N(4)	0.6125(5)	0.6276(1)	0.7673(2)	0.029(1)
N(5)	0.6860(6)	0.5908(1)	0.9852(2)	0.038(1)
N(6)	0.4147(5)	0.5228(1)	0.8260(2)	0.028(1)
N(7)	1.0495(5)	0.7903(1)	0.7329(2)	0.033(1)
C(1)	0.4758(6)	0.6179(1)	0.6378(2)	0.026(1)
C(2)	0.5696(6)	0.5797(1)	0.8601(2)	0.026(1)
C(3)	0.2899(6)	0.5164(1)	0.6965(2)	0.025(1)
H(1)	0.424(7)	0.660(1)	0.466(3)	0.044(7)
H(2)	0.619(7)	0.703(1)	0.579(2)	0.038(7)
H(3)	0.023(7)	0.457(1)	0.579(3)	0.037(7)
H(4)	0.099(7)	0.432(1)	0.718(2)	0.031(6)
H(5)	0.655(9)	0.557(2)	1.041(3)	0.070(10)
H(6)	0.757(8)	0.631(2)	1.010(3)	0.054(8)
H(7)	0.728(8)	0.666(1)	0.789(3)	0.045(7)

U(eq) is defined as one third of the trace of the orthogonalized U_{ij} tensor.

Table 5. Selected distances (Å) and angles (°) for melaminium nitrate (II)Bond lengths

O(1)-N(7)	1.244(2)	N(1)-C(1)	1.311(3)
O(2)-N(7)	1.245(2)	N(2)-C(1)	1.327(3)
O(3)-N(7)	1.250(2)	N(2)-C(3)	1.349(3)
		N(3)-C(3)	1.319(3)
		N(4)-C(2)	1.370(3)
		N(4)-C(1)	1.374(3)
		N(5)-C(2)	1.317(3)
		N(6)-C(2)	1.326(3)
		N(6)-C(3)	1.354(3)

Bond angles

O(1)-N(7)-O(2)	120.4(2)	C(1)-N(2)-C(3)	116.15(18)
O(1)-N(7)-O(3)	119.66(19)	C(2)-N(4)-C(1)	119.53(18)
O(2)-N(7)-O(3)	119.94(19)	C(2)-N(6)-C(3)	115.96(18)
		N(1)-C(1)-N(2)	121.1(2)
		N(1)-C(1)-N(4)	118.0(2)
		N(2)-C(1)-N(4)	120.94(19)
		N(5)-C(2)-N(6)	119.8(2)
		N(5)-C(2)-N(4)	119.1(2)
		N(6)-C(2)-N(4)	121.17(18)
		N(3)-C(3)-N(2)	116.82(19)
		N(3)-C(3)-N(6)	117.03(19)
		N(2)-C(3)-N(6)	126.13(19)

Deviation from best plane through C(1)C(2)C(3)N(2)N(4)N(6)

C(1)	-0.005(1)
C(2)	0.020(1)
C(3)	-0.012(1)
N(2)	0.018(1)
N(4)	-0.013(1)
N(6)	-0.007(1)
N(1)	-0.016(3)
N(3)	-0.025(3)
N(5)	0.075(3)

Hydrogen bonds

D-H...A	d(D-H)	d(H...A)	d(D...A)	<(DHA)
N(4)-H(7)...O(1)	0.90(3)	1.98(3)	2.869(3)	168(2)
N(1)-H(2)...O(2)	0.90(3)	1.97(3)	2.858(3)	173(2)
N(5)-H(6)...O(2C)	0.88(3)	2.08(3)	2.934(3)	164(3)
N(3)-H(4)...O(3D)	0.83(2)	2.16(2)	2.823(3)	137(2)
N(1)-H(1)...O(3E)	0.91(3)	2.09(3)	2.995(3)	174(2)
N(3)-H(3)...N(2A)	0.88(3)	2.13(3)	3.003(3)	170(2)
N(5)-H(5)...N(6B)	0.90(3)	2.13(3)	3.038(3)	180(3)

Symmetry transformations used to generate equivalent atoms:

- (A) -x, -y+1, -z+1 (B) -x+1, -y+1, -z+2 (c) x, -y+3/2, z+1/2
 (D) -x+1, y-1/2, -z+3/2 (E) x-1, -y+3/2, z-1/2

Figure captions

Figure 1: Melaminium dinitramide (**I**) showing the atomic-numbering and hydrogen-bonding schemes (50 % probability ellipsoids). Symmetry codes: (A) $2-x, -y, -z$; (B) $1-x, 1-y, -z$; (C) $2-x, 2-y, 1-z$

Figure 2 : Melamiunium nitrate (**II**) showing the atomic-numbering and hydrogen-bonding schemes (50 % probability ellipsoids). Symmetry codes: (A) $-x, 1-y, 1-z$; (B) $1-x, 1-y, 2-z$; (C) $x, 1.5-y, 0.5+z$; (D) $1-x, -0.5+y, 1.5-z$; (E) $-1+x, 1.5-y, -0.5+z$

Figure 3: Packing diagram of melaminium dinitramide (**I**) showing the hydrogen bonding.

Figure 4: Packing diagram of melaminium nitrate (**II**) showing the hydrogen bonding.

- ¹ Bottaro, J.C.; Schmitt, R.J.; Penwell, P.E.; Ross, D.S. **1993**, US patents 5,198,204 and 5,254,324. Bottaro, J.C.; Penwell, P.E.; Schmitt, R.J. *J. Synth. Commun.* **1991**, *21*, 945.
- ² Christe, K.O.; Wilson, W.W.; Petrie, M. A.; Michels, H.H.; Bottaro, J.C.; Gilardi, R. *Inorg. Chem.* **1996**, *35*, 5068.
- ³ Luk'yanov, O.A., Gorelik, V.P., Tartakovskii, V.A. *Russ. Chem. Bull.* **1994**, *43*, 89.
- ⁴ Shlyapochnikov, V.A.; Oleneva, G.I.; Cherskaya, N.O.; Luk'yanov, O.A.; Gorelik, V.P.; Anikin, O.V.; Tartakovsky, V.A. *J. Mol. Struc.* **1995**, *348*, 103.
- ⁵ Doyle, Jr., R.J. *Org. Mass Spectrom.* **1993**, *28*, 83.
- ⁶ Russell, T.P.; Piermarini, G.J.; Block, S.; Miller, P.J. *J. Phys. Chem.* **1996**, *100*, 3248.
- ⁷ Pace, M.D. *J. Phys. Chem* **1994**, *98*, 6251.
- ⁸ Pace, M.D.; Carmichael, A.J. *J. Phys. Chem. A* **1997**, *101*, 1848.
- ⁹ Brill, T.B.; Brush, P.J.; Patil, D.G. *Combust. Flame* **1993**, *92*, 178.
- ¹⁰ Rossi, M.J.; Bottaro, J.C.; McMillen, D.F. *Int. J. Chem. Kinet.* **1993**, *25*, 549.
- ¹¹ Vyazovkin, S.; Wight, C.A. *J. Phys. Chem. A* **1997**, *101*, 7217.
- ¹² Oxley, J.C.; Smith, J.L.; Zheng, W.; Rogers, E.; Coburn, M.D. *J. Phys. Chem. A* **1997**, *101*, 5646.
- ¹³ Vyazovkin, S.; Wight, C.A. *J. Phys. Chem. A* **1997**, *101*, 5653.
- ¹⁴ Vyazovkin, S.; Wight, C.A. *J. Phys. Chem. A* **1997**, *101*, 8279.
- ¹⁵ Fetherolf, B.L.; Litzinger, T.A. *Combust. Flame* **1998**, *114*, 515.
- ¹⁶ Kazakov, A.I.; Rubtsov, Y.I.; Andrienko, L.P.; Manelis, G.B. *Russ. Chem. Bull.* **1998**, *47*, 379.
- ¹⁷ Lobbecke, S.; Keicher, T.; Krause, H.; Pfeil, A. *Solid State Ionics* **1997**, *101*, 945.
- ¹⁸ Politzer, P.; Seminario, J.M.; Concha, M.C. *J. Mol. Struc. THEOCHEM* **1998**, *427*, 123.

- ¹⁹ Mebel, A.M.; Lin, M.C.; Morokuma, K.; Melius, C.F. *J. Phys. Chem.* **1995**, *99*, 6842.
- ²⁰ Odintsov, V.V.; Pepekin, V.I.; Korsunskii, B.L. *Chem. Phys. Rep.* **1997**, *16*, 689.
- ²¹ Agrawal, J.P.; Walley, S.M.; Field, J.E. *J. Propul. Power* **1997**, *13*, 463.
- ²² SteelGoodwin, L.; Kuhlman, K.J.; Miller, C.; Pace, M.D.; Carmichael, A.J. *Ann. Clin. Lab. Sci.* **1997**, *27*, 236.
- ²³ Kinkead, E.R.; Wolfe, R.E.; Feldmann, M.L. *Toxicol. Ind. Health* **1996**, *12*, 59.
- ²⁴ Kinkead, E.R.; Wolfe, R.E.; Flemming, C.D.; Leahy, H.F.; Caldwell, D.J.; Miller, C.R.; Marit, G.B. *Toxicol. Ind. Health* **1995**, *11*, 437.
- ²⁵ Schmitt, R.J.; Krempp, M.; Bierbaum, V.M. *Int. J. Mass Spectrom. Ion Processes* **1992**, *117*, 621.
- ²⁶ Luk'yanov, O.A.; Konnova, Yu.V.; Klimova, T.A.; Tartakovsky, V.A. *Russ. Chem. Bull.* **1994**, *43*, 1200.
- ²⁷ Luk'yanov, O.A.; Anikin, O.V.; Gorelik, V.P.; Tartakovsky, V.A. *Russ. Chem. Bull.* **1994**, *43*, 1457.
- ²⁸ Shlyapochnikov, V.A.; Cherskaya, N.O.; Luk'yanov, O.A.; Gorelik, V.P.; Tartakovsky, V.A. *Russ. Chem. Bull.* **1994**, *43*, 1522.
- ²⁹ Luk'yanov, O.A.; Shlykova, N.I.; Tartakovsky, V.A. *Russ. Chem. Bull.* **1994**, *43*, 1680.
- ³⁰ Luk'yanov, O.A.; Agevnin, A.R.; Leichenko, A.A.; Seregina, N.M.; Tartakovsky, V.A. *Russ. Chem. Bull.* **1995**, *44*, 108.
- ³¹ Shlyapochnikov, V.A.; Oleneva, G.I.; Cherskaya, N.O.; Luk'yanov, O.A.; Gorelik, V.P.; Anikin, O.V.; Tartakovsky, V.A. *Russ. Chem. Bull.* **1995**, *44*, 1449.
- ³² Shlyapochnikov, V.A.; Cherskaya, N.O.; Luk'yanov, O.A.; Anikin, O.V.; Tartakovsky, V.A. *Russ. Chem. Bull.* **1996**, *45*, 430.

- ³³ Luk'yanov, O.A.; Anikin, O.V.; Tartakovsky, V.A. *Russ. Chem. Bull.* **1996**, *45*, 433.
- ³⁴ Luk'yanov, O.A.; Kozlova, I.K.; Shitov, O.P.; Konnova, Y.V.; Kalinina, I.V.; Tartakovsky, V.A. *Russ. Chem. Bull.* **1996**, *45*, 863.
- ³⁵ Luk'yanov, O.A.; Shvedova, S.N.; Shepelev, E.V.; Varfolomeeva, O.N.; Malkina, N.N.; Tartakovsky, V.A. *Russ. Chem. Bull.* **1996**, *45*, 1497.
- ³⁶ Bottaro, J.C.; Penwell, P.E.; Schmitt, R.J. *J. Am. Chem. Soc.* **1997**, *119*, 9405.
- ³⁷ Dubovitskii, F.I.; Golevina, N.I.; Pavlev, A.N.; Atovmyan, L.O. *Dokl. Acad. Nauk* **1998**, *360*, 491.
- ³⁸ Gidaspov, B.V.; Tselinskii, I.V.; Shcherbinin, M.B. *Zh. Obshch. Khim.* **1997**, *67*, 972.
- ³⁹ Christe, K.O.; Wilson, W.W. *J. Fluorine Chem.* **1998**, *89*, 97.
- ⁴⁰ Kazakov, A.I.; Rubtsov, Yu.I.; Manelis, G.B.; Andrienko, L.P. *Russ. Chem. Bull.* **1998**, *47*, 39.
- ⁴¹ Kazakov, A.I.; Rubtsov, Yu.I.; Manelis, G.B.; Andrienko, L.P. *Russ. Chem. Bull.* **1997**, *46*, 2015.
- ⁴² Shcherbinin, M.B.; Tselinskii, I.V.; Gidaspov, B.V. *Zh. Org. Khim.* **1997**, *33*, 1823.
- ⁴³ Astrat'ev, A.A.; Kuznetsov, L.L.; Gidaspov, B.V. *Zh. Org. Khim.* **1997**, *33*, 1829.
- ⁴⁴ Eberson, L. *Acta Chem. Scand.* **1998**, *52*, 207.
- ⁴⁵ Babkin, S.B.; Pavlov, A.N.; Nazin, G.M. *Russ. Chem. Bull.* **1997**, *46*, 1844.
- ⁴⁶ Pavlov, A.N.; Nazin, G.M. *Russ. Chem. Bull.* **1997**, *46*, 1848.
- ⁴⁷ Petrie, M.A.; Sheehy, J.A.; Boatz, J.A.; Rasul, G.; Surya Prakash, G.K.; Olah, G.A.; Christe, K.O. *J. Am. Chem. Soc.* **1997**, *119*, 8802.
- ⁴⁸ Politzer, P.; Seminario, J. M. *Chem. Phys. Lett.* **1993**, *216*, 348.
- ⁴⁹ Tompa, A.S.; Boswell, R.F.; Skahan P.; Gotzmer, C J. *Therm. Anal.* **1997**, *49*, 1161.

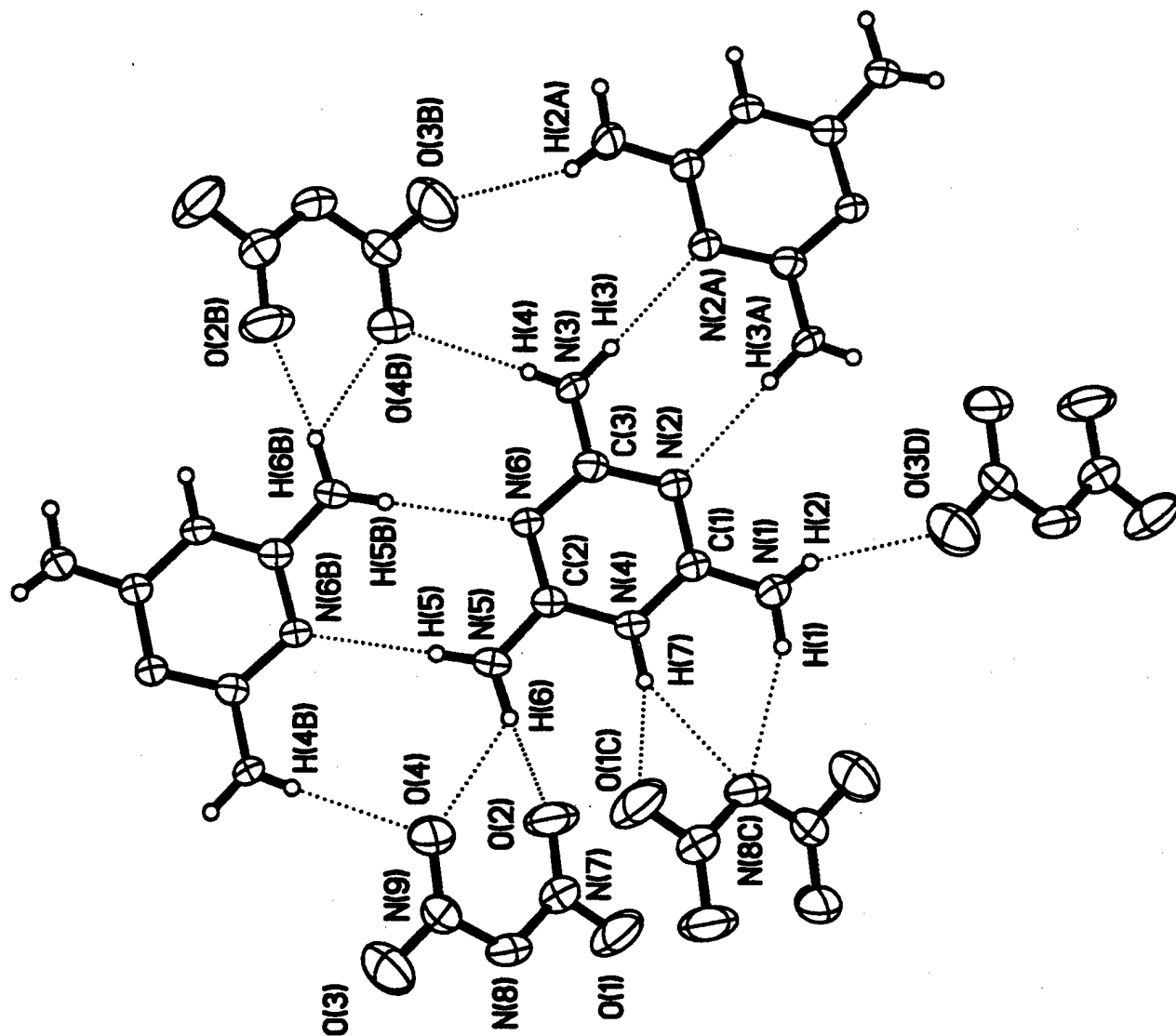
- ⁵⁰ Mebel, A.M.; Lin, M.C. *Int. Rev. Phys. Chem.* **1997**, *16*, 249.
- ⁵¹ Russell, T.P.; Piermarini, G.J.; Miller, P.J. *J. Phys. Chem. B* **1997**, *101*, 3566.
- ⁵² Dubovitskii, F.I.; Volkov, G.A.; Grebennikov, V.N.; Manelis, G.B.; Nazin, G.M. *Dokl. Acad. Nauk* **1996**, *348*, 205.
- ⁵³ Dubovitskii, F.I.; Volkov, G.A.; Grebennikov, V.N.; Manelis, G.B.; Nazin, G.M. *Dokl. Acad. Nauk* **1996**, *347*, 763.
- ⁵⁴ Gidaspov, B.V.; Tselinskii, I.V.; Mel'nikov, V.V.; Margolis, N.V.; Grigor'eva, N.V. *Zh. Obshch. Khim.* **1995**, *65*, 995.
- ⁵⁵ Michels, H.H.; Montgomery, Jr., J.A. *J. Phys. Chem.* **1993**, *97*, 6602.
- ⁵⁶ Lange, R.F.M.; Beijer, F.H.; Sijbesma, R.P.; Hooft, R.W.W.; Kooijman, H.; Spek, A.L.; Kroon, J.; Meijer, E.W. *Angew. Chem. Int. Ed.* **1997**, *36*, 969.
- ⁵⁷ Chowdhry, M.M.; Mingos, D.M.P.; White, A.J.P.; Williams, D.J. *Chem. Commun.* **1996**, 899.
- ⁵⁸ Lawrence, D.S.; Jiang, T.; Levett, M. *Chem. Rev.* **1995**, *95*, 2229 and references therein
- ⁵⁹ Simanek, E.E.; Mammen, M.; Gordon, D.M.; Chin, D.; Mathias, J.P.; Seto, C.T.; Whitesides, G.M. *Tetrahedron* **1995**, *51*, 607.
- ⁶⁰ Whitesides, G.M.; Simanek, E.E.; Mathias, J.P.; Seto, J.; Chin, D.N.; Mammen, M.; Gordon, D.M. *Accounts Chem. Res.* **1995**, *28*, 37.
- ⁶¹ Li, X.; Chin, D.N.; Whitesides, G.M. *J. Org. Chem.* **1996**, *61*, 1779.
- ⁶² Mathias, J.P.; Simanek, E.E.; Whitesides, G.M. *J. Am. Chem. Soc.* **1994**, *116*, 4326.
- ⁶³ Russell, K.C.; Lehn, J.-M.; Kyritsakas, N.; DeChian, A.; Fischer, J. *New J. Chem.* **1998**, *22*, 123.
- ⁶⁴ Philp, D.; Stoddart, J.F. *Angew. Chem. Int. Ed.* **1996**, *35*, 1155.

- ⁶⁵ Scoponi, M.; Polo, E.; Pradella, F.; Bertolasi, V.; Carassiti, V.; Goberti, P. *J. Chem. Soc., Perkin Trans. 2* **1992**, 1127.
- ⁶⁶ Zerkowski, J.A.; MacDonald, J.C.; Whitesides, G.M. *Chem. Mater.* **1994**, 6, 1250;
Zerkowski, J.A.; Seto, C.T.; Wierda, D.A.; Whitesides, G.M. *J. Am. Chem. Soc.* **1990**, 112, 9025.
- ⁶⁷ Kroenke, W.J.; Fackler, Jr., J.P.; Mazany, A.M. *Inorg. Chem.* **1983**, 22, 2412.
- ⁶⁸ Martin, A.; Pinkerton, A.A. *Acta Cryst.* **1995**, C51, 2174.
- ⁶⁹ Wang, Y.; Wei, B.; Wang, Q. *J. Cryst. Spectrosc. Res.* **1990**, 20, 79.
- ⁷⁰ Scott, B.; Geiser, U.; Willett, R.D.; Patyal, B.; Landee, C.P.; Greeney, R.E.; Manfredini, T.; Pellacani, G.C.; Corradi, A.B.; Battaglia, L.P. *Inorg. Chem.* **1988**, 27, 2454.
- ⁷¹ Colombo, A.; Menabue, L.; Motori, A.; Pellacani, G.C.; Porzio, W.; Sandrolini, F.; Willett, R. D. *Inorg. Chem.* **1985**, 24, 2900.
- ⁷² Pinkerton, A.A.; Schwarzenbach, D. J. *Chem. Soc., Dalton Trans.* **1978**, 989.
- ⁷³ Martin, A.; Pinkerton A.A.; Schiemann, A. *Acta Cryst.* **1996**, C52, 966.
- ⁷⁴ Martin, A.; Pinkerton, A.A. *Acta Cryst.* **1996**, C52, 1048; Dollimore, D.; Martin, A.; Pinkerton, A.A. *Thermochimica Acta* **1996**, 285, 109.
- ⁷⁵ Martin, A.; Pinkerton, A.A.; Gilardi, R.D.; Bottaro, J.C. *Acta Cryst.* **1997**, B53, 504.
- ⁷⁶ Donated by Dr. J.C. Bottaro; SRI International
- ⁷⁷ North, A.C.T.; Phillips, D.C.; Mathews, F.S. *Acta Cryst.* **1968**, A24, 351.
- ⁷⁸ Sheldrick, G. M. *SADABS* **1996**, University of Göttingen, Germany.
- ⁷⁹ Sheldrick, G.M. *SHELXTL Vers.5.1*. **1997**, An Integrated System for Solving, Refining and Displaying Crystal Structures from Diffraction Data, Univ. of Göttingen, Germany.
- ⁸⁰ Varghese, J.N.; O'Connell, A.M.; Maslen, E.N. *Acta Cryst.* **1977**, B33, 2102.

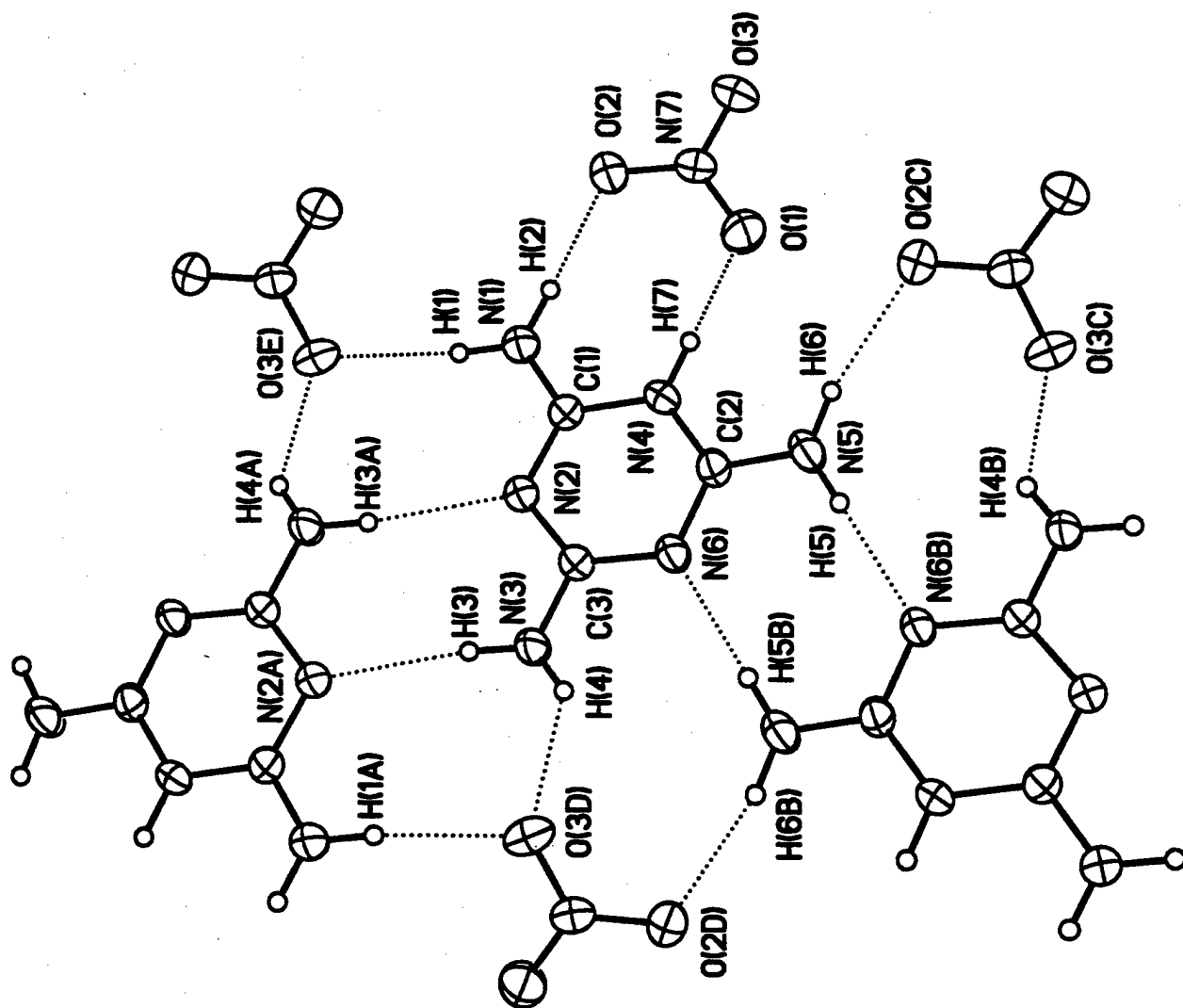
- ⁸¹ Hughes, E.W. *J. Am. Chem. Soc.* **1941**, 63, 1737.
- ⁸² Larson, A.C.; Cromer, D.T. *J. Chem. Phys.* **1974**, 60, 185.
- ⁸³ Cromer, D.T.; Larson, A.C.; Stewart, R.F. *J. Chem. Phys.* **1976**, 65, 336.
- ⁸⁴ 3D Search and Research using the Cambridge Structural Data Base, F.H. Allen and O. Kennard, *Chemical Design Automation News* **1993**, 8, 1.
- ⁸⁵ Butcher, R. J.; Gilardi, R.D. *J. Chem. Crystallogr.* **1998**, 28, 95.
- ⁸⁶ Gilardi, R.D.; Butcher, R. J. *J. Chem. Crystallogr.* **1998**, 28, 163.
- ⁸⁷ Gilardi, R.; Flippen-Anderson, J.; George, C.; Butcher, R.J. *J. Am. Chem. Soc.* **1997**, 119, 9411
- ⁸⁸ Gilardi, R.D.; Butcher, R. J. *J. Chem. Crystallogr.* **1998**, 28, 105.
- ⁸⁹ Trammell, S.; Goodson, P.A.; Sullivan, B.P. *Inorg. Chem.* **1996**, 35, 1421.
- ⁹⁰ International Tables for X-Ray Crystallography, Volume C, Kluwer Academic Publishers: Dordrecht, 1995.
- ⁹¹ Politzer, P.; Seminario, J.M.; Concha, M.C.; Redfern, P.C. *J. Mol. Struct. THEOCHEM*, **1993**, 287, 235.
- ⁹² Fair, C.K. *MolEN*. **1990**, An Interactive Intelligent System for Crystal Structure Analysis; Enraf-Nonius: Delft, The Netherlands.

SECRET

Fig 1



JCCR 494
Fig 2



100493
Fig 3

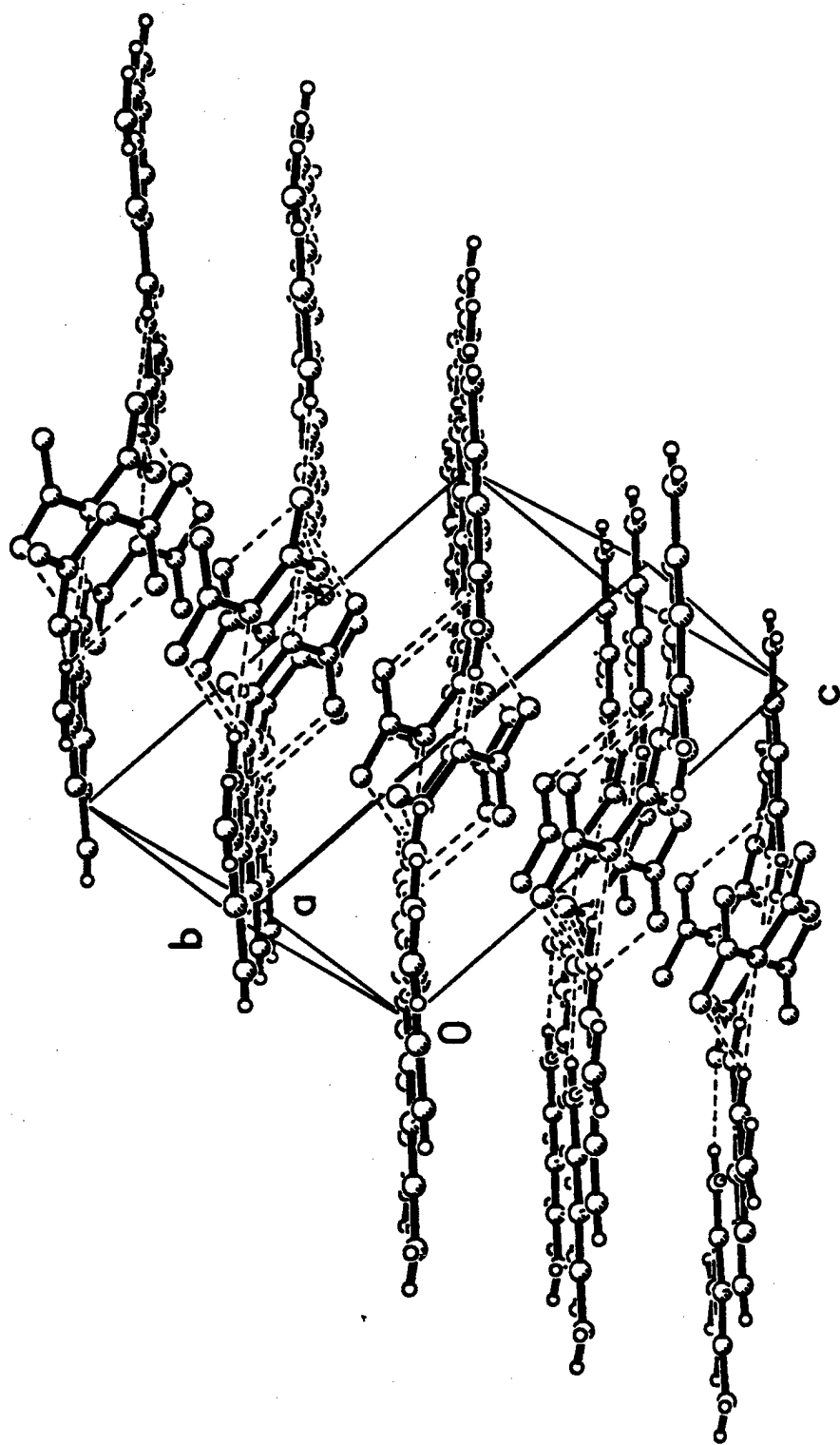
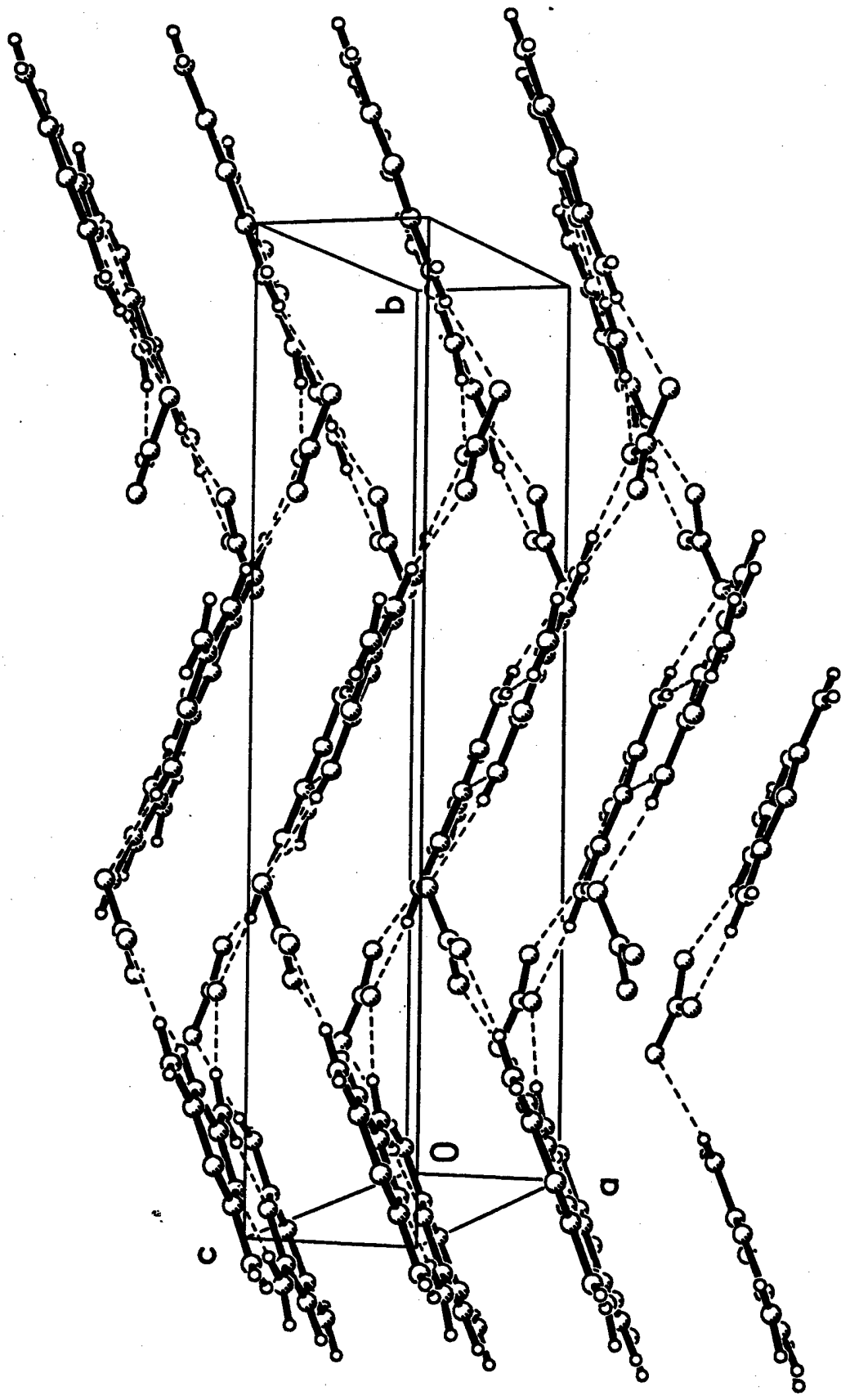


Fig. 499 1034



Contract No. N00014-95-1-0013 and N00014-97-1-0409

Program Officer: R. Miller/J. Goldwasser

**Title: Experimental Charge Densities and Electrostatic Potentials in Energetic
Materials and Infrastructure Upgrade for an X-ray Crystallography
Laboratory**

PI: A. Alan Pinkerton

Department of Chemistry, University of Toledo, Toledo, OH 43606

tel. (419) 530-4580, FAX (419) 530-4033, email apinker@uoft02.utoledo.edu

APPENDIX 5c

**Two Energetic Ionic Materials: the Biguanidinium Perchlorates.
Martin, A.; and Pinkerton, A.A., *Acta Crystallogr.*, 1996, C52, 1048-1052.**

Acta Cryst. (1996). **C52**, 1048–1052**Two Energetic Ionic Materials: the Biguanidium Perchlorates**

ANTHONY MARTIN AND A. ALAN PINKERTON

Department of Chemistry, University of Toledo, Toledo, OH 43606, USA. E-mail: apinker@uoft02.utoledo.edu

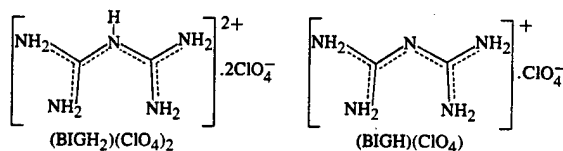
(Received 22 August 1994; accepted 23 October 1995)

Abstract

The structures of two energetic biguanidium salts have been determined from low-temperature X-ray diffraction data collected at 100 K. Biguanidium perchlorate, $C_2H_8N_5^+ \cdot ClO_4^-$, and biguanidium dperchlorate, $C_2H_9N_5^{2+} \cdot 2ClO_4^-$, have structures characterized by twisted cations and extensive hydrogen bonding.

Comment

There is a great deal of current interest in the production of energetic materials (Borman, 1994). A newly discovered class of energetic materials is based on the salts of biguanide (Bottaro, Gilardi, Martin & Pinkerton, 1996). The present paper describes two other energetic biguanidium salts, the mono- and dperchlorate. Perchlorates have a long and sometimes checkered history in the field of energetic materials due to their unpredictable nature; nevertheless, they have an important role. Ammonium perchlorate, for example, is used in the solid-fuel booster rockets of the space shuttle and an unspecified biguanidium perchlorate was included in an explosive formulation in 1917 (Manuelli & Bernardini, 1917). The two nitrate salts of biguanide (Martin, Pinkerton & Schiemann, 1996) have densities that are higher than many other organic materials, although not much higher than predicted by empirical calculations (Chichra, Holden & Dickinson, 1980; Stine, 1981). These factors encouraged us to synthesize and structurally characterize the diprotonated biguanidium dperchlorate, $(BIGH_2)(ClO_4)_2$, and the monoprotonated biguanidium perchlorate, $(BIGH)(ClO_4)$.



$(BIGH_2)(ClO_4)_2$. The structure of the dperchlorate consists of a biguanidium unit and two perchlorate anions linked by an extensive hydrogen-bond network (Fig. 1). The diprotonated biguanidium cation is fairly symmetric about the central N atom, as observed for the carbonate, sulfate and nitrate but not the free base (Pinkerton & Schwarzenbach, 1978; Martin, Pinkerton & Schiemann, 1996).

As expected, the biguanidium unit is not planar, but consists of two planar moieties twisted by $43.7(1)^\circ$ with respect to one another; this is comparable to 49.1° for the analogous sulfate. The other metric parameters are similar to those previously reported.

The bridging C—N bonds of the biguanidium unit [C1—N3 1.369(3), C2—N3 1.367(3) Å] are slightly shorter than in the analogous sulfate [room temperature data: C1—N3 1.383(5), C2—N3 1.373(5) Å]. The bond angle at the bridging N atom (C1—N3—C2) is $127.0(2)^\circ$, which is comparable to the same angle in the sulfate [$126.2(3)^\circ$]. The terminal C—N bonds are significantly shorter than the bridging bonds and range from 1.308(3) (N1—C1) to 1.313(3) Å (N2—C1); the same range is found in the sulfate [1.308(5)–1.315(5) Å].

The two perchlorate anions are well behaved with unusually small displacement parameters and have the expected tetrahedral geometry. One anion accepts five hydrogen bonds from four different biguanidium cations using three O atoms (with O...H distances less than 2.5 Å). The hydrogen-bond angles vary from $114(2)^\circ$ (O1...H7—N4) to $176(3)^\circ$ (O4...H2—N1), the latter also being the shortest of these hydrogen bonds [O4...H2 2.04(3) Å]. The other anion accepts six hydrogen bonds from four different biguanidium cations using all four O atoms (with O...H distances less than 2.5 Å); the angles vary from $135(3)^\circ$ (O6...H1—N1, O7...H4—N2) to $170(3)^\circ$ (O5...H9—N5). The shortest of these is N3—H5...O7 with an angle of $162(3)^\circ$ and an O...H distance of 2.05(3) Å. The H atom on the bridging N atom (H5) is known to be the most acidic, and is also known to form a very short hydrogen bond in the analogous nitrate, but with an angle slightly closer to linearity [$168(3)^\circ$]. We note that the more linear the

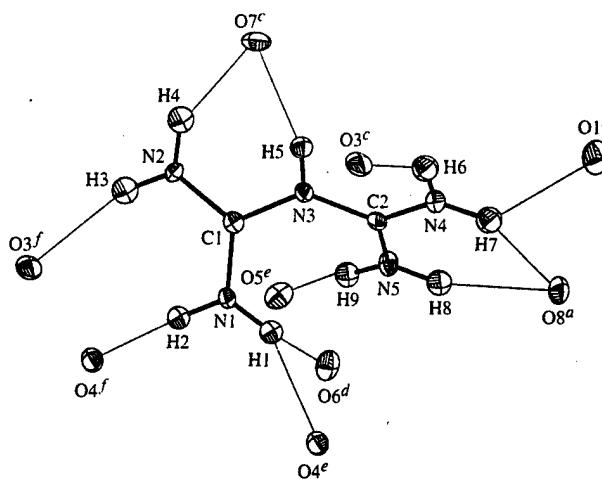


Fig. 1. The biguanidium cation in $(BIGH_2)(ClO_4)_2$ showing the hydrogen bonds. Displacement ellipsoids are shown at the 50% probability level [symmetry codes: (a) $-x, 1-y, -z$; (b) $1-x, 1-y, -z$; (c) $1+x, y, z$; (d) $1+x, 1+y, z$; (e) $x, 1+y, z$; (f) $-x, 1-y, 1-z$].

hydrogen bond, the shorter it is, and that the H atom bonded to the central N atom has a significantly different character to the others.

Examination of the biguanidium cation (Fig. 1) shows that every H atom (of which there are nine) forms a hydrogen bond to an O atom resulting in bonds to a total of six different anions. Two O atoms bind to two H atoms from the same biguanidium unit (O7 to H4 and H5, O8 to H7 and H8). We note that there are two bifurcated hydrogen bonds, involving H1 and H7.

(BIGH)(ClO₄). The structure of the monoprotonated perchlorate is more complex. There are two biguanidium units and two perchlorate anions in the asymmetric unit, again connected by an extensive hydrogen-bond network (Figs. 2 and 3). One perchlorate ion is well behaved with small displacement parameters; the other is disordered. Attempts to refine the structure in space group *P*1 were unsuccessful, thus we report the disordered structure in *P*1. The refinement of the H-atom positions was not well behaved as a result of the disorder; as these atoms are attached to planar *sp*²-hybridized N atoms the discussion of the hydrogen bonding below is based on ideal H-atom positions (N—H 0.95 Å). (We believe this to be more meaningful than an alternative description based on O...N contact distances.) We have modeled the disorder using two equally occupied sites, *A* and *B*, for each atom in the anion; refinement of the occupancies showed no significant deviation from 0.5. The Cl atom and two of the O atoms were refined isotropically due to the proximity of the disordered partner atoms (<0.4 Å); O7 and O8, however, were refined anisotropically as their partners are further away (>0.8 Å). Although it is not unusual for a perchlorate ion to show disorder, this is usually prevented by strong hydrogen bonding. In the present case the opposite is true; the hydrogen bonding to both possible perchlorate-ion orientations is very similar, with the exception that H14 forms a strong hydrogen bond to O7A in orientation *A* and to O8B in orientation *B*. We believe that this choice of two possible hydrogen-bonding schemes is the origin of the observed disorder.

The second, ordered perchlorate ion accepts eight hydrogen bonds from five different biguanidium cations using all four O atoms. The hydrogen-bond distances involving the perchlorate anions range from 1.99 (O1...H7, O1...H12) to 2.53 Å (O2...H9) with angles ranging from 103 (O5B...H9—N6) to 176° (O4...H5—N4).

Again, the biguanidium units consist of two planar halves twisted with respect to each other. One has a 43.5 (1)° twist about N3; the other has 45.6 (1)° twist about N8. This is similar to the twist of 44.0° reported for the monoprotonated biguanidium sulfate, and not very different to that in the diprotonated cation (see above).

The bridging C—N bonds range from 1.334 (3) (N8—C4) to 1.341 (3) Å (N3—C2) and are slightly longer than

the terminal C—N bonds, which range from 1.326 (3) (N2—C1) to 1.339 (3) Å (N6—C3). The bond angles at the bridging N atoms are 121.2 (2) (C1—N3—C2) and 121.3 (2)° (C3—N8—C4), and are identical to that reported for the analogous sulfate [121.2 (2)°].

There is more hydrogen bonding to describe here than for the diperchlorate because of the larger asymmetric unit. All the H atoms form at least one hydrogen bond (<2.5 Å). One interesting feature is that one of the biguanidium units is hydrogen bonded to its symmetry-related partner through a center of inversion (Fig. 2). This 'dimer' is held together by two short hydrogen bonds between H6 and N3. This is the shortest hydrogen bond in the structure (1.98 Å) and, with an N4—H6...N3 angle of 177°, it is essentially linear. Fig. 2 also shows the eight O atoms (counting all atoms, disordered or not, equally) and one additional N atom that have hydrogen-bond distances less than 2.5 Å to one biguanidium cation. Removing the disorder would reduce this to six O atoms from four different perchlorate ions. The hydrogen-bond angles involving O atoms range from 130 (O7A...H8—N5) to 176° (O4...H5—N4).

The other biguanidium unit is shown in Fig. 3, and forms hydrogen bonds to 13 O atoms (removing the disorder would reduce this to nine O atoms). The hydrogen-bond angles range from 103 (O5B...H9—N6) to 170° (O3...H10—N6). We note that H9 and H15 form bifurcated hydrogen bonds.

Clearly, the geometries of the cations in these salts are very similar to those observed previously. The increased

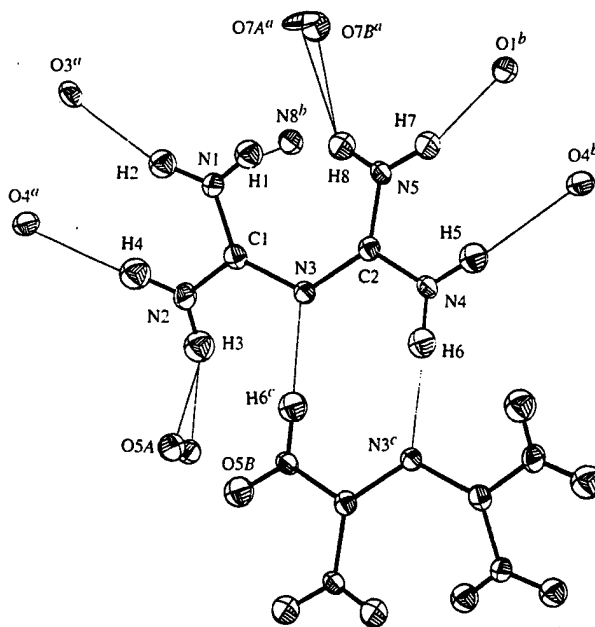


Fig. 2. The biguanidium cation 'dimer' in (BIGH)(ClO₄) showing the hydrogen bonds. Displacement ellipsoids are shown at the 50% probability level [symmetry codes: (a) $-x, -y, 1-z$; (b) $-x, 1-y, 1-z$; (c) $1-x, 1-y, 1-z$].

Table 2. Selected geometric parameters (\AA , $^\circ$) for $(\text{BIGH}_2)(\text{ClO}_4)_2$

Cl1—O1	1.424 (2)	Cl2—O8	1.439 (2)
Cl1—O2	1.424 (2)	N1—C1	1.308 (3)
Cl1—O3	1.452 (2)	N2—C1	1.313 (3)
Cl1—O4	1.446 (2)	N3—C1	1.369 (3)
Cl2—O5	1.431 (2)	N3—C2	1.367 (3)
Cl2—O6	1.429 (2)	N4—C2	1.311 (3)
Cl2—O7	1.441 (2)	N5—C2	1.311 (3)
O1—Cl1—O2	110.6 (1)	O6—Cl2—O8	109.7 (1)
O1—Cl1—O3	109.3 (1)	O7—Cl2—O8	109.4 (1)
O1—Cl1—O4	109.3 (1)	C1—N3—C2	127.0 (2)
O2—Cl1—O3	109.2 (1)	N1—C1—N2	122.0 (2)
O2—Cl1—O4	110.9 (1)	N1—C1—N3	120.6 (2)
O3—Cl1—O4	107.6 (1)	N2—C1—N3	117.3 (2)
O5—Cl2—O6	109.2 (1)	N3—C2—N4	116.5 (2)
O5—Cl2—O7	109.0 (1)	N3—C2—N5	121.1 (2)
O5—Cl2—O8	110.1 (1)	N4—C2—N5	122.4 (2)
O6—Cl2—O7	109.4 (1)		

Refinement

Refinement on F $R = 0.036$ $wR = 0.047$ $S = 2.677$

2680 reflections

233 parameters

H atoms placed in ideal positions (N—H 0.95 \AA) $w = 1/\sigma^2(F)$ $(\Delta/\sigma)_{\text{max}} = <0.001$ $\Delta\rho_{\text{max}} = 0.35 \text{ e } \text{\AA}^{-3}$ $\Delta\rho_{\text{min}} = -0.12 \text{ e } \text{\AA}^{-3}$

Extinction correction:

isotropic (Zachariasen, 1963)

Extinction coefficient:

 0.15×10^{-5}

Atomic scattering factors

from *International Tables*

for X-ray Crystallography

(1974, Vol. IV)

Table 4. Fractional atomic coordinates and isotropic or equivalent isotropic displacement parameters (\AA^2) for $(\text{BIGH})(\text{ClO}_4)$ U_{iso} for Cl2, O5 and O6, $U_{\text{eq}} = (1/3)\sum_i U_{ij}a_i^*a_j^*a_i \cdot a_j$ for all other atoms.

	x	y	z	$U_{\text{eq}}/U_{\text{iso}}$
Cl1	0.04296 (6)	0.38504 (5)	0.73141 (4)	0.0147 (1)
Cl2A†	0.4842 (1)	0.12244 (9)	0.80259 (7)	0.0121 (2)
Cl2B†	0.4697 (1)	0.0957 (1)	0.77591 (8)	0.0182 (2)
O1	0.1661 (2)	0.5207 (1)	0.7109 (1)	0.0197 (4)
O2	-0.0401 (2)	0.4397 (2)	0.8326 (1)	0.0234 (4)
O3	0.1550 (2)	0.3067 (1)	0.7545 (1)	0.0209 (4)
O4	-0.1032 (2)	0.2734 (2)	0.6245 (1)	0.0206 (4)
O5A†	0.5098 (4)	0.1876 (3)	0.7122 (2)	0.0221 (6)
O5B†	0.5062 (4)	0.2206 (3)	0.7376 (2)	0.0173 (6)
O6B†	0.6440 (4)	0.1125 (3)	0.8429 (2)	0.0203 (6)
O6A†	0.6560 (4)	0.0993 (3)	0.8174 (2)	0.0205 (6)
O7A†	0.3302 (4)	-0.0397 (3)	0.7457 (2)	0.0239 (9)
O7B†	0.3681 (5)	-0.0590 (4)	0.6821 (4)	0.052 (1)
O8B†	0.3547 (5)	0.1233 (5)	0.8660 (3)	0.059 (1)
O8A†	0.4475 (5)	0.2178 (5)	0.9087 (3)	0.042 (1)
N1	0.0788 (2)	0.0536 (2)	0.3172 (1)	0.0168 (4)
N2	0.2518 (2)	0.0883 (2)	0.4883 (1)	0.0215 (5)
N3	0.2834 (2)	0.3142 (2)	0.4654 (1)	0.0156 (4)
N4	0.3032 (2)	0.5429 (2)	0.4509 (1)	0.0185 (5)
N5	0.0078 (2)	0.3365 (2)	0.4005 (1)	0.0165 (4)
N6	-0.3967 (2)	0.5610 (2)	0.8366 (2)	0.0219 (5)
N7	-0.4395 (2)	0.7622 (2)	0.8061 (2)	0.0226 (5)
N8	-0.1359 (2)	0.8050 (2)	0.8683 (1)	0.0166 (4)
N9	0.1672 (2)	0.8462 (2)	0.9315 (1)	0.0194 (5)
N10	-0.0605 (2)	0.7448 (2)	1.0272 (1)	0.0213 (5)
C1	0.2015 (3)	0.1528 (2)	0.4230 (2)	0.0155 (5)
C2	0.1956 (3)	0.3936 (2)	0.4364 (2)	0.0150 (5)
C3	-0.3221 (3)	0.7090 (2)	0.8398 (2)	0.0174 (5)
C4	-0.0143 (3)	0.7949 (2)	0.9412 (2)	0.0164 (5)

† Site occupancy = 0.5.

Table 5. Selected geometric parameters (\AA , $^\circ$) for $(\text{BIGH})(\text{ClO}_4)$

Cl1—O1	1.445 (2)	N1—C1	1.337 (3)
Cl1—O2	1.428 (2)	N2—C1	1.326 (3)
Cl1—O3	1.444 (2)	N3—C1	1.340 (3)
Cl1—O4	1.438 (2)	N3—C2	1.341 (3)
Cl2A—O5A	1.467 (5)	N4—C2	1.331 (3)
Cl2A—O6A	1.448 (5)	N5—C2	1.334 (3)
Cl2A—O7A	1.459 (4)	N6—C3	1.339 (3)
Cl2A—O8A	1.392 (5)	N7—C3	1.332 (3)
Cl2B—O5B	1.421 (4)	N8—C3	1.338 (3)
Cl2B—O6B	1.475 (5)	N8—C4	1.334 (3)
Cl2B—O7B	1.400 (5)	N9—C4	1.331 (3)
Cl2B—O8B	1.450 (5)	N10—C4	1.335 (3)
O1—Cl1—O2	110.0 (1)	O6B—Cl2B—O8B	103.9 (3)
O1—Cl1—O3	108.5 (1)	O7B—Cl2B—O8B	108.5 (4)
O1—Cl1—O4	108.64 (9)	C1—N3—C2	121.2 (2)
O2—Cl1—O3	109.9 (1)	C3—N8—C4	121.3 (2)
O2—Cl1—O4	110.2 (1)	N1—C1—N2	118.4 (2)
O3—Cl1—O4	109.5 (1)	N1—C1—N3	124.0 (2)

Table 3. Hydrogen-bonding geometry (\AA , $^\circ$) for $(\text{BIGH}_2)(\text{ClO}_4)_2$

D—H...A	D—H	H...A	D—H...A
N1—H1...O4 ⁱ	0.83 (3)	2.36 (3)	137 (3)
N1—H1...O6 ⁱⁱ	0.83 (3)	2.30 (3)	135 (3)
N1—H2...O4 ⁱⁱⁱ	0.87 (3)	2.04 (3)	176 (3)
N2—H3...O3 ⁱⁱⁱ	0.79 (2)	2.19 (3)	159 (3)
N2—H4...O7 ^{iv}	0.80 (3)	2.42 (4)	135 (3)
N3—H5...O7 ^{iv}	0.82 (2)	2.05 (3)	162 (3)
N4—H6...O3 ^{iv}	0.80 (2)	2.12 (3)	163 (3)
N4—H7...O1 ^v	0.94 (3)	2.35 (3)	114 (2)
N4—H7...O8 ^{vi}	0.94 (3)	2.11 (4)	147 (3)
N5—H8...O8 ^{vi}	0.87 (3)	2.12 (3)	156 (3)
N5—H9...O5 ⁱ	0.81 (3)	2.21 (3)	170 (3)

Symmetry codes: (i) $x, 1+y, z$; (ii) $1+x, 1+y, z$; (iii) $-x, 1-y, 1-z$; (iv) $1+x, y, z$; (v) $1-x, 1-y, -z$; (vi) $-x, 1-y, -z$. $(\text{BIGH})(\text{ClO}_4)$

Crystal data

 $\text{C}_2\text{H}_8\text{N}_5^+\text{ClO}_4^-$ $M_r = 201.57$

Triclinic

 $P\bar{1}$ $a = 7.7421 (9) \text{\AA}$ $b = 9.874 (2) \text{\AA}$ $c = 12.267 (2) \text{\AA}$ $\alpha = 112.75 (1)^\circ$ $\beta = 91.89 (1)^\circ$ $\gamma = 111.91 (1)^\circ$ $V = 784.9 (6) \text{\AA}^3$ $Z = 4$ $D_x = 1.71 \text{ Mg m}^{-3}$

Data collection

Enraf-Nonius CAD-4 diffractometer

 $3\theta/2\theta$ scans

Absorption correction:

 ψ scans (North, Phillips & Mathews, 1968) $T_{\text{min}} = 0.9312$, $T_{\text{max}} = 0.9982$

3322 measured reflections

3069 independent reflections

Mo $K\alpha$ radiation $\lambda = 0.71073 \text{\AA}$

Cell parameters from 25 reflections

 $\theta = 9-15^\circ$ $\mu = 0.472 \text{ mm}^{-1}$ $T = 100 \text{ K}$

Parallelepiped

 $0.37 \times 0.31 \times 0.11 \text{ mm}$

Colorless

2680 observed reflections
 $[I > 3.0\sigma(I)]$ $R_{\text{int}} = 0.027$ $\theta_{\text{max}} = 25.99^\circ$ $h = 0 \rightarrow 9$ $k = -12 \rightarrow 11$ $l = -15 \rightarrow 15$

3 standard reflections

frequency: 50 min

intensity decay: 2.27%

O5A—Cl2A—O6A	103.1 (3)	N2—C1—N3	117.5 (2)
O5A—Cl2A—O7A	107.4 (3)	N3—C2—N4	117.3 (2)
O5A—Cl2A—O8A	114.1 (3)	N3—C2—N5	124.5 (2)
O6A—Cl2A—O7A	105.5 (3)	N4—C2—N5	118.1 (2)
O6A—Cl2A—O8A	115.1 (3)	N6—C3—N7	118.2 (2)
O7A—Cl2A—O8A	110.9 (3)	N6—C3—N8	124.8 (2)
O5B—Cl2B—O6B	112.1 (3)	N7—C3—N8	116.9 (2)
O5B—Cl2B—O7B	112.9 (3)	N8—C4—N9	117.6 (2)
O5B—Cl2B—O8B	105.6 (3)	N8—C4—N10	124.4 (2)
O6B—Cl2B—O7B	113.1 (3)	N9—C4—N10	117.9 (2)

Table 6. Hydrogen-bonding geometry (\AA , $^\circ$) for (BIGH)(ClO₄)

D—H...A	D—H	H...A	D—H...A
N1—H1...N8 ⁱ	0.95	2.2625	141.50
N1—H2...O3 ⁱⁱ	0.95	2.1417	162.68
N2—H3...O5A	0.95	2.0652	150.77
N2—H3...O5B	0.95	2.1877	157.64
N2—H4...O4 ⁱⁱ	0.95	2.0562	171.99
N4—H5...O4 ⁱ	0.95	2.1893	175.92
N4—H6...N3 ⁱⁱⁱ	0.95	1.9802	176.95
N5—H7...O1 ⁱ	0.95	1.9894	161.96
N5—H8...O7A ⁱⁱ	0.95	2.2240	129.83
N5—H8...O7B ⁱⁱ	0.95	2.1728	138.40
N6—H9...O2	0.95	2.5337	150.00
N6—H9...O5B ^{iv}	0.95	2.5061	102.76
N6—H10...O3 ^{iv}	0.95	2.3282	169.74
N7—H11...O6B ^v	0.95	2.2010	160.57
N7—H11...O6A ^v	0.95	2.1410	166.67
N7—H12...O1 ^{iv}	0.95	1.9873	168.42
N9—H13...O6B ^{vi}	0.95	2.0675	144.61
N9—H13...O6A ^{vi}	0.95	2.3080	139.06
N9—H14...O7A ^{vii}	0.95	2.0913	168.67
N9—H14...O8B ^{vii}	0.95	2.2183	139.99
N10—H15...O2 ^{viii}	0.95	2.4573	135.65
N10—H15...O6B ^{vi}	0.95	2.3124	136.91
N10—H15...O6A ^{vi}	0.95	2.3125	138.72
N10—H16...O8B ^{viii}	0.95	2.4163	130.00
N10—H16...O8A ^{viii}	0.95	2.3866	149.08

Symmetry codes: (i) $-x, 1-y, 1-z$; (ii) $-x, -y, 1-z$; (iii) $1-x, 1-y, 1-z$; (iv) $x-1, y, z$; (v) $x-1, 1+y, z$; (vi) $1-x, 1-y, 2-z$; (vii) $x, 1+y, z$; (viii) $-x, 1-y, 2-z$.

Preliminary examination and intensity data collection were carried out using an Enraf-Nonius CAD-4 diffractometer. Backgrounds were obtained from analysis of the scan profile (Blessing, Coppens & Becker, 1974). The crystal of the diperchlorate was lost before ψ scans were obtained, hence an absorption correction was applied using DIFABS (Walker & Stuart, 1983). All H atoms in the diperchlorate refined cleanly. This was not the case, however, for the monoperchlorate, for which all H atoms are reported in ideal positions. The computer programs used were taken from MolEN (Fair, 1990) and locally modified according to Blessing (1987). The molecular graphics were prepared with a CAChe workstation (CAChe Scientific, 1993).

For both compounds, data collection: CAD-4 Software (Enraf-Nonius, 1977); cell refinement: CAD-4 Software; data reduction: MolEN PROCESS; program(s) used to solve structures: SIR (Burla *et al.*, 1989); program(s) used to refine structures: MolEN LSFM; software used to prepare material for publication: MolEN CIF VAX.

We thank the College of Arts and Sciences of the University of Toledo for generous financial support of the X-ray diffraction facility and thank the Office of Naval Research for funding this work (contract No. N000149310597).

Lists of structure factors, anisotropic displacement parameters and H-atom coordinates have been deposited with the IUCr (Reference: BK1092). Copies may be obtained through The Managing Editor, International Union of Crystallography, 5 Abbey Square, Chester CH1 2HU, England.

References

- Blessing, R. H. (1987). *Crystallogr. Rev.* **1**, 3–57.
 Blessing, R. H., Coppens, P. & Becker, P. (1974). *J. Appl. Cryst.* **7**, 488–492.
 Borman, S. (1994). *Chem. Eng. News*, pp. 18–22.
 Bottaro, J. C., Gilardi, R. D., Martin, A. & Pinkerton, A. A. (1996). In preparation.
 Burla, M. C., Camalli, M., Cascarano, G., Giacovazzo, C., Polidori, G., Spagna, R. & Viterbo, D. (1989). *J. Appl. Cryst.* **22**, 389–393.
 CAChe Scientific (1993). *CAChe Reference Manual*. CAChe Scientific, Beaverton, Oregon, USA.
 Chichra, D. A., Holden, J. R. & Dickinson, C. (1980). Report NSWC TR79-273. Naval Research Weapons Center (White Oak), Silver Spring, MD 20910, USA.
 Dollimore, D., Martin, A. & Pinkerton, A. A. (1996). *Thermochim. Acta*. In the press.
 Enraf-Nonius (1977). *CAD-4 Operations Manual*. Enraf-Nonius, Delft, The Netherlands.
 Fair, C. K. (1990). *MolEN. An Interactive Intelligent System for Crystal Structure Analysis*. Enraf-Nonius, Delft, The Netherlands.
 Manuelli, C. & Bernardini, L. (1917). Br. Patent 155 627.
 Martin, A., Pinkerton, A. A. & Schiemann, A. (1996). *Acta Cryst. C52*. In the press.
 North, A. C. T., Phillips, D. C. & Mathews, F. S. (1968). *Acta Cryst. A24*, 351–359.
 Pinkerton, A. A. & Schwarzenbach, D. (1978). *J. Chem. Soc. Dalton Trans.* pp. 989–996.
 Stine, J. R. (1981). Report LA-8920. Los Alamos National Laboratory, Los Alamos, NM 87545, USA.
 Walker, N. & Stuart, D. (1983). *Acta Cryst. A39*, 158–166.
 Zachariasen, W. H. (1963). *Acta Cryst. B16*, 1139–1144.

Contract No. N00014-95-1-0013 and N00014-97-1-0409

Program Officer: R. Miller/J. Goldwasser

**Title: Experimental Charge Densities and Electrostatic Potentials in Energetic
Materials and Infrastructure Upgrade for an X-ray Crystallography
Laboratory**

PI: A. Alan Pinkerton

Department of Chemistry, University of Toledo, Toledo, OH 43606

tel. (419) 530-4580, FAX (419) 530-4033, email apinker@uoft02.utoledo.edu

APPENDIX 5d

Energetic Materials. The Biguanidinium Nitrates.

Martin, A.; Pinkerton, A.A.; and Schiemann, A.; *Acta Crystallogr.*, 1996, C52, 966-970.

Energetic Materials: the Biguanidium Nitrates

ANTHONY MARTIN, A. ALAN PINKERTON AND ANKE SCHIEMANN

Department of Chemistry, University of Toledo, Toledo, OH 43606, USA. E-mail: apinker@uoft02.utoledo.edu

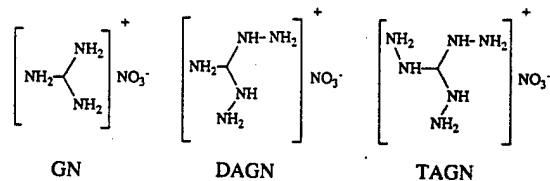
(Received 3 February 1994; accepted 31 August 1995)

Abstract

The structures of two new potentially energetic biguanidium salts, biguanidium nitrate, $\text{C}_2\text{H}_8\text{N}_5^+\cdot\text{NO}_3^-$ [(BIGH) NO_3], and biguanidium dinitrate, $\text{C}_2\text{H}_9\text{N}_5^{2+}\cdot 2\text{NO}_3^-$ [(BIGH₂)(NO_3)₂], have been determined from X-ray data collected at 193 K. The mono- and diprotonated biguanidium nitrates are dense organic materials with efficient packing of planar anions and biplanar (twisted) cations connected by multiple hydrogen bonds. The experimental densities are compared with those obtained from empirical calculations.

Comment

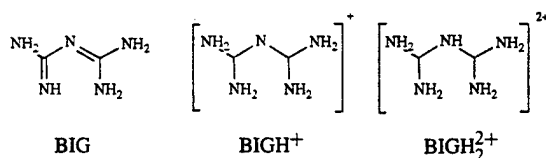
There is current interest (Borman, 1994) in the development of new energetic materials (such as explosives or propellants) and in understanding the properties of these materials, particularly with respect to their structures (Olah & Squire, 1991). One class of compounds that have solicited interest are derived from guanidinium nitrate (GN) and include, for example, diaminoguanidinium nitrate (DAGN) (Ritchie, Lee, Cromer, Kober & Lee, 1990) and triaminoguanidinium nitrate (TAGN) (Bracuti, 1979; Choi & Prince, 1979; Oyumi & Brill, 1985).



The utility of these compounds in the field of energetic materials is derived from their rapid thermal decomposition into all-gaseous products (Oyumi & Brill, 1985, and references therein). The effectiveness of materials as either explosives or propellants is related to the density of the solid, the gas volume produced and the heat of combustion (Gilardi & Karle, 1991). DAGN and TAGN have useful properties as propellants, their densities being fairly high for organic materials (1.61 and 1.59 Mg m^{-3} for DAGN and TAGN, respectively). Our

previous experience with biguanidium salts (Pinkerton & Schwarzenbach, 1978) suggested that these closely related cations might be used to prepare higher density nitrates.

Empirical calculations (Chichra, Holden & Dickinson, 1980; Stine, 1981; hereafter CHD and ST, respectively) for the monoprotonated and diprotonated biguanidium nitrates $(\text{BIGH})\text{NO}_3$ and $(\text{BIGH}_2)(\text{NO}_3)_2$, using appropriate atomic volumes, predicted densities of 1.63 (CHD) or 1.61 Mg m^{-3} (ST) for $(\text{BIGH})\text{NO}_3$ and 1.77 (CHD) or 1.74 Mg m^{-3} (ST) for $(\text{BIGH}_2)(\text{NO}_3)_2$. Analogous calculations gave 1.74 (CHD) or 1.68 Mg m^{-3} (ST) for DAGN, and 1.75 (CHD) or 1.68 Mg m^{-3} for TAGN. We note that the observed densities for DAGN and TAGN are somewhat less than the calculated densities, and that the value predicted for $(\text{BIGH}_2)(\text{NO}_3)_2$ is the highest of the four compounds. We have thus synthesized and characterized both the monoprotonated and diprotonated biguanidium nitrates and report our results herein.



The structures of the delocalized cations (Figs. 1 and 2) are very similar to those previously reported for the chloride $\text{BIGH}\cdot\text{Cl}$ (Ernst, 1977), the carbonate $(\text{BIGH})_2\text{CO}_3$ and the sulfates $(\text{BIGH})_2\text{SO}_4\cdot 2\text{H}_2\text{O}$ and $(\text{BIGH}_2)\text{SO}_4\cdot \text{H}_2\text{O}$ (Pinkerton & Schwarzenbach, 1978). Both cations are composed of two planar halves with one atom in common. The two halves are twisted with respect to each other due to the intramolecular $\text{H}\cdots\text{H}$ interaction [BIGH^+ 37.8 (1)°; BIGH_2^{2+} 47.0 (1)°]. All bonds are short due to extensive π delocalization, producing bond orders greater than one. As previously noted, protonation of the bridge N atom leads to a small increase in the C—N bridge bond lengths (compared to the monoprotonated cation) with a concomitant shortening of the terminal C—N bonds.

Both crystal structures are characterized by an extensive hydrogen-bonding network. The packing diagram for $(\text{BIGH})\text{NO}_3$ (Fig. 3) shows that there are layers of strongly hydrogen-bonded cations and anions. The layers are then connected by one additional hydrogen bond. The biguanidium cations form hydrogen-bonded dimers (Fig. 1) across an inversion center with the bridge N atom acting as the acceptor. It can also be seen from this diagram that all but two of the H atoms (H2B and H4A) take part in hydrogen bonding. However, H2B forms a square arrangement with O3 across a center of symmetry with rather longer contact distances [the sides of the 'square' are 2.43 (2) and 2.52 (2) Å, with angles at O and H of 86.5 (5) and 93.6 (6)°, respectively]. Here, the

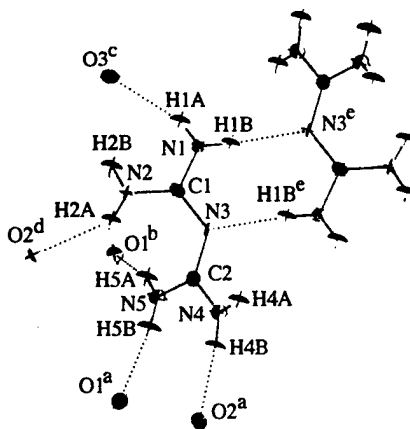


Fig. 1. The BIGH^+ cation showing the atom-numbering and hydrogen-bonding schemes (50% probability ellipsoids). [Symmetry codes: (a) $x+1, y, z$; (b) $x+\frac{1}{2}, -y+\frac{1}{2}, z-\frac{1}{2}$; (c) $x-\frac{1}{2}, -y+\frac{1}{2}, z-\frac{1}{2}$; (d) $-x+\frac{1}{2}, y+\frac{1}{2}, -z+\frac{1}{2}$; (e) $-x, -y, -z$.]

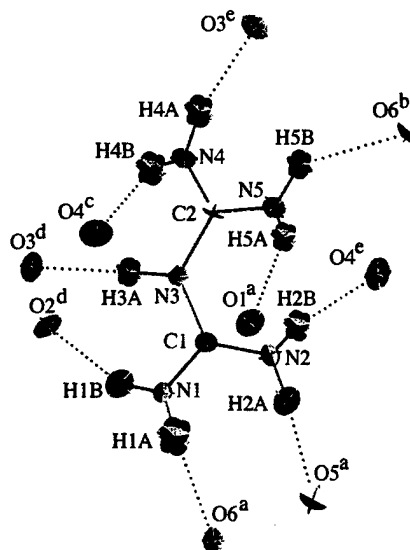


Fig. 2. The BIGH_2^{2+} cation showing the atom-numbering and hydrogen-bonding schemes (50% probability ellipsoids). [Symmetry codes: (a) $x+\frac{1}{2}, -y+2, z$; (b) $-x+1, -y+1, z+\frac{1}{2}$; (c) $-x+1, -y+1, z-\frac{1}{2}$; (d) $-x+\frac{1}{2}, y, z-\frac{1}{2}$; (e) $x+\frac{1}{2}, -y+1, z$.]

competing O atoms seem to force H2B into a less favorable position. It would appear that the putative square is distorted by the additional hydrogen bonds to the nitrate groups. The nitrate anion is unremarkable and accepts five hydrogen bonds.

The diprotonated biguanidium cation in $(\text{BIGH}_2)(\text{NO}_3)_2$ has a hydrogen bond from every H atom to a nitrate O atom (Fig. 2). The nitrate groups have the expected geometry, and every O atom accepts at least one hydrogen bond. The hydrogen-bonding scheme for $(\text{BIGH}_2)(\text{NO}_3)_2$ is now truly three-dimensional (Fig.

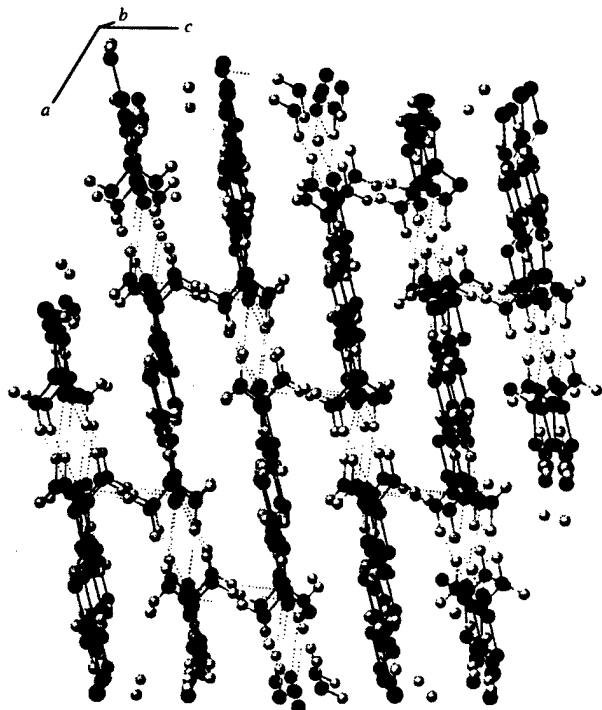


Fig. 3. Packing diagram for $(BIGH)NO_3$ showing the hydrogen bonding and layer structure.

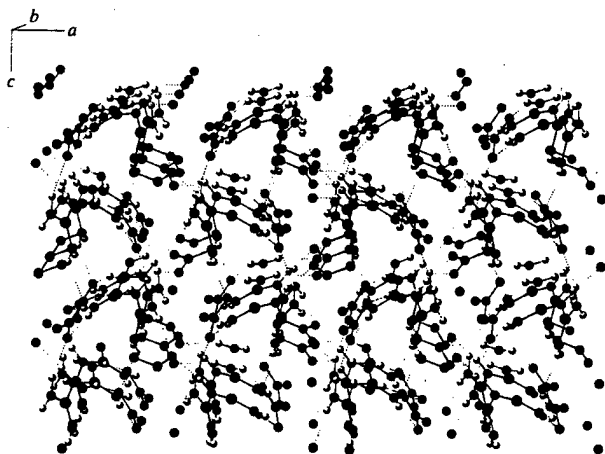


Fig. 4. Packing diagram for $(BIGH_2)(NO_3)_2$ showing the three-dimensional hydrogen-bonding scheme.

4) and, for this reason, the packing diagram is less informative because there are no obvious viewing directions. It is worth noting, however, that the H atom on the bridging N atom (H3A) forms a particularly strong hydrogen bond [$O \cdots H$ 1.83 (3) Å].

The crystals of both compounds are very compact, as evidenced by their densities [$(BIGH)NO_3$ 1.62 (193 K), 1.59 Mg m^{-3} (298 K); $(BIGH_2)(NO_3)_2$ 1.75 (193 K),

1.73 Mg m^{-3} (298 K)], which are very close to the values predicted above. Indeed, both compounds have higher densities than either DAGN or TAGN, which would not have been predicted. It is tempting to ascribe this to more efficient packing or more favorable hydrogen bonding; however, the evidence is weak. It has been noted that density predictions for energetic-material salts tend to be less reliable than for neutral energetic molecules (Gilardi, 1994).

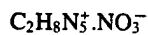
It is thus demonstrated that the protonated biguanidinium species are good cations for preparing high-density solids with flat anions capable of accepting hydrogen bonds.

Experimental

$(BIGH)NO_3$ was prepared easily from aqueous solutions of biguanidium sulfate and barium nitrate followed by filtration and slow evaporation. $(BIGH_2)(NO_3)_2$ was prepared by acidifying the above solution with nitric acid, followed by slow evaporation.

$(BIGH)NO_3$

Crystal data



$M_r = 164.12$

Monoclinic

$P2_1/n$

$a = 6.959 (1) \text{ Å}$

$b = 10.778 (2) \text{ Å}$

$c = 9.489 (2) \text{ Å}$

$\beta = 109.28 (2)^\circ$

$V = 671.8 (4) \text{ Å}^3$

$Z = 4$

$D_x = 1.62 \text{ Mg m}^{-3}$

Mo $K\alpha$ radiation

$\lambda = 0.7107 \text{ Å}$

Cell parameters from 25 reflections

$\theta = 9-15^\circ$

$\mu = 0.136 \text{ mm}^{-1}$

$T = 193 \text{ K}$

Prism

$0.40 \times 0.21 \times 0.19 \text{ mm}$

Colorless

Data collection

Enraf-Nonius CAD-4 diffractometer

ω scans

Absorption correction:

ψ scans (North, Phillips & Mathews, 1968)

$T_{\min} = 0.848$, $T_{\max} = 0.998$

1518 measured reflections

1403 independent reflections

1321 observed reflections

$[I > 3\sigma(I)]$

$R_{\text{int}} = 0.022$

$\theta_{\max} = 25.97^\circ$

$h = 0 \rightarrow 8$

$k = 0 \rightarrow 13$

$l = -11 \rightarrow 11$

3 standard reflections

frequency: 50 min

intensity decay: 0.01%

Refinement

Refinement on F

$R = 0.046$

$wR = 0.048$

$S = 1.420$

1321 reflections

132 parameters

All H-atom parameters refined

$w = 4F_o^2/[\sigma^2(F_o^2) + 0.0016F_o^2]$

$(\Delta/\sigma)_{\max} = 0.001$

$\Delta\rho_{\max} = 0.301 \text{ e Å}^{-3}$

$\Delta\rho_{\min} = -0.354 \text{ e Å}^{-3}$

Extinction correction: none

Atomic scattering factors from *International Tables for X-ray Crystallography* (1974, Vol. IV)

(BIGH₂)(NO₃)₂*Crystal data*C₂H₉N₅²⁺·2NO₃⁻*M_r* = 227.14

Orthorhombic

*Pca*2₁*a* = 14.0232 (8) Å*b* = 6.8842 (5) Å*c* = 8.9541 (5) Å*V* = 864.4 (2) Å³*Z* = 4*D_x* = 1.75 Mg m⁻³Mo *K*α radiation*λ* = 0.7107 Å

Cell parameters from 25

reflections

θ = 10–14°*μ* = 0.157 mm⁻¹*T* = 193 K

Prism

0.35 × 0.22 × 0.19 mm

Colorless

Data collection

Enraf–Nonius CAD-4

diffractometer

ω/2*θ* scans

Absorption correction:

ψ scans (North, Phillips

& Mathews, 1968)

T_{min} = 0.949, *T_{max}* =

0.998

1026 measured reflections

1026 independent reflections

841 observed reflections

[I > 3*σ*(*I*)*θ_{max}* = 25.97°*h* = –8 → 0*k* = 0 → 11*l* = –17 → 0

3 standard reflections

frequency: 50 min

intensity decay: 0.22%

*Refinement*Refinement on *F**R* = 0.027*wR* = 0.037*S* = 0.854

841 reflections

172 parameters

All H-atom parameters

refined

w = 4*F_o*²/*[σ*²(*F_o*²)+ 0.0064*F_o*⁴](Δ/*σ*)_{max} = 0.006Δ*ρ*_{max} = 0.181 e Å⁻³Δ*ρ*_{min} = –0.205 e Å⁻³

Extinction correction: none

Atomic scattering factors

from *International Tables*for *X-ray Crystallography*

(1974, Vol. IV)

Table 1. Fractional atomic coordinates and isotropic or equivalent isotropic displacement parameters (Å²) for (BIGH)NO₃

*U*_{iso} for H atoms, *U*_{eq} = (1/3)Σ_{*i*}Σ_{*j*}*U_{ij}**a_i*[†]*a_j* for all others.

	<i>x</i>	<i>y</i>	<i>z</i>	<i>U</i> _{eq} / <i>U</i> _{iso}
O1	–0.0128 (2)	0.18355 (9)	0.3222 (1)	0.0308 (3)
O2	–0.0235 (1)	–0.01718 (9)	0.3236 (1)	0.0299 (3)
O3	0.2577 (1)	0.07882 (9)	0.4369 (1)	0.0299 (3)
N1	–0.0627 (2)	0.1670 (1)	–0.0557 (1)	0.0253 (3)
N2	0.1916 (2)	0.3048 (1)	0.0504 (1)	0.0280 (3)
N3	0.2420 (2)	0.0877 (1)	0.0852 (1)	0.0224 (3)
N4	0.5335 (2)	0.0045 (1)	0.2425 (1)	0.0282 (3)
N5	0.5651 (2)	0.1690 (1)	0.1024 (1)	0.0282 (3)
N6	0.0741 (2)	0.0813 (1)	0.3608 (1)	0.0215 (3)
C1	0.1288 (2)	0.1874 (1)	0.0262 (1)	0.0200 (3)
C2	0.4448 (2)	0.0902 (1)	0.1419 (1)	0.0204 (3)
H1A	–0.138 (2)	0.227 (2)	–0.074 (2)	0.031 (4)
H1B	–0.106 (2)	0.092 (1)	–0.067 (2)	0.026 (4)
H2A	0.310 (2)	0.323 (1)	0.102 (2)	0.028 (4)
H2B	0.112 (2)	0.361 (2)	–0.003 (2)	0.035 (4)
H4A	0.460 (2)	–0.036 (2)	0.275 (2)	0.032 (4)
H4B	0.668 (2)	–0.008 (2)	0.274 (2)	0.031 (4)
H5A	0.515 (2)	0.211 (2)	0.018 (2)	0.037 (5)
H5B	0.694 (3)	0.167 (2)	0.151 (2)	0.046 (5)

Table 2. Fractional atomic coordinates and isotropic or equivalent isotropic displacement parameters (Å²) for (BIGH₂)(NO₃)₂

*U*_{iso} for H atoms, *U*_{eq} = (1/3)Σ_{*i*}Σ_{*j*}*U_{ij}**a_i*[†]*a_j* for all others.

	<i>x</i>	<i>y</i>	<i>z</i>	<i>U</i> _{eq} / <i>U</i> _{iso}
O1	0.1254 (1)	0.9811 (2)	0.9719	0.0265 (3)
O2	0.0079 (1)	1.0753 (2)	1.1095 (2)	0.0246 (3)
O3	–0.00228 (9)	0.8047 (2)	0.9843 (2)	0.0262 (3)
O4	0.3722 (1)	0.5305 (2)	0.9179 (2)	0.0335 (4)
O5	0.3972 (1)	0.8212 (2)	0.8372 (2)	0.0381 (4)
O6	0.3126 (1)	0.6208 (2)	0.7072 (2)	0.0270 (3)
N1	0.6960 (1)	1.0265 (2)	0.6430 (2)	0.0205 (4)
N2	0.7889 (1)	0.8210 (2)	0.7831 (2)	0.0223 (4)
N3	0.6380 (1)	0.7262 (2)	0.6973 (2)	0.0183 (3)
N4	0.5723 (1)	0.4265 (2)	0.7359 (2)	0.0233 (4)
N5	0.6390 (1)	0.5902 (2)	0.9359 (2)	0.0240 (4)
N6	0.0440 (1)	0.9560 (2)	1.0223 (2)	0.0188 (3)
N7	0.3610 (1)	0.6590 (2)	0.8222 (2)	0.0195 (4)
C1	0.7099 (1)	0.8608 (3)	0.7121 (2)	0.0166 (4)
C2	0.6173 (1)	0.5769 (3)	0.7933 (3)	0.0178 (4)
H1A	0.742 (2)	1.109 (4)	0.636 (4)	0.056 (9)
H1B	0.638 (2)	1.064 (4)	0.608 (4)	0.036 (7)
H2A	0.830 (2)	0.927 (3)	0.799 (4)	0.036 (7)
H2B	0.806 (1)	0.708 (4)	0.818 (4)	0.038 (8)
H3A	0.596 (1)	0.740 (5)	0.617 (4)	0.031 (6)
H4A	0.545 (2)	0.327 (4)	0.794 (5)	0.041 (7)
H4B	0.576 (2)	0.409 (4)	0.634 (4)	0.045 (8)
H5A	0.645 (2)	0.702 (3)	0.978 (4)	0.031 (6)
H5B	0.629 (2)	0.483 (4)	0.998 (4)	0.032 (7)

Table 3. Selected geometric parameters (Å, °) for (BIGH)NO₃ and (BIGH₂)(NO₃)₂

(BIGH)NO ₃		(BIGH ₂)(NO ₃) ₂	
O1–N6	1.253 (1)	O1–N6	1.239 (2)
O2–N6	1.246 (1)	O2–N6	1.241 (2)
O3–N6	1.244 (1)	O3–N6	1.274 (2)
		O4–N7	1.241 (2)
		O5–N7	1.234 (2)
		O6–N7	1.261 (2)
N1–C1	1.320 (2)	N1–C1	1.313 (3)
N2–C1	1.334 (2)	N2–C1	1.307 (2)
N3–C1	1.340 (2)	N3–C1	1.376 (2)
N3–C2	1.334 (2)	N3–C2	1.371 (3)
N4–C2	1.325 (2)	N4–C2	1.317 (3)
N5–C2	1.330 (2)	N5–C2	1.316 (3)
O1–N6–O3	119.5 (1)	O1–N6–O2	120.9 (2)
O2–N6–O3	120.4 (1)	O1–N6–O3	119.1 (2)
O1–N6–O2	120.1 (1)	O2–N6–O3	120.0 (2)
		O4–N7–O5	121.1 (2)
		O4–N7–O6	118.9 (2)
		O5–N7–O6	120.0 (2)
C1–N3–C2	123.4 (1)	C1–N3–C2	126.8 (2)
N1–C1–N2	117.9 (1)	N1–C1–N2	122.5 (2)
N1–C1–N3	116.9 (1)	N1–C1–N3	115.5 (2)
N2–C1–N3	125.0 (1)	N2–C1–N3	121.9 (2)
N3–C2–N4	117.2 (1)	N3–C2–N4	116.5 (2)
N3–C2–N5	125.4 (1)	N3–C2–N5	120.5 (2)
N4–C2–N5	117.4 (1)	N4–C2–N5	123.0 (2)

Table 4. Hydrogen-bonding geometry (Å, °) for (BIGH)NO₃ and (BIGH₂)(NO₃)₂

D–H...A	D–H	H...A	D–H...A
(BIGH)NO ₃			
N1–H1A...O3 ⁱ	0.82 (2)	2.22 (2)	159 (1)
N1–H1B...N3 ⁱⁱ	0.86 (2)	2.14 (2)	173 (2)
N2–H2A...O2 ⁱⁱⁱ	0.83 (1)	2.23 (1)	143 (1)
N4–H4B...O2 ^{iv}	0.89 (2)	2.05 (2)	171 (2)
N5–H5A...O1 ^v	0.89 (2)	2.13 (2)	163 (2)
N5–H5B...O1 ^{iv}	0.86 (2)	2.15 (2)	164 (2)

Symmetry codes: (i) *x* – ½, ½ – *y*, *z* – ½; (ii) –*x*, –*y*, –*z*; (iii) ½ – *x*, ½ + *y*, ½ – *z*; (iv) 1 + *x*, *y*, *z*; (v) ½ + *x*, ½ – *y*, *z* – ½.

$(BIGH_2)(NO_3)_2$			
N1—H1A...O6 ⁱ	0.86 (3)	2.20 (3)	151 (3)
N1—H1B...O2 ⁱⁱ	0.91 (3)	2.05 (3)	154 (3)
N2—H2A...O5 ⁱ	0.94 (3)	2.00 (2)	170 (2)
N2—H2B...O4 ⁱⁱⁱ	0.87 (3)	2.09 (3)	167 (2)
N3—H3A...O3 ⁱⁱ	0.93 (3)	1.83 (3)	168 (3)
N4—H4A...O3 ⁱⁱⁱ	0.94 (3)	2.04 (4)	157 (3)
N4—H4B...O4 ^{iv}	0.92 (4)	2.11 (4)	155 (2)
N5—H5A...O1 ⁱ	0.86 (3)	2.20 (2)	150 (3)
N5—H5B...O6 ^v	0.93 (3)	2.17 (3)	136 (2)

Symmetry codes: (i) $\frac{1}{2} + x, 2 - y, z$; (ii) $\frac{1}{2} - x, y, z - \frac{1}{2}$; (iii) $\frac{1}{2} + x, 1 - y, z$; (iv) $1 - x, 1 - y, z - \frac{1}{2}$; (v) $1 - x, 1 - y, \frac{1}{2} + z$.

Preliminary examinations and intensity data collection were carried out using an Enraf-Nonius CAD-4 diffractometer. Backgrounds were obtained from analysis of the scan profiles (Blessing, Coppens & Becker, 1974). Both structures were solved by direct methods and all atoms, including H atoms, refined cleanly.

For both compounds, data collection: CAD-4 software (Enraf-Nonius, 1977); cell refinement: CAD-4 software; data reduction: *MolEN PROCESS* (Fair, 1990); program(s) used to solve structures: *MULTAN80* (Main *et al.*, 1980); program(s) used to refine structures: *MolEN LSF*; molecular graphics: *CAChe* (CAChe Scientific, 1993); software used to prepare material for publication: *MolEN CIF IN*.

We thank Dr R. D. Gillardi for his helpful criticism and comments, and the College of Arts and Sciences of the University of Toledo for generous financial support of the X-ray diffraction facility. This work was carried out in part under contract No. N000149310597 from the Office of Naval Research.

Lists of structure factors, anisotropic displacement parameters and complete geometry have been deposited with the IUCr (Reference: BK1041). Copies may be obtained through The Managing Editor, International Union of Crystallography, 5 Abbey Square, Chester CH1 2HU, England.

References

- Blessing, R. H., Coppens, P. & Becker, P. (1974). *J. Appl. Cryst.* **7**, 488–492.
- Borman, S. (1994). *Chem. Eng. News*, pp. 18–22.
- Bracuti, A. J. (1979). *Acta Cryst.* **B35**, 760–761.
- CAChe Scientific (1993). *CAChe Reference Manual*. CAChe Scientific, Beaverton, Oregon, USA.
- Chichra, D. A., Holden, J. R. & Dickinson, C. (1980). Report NSWC TR79-273. Naval Surface Weapons Center (White Oak), Silver Spring, MD 20910, USA.
- Choi, C. S. & Prince, E. (1979). *Acta Cryst.* **B35**, 761–763.
- Enraf-Nonius (1977). *CAD-4 Operations Manual*. Enraf-Nonius, Delft, The Netherlands.
- Ernst, S. R. (1977). *Acta Cryst.* **B33**, 237–240.
- Fair, C. K. (1990). *MolEN. An Interactive Intelligent System for Crystal Structure Analysis*. Enraf-Nonius, Delft, The Netherlands.
- Gilardi, R. D. (1994). Personal communication.
- Gilardi, R. D. & Karle, J. (1991). *Chemistry of Energetic Materials*, edited by G. A. Olah & D. R. Squire, pp. 1–26. San Diego: Academic Press.
- Main, P., Fiske, S. J., Hull, S. E., Lessinger, L., Germain, G., Declercq, J.-P. & Woolfson, M. M. (1980). *MULTAN80. A System of Computer Programs for the Automatic Solution of Crystal Structures from X-ray Diffraction Data*. Universities of York, England, and Louvain, Belgium.

- North, A. C. T., Phillips, D. C. & Mathews, F. S. (1968). *Acta Cryst.* **A24**, 351–359.
- Olah, G. A. & Squire, D. R. (1991). *Chemistry of Energetic Materials*. San Diego: Academic Press.
- Oyumi, Y. & Brill, T. B. (1985). *J. Phys. Chem.* **89**, 4325–4329.
- Pinkerton, A. A. & Schwarzenbach, D. (1978). *J. Chem. Soc. Dalton Trans.* pp. 989–996.
- Ritchie, J. P., Lee, K.-L., Cromer, D. T., Kober, E. M. & Lee, D. D. (1990). *J. Org. Chem.* **55**, 1994–2000.
- Stine, J. R. (1981). Report LA-8920. Los Alamos National Laboratory, Los Alamos, NM 87545, USA.

Contract No. N00014-95-1-0013 and N00014-97-1-0409

Program Officer: R. Miller/J. Goldwasser

**Title: Experimental Charge Densities and Electrostatic Potentials in Energetic
Materials and Infrastructure Upgrade for an X-ray Crystallography
Laboratory**

PI: A. Alan Pinkerton

Department of Chemistry, University of Toledo, Toledo, OH 43606

tel. (419) 530-4580, FAX (419) 530-4033, email apinker@uoft02.utoledo.edu

APPENDIX 5e

**Energetic Materials - The Preparation and Structural Characterization of
Three Biguanidinium Dinitramides.**

**Martin, A.; Pinkerton, A.A.; Gilardi, R.D.; and Bottaro, J.C., *Acta
Crystallogr.*, 1997, *B53*, 504-512.**

Energetic Materials: The Preparation and Structural Characterization of Three Biguanidinium Dinitramides

ANTHONY MARTIN,^a A. ALAN PINKERTON,^{a*} RICHARD D. GILARDI^b AND JEFFREY C. BOTTARO^c

^aDepartment of Chemistry, University of Toledo, Toledo, OH 43606, USA, ^bNaval Research Laboratory, Code 6030, Washington DC 20375-5001, USA, and ^cSRI International, Ravenswood Ave., Menlo Park, CA 94025, USA. E-mail: apinker@uoft02.utoledo.edu

(Received 18 March 1996; accepted 21 October 1996)

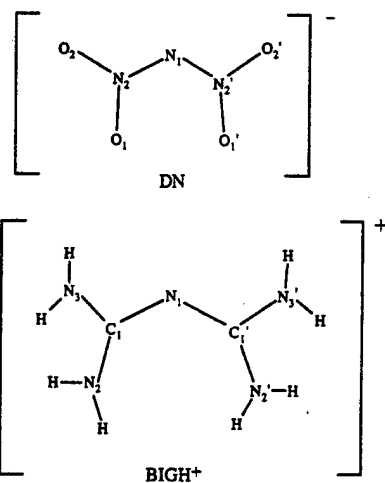
Abstract

Three biguanidinium salts of the energetic dinitramide anion have been prepared and structurally characterized from room-temperature X-ray diffraction data. Biguanidinium mono-dinitramide, (BIGH)(DN), triclinic, $P\bar{1}$, $a = 4.3686(4)$, $b = 9.404(2)$, $c = 10.742(1)$ Å, $\alpha = 83.54(1)$, $\beta = 80.386(9)$, $\gamma = 79.93(1)^\circ$, $V = 426.8(1)$ Å³, $Z = 2$, $D_x = 1.62$ g cm⁻³. Biguanidinium bis-dinitramide, (BIGH₂)(DN)₂, monoclinic, $C2/c$, $a = 11.892(2)$, $b = 8.131(1)$, $c = 13.038(2)$ Å, $\beta = 115.79(1)^\circ$, $V = 1135.1(3)$ Å³, $Z = 4$, $D_x = 1.84$ g cm⁻³. Biguanidinium bis-dinitramide monohydrate, (BIGH₂)(DN)₂·H₂O, orthorhombic, $P2_12_12_1$, $a = 6.4201(6)$, $b = 13.408(1)$, $c = 14.584(2)$ Å, $V = 1255.4(4)$ Å³, $Z = 4$, $D_x = 1.76$ g cm⁻³. All three structures are characterized by extensive hydrogen bonding. Both the mono- and diprotonated cations consist of two planar halves twisted with respect to each other. The dinitramide anion has a surprisingly variable and asymmetric structure. The two halves of the anion are twisted with respect to each other; however, the twist varies from 5.1 to 28.9°. In addition, the two ends of the anion have significantly different geometries, e.g. the 'equivalent' N—N bond lengths differ by up to 0.045 Å.

1. Introduction

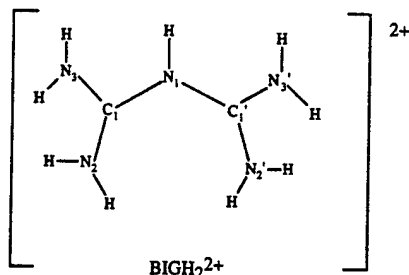
There is a great deal of current interest in the production of energetic materials (Borman, 1994). A newly discovered class of solid energetic materials is composed of the salts of the dinitramide anion, $N(NO_2)_2^-$, DN, a potent oxidizer. The preparation, characterization and thermal decomposition of the ammonium salt has been described previously (Bottaro, Schmitt, Penwell & Ross, 1991; Schmitt, Krempf & Bierbaum, 1992; Brill, Brush & Patil, 1993; Rossi, Bottaro & McMillen, 1993; Doyle, 1993). More recently, a series of papers has described the preparation and spectral (UV-vis, IR) characterization of the parent acid and a number of other salts (Luk'yanov, Gorelik & Tartakovsky, 1994; Luk'yanov, Konnova, Klimova & Tartakovsky, 1994; Luk'yanov, Anikin, Gorelik & Tartakovsky, 1994; Shlyapochnikov,

Cherskaya, Luk'yanov, Gorelik & Tartakovsky, 1994; Luk'yanov, Shlykova & Tartakovsky, 1994; Luk'yanov, Agevnin, Leichenko Serigina & Tartakovsky, 1995; Shlyapochnikov, Oleneva, Cherskaya, Luk'yanov, Gorelik, Anikin & Tartakovsky, 1995). There have also been reports of theoretical studies of the anion and the parent acid to gain insight into the possible mechanism of decomposition (Michels & Montgomery, 1993; Politzer & Seminario, 1993; Politzer, Seminario, Concha & Redfern, 1993; Mebel, Lin, Morokuma & Melius, 1995). The current paper describes the preparation and structural characterization of three new dinitramide salts, biguanidinium mono-dinitramide, (BIGH)DN (I), biguanidinium bis-dinitramide, (BIGH₂)(DN)₂ (II), and biguanidinium bis-dinitramide monohydrate, (BIGH₂)(DN)₂·H₂O (III).^{*†}



^{*} Due to this work being inadvertently partially duplicated in two different laboratories, the authors have decided that a joint publication would be appropriate. The results of an independent determination of the structure of (I), in close agreement with that reported here, have been deposited with the supplementary material.

[†] Lists of atomic coordinates, anisotropic displacement parameters and structure factors have been deposited with the IUCr (Reference: BK0035). Copies may be obtained through The Managing Editor, International Union of Crystallography, 5 Abbey Square, Chester CH1 2HU, England.



2. Experimental

CAUTION: Dinitramide salts are photosensitive and explosive.

2.1. Preparation of biguanidinium mono-dinitramide, (BIGH)DN

Barium hydroxide (15.7 g, 50 mmol) was suspended in 100 ml of H₂O and ammonium dinitramide [12.5 g, 100 mmol (Bottaro, Schmitt, Penwell & Ross, 1991)] added. The resulting mixture was heated under vacuum in a rotary evaporator until all the ammonia had been removed and the pH was <8. At this point the aqueous barium dinitramide solution was clear. This was then treated with bis(biguanidinium) sulfate (15 g, 50 mmol) and stirred in the dark for 12 h, followed by filtration. The filtrate was concentrated *in vacuo* and diluted with warm acetonitrile. The resulting solution was passed through a 2.5 × 10 cm silica gel column, eluting with acetonitrile until all the yellow effluent had been collected. This was concentrated to 100 ml and diluted with 200 ml of ethyl acetate. The resulting crystalline precipitate was collected by filtration. Yield 15 g (75%).

2.2. Preparation of biguanidinium bis-dinitramide, (BIGH₂)(DN)₂

Barium dinitramide (100 mmol) in 100 ml of H₂O was prepared as described above and this solution was added to a vigorously stirred suspension of biguanidinium monosulfate (21 g, 100 mmol) in 100 ml of H₂O. The resulting suspension was stirred for 2 h, filtered, concentrated and dissolved in ~500 ml of hot acetonitrile; this solution was immediately passed through a 2.5 × 10 cm column of silica, eluting with acetonitrile until all the yellow effluent was recovered. The acetonitrile effluent was concentrated to 100 ml and biguanidinium bis-dinitramide precipitated as dense prisms, mp 399–402 K. Yield 20 g (65%).

Crystals of (BIGH₂)(DN)₂ and (BIGH)(DN) suitable for X-ray analysis were obtained by slow evaporation of acetonitrile solutions. While attempting to obtain crystals of (BIGH₂)(DN)₂ from presumably wet acetonitrile solution, we obtained X-ray quality crystals of (BIGH₂)(DN)₂·H₂O.

Preliminary examination and intensity data collection for (BIGH)DN (sample I) and (BIGH₂)(DN)₂·H₂O

(sample III) were carried out with an Enraf–Nonius CAD-4 diffractometer and for (BIGH₂)(DN)₂ (sample II) with a Siemens R3m/V diffractometer. For (I) and (III) backgrounds were obtained from analysis of the scan profile (Blessing, Coppens & Becker, 1974). The crystal of the hydrate (III) decomposed (presumably desolvated) badly during data collection; however, the corrected data was still of sufficient quality to solve the structure. All H atoms for (I) and (II) were found and refined cleanly; however, this was not possible for (III). In this case the H atoms of the cation were fixed in ideal positions for *sp*² nitrogen (N–H 0.95 Å) and those for the water molecule constrained to keep the geometry found from a difference-Fourier map. Computer programs for structures (I) and (III) were taken from *MoLEN* (Fair, 1990) and those for (II) were taken from *SHELXTL* (Sheldrick, 1985). The figures were prepared with a CAChe workstation (CAChe, 1993). Scattering factors in all cases were taken from the *International Tables for X-ray Crystallography* (1974, Vol. IV). A summary of crystal data, data collection, structure solution and refinement is given in Table 1. Final refined parameters and derived geometrical values are reported in Tables 2–10. Drawings of the cations and anions along with the hydrogen-bonding schemes are presented in Figs. 1–3. Semi-empirical molecular orbital calculations (AM1 basis set) were carried out for various geometries of the dinitramide anion with a CAChe workstation (CAChe, 1993).

3. Results and discussion

Compound (I) is composed of one dinitramide anion and one monoprotonated biguanidinium cation in a hydrogen-bonded lattice. Compound (II) contains a diprotonated biguanidinium cation which lies on a crystallographic twofold axis and two dinitramide anions per biguanidinium moiety, again in a hydrogen-bonded network. Compound (III) is composed of two unique dinitramide anions, a diprotonated biguanidinium cation and a water molecule in a lattice which is also characterized by strong hydrogen bonds.

3.1. Biguanidinium cations

The mono- and diprotonated biguanidinium cations in these salts present no surprises. They are composed of two planar halves twisted with respect to each other [with approximate (I, III) or exact (II) twofold symmetry], as has been previously observed for other salts of these cations (Martin, Pinkerton & Schiemann, 1996; Martin & Pinkerton, 1996; Pinkerton & Schwarzenbach, 1978; Ernst, 1977). For (BIGH)⁺ all the bond lengths and angles fall close to values previously observed; however, (I) has the smallest twist yet observed for this cation [34.2(1)° compared with the literature range 37.8–49.1°]. In the diprotonated cation we again find distances and angles close to known structures, how-

Table 1. *Experimental details*

	(I)	(II)	(III)
Crystal data			
Chemical formula	$C_2H_8N_5^+ \cdot N_3O_4^-$	$C_2H_9N_5^{2+} \cdot 2N_3O_4^-$	$C_2H_9N_5^{2+} \cdot 2N_3O_4^- \cdot H_2O$
Chemical formula weight	208.14	315.20	333.18
Cell setting	Triclinic	Monoclinic	Orthorhombic
Space group	$P\bar{1}$	$C2/c$	$P2_12_12_1$
a (Å)	4.3686 (4)	11.892 (2)	6.4201 (6)
b (Å)	9.404 (2)	8.131 (1)	13.408 (1)
c (Å)	10.742 (1)	13.038 (2)	14.584 (2)
α (°)	83.54 (1)		
β (°)	80.386 (9)	115.79 (1)	
γ (°)	79.93 (1)		
V (Å ³)	426.8 (1)	1135.1 (3)	1255.4 (4)
Z	2	4	4
D_x (Mg m ⁻³)	1.62	1.844	1.76
Radiation type	Mo $K\alpha$	Cu $K\alpha$	Mo $K\alpha$
Wavelength (Å)	0.71073	1.54178	0.71073
No. of reflections for cell parameters	25	25	91
θ range (°)	8–17	39–50	9–14
μ (mm ⁻¹)	0.14	1.59	0.16
Temperature (K)	294 (1)	293 (2)	294 (1)
Crystal form	Parallelepiped	Clear chunky bipyramids	Tabular
Crystal size (mm)	0.28 × 0.22 × 0.10	0.38 × 0.36 × 0.22	0.33 × 0.24 × 0.24
Crystal color	Colorless	Colorless	Colorless
Data collection			
Diffractometer	Enraf–Nonius CAD-4	Siemens R3m/V	Enraf–Nonius CAD-4
Data collection method	$\theta/2\theta$ scans	$\theta/2\theta$ scans	$\theta/2\theta$ scans
Absorption correction	ψ scans (North, Phillips & Mathews, 1968)	None	ψ scans (North, Phillips & Mathews, 1968)
T_{min}	0.9667	—	0.8915
T_{max}	0.9989	—	0.9784
No. of measured reflections	1917	927	1462
No. of independent reflections	1683	845	1439
No. of observed reflections	1227	812	992
Criterion for observed reflections	$I > 3\sigma(I)$	$I > 2\sigma(I)$	$I > 3\sigma(I)$
R_{int}	0.025	0.0211	0.030
θ_{max} (°)	25.97	60.05	25.97
Range of h, k, l	0 → h → 5 −11 → k → 11 −13 → l → 13	0 → h → 13 −9 → k → 0 −14 → l → 13	0 → h → 7 0 → k → 16 0 → l → 17
No. of standard reflections	3	3	3
Frequency of standard reflections	50 min	Every 100 reflections	50 min
Intensity decay (%)	2.81	0.50	77.31
Refinement			
Refinement on	F	F^2	F
R	0.041	0.0533(F)	0.040
wR	0.038	0.1379	0.032
S	2.231	1.128	2.565
No. of reflections used in refinement	1227	845	992
No. of parameters used	160	115	205
H-atom treatment	All H-atom parameters refined	All H-atom parameters refined	H atoms riding
Weighting scheme	$w = 1/\sigma^2(F)$	$w = 1/[\sigma^2(F_o^2) + (0.0962P)^2 + 0.9237P]$ where $P = (F_o^2 + 2F_c^2)/3$	$w = 1/\sigma^2(F)$
$(\Delta/\sigma)_{max}$	0.010	<0.001	0.001
$\Delta\rho_{max}$ (e Å ⁻³)	0.28	0.314	0.41
$\Delta\rho_{min}$ (e Å ⁻³)	−0.23	−0.403	−0.24
Extinction method	Isotropic (Zachariasen, 1963)	SHELXL (Sheldrick, 1985)	None
Extinction coefficient	0.12×10^{-4}	0.0343 (27)	—
Source of atomic scattering factors	<i>International Tables for X-ray Crystallography</i> (1974, Vol. IV)	<i>International Tables for Crystallography</i> (1992, Vol. C, Tables 4.2.6.8 and 6.1.1.4)	<i>International Tables for X-ray Crystallography</i> (1974, Vol. IV)
Computer programs			
Data collection	CAD-4 (Enraf–Nonius, 1977)	P3/PC (Siemens, 1989a)	CAD-4 (Enraf–Nonius, 1977)
Cell refinement	CAD-4 (Enraf–Nonius, 1977)	P3/PC (Siemens, 1989a)	CAD-4 (Enraf–Nonius, 1977)
Data reduction	PROCESS, MolEN (Fair, 1990), SORTAV (Blessing, 1987)	XDISK (Siemens, 1989b)	PROCESS, MolEN (Fair, 1990), SORTAV (Blessing, 1987)
Structure solution	Direct methods (SIR; Burla <i>et al.</i> , 1989)	SHELXS86 (Sheldrick, 1990)	Direct methods (SIR; Burla <i>et al.</i> , 1989)
Structure refinement	LSFM MolEN (Fair, 1990)	SHELXL92 (Sheldrick, 1992)	LSFM MolEN (Fair, 1990)
Preparation of material for publication	CIF VAX, MolEN (Fair, 1990)	SHELXTL (Sheldrick, 1985)	CIF VAX, MolEN (Fair, 1990)

Table 2. Fractional atomic coordinates and equivalent isotropic displacement parameters (\AA^2) for (I)
$$U_{eq} = (1/3) \sum_i \sum_j U^{ij} a_i^* a_j^* a_i \cdot a_j$$

	x	y	z	U_{eq}
O1	0.8727 (5)	0.2858 (2)	0.5605 (2)	0.0756 (6)
O2	1.2289 (4)	0.0993 (2)	0.5560 (2)	0.0581 (5)
O3	0.4431 (4)	0.2823 (2)	0.7474 (2)	0.0531 (5)
O4	0.4503 (4)	0.0766 (2)	0.8587 (1)	0.0518 (5)
N1	0.9784 (4)	0.1661 (2)	0.6033 (2)	0.0392 (5)
N2	0.8413 (4)	0.0882 (2)	0.7083 (2)	0.0379 (5)
N3	0.5687 (4)	0.1571 (2)	0.7706 (2)	0.0365 (5)
N4	1.6236 (6)	-0.4174 (2)	0.6553 (2)	0.0564 (7)
N5	1.4776 (5)	-0.1840 (2)	0.7044 (2)	0.0482 (6)
N6	1.3878 (4)	-0.3812 (2)	0.8562 (2)	0.0369 (5)
N8	1.1499 (5)	-0.3622 (2)	1.0591 (2)	0.0445 (6)
N7	0.9755 (5)	-0.1878 (2)	0.9122 (2)	0.0471 (6)
C1	1.4884 (5)	-0.3244 (2)	0.7405 (2)	0.0361 (6)
C2	1.1737 (5)	-0.3076 (2)	0.9390 (2)	0.0335 (6)
H1	1.612 (6)	-0.510 (3)	0.672 (2)	0.076 (9)
H2	1.719 (6)	-0.388 (3)	0.587 (2)	0.067 (8)
H3	1.408 (5)	-0.117 (3)	0.768 (2)	0.064 (8)
H4	1.544 (5)	-0.159 (2)	0.633 (2)	0.046 (7)
H5	0.834 (5)	-0.145 (2)	0.981 (2)	0.055 (7)
H6	0.972 (5)	-0.153 (2)	0.843 (2)	0.048 (7)
H7	0.993 (5)	-0.331 (2)	1.113 (2)	0.059 (7)
H8	1.293 (5)	-0.442 (2)	1.081 (2)	0.059 (7)

Table 3. Selected geometric parameters (\AA , $^\circ$) for (I)

O1—N1	1.210 (2)	N4—C1	1.330 (3)
O2—N1	1.223 (2)	N5—C1	1.329 (3)
O3—N3	1.226 (2)	N6—C1	1.332 (3)
O4—N3	1.245 (2)	N6—C2	1.334 (3)
N1—N2	1.382 (2)	N8—C2	1.329 (3)
N2—N3	1.359 (2)	N7—C2	1.330 (3)
O1—N1—O2	122.2 (2)	C1—N6—C2	122.9 (2)
O1—N1—N2	126.1 (2)	N4—C1—N5	117.4 (2)
O2—N1—N2	111.7 (2)	N4—C1—N6	116.7 (2)
N1—N2—N3	115.7 (2)	N5—C1—N6	125.8 (2)
O3—N3—O4	121.4 (2)	N6—C2—N8	116.6 (2)
O3—N3—N2	126.9 (2)	N6—C2—N7	126.3 (2)
O4—N3—N2	111.6 (2)	N8—C2—N7	117.1 (2)

Table 4. Hydrogen-bonding parameters (\AA , $^\circ$) for (I)

D—H...A	D—H	H...A	D—H...A
N4—H1...O1 ⁱ	0.88 (3)	2.39 (3)	131 (2)
N4—H1...O3 ⁱ	0.88 (3)	2.23 (3)	163 (3)
N4—H2...O1 ⁱⁱ	0.82 (3)	2.44 (3)	159 (3)
N5—H3...O4 ⁱⁱⁱ	0.96 (3)	2.21 (3)	152 (2)
N5—H4...O2 ⁱⁱ	0.80 (2)	2.16 (2)	174 (3)
N7—H5...O4 ^{iv}	0.96 (2)	2.04 (3)	173 (2)
N7—H6...N2	0.78 (2)	2.58 (3)	144 (2)
N8—H7...O3 ^{iv}	0.86 (3)	2.23 (3)	171 (3)
N8—H8...N6 ^v	0.92 (3)	2.10 (3)	176 (2)

Symmetry codes: (i) $x+1, y-1, z$; (ii) $3-x, -y, 1-z$; (iii) $x+1, y, z$; (iv) $1-x, -y, 2-z$; (v) $3-x, -y-1, 2-z$.

ever, the bond angle at the bridging nitrogen in (II) is the largest observed to date [$130.8(3)^\circ$ compared with the literature range $122.5\text{--}127.1^\circ$]. The twist angles of $36.2(1)$ and $45.2(2)^\circ$ for (II) and (III), respectively, also extend the previous range $43.7\text{--}48.4^\circ$. The nature of the multiple bonding in these cations has been discussed elsewhere (Pinkerton & Schwarzenbach, 1978).

We note that the monoprotonated biguanidinium cations in structure (I) form hydrogen-bonded dimers

Table 5. Fractional atomic coordinates and equivalent isotropic displacement parameters (\AA^2) for (II)
$$U_{eq} = (1/3) \sum_i \sum_j U^{ij} a_i^* a_j^* a_i \cdot a_j$$

	x	y	z	U_{eq}
N1	0.1469 (2)	-0.4843 (2)	0.9129 (2)	0.0316 (6)
N2	0.1446 (2)	-0.4146 (2)	1.00920 (15)	0.0302 (6)
O1	0.1625 (2)	-0.4891 (2)	1.09534 (15)	0.0580 (7)
O2	0.1298 (2)	-0.2645 (2)	0.99970 (15)	0.0407 (6)
N3	0.1257 (2)	-0.6478 (2)	0.90013 (15)	0.0287 (6)
O3	0.0901 (2)	-0.7336 (2)	0.9577 (2)	0.0456 (6)
O4	0.1413 (2)	-0.7042 (2)	0.8189 (2)	0.0502 (7)
N4	0	-0.0261 (3)	3/4	0.0339 (8)
H4	0	0.074 (5)	3/4	0.043 (10)
C1	0.0750 (2)	-0.0959 (2)	0.7074 (2)	0.0223 (6)
N5	0.1071 (2)	-0.0021 (2)	0.6427 (2)	0.0298 (6)
H5A	0.073 (3)	0.095 (4)	0.619 (2)	0.042 (7)
H5B	0.165 (3)	-0.036 (3)	0.622 (2)	0.045 (7)
N6	0.1139 (2)	-0.2471 (2)	0.7307 (2)	0.0317 (6)
H6A	0.109 (3)	-0.300 (4)	0.783 (3)	0.045 (8)
H6B	0.153 (3)	-0.285 (4)	0.691 (3)	0.056 (9)

Table 6. Selected geometric parameters (\AA , $^\circ$) for (II)

N1—N3	1.350 (3)	N3—O4	1.240 (2)
N1—N2	1.388 (3)	N4—C1	1.363 (2)
N2—O1	1.211 (2)	C1—N6	1.302 (3)
N2—O2	1.231 (2)	C1—N5	1.312 (3)
N3—O3	1.227 (2)		
N3—N1—N2	116.0 (2)	O4—N3—N1	112.3 (2)
O1—N2—O2	123.3 (2)	C1 ⁱ —N4—C1	130.8 (3)
O1—N2—N1	124.7 (2)	N6—C1—N5	121.8 (2)
O2—N2—N1	111.8 (2)	N6—C1—N4	121.8 (2)
O3—N3—O4	122.2 (2)	N5—C1—N4	116.4 (2)
O3—N3—N1	125.4 (2)		

Symmetry codes: (i) $-x, y, \frac{1}{2} - z$.

Table 7. Hydrogen-bonding parameters (\AA , $^\circ$) for (II)

D—H...A	D—H	H...A	D—H...A
N4—H4...O4 ⁱ	0.81 (4)	2.36 (3)	139.8 (7)
N5—H5A...O2 ⁱⁱ	0.88 (3)	2.39 (3)	122 (3)
N5—H5A...O3 ⁱⁱⁱ	0.88 (3)	2.24 (3)	153 (3)
N5—H5B...O4 ^{iv}	0.89 (4)	2.49 (3)	144 (2)
N5—H5B...N1 ^{iv}	0.89 (4)	2.50 (4)	151 (2)
N6—H6A...N1	0.82 (4)	2.16 (3)	161 (3)
N6—H6B...O1 ^v	0.88 (4)	2.25 (3)	141 (3)

Symmetry codes: (i) $x, y+1, z$; (ii) $x, -y, z - \frac{1}{2}$; (iii) $-x, y+1, \frac{1}{2} - z$; (iv) $\frac{1}{2} - x, y+\frac{1}{2}, \frac{3}{2} - z$; (v) $x, -y-1, z - \frac{1}{2}$.

across a center of symmetry (Fig. 1a), a motif previously observed for this cation in the analogous nitrate and perchlorate salts (Martin, Pinkerton & Schiemann, 1996; Martin & Pinkerton, 1996).

3.2. Dinitramide anions

The dinitramide anions are composed of two trigonal nitro groups joined by a common N atom. Their overall shape is similar to that of the cations. Short N—N and N—O bonds are indicative of multiple bonding. Thus, one might expect the dinitramide anions to be as symmetrical as the biguanidinium cations, with twofold symmetry and perhaps a twist to remove steric interference between the 'inner' O atoms (O1, O1'). However, this is far from the case

Table 8. Fractional atomic coordinates and equivalent isotropic displacement parameters (\AA^2) for (III)
$$U_{eq} = (1/3) \sum_i \sum_j U^{ij} a_i^* a_j^* a_i \cdot a_j$$

	x	y	z	U_{eq}
O1	0.7839 (7)	-0.2174 (2)	0.0337 (2)	0.065 (1)
O2	0.8055 (6)	-0.2011 (2)	0.1792 (2)	0.061 (1)
O3	0.9628 (5)	-0.0717 (2)	-0.0450 (2)	0.0434 (9)
O4	0.8943 (5)	0.0680 (2)	0.0206 (2)	0.0410 (9)
O5	0.3361 (5)	-0.0874 (2)	0.1207 (2)	0.053 (1)
O6	0.3511 (6)	0.0380 (2)	0.2144 (2)	0.050 (1)
O7	0.3949 (6)	0.2054 (2)	0.0018 (2)	0.049 (1)
O8	0.2300 (5)	0.1954 (2)	0.1322 (2)	0.0437 (9)
O9	0.4366 (5)	-0.1227 (2)	0.3400 (2)	0.0482 (9)
N1	0.8097 (6)	-0.1663 (2)	0.1017 (2)	0.042 (1)
N2	0.8286 (6)	-0.0637 (2)	0.1011 (2)	0.033 (1)
N3	0.8961 (6)	-0.0240 (2)	0.0208 (2)	0.034 (1)
N4	0.3446 (5)	0.0024 (2)	0.1359 (2)	0.035 (1)
N5	0.3603 (6)	0.0567 (2)	0.0585 (2)	0.034 (1)
N6	0.3258 (6)	0.1587 (2)	0.0679 (2)	0.033 (1)
N7	0.7561 (6)	0.1932 (2)	0.1731 (2)	0.035 (1)
N8	0.7253 (6)	0.2108 (2)	0.3274 (2)	0.039 (1)
N9	0.8456 (6)	0.0614 (2)	0.2645 (2)	0.0283 (9)
N10	0.9236 (5)	-0.0769 (2)	0.3495 (2)	0.035 (1)
N11	1.0474 (6)	0.0742 (2)	0.3968 (2)	0.040 (1)
C1	0.7751 (7)	0.1575 (3)	0.2557 (3)	0.029 (1)
C2	0.9400 (7)	0.0196 (3)	0.3400 (2)	0.028 (1)

Table 9. Selected geometric parameters (\AA , $^\circ$) for (III)

O1—N1	1.216 (5)	N2—N3	1.358 (5)
O2—N1	1.223 (5)	N4—N5	1.347 (5)
O3—N3	1.229 (4)	N5—N6	1.392 (5)
O4—N3	1.234 (4)	N7—C1	1.302 (5)
O5—N4	1.226 (4)	N8—C1	1.306 (5)
O6—N4	1.241 (4)	N9—C1	1.373 (5)
O7—N6	1.232 (5)	N9—C2	1.376 (5)
O8—N6	1.225 (5)	N10—C2	1.306 (5)
N1—N2	1.381 (5)	N11—C2	1.303 (5)
O1—N1—O2	122.4 (4)	O7—N6—O8	125.1 (4)
O1—N1—N2	124.6 (4)	O7—N6—N5	111.4 (4)
O2—N1—N2	112.7 (4)	O8—N6—N5	123.4 (4)
N1—N2—N3	115.0 (4)	C1—N9—C2	127.1 (4)
O3—N3—O4	121.5 (4)	N7—C1—N8	121.1 (4)
O3—N3—N2	125.5 (4)	N7—C1—N9	117.6 (4)
O4—N3—N2	113.0 (4)	N8—C1—N9	121.3 (4)
O5—N4—O6	123.1 (4)	N9—C2—N10	116.9 (4)
O5—N4—N5	112.5 (4)	N9—C2—N11	120.9 (4)
O6—N4—N5	124.3 (4)	N10—C2—N11	122.2 (4)
N4—N5—N6	115.9 (4)		

and a wide range of 'equivalent' bond lengths and angles is observed. In these three structures the N—N bond lengths vary from 1.347 (5) to 1.392 (5) \AA and the difference in the same molecule from 0.023 to 0.045 \AA . The N—O bond lengths vary from 1.210 (2) to 1.245 (2) \AA , with the 'inner' N2—O1 bonds being shorter than the 'outer' N2—O2 bonds (Table 11). There is some indication that lengthening of the N—N bond tends to shorten the neighboring N—O bonds, but the evidence is weak. The angle at the bridging nitrogen, however, is fairly constant [115.0 (4)–116.0 (2) $^\circ$]. The bond angles at the terminal N atoms show a striking asymmetry. The N1—N2—O1 angles are all greater than 120 $^\circ$ [123.4 (4)–126.9 (2) $^\circ$], perhaps due to steric interaction between the 'inner' O atoms. However, the O1—N2—O2 angles, although smaller, are also

Table 10. Hydrogen-bonding parameters (\AA , $^\circ$) for (III)

D—H...A	D—H	H...A	D—H...A
N7—H1...O4	0.95*	1.98	175
N7—H2...O9 ⁱ	0.95*	1.83	169
N8—H3...O1 ⁱⁱ	0.95*	2.19	144
N8—H3...O3 ⁱⁱⁱ	0.95*	2.22	128
N8—H4...O5 ⁱ	0.95*	2.02	143
N9—H5...N2	0.95*	1.97	172
N10—H6...O7 ⁱⁱ	0.95*	2.10	169
N10—H7...O2	0.95*	2.19	156
N11—H8...N5 ⁱⁱ	0.95*	2.11	156
N11—H9...O1 ⁱⁱⁱ	0.95*	2.41	136
N11—H9...O2 ⁱⁱⁱ	0.95*	2.44	159
O9—H10...O4 ⁱⁱ	0.93†	2.10	150
O9—H11...O6	0.93†	1.97	166

* Calculated hydrogen positions. † Observed hydrogen positions (but not refined). Symmetry codes: (i) $1 - x, y + \frac{1}{2}, \frac{1}{2} - z$; (ii) $\frac{3}{2} - x, -y, z + \frac{1}{2}$; (iii) $2 - x, y + \frac{1}{2}, \frac{1}{2} - z$.

Table 11. Comparison of bond lengths in the dinitramide anion using the atom numbering of the scheme with N1—N2' defined as the longest N—N bond

	(I)	(II)	(IIIa)	(IIIb)
N1—N2	1.382 (2)	1.388 (3)	1.381 (5)	1.392 (5)
N1—N2'	1.359 (2)	1.350 (3)	1.358 (5)	1.347 (5)
N2—O1	1.210 (2)	1.211 (2)	1.216 (5)	1.225 (5)
N2—O2	1.223 (2)	1.231 (2)	1.223 (5)	1.232 (5)
N2'—O1'	1.226 (2)	1.227 (2)	1.229 (4)	1.241 (4)
N2'—O2'	1.245 (2)	1.240 (2)	1.234 (4)	1.226 (4)

greater than 120 $^\circ$ [121.4 (2)–125.1 (4) $^\circ$]. In contrast, the N1—N2—O2 angles are all significantly smaller [111.4 (4)–113.0 (4) $^\circ$]. It is difficult to explain this geometry on the basis of simple steric interactions, especially after consideration of the different amounts of twist observed in these molecules. Defining a pseudotorsion angle O1—N2—N2'—O1', we observe a value of 5.1 $^\circ$ in (I) and the range 24.0–28.9 $^\circ$ for the other molecules. Even this wide range underestimates the possibilities for this anion, a twist of 42.7 $^\circ$ being observed in the ammonium salt (Gilardi, 1996).

3.3. Hydrogen bonding

In (I) the lattice may be described as planes of ions joined by the twisted ends of a biguanidinium 'dimer' (see above), as shown in Figs. 1(a) and (b). The hydrogen-bonding scheme in (II) forms ribbons in the *b* direction. The hydrogen-bonded network of (III) is more complicated and completely three-dimensional.

3.4. Compound (I)

The dinitramide anion accepts eight hydrogen bonds from five different biguanidinium cations (Fig. 1b). The two shortest hydrogen bonds are associated with the two 'outer' O atoms [O2...H4 2.16 (2), O4...H5 2.04 (3) \AA]. Both these bonds are almost linear [174 (3) and 173 (2) $^\circ$, respectively]. O4 participates in another hydrogen bond to H3 [O4...H3 2.21 (3) \AA] and this is clearly bent [N5—H3...O4 152 (2) $^\circ$]. The two 'inner' O atoms have

four hydrogen bonds involving three H atoms from three different biguanidinium cations associated with them. O1 and O3 are bridged by hydrogen bonds from H1 [O1...H1 2.39(3), O3...H1 2.23(3) Å]. Both O1 and O3 accept an additional hydrogen bond [O1...H2 2.44(3), O3...H7 2.23 Å], as expected, the shorter having the more linear bond [159(3) *versus* 171(3)°]. The longest hydrogen bond [2.58(3) Å] is formed by the bridging nitrogen with a N7—H6...N2 bond angle of 144(2)°. Although this is a rather long bond with a small bond angle, its absence would imply no hydrogen bond to the lone pair on the bridging N atom of the anion.

Every hydrogen of the biguanidinium cation is involved in at least one hydrogen bond. The two

hydrogen bonds which hold the dimer together (see above) are symmetry related. The N6...H8 distance is 2.10(3) Å and the bond is almost linear [N6...H8—N8 176(2)°].

3.5. Compound (II)

The twofold axis considerably reduces the complexity of the hydrogen bonding (Figs. 2*a* and *b*). All the biguanidinium H atoms are hydrogen bonded, with a H...X (X = N, O) contact distance less than 2.5 Å. The H4 atom has a bifurcated bond about the twofold axis [O4...H4 2.36(4) Å]. H5A is also involved in a bifurcated hydrogen bond, although it is less symmetrical than H4 [O3...H5A 2.24(3), O2...H5A 2.39(3) Å]. There are three hydrogen bonds remaining, O1...H6B [2.25(3) Å], which is

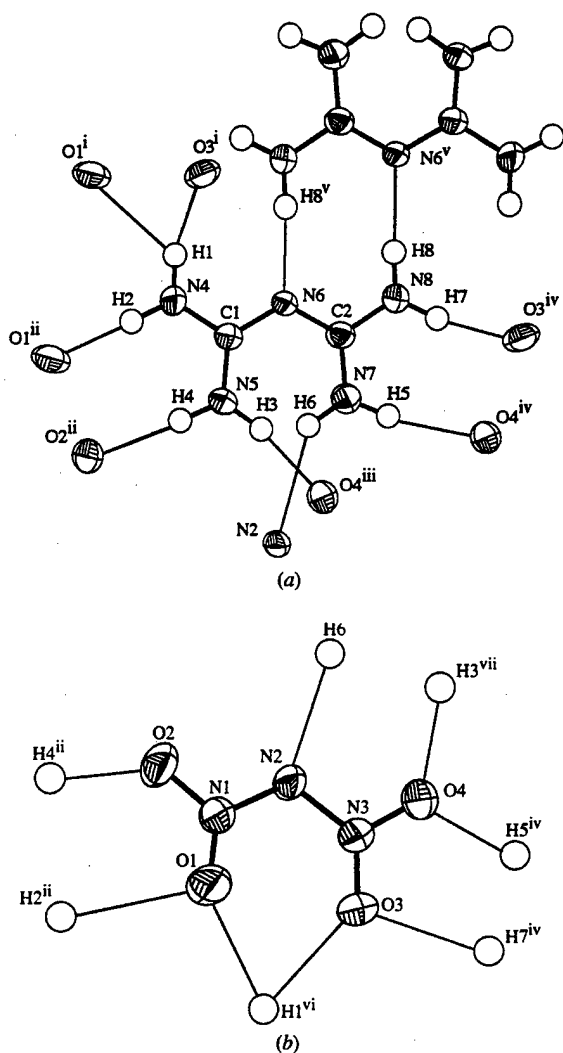


Fig. 1. ORTEP (CACH, 1993; Johnson, 1965) plots of (a) the monoprotonated biguanidinium cation and (b) the dinitramide anion in (I), showing the atom labeling and hydrogen-bonding scheme; symmetry codes: (i) $x + 1, y - 1, z$; (ii) $3 - x, -y, 1 - z$; (iii) $x + 1, y, z$; (iv) $1 - x, -y, 2 - z$; (v) $3 - x, -y - 1, 2 - z$; (vi) $x - 1, y + 1, z$; (vii) $x - 1, y, z$.

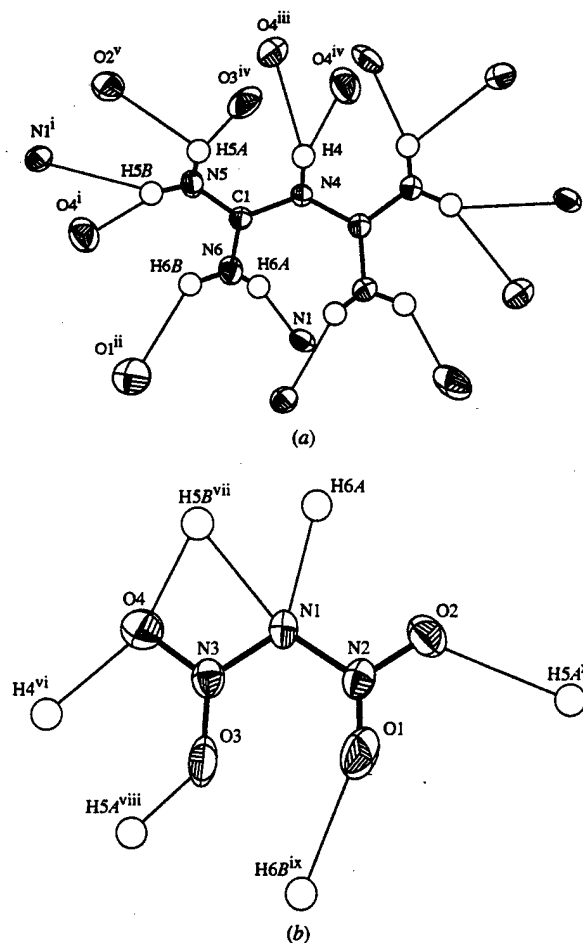


Fig. 2. ORTEP (CACH, 1993; Johnson, 1965) plots of (a) the diprotonated biguanidinium cation and (b) the dinitramide anion in (II), showing the atom labeling and hydrogen-bonding scheme; symmetry codes: (i) $\frac{1}{2} - x, y + \frac{1}{2}, \frac{3}{2} - z$; (ii) $x, -y - 1, z - \frac{1}{2}$; (iii) $x, y + 1, z$; (iv) $-x, y + 1, \frac{3}{2} - z$; (v) $x, -y, z - \frac{1}{2}$; (vi) $x, y - 1, z$; (vii) $\frac{1}{2} - x, y - \frac{1}{2}, \frac{3}{2} - z$; (viii) $-x, y - 1, \frac{3}{2} - z$; (ix) $x, -y - 1, z + \frac{1}{2}$; (x) $x, -y, z + \frac{1}{2}$.

unremarkable, $N1 \cdots H6A$ [2.16 (3) Å], which is the shortest hydrogen bond in the structure, and the bifurcated bonds of $H5B$ ($O4 \cdots H5B$ and $N1 \cdots H5B$), which are the longest [2.50 (4) Å]. Looking at the hydrogen bonding to the dinitramide, a pattern quickly emerges, bridging nitrogen < inner oxygen (agrees to within 0.01 Å) < outer oxygen (agrees to within 0.03 Å), each being ~ 0.1 Å longer than the previous.

3.6. Compound (III)*

In the hydrate there are 13 hydrogen bonds which are all less than 2.5 Å in length. All the H atoms on the biguanidinium cation participate in 11 hydrogen bonds

* Although the H-atom positions were not refined in this structure, reasonable positions can be calculated for the NH_2 groups assuming sp^2 geometry at nitrogen and, although unrefinable, the water hydrogens were observed in the difference-Fourier map. The discussion of the hydrogen bonding is based on these positions.

(Figs. 3a–d), of which four are bifurcated ($O1 \cdots H3$ 2.19 and $O3 \cdots H3$ 2.22, $O1 \cdots H9$ 2.41 and $O2 \cdots H9$ 2.44 Å). We note that H3 is bound to the two inner O atoms of a dinitramide anion and that H9 is bound to the inner and outer oxygen of one end of the same dinitramide anion. Two of the short hydrogen bonds and a longer one are also formed with this dinitramide anion in an almost planar 'W' motif; these are $O4 \cdots H1$, $N2 \cdots H5$ and $O2 \cdots H7$ (1.98, 1.97 and 2.19 Å, respectively). It also suggests that the central nitrogen on the dinitramide has a lone pair associated with it. The two short bonds are almost linear ($N7-H1 \cdots O4$ 175 and $N9-H5 \cdots N2$ 172°), while the longer bond is bent ($N10-H7 \cdots O2$ 156°). The second dinitramide anion is less strongly hydrogen bonded, however, the $N5 \cdots H8$ interaction (2.11 Å) again implies a lone pair on the bridging nitrogen.

The water molecule has three hydrogen bonds associated with it. The O9 atom accepts the shortest

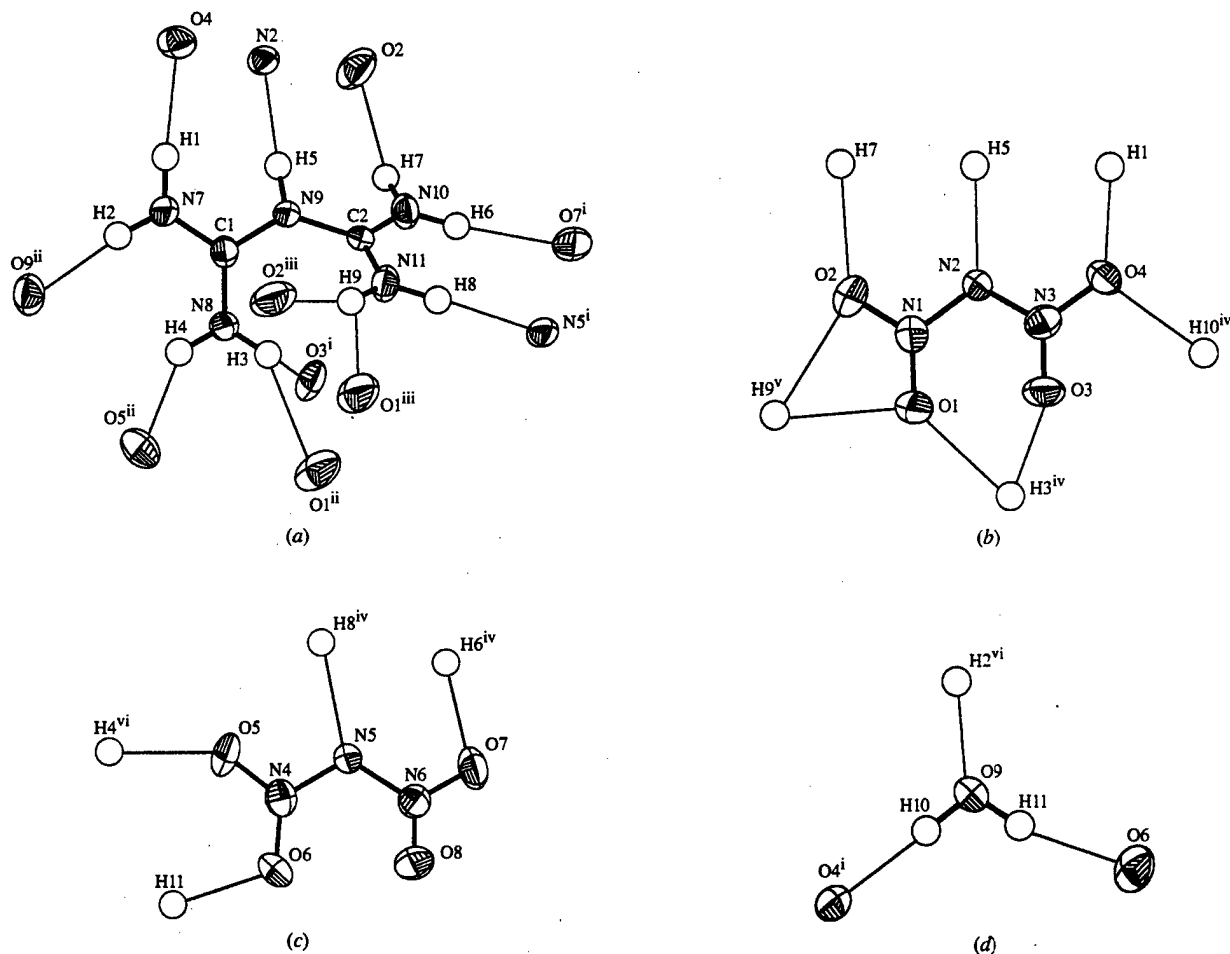


Fig. 3. ORTEP (CACH, 1993; Johnson, 1965) plot of (a) the diprotonated biguanidinium cation, (b) the first dinitramide anion, (c) the second dinitramide anion and (d) the water molecule in (III), showing the atom labeling and hydrogen-bonding scheme; symmetry operations: (i) $\frac{3}{2} - x, -y, z + \frac{1}{2}$; (ii) $1 - x, y + \frac{1}{2}, \frac{1}{2} - z$; (iii) $2 - x, y + \frac{1}{2}, \frac{1}{2} - z$; (iv) $\frac{3}{2} - x, -y, z - \frac{1}{2}$; (v) $2 - x, y - \frac{1}{2}, \frac{1}{2} - z$; (vi) $1 - x, y - \frac{1}{2}, \frac{1}{2} - z$.

hydrogen bond in the molecule ($O9 \cdots H2$ 1.83 Å), which is almost linear ($N7-H2 \cdots O9$ 169°). The two water H atoms donate to O atoms on different dinitramide anions ($O4 \cdots H10$ 2.10, $O6 \cdots H11$ 1.97 Å) and are less linear ($O9-H10 \cdots O4$ 150, $O9-H11 \cdots O6$ 166°). Thus, the water molecule can be considered as hydrogen bonding 'glue' in this structure, bonding to each of the unique ions.

3.7. Bonding in the dinitramide anion

The dinitramide ion is a relatively new anion and there are no reported crystal structures. As discussed above, it shows some very unusual geometrical variations, in particular, the nonequivalence of the N—N bonds and the variation in the pseudotorsion angle.

Two theoretical descriptions of the central nitrogen have been presented by Politzer, Seminario, Concha & Redfern (1993), depending on whether the anion is twisted or not. If the dinitramide is twisted with an N—N—N angle of 112.4° (their *ab initio* minimum structure, see below), they suggest that the electron pairs are tetrahedrally distributed, thus allowing the NO_2 to twist, separating the inner O atoms and yet remaining conjugated to the central nitrogen. The second interpretation refers to planar dinitramide with the lone pairs in different orbitals on the bridging nitrogen, an sp^2 orbital in the NNN plane and a p -orbital perpendicular to it to conjugate to both NO_2 groups.

The experimental N—N—N angles are intermediate between the ideal tetrahedral and trigonal planar geometries. The bridge and pseudotorsion angles appear to be uncorrelated. The ammonium salt (Gilardi, 1996) is an outlier having the smallest bridge angle yet observed (N—N—N, 113.2°). The most reasonable conclusion is that the best description of the bridging nitrogen lies between the two extremes. This has the advantage of delocalizing all the lone pairs on the bridging nitrogen by allowing conjugation with both NO_2 groups. None of these interpretations of the electronic structure of the central nitrogen explain the N—N bond inequivalence.

There have been high-level gas-phase *ab initio* calculations (Michels & Montgomery, 1993) on the dinitramide anion. These calculations used RHF/6-31G** and MP2/6-31G** geometry optimizations to produce a minimum energy structure with C_2 symmetry in both cases. The paper also reported two other structures as transition states, one of which had C_{2v} symmetry. The reported barrier to rotation about the N—N bond was $< 1.26 \text{ kJ mol}^{-1}$, which would account for the wide range of observed pseudotorsion angles. Using their minimized geometry we calculate a pseudotorsion angle of 43.0°. Clearly, the twofold symmetry does not allow any difference in the N—N bond lengths.

Michels & Montgomery (1993) point out that rotation of one NO_2 group perpendicular to the other produces a transition state structure that has N—N bond lengths

that differ by ~ 0.1 Å. If this rotation were responsible for the experimental difference, there should be a strong correlation between the pseudotorsion angle and bond inequivalence; however, there is none. There have also been nonlocal density functional theory calculations carried out on the dinitramide anion (Poltzer, Seminario, Concha & Redfern, 1993). This approach, like the *ab initio* calculations, produced a twisted dinitramide group. Using their bond lengths and angles we find a pseudotorsion angle of 40.6°. The N—N bond lengths did not significantly differ in length (1.407, 1.402 Å); however, the inner N—O bond lengths are shorter than the outer ones, in agreement with the crystal structures, and in contrast to the results of Michels & Montgomery (1993).

In order to gain some insight into the possible cause of these variations we have examined the shapes of the frontier orbitals obtained from semi-empirical calculations (AM1). Point calculations were carried out using the geometries of the dinitramide anion obtained from the crystal structures of the mono-protonated biguanidinium and di-protonated biguanidinium salts described above, and also from the crystal structure of the ammonium salt (Gilardi, 1996), which all produced noticeably asymmetric frontier orbitals. A similar point calculation was carried out using the *ab initio* minimum geometry, however, the frontier orbitals now had quite different shapes.

By carrying out additional point calculations, it was found that, in order to produce MO's of similar shape to those found with the experimental geometries, it is necessary that the N—N bonds be inequivalent and that there be some twist (an asymmetric planar geometry was also tested). The orbital shapes are also sensitive to the N—N—N angle. We conclude that symmetry breaking is important and that, because reducing the symmetry from C_{2v} to C_2 did not produce much change in the orbitals, A/B orbital mixing must be important. The result of the symmetry breaking is that there are two different frontier orbitals with significant contributions along the N—N bonds.

We thank the College of Arts and Sciences of the University of Toledo for generous financial support of the X-ray diffraction facility and thank the Office of Naval Research for funding this work. (Contract No. N000149310597).

References

- Blessing, R. H. (1987). *Cryst. Rev.* **1**, 3–57.
- Blessing, R. H., Coppens, P. & Becker, P. (1974). *J. Appl. Cryst.* **7**, 488–492.
- Borman, S. (1994). *Chem. Eng. News*, pp. 18–22.
- Bottaro, J. C., Schmitt, R. J., Penwell, P. E. & Ross, D. S. (1991). US Patents 5,198,204 and 5,254,324.
- Brill, T. B., Brush, P. J. & Patil, D. G. (1993). *Combust. Flame*, **92**, 178–186.

- Burla, M. C., Camalli, M., Cascarano, G., Giacovazzo, C., Polidori, G., Spagna, R. & Viterbo, D. (1989). *J. Appl. Cryst.* **22**, 389–393.
- CAChe Scientific (1993). *CAChe Reference Manual*. CAChe Scientific, Beaverton, Oregon.
- Doyle, R. J. (1993). *Org. Mass Spectrom.* **28**, 83–91.
- Ernst, S. R. (1977). *Acta Cryst.* **B33**, 237–240.
- Enraf-Nonius (1977). *CAD-4 Operations Manual*. Enraf-Nonius, Delft, The Netherlands.
- Fair, C. K. (1990). *MolEN. An Interactive Intelligent System for Crystal Structure Analysis*. Enraf-Nonius, Delft, The Netherlands.
- Gilardi, R. D. (1996). To be published.
- Johnson, C. K. (1965). *ORTEP*. Report ORNK-3794. Oak Ridge National Laboratory, Tennessee, USA.
- Luk'yanov, O. A., Anikin, O. V., Gorelik, V. P. & Tartakovsky, V. A. (1994). *Russ. Chem. Bull.* **43**, 1457–1461.
- Luk'yanov, O. A., Agevnin, A. R., Leichenko, A. A., Serigina, N. M. & Tartakovsky, V. A. (1995). *Russ. Chem. Bull.* **44**, 108–112.
- Luk'yanov, O. A., Gorelik, V. P. & Tartakovsky, V. A. (1994). *Russ. Chem. Bull.* **43**, 89–92.
- Luk'yanov, O. A., Konnova, Yu. V., Klimova, T. A. & Tartakovsky, V. A. (1994). *Russ. Chem. Bull.* **43**, 1200–1202.
- Luk'yanov, O. A., Shlykova, N. I. & Tartakovsky, V. A. (1994). *Russ. Chem. Bull.* **43**, 1680–1683.
- Martin, A. & Pinkerton, A. A. (1996). *Acta Cryst.* **C52**, 1048–1052.
- Martin, A., Pinkerton, A. A. & Schiemann, A. (1996). *Acta Cryst.* **C52**, 966–970.
- Mebel, A. M., Lin, M. C., Morokuma, K. & Melius, C. F. (1995). *J. Phys. Chem.* **99**, 6842–6848.
- Michels, H. H. & Montgomery Jr, J. A. (1993). *J. Phys. Chem.* **97**, 6602–6606.
- North, A. C. T., Phillips, D. C. & Mathews, F. S. (1968). *Acta Cryst.* **A24**, 351–359.
- Pinkerton, A. A. & Schwarzenbach, D. (1978). *J. Chem. Soc. Dalton Trans.* pp. 989–996.
- Politzer, P. & Seminario, J. M. (1993). *Chem. Phys. Lett.* **216**, 348–352.
- Politzer, P., Seminario, J. M., Concha, M. C. & Redfern, P. C. (1993). *J. Mol. Struct. Theor. Chem.* **287**, 235–240.
- Rossi, M. J., Bottaro, J. C. & McMillen, D. F. (1993). *Int. J. Chem. Kinet.* **25**, 549–570.
- Schmitt, R. J., Krempp, M. & Bierbaum, V. M. (1992). *Int. J. Mass Spectrom. Ion Processes*, **117**, 621–632.
- Sheldrick, G. M. (1985). *SHELXTL User's Manual*. Revision 5.1. Nicolet XRD Corporation, Madison, Wisconsin, USA.
- Sheldrick, G. M. (1990). *Acta Cryst.* **A46**, 467–473.
- Sheldrick, G. M. (1992). *SHELXL92. Program for the Refinement of Crystal Structures*. University of Göttingen, Germany.
- Shlyapochnikov, V. A., Cherskaya, N. O., Luk'yanov, O. A., Gorelik, V. P. & Tartakovsky, V. A. (1994). *Russ. Chem. Bull.* **43**, 1522–1525.
- Shlyapochnikov, V. A., Oleneva, G. I., Cherskaya, N. O., Luk'yanov, O. A., Gorelik, V. P., Anikin, O. V. & Tartakovsky, V. A. (1995). *Russ. Chem. Bull.* **44**, 1449–1453.
- Siemens (1989a). *P3/PC Diffractometer Program*. Version 3.13. Siemens Analytical X-ray Instruments Inc., Madison, Wisconsin, USA.
- Siemens (1989b). *XDISK. Data Reduction Program*. Version 3.11. Siemens Analytical X-ray Instruments Inc., Madison, Wisconsin, USA.
- Zachariasen, W. H. (1963). *Acta Cryst.* **16**, 1139–1144.

Contract No. N00014-95-1-0013 and N00014-97-1-0409

Program Officer: R. Miller/J. Goldwasser

**Title: Experimental Charge Densities and Electrostatic Potentials in Energetic
Materials and Infrastructure Upgrade for an X-ray Crystallography
Laboratory**

PI: A. Alan Pinkerton

Department of Chemistry, University of Toledo, Toledo, OH 43606

tel. (419) 530-4580, FAX (419) 530-4033, email apinker@uoft02.utoledo.edu

APPENDIX 5f

**A Study of the Thermal Decomposition of Biguanidinium Diperchlorate using
Thermogravimetry and Mass Spectroscopy.**

**Dollimore, D.; Martin, A.; and Pinkerton, A.A., *Thermochim. Acta*, 1996, 285,
109-117.**

A study of the thermal decomposition of biguanidinium diperchlorate using thermogravimetry and mass spectroscopy

David Dollimore*, Anthony Martin, A. Alan Pinkerton

The Chemistry Department, The University of Toledo, Toledo, OH 43606, USA

Received 31 July 1995; accepted 28 January 1996

Abstract

The thermal decomposition of biguanidinium diperchlorate has been studied by thermogravimetry in a nitrogen atmosphere and by mass spectrometry. The kinetics of the decomposition have been found from these experiments to be very rapid and exothermic. A first order (F1) mechanism has been fitted to the decomposition up to the point of inflection.

Keywords: Biguanidinium perchlorate; Differential thermal analysis; Energetic reactions; Kinetic analysis; Thermogravimetric analysis

1. Introduction

It is known that most simple guanidinium salts decompose by a vigorous exothermic reaction [1]. A number of these salts have been examined using thermogravimetry. Biguanidinium diperchlorate was prepared as described in the experimental section. A mixture containing both biguanidinium perchlorate and biguanidinium di-perchlorate was reported as explosive [2]. A search of the literature failed to reveal any other relevant information concerning the thermal decomposition of biguanidinium salts. Upon heating in air, biguanidinium diperchlorate decomposed rapidly with larger amounts (more than 3 mg) exploding with a green flash. Those results are not included here, as the thermocouple registered the explosion as a spike in the heating rate. A detailed report on this light emission is the subject of a future publication. Guanidinium salts have also displayed light emission during decomposition [3].

* Corresponding author.

2. Experimental

2.1. Materials

Biguanidinium perchlorate has the formula $[\text{C}_2\text{N}_5\text{H}_9]^+[\text{ClO}_4]^-$. The biguanidinium diperchlorate was prepared by taking stoichiometric amounts of $[\text{C}_2\text{N}_5\text{H}_8]^{2+}[\text{SO}_4]^{2-} \cdot \text{H}_2\text{O}$ and $\text{Ba}(\text{ClO}_4)_2 \cdot 3\text{H}_2\text{O}$. These two compounds were dissolved in water. The insoluble BaSO_4 was filtered off. The resultant solution was left to crystallize.

2.2. Equipment and procedures

The thermal analysis was carried out using a DuPont 1090 unit. The technique applied here was to use a small sample of biguanidinium diperchlorate (less than 3 mg) and a variety of heating rates (noted in the tables and figures). A platinum pan and an atmosphere of flowing nitrogen were used in all the TG runs. Temperature calibration was carried out using the fusible link method. The temperature could be read from the record to one decimal point but it is better to regard the temperature as correct to within one degree.

A stand-alone HP 5988 Mass Spectrometer was used with a direct insertion probe. The temperature at the probe started at 30°C and was increased at 5°C min⁻¹ up to 350°C. Scans were made approximately every second.

3. Results and discussion

The small sample size (less than 3 mg) used in the TG experiments means that the final amount of material left is not well defined. A typical TG plot for biguanidinium diperchlorate is given in Fig. 1. On this figure is noted a start temperature representing the beginning of the main reaction, an inflection point representing the maximum in the peak temperature (DTG) and an end temperature at which the main peak in the DTG is overlapped by the next stage. In the kinetic analysis the stage up to the peak temperature is shown to correspond to the decelerating mechanism (F1). The decomposition of biguanidinium diperchlorate is exothermic and very rapid. Table 1 summarizes the TG data for 17 experiments in which the heating was varied and shows the important parameters noted in Fig. 1 for each experiment. The final column in this table indicates if the run was included in the kinetic analysis. An examination of the results for which a kinetic analysis was not possible indicates that the amount of material used in three instances was too small to give accurate results. The sample containing 2.09 mg for which the kinetic analysis was also not possible was a TG run where an explosion occurred, possibly resulting in mechanical mass loss. The belief for an explosive event is based on the time versus temperature plot, Fig. 2, which shows a deviation from a constant heating rate, consistent with those found in larger examples that produced a green flash. The temperature data is retained, however, in Table 1 as the characteristic stages in the sequence of events can still be recognized.

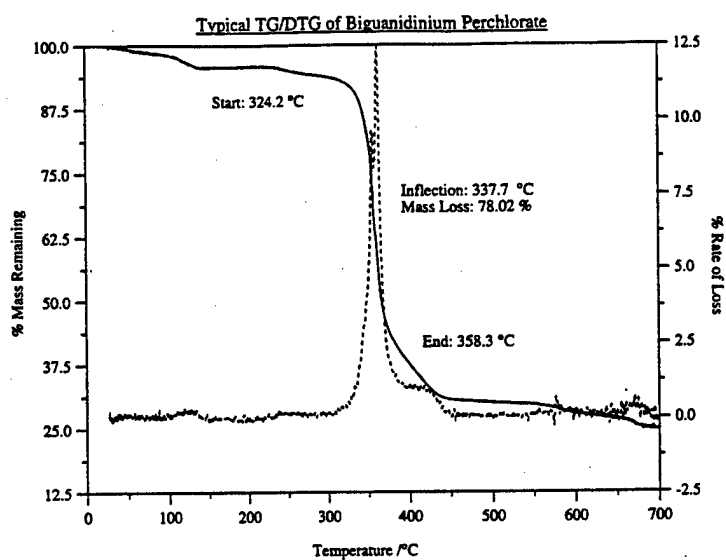


Fig. 1. TG/DTG plot showing the typical decomposition.

Table 1
Analysis of the main decomposition event

Mass/mg	Rate/ K min ⁻¹	Start/K	Inflect./K	End/K	% Loss	Kinetic Analysis
2.18	1	288	310	362.7	77.29	Y
1.77	2	297	314	344	69.7	N
1.85	3	295	317	343	73.2	Y
2.45	4	301	314	333	70.72	Y
2.24	5	343	358	377	66.1	Y
2.46	6	324	338	358	78.02	Y
3.07	7	348	366	392	70.13	Y
2.53	8	316	331	350	69.86	Y
1.85	9	302	317	346	66	N
2.17	10	311	324	343	70.64	Y
1.98	10	321	336	359	64.85	Y
2.76	10	355	375	399	70.04	Y
2.05	20	348	360	361	76.39	Y
2.01	20	304	320	342	69.4	Y
2.09	30	349	360	367	83.37	N
1.46	30	318	334	352	67.35	Y
1.47	40	377	388	399	72.8	N

An examination of Fig. 1 shows that the main step is preceded by an initial loss of volatile material. This is the loss of adsorbed water, which accounts for a mass loss of about 10% for each sample.

The second step is a decomposition where the data fits a first-order (F1) mechanism. It is postulated that this mechanism changes at the maximum in the DTG trace

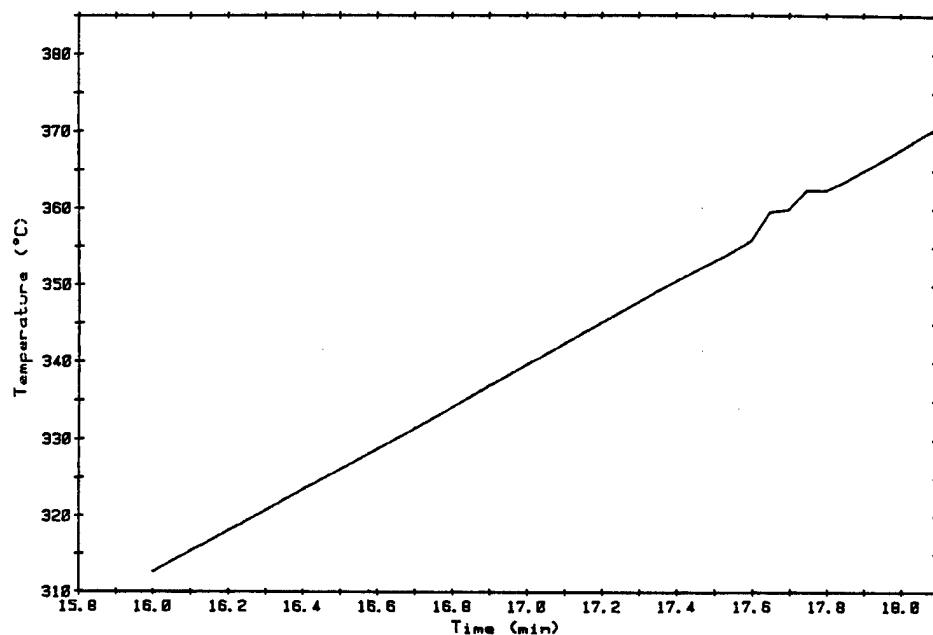


Fig. 2. Temperature versus time plot for 2.09 mg sample heated at 30 K min^{-1} .

(identical with the point of inflection in the TG curve). A third stage of the decomposition is continued decomposition after the point of inflection. This cannot be modelled with the F1 mechanism. These two stages account for a loss of about 70–80% of the sample (depending on the initial mass and the heating rate). In both stages the kinetic analysis shows a massive pre-exponential factor and a large activation energy (see next section for details).

It is likely there is fourth decomposition stage around 650°C . However, this trace only appeared on the slow heating rate experiments and there was insufficient data to analyze it properly. It typically accounted for 10% of the mass loss.

The mass spectrometry data was used to try and obtain a mechanism for the decomposition. A rising temperature direct insertion probe experiment was performed on a sample of biguanidinium diperchlorate. The data collected from the mass spectroscopy is shown in Figs. 3–6. To begin with, water, nitrogen and oxygen were detected from the sample. This was assumed to be adsorbed gas. Then, the most obvious feature of the mass spectrum of biguanidinium diperchlorate is the non-molecular ion peak of $m/z = 126$. This corresponds to a melamine radical ion ($[\text{C}_3\text{N}_6\text{H}_6]^+$). This is not unexpected and this type of rearrangement has been seen before [4]. The mass spectrum of melamine was also obtained. This was considered necessary to ensure that the biguanidinium diperchlorate spectrum was not going to simply be the decomposition of melamine. Melamine shows several peaks in its decomposition. These were compared against the biguanidinium perchlorate data.

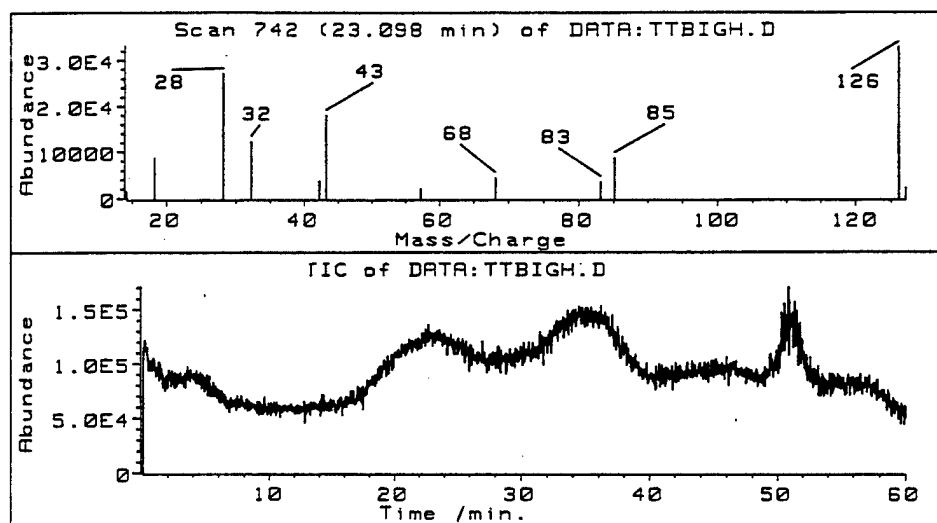


Fig. 3. Mass spectra of biguanidinium perchlorate after 23 min.

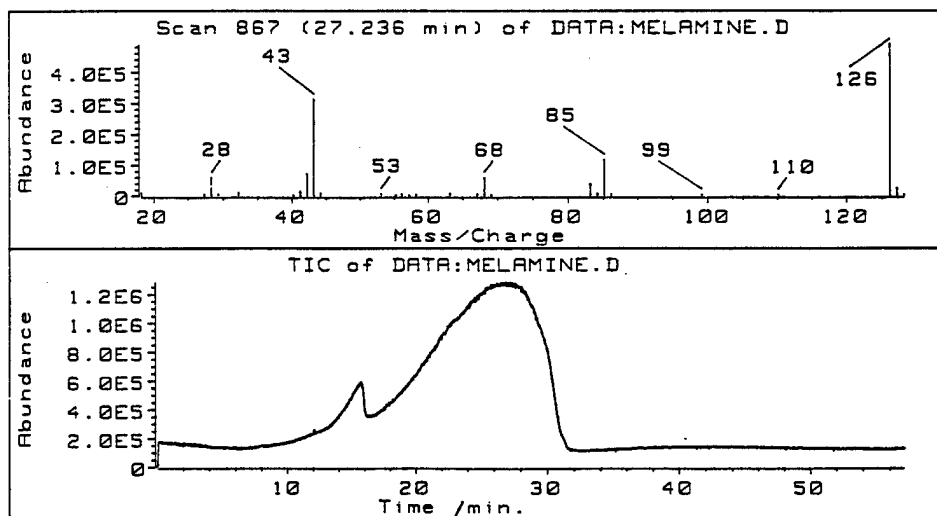


Fig. 4. Mass spectra of melamine after 27 min.

Early on (23 min, Fig. 3), the biguanidinium diperchlorate data showed essentially the same major peaks as pure melamine (Fig. 4), with some additional lower mass peaks corresponding to air and water. However, as the temperature at the dip probe continued to rise (35 min, Fig. 5), a number of additional peaks appeared in the spectra produced, and some peak relative intensities changed significantly compared to

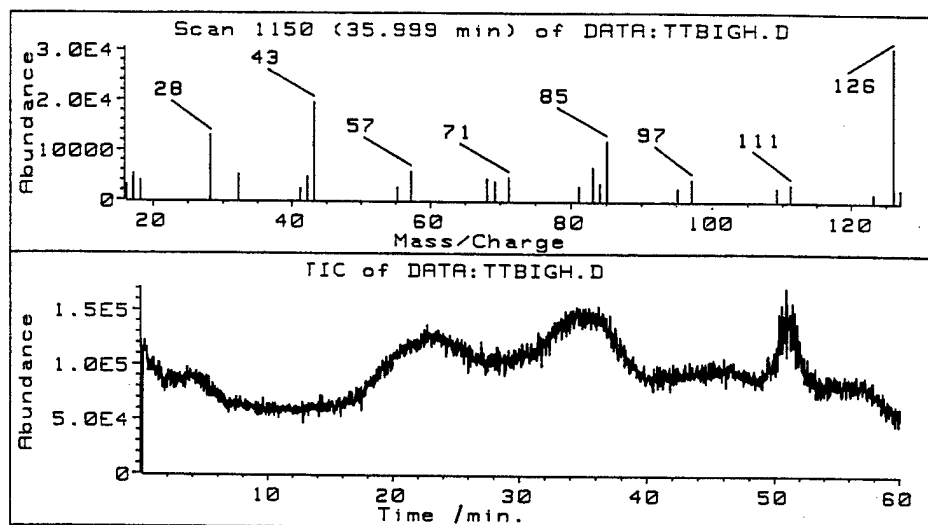


Fig. 5. Mass spectra of biguanidinium perchlorate after 35 min.

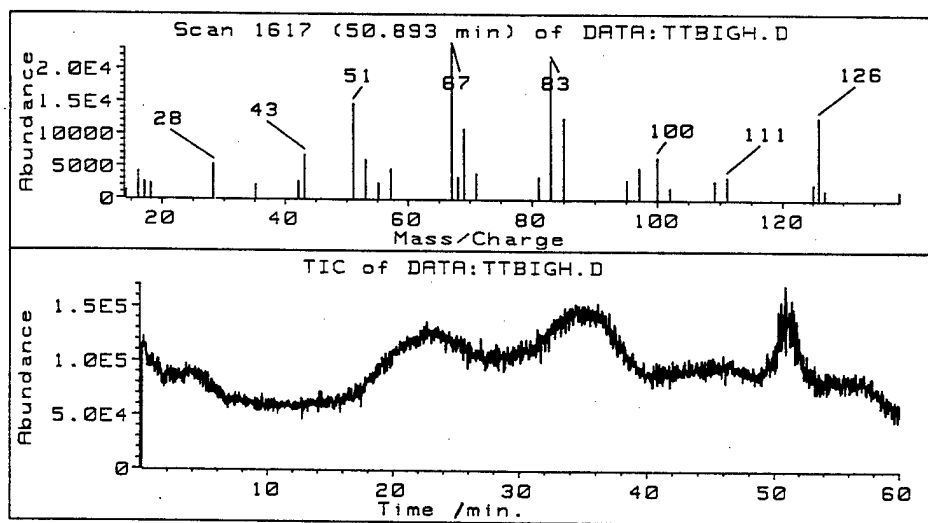


Fig. 6. Mass spectra of biguanidinium perchlorate after 50 min.

melamine. These changes were assumed to be due to the biguanidinium ion and not some more obscure rearrangement. The familiar chlorine peak pair was not seen at all. The peaks that did not appear in melamine or were significantly enhanced compared to melamine at 35 min were 32, 57, 84.

At the final peak in the total ion count (50 min, Fig. 5) an m/z peak of 102 was observed. This peak was not found at all in the melamine spectra, and we believe that this is the biguanidinium ion. It appears to decompose by initially losing pairs of hydrogen atoms and then an amine group with mass losses of 2 and 15. The peak sizes suggest that the hydrogen atoms are lost first. Peak 67 which is the most abundant at this time was seen to build slowly over the course of the experiment. There are many speculative structures that could be drawn for this, but it seems nonsensical to choose one over another. It should be noted that small peaks were seen at 137 and 153, suggesting that the melamine radical is formed from a less stable higher molecular weight ion.

4. Kinetic analysis

The procedure chosen to identify a kinetic mechanism was based on the fit of the data to the mechanism selected. When two mechanisms gave similar fits to the data (based on the correlation coefficient) the simpler mechanism was preferred. No one mechanism appears to fit all data over all the heating rates. The mechanisms investigated are listed by Dollimore and Reading [5] and the differential method of calculating the specific reaction rate was used. When the two mechanisms gave similar fits to the data (based on the correlation coefficients for the Arrhenius plots of $\log k$ against $1/T$) the simpler mechanism was preferred [6]. The main decomposition event can be split into two parts. The division between these two mechanisms can be approximated to the maximum in the DTG trace. This was done for all the data, and was not always successful, but it worked well enough for most of the samples. The reason why some of the data was not subjected to a kinetic analysis (see Table 1) has already been explained. Some data in the kinetic analysis fitted to the F1 mechanism had a correlation coefficient. The mechanism that best fitted the data up to the point of inflection (as noted in the TG trace) was found to be an F1 mechanism with a large pre-exponential factor and a large activation energy. The average correlation coefficient of the data fitted to the F1 mechanism was 0.977. The slower rate data fitted the F1 mechanism significantly less well than the more rapidly heated data. Values for the activation energy and pre-exponential factor for each run were evaluated and tabulated (Table 2). A compensation plot (Fig. 7) shows a linear relationship which could be interpreted as indicating that the mechanisms are related [7]. The occurrence of two or more kinetic models of decomposition has been previously noted [8–10]. The reason is that any change in the morphology of a solid material, e.g. abrupt changes in form, changes in surface area, or as in this case changes caused by explosions, must result in corresponding changes in the kinetics, especially if they are based on the models of an altering reaction interface. A further reason exists in extremely exothermic reactions, namely that the transfer of heat from the highly energetic processes might be reflected in the kinetic analysis. However, this was thought to be a significant contribution only after the inflection temperature and was one of the considerations why the kinetic analysis was not progressed beyond the DTG temperature. The point of inflection noted in Table

Table 2
Results of kinetic analysis using F1 mechanism

Rate/K min ⁻¹	ln A	E _a /(kJ mol ⁻¹)	Correlation
1	51	243.5	0.919
3	60	275.6	0.944
4	116	534.1	0.989
5	90	439.3	0.967
6	120	567.7	0.986
7	84	409.8	0.907
8	94	437.3	0.993
10	78	400.7	0.994
10	110	513.7	0.981
10	120	552.4	0.988
20	100	450.4	0.992
20	165	882.3	0.992
30	98	443.4	0.983

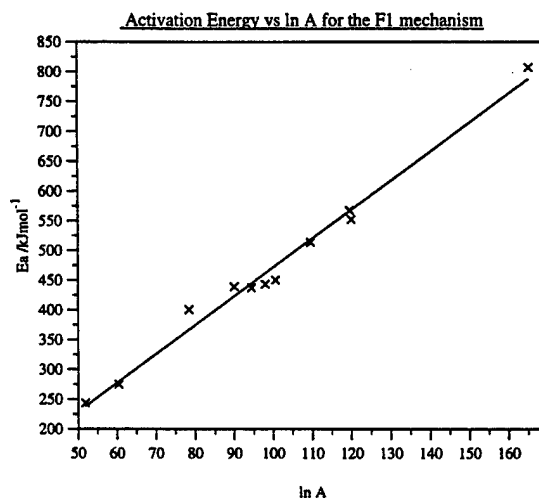


Fig. 7. The compensation plot for the data obeying the first-order (F1) mechanism.

1 can be taken as the point where the F1 mechanism ended and some new mechanism began.

At faster heating rates, the correlation in the Arrhenius plots based on the F1 mechanism is generally higher than in the slower heating rate experiments. The mass spectroscopy data offer an explanation as to why this is so. Clearly biguanidinium diperchlorate at lower decomposition temperatures can rearrange to form a more stable product, melamine. Thus slow heating rates will allow a larger portion of the

sample to rearrange without mass loss. Then, as the biguanidinium diperchlorate decomposes, this other material interferes with the F1 mechanism, promoting another. This explanation also has the advantage of simplicity, although it should be noted that the environment of the mass spectroscopy experiments is very different to those in the TG experiments.

References

- [1] M.I. Fauth, *Anal Chem.*, 32 (1960) 655.
- [2] C. Manuelli and L. Bernardini, *Brit. Pat.* (1917) # 155, 627.
- [3] W.W. Wendlandt, *Thermochim. Acta*, 70 (1983) 379.
- [4] T.M. Grahek and P. Bukovec, *Thermochim. Acta*, 215 (1993) 241.
- [5] D. Dollimore and M. Reading, in J.D. Wineforder, D. Dollimore and J.G. Dunn, (Eds.), *Treatise on Analytical Chemistry, Part I, Vol. 13, 2nd edn., Thermal Methods*, J. Wiley, New York, 1993, Chapter 1.
- [6] X. Gao and D. Dollimore, *Thermochim. Acta*, 215 (1993) 47.
- [7] M.E. Brown, D. Dollimore and A.K. Galway, in C.H. Bamford and C.F. Tipper (Eds.) *Comprehensive Chemical Kinetics*, Vol. 22 Elsevier, Amsterdam, 1980, p. 340.
- [8] D. Dollimore, J. Dollimore and D. Nicholson in J.H. de Boer (Ed.), *Proc. Fourth International Symposium on the Reactivity of Solids*, Elsevier, Amsterdam, 1960, p. 627.
- [9] D. Dollimore and D. Tinsley, *J. Chem. Soc. A*, (1971) 3034.
- [10] D. Dollimore, *J. Therm. Anal.*, 39 (1992) 111.

Contract No. N00014-95-1-0013 and N00014-97-1-0409

Program Officer: R. Miller/J. Goldwasser

**Title: Experimental Charge Densities and Electrostatic Potentials in Energetic
Materials and Infrastructure Upgrade for an X-ray Crystallography
Laboratory**

PI: A. Alan Pinkerton

Department of Chemistry, University of Toledo, Toledo, OH 43606

tel. (419) 530-4580, FAX (419) 530-4033, email apinker@uoft02.utoledo.edu

APPENDIX 6a

**Intermolecular [2 + 2] Photocyclization of Ethyl 5-oxo-1a,2,5,5a,6,6a-hexahydro-2,6-methano-2aH-indeno-[5,6-b]oxirene-2a-carboxylate.
Pinkerton, A.A.; Martin, A.; Marchand, A.P.; and Devasagayaraj, A.; *J. Chem. Crystallogr.*, 1997, 27, 701-705.**

Intermolecular [2 + 2] photocyclization of ethyl 5-oxo-1a,2,5,5a,6,6a-hexahydro-2,6-methano-2a*H*-indeno-[5,6-*b*]oxirene-2a-carboxylate

A. Alan Pinkerton,^{(1)*} Anthony Martin,⁽¹⁾ Alan P. Marchand,^{(2)*} and Arokiasamy Devasagayaram⁽²⁾

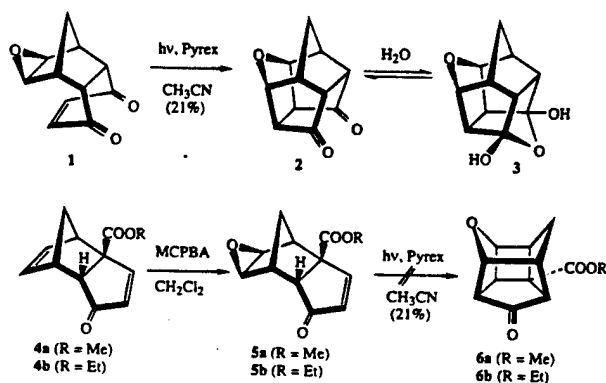
Received August 25, 1997

The photodimer, **7**, of ethyl 5-oxo-1a,2,5,5a,6,6a-hexahydro-2,6-methano-2a*H*-indeno-[5,6-*b*]oxirene-2a-carboxylate has been isolated and structurally characterized. Triclinic, $P\bar{1}$, $a = 9.7783(6)$, $b = 11.2782(7)$, $c = 11.3445(7)$ Å, $\alpha = 105.461(9)$, $\beta = 113.3759(10)$, $\gamma = 92.9155(11)^\circ$, $V = 1089.36(12)$ Å³, $R = 0.049$ for 3557 unique observed reflections. Two independent molecules lying on inversion centers occupy the unit cell. The influence of the orientation of the ester group on the polycyclic skeleton is discussed.

KEY WORDS: Photodimer; X-ray structure.

Introduction

Recently, a novel cage oxapentacyclic diketone, **2** (characterized via the corresponding hydrate, **3**) was reported to result via intramolecular [2 + 2] photocyclization of polycyclic epoxyenedione **1** (Scheme 1).¹



Scheme 1.

⁽¹⁾ Department of Chemistry, University of Toledo, Toledo, Ohio 43606.

⁽²⁾ Department of Chemistry, University of North Texas, Denton, Texas 76203-0068.

* To whom correspondence should be addressed.

At that time, it was reported that irradiation of polycyclic epoxyenone **5a**² under a variety of experimental conditions failed to afford the corresponding intramolecular [2 + 2] photocycloadduct, **6a**. The reasons for the failure of **5a** to undergo intramolecular cycloaddition were not clear at that time. Accordingly, we deemed it desirable to investigate the photochemical behavior of system **5** in greater detail; we now report the results of this reinvestigation.

Experimental section

Melting points are uncorrected. Elemental micro-analytical data were obtained by personnel at M-H-W Laboratories, Phoenix, AZ.

*Ethyl 5-oxo-1a,2,5,5a,6,6a-hexahydro-2,6-methano-2a*H*-indeno-[5,6-*b*]oxirene-2a-carboxylate, (1a α ,2 β ,2a β ,5a β ,6 β ,6a α) (5b)*

A solution of **4b** (480 mg, 2.2 mmol) in CH_2Cl_2 (50 mL) was cooled to 0°C via application of an external ice-water bath. To this cooled solution was added

Table 1. Crystal data and summary of intensity data collection and structure refinement

Compound	C ₂₆ H ₂₈ O ₈	Crystal dimensions, mm	0.34 × 0.31 × 0.15
Color/shape	Colorless/parallelepiped	Scan width	0.3°
Formula weight	468.48	Reflections measured	12197
Temp., °C	21(1)	Unique reflections	5327
Space group	$P\bar{1}$	$R(\text{merge})$	0.026
Cell constants ^a		2 θ range, deg.	5.6–57.0
<i>a</i> , Å	9.7783(6)	Range of <i>h</i> , <i>k</i> , <i>l</i>	±13 ±15 ±15
<i>b</i> , Å	11.2782(7)	Reflections observed	3557
<i>c</i> , Å	11.3445(7)	[$F_o^2 > 2\sigma(F_o^2)$]	
α , deg	105.461(9)	Computer programs ^b	SMART, SAINT, SADABS ⁴
β , deg	113.3759(10)	Structure solution	SHELXS-86 ⁵
γ , deg	92.9155(11)	Structure refinement	SHELXL-93 ⁶ (F^2)
Cell volume, Å ³	1089.36(12)	No. of parameters varied	309
		Weights	$w = 1/[\sigma^2(F_o^2) + (0.0694P)^2 + 0.1766P]$ where $P = (F_o^2 + 2Fc^2)/3$
Formula units/unit cell	2	GOF	1.019
D_{calc} , g cm ⁻³	1.428	$R = \sum \ F_o - F_c \ / \sum F_o $	0.0483
μ_{calc} , cm ⁻¹	1.06	$R_w(F^2)$ —all reflections	0.1353
Diffractometer/scan	Siemens platform/ ω	Largest feature final diff. map	0.297
Radiation, graphite	Mo-K α , 0.71073 Å		
Monochromator			

^a Determined from the *x,y,z* centroids of the complete data set.^b Data collection, integration, Lorentz-polarization, absorption, and decay corrections.

with stirring *m*-chloroperbenzoic acid (MCPBA, 770 mg, 3.12 mmol). After the addition of the oxidizing agent had been completed, the external ice-water bath was removed. The reaction mixture was allowed to warm gradually to ambient temperature and then was stirred at this temperature for 2 days. The resulting mixture was washed sequentially with 5% aqueous NaHCO₃ (3 × 20 mL), water (2 × 20 mL), and brine (2 × 20 mL). The organic layer was dried (Na₂SO₄) and filtered, and the filtrate was concentrated *in vacuo*. The residue was purified via column chromatography on silica gel by eluting with 25% EtOAc-hexane. Pure **5b** (460 mg, 88%) was thereby obtained as colorless oil; IR (film) 2974 (vs), 1725 (br, vs), 1585 (w), 1465 cm⁻¹ (m); ¹H NMR (CDCl₃) δ 1.19–1.34 (m, 4 H), 1.58 (d, *J* = 10.6 Hz, 1 H), 2.85–3.20 (m, 5 H), 4.17 (q, *J* = 7.3 Hz, 2 H), 6.09 (d, *J* = 5.7 Hz, 1 H), 7.48 (d, *J* = 5.7 Hz, 1 H); ¹³C NMR (CDCl₃) δ 14.6 (q), 29.2 (t), 39.7 (d), 42.8 (d), 49.2 (d), 49.7 (d), 55.2 (d), 62.5 (t), 65.7 (s), 136.7 (d), 160.4 (d), 171.9 (s), 207.5 (s). Anal. Calcd for C₁₃H₁₄O₄: C, 66.66; H, 6.02. Found: C, 66.42; H, 5.79.

Photodimerization of **5b**

A solution of **5b** (400 mg, 1.7 mmol) in CH₃CN (500 mL) under argon was irradiated by using a 450

W medium pressure Hg lamp (Pyrex filter). The progress of the reaction was monitored by thin-layer chromatographic (tlc) analysis. After the reaction mixture had been irradiated for 2 h, tlc analysis indicated the complete absence of starting material. The reaction mixture then was concentrated *in vacuo*, and the residue was purified via column chromatography on silica gel by using 20% MeOH–CHCl₃ as eluent. Recrystallization of the material thereby obtained from CHCl₃ afforded pure **7** (284 mg, 71%) as a colorless microcrystalline solid: mp 296–297 °C; IR (KBr) 2851 (vs), 1723 (s), 1461 (s), 1383 cm⁻¹ (s); ¹H NMR (CDCl₃) δ 0.88–0.96 (m, 2 H), 1.35 (t, *J* = 7.1 Hz, 6 H), 1.45–1.54 (m, 2 H), 2.42–2.50 (m, 2 H), 2.85–2.93 (m, 2 H), 3.20–3.01 (m, 8 H), 3.60 (d, *J* = 5.5 Hz, 2 H), 4.25 (q, *J* = 7.2 Hz, 4 H); ¹³C NMR (CDCl₃) δ 14.6 (q), 27.5 (t), 39.5 (d), 42.5 (d), 47.0 (d), 48.2 (d), 49.9 (d), 53.8 (d), 57.5 (d), 62.6 (t), 62.9 (s), 173.5 (s), 217.3 (s). Anal. Calcd for C₂₆H₂₈O₈: C, 66.66; H, 6.02. Found: C, 66.74; H, 6.03. A single crystal of **7** of suitable quality for X-ray structural analysis was obtained via repeated recrystallization from CH₃CN.

X-ray structure of **7**

Preliminary examination and data collection were carried out using a Siemens SMART platform diffrac-

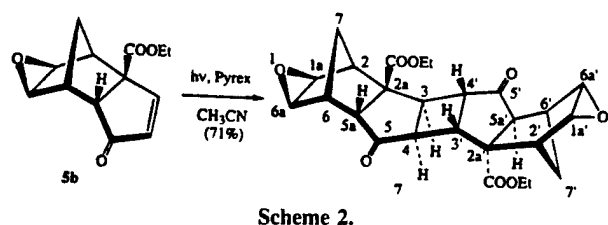
tometer. Intensity data was collected using 4 different Φ settings and 0.3° increment ω scans, $2\theta \leq 57^\circ$, which corresponds to a nominal complete sphere of data. Corrections for absorption and decay were applied using SADABS.⁴ Solution by direct methods⁵ and refinement by full matrix least squares⁶ on F^2 using all 5327 unique data. The final refinement included anisotropic thermal parameters for all nonhydrogen atoms and idealized riding hydrogen atoms with fixed isotropic thermal parameters. The refinement converged to $wR_2 = 0.1353$ (F^2 , all data) and $R_1 = 0.0483$ (F , 3557 reflections with $I > 2\sigma(I)$). A summary of the crystallographic data is presented in Table 1, final refined atomic coordinates in Table 2, and selected bond lengths and angles in Table 3.

Table 2. Final refined atomic coordinates of nonhydrogen atoms

Atom	x	y	z	U_{eq}
O1	1.00915(13)	-0.11236(13)	0.25354(13)	0.0423(3)
O2	0.7522(2)	0.06370(13)	-0.1003(2)	0.0522(4)
O3	0.4476(2)	0.33651(14)	-0.20575(14)	0.0523(4)
O4	0.4239(2)	-0.32629(12)	-0.01482(14)	0.0436(3)
O5	0.1810(2)	0.58244(12)	0.17992(13)	0.0453(3)
O6	0.2793(2)	0.88667(13)	0.6062(2)	0.0506(4)
O7	0.75431(15)	0.7823(2)	0.63335(14)	0.0553(4)
O8	0.76875(14)	0.79446(14)	0.44564(14)	0.0436(3)
C1A	0.8508(2)	-0.1008(2)	0.2122(2)	0.0319(4)
C2	0.7410(2)	-0.21988(15)	0.1152(2)	0.0285(4)
C2A	0.6149(2)	-0.17923(14)	0.0033(2)	0.0239(3)
C3	0.5493(2)	-0.06519(14)	0.0577(2)	0.0230(3)
C4	0.6139(2)	0.04931(14)	0.0325(2)	0.0253(3)
C5	0.6987(2)	0.0012(2)	-0.0517(2)	0.0300(4)
C5A	0.7043(2)	-0.13599(15)	-0.0699(2)	0.0271(3)
C6	0.8675(2)	-0.1637(2)	0.0029(2)	0.0318(4)
C6A	0.9352(2)	-0.0661(2)	0.1407(2)	0.0336(4)
C7	0.8287(2)	-0.2812(2)	0.0355(2)	0.0344(4)
C8	0.4878(2)	-0.2892(2)	-0.0872(2)	0.0298(4)
C9	0.2960(3)	-0.4290(2)	-0.0857(3)	0.0588(6)
C10	0.1512(3)	-0.3834(3)	-0.1400(3)	0.0745(8)
C11A	0.2942(2)	0.6944(2)	0.2360(2)	0.0348(4)
C12	0.4557(2)	0.6756(2)	0.3116(2)	0.0304(4)
C12A	0.5272(2)	0.7884(2)	0.4442(2)	0.0259(3)
C13	0.5024(2)	0.91784(14)	0.4223(2)	0.0258(3)
C14	0.3824(2)	0.9629(2)	0.4727(2)	0.0291(4)
C15	0.3536(2)	0.8718(2)	0.5410(2)	0.0321(4)
C15A	0.4349(2)	0.7625(2)	0.5222(2)	0.0292(4)
C16	0.3295(2)	0.6357(2)	0.4308(2)	0.0338(4)
C16A	0.2119(2)	0.6662(2)	0.3113(2)	0.0353(4)
C17A	0.4310(2)	0.5712(2)	0.3690(2)	0.0359(4)
C18	0.6943(2)	0.7870(2)	0.5203(2)	0.0309(4)
C19	0.9302(2)	0.7918(2)	0.5062(2)	0.0454(5)
C20	0.9576(3)	0.6611(2)	0.4902(3)	0.0718(8)

Results and discussion

The starting material for this study, **5b**, was synthesized from **4b**^{2a,3} via a modification of a procedure that has been reported previously^{2b} for the preparation of **5a** from **4a**. Subsequent photolysis of an acetonitrile solution of **5b**, performed by using Pyrex filtered light from a 450 W medium pressure Hg lamp, failed to produce the corresponding oxapentacyclic ketoester, **6b**. Instead, this reaction afforded a single product in high yield (71%) whose structure subsequently was established unequivocally as being that of **7** (Scheme 2) via application of single crystal X-ray crystallographic methods.



Interestingly, the intermolecular [2 + 2] photocyclization of **5b** proceeds with remarkable regioselectivity to afford a single photodimer, **7**. By considering the stereochemistries at C(2a)–C(5a) vs. C(3)–C(4), C(3)–C(4) vs. C(3')–C(4') and C(3')–C(4') vs. C(2a')–C(5a'), it should be noted that any (or all) of eight stereoisomeric photodimers might have resulted via intermolecular [2 + 2] photodimerization of **5b**. The origin of the unusually high regioselectivity of this photodimerization process is under active investigation.

The crystal of **7** contains two independent molecules in the unit cell both of which lie on centers of inversion. These remarkably symmetrical dimers are only differentiated by the orientation of the ester groups (Figure 1). The planar cyclobutane rings are almost ideal squares, the maximum difference of sides being 0.016 Å and of angles 1.3° (Table 3). The bonds adjacent to the ketone in the cyclopentanone ring are shortened by 0.04 Å with respect to the other three bonds. The three rings about the center of **7** are slightly "flattened" compared to the parent compound tricyclo(5.3.0.0^{2,6})decan-3,8-dione⁸ as indicated by the angles C(4')–C(3)–C(2A) {C(14')–C(13)–C(12A)}: 119.06(13) {119.01(13)}, C(5)–C(4)–C(3') {C(15)–C(14)–C(13')}: 111.42(13) {111.39(14)}° relative to the analogous angles of 113.2 and 109.5° in the parent compound.⁸ In general, the C–C distances and angles in **7** compare well with those of the monomeric starting

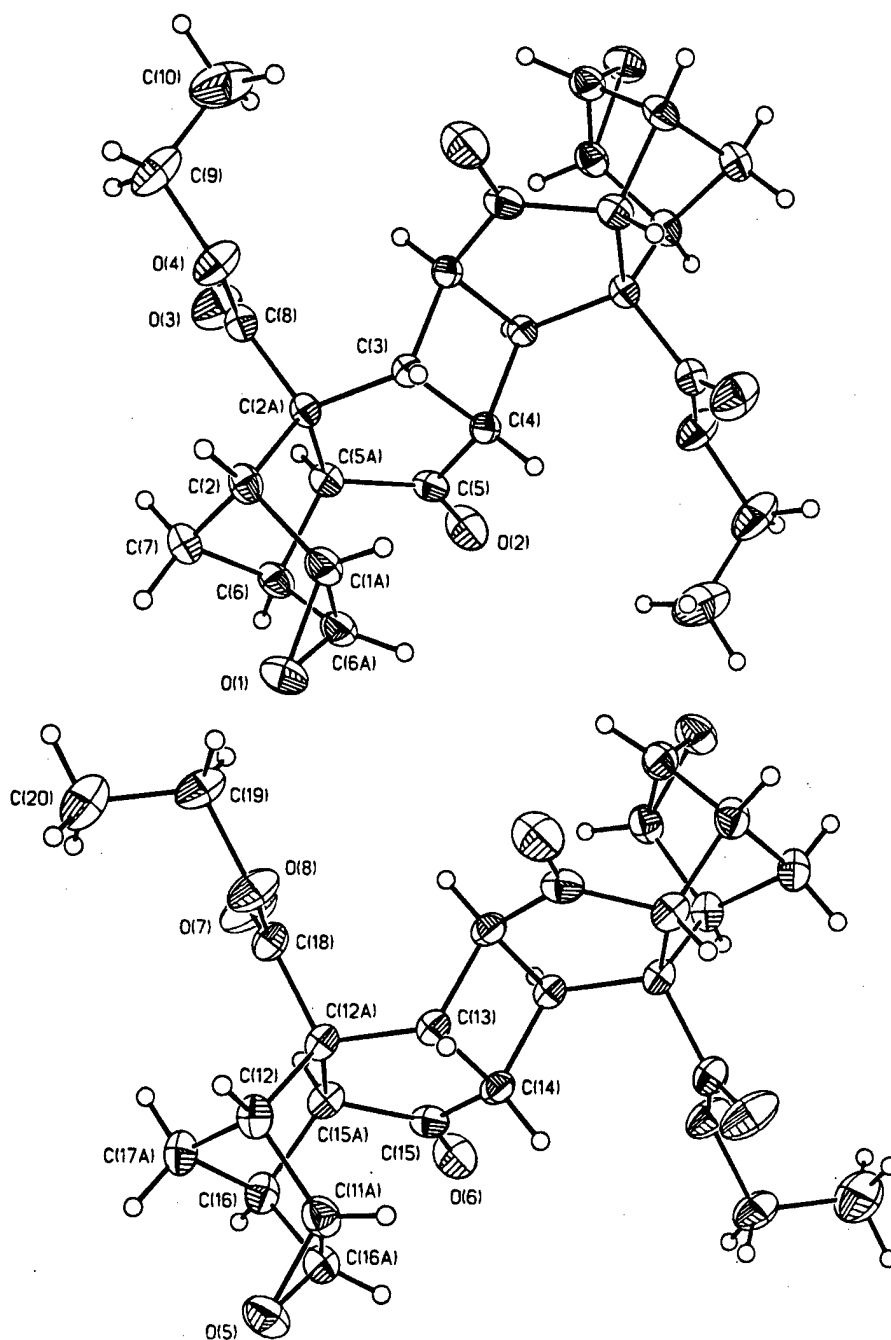


Fig. 1. ORTEP drawings of the two independent molecules of **7** (40% probability ellipsoids).

product **4b**⁹ except for the C(3)–C(4) {C(13)–C(14)} distance of 1.551(2) {1.549(2) Å} compared to the related one in **4b** {1.327(4) Å} concomitant with the decrease in bond order.

The C–C bonds in the cyclohexane ring are clearly differentiated by two different effects. The two bonds closest to the epoxide are shorter than those to the cyclopentanone ring. More surprisingly, this

differentiation is significantly modified by the orientation of the ester group, 0.06 Å in the first molecule and 0.03 Å in the second. However, the only modification in the ester group is a minor change in the C–O bond length (0.01 Å).

It is interesting to note, that the overall shape of the “monomeric” **4b** is very similar to the appropriate parts of **7**. This includes the non-bonding C···C dis-

Table 3. Selected bond lengths and angles in 7

Fragment	Molecule 1		Molecule 2	
C ₄	C(3)–C(4)	1.551(2)	C(13)–C(14)	1.549(2)
	C(4)–C(3')	1.567(2)	C(14)–C(13')	1.557(2)
	C(4)–C(3)–C(4')	88.69(11)	C(14)–C(13)–C(14')	89.36(12)
	C(3)–C(4)–C(3')	91.31(11)	C(13)–C(14)–C(13')	90.64(12)
C ₅	C(2a)–C(3)	1.556(2)	C(12a)–C(13)	1.560(2)
	C(3)–C(4)	1.551(2)	C(13)–C(14)	1.549(2)
	C(4)–C(5)	1.514(2)	C(14)–C(15)	1.518(2)
	C(5)–C(5a)	1.512(2)	C(15)–C(15a)	1.514(2)
	C(2a)–C(5a)	1.562(2)	C(12a)–C(15a)	1.559(2)
C ₆	C(1a)–C(2)	1.515(2)	C(11a)–C(12)	1.526(2)
	C(2)–C(2a)	1.571(2)	C(12)–C(12a)	1.557(2)
	C(5a)–C(6)	1.571(2)	C(15a)–C(16)	1.548(3)
	C(6)–C(6a)	1.510(3)	C(16)–C(16a)	1.527(3)
Ester	C(8)–O(4)	1.343(2)	C(18)–O(8)	1.332(2)

tances C(1A)–C(3), C(6A)–C(4), C(11A)–C(13), C(16A)–C(14) which range from 2.861(2) to 3.358(2) Å compared to 2.90 to 3.39 Å for the analogous distances in 4b. These distances are of interest because they may provide insights into factors governing possible intramolecular [2 + 2] cycloaddition as observed for 1. However, to the best of our knowledge no X-ray structure of 1 is available.¹⁰

The geometry of the epoxy group does not show any unusual features and is in close agreement with comparable compounds.^{11–13}

Acknowledgments

We thank the Robert A. Welch Foundation [Grant B-963 (A.P.M.)] and the Office of Naval Research [Grants N00014-94-1-1039 (APM) and N00014-95-1-0013 (AAP)] for financial support of this study.

Supplementary material. Crystallographic data (excluding structure factors) for the structure reported in this paper have been deposited with the Cambridge Crystallographic Data Centre as supplementary publication CCDC-1003/5255. Copies of available material can be obtained, free of charge, on application to the

CCDC, 12 Union Road, Cambridge CB2 1EZ, UK, (fax: +44-(0)1223-336033 or email: deposit@ccdc.cam.ac.uk).

References

1. Marchand, A.P.; Reddy, G.M.; Watson, W.H.; Kashyap, R. *Tetrahedron* **1990**, *46*, 3409.
2. Synthesis of 5a: (a) Herz, W.; Iyer, V.S.; Nair, M.G. *J. Org. Chem.* **1975**, *40*, 3519. (b) Marchand, A.P.; Suri, S.C. *J. Org. Chem.* **1984**, *49*, 2041.
3. Synthesis of 4b: Klunder, A.J.H.; de Valk, W.C.G.M.; Verlaak, J.M.J.; Schellekens, J.W.M.; Noordik, J.H.; Parthasarathi, V.; Zwanenburg, B. *Tetrahedron* **1985**, *41*, 963.
4. Sheldrick, G.M. *SADABS*; Sheldrick, G.M., Ed.; Univ. Göttingen, **1996**.
5. Sheldrick, G.M. *SHELXS-86*; Sheldrick, G.M., Ed.; Univ. Göttingen, **1986**.
6. Sheldrick, G.M. *SHELXL-93*; Sheldrick, G.M., Ed.; Univ. Göttingen, **1993**.
7. Matsuura, H.; Koshibe, S.; Kai, Y.; Yasuoka, N.; Kasai, N. *Acta Crystallogr.* **1979**, *B35*, 989.
8. Margulis, T.N. *Acta Crystallogr.* **1965**, *18*, 742.
9. Lange, J.H.M.; Sessink, P.J.M.; Klunder, A.J.H.; Smits, J.M.M.; Bosman, W.P.; Behm, H.; Beurskens, P. *J. Crystallogr. Spectrosc. Res.* **1988**, *18*, 779.
10. Allen, F.H.; Kennard, O. *3D Search and Research Using the Cambridge Structural Data Base*; Chemical Design Automation News, **1993**, Vol. 8, p 1.
11. Gress, M.E.; Jacobson, R.A. *Crystallogr. Struct. Commun.* **1973**, *2*, 485.
12. DeLacy, T.P.; Kennard, C.H.L. *J. Chem. Soc., Perkin Trans. 2* **1972**, 2153.
13. Bartlett, P.D.; Combs Jr., G.L.; Le, A.-X.T.; Watson, W.H.; Galloy, J.; Kimura, M. *J. Am. Chem. Soc.* **1982**, *104*, 3131.

Contract No. N00014-95-1-0013 and N00014-97-1-0409

Program Officer: R. Miller/J. Goldwasser

**Title: Experimental Charge Densities and Electrostatic Potentials in Energetic
Materials and Infrastructure Upgrade for an X-ray Crystallography
Laboratory**

PI: A. Alan Pinkerton

Department of Chemistry, University of Toledo, Toledo, OH 43606

tel. (419) 530-4580, FAX (419) 530-4033, email apinker@uoft02.utoledo.edu

APPENDIX 6b

**Structure of 1,2,3,4,9,9-Hexachloro-6,7-tetrahydro-1,4-methanonaphthalene:
A Facially Differentiated, Annulated 1,3-Cyclohexadiene.
Pinkerton, A.A.; Burckel, P.M.; Marchand, A.P.; and Dong, E.Z.; *J. Chem.
Crystallogr.*, in press.**

Structure of 1,2,3,4,9,9-Hexachloro-6,7-tetrahydro-1,4-methanonaphthalene: A Facially Differentiated, Annulated 1,3-Cyclohexadiene

A. Alan Pinkerton* and Pannee M. Burckel

Department of Chemistry, University of Toledo, Toledo, Ohio 43606

Alan P. Marchand* and Eric Zhiming Dong

Department of Chemistry, University of North Texas, Denton, Texas 76203-5070

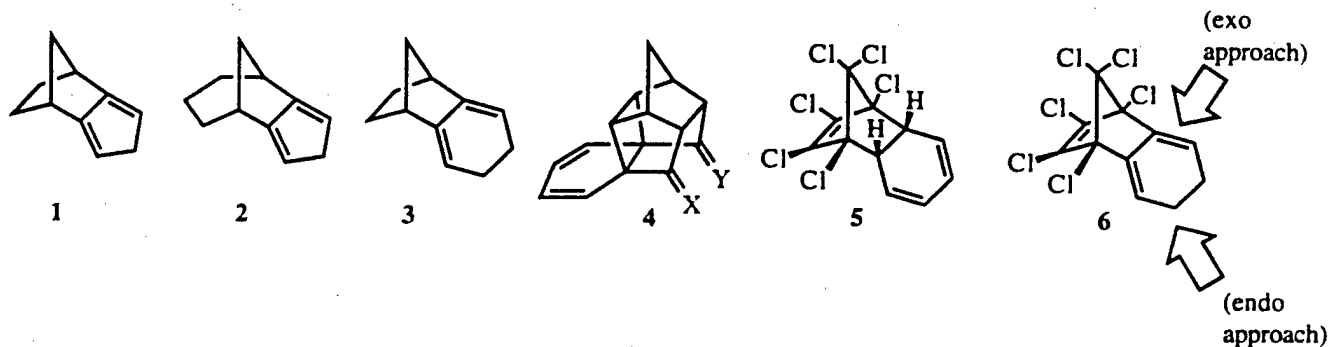
Abstract. The X-ray crystal structure of the title compound is reported. Crystal data: $T = 100\text{ K}$, monoclinic, $P2_1/n$, $a = 8.2990(17)\text{ \AA}$, $b = 13.2300(26)\text{ \AA}$, $c = 12.0350(24)\text{ \AA}$, $\beta = 93.676(30)^\circ$, $V = 1318.7(5)\text{ \AA}^3$, $R = 0.0368$. The methylene carbon atoms in the cyclohexadiene ring are disordered over two positions above and below the ring plane. The chlorine substituted endocyclic double bond deviates from planarity with an angle of $8.10(13)^\circ$ toward the *endo*-face. The facially differentiated 1,3-cyclohexadiene moiety is only slightly pyramidalized, deviating $1.75(20)^\circ$ also toward the *endo*-face of the tricyclic system.

KEY WORDS: X-ray structure, pyramidalized sp^2 carbon, facial differentiation, stereoselectivity

Introduction. The results of numerous studies of the stereoselectivities of Diels-Alder cycloadditions of various dienophiles to facially differentiated dienes have been reported in recent years. Examples in this regard include "isodicyclopentadiene" (1),¹ unsymmetrically annulated diene 2,² and unsymmetrically annulated cyclohexa-1,3-dienes 3³ and 4⁴ (Scheme 1). In each case, the stereoselectivity exhibited by the diene during $[4 + 2]$ cycloaddition to various dienophiles has been investigated, and explanations to account for observed π -facial diastereoselectivities have been forwarded.

As part of a continuing study of π -facial diastereoselectivity in Diels-Alder cycloadditions of dienophiles to facially dissymmetric, cyclic 1,3-dienes,^{4d,5} a detailed investigation of Diels-Alder cycloadditions of 4-methyl- and 4-phenyl-1,2,4-triazoline-3,5-dione [MTAD and PTAD, respectively] to two isomeric annulated cyclohexadienes, i.e., 5 and 6, was undertaken.⁶ In addition, the corresponding Diels-Alder cycloaddition of *N*-methylmaleimide (NMM) to diene 5 was studied.⁶ Insight into the various transition states for these reactions has been gleaned via application of *ab initio* and semiempirical computational methods.⁷ The structure determination of 6 is reported herein.

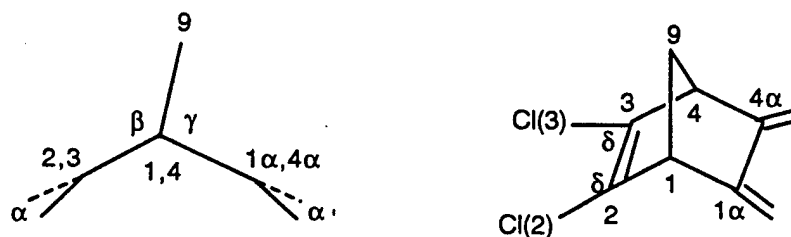
Scheme 1



Structure Determination. Preliminary examination and data collection were carried out using a Siemens SMART platform diffractometer. Intensity data was collected using three different ϕ settings and 0.3° increment ω scans, $2\theta \leq 56^\circ$, which corresponds to a nominal complete sphere of data. Corrections for absorption decay were applied using SADABS⁸. Solution was by direct methods⁹ and refinement by full matrix least squares¹⁰ on F^2 using all 3182 unique data. The final refinement included anisotropic thermal parameters for non hydrogen atoms and idealized riding hydrogen atoms (except H(5) and H(8)) with isotropic thermal parameters. The refinement converged to $wR^2 = 0.0880$ (for F^2 , all data) and $R_1 = 0.0368$ (F, 2443 reflections with $I > 2\sigma(I)$). A summary of the crystallographic data is presented in Tables 1 to 3.

Results and Discussion. The synthesis of **6** has been reported elsewhere.⁶ A suitable single crystal was obtained via careful recrystallization from hexane-acetone mixed solvent. Two ORTEP drawings with thermal ellipsoids at the 50% probability level are shown in Figure 1. The distortion of the cyclohexadiene ring shown in the figure represents one orientation of atoms C(6) and C(7) which are disordered over two positions above and below the mean plane of the cyclohexadiene ring. The disorder was modelled with the population parameters of 0.6 and 0.4 for C(6A), C7(A) and their hydrogen atoms, and C(6B), C(7B) and their hydrogen atoms, respectively. Atoms C(6B) and C(7B) have been omitted from Figure 1 for clarity.

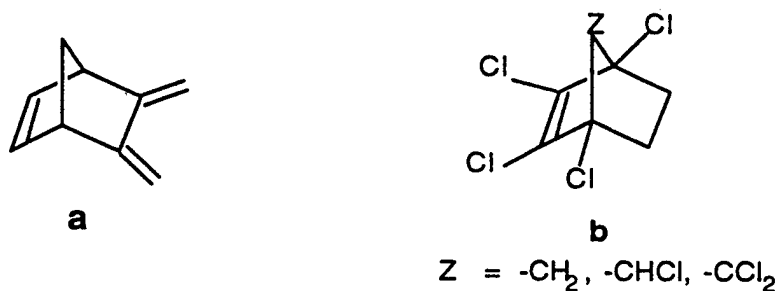
The out-of-plane deformations of the endocyclic and the exocyclic double bonds of **6** were investigated. Dihedral angles between mean planes and the exocyclic bond angles of the endocyclic double bond are defined below.



The out-of-plane deviation angle, α , of Cl(2) and Cl(3) toward the *endo*-face is significant, $8.10(13)^\circ$; whereas only a small deviation, $1.78(20)^\circ$, α' , of the diene moiety toward the *endo*-face was observed. The angles between the mean planes C(1), C(9), C(4); with C(2), C(1), C(4), C(3) (β), and C(1 α), C(1), C(4), C(4 α) (γ), are $125.62(14)^\circ$ and $122.12(15)^\circ$, respectively. The angles Cl(2)-C(2)-C(3) and Cl(3)-C(3)-C(2) (δ), are $128.3(2)^\circ$ and $127.7(2)^\circ$, respectively. Values of α , α' , β , γ and δ have been compared with literature values obtained from the analysis of data in the Cambridge Crystallographic Data Center (CCDC), Database 5.14, October 1997.

There was no matching structure for **6** from the CCDC search, thus the search for values of α , α' , β and γ for similar structures was carried out for the two fragments **a** and **b**, as shown below. Five values of α' , β and γ were obtained from searching for fragment **a**. The α' values of three structures range from

0.68 to 3.54° toward the *endo*- face, and the values from two structures were 3.24° and 4.43° toward the *exo*- face. Thus the current value (1.78(20)°) is quite typical, however, interpretation of the value is complicated by the disorder of C(6) and C(7). The difference between mean dihedral angles β - γ from 4 structures range from +3.90° to +6.55°, however, that from one structure was -0.33° again in agreement with the current study (3.50(15)°). A search for fragment **b** returned values of α , β , γ and δ from 52 matching structures. Values of α are shown as a histogram in Figure 2, negative and positive values indicating deviation toward the *endo*- and *exo*- faces, respectively. Thus molecule **6** has one of the largest out-of-plane deviations observed for this fragment (8.10(13)°). Values of the difference between dihedral angles β - γ are shown as a histogram in Figure 3. The histogram of angles δ obtained from 52 structures are shown in Figure 4.



Structure **6** shows significantly higher out-of-plane deformation (α) than the average value, whereas values of angles β , γ , and δ fall close to the average literature values. The hypothesis that the high observed α value is due to interaction of the endocyclic double bond with the Cl atoms at the bridgehead is not supported by inspection of similar structures in the database.

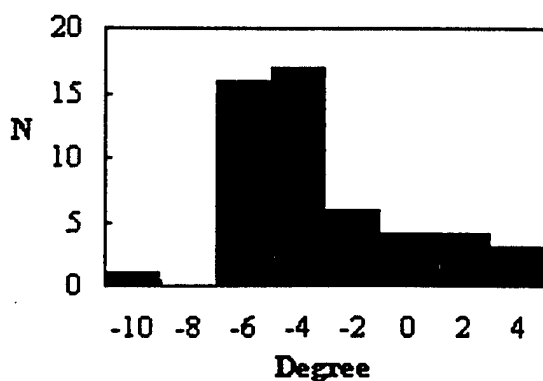


Figure 2 Histogram of the out-of-plane deviation angle, α , from 52 structures containing fragment **b**.

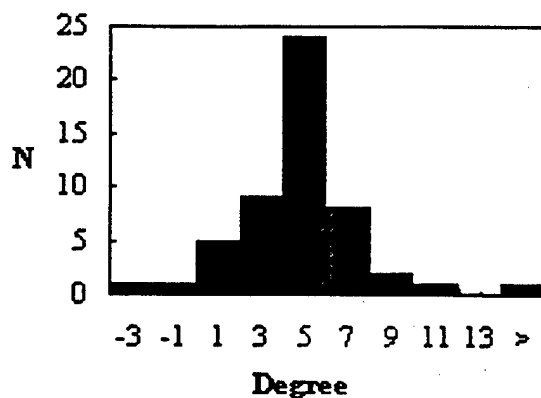


Figure 3 Histogram of the difference between dihedral angles $\beta-\gamma$ from 52 structures containing fragment b.

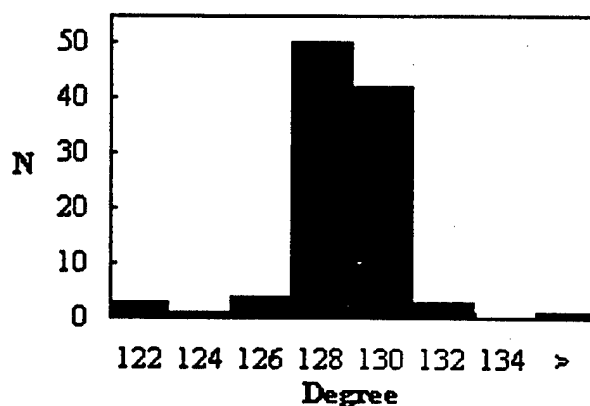


Figure 4 Histograms of angle δ from 52 structures containing fragment b.

Acknowledgment. We thank the Office of Naval Research Grants N00014-94-1-1039 (APM), N00014-95-1-0013 and N00014-95-1-1252 (AAP) and the Robert A. Welch Foundation Grant B-963 (APM) for financial support of this work.

Supplementary Material. Crystallographic data (excluding structure factors) for the structure reported in this paper have been deposited with the Cambridge Crystallographic Data Centre as supplementary publication CCDC-0000. Copies of available material can be obtained, free of charge, on application to the CCDC, 12 Union Road, Cambridge CB2 1EZ, UK (fax: +44-(0)1223-336033 or email: deposit@ccdc.cam.ac.uk).

References

1. Subramanyam, R.; Bartlett, P. D.; Iglesias, G. Y. M.; Watson, W. H.; Galloy, J. J. *Org. Chem.* **1982**, *47*, 4491.
2. (a) For a review, see: Gleiter, R.; Paquette, L. A. *Acc. Chem. Res.* **1983**, *16*, 328. (b) Paquette, L. A.; Gugelchuk, M. *J. Org. Chem.* **1988**, *53*, 1835 and references cited therein.
3. Hickey, E. R.; Paquette, L. A. *J. Am. Chem. Soc.* **1995**, *117*, 163.
4. (a) Coxon, J. M.; O'Connell, M. J.; Steel, P. J. *J. Org. Chem.* **1987**, *52*, 4726. (b) Coxon, J. M.; MacLagan, R. G. A. R.; McDonald, D. Q.; Steel, P. J. *J. Org. Chem.* **1991**, *56*, 2542. (c) Coxon, J. M.; McDonald, D. Q.; Steel, P. J. In: *Advances in Detailed Reaction Mechanisms*, Coxon, J. M., Ed., JAI Press: Greenwich, CT; Vol. 3, 1994, pp. 131-166. (d) Coxon, J. M.; Fong, S. T.; Lundie, K.; McDonald, D. Q.; Steel, P. J.; Marchand, A. P.; Zaragoza, F.; Zope, U. R.; Rajagopal, D.; Bott, S. G.; Watson, W. H.; Kashyap, R. P. *Tetrahedron* **1994**, *50*, 13037.
5. (a) Marchand, A. P.; Zope, U. R.; Burritt, A.; Bott, S. G.; Coxon, J. M. *Tetrahedron* **1995**, *51*, 9319. (b) Marchand, A. P.; Shukla, R.; Burritt, A.; Bott, S. G. *Tetrahedron* **1995**, *51*, 8733.
6. Marchand, A. P.; Dong, E. Z.; Shukla, R. S.; Prasad, A. D.; Bott, S. G. *Tetrahedron* **1997**, *53*, 14895.
7. Marchand, A. P.; Ganguly, B.; Shukla, R. S. *Tetrahedron* **1998**, *54*, 4477.
8. Sheldrick, G. M. *SADABS*, Sheldrick, G. M. Ed.; Univ. Göttingen, 1996.
9. Sheldrick, G. M. *SHELXS-86*, Sheldrick, G. M. Ed.; Univ. Göttingen, 1986.
10. Sheldrick, G. M. *SHELXL-93*, Sheldrick, G. M. Ed.; Univ. Göttingen, 1993.

Table 1. Crystal data and summary of intensity data collection and structure refinement

Compound	C ₁₁ H ₆ Cl ₁₆	Crystal dimensions, mm	0.30 x 0.10 x 0.05
Color/shape	colorless/parallelepiped	Scan width	0.3°
Formula weight	350.86	Reflections measured	8991
Temp., °C	-173(1)	Unique reflections	3182
Space group	P2 ₁ /n	Reflections observed [$F_o^2 > 2\sigma(F_o^2)$]	2443
Cell constants ^a		2 θ range, deg.	4.6 - 56.5
a, Å	8.2990(17)	Range of h, k, l	$\pm 10 \pm 12 \pm 15$
b, Å	13.2300(26)	R (merge)	0.0476
c, Å	12.0350(24)	Computer programs ^b	SMART, SAINT, SADABS ⁸
β , deg	93.676(30)	Structure solution	SHELXS-86 ⁹
		Structure refinement	SHELXL-93 ¹⁰ (F ²)
		No. of parameters varied	161
Cell volume, Å ³	1318.7(5)	Weights	$w = 1/[\sigma^2(F_o^2) + (0.0381P)^2 + 0.0838P]$ where $P = (F_o^2 + 2F_c^2)/3$
Formula units/unit cell	4	GOF	1.024
D _{calc} , g cm ⁻³	1.767	$R = \sum F_o - F_c / \sum F_o $	0.0368
μ_{calc} , cm ⁻¹	1.27	$R_w(F^2)$ - all reflections	0.0880
Diffractometer/scan	Siemens Platform/ ω	Largest feature final diff.map	0.500
Radiation, graphite monochromator	Mo-K α , 0.71073 Å		

^a Determined from the x,y,z centroids of the complete data set.

^b Data collection, integration, Lorentz-polarization, absorption and decay corrections.

Table 2. Final refined atomic coordinates of non-hydrogen atoms

Atom	x	y	z	U _{eq} ^a
Cl(1)	0.08310(8)	0.16811(5)	0.79688(5)	0.0218(2)
Cl(2)	0.30160(8)	0.36958(6)	0.73773(6)	0.0265(2)
Cl(3)	0.04790(8)	0.55369(5)	0.62917(5)	0.0224(2)
Cl(4)	-0.32834(8)	0.46155(5)	0.60962(5)	0.0203(2)
Cl(A)	-0.11398(8)	0.24768(5)	0.55025(5)	0.01846(15)
Cl(B)	-0.32241(8)	0.21991(5)	0.72949(5)	0.01790(15)
C(1)	-0.0076(3)	0.2855(2)	0.7724(2)	0.0145(5)
C(1A)	-0.0829(3)	0.3363(2)	0.8705(2)	0.0143(5)
C(2)	0.0967(3)	0.3676(2)	0.7224(2)	0.0167(5)
C(3)	-0.0023(3)	0.4384(2)	0.6787(2)	0.0167(5)
C(4)	-0.1755(3)	0.4064(2)	0.6965(2)	0.0139(5)
C(4A)	-0.1932(3)	0.4135(2)	0.8217(2)	0.0140(5)
C(5)	-0.2853(3)	0.4707(2)	0.8823(2)	0.0184(5)
C(6A) ^b	-0.2914(7)	0.4526(5)	1.0033(4)	0.0214(15)
C(6B) ^b	-0.2490(11)	0.4625(6)	1.0105(7)	0.018(2)
C(7A) ^b	-0.1411(6)	0.3985(4)	1.0550(4)	0.0186(10)
C(7B) ^b	-0.1831(9)	0.3625(6)	1.0518(6)	0.021(2)
C(8)	-0.0665(3)	0.3194(2)	0.9795(2)	0.0237(6)
C(9)	-0.1560(3)	0.2887(2)	0.6853(2)	0.0143(5)

$$^a U_{eq} = (1/3) \sum_i \sum_j U^{ij} a_i^* a_j^* a_i \cdot a_j$$

^b Occupancy of A and B sites, 0.6 and 0.4 respectively.

Table 3 Bond lengths and bond angles in 6.

Bond Lengths

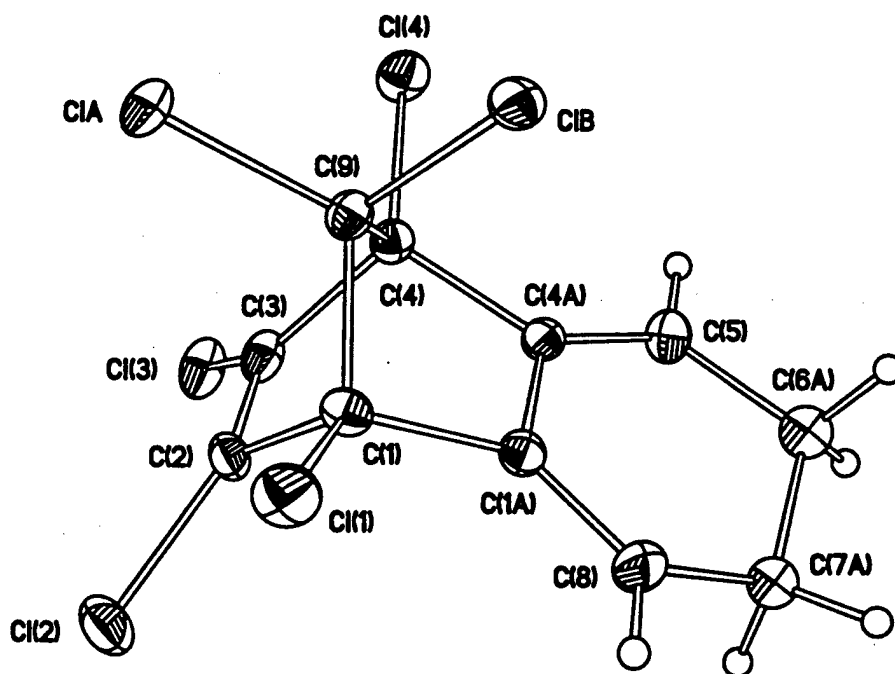
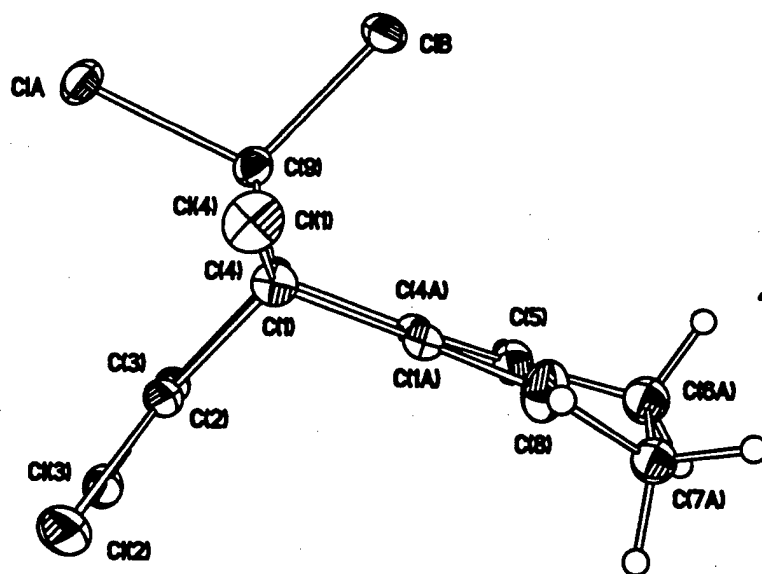
Cl(1)-C(1)	1.743(3)	C(2)-C(3)	1.331(4)
Cl(2)-C(2)	1.699(3)	C(3)-C(4)	1.527(3)
ClB-C(9)	1.764(3)	C(4)-C(9)	1.573(3)
Cl(3)-C(3)	1.699(3)	C(4A)-C(4)	1.526(3)
Cl(4)-C(4)	1.750(3)	C(4A)-C(5)	1.327(4)
ClA-C(9)	1.769(2)	C(5)-C(6A)	1.479(6)
C(1)-C(2)	1.535(3)	C(5)-C(6B)	1.556(8)
C(1)-C(9)	1.566(3)	C(6A)-C(7A)	1.535(7)
C(1A)-C(1)	1.527(3)	C(6B)-C(7B)	1.504(11)
C(1A)-C(4A)	1.468(3)	C(7A)-C(8)	1.542(5)
C(1A)-C(8)	1.329(3)	C(7B)-C(8)	1.458(7)

Bond angles

Cl(1)-C(1)-C(1A)	117.1(2)	C(1A)-C(4A)-C(5)	122.9(2)
Cl(1)-C(1)-C(2)	116.7(2)	C(4)-C(4A)-C(5)	132.3(2)
Cl(1)-C(1)-C(9)	116.7(2)	C(4A)-C(5)-C(6A)	120.4(3)
C(1A)-C(1)-C(2)	105.1(2)	C(4A)-C(5)-C(6B)	115.1(4)
C(1A)-C(1)-C(9)	99.3(2)	C(3)-C(4)-C(9)	99.2(2)
C(2)-C(1)-C(9)	99.1(2)	C(4A)-C(4)-C(9)	99.3(2)
C(1)-C(1A)-C(4A)	105.8(2)	C(1A)-C(4A)-C(4)	104.8(2)
C(1)-C(1A)-C(8)	131.9(2)	C(5)-C(6A)-C(7A)	113.4(4)
C(4A)-C(1A)-C(8)	122.3(2)	C(5)-C(6B)-C(7B)	115.6(6)
Cl(2)-C(2)-C(1)	123.6(2)	C(6A)-C(7A)-C(8)	115.1(4)
Cl(2)-C(2)-C(3)	128.3(2)	C(6B)-C(7B)-C(8)	112.8(6)
C(1)-C(2)-C(3)	107.7(2)	C(1A)-C(8)-C(7A)	116.6(3)
Cl(3)-C(3)-C(2)	127.7(2)	C(1A)-C(8)-C(7B)	119.6(4)
Cl(3)-C(3)-C(4)	123.5(2)	ClA-C(9)-ClB)	108.87(13)
C(2)-C(3)-C(4)	108.2(2)	ClA-C(9)-C(1)	114.4(2)
Cl(4)-C(4)-C(3)	117.0(2)	ClA-C(9)-C(4)	114.2(2)
Cl(4)-C(4)-C(4A)	116.9(2)	ClB-C(9)-C(1)	112.4(2)
Cl(4)-C(4)-C(9)	115.9(2)	ClB-C(9)-C(4)	113.5(2)
C(3)-C(4)-C(4A)	105.8(2)	C(1)-C(9)-C(4)	92.8(2)

Figure Caption

Figure 1 ORTEP drawings of **6** (50% probability ellipsoids) showing only the A component of the disorder for clarity.



Contract No. N00014-95-1-0013 and N00014-97-1-0409

Program Officer: R. Miller/J. Goldwasser

**Title: Experimental Charge Densities and Electrostatic Potentials in Energetic
Materials and Infrastructure Upgrade for an X-ray Crystallography
Laboratory**

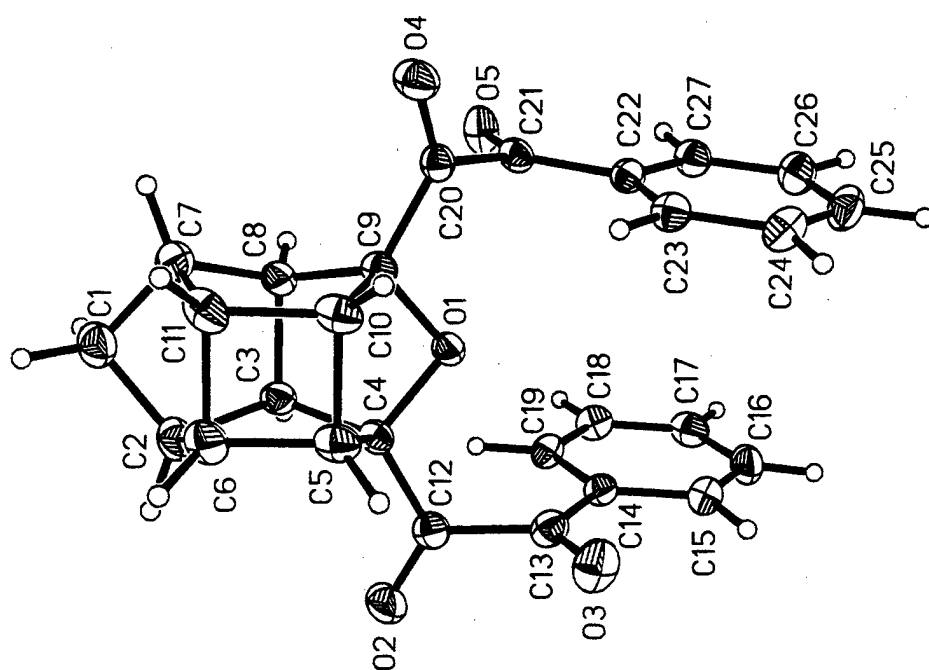
PI: A. Alan Pinkerton

Department of Chemistry, University of Toledo, Toledo, OH 43606

tel. (419) 530-4580, FAX (419) 530-4033, email apinker@uoft02.utoledo.edu

APPENDIX 6c

An Unusual Cage Functionalized Molecular Cleft from the Oxidation of 3,5-bis(2'-phenylethynyl)hexacyclo[5.4.1-0^{2,6}.0^{3,10}.0^{5,9}]dodecane.



Crystallography

A colourless fragment of K-512 was mounted on a fine glass fiber with epoxy resin. Preliminary examination and data collection were carried out at 100(1) K on a Siemens SMART Platform diffractometer. 0.1° omega scans with 60 second exposure time were carried out at three different phi settings corresponding to a nominal hemisphere of data. The intensities were corrected for absorption and decay (SADABS [1]). The structure was solved by direct methods (SHELXS-86 [2]) in the space group C2/c. All non-hydrogen atoms were refined using full matrix least-squares (SHELXL-93 [3]) with anisotropic displacement parameters. Positional parameters and isotropic displacement parameters were refined for all hydrogen atoms. Structure solution and refinement are summarized in Table 1. Complete details including tables of all atomic coordinates, bond lengths, angles and lists of observed and calculated structure factors are available upon request.

The structure consists of two crystallographically distinct molecules. The atoms of one molecule (O1-O5, C1-C27) lie on general positions. The second molecule has a symmetry imposed disorder with the molecule lying across the two-fold axis with O6 lying on the two-fold axis. The CH₂ group of the cage is disordered with atoms C28, H28A and H28B having 50% site occupancies. The probability ellipsoids of C29 and C33 are slightly elongated along the C29-C33^I and C33-C29^I bonds as would be anticipated for this type of disorder. A structurally similar disorder was also apparent for the solution obtained in the noncentrosymmetric space group Cc.

1. SADABS, G. M. Sheldrick, University of Göttingen (1996).
2. SHELXS-86, G. M. Sheldrick, *Acta Cryst.*, A46 (1990) 467.
3. SHELXL-93, G. M. Sheldrick, University of Göttingen (1993).

Table 1. Crystal data and structure refinement for K-512.

Empirical formula	C ₂₇ H ₂₀ O ₅
Formula weight	424.46
Temperature	100(1) K
Wavelength	0.71073 Å
Crystal system	Monoclinic
Space group	C2/c
Unit cell dimensions	$a = 35.6383(2)$ Å $b = 11.8110(1)$ Å, $\beta = 110.7745(2)^\circ$ $c = 15.6319(2)$ Å
Volume, Z	6152.04(9) Å ³ , 12
Density (calculated)	1.375 Mg/m ³
F(000)	2664
Absorption coeff.	0.095 mm ⁻¹
Crystal size	0.28 x 0.26 x 0.15 mm
Instrument	Siemens SMART CCD
Scan width and axis	-0.1° in ω
θ range	2.16 to 28.29°
Limiting indices	-47 < h < 46, -15 < k < 14, -16 < l < 20
Reflections collected	19839
Independent reflections	7597 (R _{int} = 0.0465)
Observed reflections [I > 2 σ (I)]	5203
Refinement method	Full-matrix least-squares on F ²
Data / restraints / parameters	7597 / 0 / 562
Goodness-of-fit on F ²	1.030
Final R indices [I > 2 σ (I)]	R ₁ = 0.0691, wR ₂ = 0.1849
R indices (all data)	R ₁ = 0.1000, wR ₂ = 0.2043
Maximum shift/e.s.d.	0.000
Largest diff. peak and hole	0.562 and -0.328 eÅ ⁻³

Table 2. Atomic coordinates and equivalent isotropic displacement parameters (\AA^2) for K-512. U(eq) is defined as one third of the orthogonalized U_{ij} tensor.

	x	y	z	U(eq)
O1	0.16927(4)	0.20348(11)	0.25468(9)	0.0199(3)
O2	0.15894(5)	0.14502(13)	0.02803(11)	0.0362(4)
O3	0.22483(4)	0.31059(13)	0.14519(12)	0.0364(4)
O4	0.17970(5)	0.15128(12)	0.48265(10)	0.0298(4)
O5	0.11144(4)	0.30644(12)	0.36845(11)	0.0294(4)
O6	0.0000	0.31017(14)	0.2500	0.0167(4)
O7	0.01149(4)	0.36402(12)	0.47805(9)	0.0263(3)
O8	-0.05612(4)	0.20547(12)	0.36355(11)	0.0302(4)
C1	0.12554(7)	-0.1477(2)	0.2219(2)	0.0309(5)
C2	0.14452(6)	-0.0794(2)	0.16487(15)	0.0272(4)
C3	0.13277(6)	0.0441(2)	0.17508(14)	0.0209(4)
C4	0.16893(5)	0.1216(2)	0.18613(13)	0.0191(4)
C5	0.20498(6)	0.0423(2)	0.23626(14)	0.0252(4)
C6	0.18971(6)	-0.0805(2)	0.2242(2)	0.0288(5)
C7	0.14372(7)	-0.0765(2)	0.3085(2)	0.0280(5)
C8	0.13196(6)	0.0461(2)	0.27503(13)	0.0213(4)
C9	0.16855(6)	0.1238(2)	0.32372(13)	0.0199(4)
C10	0.20430(6)	0.0444(2)	0.33540(14)	0.0245(4)
C11	0.18892(6)	-0.0787(2)	0.32501(14)	0.0283(5)
C12	0.16998(6)	0.1854(2)	0.10419(14)	0.0232(4)
C13	0.18837(6)	0.3044(2)	0.12251(14)	0.0242(4)
C14	0.16162(5)	0.4032(2)	0.10975(13)	0.0198(4)
C15	0.17825(6)	0.5121(2)	0.11938(15)	0.0259(4)
C16	0.15354(7)	0.6061(2)	0.1055(2)	0.0291(5)
C17	0.11233(7)	0.5924(2)	0.08287(15)	0.0280(5)
C18	0.09561(6)	0.4849(2)	0.07398(14)	0.0249(4)
C19	0.12025(6)	0.3896(2)	0.08761(14)	0.0222(4)
C20	0.16786(5)	0.1893(2)	0.40553(13)	0.0202(4)
C21	0.14757(6)	0.3057(2)	0.38621(13)	0.0205(4)
C22	0.17257(6)	0.4076(2)	0.39371(13)	0.0202(4)
C23	0.21373(6)	0.3995(2)	0.41072(14)	0.0236(4)

C24	0.23673(6)	0.4970(2)	0.4198(2)	0.0291(5)
C25	0.21843(7)	0.6026(2)	0.4117(2)	0.0305(5)
C26	0.17763(7)	0.6114(2)	0.3949(2)	0.0292(5)
C27	0.15459(6)	0.5142(2)	0.38552(14)	0.0239(4)
C28	0.04195(11)	0.6641(3)	0.2833(3)	0.0194(7)
C29	0.02226(6)	0.5934(2)	0.3298(2)	0.0283(5)
C30	0.03586(5)	0.46981(15)	0.32996(12)	0.0159(4)
C31	-0.00012(5)	0.39117(14)	0.31897(12)	0.0159(4)
C32	-0.03649(5)	0.46971(15)	0.26956(13)	0.0161(4)
C33	-0.02296(6)	0.5930(2)	0.2926(2)	0.0333(5)
C34	-0.00051(5)	0.32637(15)	0.40087(13)	0.0182(4)
C35	-0.01993(5)	0.2084(2)	0.38246(13)	0.0196(4)
C36	0.00580(5)	0.10730(15)	0.39278(13)	0.0190(4)
C37	-0.01139(6)	-0.0004(2)	0.38452(15)	0.0234(4)
C38	0.01236(7)	-0.0960(2)	0.3973(2)	0.0285(5)
C39	0.05351(7)	-0.0848(2)	0.41887(15)	0.0284(5)
C40	0.07095(6)	0.0220(2)	0.42653(14)	0.0254(4)
C41	0.04705(6)	0.1184(2)	0.41324(13)	0.0209(4)

Table 3. Anisotropic displacement parameters (\AA^2) for K-512. The anisotropic displacement factor takes the form: $-2\pi^2[(ha^*)^2U_{11} + \dots + 2hka^*b^*U_{12}]$

	U11	U22	U33	U23	U13	U12
O1	0.0245(7)	0.0170(6)	0.0190(7)	-0.0008(5)	0.0086(6)	0.0015(5)
O2	0.0580(11)	0.0283(8)	0.0233(8)	-0.0023(6)	0.0158(8)	-0.0024(7)
O3	0.0233(8)	0.0334(8)	0.0538(11)	0.0026(7)	0.0152(7)	0.0029(6)
O4	0.0395(8)	0.0267(8)	0.0223(8)	0.0009(6)	0.0098(7)	0.0071(6)
O5	0.0205(7)	0.0226(7)	0.0452(9)	-0.0047(6)	0.0118(7)	0.0010(5)
O6	0.0231(9)	0.0100(8)	0.0189(9)	0.000	0.0099(7)	0.000
O7	0.0361(8)	0.0231(7)	0.0210(7)	-0.0008(6)	0.0118(6)	-0.0019(6)
O8	0.0201(7)	0.0235(7)	0.0483(10)	0.0068(6)	0.0136(7)	0.0006(5)
C1	0.0360(12)	0.0228(10)	0.0336(12)	0.0004(9)	0.0118(10)	0.0031(9)
C2	0.0354(11)	0.0196(10)	0.0229(11)	0.0007(8)	0.0057(9)	0.0006(8)
C3	0.0226(9)	0.0208(9)	0.0211(10)	0.0000(7)	0.0098(8)	0.0025(7)
C4	0.0192(9)	0.0182(9)	0.0198(9)	-0.0009(7)	0.0071(7)	0.0031(7)
C5	0.0258(10)	0.0273(10)	0.0241(10)	0.0025(8)	0.0110(8)	0.0100(8)
C6	0.0317(11)	0.0230(10)	0.0346(12)	0.0014(9)	0.0153(9)	0.0119(8)
C7	0.0355(11)	0.0195(9)	0.0339(12)	0.0012(9)	0.0185(10)	0.0040(8)
C8	0.0239(10)	0.0192(9)	0.0220(10)	-0.0016(7)	0.0096(8)	0.0018(7)
C9	0.0224(9)	0.0186(9)	0.0189(9)	0.0014(7)	0.0075(7)	0.0049(7)
C10	0.0241(10)	0.0271(10)	0.0218(10)	0.0011(8)	0.0075(8)	0.0115(8)
C11	0.0340(11)	0.0232(10)	0.0231(10)	0.0011(8)	0.0042(9)	0.0136(8)
C12	0.0252(10)	0.0201(9)	0.0255(10)	0.0021(8)	0.0105(8)	0.0052(7)
C13	0.0227(10)	0.0249(10)	0.0270(10)	0.0019(8)	0.0115(8)	0.0007(7)
C14	0.0206(9)	0.0200(9)	0.0196(9)	0.0015(7)	0.0082(7)	0.0011(7)
C15	0.0260(10)	0.0248(10)	0.0278(11)	-0.0002(8)	0.0106(9)	-0.0029(8)
C16	0.0369(12)	0.0199(10)	0.0298(11)	-0.0011(8)	0.0112(9)	-0.0040(8)
C17	0.0370(12)	0.0219(10)	0.0257(11)	0.0027(8)	0.0118(9)	0.0080(8)
C18	0.0219(10)	0.0270(10)	0.0256(11)	0.0034(8)	0.0080(8)	0.0042(8)
C19	0.0222(9)	0.0218(9)	0.0226(10)	0.0032(8)	0.0077(8)	-0.0006(7)
C20	0.0197(9)	0.0181(9)	0.0228(10)	-0.0006(7)	0.0077(7)	0.0011(7)
C21	0.0225(9)	0.0184(9)	0.0216(10)	-0.0019(7)	0.0090(7)	0.0036(7)
C22	0.0223(9)	0.0190(9)	0.0190(9)	0.0013(7)	0.0070(7)	0.0012(7)

C23	0.0246(10)	0.0224(10)	0.0230(10)	0.0026(8)	0.0076(8)	0.0026(8)
C24	0.0244(10)	0.0325(12)	0.0301(12)	0.0078(9)	0.0093(9)	-0.0006(8)
C25	0.0340(12)	0.0249(11)	0.0304(12)	0.0065(9)	0.0087(9)	-0.0063(9)
C26	0.0346(11)	0.0208(10)	0.0318(12)	0.0043(8)	0.0110(9)	0.0028(8)
C27	0.0255(10)	0.0217(10)	0.0245(10)	0.0003(8)	0.0087(8)	0.0021(8)
C28	0.022(2)	0.012(2)	0.024(2)	-0.0034(14)	0.009(2)	-0.0028(13)
C29	0.0209(10)	0.0146(9)	0.0490(14)	0.0012(9)	0.0121(9)	0.0009(7)
C30	0.0160(8)	0.0140(8)	0.0183(9)	0.0007(7)	0.0069(7)	0.0001(6)
C31	0.0170(8)	0.0115(8)	0.0202(9)	-0.0011(6)	0.0079(7)	0.0007(6)
C32	0.0154(8)	0.0130(8)	0.0211(9)	0.0001(7)	0.0078(7)	0.0009(6)
C33	0.0211(10)	0.0128(9)	0.056(2)	-0.0039(9)	0.0014(10)	0.0017(7)
C34	0.0181(8)	0.0154(8)	0.0234(10)	0.0016(7)	0.0102(7)	0.0035(6)
C35	0.0221(9)	0.0168(9)	0.0216(10)	0.0040(7)	0.0100(8)	-0.0004(7)
C36	0.0223(9)	0.0170(9)	0.0186(9)	0.0022(7)	0.0085(7)	0.0000(7)
C37	0.0247(10)	0.0182(9)	0.0273(11)	-0.0006(7)	0.0091(8)	-0.0033(7)
C38	0.0372(12)	0.0154(9)	0.0324(12)	-0.0031(8)	0.0115(9)	-0.0012(8)
C39	0.0356(11)	0.0194(10)	0.0284(11)	-0.0017(8)	0.0092(9)	0.0060(8)
C40	0.0251(10)	0.0255(10)	0.0250(11)	-0.0011(8)	0.0079(8)	0.0039(8)
C41	0.0217(9)	0.0189(9)	0.0226(10)	-0.0010(7)	0.0083(8)	-0.0016(7)

Table 4. Bond lengths (Å) and angles (°) for K-512.

Molecule 1:		Molecule 2:	
O1-C4	1.441(2)	C28-C29	1.442(4)
O1-C9	1.439(2)	C28-C33 ^I	1.415(4)
O2-C12	1.211(2)	C29-C30	1.538(3)
O3-C13	1.222(2)	C29-C33	1.507(3)
O4-C20	1.214(2)	C30-C31	1.543(2)
O5-C21	1.217(2)	C30-C32 ^I	1.564(3)
O6-C31	1.442(2)	C31-C32	1.558(2)
O7-C34	1.212(2)	C31-C34	1.496(2)
O8-C35	1.217(2)	C32-C30 ^I	1.564(3)
C1-C2	1.526(3)	C32-C33	1.536(3)
C2-C3	1.542(3)	C33-C28 ^I	1.414(4)
C3-C4	1.539(3)	C33-C29 ^I	1.922(4)
C5-C4	1.558(3)	C34-C35	1.536(3)
C5-C6	1.537(3)	C35-C36	1.480(2)
C5-C10	1.559(3)	C36-C37	1.398(3)
C6-C2	1.547(3)	C36-C41	1.395(3)
C6-C11	1.586(3)	C37-C38	1.383(3)
C7-C1	1.529(3)	C38-C39	1.390(3)
C7-C8	1.546(3)	C39-C40	1.393(3)
C7-C11	1.539(3)	C40-C41	1.393(3)
C8-C3	1.573(3)		
C8-C9	1.555(3)		
C9-C10	1.540(2)		
C9-C20	1.502(3)		
C10-C11	1.543(3)		
C12-C4	1.498(3)		
C12-C13	1.534(3)		
C13-C14	1.475(3)		
C14-C15	1.403(3)		
C14-C19	1.399(3)		
C15-C16	1.385(3)		
C16-C17	1.393(3)		

C17-C18	1.389(3)
C18-C19	1.397(3)
C20-C21	1.532(2)
C21-C22	1.477(3)
C22-C23	1.398(3)
C22-C27	1.398(3)
C23-C24	1.391(3)
C24-C25	1.392(3)
C25-C26	1.387(3)
C26-C27	1.389(3)

C9-O1-C4	96.95(13)
C7-C1-C2	95.2(2)
C1-C2-C3	104.3(2)
C6-C2-C1	103.2(2)
C6-C2-C3	102.1(2)
C2-C3-C4	109.1(2)
C8-C3-C2	102.6(2)
C8-C3-C4	100.89(15)
O1-C4-C3	105.56(14)
O1-C4-C5	103.99(15)
O1-C4-C12	107.56(15)
C5-C4-C3	101.97(15)
C5-C4-C12	117.8(2)
C12-C4-C3	118.5(2)
C6-C5-C4	108.2(2)
C6-C5-C10	90.4(2)
C10-C5-C4	100.92(14)
C5-C6-C2	108.3(2)
C5-C6-C11	89.8(2)
C11-C6-C2	102.4(2)
C8-C7-C1	103.7(2)
C8-C7-C11	102.4(2)
C11-C7-C1	103.2(2)
C7-C8-C3	102.90(15)
C7-C8-C9	107.9(2)

C29-C28-C33 ^I	84.6(2)
C28-C29-C30	109.9(2)
C28-C29-C33	116.9(2)
C30-C29-C33 ^I	83.31(14)
C30-C29-C33	106.9(2)
C33-C29-C33 ^I	90.3(2)
C29-C30-C31	108.81(14)
C29-C30-C32 ^I	96.60(15)
C31-C30-C32 ^I	101.15(14)
O6-C31-C30	105.07(13)
O6-C31-C32	104.29(13)
O6-C31-C34	107.68(14)
C30-C31-C32	102.08(14)
C30-C31-C34	118.2(2)
C32-C31-C34	118.05(14)
C31-C32-C30 ^I	100.99(13)
C31-C32-C33	108.16(14)
C33-C32-C30 ^I	96.8(2)
C28-C33-C29 ^I	116.7(2)
C28-C33-C32	110.5(2)
C29-C33-C29 ^I	89.7(2)
C29-C33-C32	107.3(2)
C32-C33-C29 ^I	83.31(15)
O7-C34-C31	123.8(2)
O7-C34-C35	119.7(2)

C9-C8-C3	100.82(15)	C31-C34-C35	116.4(2)
O1-C9-C8	104.70(14)	O8-C35-C34	116.1(2)
O1-C9-C10	104.66(15)	O8-C35-C36	124.4(2)
O1-C9-C20	108.15(15)	C34-C35-C36	119.4(2)
C8-C9-C10	102.4(2)	C35-C36-C37	119.4(2)
C8-C9-C20	117.2(2)	C35-C36-C41	120.7(2)
C10-C9-C20	118.4(2)	C37-C36-C41	119.9(2)
C5-C10-C9	101.30(15)	C36-C37-C38	120.3(2)
C5-C10-C11	90.6(2)	C37-C38-C39	119.8(2)
C9-C10-C11	108.3(2)	C38-C39-C40	120.5(2)
C6-C11-C7	102.7(2)	C39-C40-C41	119.8(2)
C6-C11-C10	89.2(2)	C36-C41-C40	119.7(2)
C7-C11-C10	108.2(2)		
O2-C12-C4	123.0(2)		
O2-C12-C13	120.8(2)		
C13-C12-C4	116.1(2)		
O3-C13-C12	116.7(2)		
O3-C13-C14	124.2(2)		
C12-C13-C14	119.1(2)		
C13-C14-C15	118.9(2)		
C13-C14-C19	121.1(2)		
C15-C14-C19	120.0(2)		
C14-C15-C16	119.8(2)		
C15-C16-C17	120.1(2)		
C16-C17-C18	120.5(2)		
C17-C18-C19	119.8(2)		
C14-C19-C18	119.7(2)		
O4-C20-C9	123.4(2)		
O4-C20-C21	120.1(2)		
C9-C20-C21	116.3(2)		
O5-C21-C20	116.0(2)		
O5-C21-C22	124.9(2)		
C20-C21-C22	119.1(2)		
C21-C22-C23	121.5(2)		
C21-C22-C27	118.9(2)		
C23-C22-C27	119.7(2)		

C22-C23-C24	120.2(2)
C23-C24-C25	119.5(2)
C24-C25-C26	120.7(2)
C25-C26-C27	119.9(2)
C22-C27-C26	120.0(2)

Symmetry operation to generate equivalent atoms:

I -x, y, -z+1/2

Table 5. Hydrogen atomic coordinates and isotropic displacement parameters (\AA^2) for K-512.

	x	y	z	U(iso)
H1A	0.0918(8)	-0.1439(23)	0.1936(18)	0.050(8)
H1B	0.1365(8)	-0.2331(21)	0.2297(17)	0.042(7)
H2	0.1406(6)	-0.1045(17)	0.1017(15)	0.019(5)
H3	0.1085(7)	0.0711(19)	0.1291(16)	0.026(6)
H5	0.2314(6)	0.0603(18)	0.2259(14)	0.021(5)
H6	0.2060(8)	-0.1411(23)	0.2103(19)	0.048(8)
H7	0.1356(7)	-0.0988(20)	0.3610(17)	0.037(7)
H8	0.1071(7)	0.0768(19)	0.2765(15)	0.026(6)
H10	0.2295(8)	0.0652(23)	0.3868(19)	0.050(8)
H11	0.2042(7)	-0.1343(21)	0.3711(18)	0.039(7)
H15	0.2078(8)	0.5189(21)	0.1323(18)	0.039(7)
H16	0.1634(8)	0.6828(23)	0.1064(18)	0.046(7)
H17	0.0945(7)	0.6576(22)	0.0731(17)	0.037(7)
H18	0.0685(8)	0.4731(20)	0.0610(16)	0.031(6)
H19	0.1084(7)	0.3109(20)	0.0815(16)	0.027(6)
H23	0.2259(7)	0.3234(20)	0.4141(17)	0.031(6)
H24	0.2659(8)	0.4924(21)	0.4273(17)	0.037(7)
H25	0.2348(7)	0.6714(22)	0.4197(18)	0.039(7)
H26	0.1667(8)	0.6940(22)	0.3925(18)	0.042(7)
H27	0.1243(8)	0.5216(21)	0.3754(18)	0.042(7)
H28A	0.0318(12)	0.7371(36)	0.2770(28)	0.019(10)
H28B	0.0727(12)	0.6608(33)	0.3107(27)	0.016(10)
H29	0.0323(11)	0.6254(30)	0.3885(26)	0.090(12)
H30	0.0615(7)	0.4437(19)	0.3776(16)	0.030(6)
H32	-0.0623(7)	0.4498(18)	0.2750(15)	0.021(5)
H33	-0.0362(13)	0.6365(36)	0.3230(29)	0.118(15)
H37	-0.0385(8)	-0.0077(22)	0.3746(18)	0.038(7)
H38	0.0015(8)	-0.1756(22)	0.3978(18)	0.039(7)
H39	0.0702(7)	-0.1505(20)	0.4296(16)	0.027(6)
H40	0.0999(7)	0.0301(19)	0.4399(16)	0.028(6)
H41	0.0584(7)	0.1930(20)	0.4170(15)	0.025(6)

Contract No. N00014-95-1-0013 and N00014-97-1-0409

Program Officer: R. Miller/J. Goldwasser

**Title: Experimental Charge Densities and Electrostatic Potentials in Energetic
Materials and Infrastructure Upgrade for an X-ray Crystallography
Laboratory**

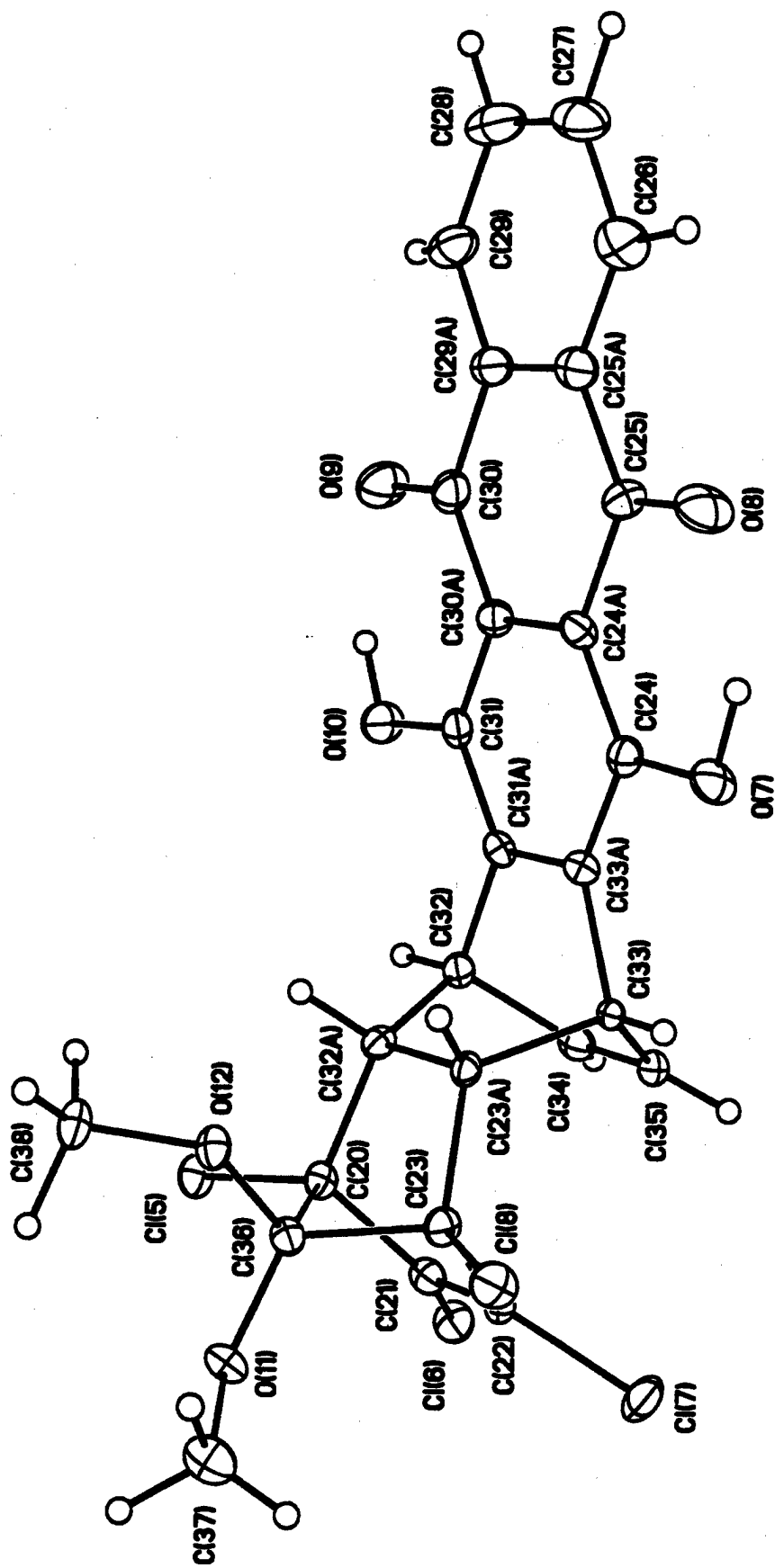
PI: A. Alan Pinkerton

Department of Chemistry, University of Toledo, Toledo, OH 43606

tel. (419) 530-4580, FAX (419) 530-4033, email apinker@uoft02.utoledo.edu

APPENDIX 6d

An Unusual Hydroquinone Grafted to a Bicyclo[2.2.2]octene moiety.



X-ray crystallography.

A red crystal of approximate dimensions 0.45 x 0.30 x 0.25 mm was mounted on a fine glass capillary with epoxy resin. Preliminary examination and data collection were performed at 150(1) K on a Siemens SMART Platform diffractometer equipped with a CCD detector. 0.3° Omega scans were carried out at three different phi settings corresponding to a nominal sphere of data, with frame time set at <20> seconds. The final unit cell was obtained from the refinement of 8192 reflections after integration (SAINT [1]). The intensity data were corrected for decay and absorption (SADABS [2]). The structure was solved in the noncentrosymmetric space group $Pna2_1$ by direct methods (SHELXS-86 [3]) and refined as a racemic twin. There are two molecules in the asymmetric unit. All nonhydrogen atoms were refined with anisotropic displacement parameters by full matrix least-squares on F^2 (SHELXL-93 [4]). The atoms C(5)/C(24) and C(6)/C(25) were constrained to have the same displacement parameters. Hydrogen atoms were included with their isotropic displacement parameters refined, methyl hydrogen atoms bonded to C(19) and C(37) were constrained to have the same displacement parameter, respectively.

Details of the data collection and refinement are given in Table 1. Fractional atomic coordinates, anisotropic displacement parameters, bond lengths and bond angles are presented in Tables 2 to 5.

1. SAINT, Siemens Energy and Automation (1994-1996).
2. SADABS, G. M. Sheldrick, University of Göttingen (1996)
3. SHELXS-86, G. M. Sheldrick, *Acta Cryst.*, A46 (1990) 467.
4. SHELXL-93, G. M. Sheldrick, University of Göttingen (1993).

Table 1. Crystal data and structure refinement for sad.

Empirical formula	C ₂₇ H ₁₈ Cl ₄ O ₆
Formula weight	580.21
Temperature	150(2) K
Wavelength	0.71073 Å
Crystal system, space group	Orthorhombic, Pna2(1)
Unit cell dimensions	a = 13.4677(6) Å alpha = 90 deg. b = 8.5420(4) Å beta = 90 deg. c = 41.5458(17) Å gamma = 90 deg.
Volume	4779.5(4) Å ³
Z, Calculated density	8, 1.613 Mg/m ³
Absorption coefficient	0.540 mm ⁻¹
F(000)	2368
Crystal size	0.45 x 0.30 x 0.25 mm
Theta range for data collection	2.43 to 28.29 deg.
Limiting indices	-17<=h<=7, -11<=k<=10, -55<=l<=55
Reflections collected / unique	31623 / 11798 [R(int) = 0.0481]
Completeness to theta = 28.29	99.9 %
Refinement method	Full-matrix least-squares on F ²
Data / restraints / parameters	11798 / 1 / 796
Goodness-of-fit on F ²	1.047
Final R indices [I>2sigma(I)]	R1 = 0.0414, wR2 = 0.0977
R indices (all data)	R1 = 0.0502, wR2 = 0.1024
Absolute structure parameter	0.22(5)
Largest diff. peak and hole	0.521 and -0.376 e.Å ⁻³

Table 2. Atomic coordinates ($\times 10^4$) and equivalent isotropic displacement parameters ($\text{\AA}^2 \times 10^3$) for sad.
 $U(\text{eq})$ is defined as one third of the trace of the orthogonalized U_{ij} tensor.

	x	y	z	U(eq)
Cl(1)	5616(1)	7283(1)	6568(1)	19(1)
Cl(2)	4951(1)	10489(1)	6201(1)	23(1)
Cl(3)	6971(1)	12741(1)	6050(1)	26(1)
Cl(4)	8978(1)	10933(1)	6330(1)	24(1)
Cl(5)	6893(1)	2257(1)	9954(1)	20(1)
Cl(6)	7565(1)	5461(1)	10325(1)	24(1)
Cl(7)	5535(1)	7717(1)	10476(1)	30(1)
Cl(8)	3540(1)	5944(1)	10190(1)	23(1)
O(1)	8725(2)	13402(3)	7470(1)	26(1)
O(2)	9220(2)	13241(4)	8069(1)	34(1)
O(3)	6098(2)	9510(4)	8335(1)	33(1)
O(4)	5558(2)	9525(4)	7744(1)	25(1)
O(5)	7436(2)	7872(4)	6131(1)	19(1)
O(6)	8176(3)	7797(4)	6635(1)	18(1)
O(7)	3798(2)	8399(3)	9052(1)	25(1)
O(8)	3303(2)	8247(4)	8452(1)	34(1)
O(9)	6427(2)	4519(4)	8186(1)	35(1)
O(10)	6969(2)	4521(4)	8776(1)	26(1)
O(11)	5084(2)	2875(4)	10393(1)	20(1)
O(12)	4339(3)	2786(4)	9888(1)	17(1)
C(1)	6434(2)	8884(3)	6561(1)	14(1)
C(2)	6140(2)	10164(4)	6324(1)	17(1)
C(3)	6927(2)	11040(4)	6263(1)	18(1)
C(4)	7776(2)	10377(4)	6454(1)	16(1)
C(4A)	7606(2)	10641(3)	6821(1)	15(1)
C(5)	7966(6)	12462(3)	7550(2)	18(1)
C(5A)	7806(2)	11931(4)	7874(1)	19(1)
C(6)	8499(5)	12417(4)	8112(2)	21(1)
C(6A)	8304(3)	11857(4)	8461(1)	24(1)
C(7)	8926(5)	12360(5)	8712(2)	28(1)
C(8)	8730(3)	11880(6)	9025(1)	36(1)
C(9)	7950(3)	10909(5)	9088(1)	35(1)
C(10)	7326(4)	10389(6)	8846(1)	33(1)
C(10A)	7497(3)	10885(4)	8529(1)	25(1)
C(11)	6804(3)	10373(4)	8273(1)	23(1)
C(11A)	6990(2)	10942(4)	7943(1)	19(1)
C(12)	6342(2)	10480(4)	7699(1)	18(1)
C(12A)	6508(2)	11026(3)	7384(1)	16(1)
C(13)	5904(2)	10527(4)	7092(1)	16(1)
C(13A)	6689(2)	9572(3)	6897(1)	14(1)
C(14)	7374(5)	12307(5)	6954(2)	23(1)
C(14A)	7300(2)	11982(4)	7315(1)	18(1)
C(15)	5637(3)	12010(5)	6913(1)	19(1)
C(16)	6401(3)	12917(5)	6841(1)	20(1)
C(17)	7519(2)	8561(3)	6431(1)	15(1)
C(18)	8330(5)	7711(6)	5946(1)	23(1)
C(19)	7996(3)	6165(4)	6690(1)	23(1)
C(20)	6077(2)	3876(3)	9963(1)	15(1)
C(21)	6378(2)	5154(4)	10198(1)	18(1)
C(22)	5590(2)	6032(4)	10260(1)	18(1)
C(23)	4738(2)	5361(4)	10067(1)	18(1)
C(23A)	4915(2)	5625(3)	9699(1)	14(1)
C(24)	4560(6)	7458(3)	8962(2)	18(1)
C(24A)	4717(2)	6925(4)	8652(1)	18(1)
C(25)	4032(5)	7413(4)	8382(2)	21(1)

C(25A)	4222(3)	6860(4)	8061(1)	24(1)
C(26)	3599(6)	7353(6)	7816(2)	32(2)
C(27)	3790(3)	6883(6)	7500(1)	37(1)
C(28)	4577(3)	5900(5)	7429(1)	37(1)
C(29)	5207(4)	5398(6)	7676(1)	30(1)
C(29A)	5024(3)	5878(4)	7992(1)	23(1)
C(30)	5715(3)	5389(5)	8252(1)	23(1)
C(30A)	5535(2)	5944(4)	8579(1)	17(1)
C(31)	6187(2)	5481(3)	8826(1)	18(1)
C(31A)	6018(2)	6011(3)	9138(1)	16(1)
C(32)	6614(2)	5515(4)	9431(1)	16(1)
C(32A)	5830(2)	4566(4)	9625(1)	15(1)
C(33)	5091(4)	7328(4)	9566(1)	11(1)
C(33A)	5227(2)	6981(4)	9209(1)	17(1)
C(34)	6878(3)	7001(5)	9612(1)	20(1)
C(35)	6118(3)	7906(5)	9682(1)	20(1)
C(36)	4994(2)	3577(4)	10093(1)	16(1)
C(37)	4199(5)	2809(7)	10591(1)	27(1)
C(38)	4505(3)	1156(4)	9836(1)	23(1)

Table 3. Bond lengths [Å] and angles [deg] for sad.

Cl(1)-C(1)	1.756(3)
Cl(2)-C(2)	1.704(3)
Cl(3)-C(3)	1.701(3)
Cl(4)-C(4)	1.766(3)
Cl(5)-C(20)	1.767(3)
Cl(6)-C(21)	1.704(3)
Cl(7)-C(22)	1.697(3)
Cl(8)-C(23)	1.764(3)
O(1)-C(5)	1.342(7)
O(1)-H(10)	0.75(5)
O(2)-C(6)	1.214(7)
O(3)-C(11)	1.231(5)
O(4)-C(12)	1.347(4)
O(4)-H(40)	0.77(5)
O(5)-C(17)	1.383(4)
O(5)-C(18)	1.435(7)
O(6)-C(17)	1.387(5)
O(6)-C(19)	1.434(4)
O(7)-C(24)	1.355(7)
O(7)-H(70)	0.96(5)
O(8)-C(25)	1.246(7)
O(9)-C(30)	1.245(5)
O(10)-C(31)	1.350(4)
O(10)-H(100)	0.90(7)
O(11)-C(36)	1.388(4)
O(11)-C(37)	1.449(7)
O(12)-C(36)	1.399(4)
O(12)-C(38)	1.427(4)
C(1)-C(2)	1.523(4)
C(1)-C(13A)	1.553(4)
C(1)-C(17)	1.583(4)
C(2)-C(3)	1.322(5)
C(3)-C(4)	1.504(4)
C(4)-C(4A)	1.557(4)
C(4)-C(17)	1.592(4)
C(4A)-C(14)	1.558(6)
C(4A)-C(13A)	1.568(4)
C(4A)-H(4A)	0.97(3)
C(5)-C(14A)	1.388(8)
C(5)-C(5A)	1.436(8)
C(5A)-C(11A)	1.415(5)
C(5A)-C(6)	1.422(8)
C(6)-C(6A)	1.547(7)
C(6A)-C(10A)	1.397(6)
C(6A)-C(7)	1.406(7)
C(7)-C(8)	1.387(8)
C(7)-H(7)	0.82(4)
C(8)-C(9)	1.364(7)
C(8)-H(8)	0.91(7)
C(9)-C(10)	1.384(6)
C(9)-H(9)	0.85(6)
C(10)-C(10A)	1.406(6)
C(10)-H(10)	1.13(4)
C(10A)-C(11)	1.480(5)
C(11)-C(11A)	1.475(5)
C(11A)-C(12)	1.395(4)
C(12)-C(12A)	1.407(4)
C(12A)-C(14A)	1.373(5)
C(12A)-C(13)	1.523(4)
C(13)-C(15)	1.511(5)
C(13)-C(13A)	1.561(4)
C(13)-H(13)	0.96(4)

C(13A)-H(13A)	0.99(3)
C(14)-C(16)	1.487(8)
C(14)-C(14A)	1.527(7)
C(14)-H(14)	0.92(4)
C(15)-C(16)	1.322(6)
C(15)-H(15)	1.09(4)
C(16)-H(16)	0.92(4)
C(18)-H(181)	1.00(7)
C(18)-H(182)	0.94(5)
C(18)-H(183)	1.06(4)
C(19)-H(191)	0.98(4)
C(19)-H(192)	1.06(4)
C(19)-H(193)	0.99(5)
C(20)-C(21)	1.520(4)
C(20)-C(32A)	1.557(4)
C(20)-C(36)	1.576(4)
C(21)-C(22)	1.326(5)
C(22)-C(23)	1.512(4)
C(23)-C(23A)	1.563(4)
C(23)-C(36)	1.566(4)
C(23A)-C(32A)	1.560(4)
C(23A)-C(33)	1.574(5)
C(23A)-H(23A)	0.98(4)
C(24)-C(24A)	1.385(8)
C(24)-C(33A)	1.422(8)
C(24A)-C(30A)	1.417(4)
C(24A)-C(25)	1.510(7)
C(25)-C(25A)	1.440(7)
C(25A)-C(26)	1.383(8)
C(25A)-C(29A)	1.397(6)
C(26)-C(27)	1.397(8)
C(26)-H(26)	1.02(5)
C(27)-C(28)	1.383(7)
C(27)-H(27)	1.00(5)
C(28)-C(29)	1.398(7)
C(28)-H(28)	0.93(5)
C(29)-C(29A)	1.395(6)
C(29)-H(29)	0.63(4)
C(29A)-C(30)	1.488(5)
C(30)-C(30A)	1.457(5)
C(30A)-C(31)	1.406(4)
C(31)-C(31A)	1.394(4)
C(31A)-C(33A)	1.380(5)
C(31A)-C(32)	1.520(4)
C(32)-C(34)	1.516(5)
C(32)-C(32A)	1.556(4)
C(32)-H(32)	1.05(4)
C(32A)-H(32A)	0.99(4)
C(33)-C(33A)	1.526(6)
C(33)-C(35)	1.546(6)
C(33)-H(33)	0.92(4)
C(34)-C(35)	1.316(6)
C(34)-H(34)	0.71(5)
C(35)-H(35)	0.92(4)
C(37)-H(371)	1.00(4)
C(37)-H(372)	0.90(5)
C(37)-H(373)	0.89(4)
C(38)-H(381)	0.94(5)
C(38)-H(382)	1.12(4)
C(38)-H(383)	0.99(5)

C(5)-O(1)-H(10)	110(4)
C(12)-O(4)-H(40)	117(4)
C(17)-O(5)-C(18)	117.1(3)
C(17)-O(6)-C(19)	116.6(3)
C(24)-O(7)-H(70)	107(3)

C(31)-O(10)-H(100)	105(4)
C(36)-O(11)-C(37)	117.1(3)
C(36)-O(12)-C(38)	117.7(3)
C(2)-C(1)-C(13A)	111.5(2)
C(2)-C(1)-C(17)	98.3(2)
C(13A)-C(1)-C(17)	99.7(2)
C(2)-C(1)-Cl(1)	114.1(2)
C(13A)-C(1)-Cl(1)	114.7(2)
C(17)-C(1)-Cl(1)	116.7(2)
C(3)-C(2)-C(1)	108.8(3)
C(3)-C(2)-Cl(2)	127.1(3)
C(1)-C(2)-Cl(2)	123.7(2)
C(2)-C(3)-C(4)	107.1(3)
C(2)-C(3)-Cl(3)	127.7(3)
C(4)-C(3)-Cl(3)	124.7(2)
C(3)-C(4)-C(4A)	110.6(3)
C(3)-C(4)-C(17)	99.8(2)
C(4A)-C(4)-C(17)	99.7(2)
C(3)-C(4)-Cl(4)	116.1(2)
C(4A)-C(4)-Cl(4)	112.5(2)
C(17)-C(4)-Cl(4)	116.3(2)
C(4)-C(4A)-C(14)	120.6(3)
C(4)-C(4A)-C(13A)	103.2(2)
C(14)-C(4A)-C(13A)	107.6(3)
C(4)-C(4A)-H(4A)	106.5(18)
C(14)-C(4A)-H(4A)	107.8(19)
C(13A)-C(4A)-H(4A)	110.9(19)
O(1)-C(5)-C(14A)	119.6(6)
O(1)-C(5)-C(5A)	122.5(6)
C(14A)-C(5)-C(5A)	117.9(5)
C(11A)-C(5A)-C(6)	122.9(4)
C(11A)-C(5A)-C(5)	119.6(4)
C(6)-C(5A)-C(5)	117.5(5)
O(2)-C(6)-C(5A)	126.2(5)
O(2)-C(6)-C(6A)	117.0(5)
C(5A)-C(6)-C(6A)	116.7(5)
C(10A)-C(6A)-C(7)	119.7(4)
C(10A)-C(6A)-C(6)	120.3(4)
C(7)-C(6A)-C(6)	120.0(5)
C(8)-C(7)-C(6A)	119.5(6)
C(8)-C(7)-H(7)	126(3)
C(6A)-C(7)-H(7)	115(3)
C(9)-C(8)-C(7)	120.5(4)
C(9)-C(8)-H(8)	120(4)
C(7)-C(8)-H(8)	119(5)
C(8)-C(9)-C(10)	121.5(4)
C(8)-C(9)-H(9)	120(4)
C(10)-C(9)-H(9)	118(4)
C(9)-C(10)-C(10A)	119.1(5)
C(9)-C(10)-H(10)	125(2)
C(10A)-C(10)-H(10)	116(2)
C(6A)-C(10A)-C(10)	119.8(4)
C(6A)-C(10A)-C(11)	121.4(3)
C(10)-C(10A)-C(11)	118.8(4)
O(3)-C(11)-C(11A)	121.6(4)
O(3)-C(11)-C(10A)	120.8(3)
C(11A)-C(11)-C(10A)	117.6(3)
C(12)-C(11A)-C(5A)	120.5(3)
C(12)-C(11A)-C(11)	118.4(3)
C(5A)-C(11A)-C(11)	121.1(3)
O(4)-C(12)-C(11A)	124.0(3)
O(4)-C(12)-C(12A)	117.2(3)
C(11A)-C(12)-C(12A)	118.8(3)
C(14A)-C(12A)-C(12)	121.0(3)
C(14A)-C(12A)-C(13)	114.5(3)
C(12)-C(12A)-C(13)	124.3(3)

C(15)-C(13)-C(12A)	106.5(2)
C(15)-C(13)-C(13A)	110.2(2)
C(12A)-C(13)-C(13A)	101.4(2)
C(15)-C(13)-H(13)	114(2)
C(12A)-C(13)-H(13)	112(2)
C(13A)-C(13)-H(13)	112(2)
C(1)-C(13A)-C(13)	120.9(2)
C(1)-C(13A)-C(4A)	102.4(2)
C(13)-C(13A)-C(4A)	109.5(2)
C(1)-C(13A)-H(13A)	107(2)
C(13)-C(13A)-H(13A)	104(2)
C(4A)-C(13A)-H(13A)	113(2)
C(16)-C(14)-C(14A)	108.4(5)
C(16)-C(14)-C(4A)	112.6(4)
C(14A)-C(14)-C(4A)	101.3(3)
C(16)-C(14)-H(14)	109(2)
C(14A)-C(14)-H(14)	109(2)
C(4A)-C(14)-H(14)	116(2)
C(12A)-C(14A)-C(5)	122.1(4)
C(12A)-C(14A)-C(14)	111.3(3)
C(5)-C(14A)-C(14)	126.4(4)
C(16)-C(15)-C(13)	114.7(3)
C(16)-C(15)-H(15)	126(2)
C(13)-C(15)-H(15)	119(2)
C(15)-C(16)-C(14)	114.1(4)
C(15)-C(16)-H(16)	124(3)
C(14)-C(16)-H(16)	122(3)
O(5)-C(17)-O(6)	113.7(3)
O(5)-C(17)-C(1)	107.8(2)
O(6)-C(17)-C(1)	117.5(3)
O(5)-C(17)-C(4)	119.2(3)
O(6)-C(17)-C(4)	106.4(3)
C(1)-C(17)-C(4)	90.6(2)
O(5)-C(18)-H(181)	109(4)
O(5)-C(18)-H(182)	106(3)
H(181)-C(18)-H(182)	133(4)
O(5)-C(18)-H(183)	114(2)
H(181)-C(18)-H(183)	100(4)
H(182)-C(18)-H(183)	92(3)
O(6)-C(19)-H(191)	113(2)
O(6)-C(19)-H(192)	106(2)
H(191)-C(19)-H(192)	118(3)
O(6)-C(19)-H(193)	108(3)
H(191)-C(19)-H(193)	104(3)
H(192)-C(19)-H(193)	107(3)
C(21)-C(20)-C(32A)	111.3(2)
C(21)-C(20)-C(36)	98.2(2)
C(32A)-C(20)-C(36)	100.0(2)
C(21)-C(20)-Cl(5)	114.2(2)
C(32A)-C(20)-Cl(5)	114.2(2)
C(36)-C(20)-Cl(5)	117.1(2)
C(22)-C(21)-C(20)	108.6(3)
C(22)-C(21)-Cl(6)	127.1(3)
C(20)-C(21)-Cl(6)	124.1(2)
C(21)-C(22)-C(23)	106.8(3)
C(21)-C(22)-Cl(7)	128.2(3)
C(23)-C(22)-Cl(7)	124.6(2)
C(22)-C(23)-C(23A)	110.4(3)
C(22)-C(23)-C(36)	99.6(2)
C(23A)-C(23)-C(36)	99.9(2)
C(22)-C(23)-Cl(8)	115.7(2)
C(23A)-C(23)-Cl(8)	112.4(2)
C(36)-C(23)-Cl(8)	117.1(2)
C(32A)-C(23A)-C(23)	103.3(2)
C(32A)-C(23A)-C(33)	110.4(3)
C(23)-C(23A)-C(33)	120.0(3)

C(32A)-C(23A)-H(23A)	114(2)
C(23)-C(23A)-H(23A)	107(2)
C(33)-C(23A)-H(23A)	102(2)
O(7)-C(24)-C(24A)	124.5(6)
O(7)-C(24)-C(33A)	116.9(5)
C(24A)-C(24)-C(33A)	118.7(5)
C(24)-C(24A)-C(30A)	120.8(4)
C(24)-C(24A)-C(25)	120.5(4)
C(30A)-C(24A)-C(25)	118.7(3)
O(8)-C(25)-C(25A)	122.8(6)
O(8)-C(25)-C(24A)	117.8(5)
C(25A)-C(25)-C(24A)	119.3(4)
C(26)-C(25A)-C(29A)	120.1(4)
C(26)-C(25A)-C(25)	118.3(5)
C(29A)-C(25A)-C(25)	121.6(4)
C(25A)-C(26)-C(27)	119.4(6)
C(25A)-C(26)-H(26)	126(2)
C(27)-C(26)-H(26)	114(2)
C(28)-C(27)-C(26)	121.0(5)
C(28)-C(27)-H(27)	120(3)
C(26)-C(27)-H(27)	119(3)
C(27)-C(28)-C(29)	119.8(4)
C(27)-C(28)-H(28)	118(3)
C(29)-C(28)-H(28)	122(3)
C(29A)-C(29)-C(28)	119.4(5)
C(29A)-C(29)-H(29)	116(4)
C(28)-C(29)-H(29)	124(4)
C(29)-C(29A)-C(25A)	120.3(4)
C(29)-C(29A)-C(30)	119.4(4)
C(25A)-C(29A)-C(30)	120.2(3)
O(9)-C(30)-C(30A)	121.9(4)
O(9)-C(30)-C(29A)	119.3(4)
C(30A)-C(30)-C(29A)	118.8(3)
C(31)-C(30A)-C(24A)	119.8(3)
C(31)-C(30A)-C(30)	118.9(3)
C(24A)-C(30A)-C(30)	121.4(3)
O(10)-C(31)-C(31A)	117.9(3)
O(10)-C(31)-C(30A)	123.1(3)
C(31A)-C(31)-C(30A)	119.0(3)
C(33A)-C(31A)-C(31)	121.3(3)
C(33A)-C(31A)-C(32)	113.9(3)
C(31)-C(31A)-C(32)	124.7(3)
C(34)-C(32)-C(31A)	106.6(2)
C(34)-C(32)-C(32A)	109.8(2)
C(31A)-C(32)-C(32A)	101.6(2)
C(34)-C(32)-H(32)	114(2)
C(31A)-C(32)-H(32)	115(2)
C(32A)-C(32)-H(32)	109(2)
C(32)-C(32A)-C(20)	121.2(3)
C(32)-C(32A)-C(23A)	109.7(2)
C(20)-C(32A)-C(23A)	102.1(2)
C(32)-C(32A)-H(32A)	113(2)
C(20)-C(32A)-H(32A)	103(2)
C(23A)-C(32A)-H(32A)	107(2)
C(33A)-C(33)-C(35)	104.9(4)
C(33A)-C(33)-C(23A)	100.4(3)
C(35)-C(33)-C(23A)	108.7(3)
C(33A)-C(33)-H(33)	115(2)
C(35)-C(33)-H(33)	120(3)
C(23A)-C(33)-H(33)	106(3)
C(31A)-C(33A)-C(24)	120.5(4)
C(31A)-C(33A)-C(33)	114.6(3)
C(24)-C(33A)-C(33)	124.6(4)
C(35)-C(34)-C(32)	114.9(3)
C(35)-C(34)-H(34)	120(4)
C(32)-C(34)-H(34)	125(4)

C(34)-C(35)-C(33)	116.0(4)
C(34)-C(35)-H(35)	122(3)
C(33)-C(35)-H(35)	122(3)
O(11)-C(36)-O(12)	113.1(3)
O(11)-C(36)-C(23)	120.0(3)
O(12)-C(36)-C(23)	106.9(3)
O(11)-C(36)-C(20)	107.3(2)
O(12)-C(36)-C(20)	117.0(3)
C(23)-C(36)-C(20)	91.3(2)
O(11)-C(37)-H(371)	105(2)
O(11)-C(37)-H(372)	108(4)
H(371)-C(37)-H(372)	102(3)
O(11)-C(37)-H(373)	102(2)
H(371)-C(37)-H(373)	115(3)
H(372)-C(37)-H(373)	123(3)
O(12)-C(38)-H(381)	109(3)
O(12)-C(38)-H(382)	109(2)
H(381)-C(38)-H(382)	106(3)
O(12)-C(38)-H(383)	108(3)
H(381)-C(38)-H(383)	108(3)
H(382)-C(38)-H(383)	117(3)

Symmetry transformations used to generate equivalent atoms:

Table 4. Anisotropic displacement parameters ($\text{\AA}^2 \times 10^3$) for sad.
The anisotropic displacement factor exponent takes the form:
 $-2 \pi^2 [h^2 a^{*2} U_{11} + \dots + 2 h k a^* b^* U_{12}]$

	U11	U22	U33	U23	U13	U12
Cl(1)	15(1)	17(1)	26(1)	-1(1)	0(1)	-5(1)
Cl(2)	21(1)	24(1)	25(1)	-1(1)	-6(1)	7(1)
Cl(3)	39(1)	18(1)	22(1)	6(1)	2(1)	1(1)
Cl(4)	21(1)	24(1)	26(1)	0(1)	6(1)	-9(1)
Cl(5)	16(1)	17(1)	27(1)	0(1)	-4(1)	5(1)
Cl(6)	21(1)	24(1)	26(1)	0(1)	-7(1)	-6(1)
Cl(7)	42(1)	22(1)	25(1)	-10(1)	-6(1)	5(1)
Cl(8)	21(1)	26(1)	24(1)	2(1)	5(1)	10(1)
O(1)	24(1)	31(1)	22(1)	-1(1)	-2(1)	-13(1)
O(2)	34(2)	42(2)	28(1)	-5(1)	-4(1)	-14(1)
O(3)	38(2)	40(2)	22(1)	12(1)	0(1)	-8(1)
O(4)	26(2)	27(2)	21(1)	2(1)	7(1)	-9(1)
O(5)	18(1)	21(1)	18(1)	-4(1)	2(1)	-1(1)
O(6)	14(1)	14(1)	24(1)	1(1)	-2(1)	-2(1)
O(7)	26(1)	27(1)	23(1)	4(1)	1(1)	13(1)
O(8)	31(1)	44(2)	28(1)	4(1)	-8(1)	14(1)
O(9)	38(2)	39(2)	28(2)	-7(1)	2(1)	11(1)
O(10)	27(2)	26(2)	25(2)	-3(1)	-1(1)	12(1)
O(11)	18(1)	23(1)	18(1)	7(1)	1(1)	0(1)
O(12)	14(1)	15(1)	23(1)	0(1)	-4(1)	-2(1)
C(1)	15(1)	10(1)	17(1)	1(1)	0(1)	-2(1)
C(2)	18(2)	16(1)	17(1)	-1(1)	-2(1)	3(1)
C(3)	24(2)	15(1)	16(1)	1(1)	1(1)	0(1)
C(4)	16(1)	13(1)	18(1)	0(1)	2(1)	-4(1)
C(4A)	15(1)	14(1)	16(1)	1(1)	1(1)	-2(1)
C(5)	18(1)	16(1)	20(1)	-1(1)	2(1)	1(1)
C(5A)	20(2)	19(2)	20(2)	-2(1)	-1(1)	4(1)
C(6)	22(1)	24(1)	17(1)	-4(1)	1(1)	1(1)
C(6A)	25(2)	30(2)	16(1)	-3(1)	-5(1)	7(2)
C(7)	26(3)	33(2)	27(3)	-7(2)	-20(2)	7(2)
C(8)	41(2)	48(3)	18(2)	-6(2)	-8(2)	18(2)
C(9)	45(2)	44(2)	17(2)	3(2)	-5(2)	16(2)
C(10)	39(3)	36(2)	25(2)	5(2)	-1(2)	10(2)
C(10A)	32(2)	24(2)	20(2)	1(1)	-1(1)	6(2)
C(11)	28(2)	23(2)	17(2)	4(1)	0(1)	7(2)
C(11A)	23(2)	16(2)	18(1)	-2(1)	1(1)	5(1)
C(12)	17(2)	17(2)	21(1)	1(1)	3(1)	0(1)
C(12A)	18(1)	14(1)	17(1)	-2(1)	1(1)	1(1)
C(13)	15(1)	17(1)	17(1)	-1(1)	1(1)	-2(1)
C(13A)	14(1)	11(1)	16(1)	0(1)	-1(1)	-1(1)
C(14)	30(3)	14(2)	24(2)	1(2)	3(2)	-12(2)
C(14A)	21(2)	13(2)	19(1)	-1(1)	3(1)	2(1)
C(15)	21(2)	15(2)	22(2)	-1(1)	-2(1)	6(1)
C(16)	26(2)	12(2)	21(2)	0(2)	-1(1)	5(2)
C(17)	16(1)	13(1)	17(1)	0(1)	0(1)	-3(1)
C(18)	22(2)	35(2)	13(2)	-5(2)	5(2)	4(2)
C(19)	23(2)	18(2)	29(2)	0(1)	0(1)	1(1)
C(20)	12(1)	13(1)	19(1)	0(1)	-2(1)	4(1)
C(21)	16(1)	18(1)	18(1)	2(1)	-4(1)	-5(1)
C(22)	25(2)	12(1)	16(1)	-1(1)	-4(1)	1(1)
C(23)	17(1)	17(2)	18(1)	-1(1)	-1(1)	5(1)
C(23A)	15(1)	12(1)	15(1)	-2(1)	-1(1)	2(1)
C(24)	18(1)	16(1)	20(1)	-1(1)	2(1)	1(1)
C(24A)	20(2)	18(2)	16(1)	4(1)	2(1)	1(1)
C(25)	22(1)	24(1)	17(1)	-4(1)	1(1)	1(1)
C(25A)	25(2)	24(2)	23(2)	4(1)	-3(1)	-11(2)

C(26)	35(3)	36(3)	26(3)	6(2)	10(2)	-11(2)
C(27)	39(2)	44(3)	29(2)	8(2)	-14(2)	-16(2)
C(28)	41(2)	49(2)	21(2)	-2(2)	-2(2)	-16(2)
C(29)	35(3)	35(2)	21(2)	-5(2)	3(2)	-6(2)
C(29A)	27(2)	24(2)	19(2)	2(1)	-1(1)	-10(2)
C(30)	28(2)	20(2)	22(2)	-1(1)	6(2)	-1(2)
C(30A)	18(2)	18(2)	16(1)	0(1)	3(1)	0(1)
C(31)	20(2)	13(1)	21(1)	1(1)	3(1)	0(1)
C(31A)	16(1)	14(1)	18(1)	3(1)	1(1)	-1(1)
C(32)	16(1)	14(1)	18(1)	1(1)	1(1)	1(1)
C(32A)	14(1)	16(1)	15(1)	-2(1)	-2(1)	2(1)
C(33)	11(2)	10(1)	12(2)	0(1)	-1(1)	-4(1)
C(33A)	20(2)	18(2)	15(1)	2(1)	1(1)	0(1)
C(34)	20(2)	21(2)	19(2)	3(1)	-2(1)	-6(2)
C(35)	29(2)	14(2)	17(2)	0(2)	-2(1)	-4(2)
C(36)	15(1)	15(1)	18(1)	1(1)	-2(1)	-1(1)
C(37)	20(2)	33(2)	28(2)	6(2)	1(2)	-2(2)
C(38)	23(2)	15(2)	30(2)	-4(1)	-3(1)	-2(1)

Table 5. Hydrogen coordinates ($\times 10^4$) and isotropic displacement parameters ($\text{\AA}^2 \times 10^3$) for sad.

	x	y	z	U(eq)
H(4A)	8200(20)	10260(40)	6929(7)	2(7)
H(7)	9370(30)	12960(50)	8657(9)	12(9)
H(8)	9150(50)	12170(80)	9185(17)	53(18)
H(9)	7820(40)	10630(60)	9282(14)	57(16)
H(10)	6640(30)	9640(50)	8884(9)	24(10)
H(13)	5340(30)	9900(50)	7151(8)	14(8)
H(13A)	6860(30)	8680(40)	7039(8)	10(8)
H(14)	7850(20)	13050(40)	6919(7)	0(7)
H(15)	4870(30)	10220(50)	6850(10)	18(10)
H(16)	6350(30)	13800(50)	6719(9)	25(10)
H(181)	8900(50)	7460(50)	6094(17)	36(7)
H(182)	8140(30)	7320(50)	5744(11)	36(7)
H(183)	8590(30)	8770(50)	5843(10)	36(7)
H(191)	7740(30)	5630(50)	6500(9)	16(9)
H(192)	8650(30)	5720(40)	6795(8)	15(8)
H(193)	7460(40)	6060(50)	6853(12)	39(12)
H(23A)	4310(30)	5310(40)	9588(8)	11(8)
H(26)	2980(30)	8020(50)	7842(10)	26(10)
H(27)	3330(40)	7210(50)	7326(13)	22(12)
H(28)	4670(40)	5590(60)	7218(12)	44(14)
H(29)	5580(30)	4950(60)	7656(11)	24(13)
H(32)	7220(30)	4790(50)	9380(9)	17(9)
H(32A)	5580(30)	3650(50)	9505(9)	22(10)
H(33)	4530(30)	7890(50)	9616(10)	21(10)
H(34)	7370(40)	7250(50)	9648(11)	23(13)
H(35)	6200(30)	8840(50)	9787(9)	23(10)
H(371)	4240(30)	1790(50)	10706(9)	21(9)
H(372)	3670(40)	2650(40)	10462(13)	10(9)
H(373)	4260(30)	3660(50)	10714(8)	15(8)
H(381)	3910(30)	690(50)	9764(10)	30(6)
H(382)	4680(30)	590(50)	10072(10)	30(6)
H(383)	5000(30)	1060(50)	9663(10)	30(6)
H(70)	3430(30)	8630(50)	8859(11)	35(11)
H(10)	9080(40)	13470(60)	7608(12)	47(15)
H(40)	5390(40)	9400(50)	7919(13)	36(14)
H(100)	6960(50)	4300(70)	8564(16)	70(20)